

30 copies

NATIONAL AERONAUTICS AND SPACE ADMINISTRATION

*Technical Report 32-1246**Surveyor V Mission Report**Part I. Mission Description and Performance**Prepared by the Surveyor Project Staff*

FACILITY FORM 602	NOV 21 1968	
	(ACCESSION NUMBER)	(THRU)
	240	
	(PAGES)	(CODE)
	01-96251	31 11
	(NASA CR OR TMX OR AD NUMBER)	(CATEGORY)

JET PROPULSION LABORATORY

CALIFORNIA INSTITUTE OF TECHNOLOGY

PASADENA, CALIFORNIA

March 15, 1968

PO PRICE \$ \_\_\_\_\_

POSTAGE PRICE(S) \$ \_\_\_\_\_

Hard copy (HC) 3.50Microfiche (MF) 65

NATIONAL AERONAUTICS AND SPACE ADMINISTRATION

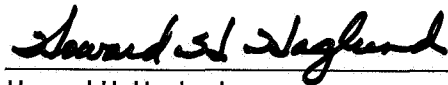
*Technical Report 32-1246*

*Surveyor V Mission Report*

*Part I. Mission Description and Performance*

*Prepared by the Surveyor Project Staff*

Approved by:

A handwritten signature in dark ink, reading "Howard H. Haglund", is written over a horizontal line.

Howard H. Haglund  
Surveyor Project Manager

JET PROPULSION LABORATORY  
CALIFORNIA INSTITUTE OF TECHNOLOGY  
PASADENA, CALIFORNIA

March 15, 1968



**TECHNICAL REPORT 32-1246**

Copyright © 1968  
Jet Propulsion Laboratory  
California Institute of Technology  
Prepared Under Contract No. NAS 7-100  
National Aeronautics & Space Administration

## Preface

This three-part document constitutes the Project Mission Report on *Surveyor V*, the fifth in a series of unmanned missions designed to soft-land on the moon and return data from the lunar surface.

Part I of this report consists of a technical description and a performance evaluation of the systems utilized in the *Surveyor V* mission. Part I was compiled using contributions of many individuals in the major systems which support the Project, and is based on data evaluation prior to approximately November 1, 1967. Some of the information in this report was obtained from other published documents; a list of these documents is presented in a bibliography.

Part II of this report presents the scientific data derived from the mission and the results of scientific analyses which have been conducted. Part III consists of selected pictures from *Surveyor V* and appropriate explanatory material.



## Contents

<b>I. Introduction and Summary . . . . .</b>	<b>1</b>
A. Surveyor Project Objectives . . . . .	1
B. Project Description . . . . .	2
C. Mission Objectives . . . . .	4
D. Mission Summary . . . . .	4
<b>II. Space Vehicle Preparations and Launch Operations . . . . .</b>	<b>11</b>
A. Spacecraft Assembly and Testing . . . . .	11
B. Combined Systems Test at San Diego . . . . .	12
C. Launch Operations at AFETR . . . . .	13
D. Launch Phase Mission Analysis . . . . .	19
<b>III. Launch Vehicle System . . . . .</b>	<b>23</b>
A. Atlas Stage . . . . .	23
B. Centaur Stage . . . . .	24
C. Launch Vehicle/Spacecraft Interface . . . . .	26
D. Vehicle Flight Sequence of Events . . . . .	28
E. Performance . . . . .	30
<b>IV. Surveyor Spacecraft . . . . .</b>	<b>35</b>
A. Spacecraft System . . . . .	35
B. Structures and Mechanisms . . . . .	55
C. Thermal Control . . . . .	62
D. Electrical Power . . . . .	64
E. Propulsion . . . . .	70
F. Flight Control . . . . .	84
G. Radar . . . . .	89
H. Telecommunications . . . . .	99
I. Television . . . . .	108
J. Alpha Scattering Instrument . . . . .	113
<b>V. Tracking and Data System . . . . .</b>	<b>121</b>
A. Air Force Eastern Test Range . . . . .	121
B. Manned Space Flight Network . . . . .	129
C. Deep Space Network . . . . .	132

## Contents (contd)

<b>VI. Mission Operations System</b>	145
A. Functions and Organization	145
B. Mission-Dependent Equipment	149
C. Mission Operations Chronology	152
<b>VII. Flight Path and Events</b>	171
A. Prelaunch	171
B. Launch Phase	171
C. Cruise Phase	172
D. Midcourse Maneuver Phase	177
E. Terminal Phase	183
F. Landing Site	189
<b>Appendix A. Surveyor V Flight Events</b>	191
<b>Appendix B. Surveyor V Spacecraft Configuration</b>	207
<b>Appendix C. Surveyor V Spacecraft Data Content of Telemetry Modes</b>	211
<b>Appendix D. Surveyor V Spacecraft Temperature Histories</b>	215
<b>Glossary</b>	223
<b>Bibliography</b>	225

## Tables

II-1. Major Surveyor V operations at Cape Kennedy	14
II-2. Surveyor V countdown time summary	19
III-1. Differences between <i>Atlas</i> LV-3C and SLV-3C	25
III-2. <i>Atlas</i> propellant residuals	31
III-3. <i>Centaur</i> usable propellant residuals	32
IV-1. Surveyor V spacecraft telemetry mode summary	40
IV-2. Surveyor V instrumentation	42
IV-3. Notable differences between <i>Surveyors IV</i> and <i>V</i>	43
IV-4. Surveyor spacecraft subsystem and system reliability estimates	43
IV-5. Surveyor V maximum measured zero-to-peak acceleration during launch phase events	48
IV-6. Summary of vernier firings conducted on Surveyor V mission	49

## Contents (contd)

### Tables (contd)

IV-7. Predicted and actual terminal descent phase events . . . . .	50
IV-8. Predicted and actual values of terminal descent parameters . . . . .	51
IV-9. Maximum axial forces in the shock absorbers and times of initial ground impact of footpads . . . . .	56
IV-10. Thermal compartment component installation . . . . .	59
IV-11. Pyrotechnic devices . . . . .	61
IV-12. Electrical power performance during transit . . . . .	67
IV-13. Vernier pressurization system functional parameters during test and flight . . . . .	76
IV-14. Flight control modes . . . . .	86
IV-15. Surveyor V star map results . . . . .	88
IV-16. AMR temperatures just before turn-on . . . . .	90
IV-17. Telecommunications performance values during transit . . . . .	106
IV-18. Typical signal processing parameter values . . . . .	108
IV-19. Characteristics of alpha scattering instrument data channels . . . . .	117
IV-20. Engineering parameters telemetered from alpha scattering instrument . . . . .	118
V-1. AFETR configuration for Surveyor V mission . . . . .	123
V-2. Real-time telemetry data retransmission . . . . .	125
V-3. Atlas/Centaur Mark Event readouts . . . . .	128
V-4. GSFC Network configuration . . . . .	129
V-5. DSN tracking data requirements . . . . .	132
V-6. Characteristics for S-band and tracking systems . . . . .	134
VI-1. CDC mission-dependent equipment support of Surveyor V at DSIF stations . . . . .	150
VI-2. Surveyor V command, TV, and alpha scattering activity before shutdown during first lunar night . . . . .	150
VII-1. Surveyor V encounter conditions based on selected pre-midcourse orbit determination . . . . .	176
VII-2. First midcourse correction alternatives comparison . . . . .	181
VII-3. Midcourse correction data . . . . .	182
VII-4. Injection and terminal conditions for pre-midcourse and post-midcourse (fifth and sixth) trajectories . . . . .	185
VII-5. Surveyor V encounter conditions based on selected post-midcourse (first) orbit determinations . . . . .	187
A-1. Mission flight events . . . . .	192
A-2. Lunar operations . . . . .	203

## Contents (contd)

### Figures

I-1. Earth-moon trajectory and major events . . . . .	5
I-2. Soft-landing sites of Surveyor V and previous missions . . . . .	7
II-1. Combined System Test Stand at San Diego . . . . .	13
II-2. Surveyor V undergoing TV calibration in SCF of Building AO . . . . .	15
II-3. Surveyor V mating to adaptor in ESF . . . . .	16
II-4. Atlas/Centaur AC-13 launching Surveyor V . . . . .	18
II-5. Final Surveyor V launch window design for September 1967 . . . . .	20
III-1. Atlas (SLV-3C)/Centaur/Surveyor space vehicle configuration . . . . .	24
III-2. Surveyor/Centaur interface configuration . . . . .	27
III-3. Surveyor V launch phase nominal events . . . . .	29
III-4. Centaur roll attitude relative to local vertical . . . . .	31
IV-1. Surveyor spacecraft in cruise mode . . . . .	36
IV-2. Simplified spacecraft functional block diagram . . . . .	37
IV-3. Spacecraft coordinates relative to celestial references . . . . .	38
IV-4. Surveyor spacecraft system reliability estimates . . . . .	43
IV-5. Terminal descent nominal events for a normal mission . . . . .	44
IV-6. Main retro phase sequence for a normal mission . . . . .	45
IV-7. Range-velocity diagram . . . . .	46
IV-8. Comparison of nominal, predicted, and actual Surveyor V terminal descent event time intervals . . . . .	50
IV-9. Surveyor V descent profile . . . . .	52
IV-10. Trench produced by Footpad 2 during landing . . . . .	53
IV-11. Surveyor V landed attitude and local lunar topography . . . . .	53
IV-12. Alpha scattering instrument sensor head positions on lunar surface . . . . .	54
IV-13. Landing leg assembly . . . . .	55
IV-14. Loads on spacecraft shock absorbers during landing . . . . .	56
IV-15. Antenna/solar panel configuration . . . . .	58
IV-16. Thermal switch . . . . .	60
IV-17. Thermal design . . . . .	63
IV-18. Predicted Surveyor V temperature response after shutdown during first lunar night . . . . .	65
IV-19. Functional diagram of Surveyor V redesigned electrical power subsystem . . . . .	66
IV-20. Battery energy profile during transit . . . . .	68

## Contents (contd)

### Figures (contd)

IV-21. Postlanding regulated power requirement . . . . .	69
IV-22. Solar panel/sun angle during lunar day . . . . .	69
IV-23. Solar panel output characteristics during lunar day . . . . .	70
IV-24. Battery performance during lunar day . . . . .	71
IV-25. Vernier propulsion system schematic including locations of pressure and temperature sensors . . . . .	72
IV-26. Vernier propulsion system installation . . . . .	73
IV-27. Helium tank assembly . . . . .	74
IV-28. Vernier engine thrust chamber assembly . . . . .	75
IV-29. Vernier propellant tank pressurization prior to Surveyor V midcourse correction . . . . .	76
IV-30. Helium tank pressure decay following midcourse correction . . . . .	77
IV-31. Surveyor V vernier engine flow test results . . . . .	78
IV-32. Propellant supply pressure decay during terminal descent . . . . .	79
IV-33. Propulsion system temperature ranges during transit and lunar day . . . . .	80
IV-34. Engine thrust during vernier static firing experiment on lunar surface . . . . .	81
IV-35. Vernier propulsion system pressures during first lunar day . . . . .	82
IV-36. Oxidizer Tank 1 thermal wrap before oxidizer leak . . . . .	83
IV-37. Oxidizer Tank 1 thermal wrap after oxidizer leak . . . . .	83
IV-38. Main retrorocket motor . . . . .	84
IV-39. Simplified flight control functional diagram . . . . .	85
IV-40. Gas-jet attitude control system . . . . .	86
IV-41. Altitude marking radar functional diagram . . . . .	49
IV-42. Altitude marking radar AGC . . . . .	91
IV-43. Simplified RADVS functional block diagram . . . . .	92
IV-44. RADVS beam orientation . . . . .	93
IV-45. Slant range vs time during terminal descent . . . . .	95
IV-46. Reflectivity of RADVS beams during terminal descent . . . . .	96
IV-47. X-component of velocity $V_x$ during descent . . . . .	98
IV-48. Y-component of velocity $V_y$ during descent . . . . .	98
IV-49. Z-component of velocity $V_z$ during descent . . . . .	98
IV-50. Radio subsystem block diagram . . . . .	99
IV-51. Spacecraft Receiver B signal level during star verification/ acquisition roll . . . . .	101



## Contents (contd)

### Figures (contd)

IV-52. Receiver A/Omniantenna A total received power during transit . . . . .	102
IV-53. Receiver B/Omniantenna B total received power during transit . . . . .	103
IV-54. DSIF received power during transit . . . . .	105
IV-55. Simplified signal processing functional block diagram . . . . .	107
IV-56. Survey TV camera . . . . .	109
IV-57. Simplified survey TV camera functional block diagram . . . . .	110
IV-58. TV photometric/colorimetric reference chart . . . . .	111
IV-59. Alpha scattering instrument components . . . . .	114
IV-60. View of bottom of alpha scattering instrument sensor head . . . . .	115
IV-61. Diagrammatic view of sensor head illustrating functional operation . . . . .	116
IV-62. Alpha scattering instrument deployment mechanism . . . . .	117
V-1. Planned launch phase TDS coverage for September 8, 1967 . . . . .	122
V-2. AFETR C-band radar coverage . . . . .	124
V-3. AFETR VHF telemetry coverage . . . . .	126
V-4. AFETR S-band telemetry coverage . . . . .	127
V-5. MSFN VHF telemetry coverage . . . . .	130
V-6. MSFN C-band radar coverage . . . . .	131
V-7. DSS 51 antenna system at Johannesburg . . . . .	133
V-8. DSIF station tracking periods and command activity: transit phase . . . . .	135
V-9. DSIF received signal level . . . . .	137
V-10. DSIF station tracking periods and command activity: postlanding (first lunar day) . . . . .	139
V-11. DSN/GCF communications links . . . . .	141
V-12. General configuration of SFOF data processing system . . . . .	143
VI-1. Organization of the MOS during the Surveyor V mission . . . . .	146
VI-2. Surveyor V telemetry bit rate/mode profile . . . . .	155
VI-3. Key spacecraft thermal and power parameters controlled during first lunar night operations before shutdown . . . . .	165
VI-4. Surveyor V lunar night survival plan and predicted battery temperature profile . . . . .	168
VII-1. Surveyor and Centaur trajectories in earth's equatorial plane . . . . .	173
VII-2. Surveyor V earth track . . . . .	174
VII-3. Computed Surveyor V pre-midcourse unbraked impact points . . . . .	175

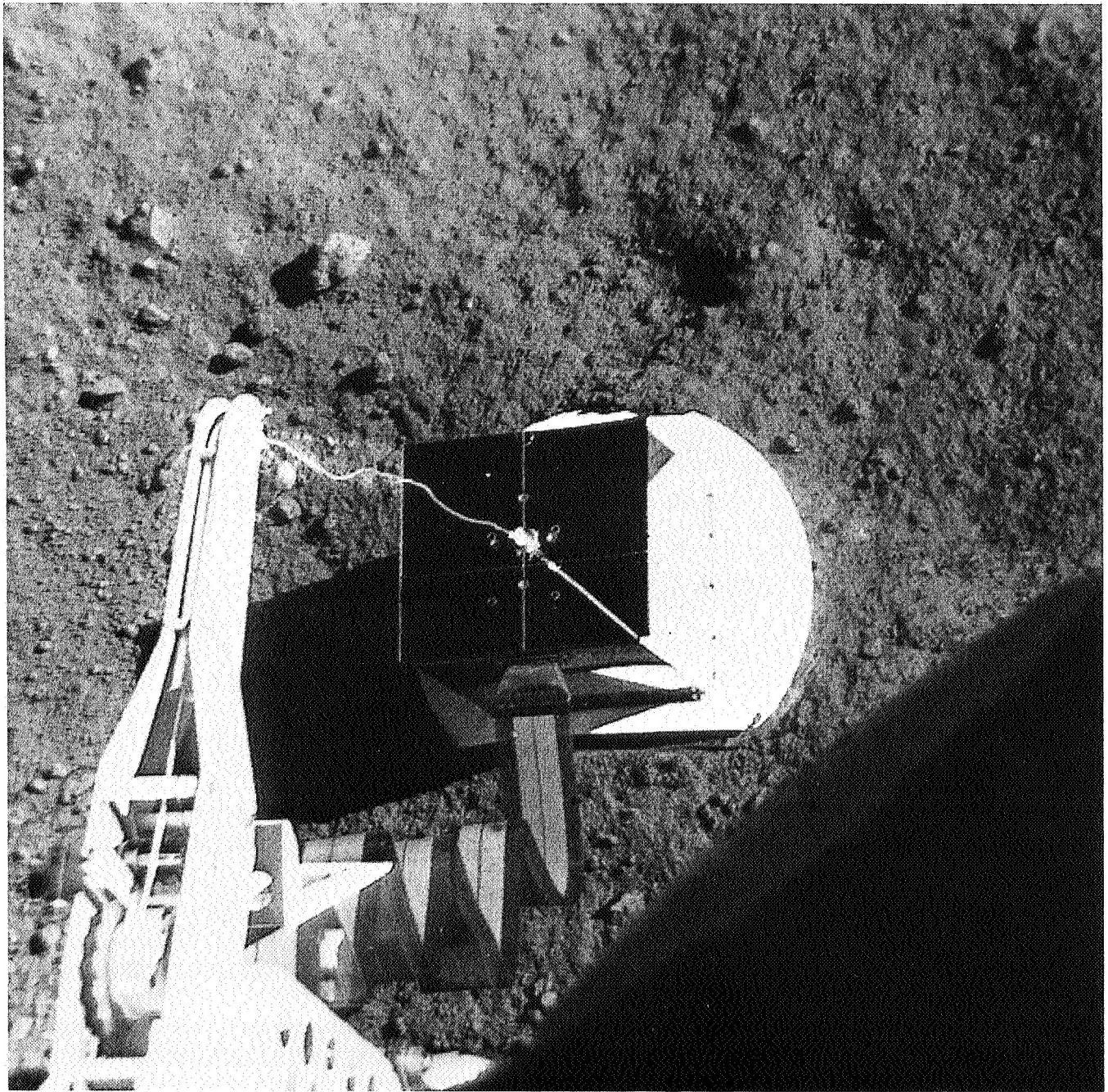
## Contents (contd)

### Figures (contd)

VII-4. Surveyor V landing location . . . . .	178
VII-5. Midcourse correction capability contours . . . . .	179
VII-6. Effect of noncritical velocity component on terminal descent parameters for first midcourse correction . . . . .	180
VII-7. Computed Surveyor V impact points for each midcourse correction . . . . .	182
VII-8. Surveyor V main retro burnout conditions compared with previous missions . . . . .	184
VII-9. Vernier descent phase capability contours—initial estimates . . . . .	184
VII-10. Main retro phase velocity diagram . . . . .	188
D-1. Landing gear transit temperatures . . . . .	216
D-2. Compartment A transit temperatures . . . . .	217
D-3. Compartment B temperatures . . . . .	217
D-4. Vernier propulsion system temperatures . . . . .	218
D-5. Main retromotor transit temperatures . . . . .	220
D-6. Radar and flight control temperatures . . . . .	220
D-7. Solar panel and planar array transit temperatures . . . . .	221
D-8. Alpha scattering instrument transit temperatures . . . . .	221
D-9. Electrical power subsystem postlanding temperatures . . . . .	221
D-10. Vernier propulsion subsystem postlanding temperatures . . . . .	222
D-11. Television camera and alpha scattering instrument postlanding temperatures . . . . .	222

## Abstract

*Surveyor V*, the fifth in a series of seven unmanned spacecraft designed to soft-land on the moon and return engineering and scientific data, was launched from Cape Kennedy, Florida, on September 8, 1967. All established objectives for the mission were achieved. Several extra midcourse corrections were performed during the transit phase in an attempt to correct a helium leak in the vernier propulsion pressurization system. Although the leak persisted, a completely successful soft landing was achieved in the Sea of Tranquility on September 11, 1967, by modifying the terminal descent sequence during the flight. *Surveyor V* performed extensive operations before shutdown after sunset of the first lunar day and also was operated the second and fourth lunar days. A large quantity of television pictures and other new data were provided on the inside of a small crater in which the spacecraft landed and the relatively level mare surface visible surrounding the crater. Of special interest are the results obtained by an alpha scattering instrument, included for the first time on this mission, which provide the first direct information on the chemical composition of the moon. Unique results were also obtained on this mission from a postlanding vernier engine static firing, which produced lunar surface erosion, and from a test of the lunar surface magnetic properties using a bar magnet.



(Photograph received September 12, 1967, 00:39:54 GMT)

# I. Introduction and Summary

*Surveyor V* was launched from Cape Kennedy, Florida, at 07:57:01.257 GMT on September 8, 1967. A completely successful soft landing was achieved in spite of a very serious vernier propulsion system helium leak which developed during midcourse correction and persisted even after several additional vernier firings were made in an attempt to correct the problem. Touchdown occurred at 00:46:44.284 GMT on September 11, 1967, in the Sea of Tranquility at 1.41 deg north latitude and 23.18 deg east longitude based on preliminary postlanding tracking analysis. Very extensive spacecraft operations were conducted through the first lunar day before shutdown during the lunar night. The spacecraft also responded during the second lunar day, permitting resumption of operations\*

*Surveyor V* landed on a 17-deg slope and came to rest with a 20-deg tilt inside a small, 30-ft-diameter crater. An alpha scattering instrument for chemical analysis of surface material and a soil magnet were utilized for the first time on this mission. Abundant data from the alpha scattering instrument, television camera, soil magnet, and other spacecraft instrumentation, together with the results of a unique postlanding vernier engine test, completely satisfies the mission objectives and provides a significant extension to, as well as confirmation of, the important findings already obtained from the *Surveyor I* and *III* missions.

\**Surveyor V* did not respond the third lunar day, but was reawakened and operated the fourth lunar day.

The success of the *Surveyor V* mission can be attributed to the intensive and resourceful effort put forth by the special HAC/JPL task force team which was assembled during the flight phase of the mission and redesigned the terminal descent sequence by taking full advantage of the inherent flexibility in the basic spacecraft design.

## A. *Surveyor* Project Objectives

The *Surveyor* Project is being conducted to explore the moon with unmanned, automated soft-landing spacecraft which are equipped to respond to earth commands and transmit back scientific and engineering data from the lunar surface.

The overall objectives of the *Surveyor* Project are:

- (1) To accomplish successful soft landings on the moon as demonstrated by operations of the spacecraft subsequent to landing.
- (2) To provide basic data in support of *Apollo*.
- (3) To perform operations on the lunar surface which will contribute new scientific knowledge about the moon and provide further information in support of *Apollo*.

The first two *Surveyor* spacecraft carried a survey television camera in addition to engineering instrumentation

for obtaining in-flight and postlanding data. As an additional instrument, *Surveyors III* and *IV* carried a soil mechanics/surface sampler (SM/SS) device to provide data based on picking, digging, and handling of lunar surface material. On *Surveyor V*, an alpha scattering instrument was substituted for the SM/SS device to obtain data from which a chemical analysis of the lunar surface material could be made. A magnet was also attached to one of the footpads of the *Surveyor IV* and *V* spacecraft to determine magnetic properties of the soil.

*Surveyor I* was launched on May 30, 1966, and soft-landed near the western end of the *Apollo* zone of interest at 2.45 deg south latitude and 43.21 deg west longitude (based on *Lunar Orbiter III* data). Operations on the lunar surface were highly successful. In addition to a wide variety of other types of lunar surface data, over 11,000 television pictures were received in the course of operations during the first two lunar days. *Surveyor I* exhibited a remarkable capability to survive eight lunar day and night cycles involving temperature extremes of +250 and -250°F.

*Surveyor II* was launched on September 20, 1966, and achieved a nominal mission until execution of the mid-course velocity correction. One of the three vernier engines did not fire, which caused the spacecraft to tumble. Attempts to stabilize the spacecraft by repeatedly firing the verniers were unsuccessful. When nearly all the spacecraft battery energy had been consumed prior to lunar encounter, the mission was terminated shortly after firing of the main retromotor 45 hr after launch. A thorough investigation by a specially appointed Failure Review Board was unable to disclose the exact cause of failure. A number of recommendations were made to assure against a similar failure and to provide better diagnostic data on future missions.

*Surveyor III* was launched on April 17, 1967, and achieved a successful soft landing, although the spacecraft lifted off twice after initial touchdown before finally coming to rest. Based on correlation with *Lunar Orbiter III* photographs, the *Surveyor III* landing site has been located in the Ocean of Storms at 2.94 deg south latitude and 23.34 deg west longitude, about 625 km east of the *Surveyor I* landing site. Important new data was obtained as a result of extensive postlanding operations with the SM/SS, television, and other spacecraft equipment. The lunar surface characteristics determined by *Surveyor III* confirmed the findings of *Surveyor I* and indicated the

suitability of an additional site for *Apollo*, which will utilize final descent and landing system technology similar to that of *Surveyor*.

*Surveyor IV* was launched on July 14, 1967, and achieved a very nominal mission until the spacecraft radio signal was abruptly lost on July 16, 1967, about 2½ min before expected soft landing. The loss of signal occurred during the main retro phase just 1.4 sec before predicted retromotor burnout, when the spacecraft was about 49,000 ft above the lunar surface and traveling 1070 ft/sec. Exhaustive attempts to reestablish telecommunications with *Surveyor IV* through July 18, 1967, were unsuccessful. A formally appointed Technical Review Board conducted a detailed examination of the *Surveyor IV* mission, but was unable to find evidence of any single or multiple cause for the failure.

The all-out effort to salvage the *Surveyor V* mission after the helium leak enabled the spacecraft to achieve a completely successful soft landing, after which it was operated very extensively on the lunar surface to fully satisfy the Project Objectives at a new site. By means of the alpha scattering instrument and soil magnet, important new data was obtained which can be used for chemical analysis and determination of magnetic properties of the lunar surface material. Data was also obtained for the first time on the lunar surface erosion effects of a vernier rocket engine firing which was conducted after landing. In addition, an abundance of television and other data was obtained through the very extensive operation of the spacecraft camera and other equipment. In supporting and extending the findings of *Surveyors I* and *III*, the data obtained from *Surveyor V* provides additional assurance of the suitability of the *Surveyor* landing sites for *Apollo*.

## B. Project Description

The *Surveyor* Project is managed by the Jet Propulsion Laboratory for the NASA Office of Space Science and Applications. The Project is supported by four major administrative and functional elements or systems: Launch Vehicle System, Spacecraft System, Tracking and Data System (TDS), and Mission Operations System (MOS). In addition to overall project management, JPL has been assigned the management responsibility for the Spacecraft, Tracking and Data Acquisition, and Mission Operations Systems. NASA/Lewis Research Center (LeRC) has been assigned responsibility for the *Atlas/Centaur* launch vehicle system.

## 1. Launch Vehicle System

*Atlas/Centaur* launch vehicle development began as an Advanced Research Projects Agency program for synchronous-orbit missions. In 1958, General Dynamics/Convair was given the contract to modify the *Atlas* first stage and develop the *Centaur* upper stage; Pratt & Whitney was given the contract to develop the high-impulse  $\text{LH}_2/\text{LO}_2$  engines for the *Centaur* stage.

The Kennedy Space Center, Unmanned Launch Operations branch, working with LeRC, is assigned the *Centaur* launch operations responsibility. The *Centaur* vehicle utilizes Launch Complex 36, which consists of two launch pads (A and B) connected to a common blockhouse. The blockhouse has separate control consoles for each of the pads. Pad 36B was utilized for the *Surveyor V* mission.

The launch of *Atlas/Centaur* AC-13 on the *Surveyor V* mission was the fifth operational flight of an *Atlas/Centaur* vehicle, all of which have been very successful. This mission and the third operational flight of AC-12 on *Surveyor III* utilized the "parking orbit" mode of ascent, wherein the *Centaur* stage burns twice. The first burn injects the vehicle into a temporary parking orbit with a nominal altitude of 90 nm. After a coast period of up to 25 min, the *Centaur* reignites and provides the additional impulse necessary to achieve a lunar intercept trajectory. The parking orbit ascent mode, which will also be used on the remaining *Surveyor* missions, permits launching for all values of lunar declinations. This allows the design of launch periods which are compatible with favorable postlanding lunar lighting. In contrast, the *Surveyor* direct ascent missions (*Surveyors I, II, and IV*) could utilize only those days (about 8 per month) for which the lunar declination was less than approximately  $-14^\circ$ .

The *Surveyor V* mission was the first flight of the new *Atlas* SLV-3C booster which has been uprated from the previous LV-3C configuration by incorporating a 51-in. extension of the tank section, to provide greater propellant capacity, and by increasing the engine thrust levels sufficiently to maintain adequate liftoff acceleration.

## 2. Spacecraft System

Design, fabrication, and test operations of the *Surveyor* spacecraft are performed by Hughes Aircraft Company under the technical direction of JPL.

*Surveyor* is a fully attitude-stabilized spacecraft designed to receive and execute a wide variety of earth

commands, as well as perform certain automatic functions including the critical terminal descent and soft-landing sequences. Overall spacecraft dimensions and weight of 2200 to 2300 lb were established in accordance with the *Atlas/Centaur* vehicle capabilities. *Surveyor* has made significant new contributions to spacecraft technology through the development of new and advanced subsystems required for successful soft landing on the lunar surface. New features which are employed to execute the complex terminal phase of flight include: a solid-propellant main retromotor with throttlable vernier engine (also used for midcourse velocity correction), extremely sensitive velocity- and altitude-sensing radars, and an automatic closed-loop guidance and control system. The demonstration of these devices on *Surveyor* missions is a direct benefit to the *Apollo* program, which will employ similar techniques.

A survey television camera is included in the payload of all *Surveyor* spacecraft. The *Surveyor V* spacecraft was the first to carry an alpha scattering instrument (which was substituted for the soil mechanics/surface sampler device carried on *Surveyor III* and *IV*) to provide data for chemical analysis of lunar surface material. *Surveyor V*, like *Surveyor IV*, had a soil magnet attached to one footpad in view of the camera. Significant changes were made to the *Surveyor V* spacecraft power subsystem to achieve greater efficiency and simplification.

## 3. Tracking and Data System

The TDS system provides the tracking and communications link between the spacecraft and the Mission Operations System. For *Surveyor* missions, the TDS system uses the facilities of (1) the Air Force Eastern Test Range for tracking and telemetry of the spacecraft and vehicle during the launch phase, (2) the Deep Space Network for precision tracking communications, data transmission and processing, and computing, and (3) the Manned Space Flight Network and the World-Wide Communications Network (NASCOM), both of which are operated by Goddard Space Flight Center.

The critical flight maneuvers and most television operations on *Surveyor* missions are commanded and recorded by the Deep Space Station at Goldstone, California (DSS 11), during its view periods. Other stations which provided prime support for the *Surveyor V* mission were DSS 42, near Canberra, Australia, and DSS 61, near Madrid, Spain. During postlanding operations on the *Surveyor V* mission, DSS 42 and DSS 61 also obtained

many television pictures, an abundance of alpha scattering data, and other engineering and scientific data. Additional support on a limited basis was provided by DSS 71 (Cape Kennedy) during prelaunch and launch phase, DSS 72 at Ascension Island for backup command support and early telemetry coverage, DSS 51 at Johannesburg, South Africa, which provided initial two-way acquisition and coverage during the transit phase, DSS 14 (with a 210-ft antenna at Goldstone) to back up DSS 11 during the midcourse and terminal descent phases and to provide telemetry data during touchdown, and DSS 12 (Goldstone) for additional backup to DSS 11 during terminal descent.

#### 4. Mission Operations System

The Mission Operations System essentially controls the spacecraft from launch through termination of the mission. In carrying out this function, the MOS constantly evaluates the spacecraft performance and prepares and issues appropriate commands. The MOS is supported in its activities by the TDS system as well as with special hardware provided exclusively by the *Surveyor* project and referred to as mission-dependent equipment. Included in this category are the Command and Data Handling Consoles installed at each of the prime DSIF stations and at DSS 71, the Television Ground Data Handling System (TV-GDHS) installed at DSS 11 (TV-11) and the SFOF (TV-1), and other special display equipment.

#### C. Mission Objectives

All *Surveyor V* mission objectives were satisfied. These objectives, which were established before launch, were as follows:

- (a) Perform a soft landing on the moon in Mare Tranquillitatis.
- (b) Obtain postlanding television pictures of the lunar surface.
- (c) Conduct a vernier engine erosion experiment.
- (d) Determine the relative abundance of the chemical elements in the lunar soil by operation of the alpha scattering instrument.
- (e) Obtain touchdown dynamics data.
- (f) Obtain thermal and radar reflectivity data on the lunar surface.

For the *Surveyor V* mission, a six-day launch period from September 8 through September 13, 1967, was

selected which optimized the postlanding lunar lighting conditions at the selected landing site and satisfied the other mission constraints.

#### D. Mission Summary

*Surveyor V* was launched on September 8, 1967, the first day of the selected launch period, from Launch Pad 36B at Cape Kennedy. This launch with the *Atlas/Centaur* AC-13 vehicle was the first use of an uprated *Atlas* SLV-3C, which has a 51-in. extension of the tank section. Liftoff ( $L + 00:00$ ) occurred at 07:57:01.257 GMT, 18 min after opening of the launch window, the delay being required to confirm adequate hydraulic pressure of the launcher stabilization system. Very satisfactory launch phase performance was achieved. Following *Atlas* powered flight on a 79.5-deg flight azimuth, the *Centaur* first burn injected the spacecraft into a temporary parking orbit with an altitude close to the nominal 90 nm. After a 6.7-min coast period, the *Centaur* was reignited and injected the spacecraft into a lunar transfer trajectory. The injection was extremely precise, with the estimated uncorrected impact point only 46 km from the prelaunch target point.

The earth-moon trajectory and major events are depicted in Fig. I-1. Following spacecraft separation, the *Centaur* performed a required retromaneuver sequence to provide increased separation distance from the spacecraft and to miss the moon. After separation, the spacecraft properly executed the automatic antenna/solar panel positioning and sun acquisition sequences. These sequences established the desired attitude of the spacecraft roll axis and insured an adequate supply of solar energy during the coast period.

Tracking and telemetry data received in one-way lock by stations of the AFETR, MSFN, and DSIF confirmed a normal mission during the near-earth portion of flight. As planned, DSS 51 was the first station to establish two-way lock and exercise control of the spacecraft by command. Thereafter, the DSIF stations received and recorded all desired spacecraft data and transmitted necessary earth commands. Nearly continuous two-way coverage of the transit phase was provided, including two-way tracking coverage during each of the midcourse corrections.

Spacecraft lock-on with the star Canopus was achieved according to plan about 6½ hr after launch. This provided 3-axes attitude reference, which is required before the midcourse and terminal maneuvers can be executed.



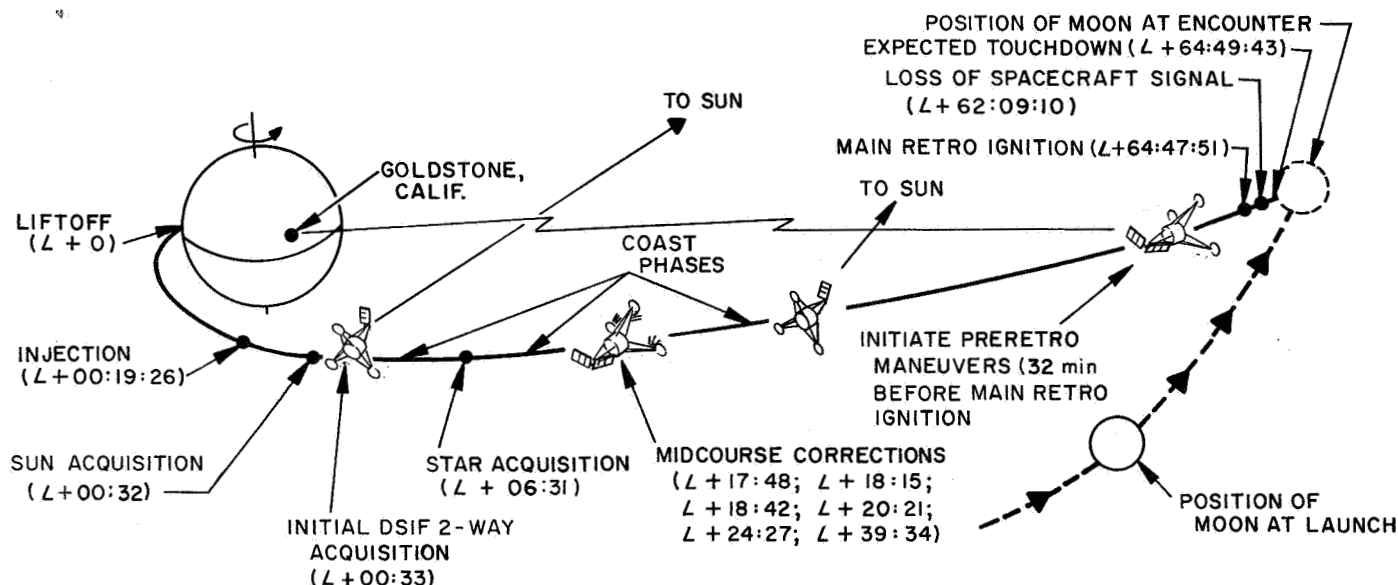


Fig. I-1. Earth-moon trajectory and major events

Spacecraft system performance during the pre-midcourse coast phase was excellent, with all system parameters near nominal values.

During the first "pass" over DSS 11, Goldstone, a roll-yaw maneuver sequence was performed in preparation for a midcourse velocity correction. The midcourse aim point was biased 0.12 deg northeast of the prelaunch target point in order to maximize probability of landing in the area covered by high-resolution *Lunar Orbiter* photographs. At 01:45 GMT on September 9, 1967, almost 18 hr after liftoff, a velocity correction of 14.01 m/sec was executed by commanding the vernier engines to burn for a period of 14.29 sec. Only a very small fraction of this velocity change was required to correct to the aim point. The larger maneuver was selected to optimize the terminal descent conditions, including main retro burnout velocity, vernier system propellant margin, and arrival time.

After the required midcourse correction had been performed, the vernier propulsion system helium regulator did not reseal tightly, thus allowing helium to vent overboard through relief valves on the low pressure side of the propellant pressurization system. Two additional vernier engine firings were then made in quick succession along the sunline and anti-sunline in an attempt to clear and reseal the regulator. Shortly thereafter, it was determined, from the preliminary results of an intensive analysis including special vernier engine flow tests at low supply pressure conditions, that a soft landing might still

be accomplished if (1) critical spacecraft system parameters were adjusted and (2) the spacecraft would perform in a very predictable manner during a descent sequence that would be modified to minimize the required total vernier engine impulse. Three additional vernier engine firings\* were made to achieve the desired spacecraft system parameters of reduced spacecraft weight for maximum deceleration during the main retromotor burn phase and increased helium ullage volume to assure minimum pressure drop during the vernier phase of terminal descent. The last midcourse correction (there were six altogether) also was used for final adjustment of the predicted landing site.

The helium leak persisted after each of the vernier firings, and, by about 10 hr before terminal descent, the helium tank pressure had dropped to and stabilized at the relief valve setting of about 825 psia. Except for the helium leak, spacecraft performance during the post-midcourse coast phase was excellent. The battery charge level was satisfactory, although it dropped below the predicted level owing to the special corrective operations performed.

In preparation for terminal descent, a roll-yaw maneuver combination was executed, beginning about 32 min before retroignition, to properly align the retrorocket nozzle in the direction of the velocity vector. The actual descent sequence was initiated automatically by a *mark*

\*The first of the three firings actually consisted of a 12-sec burn followed by two 0.5-sec burns with 1.0-sec interruptions.

signal from the spacecraft altitude marking radar (AMR) when the spacecraft was 60 miles slant range from the lunar surface. After a timed delay of 12.33 sec, the three liquid-propellant vernier engines ignited, followed (after an additional 1.1-sec delay) by ignition of the solid-propellant main retromotor. The larger-than-normal 12.33-sec delay had been preset earlier by earth command to delay the main retro phase such that retromotor burnout would occur at an altitude of only about 4600 ft instead of about 30,000 ft for a normal mission. Actual main retro burnout is estimated to have occurred at 4150 ft, with a spacecraft velocity of only about 80 ft/sec instead of the normally planned burnout velocity of 400 to 500 ft/sec. The lower main retro burnout velocity and altitude were necessary on this mission to reduce the total impulse required during the final vernier descent phase. After retro case ejection, the timing of which was adjusted to be earlier than normal by a carefully timed earth-command that overrode the flight control programmer, the radar altimeter and doppler velocity sensor (RADVS) became operational and throttled the vernier engines to allow the spacecraft to reach conditions of altitude and velocity specified by a descent contour that had been programmed in the spacecraft before launch. Once reaching the descent contour at about 800 ft altitude, the spacecraft closely followed the contour down to the *13-ft altitude mark*, at which time the vernier engines were shut off. The spacecraft touched down 1.6 sec later, at 00:46:44.284 GMT on September 11, 1967, with a velocity of about 14 ft/sec. As a result of very close to predicted performance by the spacecraft throughout the terminal descent sequence, a completely successful soft landing was achieved with no resulting damage to the spacecraft.

Landing occurred inside the rimless edge of a small, 30-ft-diameter crater, on a slope of about 17 deg. Because of the steep slope, one spacecraft leg touched down approximately 0.2 sec before the nearly simultaneous contacts of the other two. The spacecraft moved about 32 in. down the slope and also turned about 6 deg before finally coming to rest with a tilt of about 20 deg.

The landing site of *Surveyor V* is indicated in Fig. I-2 together with sites associated with previous *Surveyor* missions. The current estimate of the *Surveyor V* landing site, based on in-flight tracking data, is in the Sea of Tranquility (Mare Tranquillitatis) at 1.50 deg north latitude and 23.19 deg east longitude,\* which is about 32 km

\*Preliminary analysis of postlanding tracking data indicates the landing site is located at 1.41 deg north latitude, 23.18 deg east longitude.

northwest of the pre-midcourse aim point. This miss distance is not very large considering the large uncertainty in the trajectory at the time of the final midcourse correction which was due to the limited tracking time available between the last two corrections.

Communication had been maintained with the spacecraft throughout the terminal descent and landing sequence, making it possible to immediately proceed with postlanding operations. Landing had occurred shortly after local sunrise, and the initial assessment of postlanding telemetry data indicated the spacecraft condition to be excellent. Spacecraft performance remained excellent throughout the lunar day, permitting very extensive operations to be conducted.

A total of 18 high-quality 200-line television pictures were obtained after touchdown, before the spacecraft was reconfigured for transmission of 600-line pictures. The 600-line mode required positioning of the solar panel to receive maximum solar power and precise pointing of the planar array toward the earth to provide maximum signal strength. Because of the large tilt of the spacecraft, which was not known at that time, this operation required more time than expected, and it was necessary to transfer control of the spacecraft to DSS 42 near Canberra, Australia, before any 600-line pictures could be received. A total of 142 600-line pictures were received by DSS 42 on its first posttouchdown pass, the first few of these pictures being received simultaneously by Goldstone.

The *Surveyor V* spacecraft camera operated without trouble and provided over 18,000 pictures before shutdown after sunset of the first lunar day. This is a larger quantity of pictures than was obtained by the combined operations of the previous two successful missions (*Surveyors I* and *III*). Also, *Surveyor V* provided the highest quality pictures yet received.

The *Surveyor V* television sequences included (1) a large number of wide- and narrow-angle panoramas of the lunar surface out to the horizon, (2) pictures of stars to aid in spacecraft attitude determination, (3) images obtained with different lens filters which can be reconstructed on earth in true color, (4) images obtained with different focus settings to provide a means of determining the distance of objects from the cameras, (5) pictures of the visible parts of the spacecraft, (6) pictures showing disturbances of the lunar soil caused by the spacecraft footpads during landing and vernier engines during static firing, and (7) pictures of the solar corona after sunset.

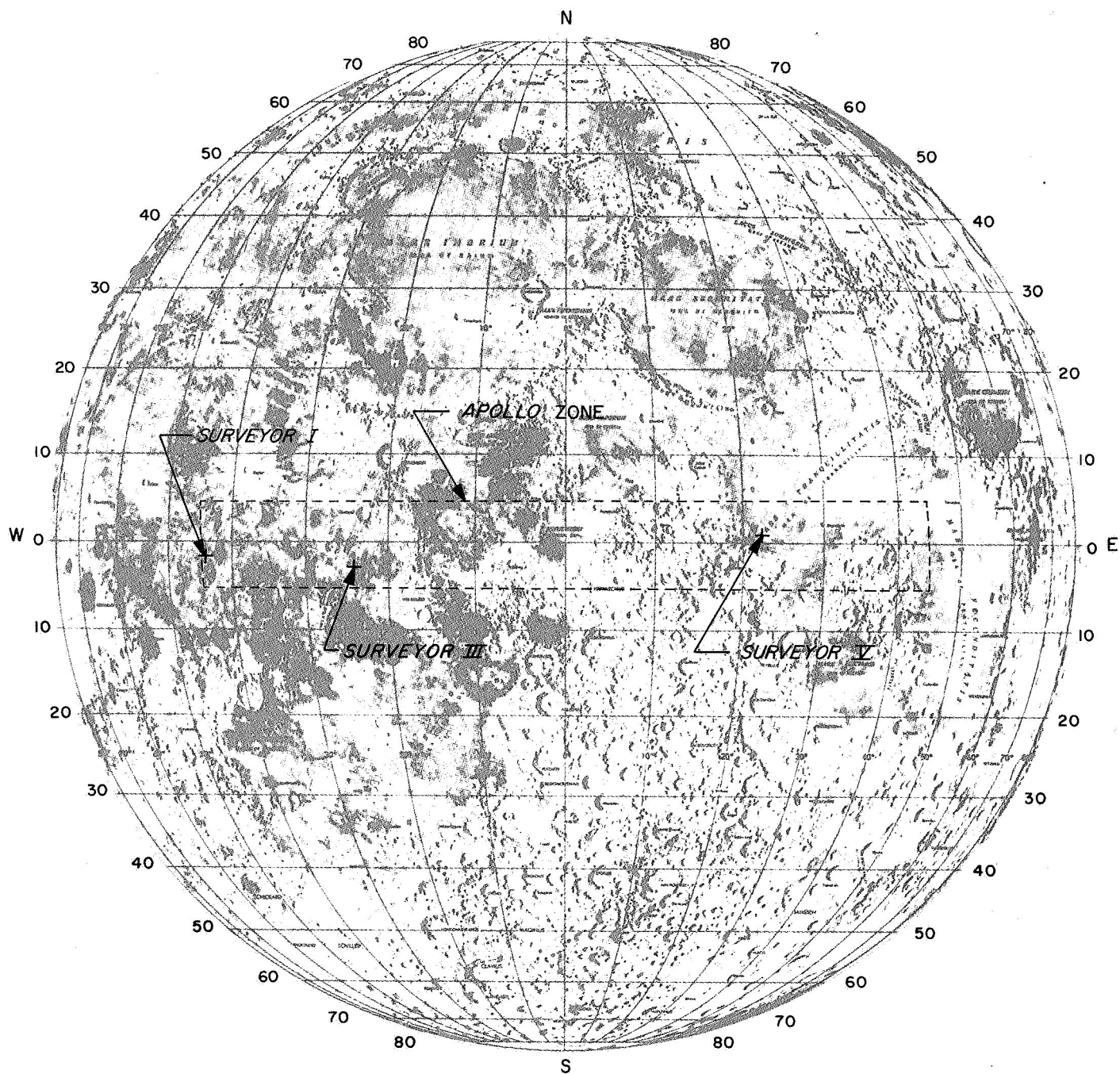


Fig. I-2. Soft-landing sites of Surveyor V and previous missions

Many television pictures were repeated during the lunar day to obtain views under different lighting conditions, and a series of frames was obtained toward the end of the lunar day showing the progression of shadows cast by spacecraft and lunar surface features.

*Surveyor V* carried a magnetic bar and a nonmagnetized control bar attached to the side of one of the footpads in view of the television camera. These bars came in direct contact with lunar surface material when the spacecraft slid downslope during landing, and pictures taken of the bars provide, for the first time, data on the magnetic properties of the lunar surface.

Most of the *Surveyor V* pictures were obtained during the Goldstone view periods, when the special TV ground data handling system could be used to relay the pictures from Goldstone to the SFOF for evaluation in real-time. However, on this mission, DSS 42 and DSS 61, near Madrid, participated more actively in television operations and received many more pictures than on previous missions.

Approximately 53 hr after landing, the vernier engines were fired briefly (0.55 sec) to determine lunar surface erosion effects. Erosion of the lunar surface was clearly evident in pictures taken after the firing. There was no apparent degradation of the spacecraft due to the firing, and only a very slight shift in spacecraft attitude resulted. However, television pictures revealed that the firing caused the alpha scattering head (which had been deployed to the surface) to move a few inches down the slope.

The alpha scattering instrument was also operated extensively to provide, for the first time, an abundance of useful data for chemical analysis of the lunar surface material. After obtaining calibration data in the stowed position, the sensor head was first deployed outwardly to obtain data on background radiation above the lunar surface; then it was lowered to the surface for gathering of lunar back-scattering data. About 18 hr of alpha and proton back-scattering data (Sample I) was obtained on the surface prior to the vernier static firing. After movement of the sensor head as a result of the firing, an additional 65 hr of data (Sample II) was obtained before the end of the first lunar day.

Spacecraft engineering data was received frequently throughout the lunar day to enable repeated assessment of the spacecraft condition. In addition, two-way doppler

tracking data was obtained whenever possible, and several special engineering tests were conducted, many of which were for the purpose of determining the performance and other characteristics of the spacecraft/DSIF telecommunications link.

Around lunar noon, the spacecraft was not operated for several periods of time, totaling about 28 hr, because of excessive temperatures (which were even higher than anticipated since the spacecraft was in a crater and the thermal view factors were therefore greater). The restricting effect of high lunar temperatures on spacecraft operations was greatly reduced by shading of critical components with other spacecraft elements, notably the solar panel and planar array.

As the first lunar day came to a close, the condition of *Surveyor V* was considered excellent, although two anomalies occurred shortly before sunset: (1) Even though commands had been sent to lock the spacecraft legs, two of the legs sagged, causing the spacecraft to rest on the crushable blocks. (2) The focus, focal length, and filter controls of the camera became inoperative, but the scheduled television sequences were successfully performed anyway, using the fixed camera settings.

In order to enhance the chances of spacecraft survival through the lunar night, operations near the end of the lunar day were carefully planned to provide nearly a fully charged battery at sunset. This was accomplished while still obtaining desired television pictures and other data.

Sunset relative to the top of the spacecraft antenna mast occurred at 10:56 GMT on September 24, 1967, during Goldstone view. During the final hours before sunset, narrow-angle surveys and shadow progression sequences were obtained with the camera. After sunset, solar corona pictures were taken, followed by three pictures of the spacecraft and lunar surface taken in earthshine. When the last television picture had been taken, about 4 hr after sunset, the solar panel and planar array were placed in the optimum position for resumption of operations during the second lunar day.

The spacecraft was operated on a low duty cycle as long as possible into the lunar night in order to prevent the battery, which is located in a superinsulated compartment, from cooling to the low temperature of the lunar night environment. Interrogations of the spacecraft were continued periodically during this time for engineering assessment and to obtain thermal data of scientific interest. Finally, since the battery capacity is not sufficient to

permit operation through the entire lunar night, it was necessary to shut down the spacecraft at 06:36 GMT on September 29, 1967, about 115 hr after sunset. Because the battery was kept warm until that time, it is estimated that it should not have cooled below  $-180^{\circ}\text{F}$  before sunrise, compared to a possible lunar night temperature as low as  $-240^{\circ}\text{F}$ .

During the second lunar day, after being shut down for over 16 days, *Surveyor V* responded immediately to the first series of commands sent by DSS 42 at 08:07 on October 15, 1967. The reawakening attempt had been scheduled for several days after sunrise to permit the spacecraft to warm sufficiently. Although a few spacecraft subsystems had suffered some degradation from the lunar night, it was possible to resume operation and obtain additional useful data, including television pictures and alpha scattering data. The television picture quality was degraded because of an apparent video amplifier problem, but this was partially offset by enhancement of the signal on earth. Many hours of alpha scattering data were obtained on the second lunar day. However, this data contains significant detector noise, and will be useful primarily for engineering purposes.

The spacecraft had overcome both problems which had been observed near the end of the first lunar day (two legs sagged and TV filter, focus, and focal length controls were inoperative). However, near the end of the second lunar day, these problems, which are apparently temperature-related, appeared again with only one leg sagging on that occasion.

The spacecraft experienced a total eclipse of the sun by the earth on October 18, 1967. During the event, thermal data reflecting the cooldown of the spacecraft and surrounding lunar surface was obtained which appears like the data obtained by *Surveyor III* during a similar event.

As the second lunar day approached an end, the spacecraft was again prepared for the lunar night survival by fully charging the battery. Shutdown during the second lunar night occurred on November 1, 1967, about 200 hr after sunset.\*

---

\*The spacecraft did not respond to any of several reawakening attempts during the third lunar day; however, it was reawakened and operated on the fourth lunar day.



## II. Space Vehicle Preparations and Launch Operations

The *Surveyor V* spacecraft was assembled and flight-acceptance-tested at the Hughes Aircraft Company facility, El Segundo, California. After completion of these tests, the spacecraft was shipped to the Combined System Test Stand (CSTS) at San Diego on June 17, 1967, for compatibility tests with the *Atlas/Centaur* (AC-13) launch vehicle. Spacecraft/launch vehicle compatibility was verified and the spacecraft was airlifted to the Air Force Eastern Test Range (AFETR), Cape Kennedy, arriving on June 28, 1967.

The *Atlas/Centaur* launch vehicle stages arrived at AFETR on June 30 and July 3, 1967, respectively. Pre-launch assembly, checkout, and systems tests were performed successfully at AFETR, and launch was accomplished on September 8, 1967 at 07:57:01.257 GMT 18 min, 1.257 sec after opening of the launch window on the first day of the launch period.

### A. Spacecraft Assembly and Testing

Tests and operations on the spacecraft were conducted by a test team and data analysis team which worked with the spacecraft throughout the period from the beginning of testing until launch. The test equipment used to control and monitor the spacecraft performance at all test facilities includes (1) a system test equipment assembly (STEA) containing equipment for testing each of the spacecraft subsystems, (2) a command and data handling

console (CDC) similar to units located at the DSIF stations (see Section VI) for receiving telemetry and TV data and sending commands, and (3) a computer data system (CDS) for automatic monitoring of telemetry during spacecraft testing.

### 1. Spacecraft Ambient Testing

The ambient test phase consists of initial system check-out (ISCO) and mission sequence tests. During ISCO, each subsystem is first checked out and then is tested for compatibility and calibration with the other spacecraft subsystems. A system readiness test is performed for initial system operational verification. This phase was completed February 25, 1967.

The mission sequence (MS) tests are performed to obtain system performance characteristics of the spacecraft under ambient conditions and in the electromagnetic (EM) environment expected on the launch pad and in flight prior to separation from the *Centaur*. Mission Sequences 1 and 2 are compressed (32-hr) mission sequence runs without the expected EM environment. Mission Sequence 3 is a full (68-hr) mission with plugs out and the expected launch EM environment. This test phase was completed March 15, 1967. The major anomalies that occurred during this phase included: radar altimeter doppler velocity sensor (RADVS) induced telemetry noise which was corrected by adding a zener diode to the

signal processing; a suspected 4-db shift in receiver AGC which was corrected by replacing Receiver B; and a television camera black-level shift which was corrected by adding filtering on the 22-V input.

## 2. Solar-Thermal-Vacuum (STV) Testing

The STV test sequences are conducted to verify proper spacecraft performance in simulated missions at various solar intensities (test phases) and in a vacuum environment. During STV tests, as well as the vibration tests which follow, the propellant tanks are loaded with "referee" fluids to simulate flight weight and thermal characteristics.

The STV testing was begun on the *Surveyor V* spacecraft in mid-April, 1967. A Phase A sequence was first conducted at 112% of nominal sun intensity (high sun). During this sequence, the nitrogen tank temperature was observed to be running 40 to 45 deg cooler than expected, while the helium relief valve assembly was running hotter. These anomalies were brought about by the fact that the helium relief valves were moved to a new and more exposed location on the *Surveyor V* spaceframe while the addition of Compartment C, which houses the alpha scattering instrument electronics, provided additional shading of the nitrogen tank. Due primarily to these anomalies plus the fact that undesirable "spurs" were noted in the Transmitter A spectrum, the STV chamber was opened and Phase B was delayed until the transmitter had been replaced and changes affecting the thermal characteristics of both the nitrogen tank and helium relief valves had been incorporated.

Phase B was initiated May 4, 1967, at 87% of nominal sun intensity (low sun). Two hours after simulated launch, a fuel leak was noted near the fuel port of Vernier Engine 3. The mission sequence was aborted and the engine was replaced. The spacecraft was then commanded through two modified STV test sequences to verify satisfactory spacecraft operation and to obtain thermal data. The first modified STV test was a Phase B sequence performed at low sun intensity, followed immediately (back-to-back) by a Phase A sequence at high sun intensity. These two STV sequences were considered to be successful although two problems were noted: the helium relief valve temperatures exceeded the specification limit of 125°F, and the alpha scattering instrument guard event monitor voltage was higher than expected. The relief valves were considered acceptable for flight after similar units were qualified for the higher temperatures. The alpha scattering electronics was reworked to minimize the problem, which was considered minor. The STV test

phase was completed May 15, 1967, and preparations commenced for the vibration phase of system testing.

## 3. System Vibration Testing

Vibration tests are conducted in each of the three orthogonal axes of the spacecraft to verify spaceframe integrity and proper functional operation during and after exposure to a simulated launch environment. During these tests the spacecraft is placed in the launch configuration, with the landing legs and omniantennas in the folded position. In addition, a vernier engine vibration (VEV) test is conducted, with the vibration input at the vernier engine mounting points to simulate the vibration environment during the midcourse and terminal descent phases of flight. The spacecraft is checked functionally during each phase and pre- and postvibration alignments are performed to verify that the spacecraft is not degraded by exposure to the vibration environment. The *Surveyor V* vibration test phase began on May 18, 1967, and ended with the successful completion of VEV tests on June 8, 1967. In addition to the vibration tests, an abbreviated "plugs out" mission sequence was performed on May 29, 1967. The only significant problem noted during this test phase was Transmitter A phase jitter, which developed prior to vibration. This required temporary replacement of the transmitter just prior to VEV. After transport preparations, the spacecraft was shipped by van to the Combined Systems Test Stand (CSTS) in San Diego on June 17, 1967.

### B. Combined Systems Test (CST) at San Diego

The Combined Systems Test is performed to demonstrate electrical and mechanical compatibility of the *Surveyor* spacecraft, the *Atlas/Centaur* launch vehicle, and the ground support equipment (GSE) during a simulated countdown and launch. The configuration for the tests is shown in Fig. II-1. After successful completion of assembly, factory checkout, and acceptance testing, the *Centaur* was erected in the test tower on May 5, 1967, followed by installation of the *Atlas* in its horizontal test position on May 22, 1967.

After arrival at the CSTS on June 17, 1967, the *Surveyor V* spacecraft proceeded through receiving, inspection, assembly, and checkout with the STEA with no significant problems. The spacecraft was then mated to the *Centaur* forward adapter and a System Readiness Test (SRT) was performed to verify the functional integrity of the spacecraft prior to encapsulation. On June 21, the spacecraft was encapsulated within the nose



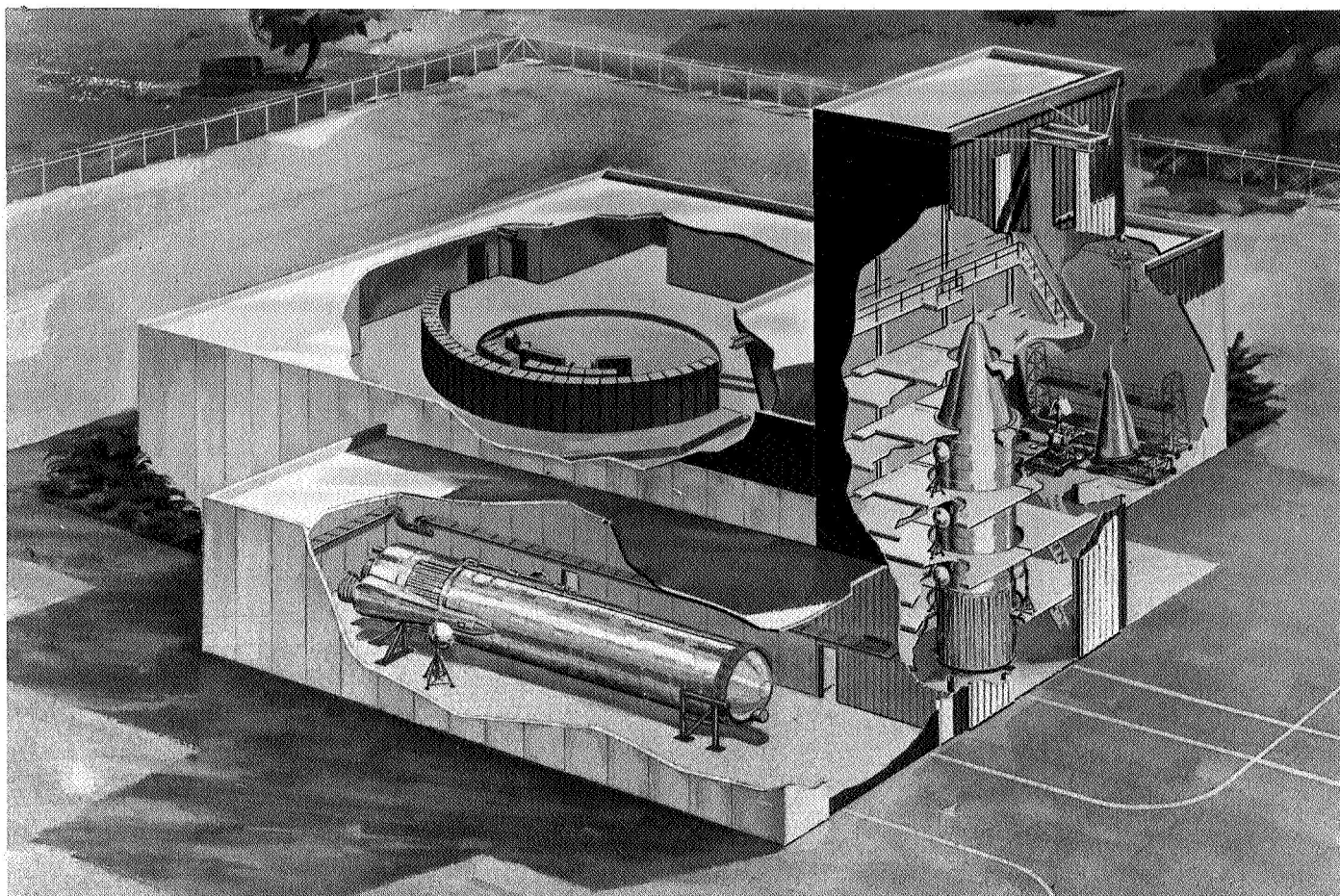


Fig. II-1. Combined system test stand at San Diego

fairing and mated to the *Centaur*. This was followed by another SRT on June 22, 1967.

The CST Joint Flight Acceptance Composite Test (J-FACT) was performed on June 23, 1967. During the test the *retro arm* indicator light did not illuminate. Failure to remove the safe-and-arm pin from the retromotor prior to encapsulation was found to be the cause of this problem. The only other significant problem noted was that the Compartment A temperature control and heater assembly failed to function when commanded. The latter problem reoccurred at AFETR, where the assembly was replaced.

Following CST, the flight transmitter was reinstalled and the spacecraft was readied for shipment and airlifted from Montgomery Field in San Diego to AFETR, arriving on June 28, 1967. The *Atlas* was also shipped by air to AFETR and arrived on June 30, followed by the *Centaur* on July 3, and the nose fairing and interstage adapter on July 5, 1967.

## C. Launch Operations at AFETR

The major operations performed at AFETR after arrival of the launch vehicle and the spacecraft are listed in Table II-1.

### 1. Initial Preparations

Modifications to Launch Complex 36B began on April 17, 1967, immediately after the launch of *Surveyor III*. These modifications, which included replacement of the launcher system, relocation of service tower levels, changes to the launch control system, and checkout of the entire complex, were required in order to accommodate the new SLV-3C *Atlas* used for the first time on the *Surveyor V* mission. A description of the new features incorporated in the SLV-3C is contained in Section III.

The *Atlas* and *Centaur* stages of AC-13 were erected on Launch Pad 36B on July 3 and 6, 1967, respectively. All required launch vehicle operations preliminary to mating

**Table II-1. Major Surveyor V operations at Cape Kennedy**

Operation	Location	Date completed, 1967
AC-13 <sup>a</sup> erection (Atlas stage)	Launch Complex 36B	July 3
AC-13 erection (Centaur stage)	Launch Complex 36B	July 6
SC-5 <sup>b</sup> inspection, reassembly and initial checkout	Building AO	July 8
SC-5 vernier engine functional test	Building AO	July 12
SC-5 Performance Verification Test (PVT) 3	Building AO	July 15
SC-5 PVT 4 system calibration	Building AO	July 20
SC-5 solar panel field test	Building AO	July 24
SC-5 mate to adapter	Explosive Safe Facility (ESF)	July 25
SC-5 mate to Centaur	Launch Complex 36B	July 28
SC-5 Spacecraft/DSS 71 compatibility test	Launch Complex 36B	July 30
AC-13/SC-5 Joint Flight Acceptance Composite Test (J-FACT)	Launch Complex 36B	July 31
SC-5 demate from Centaur	Launch Complex 36B	July 31
SC-5 decapsulation, depressurization, removal of J-FACT items and preparation for alignment	ESF	August 1
SC-5 spacecraft alignment	ESF	August 3
SC-5 PVT 5 mission sequence	Building AO	August 10
AC-13 propellant tanking test	Launch Complex 36B	August 18
SC-5 vernier system pressure leak test	ESF	August 20
SC-5 vernier system propellant loading and high pressure leak test	ESF	August 22
AC-13 FACT	Launch Complex 36B	August 25
SC-5 retromotor installation, and final weight, balance, and alignment	ESF	August 26
SC-5 PVT 6	ESF	August 30
SC-5 Encapsulation and System Readiness Test (SRT)	ESF	August 31
AC-13 Composite Readiness Test (CRT)	Launch Complex 36B	September 1
SC-5 final mate to Centaur	Launch Complex 36B	September 1
SC-5 commutator assessment and final SRT	Launch Complex 36B	September 7
Surveyor V Launch	Launch Complex 36B	September 8
<sup>a</sup> Atlas/Centaur vehicle designation.		
<sup>b</sup> Surveyor V spacecraft designation.		

of the spacecraft and performance of the Joint Flight Acceptance Composite Test (J-FACT) were culminated with a successful guidance/autopilot (GAP) test on July 26 and a *Centaur* programmer functional test in the armed configuration on July 27.

Receiving inspection and reassembly of the spacecraft at Building AO started on July 5, 1967. During this time, the television camera was replaced by a unit which had a vidicon of the type flown on previous *Surveyor* spacecraft. Starting on July 8, 1967, a series of Performance Verification Tests (PVT 1 through 4) and television calibrations (Fig. II-2) were performed to verify flight readiness of the spacecraft. Two significant problems were noted during this period. First, a RADVS ranging test performed on July 12 revealed that the Beam 4 range tracker would not maintain lock on the test target. As a result, the klystron power supply modulator (KPSM) was returned to Ryan Aeronautical Company for troubleshooting. (The klystron exhibited a wide spectrum, and on August 7 the spare KPSM was installed for flight.) The second problem occurred during the vernier propulsion system bladder leak checks. Fuel Tank 1 bladder exhibited an excessive leak rate, and the tank was replaced.

## 2. Flight Acceptance Composite Tests and Launch Vehicle Propellant Tanking Test

Following initial testing at the Spacecraft Checkout Facility (SCF) in Building AO, which was concluded on July 23, the spacecraft was moved to the Explosive Safe Facility (ESF), where it was prepared for the Joint Flight Acceptance Composite Test (J-FACT). The spacecraft was built up to flight configuration except for a dummy retromotor, nonflight shock absorbers, referee fluids instead of liquid propellants, leg and omniantenna deploy squibs in mufflers, and no flight calibration sources in the sensor head of the alpha scattering instrument. After the spacecraft was mated to the forward adapter (Fig. II-3), the helium and nitrogen tanks were pressurized, the spacecraft was encapsulated, and an SRT was performed. There were no spacecraft anomalies except that the TV camera electronics temperature indicated cooler than expected, requiring the telemetry coefficients to be adjusted for a proper ambient reading.

The spacecraft was mated to the *Centaur* vehicle on Launch Pad 36B on July 28, 1967. After mating, an RF air link optimization test and an SRT were performed independent of the launch vehicle to verify proper operation of the spacecraft and GSE. There were no anomalies. An integrated launch control test to check out the space vehicle countdown sequence was also conducted on July 28.

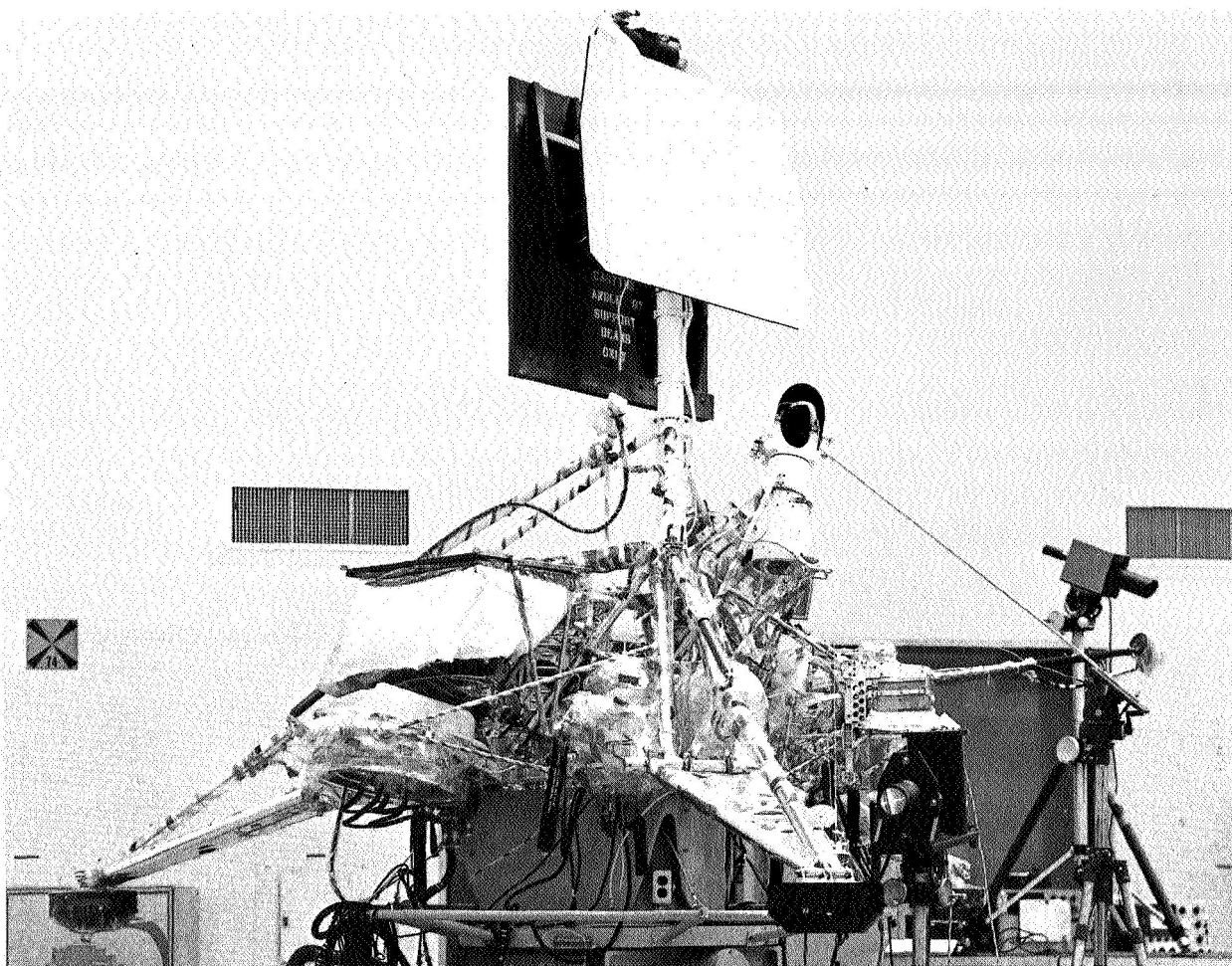


Fig. II-2. *Surveyor V* undergoing TV calibration in SCF of Building AO

On July 29, a spacecraft/DSS 71 compatibility test with the spacecraft was performed. The only significant anomaly noted was the reappearance of Transmitter A phase jitter, which had been noted prior to the last repair cycle of the transmitter. However, there was no loss of lock.

J-FACT was performed satisfactorily on July 31. This test, involving all systems, covered launch through spacecraft separation and *Centaur* retromaneuver. Spacecraft/*Centaur* separation was simulated by manually disconnecting the adapter field joint electrical connector.

During the J-FACT, between  $T - 120$  and  $T - 60$  min in the countdown, a launch vehicle electromechanical interference (EMI) test was conducted. The purpose of this test is to verify spacecraft electrical compatibility with the launch complex and vehicle propellant storage and handling systems in lieu of a cryogenic tanking operation. During the EMI test, a procedural error in turning

off the service tower lights resulted in the inadvertent tripping of a circuit breaker, which removed power from the S-band repeater amplifier. Also while the EMI test was in progress, vehicle dc power was lost for a few seconds while ac power remained on. This condition violated a test constraint for the *Atlas* programmer in that the transistors in the high-power circuits could be overstressed. The anomaly could not be repeated, so the programmer was left installed on the vehicle for the balance of the J-FACT and later replaced. No spacecraft anomalies were observed during performance of the EMI test.

After on-pad calibration of the spacecraft receivers with the service tower in place, *Surveyor V* was demated from the *Centaur* and returned to the ESF on July 31. The portion of the spacecraft receiver calibration with the service tower in the launch position (removed) was rescheduled for accomplishment after final mating due to an electrical storm and a problem with the service tower drive system.



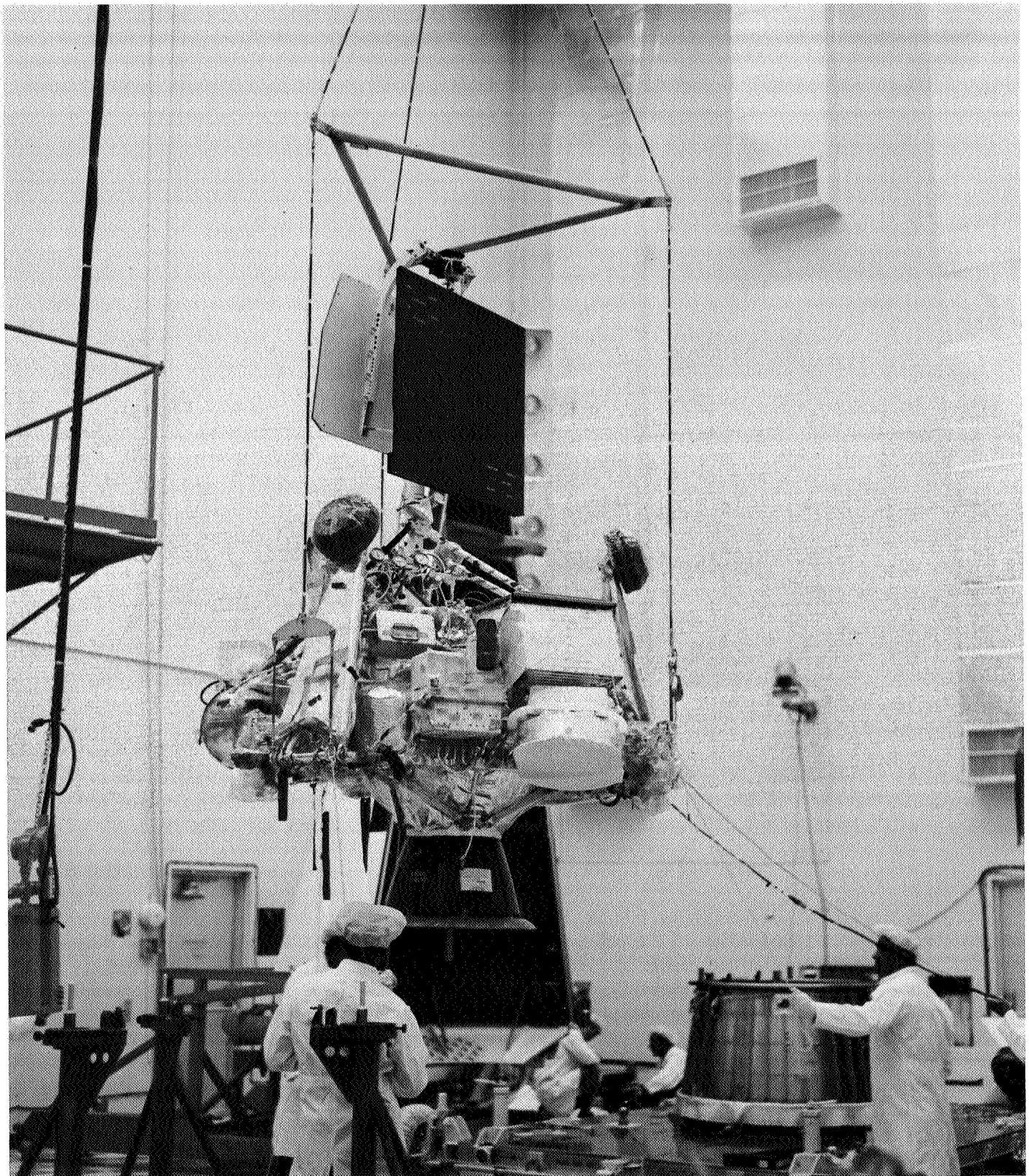


**Fig. II-3. Surveyor V mating to adaptor in ESF**

Following the J-FACT, several launch vehicle airborne and GSE equipment components were replaced, including the propellant utilization (PU) valve electronic package and constant flow valve, *Atlas* displacement and rate gyros, the *Atlas* inverter, the hydrogen inlet valve to *Centaur* Engine C2, the *Atlas* fuel regulator and relief valve, a pyrotechnic relay assembly, and several transducers. After satisfactory operation of these components was confirmed by appropriate retest, the *Atlas/Centaur* integrated flight control and propellant tanking test was successfully conducted on August 18. *Atlas* fuel (RP-1) tanking was accomplished using a new liquid level sight gage for determination of fuel level.

Anomalies occurring during the tanking test included loss of optical acquisition while conducting vehicle alignment checks due to misalignment of the theodolite, a pressure oscillation problem in the *Atlas* guidance pod cooling system, which was caused by improper setting of the cooling compressor head pressure, and erratic operation of transducers associated with telemetry measurement of the *Atlas* booster pneumatic regulator output pressure and measurements of the *Atlas* guidance pod cooling duct pressure. The faulty transducers were replaced following the tanking test. Additional posttanking checks revealed a failure of the oxidizer start tank relief valve caused by a loose piece of plastic material in the valve, a leaking liftoff disconnect on an *Atlas* helium bottle, which was corrected by replacement of the O-ring seal, and a *Centaur* forward seal failure which necessitated replacement of affected sections. Satisfactory operation of all *Atlas/Centaur* ground and airborne electrical systems was reverified by a successful Flight Acceptance Composite Test (FACT) conducted on August 25, 1967.

### 3. Final Flight Preparations

Spacecraft operations at the ESF following J-FACT included decapsulation, depressurization and calibration of the nitrogen and helium system pressure transducers, and a mechanical fit and electrical checkout of the flight shock absorbers. The spacecraft was moved to the optical dock for alignment on August 2. During this period, the antenna/solar panel positioner (A/SPP) was partially disassembled and all the A/SPP drive motor screws were replaced and safety wired. This action was taken to prevent loosening of the drive motor screws which had occurred during previous vibration testing. Additional tests performed on Transmitter A indicated that the phase jitter noted previously was not serious enough or of such a nature to warrant replacement of the transmitter prior to launch.

Performance Verification Test 5 was performed in Building AO from August 7 to 10. No significant anomalies were noted. A special TV test was performed at this time to determine the extent of TV vidicon contamination. The results were acceptable and no additional cleaning was required prior to flight. The spacecraft was then moved to the work stand where a detailed spacecraft harness and thermal inspection were performed. No significant discrepancies were noted, although a number of harness string ties were added and thermal finishes were cleaned and touched up as required.

On August 14, the alpha scattering instrument flight sources were received, and the calibration of these sources with the alpha scattering sensor head was begun. On August 12, the spacecraft was moved to the ESF Propellant Loading Building, where solvent was loaded and high- and low-pressure leak tests were performed. During high-pressure leak testing of the oxidizer system, it was noted that Tank 2 and, subsequently, Tank 1 leaked solvent around the O-ring at the base of the tanks. An investigation revealed that the O-rings on these tanks, as well as Oxidizer Tank 3, came from the same lot. Therefore, on August 16, all three oxidizer tanks were replaced. The leak test was rerun on the oxidizer tanks, and no further problems were noted. On August 17, the fuel system was again leak-tested, and solvent was noted to have penetrated the bladders of Fuel Tanks 2 and 3. These fuel tanks were replaced on August 18 and the test was rerun with no new problems being noted.

On August 22, flight propellant loading was completed and a special high-pressure test was performed to verify the integrity of the vernier propulsion system. In addition, PVT 6 was completed along with the final flight preparations, which included installation of the main retromotor, pyrotechnic devices, and the alpha scattering instrument flight sources.

The spacecraft was mated to the forward adapter on August 28, after which the helium and nitrogen systems were pressurized for flight and the spacecraft was given a final inspection and cleaning. The spacecraft was encapsulated within the nose fairing, and an SRT was performed on August 31. No problems were noted, although there was a minor recurrence of Transmitter A phase jitter.

After the completion of FACT on August 25, the launch vehicle was prepared for the Composite Readiness Test (CRT), the last multiple systems test before launch. During this period, the *Centaur* engines control regulator,

the *Atlas* PU system, a telemetry quick disconnect, and several transducers were replaced. The launch readiness of all *Atlas/Centaur* electrical and RF systems was then verified by the successful performance of the CRT on September 1. On the same day, the encapsulated spacecraft was transported to the launch pad, mated to the *Centaur*, and an SRT was performed. While conducting the gyro precession checks during the SRT, the programmed automatic telemetry evaluator limits were exceeded initially. This was caused by low inlet air temperature of the *Surveyor* air conditioning system. The gyros checked out satisfactorily after the inlet air temperature was raised to the correct setting of 75°F. On the following day, the service tower was removed to the launch position to permit completing calibration of the spacecraft receivers. A practice countdown and retro-motor safe-and-arm checks were also performed on the spacecraft.

On September 2, the *Atlas* PU system, which was installed prior to the launch vehicle CRT, was found to be inaccurate. The PU system from AC-14 (the launch vehicle scheduled to support the following *Surveyor* mission) was removed, system-calibrated, installed on AC-13, and functionally tested.

#### 4. Countdown and Launch

The final spacecraft SRT began at 19:03 GMT on September 7 at a countdown time of  $T - 680$  min, and was completed at 00:14 GMT on September 8. The spacecraft joined the launch vehicle countdown during the scheduled 60-min hold which started at  $T - 90$  min. The countdown proceeded normally down to  $T - 9$  min 49 sec, when the launcher stabilization pressure monitor light in the blockhouse went out. It relighted at  $T - 8$  min 16 sec, but went out again at  $T - 5$  min 26 sec, indicating either a loss of instrument air pressure or loss of stabilization system hydraulic pressure. Since vehicle instability under excessive wind loads would occur with insufficient hydraulic pressure, the planned 10-min hold at  $T - 5$  min was extended 18 min to investigate the problem. An analysis indicated that the stabilization system was operational. During this hold, spacecraft Receiver A experienced a severe fluctuation in received signal strength. Repositioning of the antenna on Building AO indicated this to be an air-link phenomenon.

The countdown was resumed at 07:52 GMT and proceeded without further incident through liftoff (Fig. II-4), which occurred at 07:57:01.257 GMT September 8, 1967, on a flight azimuth of 79.517 deg.

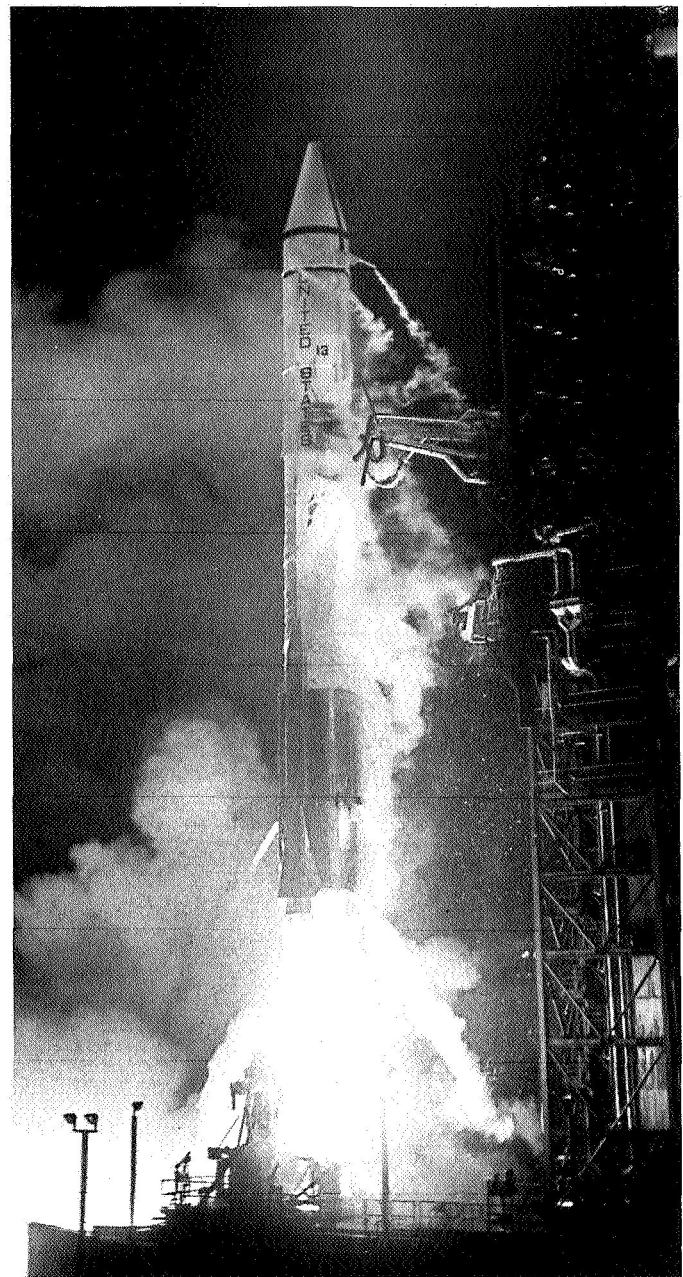


Fig. II-4. *Atlas/Centaur* AC-13 launching *Surveyor* V

The countdown included a total of 70 min of planned, built-in holds (the one of 60-min duration at  $T - 90$  min and the one of 10-min duration at  $T - 5$  min). A 120-min launch window was available on September 8, extending from 07:39 to 09:29 GMT, 18 min of which was consumed by the 18-min extension of the hold at  $T - 5$  min. A countdown time summary is shown in Table II-2.

All vehicle systems performed satisfactorily throughout the powered phases of flight, and the spacecraft was very



**Table II-2. Surveyor V countdown time summary**

Event	Countdown time, min	GMT
Started spacecraft SRT	T - 680	(September 7) 19:03
Completed spacecraft SRT	T - 369	(September 8) 00:14
Started launch vehicle countdown	T - 335	00:54
Started 60-min built-in hold (BIH)	T - 90	04:59
Spacecraft joined launch vehicle countdown	T - 90	05:35
End BIH; resumed countdown	T - 90	05:59
Started 10-min BIH	T - 5	07:24
BIH extended	T - 5	07:33
Resumed countdown	T - 5	07:52
Liftoff	T - 0	07:57:01.257

accurately injected into a lunar transfer trajectory. The *Centaur* burn time was 10 sec longer than predicted, but this was well within tolerance and had no detrimental effect on the mission. Damage to Launch Complex 36B was light. The powered flight sequence of events and launch vehicle performance are described in Section III.

The atmospheric conditions during the launch were favorable, with unusually good visibility. Surface winds were 9 knots from 310 deg. Surface temperature was 74.5°F with a relative humidity of 94% and a dew point of 73°F. Sea level atmospheric pressure was 1012.2 millibars. The cloud cover was 4/10 cumulus at 1600 ft. The maximum expected wind shear parameter was 18 ft/sec per thousand feet of altitude (velocity decreasing with increasing altitude) occurring at 46,000 ft on an azimuth of 310 deg from true north.

## D. Launch Phase Mission Analysis

The *Surveyor V* launch phase mission analysis activities during the prelaunch planning and countdown stages of the mission were devoted to launch constraint evaluations and launch window definitions. During the near-earth portion of the flight, the activities were concentrated on obtaining an early and continuing evaluation of the mission by integrating information being gathered by each system of the Project.

### 1. Prelaunch Planning Activities

The initial *Surveyor V* launch windows for the September 1967 opportunity were derived from the results of the trajectory targeting effort. Analyses were made of the

effect on launch windows of the launch constraints of each of the four Project supporting systems. These constraints and the resulting preliminary launch window design alternatives were published in a launch constraints document for the *Surveyor V* mission (see Bibliography). When the final near-earth support plans and commitments of the Tracking and Data System (TDS) were made available, so that the near-earth coverage capabilities and limitations could be identified, it was possible to establish the final launch windows for the mission. These windows, which are shown in Fig. II-5, were selected after a careful analysis of the relative risks to the TDS near-earth data gathering capabilities as a function of launch azimuth, and after these TDS risk profiles were balanced against the total mission values of launching early in the launch period.

The possibility of launching a day earlier, on September 7, had been considered, but was rejected because the unbraked impact incidence angle was slightly in excess of the upper limit (45 deg), and a predawn landing was possible for that day.

Although the unbraked incidence angle ( $\approx 46$  deg) was slightly high for September 8 also, launching on that day was approved by the Project because lunar landing would occur in daylight, shortly after sunrise. This time of landing is very desirable since it permits initial television pictures to be taken at low sun angle as well as providing maximum lunar operational time before sunset.

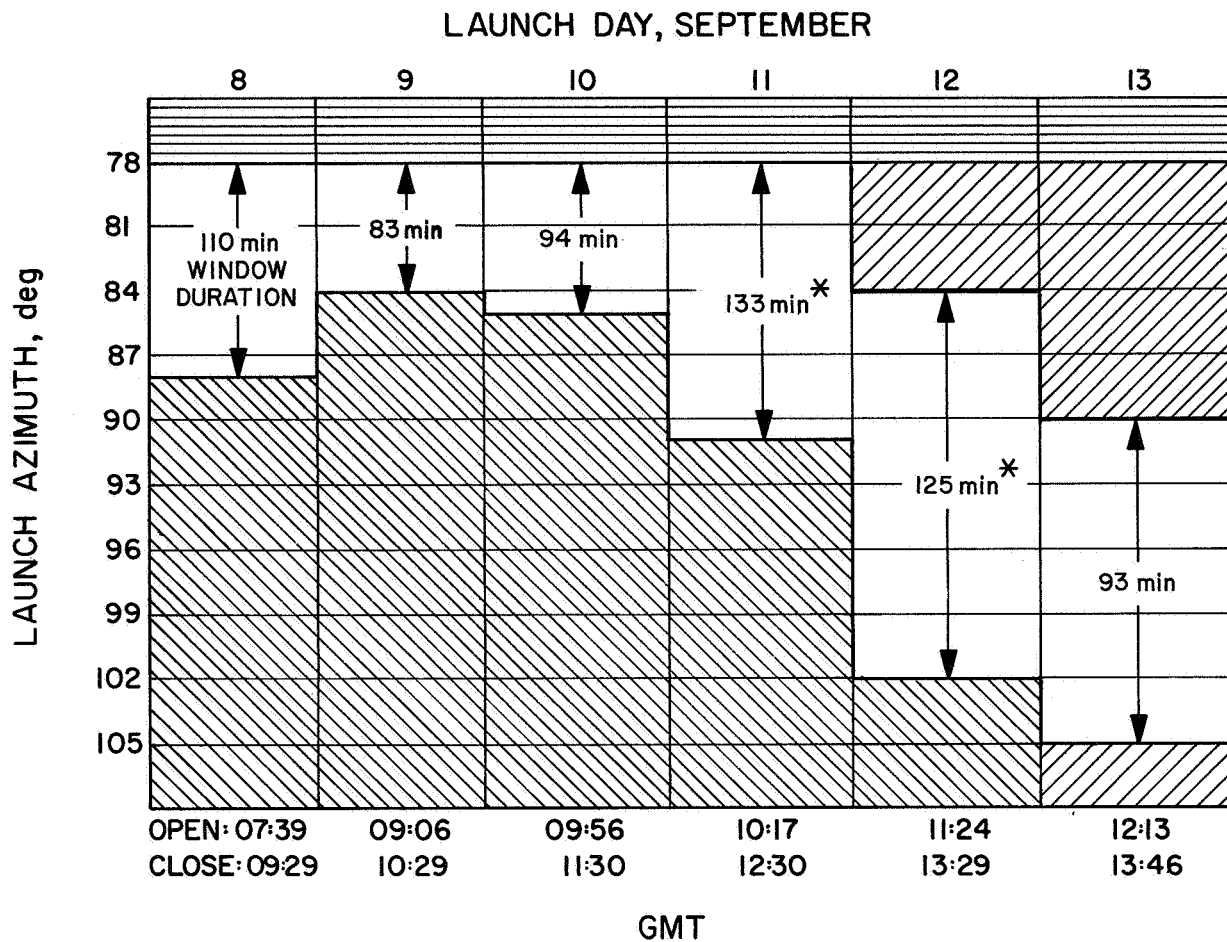
The windows for the first four days opened on a 78-deg launch azimuth, which is the minimum azimuth for which the *Surveyor* Project has Range Safety approval to launch.

Closing of the launch windows for the first five days was constrained by the 116-sec minimum parking orbit coast time limit. This time period is required by the *Centaur* to complete the propellant settling sequence between the first and second burns.

Opening of the launch windows for September 12 and 13, and closing of the window for September 13 were constrained by TDS coverage limitations. (Also refer to Section V for TDS near-earth coverage.)

### 2. Countdown to Liftoff

During the countdown, several stations of the TDS developed hardware problems. Of these stations in the "red," only one, the RIS *Coastal Crusader*, represented a



116-sec MINIMUM PARKING ORBIT  
COAST TIME CONSTRAINT

TDS COVERAGE CONSTRAINT

RANGE SAFETY CONSTRAINT

\* LAUNCH VEHICLE SYSTEM HOLD CAPABILITY COULD HAVE REDUCED THESE WINDOWS TO 2-hr MAXIMUM.

Fig. II-5. Final Surveyor V launch window design for September 1967



threat to the launch. The Mission Director was advised of the possible violation of the established launch-hold criteria. However, all but two of the stations had corrected their problems by liftoff, and neither of the stations remaining in the red, Antigua and Carnarvon, were mandatory.

Countdown operations proceeded normally except for extension of the  $T - 5$ -min built-in hold, as described earlier, to permit confirmation of adequate launcher stabilization system pressure, which delayed liftoff until about 18 min after opening of the window.

### 3. Near-Earth Phase

The near-earth mission analysis was based on space vehicle Mark Events reported in near-real-time (see Section V, Table V-3), the reported acquisition characteristics of the TDS stations, the reported space vehicle performance evaluations based on real-time telemetry data, the monitored powered flight trajectory characteristics, and the orbit determination calculations of the Real Time Computer System (RTCS) at Cape Kennedy.

The information available during launch until parking orbit insertion exceeded that expected for the actual trajectory. Consequently, normalcy of that portion of the flight was readily established. Evaluation of the subsequent portion of the near-earth phase was hampered by the loss of expected real-time spacecraft data and the poor quality of the transfer orbit data, which was due to radar acquisition of the *Centaur* C-band beacon by the Grand Canary station after start of the *Centaur* turn-around maneuver. However, real-time data from selected *Centaur* telemetry channels provided by Grand Canary did indicate that the *Centaur* second burn and retro-maneuver were normal. The very nominal spacecraft acquisition time achieved by DSS 51 also confirmed the normalcy of the powered flight phase. Furthermore, the RTCS was able to compute two consistent transfer orbits based on DSS 51 data. (Refer to Section VII for discussion of transfer orbit determination.) The RTCS orbits based on DSN data, while not up to the standards of previous missions, were sufficient to enable a timely evaluation of the flight. This evaluation did not reveal any reason to recommend that the Mission Operations System (MOS) deviate from its standard planned sequence.



### III. Launch Vehicle System

*Surveyor V* was successfully launched by a General Dynamics/Convair *Atlas/Centaur* launch vehicle (AC-13). Liftoff occurred at 07:57:01.257 GMT on September 8, 1967, from Launch Complex 36B of AFETR at Cape Kennedy, Florida. Launch was via the indirect ascent mode wherein the *Centaur* second stage coasted about 7 min in a near-circular 90-nm parking orbit before reigniting and thrusting a second time to provide the desired injection conditions. The injection was extremely precise. Without a midcourse correction, it is estimated that *Surveyor V* would have impacted the moon only 45.9 km (28.5 miles) from the prelaunch target point.

This was the fifth operational flight of an *Atlas/Centaur* vehicle and the second to utilize the indirect ascent mode. The other flights utilized the direct-ascent mode, which requires only one "burn" of the second stage to achieve injection. Several design modifications were incorporated in the *Centaur* stage for parking orbit missions in order to achieve propellant control under the low gravity environment during the coast period and to insure successful second ignition.

The *Surveyor V* mission was the first *Atlas/Centaur* flight to use the new SLV-3C *Atlas*, which has a 51-in.-longer propellant tank section and increased thrust compared with the LV-3C *Atlas* previously used. The increased length permits tanking of approximately 20,000 lb

of additional propellants. The SLV-3C *Atlas/Centaur* vehicle with the *Surveyor* spacecraft encapsulated in the nose fairing is 117 ft long and weighs about 325,000 lb at liftoff (2-in. rise). The basic diameter of the vehicle is a constant 10 ft from the aft end to the base of the conical section of the nose fairing. The configuration of the completely assembled vehicle is illustrated in Fig. III-1. Both the *Atlas* first stage and *Centaur* second stage utilize thin-wall, pressurized, main propellant tank sections of monocoque construction to provide primary structural integrity and support for all vehicle systems. The first and second stages are joined by an interstage adapter section of conventional sheet and stringer design. The clamshell nose fairing is constructed of laminated fiberglass over a fiberglass honeycomb core and attaches to the forward end of the *Centaur* cylindrical tank section.

#### A. *Atlas* Stage

The first stage of the *Atlas/Centaur* vehicle is a modified version of the *Atlas* used on many previous Air Force and NASA missions such as *Ranger* and *Mariner*. The SLV-3C *Atlas* utilizes an uprated Rocketdyne MA-5 propulsion system, which burns RP-1 kerosene and liquid oxygen in each of its five engines to provide a total liftoff thrust of approximately 395,000 lb. The individual sea-level thrust ratings of the engines are: two booster engines at 168,000 lb each, one sustainer engine at 58,000 lb, and

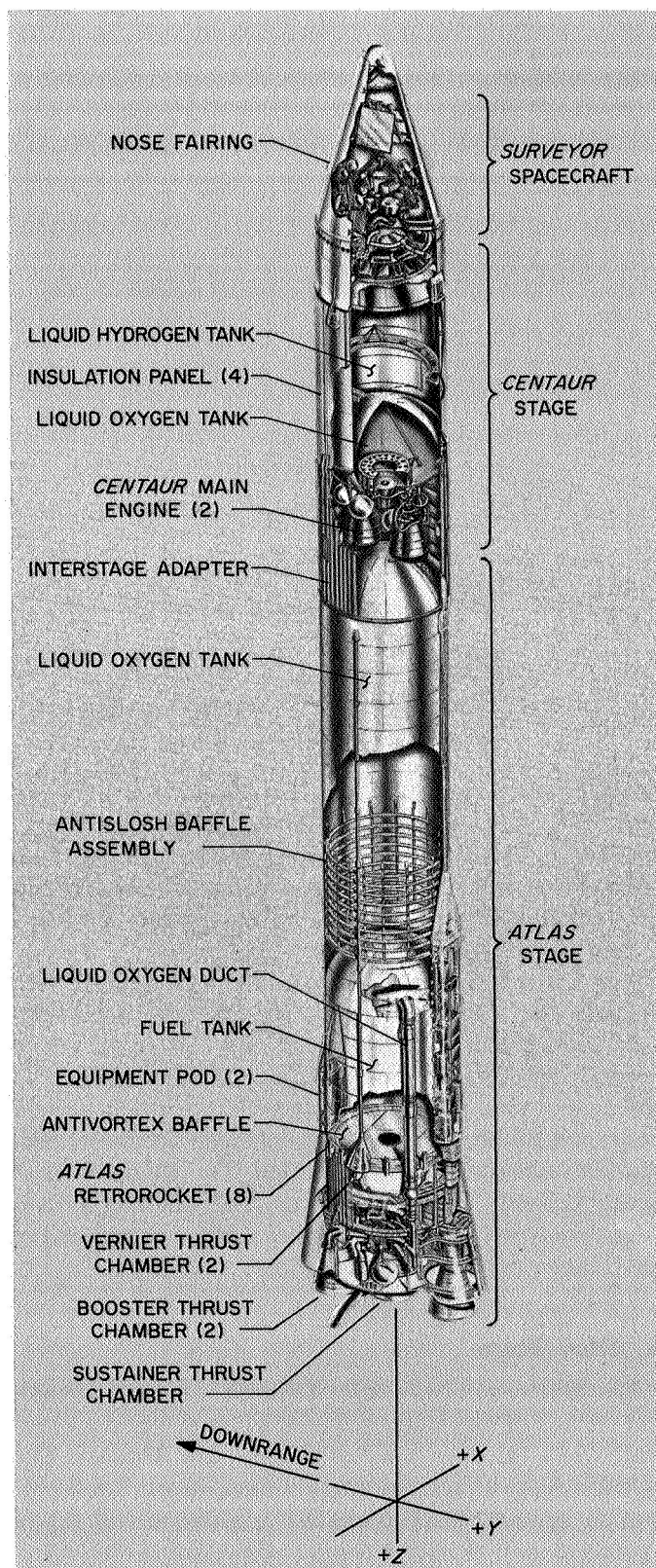


Fig. III-1. Atlas (SLV-3C)/Centaur/Surveyor space vehicle configuration

two vernier engines at 670 lb each. The *Atlas* can be considered a  $1\frac{1}{2}$ -stage vehicle because the "booster section," weighing 6000 lb and consisting of the two booster engines together with the booster turbopumps and other equipment located in the aft section, is jettisoned after about 2.6 min of flight. The sustainer and vernier engines continue to burn until propellant depletion. A mercury manometer propellant utilization system is used to control mixture ratio for the purpose of minimizing propellant residuals at *Atlas* sustainer engine cutoff.

Flight control of the first stage is accomplished by the *Atlas* autopilot, which contains displacement gyros for attitude reference, rate gyros for response damping, and a programmer to control flight sequencing until *Atlas*/*Centaur* separation. After booster jettison, the *Atlas* autopilot also is fed steering commands from the all-inertial guidance set located in the *Centaur* stage. Vehicle attitude and steering control are achieved by the coordinated gimballing of the five thrust chambers in response to autopilot signals.

The AC-13 *Atlas* contained two solid-state telemetry packages for transmission of 208 *Atlas* measurements over two VHF links (229.9 and 232.4 MHz). Both telemetry links utilize each of two antennas mounted on opposite sides of the vehicle at the forward ends of the equipment pods. Redundant range-safety command receivers and a single destructor unit are employed on the *Atlas* to provide the Range Safety Officer with means of terminating the flight by initiating engine cutoff, and/or destroying the vehicle.

Table III-1 notes the significant *Atlas* changes made between the LV-3C flown on *Surveyor III* and the SLV-3C flown on *Surveyor V*.

### B. Centaur Stage

The *Centaur* second stage is the first vehicle to utilize liquid hydrogen/liquid oxygen, high-specific-impulse propellants. The cryogenic propellants require special insulation to be used for the forward, aft, and intermediate bulkheads as well as the cylindrical walls of the tanks. The cylindrical tank section is thermally insulated by four jettisonable insulation panels having built-in fairings to accommodate antennas, conduits, and other tank protrusions. Most of the *Centaur* electronic equipment packages are mounted on the forward tank bulkhead in a compartment which is air-conditioned prior to liftoff.

**Table III-1. Differences between Atlas LV-3C and SLV-3C: notable changes incorporated in SLV-3C used for Surveyor V**

Item	Modification
Propellant tanks	Total length of Atlas tank section was increased 51 in. to provide 20,000-lb additional propellant capacity; Gross space vehicle weight including spacecraft increased from about 303,000 to 325,000 lb
Engine thrust	Rated sea level thrust was increased as follows (by raising the propellant regulator reference pressure to achieve increased propellant flow rates): Booster engines from 165,000 to 168,000 lb each Sustainer engine from 57,000 to 58,000 lb Total liftoff thrust from 387,000 to 395,000 lb
Helium supply	Number of helium tanks was increased from 6 to 8 to provide additional pressurization gas for the larger propellant tanks
Propellant utilization (PU) system	PU system inhibited for first 13 sec of flight because manometers were not lengthened for new tanks and no longer extend to top of tanks
Autopilot	Rate gyro package mounting location was moved approximately 16 in. farther forward for consistency with the dynamics of the longer vehicle structure. Appropriate gain changes were also made in the rate and displacement gyro amplifiers to accommodate the revised vehicle dynamic characteristics
Telemetry system	A second telemetry package was added together with a second telemetry battery to provide an increase in the number of measurements telemetered for evaluation of the SLV-3C
Electrical harnesses and equipment arrangement	Electrical harnesses were redesigned to eliminate splices and for standardization to facilitate installation of mission-peculiar equipment modules. Some equipment was also relocated for improved arrangement and for compatibility with the tank section extension

The *Centaur* is powered by two Pratt & Whitney constant-thrust engines rated at 15,000 lb thrust each in vacuum. Each engine can be gimballed to provide control in pitch, yaw, and roll. Propellant is fed from each of the tanks to the engines by boost pumps driven by hydrogen peroxide turbines. In addition, each engine contains integral "boot-strap" turbopumps driven by hydrogen propellant. Hydrogen propellant is also used for regenerative cooling of the thrust chambers. The AC-13 *Centaur* stage utilized RL10A-3-3 main engines, which were improved over those used on direct ascent flights to provide for operation at lower NPSH (net positive suction head) and an increased specific impulse of 444 sec.

A propellant utilization system is used on the *Centaur* stage to achieve minimum residual of one propellant at depletion of the other. The system controls the mixture ratio valves as a continuous function of propellant in the tanks by means of capacitive-type tank probes and an error ratio detector. The nominal oxygen/hydrogen mixture ratio is 5:1 by weight. Special design features were incorporated in the hydrogen tank design for parking orbit missions to insure propellant control during the coast phase. These include (1) an antiswirl/antislosh baffle located at the hydrogen level at the end of the first burn, (2) diffusers for energy dissipation at the tank inlets of propellant return and helium pressurization lines, and (3) special ducting to provide balanced thrust venting of the hydrogen tank.

The second stage utilizes a Minneapolis-Honeywell all-inertial guidance system containing a navigation computer which provides vehicle steering commands after jettison of the *Atlas* booster section. For windshear relief during the *Atlas* booster phase, the navigation computer may also be used to generate incremental pitch and yaw corrective signals to supplement the *Atlas* fixed pitch and yaw program. The incremental pitch and yaw programs are selected and fed into the navigational computer prior to launch based on measured wind conditions. The *Centaur* guidance signals are fed to the *Atlas* autopilot until *Atlas* sustainer engine cutoff and to the *Centaur* autopilot after *Centaur* main engine ignition. During flight, platform gyro drifts are compensated for analytically by the guidance system computer rather than by applying corrective gyro torquing signals. Subminiature rate gyros with higher response were used for the first time on the AC-13 flight for pitch, yaw, and roll control.

The *Centaur* autopilot system provides the primary control functions required for vehicle stabilization during powered flight, execution of guidance system steering commands, and attitude orientation during parking orbit coast and following the powered phase of flight. In addition, the autopilot system employs an electromechanical timer to control the sequence of programmed events during the *Centaur* phase of flight, including a series of commands required to be sent to the spacecraft prior to spacecraft separation. A dual-timer configuration is used to provide for the additional programmed events required on a parking orbit mission.

The *Centaur* reaction control system provides thrust to control the vehicle during parking orbit coast and after powered flight. For small corrections in yaw, pitch, and roll attitude control, the system utilizes six individually

controlled, fixed-axes, constant-thrust, hydrogen peroxide reaction engines. These engines are mounted in clusters of three, 180 deg apart, near the periphery of the main propellant tanks just aft of the interstage adapter separation plane. Each cluster contains one 6-lb-thrust engine for pitch control and two 3.5-lb-thrust engines for yaw and roll control. In addition, four 50-lb-thrust and four 3-lb-thrust hydrogen peroxide engines are installed on the aft bulkhead, with thrust axes parallel to the vehicle axis.\*

These engines are used to provide axial acceleration for propellant control during parking orbit coast, to achieve initial separation of the *Centaur* from the spacecraft prior to retromaneuver blowdown, and for executing larger attitude corrections if necessary.

The *Centaur* stage utilizes a VHF telemetry system with a single antenna transmitting through the nose fairing cylindrical section on a frequency of 225.7 MHz. The telemetry system provides data from transducers located throughout the second stage and spacecraft interface area as well as a spacecraft composite signal from the spacecraft central signal processor. On the AC-13 flight, 160 measurements were transmitted by the *Centaur* telemetry system.

Redundant range safety command receivers are employed on the *Centaur*, together with shaped-charge destruct units for the second stage and spacecraft. This provides the Range Safety Officer with means to terminate the flight by initiating *Centaur* main engine cutoff and destroying the vehicle and spacecraft retrorocket. The system can be safed by ground command, which is normally transmitted by the Range Safety Officer when the vehicle has reached orbital energy.

A waiver has been obtained for *Surveyor* missions to permit elimination of the inadvertent separation system, which was designed to provide for the automatic destruction of the *Centaur* and spacecraft in the event of premature spacecraft separation.

A C-band tracking system is contained on the *Centaur* which includes a lightweight transponder, circulator, power divider, and two antennas located under the insulation panels. The C-band radar transponder provides real-time position and velocity data for the range safety instantaneous impact predictor as well as data for early orbit determination and postflight guidance and trajectory analysis.

\*The 3-lb-thrust engines were not installed for the direct-ascent missions.

### C. Launch Vehicle/Spacecraft Interface

The general arrangement of the *Surveyor/Centaur* interface is illustrated in Fig. III-2. The spacecraft is completely encapsulated within a nose fairing/adapter system in the final assembly bay of the Explosive Safe Facility at AFETR prior to being moved to the launch pad. This encapsulation provides protection for the spacecraft from the environment before launch as well as from aerodynamic loads and heating during ascent. An ablative-type coating (Thermolag) is applied over the nose fairing and *Centaur* insulation panels to provide added thermal protection.

The spacecraft is first attached to the forward section of a two-piece, conical adapter system of aluminum sheet and stringer design by means of three latch mechanisms, each containing a dual-squib pin puller. The following equipment is located on the forward adapter: three separation spring assemblies each containing a linear potentiometer for monitoring separation; a 52-pin electrical connector with a pyrotechnic separation mechanism; three pedestals for the spacecraft-mounted separation sensing and arming devices; a shaped-charge destruct assembly directed toward the spacecraft retrorocket; a diaphragm to provide a thermal seal and to prevent contamination from passing to the spacecraft compartment from the *Centaur* forward equipment compartment; and accelerometers for monitoring vibration at the separation plane. On the AC-13 vehicle, two high-frequency accelerometers were located on the vehicle side of the separation plane just below the spacecraft attachment ring of the forward adapter section. One of these accelerometers was mounted in the radial direction near spacecraft Leg 1 attach point; the other was mounted in the longitudinal direction near Leg 3 attach point. The outputs of both accelerometers were telemetered continuously. On previous missions, one accelerometer had been mounted differently on the adapter, and four accelerometers had been installed on the spacecraft side of the separation plane.

The low-drag nose fairing is an RF-transparent, clam-shell configuration consisting of four sections fabricated of laminated fiberglass cloth faces and honeycomb fiberglass core material. Two half-cone forward sections are brought together over the spacecraft mounted on the forward adapter. An annular thermal bulkhead between the adapter and base of the conical section completes encapsulation of the spacecraft.

The encapsulated assembly is mated to the *Centaur* with the forward adapter section attaching to the aft

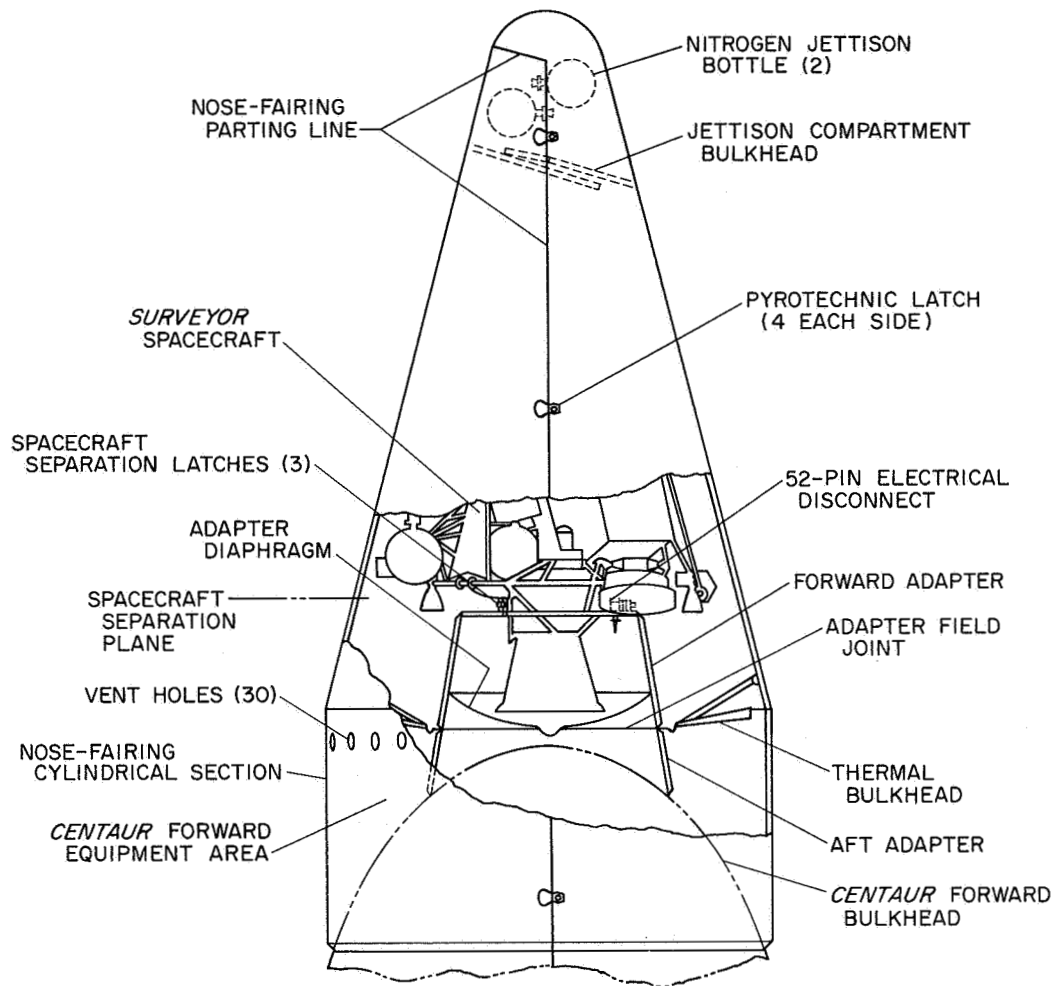


**Fig. III-2. Surveyor/Centaur interface configuration**

adapter section at a flange field joint requiring 72 bolts. The conical portion of the nose fairing is bolted to the cylindrical portion of the fairing, the two halves of which are attached to the forward end of the *Centaur* tank around the equipment compartment prior to mating of the spacecraft. Doors in the cylindrical sections provide access to the adapter field joint. The electrical leads from the forward adapter are carried through three field connectors and routed across the aft adapter to the *Centaur* umbilical connectors and to the *Centaur* programmer and telemetry units.

Special distribution ducts are built into the nose fairing and forward adapter to provide air conditioning of the spacecraft cavity after encapsulation and until liftoff. Seals are provided at the joints to prevent shroud leakage except out through vent holes in the cylindrical section. Prior to launch, the shroud cavity is monitored for possible spacecraft propellant leakage by means of a toxic

gas detector tube which disconnects at liftoff. Tubes are also inserted into each of the vernier engine combustion chambers to permit nitrogen purging for humidity control and leak detection until manual removal before the service tower is rolled away. On the *Surveyor V* mission, the spacecraft alpha scattering instrument was also purged by means of a tube which disconnected at liftoff.

The entire nose fairing is designed to be ejected by separation of two clamshell pieces, each consisting of a conical and cylindrical section. Four pyrotechnic pinpuller latches are used on each side of the nose fairing to carry the tension loads between the fairing halves. Nose fairing loads are transmitted to the *Centaur* tank through a bolted joint, which also attaches to the forward end of the *Centaur* insulation panels and contains a flexible linear shaped charge for insulation panel and nose fairing separation. A nitrogen bottle is mounted in each half of the nose fairing near the forward end to supply gas for cold



gas jets to force the panels apart. Hinge fittings are located at the base of each fairing half to control ejection, which occurs under vehicle acceleration of approximately 1 g during the *Atlas* sustainer phase of flight.

## D. Vehicle Flight Sequence of Events

All vehicle flight events occurred satisfactorily. The only significant deviation from nominal sequence times was the longer-than-expected duration of the *Centaur* first burn period, but this caused no adverse effects on the mission. Predicted and actual times for the vehicle flight sequence of events are included in Table A-1 of Appendix A. Figure III-3 illustrates the major nominal events. The times reported in near-real-time for Mark Events are listed in Section V, Table V-3. Following is a brief description of the vehicle flight sequence of events, with all times referenced to liftoff (2-in. rise) unless otherwise noted. (Refer to Section II-C for a description of the countdown.)

### 1. *Atlas* Booster Phase of Flight

Hypergolic ignition of all five *Atlas* engines was initiated 2 sec before liftoff. Vehicle liftoff occurred 18 min after opening of the launch window on the first day of the launch period at 07:57:01.257 GMT, September 8, 1967. The launcher mechanism is designed to begin a controlled release of the vehicle when all engines have reached nearly full thrust. At 2 sec after liftoff, the vehicle began a 13-sec programmed roll from the fixed launcher azimuth setting of 115 deg to a planned launch azimuth of 79.517 deg. The programmed pitchover of the vehicle began 15 sec after liftoff and lasted until booster engine cutoff (BECO). Incremental pitch program (Code 31) signals from the *Centaur* navigational computer were used to correct the *Atlas* fixed pitch program. The pitch program was selected on the basis of prelaunch wind analysis. However, no incremental yaw program was required.

The vehicle reached Mach 1 at 64 sec and maximum aerodynamic loading occurred at 81.5 sec. During the booster phase of flight, the booster engines were gimbaled for pitch, yaw, and roll control, and the vernier engines were active in roll control only, while the sustainer engine was centered.

At 153.4 sec, BECO was initiated by a signal from the *Centaur* guidance system when vehicle acceleration equalled 5.72 g (expected value:  $5.7 \pm 0.08$  g). At 3 sec after BECO, with the booster and sustainer engines centered, the booster section was jettisoned by release of

pneumatically operated latches. *Atlas* events beginning with BECO occurred later on this flight because of the increased propellant tank capacity of the SLV-3C *Atlas*.

### 2. *Atlas* Sustainer Phase of Flight

At BECO + 8 sec, the *Centaur* guidance system was enabled to provide steering commands for the *Atlas* sustainer phase of flight. During this phase the sustainer engine was gimbaled for pitch and yaw control, while the verniers were active in roll. The *Centaur* insulation panels were jettisoned by firing shaped charges at 198.0 sec at an altitude of approximately 54 nm, where the aerodynamic heating rate was rapidly decreasing. At 227.3 sec, squibs were fired to unlatch the clamshell nose fairing, which was jettisoned 0.5 sec later by means of nitrogen gas thruster jets activated by pyrotechnic valves.

Other programmed events which occurred during the sustainer phase of flight were (1) the unlocking of the *Centaur* hydrogen tank vent valve to permit venting as required to relieve hydrogen boiloff pressure, (2) starting of the *Centaur* boost pumps about 43 sec prior to *Centaur* first main engine start (MES 1), and (3) locking of the *Centaur* oxidizer tank vent valve followed by "burp" pressurization of the tank.

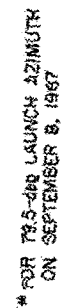
Sustainer and vernier engine cutoff (SECO and VECO) occurred at 246.4 sec as a result of oxidizer depletion, which was the predicted cutoff mode. Shutdown began with an exponential thrust decay phase of about 1-sec duration due to low oxidizer inlet pressure to the turbopump and resulting loss in turbopump performance. Then, final fast shutdown by propellant valve closure was initiated by actuation of a switch when fuel manifold pressure dropped to  $650 \pm 50$  psi. Also, at the SECO event, the *Centaur* hydrogen tank vent valve was locked and burp pressurization of the tank was begun.

Separation of the *Atlas* from the *Centaur* occurred 1.9 sec after SECO by firing of shaped charges at the forward end of the interstage adapter. This was followed by ignition of eight retrorockets located at the aft end of the *Atlas* tank section to back the *Atlas*, together with the interstage adapter, away from the *Centaur*.

### 3. *Centaur* First Burn Phase of Flight

The *Centaur* prestart sequence for providing chilldown of the propulsion system was initiated 8 sec before first ignition of the *Centaur* main engines (MES 1). MES 1 was commanded 11.4 sec after SECO, at 257.8 sec. *Centaur* guidance was reenabled 4 sec after MES 1 to provide





**VICAL REPORT 32-1246**

steering commands during the *Centaur* first burn. Main engine cutoff (MECO 1) was commanded by guidance at 587.1 sec, when sufficient impulse had been delivered for injection into the desired parking orbit. *Centaur* first-burn duration was 329.3 sec, or about 10 sec longer than predicted for the actual launch conditions.

#### 4. *Centaur* Coast Phase of Flight

Coincident with MECO 1, two of the 50-lb-thrust hydrogen peroxide engines were turned on and provided a low level of axial acceleration to overcome transient disturbances to the propellants caused by main engine shutdown. After 76 sec, the 50-lb engines were turned off and two of the 3-lb axial engines were turned on to retain the propellants at the proper location in the tanks. During the parking orbit coast period the hydrogen peroxide engines also were enabled for attitude control.

The required parking orbit coast time varies with actual liftoff time. For this flight, the coast period (MECO 1 to MES 2) lasted for 402.5 sec (6.7 min). The *Centaur* stage can support coast periods of from 116 sec to 25 min in duration. Only one brief occurrence of hydrogen tank venting was observed during the coast period, at 323 sec after MECO 1.

At 40 sec before the end of the coast period, the 3-lb engines were turned off and two of the 50-lb engines turned on again until MES 2 to insure propellant control during the events preceding ignition, which included "burp" pressurization of the propellant tanks, starting of the boost pumps 28 sec before MES 2, and initiation of the prestart (chilldown) sequence 17 sec before MES 2.

#### 5. *Centaur* Second Burn Phase of Flight Through Spacecraft Separation

Second main engine start occurred at 989.6 sec, followed 4 sec later by *guidance enable* for second burn steering control. After a burn time of 114.2 sec, when sufficient velocity had been attained, the *Centaur* engines were shut down by guidance command at 1103.8 sec. *Centaur* second burn duration was only about 1.4 sec longer than expected. At main engine cutoff, the hydrogen peroxide engines were enabled again for attitude stabilization.

During the 61.8-sec period between MECO 2 and spacecraft separation, the following signals were transmitted to the spacecraft from the *Centaur* programmer: *extend spacecraft landing gear*, *unlock spacecraft omniantennas*, and *turn on spacecraft transmitter high power*. An arming signal also was provided by the *Centaur* during this

period to enable the spacecraft to act on the preseparation commands.

The *Centaur* commanded separation of the spacecraft electrical disconnect 5.5 sec before spacecraft separation, which was initiated at 1165.6 sec. The *Centaur* attitude-control engines were disabled for 5 sec during spacecraft separation in order to minimize vehicle turning moments.

#### 6. *Centaur* Retromaneuver Phase of Flight

At 5 sec after spacecraft separation, the *Centaur* began a turnaround maneuver using the attitude-control engines to point the aft end of the stage in the direction of the flight path. About 40 sec after beginning the turn, which required approximately 100 sec to complete, two of the 50-lb-thrust hydrogen peroxide engines were fired for a period of 20 sec while the *Centaur* continued the turn. This provided initial lateral separation of the *Centaur* from the spacecraft. About 240 sec after spacecraft separation, the propellant blowdown phase of the *Centaur* retromaneuver was initiated by opening the hydrogen and oxygen prestart (chilldown) valves. Oxygen was vented through the engine nozzles while hydrogen discharged directly through the chilldown valves. The oxygen tank pressure remained relatively constant, indicating that liquid oxygen remained in the tank throughout the blowdown. At 115 sec from start of blowdown, the fuel tank pressure decay rate increased, indicating that most of the liquid hydrogen had been expelled at that time.

Coincident with termination of propellant blowdown, a hydrogen peroxide depletion experiment was initiated by firing two of the 50-lb engines for 100 sec. Owing to the relatively short parking orbit coast period, hydrogen peroxide depletion did not occur before the hydrogen peroxide experiment was concluded by energizing the *Centaur* power changeover switch at 1755.6 sec, which turned off all power except telemetry and the C-band beacon.

### E. Performance

The *Atlas/Centaur* AC-13 vehicle performance was very satisfactory, providing injection into the desired parking orbit followed by successful restart and extremely accurate injection of the *Surveyor V* spacecraft into the prescribed lunar transfer trajectory.

#### 1. Guidance and Flight Control

The guidance system performed well throughout the flight. A satisfactory parking orbit was achieved, with injection occurring near the apogee of 91 nm. Perigee was 85 nm. The spacecraft was injected on a near-perfect lunar

transfer trajectory which would have resulted in an uncorrected impact only 45.9 km from the prelaunch target point. (Refer to Section VII for a presentation of vehicle guidance accuracy results in terms of equivalent mid-course velocity correction.)

The guidance system provided the programmed incremental pitch signals during booster phase, and all guidance system discrete commands, including BECO, SECO backup, MECO 1 and MECO 2, were generated as planned. Vehicle attitude errors remained small during the closed-loop steering phases of flight except for the initial errors which existed (maximum 5 deg nose up and 1 deg nose right at BECO + 8 sec) and were quickly nulled each time guidance was enabled.

Autopilot performance was satisfactory throughout the flight, with proper initiation of programmed events and control of vehicle stability. Vehicle disturbances during the *Atlas* phase of flight were at or below the expected levels and were easily controlled following *Atlas* autopilot activation at 42-in. motion. Vehicle stability was also satisfactorily maintained during the *Centaur* phase of flight. The MES and MECO transients for both burns appeared similar to those observed on previous flights.

The *Centaur* reaction control system performed properly, maintaining desired vehicle attitude during the coast phases and providing the necessary low-level axial thrust for propellant control and initial lateral separation from the spacecraft. Disturbing torques occurred as expected due to boost pump exhaust and main engine chill-down venting. During the 100-lb thrust period following MECO 1, the 3.5-lb-thrust engines operated at approximately 50% duty cycle in roll. About 3 sec after start of *Centaur* retro turnaround, a brief loss of thrust of the attitude control engines was indicated. This anomaly has been noted on two previous flights (*Surveyors III* and *IV*) at about this time and has been attributed to gas bubbles in the hydrogen peroxide system.

During the *Centaur* phase of flight, the vehicle is rate-stabilized in roll rather than roll-position-stabilized. Vehicle roll attitude during the *Centaur* powered phase of flight is presented in Fig. III-4.

## 2. Propulsion and Propellant Utilization

*Atlas* propulsion system performance was satisfactory, although the booster engine chamber pressures indicated slightly lower levels than expected. Normal sustainer cut-off characteristics were exhibited following oxidizer deple-

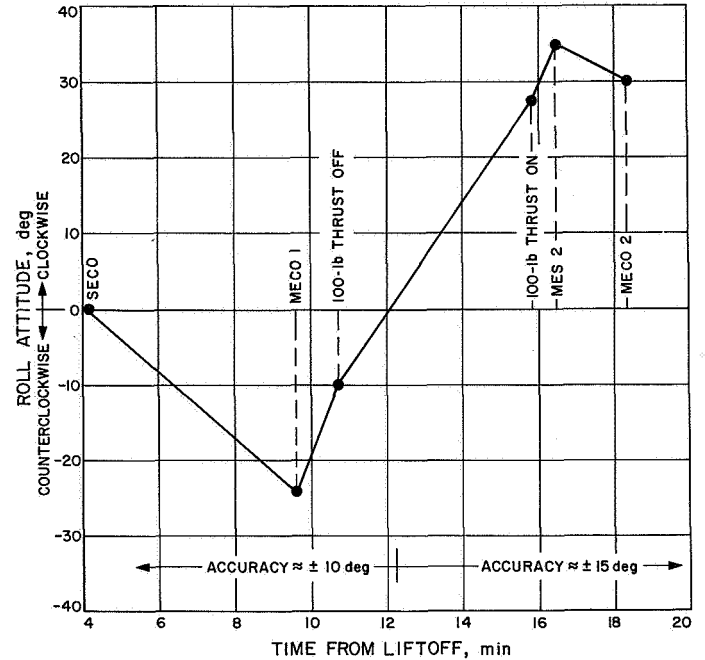


Fig. III-4. *Centaur* roll attitude relative to local vertical

tion, which had been predicted. Performance of the *Atlas* propellant utilization (PU) system was also satisfactory. The predicted *Atlas* residuals (propellant above pump) are compared in Table III-2, with preliminary values computed from flight data assuming nominal flow rates from port uncovering times until actual SECO.

Table III-2. *Atlas* propellant residuals, lb

Residuals	Actual	Predicted
Oxidizer	274	146
Fuel	186	194

The *Centaur* propulsion system performed well during both burn periods. The first burn was 10 sec longer than predicted but well within the estimated  $3\sigma$  tolerance. The thrust of one of the engines was approximately 170 lb lower than predicted based on engine acceptance testing, but well within the allowable  $\pm 300$  lb tolerance. The low thrust would account for less than 3 sec of the longer burn time. The cause of the remainder of the extra burn time is not known at this time. The *Centaur* has also burned for a period longer than expected on each of the previous *Surveyor* missions; in each case, about 4 to 6 sec of the additional burn time is unexplained.

The turbine inlet pressure and speed data of the fuel and oxidizer boost pumps exhibited unexpected trends which are indicative of gas flow through the hydrogen

peroxide catalyst beds. A very similar anomaly was observed during the AC-12 (*Surveyor III*) second burn, but there was no apparent effect on main engine operation on either mission.

The *Centaur* PU system performed very well during both burn periods. The predicted and preliminary actual *Centaur* usable residuals after MECO 1 and MECO 2 are compared in Table III-3.

Based on an average mixture ratio of 5.04:1, the usable residuals would have provided 10.2 sec additional burn time before theoretical oxidizer depletion, with an ultimate fuel residual of approximately 26 lb. Comparing this to the predicted value of 28.1 lb residual hydrogen indicates a *Centaur* PU system error of only 2.1 lb hydrogen deficiency.

**Table III-3. *Centaur* usable propellant residuals, lb**

Usable residuals	Actual	Predicted
MECO 1		
Oxidizer	7137 $\pm$ 400	7180
Fuel	1539 $\pm$ 100	1436
MECO 2		
Oxidizer	576	577
Fuel	140.2	143.6

### 3. Pneumatic, Hydraulic, and Electrical Power Systems

Operation of the *Atlas* pneumatic system, including the programmed tank pressurization and pneumatic control functions, was properly accomplished throughout the flight. Both *Centaur* propellant tanks were maintained at satisfactory levels during all phases of flight, with normal occurrences of the "burp" pressurization sequences and hydrogen tank venting.

Performance of the vehicle hydraulic and electrical power systems was satisfactory throughout the flight. There were no unexpected voltage demands or transients.

### 4. Telemetry, Tracking, and Range Safety Command

The *Atlas* and *Centaur* instrumentation and telemetry systems functioned well, with only a few minor measurement anomalies. Continuous data was obtained over all vehicle flight phases, including the critical second prestart sequence.

The *Centaur* C-band radar apparently operated normally, although, as on some previous flights, it is believed that *Centaur* roll may have contributed to weak signal strength and some loss of data by downrange receivers.

An evaluation of the system can only be made on the basis of received tracking data and station operator logs because the airborne system is not instrumented. (See also Section V.)

The *Atlas* and *Centaur* range safety command systems performed satisfactorily. About 14 sec after parking orbit injection (MECO 1), a range safety command to disable the destruct systems was sent and properly executed.

### 5. Vehicle Loads and Environment

Vehicle loads and thermal environment were within expected ranges throughout the flight. Maximum axial accelerations were 5.72 g at BECO during the booster phase and 1.73 g just before SECO during the sustainer phase. Longitudinal oscillations during launch reached a maximum (0.56 g peak-to-peak at 6 Hz) at 0.5 sec and damped out by 20 sec. Owing to the longer SLV-3C *Atlas*, higher amplitude bending was noted throughout the booster and sustainer phases of flight.

The two high-frequency accelerometers located on the forward spacecraft adapter indicated expected steady-state vibration levels during the flight which agreed well with similar measurements of previous flights. The radially oriented accelerometer indicated a maximum steady-state value during launch of 2.1 g (rms) within a 10- to 660-Hz bandwidth. The maximum longitudinal steady-state level indicated during launch was 1.6 g (rms) within a 10- to 2100-Hz bandwidth. Low-level short-duration transients were recorded throughout the launch phase and have been noted on previous flights. The exact cause of these transients is not known, but they are believed to be due to a combination of dynamic and thermal loads in the area of the *Centaur* forward bulkhead and adapter structure. (Also see Section IV-A for a discussion of launch phase vibration environment.)

The *Surveyor* compartment thermal and pressure environments were normal throughout flight. The ambient temperature within the compartment was 82°F at launch and gradually decreased to 70°F by 89 sec as a result of expansion during ascent. The ambient pressure decayed characteristically to essentially zero prior to nose fairing jettison.

### 6. Separation and Retro Maneuver Systems

All vehicle separation systems functioned normally. Booster section jettison occurred as planned, with resulting vehicle rates and high-frequency accelerometer data comparable to previous flights.

Satisfactory insulation panel jettison was confirmed by normal transient effects on vehicle rates, axial acceleration, vibration, etc. The times of 35-deg rotation of the four insulation panels during jettison are provided by a breakwire at one hinge arm of each panel. Average panel rotational rates to the 35-deg position, derived from the breakwire instrumentation, were from 78 to 83 deg/sec. These values are consistent with rates determined on previous flights.

Normal separation of the nose fairing was verified by indications of 3-deg rotation from disconnect wires which are incorporated in the pullaway electrical connectors of each fairing half. The spacecraft compartment pressure remained at zero throughout nose fairing jettison, with no pressure surge at thruster bottle discharge.

*Atlas/Centaur* separation occurred as planned. Displacement data obtained with respect to time is in close agreement with expected values and indicates successful *Atlas* retro rocket operation. Only a very small angular

motion occurred between stages before the *Atlas* cleared the *Centaur*.

At spacecraft separation, data from the extensometers (linear potentiometers) indicates that first motion of all three springs occurred within 2 msec of each other. Spring extension to the full 1-in. position was normal and nearly identical, producing a spacecraft separation rate of approximately 1 ft/sec. The spacecraft angular rates resulting from the separation event were small and well within the specified maximum acceptable rate of 3.0 deg/sec. (Refer to Section IV-F for a discussion of angular separation rates as determined from spacecraft gyro data.)

All phases of the *Centaur* retro maneuver were executed as planned. Five hours after spacecraft separation, the *Centaur/Surveyor* separation distance was computed to be about 1750 km, which is far in excess of the required minimum distance of 336 km at that time. The *Centaur* closest approach to the moon was computed to be approximately 40,000 km and occurred at about 12:40 GMT on September 11, 1967.



## IV. Surveyor Spacecraft

The basic objectives of the *Surveyor V* spacecraft system were: (1) to accomplish a soft landing on the moon at a new site within the *Apollo* zone of interest (the final pre-midcourse aim point was 0.916 deg north latitude and 24.083 deg east longitude); (2) to obtain postlanding television pictures of the lunar surface; (3) to conduct a lunar surface erosion experiment by static firing the vernier engines; (4) to determine the relative abundance of chemical elements on the lunar surface using the alpha scattering instrument; and (5) to obtain data on radar reflectivity, thermal characteristics, touchdown dynamics, and other measurements of the lunar surface through use of various spacecraft equipment.

*Surveyor V* met all of its objectives. Liftoff occurred at 07:57:01.257 GMT on September 8, 1967. Spacecraft performance was normal until midcourse correction when a leak occurred in the helium regulator of the vernier propulsion system. After execution of the planned midcourse correction, additional vernier firings were performed in an attempt to stop the leak. However, the leak persisted, reducing vernier propulsion capability. Nevertheless, by carefully adjusting critical event times in the terminal descent sequence to reduce required vernier propulsion impulse and by utilizing the last midcourse firings to adjust spacecraft weight and vernier propulsion parameters, a completely successful soft landing was achieved, with the spacecraft performing very close to predictions throughout the descent. Touchdown occurred at 00:46:44 GMT, on September 11, 1967. The spacecraft landed at

1.50 deg north latitude and 23.19 deg east longitude\* on the inside wall of a 30-ft-diameter crater, resulting in a 20-deg tilt of the spacecraft.

After landing, the spacecraft performed extensive operations, including gathering of an abundance of useful alpha scattering data, a successful static firing of the vernier engines, taking of a wide variety of high-quality television pictures (over 18,000 received before camera shutdown after sunset), and other scientific and engineering tests and experiments. The spacecraft survived the lunar night and again responded to commands to provide additional television pictures and other data on the second lunar day.

### A. Spacecraft System

In the *Surveyor* spacecraft design, the primary objective was to maximize the probability of successful spacecraft operation within the basic limitations imposed by launch vehicle capabilities, the extent of knowledge of transit and lunar environments, and the current technological state of the art. In keeping with this primary objective, design policies were established which (1) minimized spacecraft complexity by placing responsibility for mission control and decision-making on earth-based

---

\*Based on in-flight tracking data, preliminary analysis of postlanding tracking data indicates a site location of 1.41 deg north latitude, 23.18 deg east longitude.



equipment wherever possible, (2) provided the capability of transmitting a large number of different data channels from the spacecraft, (3) included provisions for accommodating a large number of individual commands from the earth, and (4) made all subsystems as autonomous as practicable.

Figure IV-1 illustrates the *Surveyor* spacecraft in the cruise mode and identifies many of the major components. A simplified functional block diagram of the

spacecraft system is shown in Fig. IV-2. The spacecraft design is discussed briefly in this section and in greater detail in the subsystem sections which follow. A detailed configuration drawing of the spacecraft is contained in Appendix B.

### 1. Spacecraft Coordinate System

The spacecraft coordinate system is an orthogonal, right-hand Cartesian system. Figure IV-3 shows the

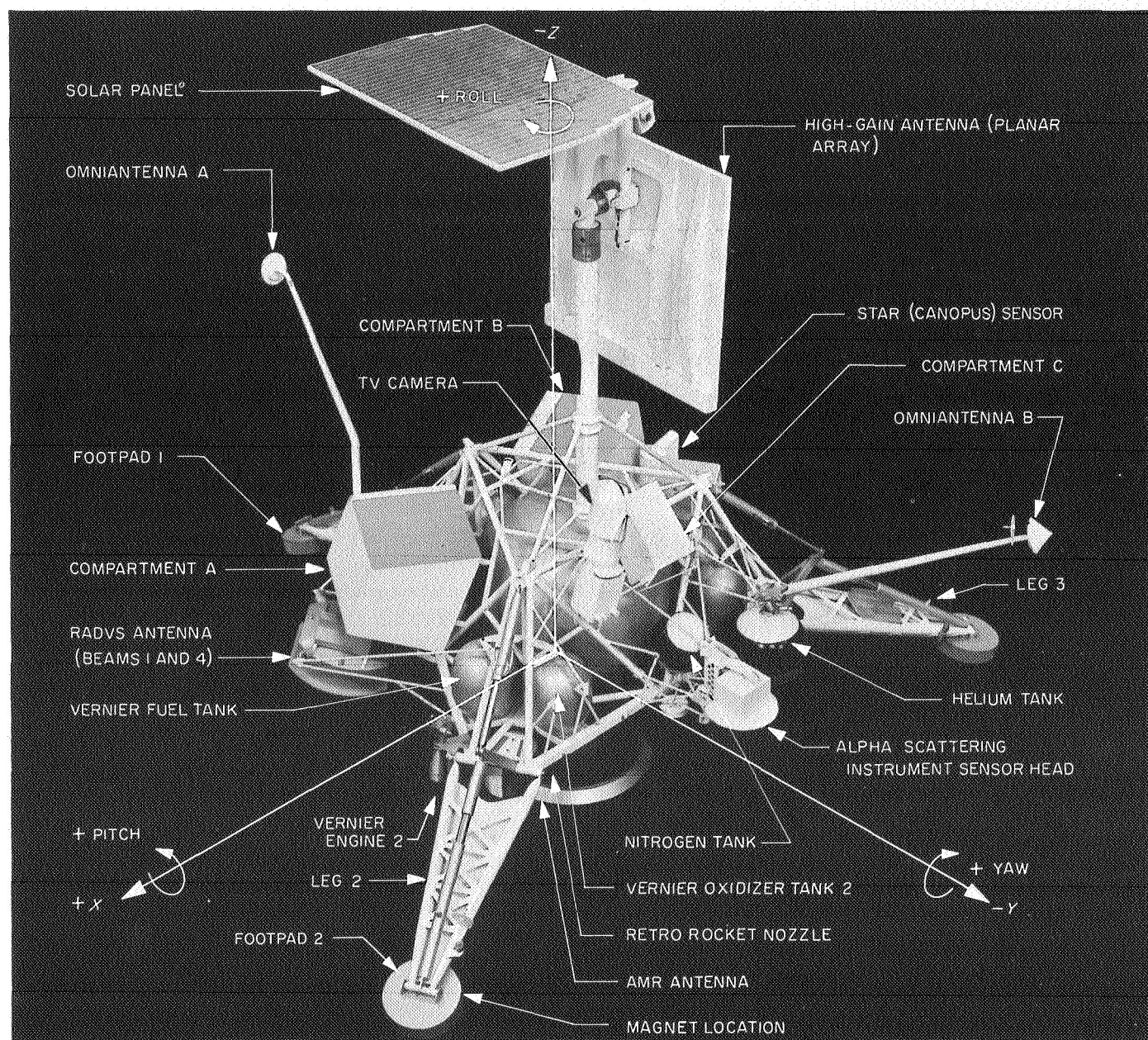


Fig. IV-1. *Surveyor* spacecraft in cruise mode



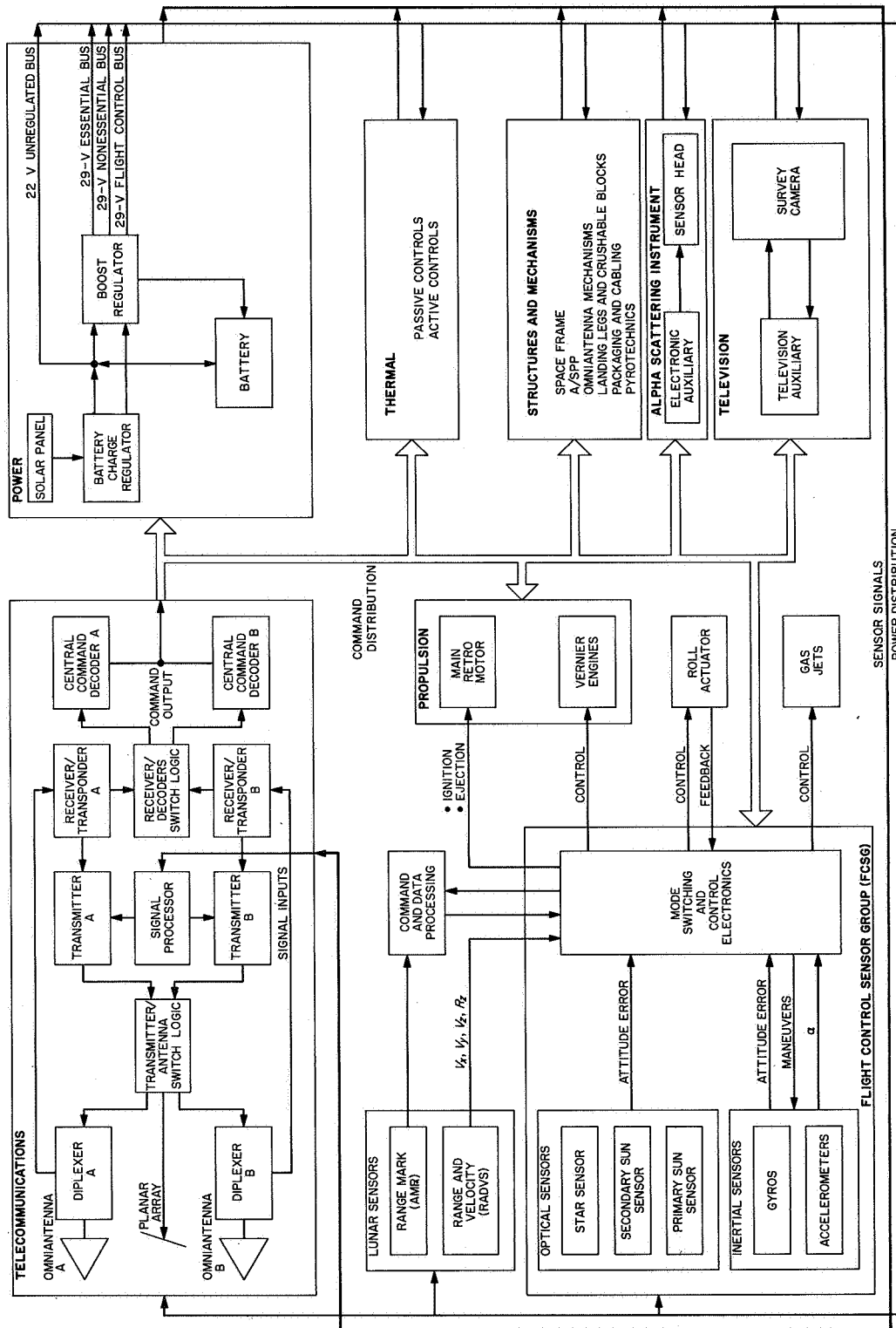
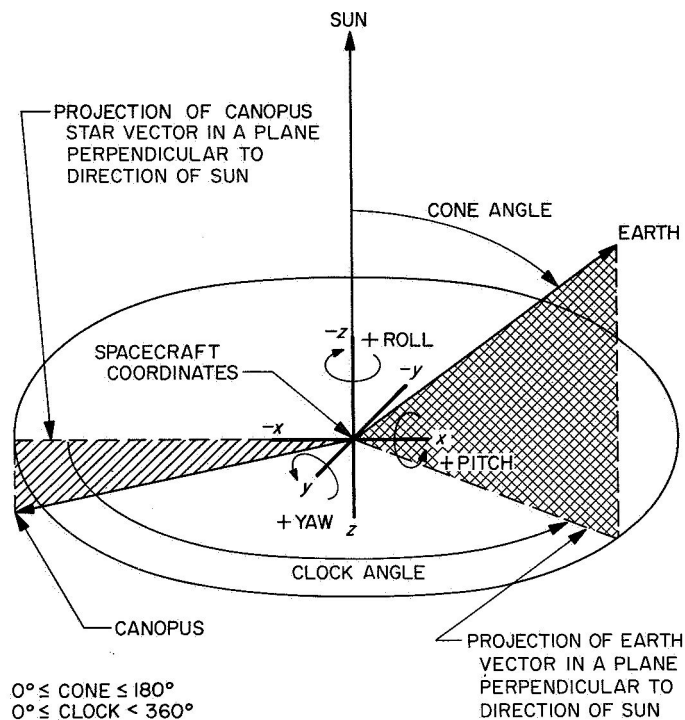


Fig. IV-2. Simplified spacecraft functional block diagram



**Fig. IV-3. Spacecraft coordinates relative to celestial references**

spacecraft motion about its coordinate axes relative to the celestial references. The cone angle of the earth is the angle between the sun vector and the earth vector as seen from the spacecraft. The clock angle of the earth is measured in a plane perpendicular to the sun vector from the projection of the star Canopus vector to the projection of the earth vector in the plane. The spacecraft coordinate system may be related to the cone and the clock angle coordinate system, provided sun and Canopus lock-on has been achieved. In this case, the spacecraft minus Z-axis is directed toward the sun, and the minus X-axis is coincident with the projection of the Canopus vector in the plane perpendicular to the direction of the sun. The spacecraft  $-Z$ -axis is in the direction of the retro motor thrust vector, and Leg 1 lies in the Y-Z plane.

## 2. Spacecraft Mass Properties

The *Surveyor V* spacecraft weighed 2216.82 lb at separation and 668 lb at touchdown. Center of gravity of the vehicle is kept low to obtain stability over a wide range of landing conditions. Center-of-gravity limits after *Surveyor/Centaur* separation for midcourse and retro maneuvers are constrained by the attitude correction capabilities of the flight control and vernier engine subsystems during retrorocket burning. Limits of travel of

the vertical center of gravity in the touchdown configuration are designed to landing site assumptions and approach angle requirements so that the spacecraft will not topple when landing.

## 3. Vehicle Structures and Mechanisms

The vehicle structures and mechanisms subsystem provides support, alignment, thermal protection, electrical interconnection, mechanical actuation, and touchdown stabilization for the spacecraft. The subsystem consists of the basic spaceframe, landing gear, crushable blocks, omnidirectional antenna mechanisms, antenna/solar panel positioner, pyrotechnic devices, electrical cabling, thermal compartments, and separation sensing and arming devices.

The spaceframe is the basic structure of the spacecraft and provides a rigid mount for all components of the spacecraft and mounting surfaces and attachments for connecting to *Centaur*. The tripodic landing gear and crushable blocks stabilize the spacecraft and absorb impact energy during touchdown. The omnidirectional antenna mechanisms provide for omniantenna deployment. The antenna/solar panel positioner (A/SPP) supports and positions (around four independent axes) the planar array antenna and solar panel. The pyrotechnic devices mechanically actuate mechanisms, switches, and valves. The electrical cabling interconnects the spacecraft subsystems and components. The thermal compartments provide thermal control for temperature-sensitive components. The separation sensing and arming devices insure that certain critical squib firing circuits will remain disabled until after *Centaur* separation.

## 4. Thermal Control

Thermal control of equipment over the extreme temperature range of the lunar surface ( $+260$  to  $-260^\circ\text{F}$ ) is accomplished by techniques representing the latest state of the art in the design of lightweight spacecraft. Included are "passive" controls such as superinsulation of electronic compartments and special surface finishes to achieve optimum absorption and emission characteristics, "active" heater systems, and "semiactive" thermal switches.

## 5. Electrical Power

For *Surveyor V*, the electrical power system was redesigned for higher efficiency and simplification. Electrical power for the spacecraft is supplied by a solar panel and a sealed, rechargeable, silver-zinc battery. Power regulation and distribution are provided by a battery

charge regulator (BCR) and a boost regulator (BR). The BCR provides solar panel switching functions and battery charge control. The battery is connected to the unregulated bus which supplies power at a voltage between 17.5 and 27.5 V (nominal 22 V) to spacecraft loads not requiring regulation. The unregulated bus voltage is converted by the BR to supply spacecraft loads requiring regulated power. The BR contains (1) a preregulator that provides power at  $30\text{ V} \pm 2\%$  for the spacecraft "essential" loads, (2) a nonessential bus that provides power at  $29\text{ V} \pm 1\%$  for "nonessential" loads, (3) a flight control regulator to provide power at 29 V for flight control loads, and (4) a shunt regulator which converts excess solar panel power for battery charging. The solar panel can be connected either to the unregulated bus or directly to the preregulator output bus, in which mode the power system operates most efficiently.

## 6. Propulsion

The propulsion subsystem provides thrust during the midcourse correction and terminal descent phases. The propulsion subsystem, consisting of a bipropellant vernier engine system and a solid-propellant main retrorocket motor, is controlled by the flight control system through preprogrammed maneuvers, commands from earth, and maneuvers initiated by flight control sensor signals.

The three thrust chambers of the vernier engine subsystem provide the thrust for midcourse velocity vector correction, attitude control during main retrorocket burning, and velocity vector and attitude control during terminal descent. Thrust Chamber 1 can be swiveled to provide a thrust vector about the roll axis. Thrust Chambers 2 and 3 are stationary and provide thrust parallel to the roll axis for pitch and yaw control. The thrust of each engine can be differentially throttled over a range of 30 to 104 lb to provide attitude control in pitch and yaw.

The main retromotor is utilized to remove the major portion of the spacecraft approach velocity during terminal descent. It is a spherical solid-propellant motor with partially submerged nozzle to minimize overall length. The motor provides a thrust of 8,000 to 10,000 lb for a duration of about 41 sec.

## 7. Flight Control

The flight control subsystem provides spacecraft velocity and attitude control during transit and terminal descent and includes the following spacecraft elements: flight control sensor group (FCSG), attitude control jets,

attitude control gas supply, and Vernier Engine 1 roll actuator.

The FCSCG contains inertial (gyros), optical (Canopus sensor, acquisition sun sensor, primary sun sensor), and acceleration sensors and flight control electronics. The outputs of each of these sensors and radar sensors are utilized by analog electronics to provide commands for operation of attitude gas jets and the spacecraft vernier and main retro propulsion systems. Flight control requires ground commands for initiation of various sequences and performance of "manual" operations. Flight control programming initiates and controls other sequences.

The celestial sensors allow the spacecraft to be locked to a specific orientation defined by the vectors to the sun and the star Canopus and the angle between them. Initial search and acquisition of the sun are accomplished by the secondary sun sensor. The primary sun sensor then maintains the orientation with the sun line.

Of the inertial sensors, integrating gyros are used to maintain spacecraft orientation inertially when the celestial references are not available. Accelerometers measure the thrust levels of the spacecraft propulsion system during midcourse correction and terminal descent phases.

A pair of attitude jets is located on each of the three legs of the spacecraft. The attitude jets provide for angular rate stabilization after spacecraft separation from the *Centaur*, attitude orientation for sun and Canopus acquisition, attitude control during coast phases, and attitude orientation for midcourse correction and terminal descent. The attitude control gas supply provides nitrogen under regulated pressure from a supply tank to the attitude jets.

The three vernier engines are controlled to provide thrust, which can be varied over a wide range, for midcourse correction of the spacecraft velocity vector and controlled descent to the lunar surface. Commands to the vernier roll actuator tilt the thrust axis of Vernier Engine 1 away from the spacecraft roll axis for attitude and roll control during thrust phases of flight when the attitude gas jets are not effective.

## 8. Radar

Two radar systems are employed by the *Surveyor* spacecraft. An altitude marking radar (AMR) provides a mark signal to initiate the main retro sequence. In addition, a radar altimeter and doppler velocity sensor (RADVS)

functions in the flight control subsystem to provide three-axis velocity, range, and altitude mark signals for flight control during the main retro and vernier phases of terminal descent. The RADVS consists of a doppler velocity sensor, which computes velocity along each of the spacecraft X, Y, and Z axes, and a radar altimeter, which computes slant range from 50,000 ft to 13 ft and generates 1000-ft mark and 13-ft mark signals.

## 9. Telecommunications

The spacecraft telecommunications subsystem provides for (1) receiving and processing commands from earth, (2) providing angle tracking and one- or two-way doppler data for orbit determination, and (3) processing and transmitting spacecraft telemetry data.

Continuous command capability is assured by two identical receivers which remain on throughout the life of the spacecraft and operate in conjunction with two omniantennas and two command decoders through switching logic.

Operation of a receiver in conjunction with a transmitter through a transponder interconnection provides a phase-coherent system for doppler tracking of the spacecraft during transit and after touchdown. Two identical

transponder interconnections (Receiver/Transponder A and Receiver/Transponder B) are provided for redundancy. Transmitter B with Receiver/Transponder B is the transponder system normally operated during transit.

Data signals from transducers located throughout the spacecraft are received and prepared for telemetry transmission by signal processing equipment which performs commutation, analog-to-digital conversion, and pulse-code and amplitude-to-frequency modulation functions. Most of the data signals are divided into six groups (commutator modes) for commutation by two commutators located within the telecommunications signal processor. (An additional commutator is located within the television auxiliary for processing television frame identification data.) The content of each commutator mode has been selected to provide essential data during particular phases of the mission (Table IV-1 and Appendix C). Other signals, such as strain gage data which is required continuously over brief intervals, are applied directly to subcarrier oscillators.

Summing amplifiers are used to combine the output of any one commutator mode with continuous data. The composite signal from the signal processor, or television data from the television auxiliary, is sent over one of the

**Table IV-1. Surveyor V spacecraft telemetry mode summary**

	Data mode	Method of transmission	Data rate	Number of signals		Signals emphasized	Primary use
				Analog	Digital		
Engineering commutator	1	PCM/FM/PM	All	42	40	Flight control, propulsion	Canopus acquisition midcourse maneuver
Engineering commutator	2	PCM/FM/PM	All	80	59	Flight control, propulsion, AMR, RADVS	Transit interrogations, backup for main retro phase
Engineering commutator	3	PCM/FM/PM	All	21	40	Inertial guidance, AMR, RADVS, vernier engines	Backup for vernier descent phase
Engineering commutator	4	PCM/FM/PM	All	75	29	Temperatures, power status, telecommunications	Transit interrogations, lunar operations
Engineering commutator	5	PCM/FM/PM	All	108	50	Flight control, power status, temperature	Midcourse and terminal attitude maneuvers, launch and primary cruise data, lunar interrogations
Engineering commutator	6	PCM/FM/PM	All	47	74	Flight control, power status, AMR, RADVS, vernier engine conditions	Terminal descent thrust phase
Television commutator	7	PCM/FM	Only 4400 bit/sec	13		TV survey camera	TV camera interrogation, TV camera operation
Shock absorber strain gages		FM/PM	Continuous	3		Strain gages	Touchdown force on spacecraft legs
Gyro speed		FM/PM	50 Hz	3		Inertial guidance unit	Verify gyro sync

two spacecraft transmitters. The commutators can be operated at five different rates (4400, 1100, 550, 137.5, and 17.2 bit/sec) and the transmitters at two different power levels (10 W or 100 mW). In addition, switching permits each of the transmitters to be operated with any one of the three spacecraft antennas (two omniantennas and a planar array) at either the high or low power level. Selection of data mode(s), data rate, transmitter power, and transmitter-antenna combination is made by ground command. A data rate is selected for each mission phase which will provide sufficient signal strength at the DSIF station to maintain the telemetry error rate within satisfactory limits. The high-gain antenna (planar array) is utilized for efficient transmission of video data.

## 10. Television

The *Surveyor* television subsystem includes a survey camera and a television auxiliary for final decoding of commands and processing of video and frame identification data for transmission by either of the spacecraft transmitters.

The survey camera is designed for postlanding operation by earth commands to provide photographs of the lunar surface panorama, portions of the spacecraft, and the lunar sky. Photographs may be obtained in either of two modes: a 200-line mode for relatively slow (61.8 sec/frame) transmission over an omniantenna or a 600-line mode for a more efficient and rapid (3.6 sec/frame) transmission over the planar array.

The survey camera is mounted about 16 deg from vertical and is pointed upward toward a mirror mounted in the camera hood. The mirror together with the hood can be rotated 360 deg and the mirror can be tilted in steps for horizontal and vertical scanning, respectively. Special mirrors are mounted on the spacecraft frame to provide additional camera coverage of areas of interest under the spacecraft.

The camera can be focused over a range from 4 ft to infinity and can be zoomed to obtain photos in narrow angle (6.4 deg) or a wide angle (25.4 deg) field of view. A lens iris provides a stop range from  $f/4$  to  $f/22$ . The camera is equipped with a focal plane shutter which normally provides an exposure time of 150 msec but can be commanded to remain open for time exposures. A sensing device, attached to the shutter, will keep it from opening if the light level is too strong. The same device automatically controls the iris setting. This device can be

overridden by ground command. A filter wheel assembly between the lens and mirror contains three colored (red, green and blue) and one clear filter.

## 11. Alpha Scattering Instrument

An alpha scattering instrument was included in the spacecraft system for the first time on the *Surveyor V* mission. This instrument contains a radioactive source of alpha-particles, the interaction of which with the lunar surface material produces back-scattering of alpha and proton particles. Detectors are used to determine the characteristics of the back-scattering, from which the relative abundance of chemical elements can be determined. The instrument consists of a sensor head, a deployment mechanism, and associated electronics contained in a thermally insulated compartment. During transit to the moon, the sensor head is held in a stowed position where it is in contact with a standard sample. Following an initial calibration period after landing, the sensor head is deployed—first to a position above the lunar surface where it obtains data on background radiation, and then to a position where it rests on the lunar surface to obtain lunar scattering data. An electronics auxiliary and digital electronics provide command decoding, signal processing, power management, and the electronics interface with the basic spacecraft bus.

## 12. Instrumentation

Transducers are located throughout the spacecraft system to provide signals that are relayed to the DSIF stations by the telecommunication subsystem. These signals are used primarily to assess the condition and performance of the spacecraft. Some of the measurements also provide data useful in deriving knowledge of certain characteristics of the lunar surface. In most cases, the individual subsystems provide the transducers and basic signal conditioning required for signals provided for data related to their equipment. All the instrumentation signals provided for the *Surveyor V* spacecraft are summarized by category and responsible subsystem in Table IV-2.

All of the temperature transducers are resistance-type units except for two microdiode bridge amplifier assemblies used in the television subsystem. The voltage (signals) and position (electronic switches) measurements consist largely of signals from the command and control circuits. A strain gage is mounted on each of the vernier engine brackets to measure thrust and on each of the three landing leg shock absorbers to monitor touchdown dynamics.

**Table IV-2. Surveyor V instrumentation**

Sensor type	Subsystem location									
	Structures, mechanisms, and thermal control	Electrical power	Propulsion	Flight control	Radar	Telecommunications		Alpha scattering instrument	Television	Total
						Signal processing	Radio and command decoding			
Temperature (thermistors)	33	4	19	9	6	4	2	2	2	76
Temperature (bridges)									2	2
Pressure		1	3	1						5
Position (potentiometers)	7								6	13
Position (mechanical switches)	10			1						11
Position (electrical switches)	1	2		34	15			8	4	68
Current		13							1	14
Voltage (power)		5							2	7
Voltage (signals)				14	7			6	2	29
Strain gages	3		3							6
Accelerometer				1					1	
Inertial sensors (gyro speed)				3					3	
RF power							2		2	
Optical				9					9	
Calibration				1		10			1	12
Totals	54	25	25	73	28	14	18	7	15	262

The flight control accelerometer is mounted on the retromotor case to verify motor ignition and provide gross retro performance data.

Additional discussion of instrumentation is included with the individual subsystem descriptions.

### 13. Design Changes

Table IV-3 presents a summary of notable differences in design between the *Surveyor IV* and *V* spacecraft.

### 14. Spacecraft Reliability

The prelaunch reliability estimate for the *Surveyor V* spacecraft was 0.72 at 50% confidence level for the flight through landing phases of the mission, assuming successful injection. The reliability estimates for the *Surveyor V* spacecraft system vs systems test experience are shown in Fig. IV-4. Table IV-4 presents the final reliability estimates for each subsystem. For comparative purposes, estimates for *Surveyor I* through *IV* are also shown. The primary source of data for these reliability estimates is the time and cycle information experienced by spacecraft units during systems tests. Test and flight data for the spacecraft used on previous missions was included where there were no significant design differences between the

units. In general, a failure is considered relevant if it could occur during a mission.

### 15. Functional Description of Spacecraft Automatic Flight Sequences

The *Surveyor* spacecraft system has been designed for automatic operation in the following flight sequences:

*a. Solar panel deployment and sun acquisition.* Immediately upon separation from the *Centaur*, the spacecraft automatically deploys the solar panel to the transit position in a two-step sequence. First, the A/SPP solar panel axis is unlocked and the solar panel is rotated 85 deg from the stowed position to an orientation normal to the spacecraft Z-axis. When this position is reached, the solar panel axis is locked and the A/SPP roll axis is unlocked. The antenna/solar panel combination is then rotated 60 deg about the roll axis and locked in the transit position.

Also upon separation from the *Centaur*, the spacecraft flight control system operates the attitude control jets in a rate-stabilization mode to reduce angular motion imparted to the spacecraft to within deadband limits of  $\pm 0.1$  deg/sec. After a 51-sec delay following spacecraft electrical disconnect, which allows time for the spacecraft

**Table IV-3. Notable differences between Surveyors IV and V: changes incorporated on Surveyor V**

Item	Description
Signal processor data channel assignments	The telemetry channels within the signal processor were reassigned to provide more optimum data for spacecraft evaluation and to provide channels for the alpha scattering instrument
Power subsystem	Major design changes were made to the power subsystem for simplification and increased efficiency, the most significant of which were: flat cell mounting and a new series/parallel arrangement in the solar panel for better performance over a wider temperature range; elimination of the auxiliary battery and auxiliary battery control; replacement of the optimum charge regulator by a solar panel switch for an increase in overall battery charge regulator efficiency
Flight control programmer	The maximum midcourse burn time which can be timed for automatic vernier engine shutoff was increased from 51 to 102 sec, and the high thrust command at retro burnout was set for a 10-sec delay
Vernier propulsion system	The helium check and relief valves were relocated on the spaceframe in a separate assembly, and additional transducers were added to the fuel lines
A/SPP	The A/SPP mechanism was strengthened and new drive motors with improved performance were incorporated
Main compartments	The compartment shells were redesigned to facilitate access to electronic components after initial spacecraft assembly
Accelerometers	The eight vibration accelerometers (including four used during launch phase) and amplifiers were removed. Two accelerometers are now located on the Centaur side of the separation plane
Alpha scattering instrument	The SM/SS was deleted and an alpha scattering instrument was installed, the sensor head of which is stowed where the auxiliary battery was mounted

to reduce the angular motion, a sun acquisition sequence is automatically initiated. First, flight control commands a roll maneuver which permits the sun to be acquired by the acquisition sun sensor, which has a 10-deg-wide by 196-deg-fan-shaped field of view that is centered about the spacecraft minus X-axis. Upon initial sun acquisition, the roll is stopped and a positive yaw maneuver is initiated to permit the narrow-view primary sun sensor to acquire and lock-on the sun. A secondary sun sensor is mounted on the solar panel to provide a means of sun acquisition by ground command if the automatic sequence fails.

Upon completion of the solar panel deployment and sun acquisition sequences, the spacecraft coasts with its roll axis (and the active face of the solar panel) held posi-

**Table IV-4. Surveyor spacecraft subsystem and system reliability estimates**

Subsystem	Surveyor				
	I	II	III	IV	V
Telecommunications	0.925	0.944	0.965	0.929	0.987
Vehicle and mechanisms	0.816	0.868	0.907	0.854	0.853
Propulsion	0.991	0.991	0.968	0.947	0.934
Electrical power	0.869	0.958	0.935	0.953	0.985
Flight control	0.952	0.889	0.971	0.931	0.945
Systems interaction factor	0.736	0.949	0.967	0.978	0.986
Overall spacecraft system	0.456	0.658	0.745	0.653	0.722

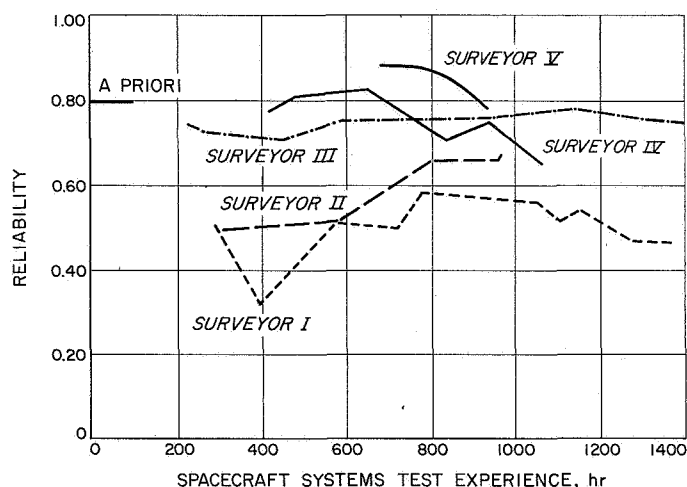


**Fig. IV-4. Surveyor spacecraft system reliability estimates**

tioned toward the sun by maintaining the sun within the field of view of the center cell of the primary sun sensor. The other axes are held inertially fixed by means of the roll gyro.

**b. Canopus acquisition.** Some time after sun acquisition, a roll maneuver is initiated by ground command for star verification and Canopus acquisition. As the spacecraft rolls about its Z-axis, the Canopus sensor provides intensity signals of objects which pass through its field of view and have intensities in the sensitivity range of the sensor. Comparison of a map constructed from these signals and a map previously prepared based on predictions permits identification of Canopus from among the signals. After sufficient spacecraft roll to permit Canopus verification, the spacecraft is switched to *star acquisition* mode by ground command to permit the spacecraft to lock-on

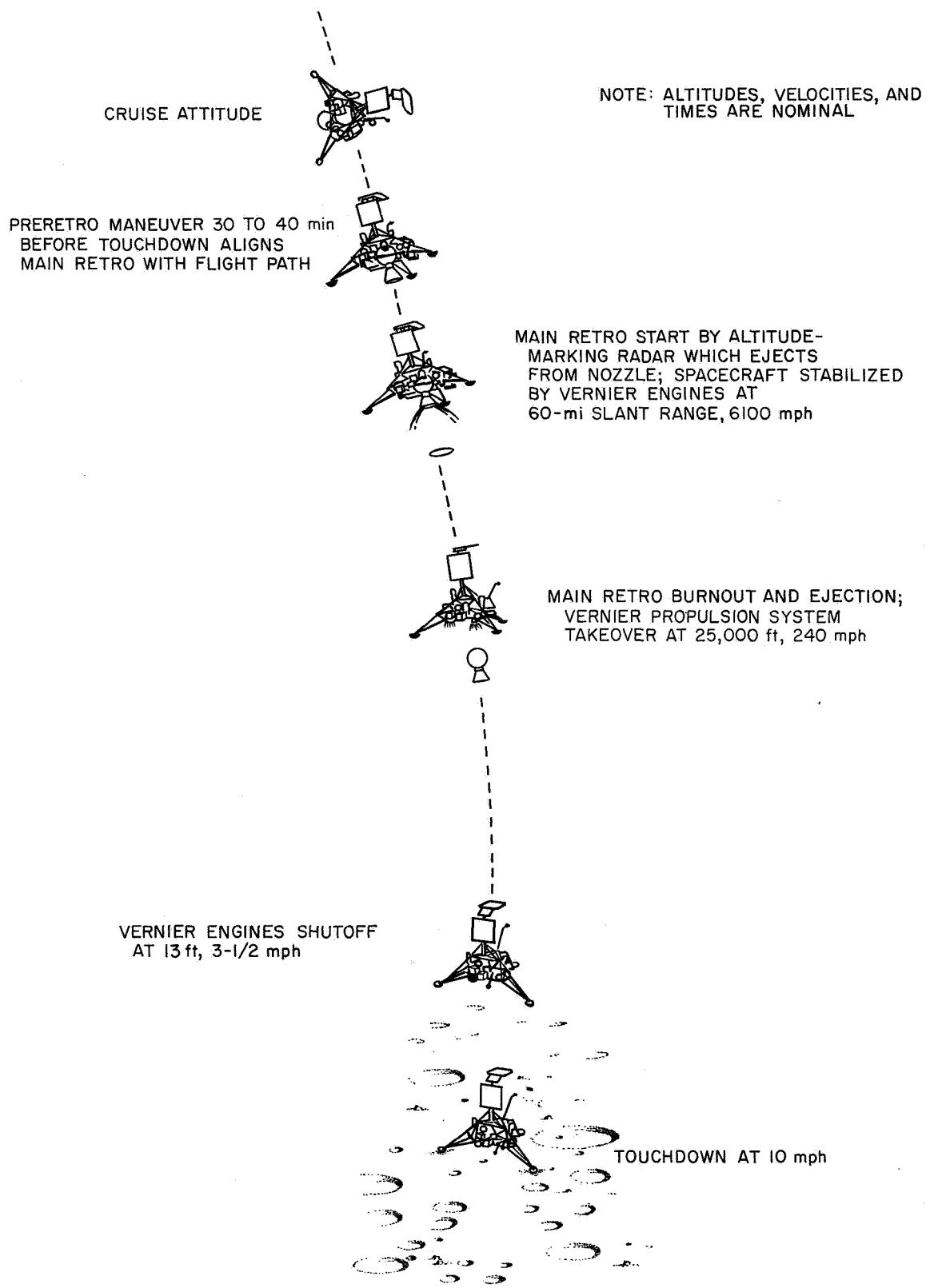


Fig. IV-5. Terminal descent nominal events for a normal mission



Canopus automatically the next time Canopus passes through the sensor field of view. Canopus acquisition establishes three-axes attitude reference, which is required before the midcourse and terminal maneuvers can be performed.

**c. Midcourse velocity correction.** The spacecraft executes each of the desired midcourse attitude maneuvers (roll, pitch, or yaw) upon initiation by ground command. The spacecraft automatically terminates each maneuver when the desired magnitude (previously transmitted by ground command and stored in the flight control programmer) of turn has been accomplished. The maneuvers must be accomplished serially since the flight control programmer can store only one magnitude at a time.

The magnitude of the desired vernier thrust time for midcourse velocity correction is also transmitted to the spacecraft, verified, and stored by the flight control. During the midcourse thrusting phase, the three vernier engines provide a constant spacecraft acceleration of about 0.1 earth  $g$  until cutoff is commanded by flight control. During thrusting, the vernier engines are differentially throttled and the roll actuator is controlled to achieve attitude stabilization.

**d. Terminal descent sequence.** The terminal phase begins with the preretro attitude maneuvers (Fig. IV-5). These maneuvers are commanded from earth in a manner similar to the midcourse maneuvers to reposition the

attitude of the spacecraft from the coast phase sun-star reference such that (1) the expected direction of the retro thrust vector will be aligned with respect to the spacecraft velocity vector, and (2) the spacecraft roll attitude will provide the most desirable landed orientation for lunar operations within the RADVS and telecommunications descent constraints. Following completion of the attitude maneuvers, the AMR is activated. It has been preset to generate a *mark* signal when the slant range to the lunar surface is 60 miles nominal. A backup *mark* signal, delayed a short interval after the AMR *mark* should occur, is transmitted to the spacecraft to initiate the automatic sequence in the event the AMR *mark* is not generated. A delay between the *altitude mark* and main retro motor ignition has been preset in the flight control programmer by ground command. Vernier engine ignition is automatically initiated 1.1 sec prior to main retro ignition. The main retro phase sequence for a nominal mission is illustrated in Fig. IV-6.

During the main retro phase, spacecraft attitude is maintained in the inertial direction established at the end of the preretro maneuvers by differential throttle control of the vernier engines while maintaining the total vernier thrust at the midthrust level. The main retro burns at essentially constant thrust for about 40 sec, after which the thrust starts to decay. This tailoff is detected by an inertial switch which increases vernier thrust to the high level and initiates a programmed time delay of about 12 sec, after which the main retro motor case is

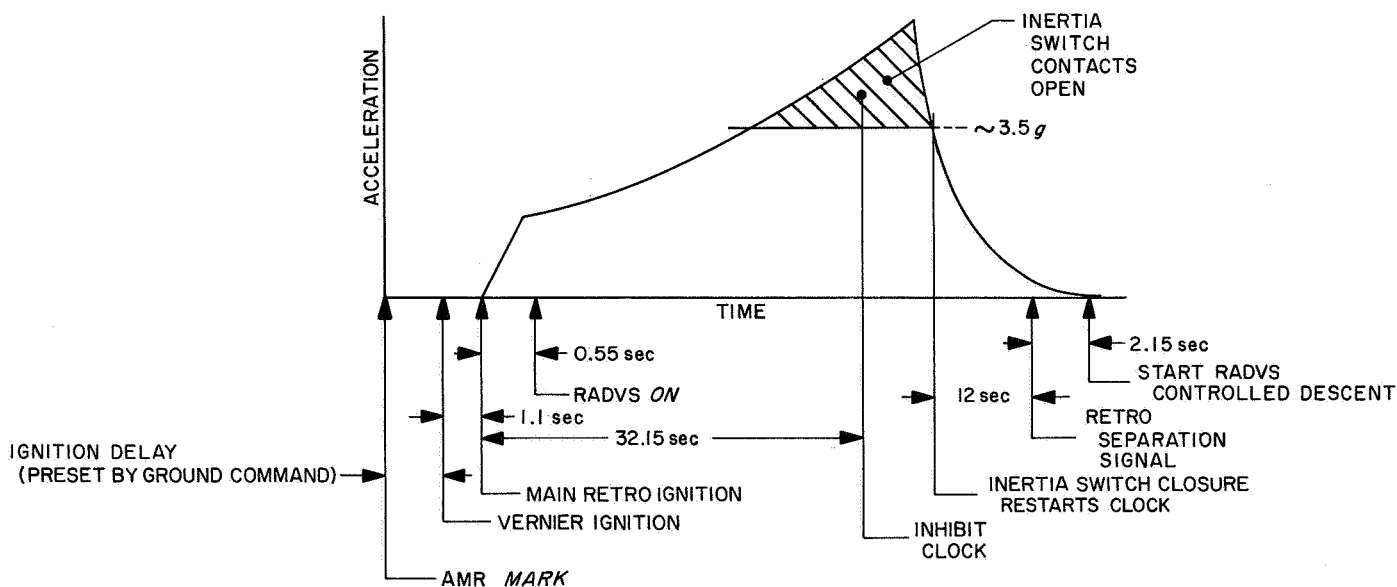


Fig. IV-6. Main retro phase sequence for a normal mission

ejected. The main retro phase removes more than 95% of the spacecraft velocity and puts the spacecraft position, velocity, and attitude relative to the lunar surface within the capability of the final, vernier phase.

The vernier phase normally begins at altitudes between 10,000 and 50,000 ft and velocities in the range of 100 to 700 ft/sec. This wide range of vernier-phase initial conditions exists because of statistical variations in parameters which affect main retro burnout. About 2 sec after separation of the main retro case, vernier thrust is reduced and controlled to produce a constant spacecraft acceleration of 0.1 lunar  $g$ , as sensed by an axially oriented accelerometer. The spacecraft attitude is held in the preretro position until the doppler velocity sensor locks onto the lunar surface. The thrust axis is then aligned and maintained to the spacecraft velocity vector throughout the remainder of the descent until the terminal sequence is initiated (when the attitude is again held inertially fixed). With the thrust axis maintained in alignment with the velocity vector, the spacecraft makes a "gravity turn," wherein gravity tends to force the flight path towards the vertical as the spacecraft decelerates.

The vehicle descends at 0.1 lunar  $g$  until the radars sense that the "descent contour" has been reached (Fig. IV-7). This contour corresponds, in the vertical case, to descent at a constant deceleration. The vernier thrust is commanded such that the vehicle follows the descent contour until shortly before touchdown, when the terminal sequence is initiated. Nominally, the terminal sequence consists of a constant-velocity descent from 40 to 13 ft at 5 ft/sec, followed by a free fall from 13 ft, resulting in touchdown at approximately 13 ft/sec.

Constraints on the allowable main retro motor burnout conditions are of major importance in *Surveyor* terminal descent design.

RADVS operational limitations contribute to constraints on the main retro burnout conditions. Linear operation of the doppler velocity sensor is expected for slant ranges below 50,000 ft and for velocities below 700 ft/sec. The altimeter limit is between 30,000 and 40,000 ft, depending on velocity. These constraints are illustrated in the range-velocity plane of Fig. IV-7.

The allowable main retro burnout region is further restricted by the maximum thrust capability of the vernier engine system. To accurately control the final descent, the minimum thrust must be less than the least

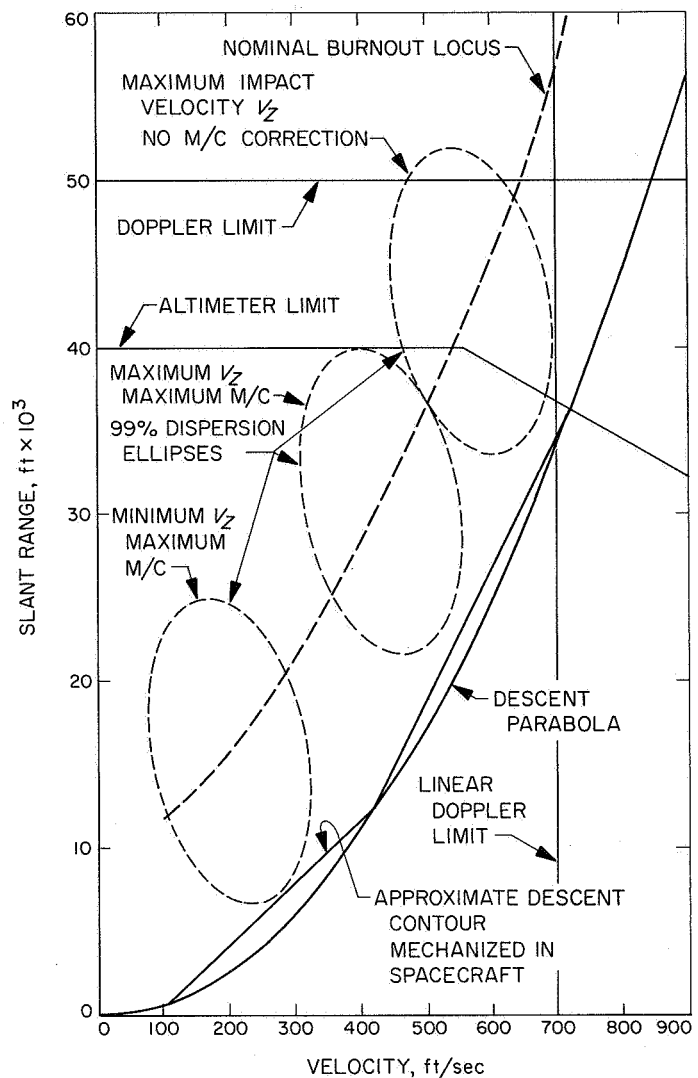


Fig. IV-7. Range-velocity diagram

possible landed weight (lunar gravity) of the vehicle. The result is a minimum thrust of 90 lb. This in turn constrains the maximum vernier thrust to 312 lb because of the limited range of throttle control which is possible.

Descent at the maximum thrust to touchdown defines a curve in the range-velocity plane below which main retro burnout cannot be allowed to occur. Actually, since the vernier engines are also used for attitude stabilization by differential thrust control, it is necessary to allow some margin from the maximum thrust level. Furthermore, since it is more convenient to sense deceleration than thrust, the vernier phase of terminal descent is performed at nearly constant deceleration rather than at constant thrust. Therefore, maximum thrust will be utilized only at the start of the vernier phase.

The maximum vernier phase deceleration defines a parabola in the altitude-velocity plane. For vertical descents at least, this curve defines the minimum altitude at which main retro burnout is permitted to occur with a resulting soft landing. This parabola is indicated in Fig. IV-7. (For ease of spacecraft mechanization, the parabola is approximated by a descent contour consisting of straight-line segments.)

Main retro burnout must occur sufficiently above the descent contour to allow time to align the thrust axis with the velocity vector before the trajectory intersects the contour. Thus, a "nominal burnout locus" (also shown in Fig. IV-7) is established which allows for altitude dispersions plus an alignment time which depends on the maximum angle between the flight path and roll axis at burnout.

The allowable burnout region having been defined, the size of the main retro motor and ignition altitude are determined such that burnout will occur within that region.

In order to establish the maximum propellant requirements for the vernier system, it is necessary to consider dispersions in main retro burnout conditions as well as midcourse maneuver fuel expenditures. The principal sources of main retro burnout velocity dispersion are the imperfect alignment of the vehicle prior to main retro ignition and the variability of the total impulse. In the case of a vertical descent, these variations cause dispersions of the type shown in Fig. IV-7, where the ellipse defines a region within which burnout will occur with probability 0.99. The design chosen provides enough fuel so that, given a maximum midcourse correction, the probability of not running out is at least 0.99.

The spacecraft landing gear is designed to withstand a horizontal component of the landing velocity. The horizontal component of the landing velocity is nominally zero. However, dispersions arise primarily because of the following two factors:

- (1) Measurement error in the doppler system resulting in a velocity error normal to the thrust axis.
- (2) Nonvertical attitude due to: (a) termination of the "gravity turn" at a finite velocity, and (b) attitude control system noise sources.

Since the attitude at the beginning of the constant-velocity descent is inertially held until vernier engine cutoff, these errors give rise to a significant lateral velocity at touchdown.

## 16. Spacecraft System Performance

A summary of *Surveyor V* spacecraft system performance is presented below by mission phases. Also refer to Sections IV-B through IV-J for spacecraft subsystem performance; Section VI-C presents a chronology of mission operations.

*a. Countdown and launch phase performance.* The spacecraft performed normally prior to launch and caused no interruptions in the countdown. Excessive AGC fluctuations of spacecraft Receiver A were noted but, as on the previous mission, the AGC variations were found to be associated with the air link between Building AO and the launch pad and were not due to a spacecraft anomaly.

Liftoff occurred at 07:57:01.257 GMT on September 8, 1967, with the spacecraft in the standard launch configuration (transmitter low power on, legs and omniantennas folded, solar panel and planar array stowed and locked, etc.). Performance during launch via parking orbit was as expected, and the spacecraft was injected into an extremely accurate transfer trajectory.

During the boost phase of flight, the *Surveyor* spacecraft is subjected to a variable vibration environment consisting of acoustically induced random vibration and the transient response to discrete flight events. The *Surveyor V* space vehicle was instrumented with two accelerometers, the output of each of which was telemetered continuously in order to obtain information on this vibration environment. These accelerometers were located on the spacecraft adapter just below the spacecraft attach points. One accelerometer was oriented in the radial direction at Leg 1 attach point, and the other in the longitudinal direction at Leg 3 attach point. On previous spacecraft, accelerometers have been located differently on the spaceframe and adapter, near the spacecraft/adapter attach points. Because of the differences in the accelerometer locations and mounting structure, the dynamic environment indicated by the accelerometers on *Surveyor V* cannot be compared directly with the dynamic environment on previous spacecraft; however, the levels are within the expected ranges. For *Surveyor V*, the accelerometers were used to identify dynamic response to launch vehicle and spacecraft events, and to indicate any anomalous dynamic environment. The responses of the accelerometers to launch phase events are shown in Table IV-5.

The spacecraft properly executed all preseparation events initiated by the *Centaur* programmer, which included turning on the transmitter high power, extending

**Table IV-5. Surveyor V maximum measured zero-to-peak acceleration, g, during launch phase events**

Event	Accelerometer	
	Radial	Longitudinal
Liftoff	1.95 rms	1.26 rms
Maximum aerodynamic loading	0.61 rms	0.50 rms
BECO	2.0	3.0
Insulation panel jettison	>10	>10
Nose fairing separation	1.0	1.0
Atlas/Centaur separation	>10	>10
Main engine start 1	<1.0	<1.0
Main engine cutoff 1	1.8	3.8
Main engine start 2	<1.0	<1.0
Main engine cutoff 2	3.2	2.8

the landing legs, and extending the omniantennas. Spacecraft separation from the *Centaur* was also accomplished as desired.

**b. Postseparation through star acquisition performance.** The automatic solar panel and A/SPP roll-axis stepping sequence was initiated by spacecraft separation and occurred normally. The solar panel was unlocked and required about 361 sec to step through  $-85$  deg and lock in its transit position. Upon locking of the solar panel, the A/SPP roll axis was unlocked and about 187 sec was required for the A/SPP to roll  $+60$  deg and lock in its transit position.

Spacecraft separation also enabled the cold gas attitude control system, and the small angular rates which had been imparted to the spacecraft were nulled in less than 20 sec. After the 51-sec built-in time delay from electrical disconnect, the sun acquisition sequence occurred properly, beginning with a negative roll through about  $342$  deg, which was terminated upon illumination of the acquisition sun sensor. Then followed a positive yaw turn through about  $18$  deg, which was terminated upon illumination of the primary sun sensor center cell.

After good two-way telecommunications were initially established by DSS 51 at about  $L + 33$  min and an assessment of spacecraft telemetry indicated all systems to be normal, the spacecraft responded correctly to an initial sequence of earth commands to place the spacecraft in the cruise configuration. In the cruise configuration, the transmitter was operated on low-power at 1100 bit/sec with the coast phase commutator (Mode 5) on.

Automatic Canopus lock-on occurred successfully about  $6\frac{1}{2}$  hr after launch, when acquisition was attempted following an initial roll to generate a star map. The total spacecraft roll was  $533$  deg. Canopus sensor performance was excellent, with the ratio of measured to predicted Canopus intensity equalling approximately 1.08.

**c. Midcourse correction performance.** Maneuvers consisting of  $+71.9$  deg roll and  $-35.7$  deg yaw were successfully performed in preparation for the midcourse velocity correction. When a helium squib valve was fired about  $2\frac{1}{2}$  min before midcourse correction to pressurize the vernier propulsion system, the helium regulator failed to lock up tight after propellant tank pressure reached the regulated pressure setting of about 730 psia. This caused the tank pressure to rise slowly to the relief valve pressure setting of about 825 psia, where it was maintained by overboard venting of the helium. The midcourse firing of 14.25-sec duration was successfully executed. However, afterward the propellant tank pressure again rose slowly until venting occurred. The helium leak caused the helium tank pressure to drop at a rate of approximately 10 psi/min. In an attempt to actuate and reseal the helium regulator, three additional vernier engine firings (Nos. 2 through 4) were performed. However, the leak persisted. Firing 3 consisted of a 12-sec burn followed by two additional 0.5-sec burn periods with 1-sec interruptions. A summary of each of the vernier firings conducted on the *Surveyor V* mission is contained in Table IV-6.

An intensive study of the situation, including special vernier engine tests at low supply pressure conditions, indicated that a soft landing would still be feasible if (1) critical spacecraft propulsion system parameters were adjusted and (2) the spacecraft would perform in a very predictable manner during a terminal descent sequence that would be modified to minimize the required total vernier engine impulse. Two additional midcourse vernier firings (Nos. 5 and 6) were performed to optimize the vernier propulsion system parameters and to make final trajectory corrections (refer also to Section VII—Flight Path and Events). Vernier engine performance was smooth and spacecraft attitude was easily maintained during all the midcourse firings. By means of the last two firings, the weight of the remaining vernier propellant was reduced to a desired minimum. The purpose of this was to reduce the total spacecraft weight so that the main retro-motor impulse would decelerate the spacecraft to a much lower than normal velocity ( $\approx 100$  ft/sec instead of 400 to 500 ft/sec) at main retro burnout and to increase the helium ullage volume. The increased helium volume

**Table IV-6. Summary of vernier firings conducted on Surveyor V mission**

No.	Ignition time, GMT	Magnitude, m/sec	Duration, sec	Propellant used, lb	Purpose
1	(September 9, 1967) 01:45:02	14.0	14.25	11.6	Trajectory correction
2	02:12:02	9.91	10.05	8.2	Attempt to stop helium leak
3	02:39:50	22.6	23.05	18.8	Attempt to stop helium leak
4	04:18:48	12.8	$\left\{ \begin{array}{c} 12.0 \\ 0.5 \\ 0.5 \end{array} \right\}$	10.6	Trajectory correction and attempt to stop helium leak
5	08:24:02	32.4	33.0	26.8	Adjust propulsion system parameters
6	23:31:00	5.3	5.45	4.4	Final trajectory correction
7	(September 11, 1967) 00:44:51	—	111	58.4	Terminal descent
8	(September 13, 1967) 07:38:08	—	0.55	—	Lunar surface erosion experiment

assured that a maximum weight of helium would be retained for blowdown during terminal descent, since the last vernier midcourse firing was made prior to the time when helium tank pressure had dropped to the relief valve setting, which occurred about 10 hr before terminal descent. It had been determined that a minimum of 500 psia helium pressure was required to maintain vernier engine thrust.

**d. Coast phase performance.** Except for the helium leak and the special operations which were conducted for corrective and compensating purposes thereof, spacecraft performance during the transit phase was normal.

Solar panel power was slightly higher than predicted, and the battery energy level followed the programmed management curve very closely during the pre-midcourse coast phase. Thereafter, battery energy fell below the predicted curve because of the extra vernier firings and because unscheduled alpha scattering calibration data was gathered during transit. Nevertheless, battery energy remaining at touchdown was estimated to be an acceptable 1830 W-hr.

Performance of the thermal control system was also excellent, with no anomalies occurring during transit, and no problems due to the extra vernier engine firings.

Curves of temperature histories of spacecraft components during transit are contained in Appendix D.

Although the gyro drift rates were found to be within specification limits, many gyro drift checks were made during transit for accurate determination of gyro drift errors. The final gyro drift rates computed for compensation of the terminal maneuvers were +0.85 deg/hr roll, +0.60 deg/hr pitch, and -0.60 deg/hr yaw. In addition, about 6½ hr before terminal descent, a 360-deg yaw turn was made for the first time on a mission specifically to determine the precession torquing rate accuracy of the attitude control loop. The gyro precession rate was found to be within the accuracy required for the terminal maneuvers.

Telecommunications system performance was satisfactory throughout transit. During the initial coast phase prior to Canopus acquisition, down-link signal level via Omnantenna B was below nominal because of the inertially held roll attitude of the spacecraft. Therefore, down-link transmission was switched to Omnantenna A until the Canopus roll maneuver with satisfactory results. After Canopus acquisition, some deviation from predicted signal level was noted. However, the gyro drift checks account for some omni antenna gain variation which was not considered in making the predictions. Allowing for the gyro checks, Receiver B received signal level was about 4 to 5 db low; this characteristic has also occurred on previous flights.

**e. Terminal maneuver and descent performance.** The spacecraft properly executed the commanded terminal maneuvers (+73.9 deg roll and +119.5 deg yaw) which were initiated about 32 min before retro ignition. In order to limit printing errors, each maneuver was initiated when the respective attitude control loop error was near a null position.

The terminal descent sequence was modified by sending the following earth commands in order to minimize vernier engine total impulse requirements.

- (1) An unusually long delay time of 12.33 sec between automatic AMR 60-mile mark and vernier engine ignition was stored in the flight control programmer to delay the start of the main retro phase so that main retro burnout (and the beginning of the RADVS-controlled vernier phase) would occur at a lower altitude.
- (2) A vernier engine thrust level of 150 lb (instead of the 200 lb level used on previous missions) was

stored in flight control to increase the available burn time.

- (3) At carefully selected times during the descent sequence, earth-commands were sent overriding the flight control programmer to achieve retro ejection about 4 sec early, to restrict the period of time that the vernier engines would be commanded to the high-thrust level following main retro burnout, and to begin the RADVS-controlled phase earlier relative to main retro burnout so that sufficient time would be available for the spacecraft to acquire the programmed descent curve.

The descent sequence was initiated automatically by the 60-mile mark signal from the AMR. All the terminal descent events occurred very close to predicted times. A comparison between the premission nominal, preretro predicted, and actual event time intervals is shown in Fig. IV-8. Predicted and actual GMT times corresponding to the events are listed in Table IV-7. Spacecraft performance was very nearly as planned in all respects as indicated by the comparison of terminal descent parameters presented in Table IV-8. In particular, note the very close agreement between predicted and actual main retro burnout conditions, which were constrained between narrow limits on this mission (see Fig. VII-9, Section VII).

**Table IV-7. Predicted and actual terminal descent phase events (GMT September 11, 1967, at the spacecraft<sup>a</sup>)**

Event	Predicted <sup>b</sup>	Actual
AMR 60-mile mark	00:44:37.73	00:44:37.85
Vernier ignition	00:44:50.05	00:44:50.19
Main retro ignition	00:44:51.15	00:44:51.26
RADVS power on (warm up)		00:44:52
RADVS high voltage on		00:45:14
RODVS		00:45:23
RORA		00:45:24
Main retro burnout (3.5-g level)	00:45:30.43	00:45:30.12
Retro case eject (by earth command)	00:45:38.43	00:45:39.16
Vernier high thrust (by earth command)		00:45:39.7
Start RADVS control (by earth command)	00:45:40.43	00:45:41.16
Programmed descent segment acquisition	00:46:09.94	00:46:21.10
1000-ft mark	00:46:14.44	00:46:18.46
10-ft/sec mark	00:46:31.44	00:46:35.86
13-ft mark	00:46:37.44	00:46:41.46
Initial touchdown	00:46:39.14	00:46:43.05

<sup>a</sup> 1.234-sec RF delay time between spacecraft and DSIF stations.

<sup>b</sup> Based upon the final computer run of the Terminal Guidance Program completed approximately 3 hr before retro ignition.

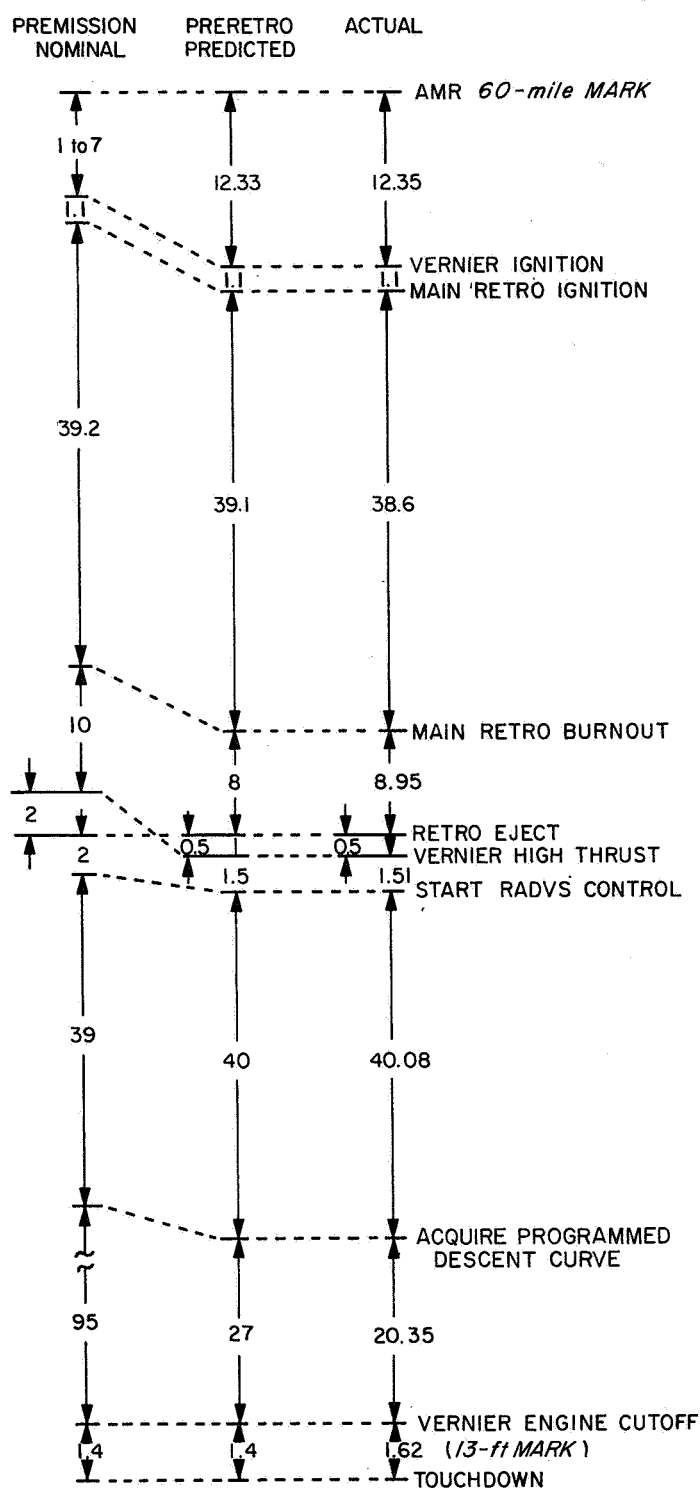


**Fig. IV-8. Comparison of nominal, predicted, and actual Surveyor V terminal descent event time intervals, sec (not to scale)**

Descent during the RADVS control phase until programmed descent contour interception and thence very

**Table IV-8. Predicted and actual values of terminal descent parameters**

Parameter	Predicted	Actual (best estimate)
<b>Main retro phase initial conditions</b>		
Altitude, ft	150,164	147,604
Velocity, ft/sec	8,485	8,487
<b>Main retro burnout conditions</b>		
Altitude, ft	4598	4139
Velocity, ft/sec	94	79.3
Flight path angle with lunar vertical, deg	-5.0	-35.67
<b>Programmed descent segment acquisition conditions</b>		
Slant range, ft	1500	806
Velocity, ft/sec	117	97
<b>Vernier engine cutoff conditions</b>		
Altitude, ft	12	14.5
Velocity, ft/sec	5	5.2
Flight path angle with lunar vertical, deg	-0.10	0.11
<b>Touchdown conditions</b>		
Longitudinal velocity, ft/sec	13	13.5
Lateral velocity, ft/sec	0	0.5
Spacecraft weight, lb		668
Roll attitude (spacecraft + X-axis relative to lunar north), deg clockwise	89.8	108.6
Surface slope, deg		17
<b>Postlanding conditions</b>		
Roll attitude (spacecraft + X-axis relative to lunar north), deg clockwise		114.5
Spacecraft tilt, deg		20

nearly along the contour is illustrated in Fig. IV-9. As expected, vernier engine thrust command saturation was indicated near the end of the descent sequence due to low propellant supply pressure. Helium tank pressure was only 575 lb at touchdown.

*f. Landing performance.* Initial touchdown occurred at 00:46:44.284 GMT on September 11, 1967, inside the edge of a small, 30-ft-diameter by 5-ft-deep crater. Leg 1 contacted first, followed by the almost simultaneous contacts of Legs 2 and 3. Having touched down on a slope of about 20 deg, the spacecraft slid along the surface approximately 30 in. while turning approximately 6 deg clockwise before coming to rest. The trench made by Leg 2 during the landing is illustrated in Fig. IV-10. The landed attitude of the spacecraft and topography of the crater in which it landed are shown in Fig. IV-11.

*g. Postlanding performance.* Engineering assessments revealed the postlanding condition of the spacecraft to

be excellent, with no damage having resulted from the landing.

The spacecraft performed extensive operations very successfully during the lunar day. Only near lunar noon was it necessary to place the spacecraft in a nonoperating mode for periods of time totalling about 28 hr. This condition is normally anticipated due to high temperatures, but was aggravated on this mission as a result of somewhat higher than expected spacecraft temperatures due to its landing in a crater.

After being unlocked following landing, the A/SPP responded normally to stepping commands. This permitted acquisition of the sun by the solar panel and the earth by the planar array, although these operations took longer than anticipated due to the large (but at that time unknown) tilt of the spacecraft. These are necessary operations to permit transmission of 600-line pictures and to obtain adequate power for continued lunar operation. The A/SPP continued to function properly throughout the lunar day when it was required to (1) reposition the solar panel as sun elevation changed, (2) change the panel shadow patterns for thermal control of critical components such as the camera, alpha scattering sensor head, and compartments, and (3) step the planar array for antenna pattern mapping and spacecraft attitude determination. The spacecraft attitude shown in Fig. IV-11 is based upon determinations made from postlanding planar array and solar panel positioning experiments.

The television camera was used extensively and provided excellent-quality pictures. The first television frames returned were 200-line pictures followed, after proper positioning of the A/SPP, by 600-line pictures. The television operations included wide- and narrow-angle panoramas, focus ranging, photometric sequences, star surveys, color surveys, shadow progressions, a solar corona sequence, and numerous special area sequences of the lunar surface and parts of the spacecraft. In addition, a television gain margin experiment was conducted in which signal strength was intentionally degraded in order to determine the point at which picture quality would be affected. Television pictures also provided data on the amount of lunar soil on the magnet attached to Footpad 2. Before spacecraft shutdown after the first lunar day, over 18,000 pictures had been returned, this being more than the combined total for the two previous successful missions. Only near the close of the lunar day did an electronic failure limit the capability to change camera focal length, focus, and filter wheel positions.

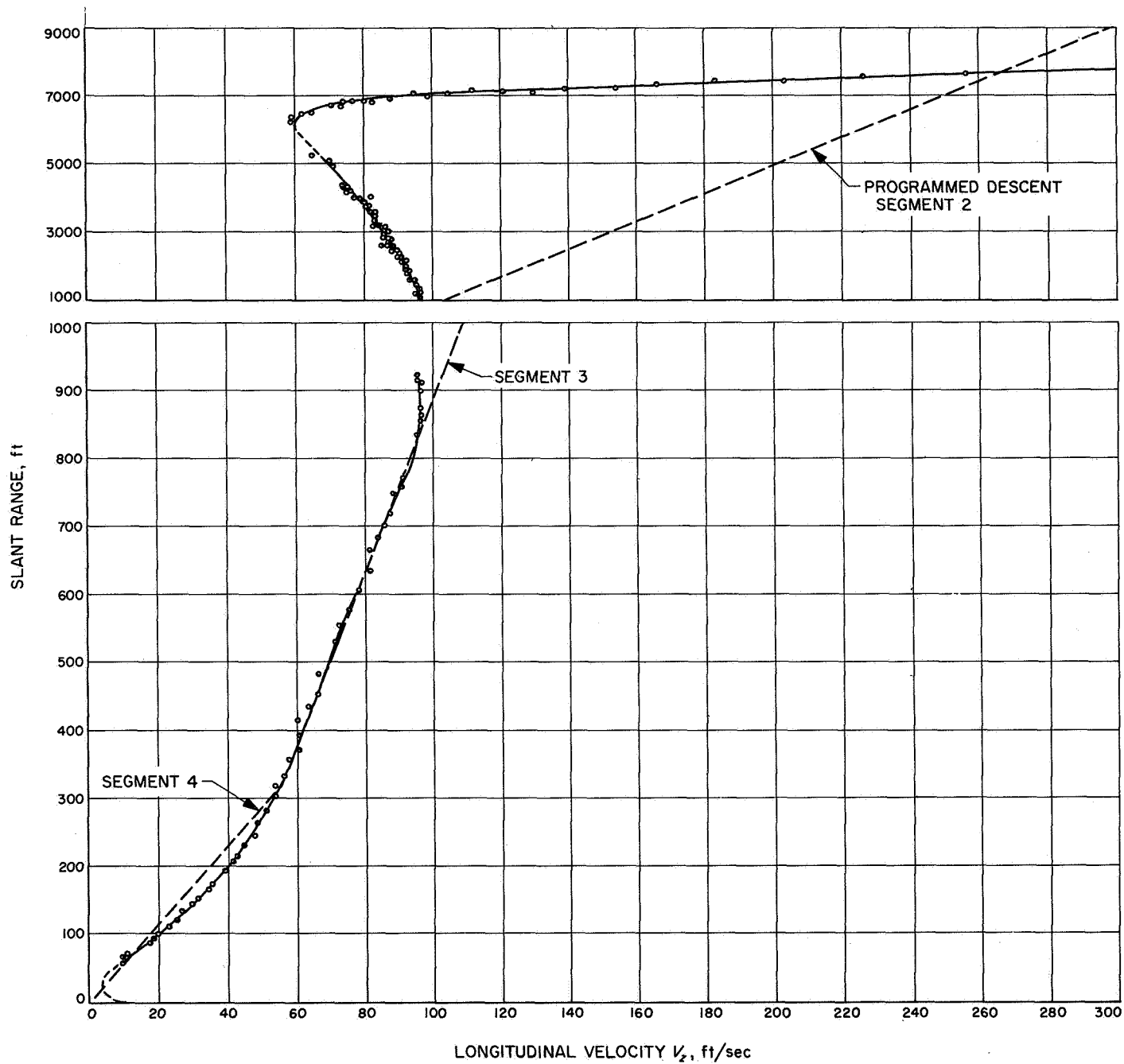


Fig. IV-9. Surveyor V descent profile



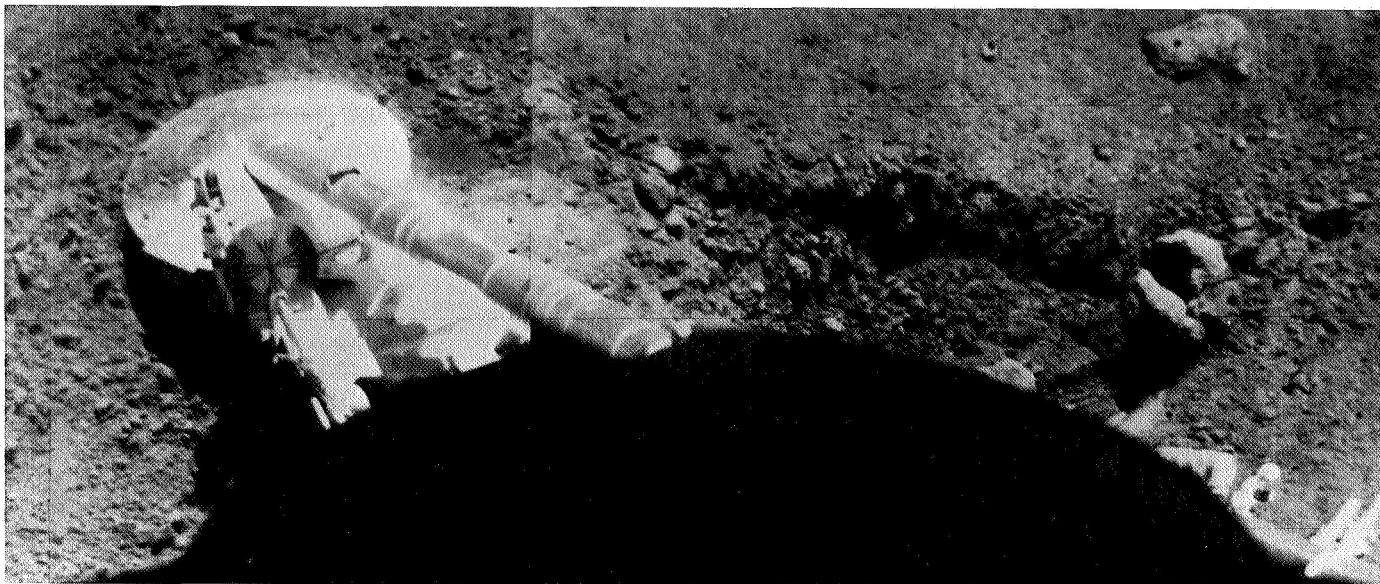


Fig. IV-10. Trench produced by Footpad 2 during landing (September 14, 1967, between 04:00 and 06:00 GMT, Catalog No. 5-MP-19)

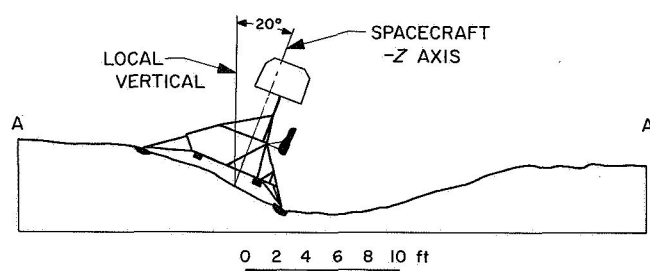
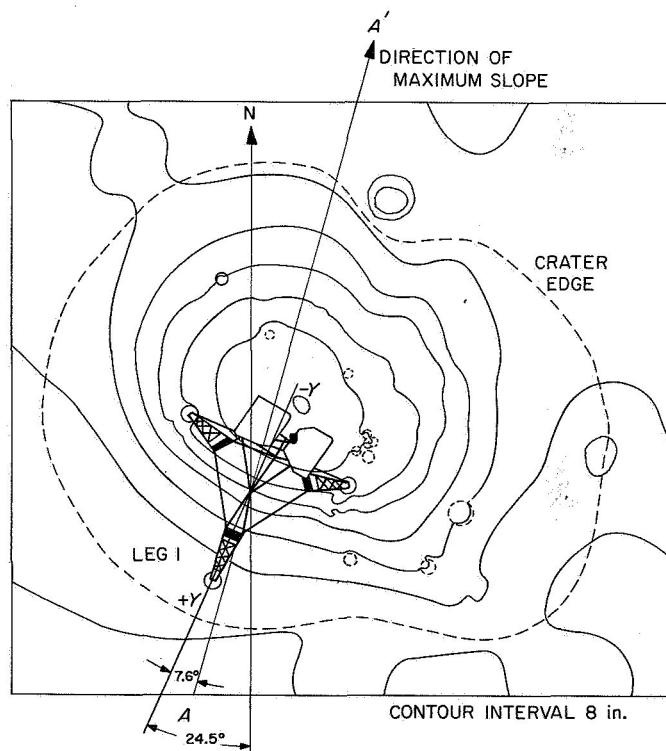


Fig. IV-11. Surveyor V landed attitude and local lunar topography

Approximately 53 hr after landing, a short (0.55-sec) vernier engine static firing was successfully performed. It is estimated that the thrust levels were about 24 lb for Engine 1, 17 lb for Engine 2, and 26 lb for Engine 3. This variation from the commanded value of about 30 lb was expected because the temperature limits for normal operation of the vernier propulsion system had been exceeded. Erosion of the lunar surface by the vernier engines was clearly evident in television pictures taken after the firing. The firing also caused the alpha scattering sensor head (which had been deployed to the surface) to move a few inches down the slope as shown in Fig. IV-12. In addition, a very slight increase in the spacecraft tilt (about 0.3 deg) was indicated by gyro data and confirmed by postfiring A/SPP attitude determinations. The firing also produced some effect on signal strength.

Later on in the lunar day, on separate occasions, pressure and temperature data indicated leaks had occurred in the oxidizer and fuel systems; this could be expected because of the high temperatures to which the systems were exposed over an extended period of time.

The alpha scattering instrument was also operated extensively to provide an abundance of useful data. About 1 hr of calibration data was obtained in the stowed posi-

tion before the sensor head was deployed outwardly to obtain data on background radiation in the lunar environment. Then, the sensor head was lowered to the surface for gathering of lunar back-scattering data. About 18 hr of alpha scattering data (Sample I) was obtained on the surface prior to the vernier static firing. After movement of the sensor head as a result of the firing, an additional 65 hr of data (Sample II) was obtained before the end of the first lunar day.

The spacecraft power subsystem performed perfectly after lunar landing and, by careful power management, the battery charge level was brought to a maximum of 163 A-hr before sunset, which is nearly the full charge condition. For operation during the lunar night, the spacecraft electronics contained in Compartment A and B must be maintained above a lower operating limit (approximately  $-10^{\circ}\text{F}$ ) to assure reliable operation. Battery capacity is not sufficient to offset heat losses from the compartments to the cold lunar environment and operate the spacecraft through the entire lunar night. However, the spacecraft was operated as long as possible in order to prevent the battery (located in Compartment A) from cooling to too low a temperature after shutdown. The spacecraft was finally shut down 115 hr after sunset when the remaining battery charge was estimated to be 45 A-hr.

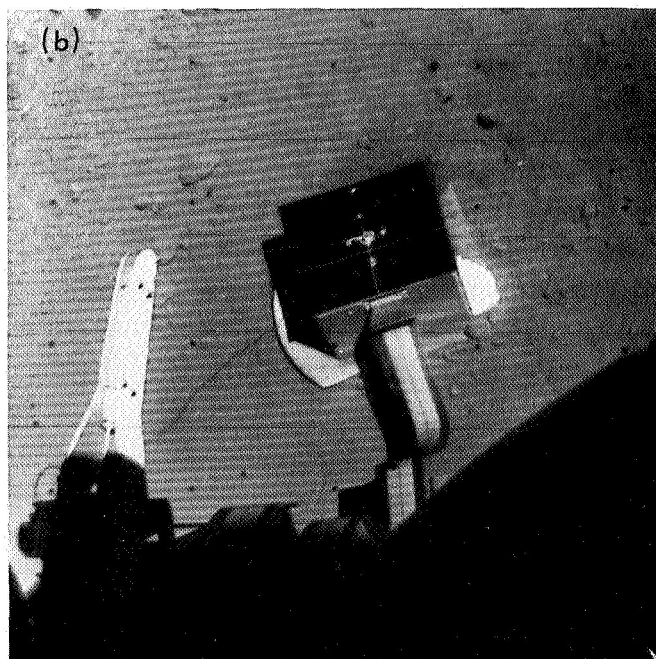
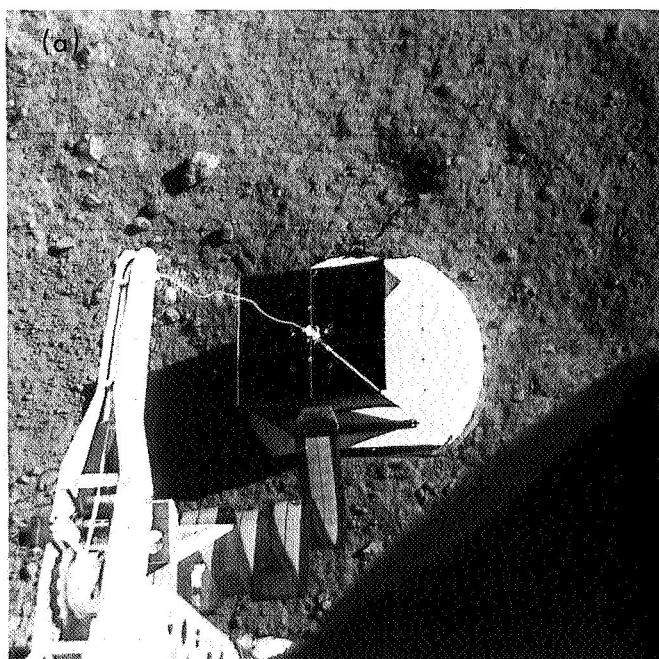


Fig. IV-12. Alpha scattering instrument sensor head positions on lunar surface  
(a) before and (b) after vernier static firing

About 147 hr after sunrise during the second lunar day, the spacecraft responded immediately to the first turn-on command at 08:07:34 on October 15, 1967. The spacecraft condition was determined to be fairly good, permitting a resumption of operations which included the gathering of additional alpha scattering data and the taking of more pictures in both the 200- and 600-line modes. Though picture quality was poor because of a suspected amplifier anomaly, the pictures were still useful for scientific and engineering evaluation. The camera focus, filter, and focal length controls, which had malfunctioned near the close of the first lunar day, were found to be operating satisfactorily. It was determined that the spacecraft should again be operated as long as possible into the lunar night in the hope that it could survive for yet another lunar day.

## B. Structures and Mechanisms

The structure and mechanisms subsystem provides support, alignment, thermal protection, electrical interconnection, mechanical actuation, and touchdown shock absorption and vehicle stabilization for the spacecraft and its components. The subsystem includes the basic spaceframe, landing gear mechanism, crushable blocks, omnidirectional antenna mechanisms, antenna/solar panel positioner (A/SPP), pyrotechnic devices, electronic packaging and cabling, thermal compartments, thermal switches, and separation sensing and arming device.

### 1. Spaceframe and Substructure

The spaceframe, constructed of thin-wall aluminum tubing, is the basic structure of the spacecraft. The landing legs and crushable blocks, the retrorocket engine, the *Centaur* interconnect structure, the vernier propulsion engines and tanks, and the A/SPP attach directly to the spaceframe. Substructures are used to provide attachment between the spaceframe and the following subsystems: the thermal compartments, TV, alpha scattering instrument, RADVS antennas, omniantennas, flight control sensor group, attitude control nitrogen tank, and the vernier system helium tank.

During the *Surveyor V* mission, there was no indication of any failures or anomalies attributable to structural malfunctions.

### 2. Landing Gear Subsystem

The landing gear subsystem consists of three landing leg assemblies and three crushable honeycomb blocks attached to the spaceframe (Fig. IV-13). Each leg assembly is made up of a tubular inverted tripod structure with a shock absorber, an A-frame, a lock strut, and a honeycomb footpad.

During launch, the legs are folded for stowage under the shroud. Shortly before spacecraft separation, upon command from the *Centaur* programmer, the legs are

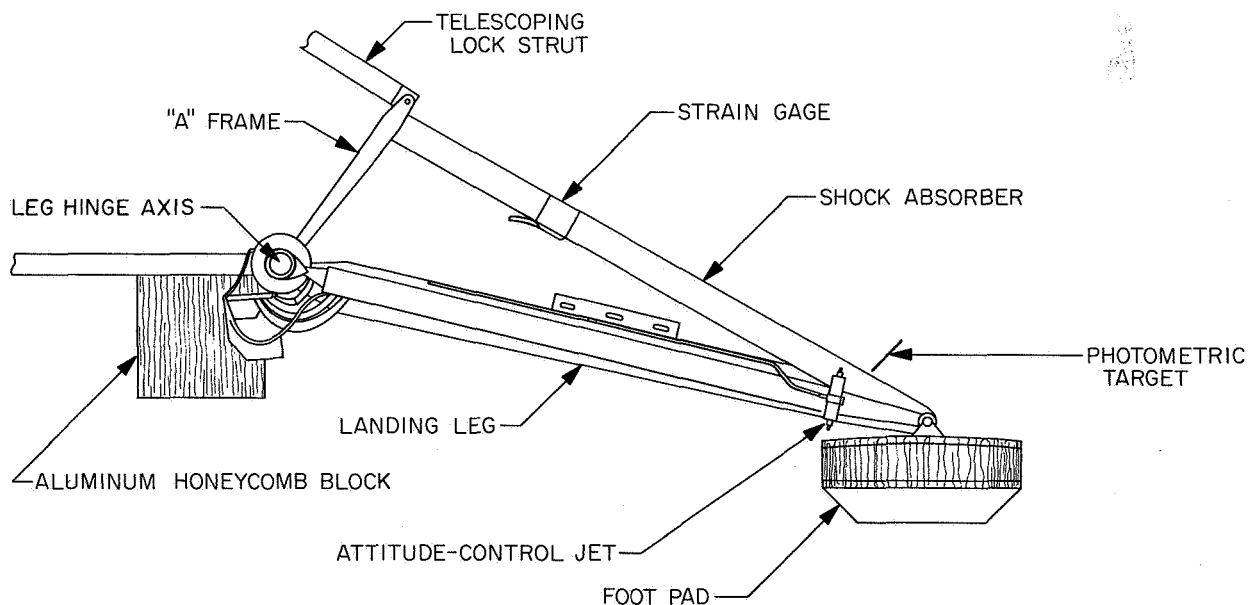


Fig. IV-13. Landing leg assembly

released by squib-actuated pin pullers and motion is initiated by a leaf-type kickout spring located near the respective release pin pullers. Torsion springs at each hinge axis continue the movement to the fully deployed positions, where they are automatically locked.

Upon landing, each leg pivots about its hinge axis. Landing loads are absorbed by compression of the upper member of the tripod, which is a combined shock absorber and spring assembly. The shock absorber columns are instrumented with strain gages. Axial loads measured by the strain gages are telemetered to provide continuous analog traces during the terminal descent and touchdown phase.

For a vertical landing on a hard, level surface at a velocity in excess of about 8.5 ft/sec, the crushable blocks will contact the surface. Energy will then be further dissipated through penetration of the surface by the blocks or by crushing of the blocks if the surface bearing strength exceeds 40 psi. Crushing of the honeycomb footpads is not expected for landing velocities below about 11.5 ft/sec or for surface bearing strength less than about 10 psi.

On the *Surveyor V* mission, shock absorbers identical to the type used on *Surveyors III* and *IV* were installed. This type of shock absorber provides the landing gear subsystem with a better controlled damping characteristic as well as a higher load carrying capability than did the *Surveyor I* and *II* design.

The performance of the landing gear subsystem on the *Surveyor V* mission was as expected; it was very satisfactory in every respect. The legs were deployed in response to a command from the *Centaur*, and all three were locked in the landing position as indicated by telemetry. Figure IV-14 shows the strain gage force histories of the three shock absorbers throughout the landing phase. The peak axial force in the shock absorbers and times of initial impact of the footpads are given in Table IV-9. The forces are considered accurate within  $\pm 80$  lb, the times within  $\pm 2$  msec.

An evaluation of the data in Table IV-9, together with other engineering telemetry and postlanding video data, has resulted in the following reconstruction of events during the landing sequence: The 10-ft/sec descent velocity *mark* signal was generated 7.21 sec prior to initial ground contact when the spacecraft was at an altitude

**Table IV-9. Maximum axial forces in the shock absorbers and times of initial ground impact of footpads**

	Leg 1	Leg 2	Leg 3
Maximum shock absorber force, lb	1240	1650	1660
Time of initial footpad impact, GMT (September 11, 1967)	00:46:44.284	00:46:44.474	00:46:44.481

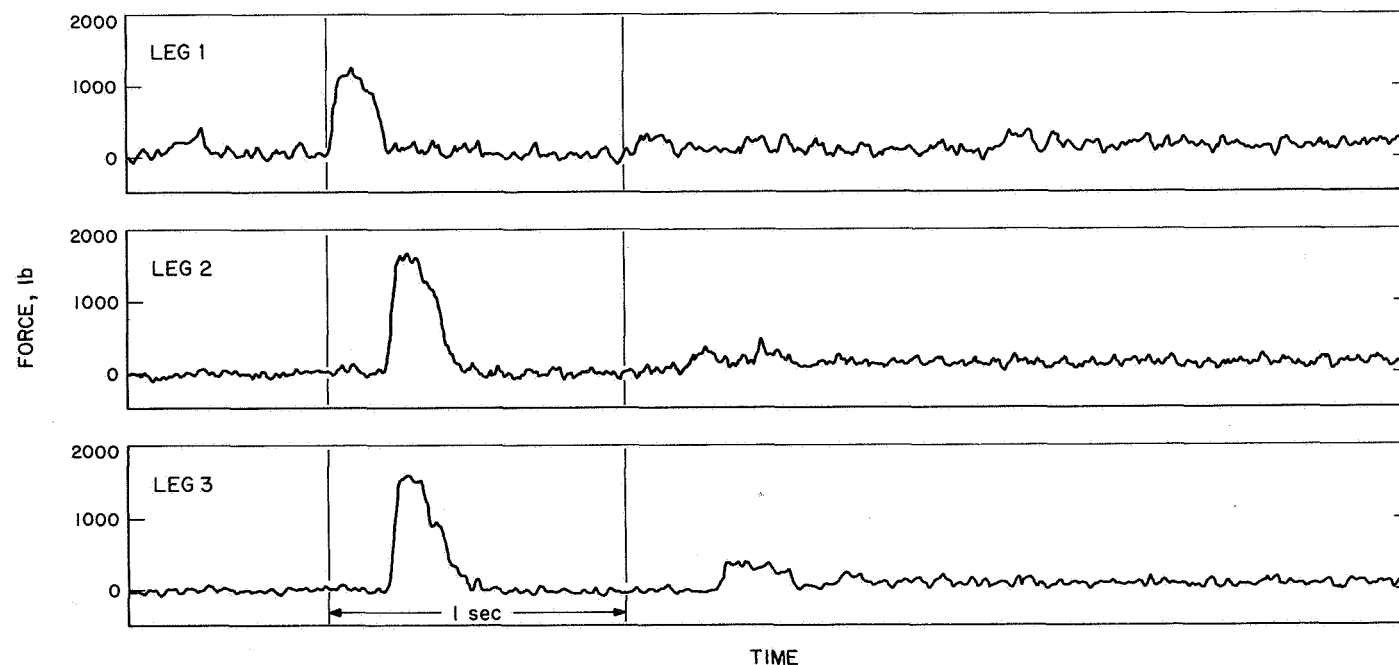


**Fig. IV-14. Loads on spacecraft shock absorbers during landing**

of  $51 \pm 4$  ft. Immediately following this mark, the spacecraft was slowed to a constant descent velocity of  $5.4 \pm 1.5$  ft/sec (nominal:  $5.0 \pm 1.5$ ), which was maintained until the 13-ft altitude mark was generated 1.62 sec before initial touchdown, at an altitude of  $15.7 \pm 2.4$  ft (nominal:  $13 \pm 4.5$ ). At this time, all three vernier engines were cut off, resulting in a free-fall period, during which time the spacecraft vertical velocity component increased to  $13.9 \pm 1.4$  ft/sec (nominal:  $12.6 \pm 2.4$ ) until Leg 1 first contacted the lunar surface. Angular spacecraft motions during the constant-velocity descent were very small; at engine cutoff, slight angular rates were induced which increased to the following values just prior to initial contact with the lunar surface:  $+0.7$  deg/sec in pitch;  $+0.5$  deg/sec in yaw; and  $-0.4$  deg/sec in roll.

Following Leg 1 impact, the spacecraft experienced a sharp negative pitch motion with a rate higher than 13 deg/sec (the gyro range was exceeded), accompanied by little roll and yaw until approximately 200 msec later, when Legs 2 and 3 impacted almost simultaneously. A "slideout" period of approximately 1.7-sec duration followed, during which the spacecraft traveled  $32 \pm 2$  in. along the surface in the direction opposite to Leg 1, while turning approximately  $+5.9$  deg about the roll axis and less than 1 deg about the yaw axis.

The shock absorber force histories exhibit an initial high force period of approximately 0.25-sec duration (very similar to those of *Surveyor I*), followed by a 0.6- to 0.8-sec-long zero-force reading. This reading indicated that the spacecraft rebounded slightly, raising the footpads by 3 to 5 in. from their initial impact positions.

The relative timing of the leg impacts indicates an angle of approximately 17 deg between the plane containing the three footpad pivot points at the time of Leg 1 contact and the plane determined by the three footpad imprints. The spacecraft was determined to have a pitch angle of approximately  $-20$  deg in the final resting position. Hence, the spacecraft flight path angle at first touchdown is estimated to have been between 0 and  $-3$  deg in pitch. Accordingly, the horizontal spacecraft velocity is estimated to have been between 0 and 1.5 ft/sec in the minus Y-direction (opposite to Leg 1).

The shock absorbers were not locked after landing, in order to permit shock absorption capability in the event that a vernier engine firing experiment should be performed. A vernier firing was later conducted successfully. Commands were sent to lock the shock absorbers about 31 hr before sunset. However, at least two of the

three legs were not locked in response to these commands, and the spacecraft was found to be resting on its crushable blocks at the end of the first lunar day. Sagging of the spacecraft may have been due to leakage of helium gas from the cylinder of the shock absorbers, compression of the helium and shrinkage of the hydraulic fluid due to cooling near sunset, or a combination of these factors. During the second lunar day, the spacecraft was found to have returned to very nearly the same attitude that it had before sagging of the shock absorbers. The cause of the sagging is now under investigation.

### 3. Omnidirectional Antennas

The omnidirectional antennas are mounted on the ends of folding booms hinged to the spaceframe. Pins retain the booms in the stowed position during launch. Squib-actuated pin pullers release the booms upon command from the *Centaur* shortly before spacecraft separation. A leaf-type kickout spring on each omniantenna boom initiates movement. Torsion springs continue the movement to the fully deployed positions, where the booms are automatically locked. On the *Surveyor V* spacecraft, Omniantenna B was painted black to reduce television picture glare. The paint had little or no effect on the thermal control of the spacecraft.

The omniantenna booms were extended by *Centaur* command, and both antennas were locked in the landing or transit position as indicated by telemetry.

### 4. Antenna and Solar Panel Positioner (A/SPP)

The A/SPP supports and positions the high-gain planar array antenna and solar panel. The A/SPP has four axes of rotation: roll, polar, solar, and elevation (Fig. IV-15). Stepping motors rotate the axes in either direction in response to ground commands or during automatic deployment following *Centaur*/spacecraft separation. This permits orienting the planar array antenna toward the earth and the solar panel toward the sun. Each ground command gives approximately  $\frac{1}{8}$  deg of rotation about the roll, solar, and elevation axes and approximately  $\frac{1}{15}$  deg about the polar axis.

The solar axis is locked with the solar panel in a vertical position for stowage in the nose fairing. After spacecraft separation from the *Centaur*, the roll and solar axes are repositioned and locked such that the planar array is parallel to Leg 1, and the solar panel is perpendicular to the A/SPP mast. The A/SPP remains locked in this position until after touchdown, at which time the roll, solar, and elevation axes can be released in any order desired

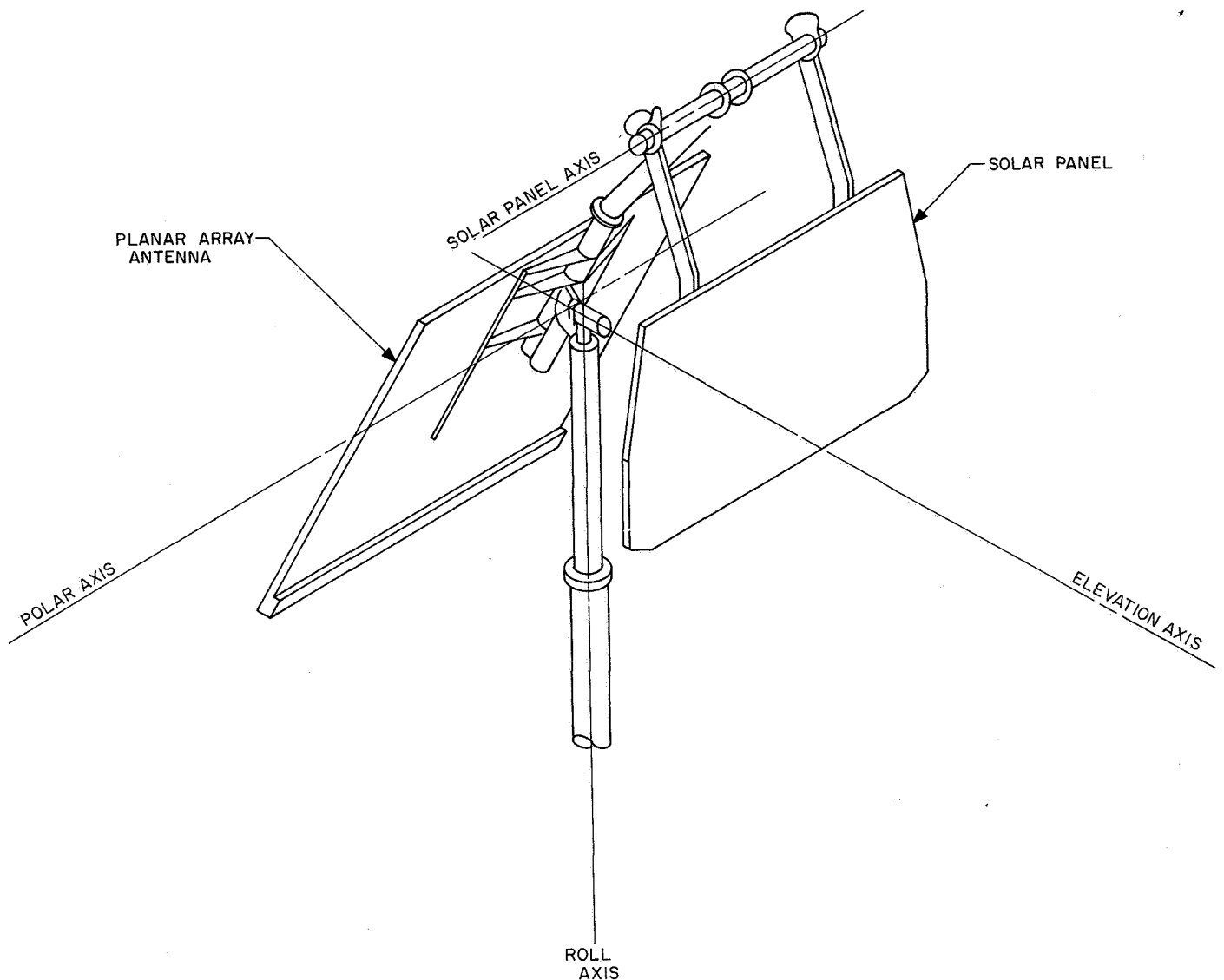


**Fig. IV-15. Antenna/solar panel configuration**

to reposition the A/SPP for solar panel acquisition of the sun and planar array acquisition of the earth. Following initial acquisition, the A/SPP is stepped periodically during the lunar day to maintain desired solar panel and planar array positioning relative to the sun and earth. Data from potentiometers on each axis can be used to determine spacecraft lunar orientation.

The A/SPP was redesigned for *Surveyor V* to increase the structural and operational margins and to incorporate new high-torque stepping motors.

After the *Surveyor V* spacecraft separated from the *Centaur*, the A/SPP operated as expected during the auto-deploy sequence, and the roll and solar axes relocked.

After touchdown, the following nonstandard earth command sequence was used to acquire the sun and earth and to determine the spacecraft attitude. The roll-axis pin puller was fired (the solar and elevation axes were left locked for later accurate attitude determination). A first attempt was made to acquire the earth by moving the roll and polar axes and comparing the observed planar array antenna gain with the known antenna pattern. This initial attempt to acquire the earth was abandoned owing to interference between the solar panel and the TV camera hood. With the solar and elevation axes still locked, the roll and polar axes were used to orient the solar panel toward the sun, using solar panel power and sun sensor signals as means of lock on. This was accomplished to an accuracy of  $\pm 2$  deg. The sun was

acquired almost 30 deg in azimuth away from its predicted position, indicating that the spacecraft was on a slope and not level. This information reduced the earth uncertainty, and the planar array was stepped along an earth-search arc which increased the antenna gain to within 2 db of the predicted value. A crude tilt estimate of 18 deg was calculated at this point.

Later, the A/SPP was also used to make more accurate attitude determinations in the following manner: The A/SPP was stepped to obtain a precise sun sighting with the secondary sun sensor. After firing the solar axis pin pullers to preclude possible solar panel/TV interference, a precise earth sighting was obtained by stepping the planar array slowly through the earth position in two orthogonal A/SPP axes and observing potentiometer positions corresponding to maximum DSIF received signal strength. The potentiometer readings were then used in a computer program to obtain an accurate attitude determination.

Throughout the lunar day, the A/SPP stepping efficiency appeared to be 100%. During lunar noon, the temperature of the planar array reached a maximum of 296°F, which is 16° above the predicted maximum. The A/SPP was not commanded at this time. The number of degrees of movement of each axis at the end of the first lunar day (September 24) were: solar, 543; polar, 370; elevation, 143; and roll, 1210.

## 5. Thermal Compartments

Three thermal compartments (A, B, and C) house the thermally sensitive spacecraft electronic equipment. Compartment C, which was added for *Surveyor V*, is an insulated and heated box that houses the additional electronics needed to operate the data system associated with the alpha scattering instrument. The main Compartments A and B contain the components identified in Table IV-10. These components are arranged on thermal trays which distribute heat from the electronic components throughout the compartments.

Each main compartment contains a thermal control and heater assembly to maintain the temperature of the thermal tray above a specified temperature (above 40°F for Compartment A and above 0°F for Compartment B). The thermal control and heater assembly is capable of automatic operation, or may be turned on or off by earth command.

Each main compartment employs thermal switches (nine in Compartment A and six in Compartment B)

**Table IV-10. Thermal compartment component installation**

Compartment A	Compartment B
Receivers (2)	Central command decoder
Transmitters (2)	Boost regulator
Battery	Central signal processor
Battery charge regulator	Signal processing auxiliary
Engineering mechanisms auxiliary	Engineering signal processor
Television auxiliary	Low data rate auxiliary
Thermal control and heater assembly	Thermal control and heater assembly
Auxiliary battery control	Auxiliary engineering signal processor

which are capable of varying the thermal conductance between the inner compartment and the external radiating surface. The thermal switches maintain thermal tray temperature below +125°F. Like the switches used on *Surveyor IV*, the switches used on *Surveyor V* were set to open at  $35 \pm 10^\circ\text{F}$ .

An insulating blanket consisting of 75 sheets of 0.25-mil-thick aluminized mylar is installed between the inner structure and the outer protective cover of each of the main compartments. The thermal blankets and protective covers for Compartments A and B were redesigned for *Surveyor V* and are now made in two pieces. One piece covers the back and bottom of the compartment; the other piece covers the top, ends, and front. The redesign provides easy access to the electronic components during all phases of systems checkout and much simpler final compartment installation. The blanket for Compartment A was also redesigned to allow cable access into the electronics during STV tests.

## 6. Thermal Switch

The thermal switch is a thermal-mechanical device which varies the conductive path between an external radiation surface and the top of the equipment tray of each compartment (Fig. IV-16). The switch has two contact surfaces which are ground to within one wavelength of being optically flat. One surface is coated with a conforming substance to form an intimate contact with the mating surface. To reduce the contact sticking condition experienced on the *Surveyor I* and *III* missions, the coating surface, which consists of a room-temperature-curing (RTV) silicone compound, is vacuum-baked at 300°F to drive off the volatiles. The coating surface is also charged with molybdenum disulfide, which serves as a parting agent. These processes increase the opening reliability of the thermal switches significantly above that



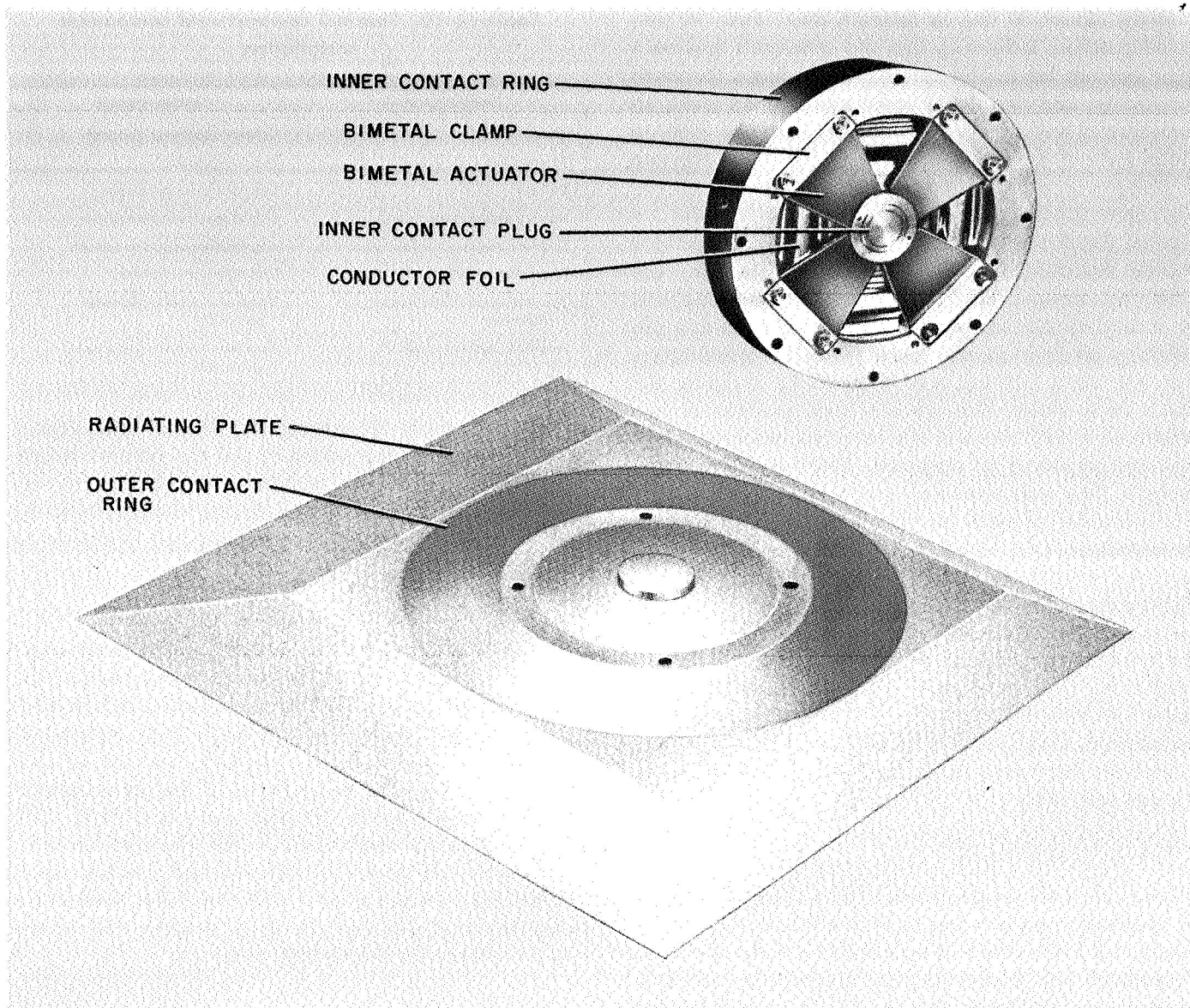


Fig. IV-16. Thermal switch

of the switches used on *Surveyors I* through *III*. Actuation of the thermal switch is accomplished by four bi-metallic elements located at the base of the switch. These elements are connected mechanically to the top of the compartment so that switch actuation is controlled by compartment temperature.

The external radiator surface is such that it absorbs only 12% of the solar energy incident on it and radiates 74% of the heat energy conducted to its surface. When the switch is closed and the compartment is hot, the switch loses its heat energy to space. When the compartment gets cold, the switch contacts are designed to open about

0.020 in., thereby opening the heat-conductive path to the radiator and thus reducing the heat loss through the switch to almost zero. Four Compartment A and three Compartment B switches are instrumented with temperature sensors attached to the radiators. The temperature sensors provide an indication of switch actuation for those switches which are monitored.

On the *Surveyor V* mission, the thermal switches were closed during flight and kept the electronics at or below the maximum allowable temperature at all times. All the thermal switches also remained closed during the lunar day after landing.



The cooling rate of the compartments shortly after sunset indicated that most of the switches were open. Four of the thermal switches on Compartment A and two on Compartment B were instrumented so that their opening temperatures could be determined. One of the Compartment B switches did not open until the temperature reached 20°F; another opened at -5°F, and it appeared that a third Compartment B switch had still not opened by the time of spacecraft shutdown during the lunar night, although the heaters had kept Compartment B very close to 0°F in the interim period. There is a question about the possibility that one uninstrumented Compartment A switch remained closed well into the lunar night, but the spacecraft conditions are not known well enough to verify that this did occur.

## 7. Pyrotechnic Devices

The pyrotechnic devices installed on *Surveyor V* are listed in Table IV-11. All the squibs used in these devices are electrically initiated, hot-bridgewire, gas-generating devices. Qualification tests for flight squibs included demonstration of reliability at a firing current level of 4 or 4.5 A. "No fire" tests were conducted at a 1-A or 1-W level for 5 min. Electrical power required to initiate pyrotechnic devices is furnished by the spacecraft main battery. Power distribution is through 19.0- and 9.5-A constant-current generators in the engineering mechanism auxiliary (EMA).

All the taper pin assemblies associated with the A/SPP pin pullers were changed for this mission. They were all made heavier in conjunction with the A/SPP redesign, which was required in order to obtain a positive struc-

tural margin. The basic operating characteristics of the pin pullers were not changed, although the axial degree of freedom of the pins used to lock the solar axis during launch was limited to keep them from backing out because of vibration during the launch phase of the flight.

Except for the shock absorber locks, all pyrotechnic devices functioned normally upon command. Mechanical operation of the squib-actuated locks, valves, switches, and pins was indicated on telemetry signals as part of the spacecraft engineering measurement data.

The shock absorber lock pins were not fired at the normal time in order to maintain the capability to fire the vernier engines. The command to fire the locks was transmitted near the end of the lunar day when some of the component temperatures had dropped below the design operating levels. The low temperatures may have affected the squib firing capability. However, the reliability history of the squibs indicates they would have fired. Therefore, it is indicated that the squibs may not have received the command or that the command signal was not of adequate energy to fire the squibs.

## 8. Electronic Packaging and Cabling

The electronic assemblies provide mechanical support for electronic components in order to insure proper operation throughout the various environmental conditions to which they are exposed during a mission. The assemblies (or control items) are constructed utilizing sheet metal structure, sandwich-type etched circuit board chassis with two-sided circuitry, plated-through holes, and/or

Table IV-11. Pyrotechnic devices

Type	Location and use	Quantity of devices	Quantity of squibs	Command source
Pin pullers	Lock and release Omnantennas A and B	2	2	Centaur programmer
Pin pullers	Lock and release landing legs	3	3	Centaur programmer
Pin pullers	Lock and release planar antenna and solar panel	7	7	Separation sensing and arming device and ground station
Pin puller	Lock and release Vernier Engine 1	1	1	DSIF station
Pin pullers	Apha scatter unlatch and lower mechanism	2	2	DSIF station
Separation nuts	Retro rocket attach and release	3	6	Flight control subsystem
Valve	Helium gas release and dump	1	2	DSIF station
Pyrotechnic switches	EMA Board 4, RADVS power on and off	4	4	DSIF station and flight control subsystem
Initiator squibs	Safe-and-arm assembly retromotor initiators	1	2	Flight control subsystem
Locking plungers	Landing leg, shock absorber locks	3	3	DSIF station
		27	32	

bifurcated terminals. In general, each control item consists of only a single functional subsystem and is located either in or out of the three thermally controlled compartments, depending on the temperature sensitivity of the particular subsystem. Electrical interconnection is accomplished primarily through the main spacecraft harness. The cabling system utilizes lightweight, minimum-bulk, and abrasion-resistant wire which is constructed of extruded teflon with a dip coating of modified polyamide.

### C. Thermal Control

The thermal control subsystem is designed to provide acceptable thermal environments for all components during all phases of spacecraft operation. Spacecraft items with close temperature tolerances were grouped together in thermally controlled compartments. Those items with wide temperature tolerances were thermally decoupled from the compartments. The thermal design fits the "basic bus" concept in that the design was conceived to require minimum thermal design changes between missions. Monitoring of the performance of the spacecraft thermal design is provided by engineering temperature sensors which are distributed throughout the spacecraft. On the *Surveyor V* spacecraft, 76 temperature sensors were located within the subsystems as follows:

Flight control	9
Mechanisms	3
Radar	6
Electrical power	4
Transmitters	2
Television	4
Vehicle structure	27
Propulsion	19
Alpha scattering instrument	2

The spacecraft thermal control subsystem is designed to function in the space environment, both in transit and on the lunar surface. Extremes in the environment as well as mission requirements on various components of the spacecraft have led to a variety of methods of thermal control. The spacecraft thermal control design is based upon the absorption, generation, conduction, and radiation of heat.

The radiative properties of the external surfaces of major items are controlled by using paints, by polishing, and by using various other surface treatments. Reflecting

mirrors are used to direct sunlight to certain components. In cases where the required radiative isolation cannot be achieved by surface finishes or treatments, the major item is covered with an insulating blanket composed of multiple-sheet aluminized mylar. This type of thermal control is called "passive" control.

The major items whose survival or operating temperature requirements cannot be achieved by surface finishing or insulation alone use heaters that are located within the unit. These heaters can be operated by external command, thermostatic actuation, or both. The thermal control design of those units using auxiliary heaters also includes the use of surface finishing and insulating blankets to optimize heater effectiveness and to minimize the electrical energy required. Heaters are considered "active control."

Items of electronic equipment whose temperature requirements cannot be met by the above techniques are located in thermally controlled compartments. Each of the main compartments (A and B) is enclosed by a shell covering the bottom and four sides and contains a structural tray on which the electronic equipment is mounted. The top of each compartment is equipped with a number of temperature-actuated switches (nine in Compartment A and six in Compartment B). These switches, which are attached to the top of the tray, vary the thermal conductance between the tray and the outer radiator surfaces, thereby varying the heat-dissipation capability of the compartments. When the tray temperature increases, heat transfer across the switch increases. During the lunar night, the switch opens, decreasing the conductance between the tray and the radiators to a very low value in order to conserve heat. When dissipation of heat from the electronic equipment is not sufficient to maintain the required minimum tray temperature, a heater on the tray supplies the necessary heat. The switches are considered "semiaactive."

Examples of units which are controlled by active, semi-active, or passive means are shown in Fig. IV-17.

The thermal control surface of the nitrogen tank was modified for *Surveyor V* to compensate for increased shadowing by Compartment C, which was added in order to contain the alpha scattering instrument electronics. Black paint was applied to most of the upper outboard quadrant to increase solar absorption, and aluminum foil was placed over the upper inboard quadrant to reduce emissivity of that area.

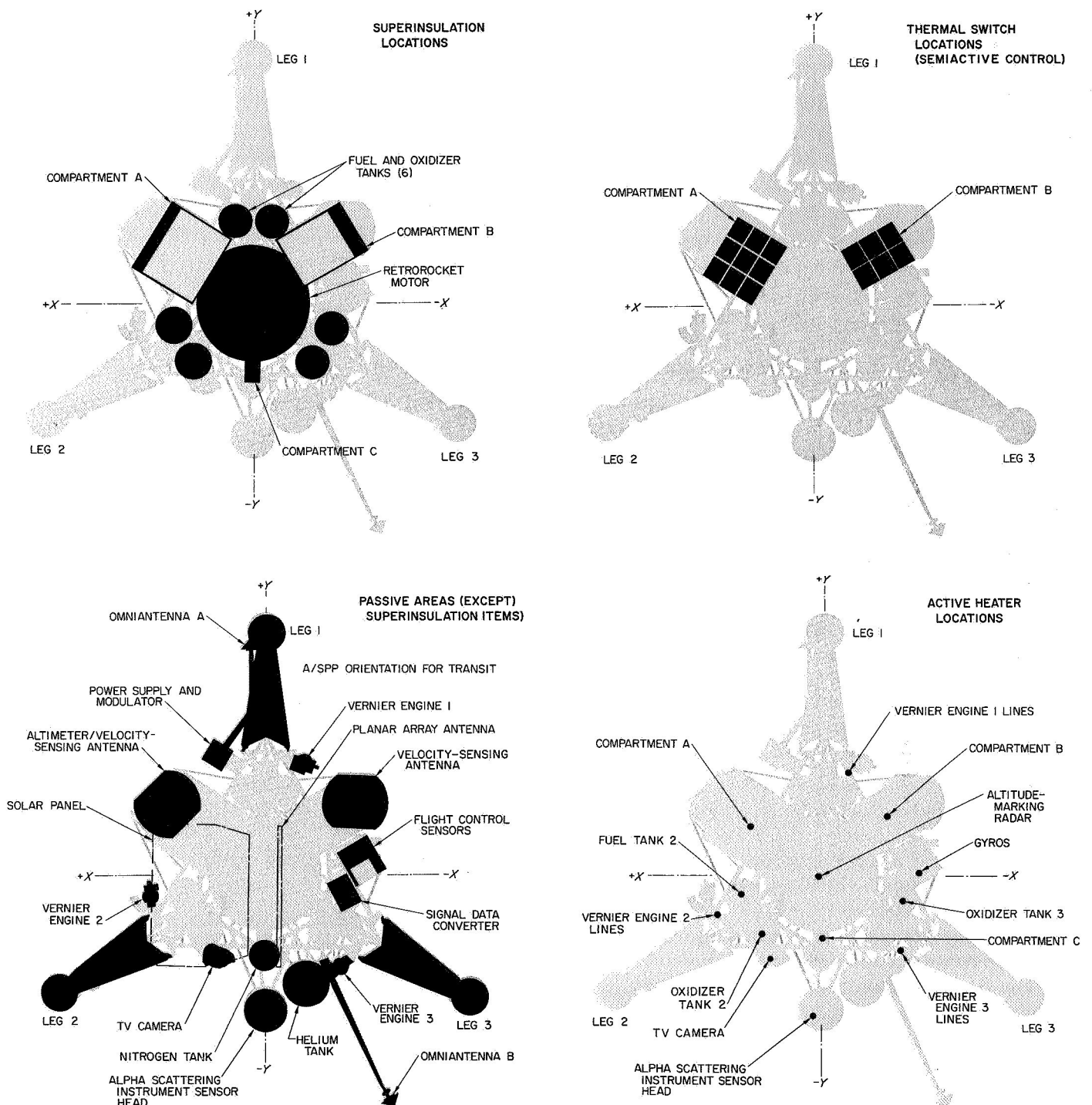


Fig. IV-17. Thermal design

A few paint pattern changes were also made to *Surveyor V* to reduce TV picture glare by limiting reflected sunlight. A black stripe was painted on Legs 2 and 3 on the top quadrant of the tubes adjacent to the TV camera. Also, the boom for Omnantenna B was painted black instead of white, but the cone of the antenna was left white as on previous spacecraft. Footpads 2 and 3 of *Surveyor V* also had the gray and white stripes which were first introduced on *Surveyor IV*. Some difference in temperature for these components was expected, but no detectable change occurred.

*Surveyor V* did not experience any thermal anomalies during the transit phase of flight. The several vernier propulsion system firings following the initial midcourse maneuver did not create any major problems in the thermal control subsystem. Plots of transit temperatures are contained in Figs. D-1 through D-8 of Appendix D.

After *Surveyor V* landed, the temperatures of most components were higher than expected. The increased temperatures were due to the spacecraft tilt of about 20 deg inside a small crater. This orientation and environment resulted in increased view factors of most components to the lunar surface. Among the critical spacecraft temperatures affected by the increased temperatures were the alpha scattering sensor head temperature, which increased more rapidly than expected in the stowed and background positions, and the vernier propulsion system temperatures, which were important parameters for satisfactory performance of a postlanding vernier firing. Post landing temperatures for the first and second lunar day are plotted in Figs. D-9 through D-11 of Appendix D.

After sunset, in accordance with an established operating plan designed to maximize the chance for spacecraft survival of the lunar night, Compartments A and B were allowed to cool to 20 and  $-15^{\circ}\text{F}$ , respectively. All thermal switches apparently opened except for one on Compartment B. The compartments were maintained at approximately these temperatures by use of heaters and by power dissipation from operation of electronics within the compartments. The rates of heat loss from Compartments A and B during this period were calculated to be 8.5 W and 10.9 W, respectively. Of the Compartment B loss, 3.8 W is attributed to the stuck switch. The predicted heat loss rates were  $12.0 \pm 3$  W for Compartment A and  $9.0 \pm 3$  W for Compartment B with no switches closed.

Figure IV-18 shows estimates of the compartment temperature profiles between the time of spacecraft shut-

down, about 115 hr after sunset, and resumption of spacecraft operations about 147 hr after sunrise on the second lunar day. The predicted minimum battery temperature was  $-180^{\circ}\text{F}$ . These curves are based on *Surveyor I* data and *Surveyor V* first lunar night data.

## D. Electrical Power

The electrical power subsystem is designed to store, convert, and distribute electrical energy. The power subsystem for *Surveyor V* was redesigned to provide better matching characteristics between power sources and power conditioning units. By this means, a number of improvements were introduced into the subsystem which increased the capability, reliability, and overall power performance.

### 1. Power Subsystem Description

A block diagram of the subsystem as redesigned for *Surveyor V* is shown in Fig. IV-19.

The spacecraft system derives its energy from two sources, a spacecraft battery and a solar panel which converts solar radiation energy to electrical energy. The spacecraft battery is a secondary or rechargeable battery. An auxiliary battery, which was part of the battery system on previous spacecraft, was eliminated from the *Surveyor V* system. This was possible because the efficiency of the power subsystem was increased so that the main battery was capable of meeting the power storage requirements of the spacecraft for the *Surveyor* missions beginning with *Surveyor V*. Deletion of the auxiliary battery made it possible also to eliminate the auxiliary battery control, which had been used for selection of the battery operation modes on previous missions.

Several changes made in the solar panel design for *Surveyor V* account for most of the increased efficiency and improved performance of the subsystem. A new series-parallel cell arrangement was used to obtain maximum power output at  $30.5 \pm 2$  V during transit. By this arrangement open circuit voltage of the solar panel was reduced, ranging from 65 V after sunrise on the lunar surface to 32 V at lunar noon. Previous solar panel open circuit voltage ranged from 100 to 50 V for the above conditions. Flat-cell rather than shingle-cell mounting has been incorporated, thus providing more uniform bonding of the cells to the substrate for better performance over a wider temperature range.

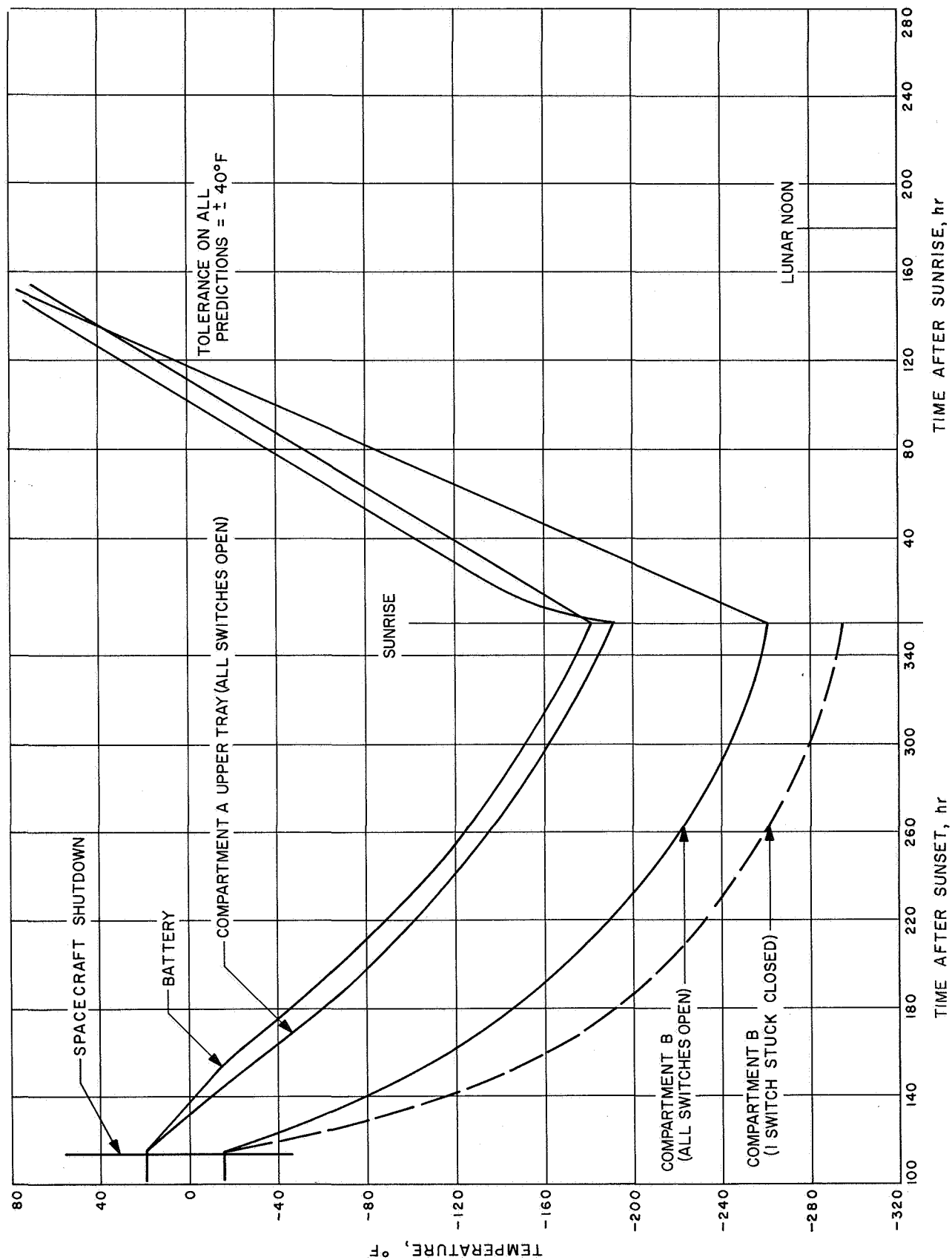
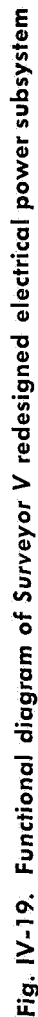


Fig. IV-18. Predicted Surveyor V temperature response after shutdown during first lunar night



**Fig. IV-19. Functional diagram of Surveyor V redesigned electrical power subsystem**

The solar panel changes have made possible the use of a simplified battery charge regulator (BCR). The optimum charge regulator (OCR) has been replaced by a solar panel transistor switch which increases the BCR efficiency and reduces power dissipation in Compartment A by 16 W. The OCR was used to track the volt/ampere characteristic curve of the solar panel and control the output for maximum power. The lower output voltage of the redesigned solar panel permits switching of the solar panel directly to: (1) the 30-V preregulated bus in the boost regulator (BR) during transit, or (2) the 22-V unregulated bus during lunar operations, when the temperature is higher and the solar panel voltage is lower. The power subsystem is in its most efficient mode of operation when the solar panel is connected to the 30-V preregulated bus. This mode of operation was not possible in the previous design. The unregulated bus is used for charging of the battery and for distribution of current from the BCR and battery to the unregulated spacecraft loads and the BR. The voltage on the unregulated bus can vary between 17.5 and 27.5 V, with a nominal value of 22 V. The BCR also has an *off* mode in which the solar panel is left floating. The *off* mode can result from earth command or automatically if the battery voltage exceeds 27.3 V or battery pressure exceeds 65 psia. The automatic turn-off feature of the BCR can be enabled or disabled by earth command.

The BR converter boosts the unregulated bus voltage, the output of which is used by the BR preregulator to supply 30 V to the preregulator bus. The essential loads are fed by the preregulated bus through a series diode which drops the preregulated bus voltage to the essential bus voltage of 29 V. The preregulator bus also feeds the flight control regulator and the nonessential regulator, which in turn feed the flight control and nonessential buses, respectively. These regulators can be turned on and off by earth commands. The nonessential regulator has a *bypass* mode which is used to connect the preregulated bus directly to the nonessential bus if the nonessential regulator fails.

The BR operates at higher efficiency as a result of the BCR changes. The higher efficiency is especially pronounced during transit because all the regulator current does not have to pass through the preregulator. In addition, a shunt regulator has been connected between the preregulated bus and the battery to supply excess solar panel current to the battery and prevent excess solar panel voltage when the spacecraft current demands are low during transit. In the previous design, the shunt output was connected to battery ground so that no battery charg-

ing was possible. Other changes in the BR include the use of higher-gain transistors in the electronic conversion unit of the preregulator for increased efficiency, the addition of a sensing resistor for added protection by providing for nonessential regulator turnoff if an overload (8-A) condition occurs, a reduction in the overload trip circuit (OTC) trip time from a 20- to 120-msec range to  $40 \pm 20$  msec, and the internal mounting of the BR bus filter.

In the redesigned power subsystem, the maximum battery storage capacity is 180 A-hr. The battery provides about 2000 W-hr during transit, the balance of the energy being supplied by the solar panel. Even though the auxiliary battery was eliminated and spacecraft power requirements were increased for *Surveyor V*, the nominal expected battery energy remaining at touchdown was increased from approximately 1000 W-hr to approximately 2000 W-hr.

## 2. Power Subsystem Performance

Performance of the electrical power subsystem was very satisfactory during the transit and postlanding phases of the *Surveyor V* mission. Expected and actual values of several power system parameters during the transit phase are presented in Table IV-12. The battery energy at liftoff was 3608 W-hr (165 A-hr), which was the predicted nominal value. Following solar panel deployment after spacecraft separation, solar panel voltage was 30.3 V, with a current of 2.53 A. The BCR was connected to the preregulated bus and remained in that position until after touchdown. The solar panel switch tripped out automatically due to high bus voltage about 6 hr after liftoff, coincident with transmission of a commutator change command. About 4 min later, the *solar panel on* command was transmitted and the switch stayed on. During the next 8 hr, the switch tripped out 10 more

Table IV-12. Electrical power performance during transit

Parameter	Time period	Predicted	Actual
Battery energy, A-hr	Liftoff	165	165
	Touchdown	100	83
Average solar panel power, W	Coast phases	84	85
Average BCR output current, A	Coast phases	2.56	2.79
BCR efficiency, %	Coast phases	94.6	94.6
Regulated loads, A	High power	3.3	3.1
	Low power	80.5	80
BR efficiency, %	High power		86

times. This was normal operation of the BCR over-voltage-protection circuit resulting from battery charging during periods of minimum heater loads, and had been predicted from results of spacecraft tests conducted in a solar-thermal-vacuum chamber. Average solar panel current was 2.84 A at an average of 30.0 V during transit. Average BCR output current during the coast phase was 2.79 A compared to 2.56 A predicted. Although the BCR efficiency is not measured directly in flight, it was estimated to be close to the expected value of 94.6%. During high-power operation, the regulated loads were 3.1 A vs the predicted value of 3.3 A. The BR efficiency for low- and high-power modes was 80% and 86%, respectively.

The average battery discharge current was 0.21 A during the first coast period; this was approximately 0.2 A lower than predicted because of higher than anticipated solar panel output. Battery temperature ranged from 83°F prior to midcourse, and battery pressure remained low, never exceeding 15.6 psia during the entire transit phase. The battery charge level followed the predicted profile closely during the first coast period until midcourse correction, as illustrated in Fig. IV-20. After the midcourse correction, however, the battery energy level fell below

the predicted curve, owing to the special vernier engine firings, which were conducted as a result of the helium leak, and calibration of the alpha scattering instrument, which had not been planned during transit. Battery energy remaining at touchdown was estimated to be 1830 W-hr (83 A-hr).

After touchdown, the power subsystem continued to perform satisfactorily. The two requirements imposed on the power system during lunar day operations are (1) to supply the power demands to perform the engineering and scientific operations, and (2) to recharge the battery to assure a fully charged battery prior to lunar sunset.

At touchdown, the solar panel output was still connected to the preregulated bus. Approximately 19 hr after touchdown, the solar panel output was switched to the unregulated bus for charging of the battery, and the spacecraft remained in that configuration when the spacecraft was shut down during the lunar night.

The spacecraft regulated power requirements to support postlanding operations, including alpha scattering

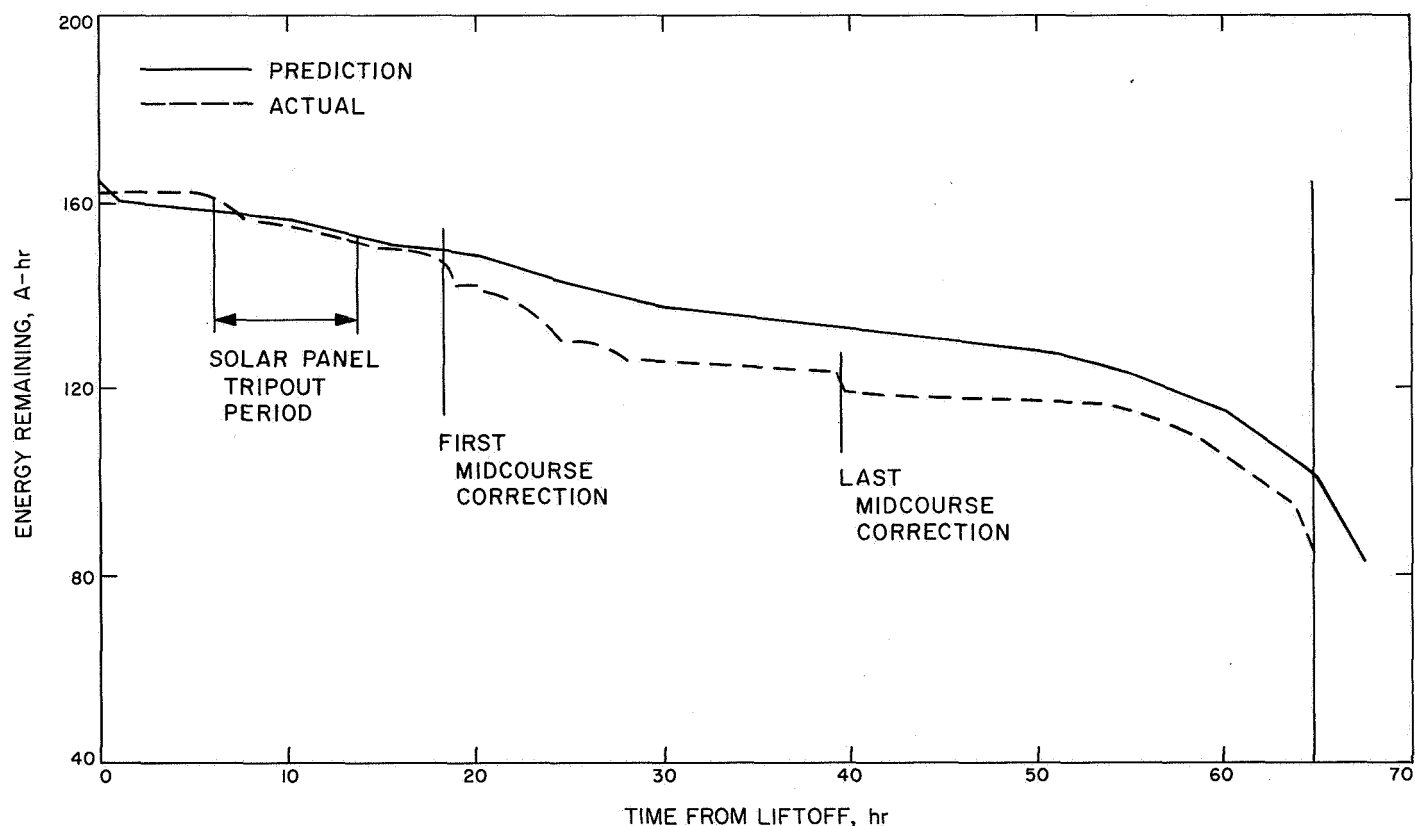


Fig. IV-20. Battery energy profile during transit



instrument and television camera operation, are shown in Fig. IV-21.

Solar panel performance continued to be satisfactory during the lunar day. In addition to supplying power to

the spacecraft for lunar operations, the solar panel was utilized to shade the compartments and TV camera in order to provide a comfortable environment for the electronics. Figure IV-22 shows the solar panel/sun angle (the angle between the plane of the solar panel and the

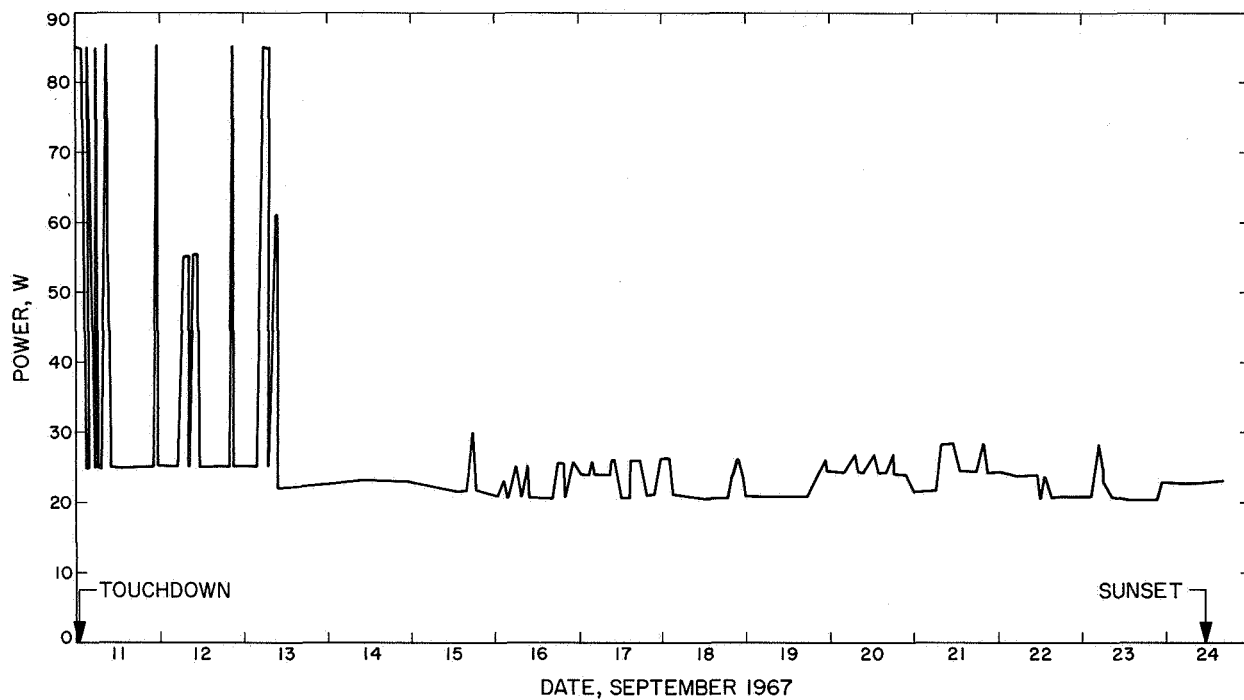


Fig. IV-21. Postlanding regulated power requirement

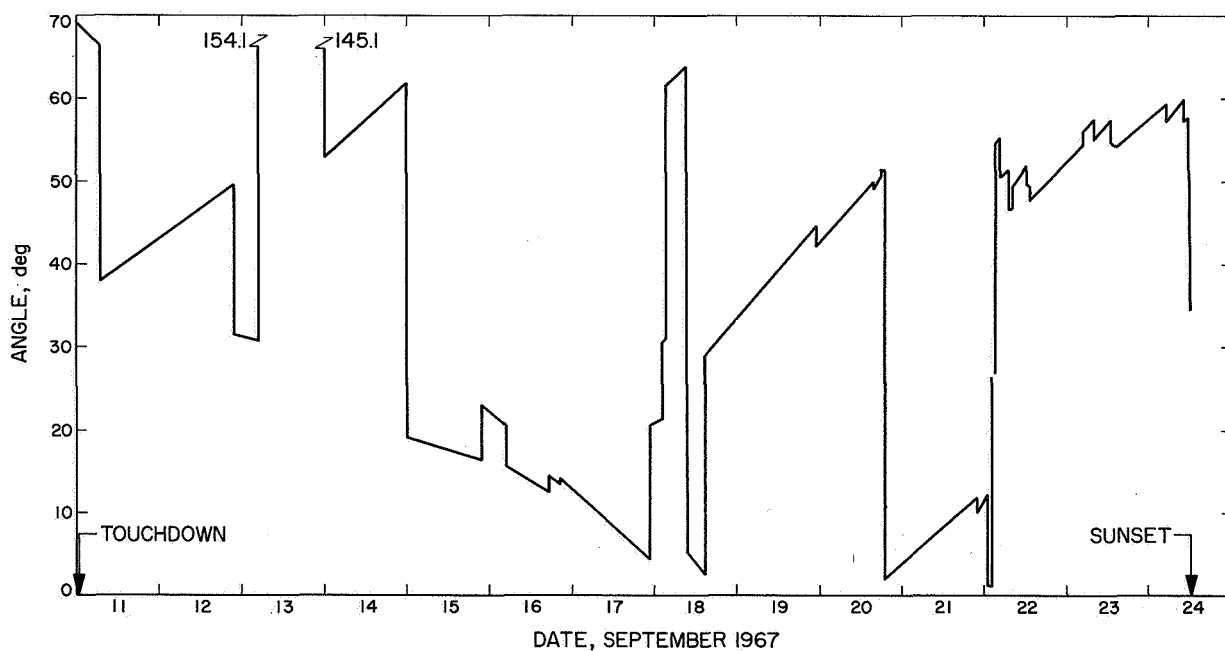


Fig. IV-22. Solar panel/sun angle during lunar day

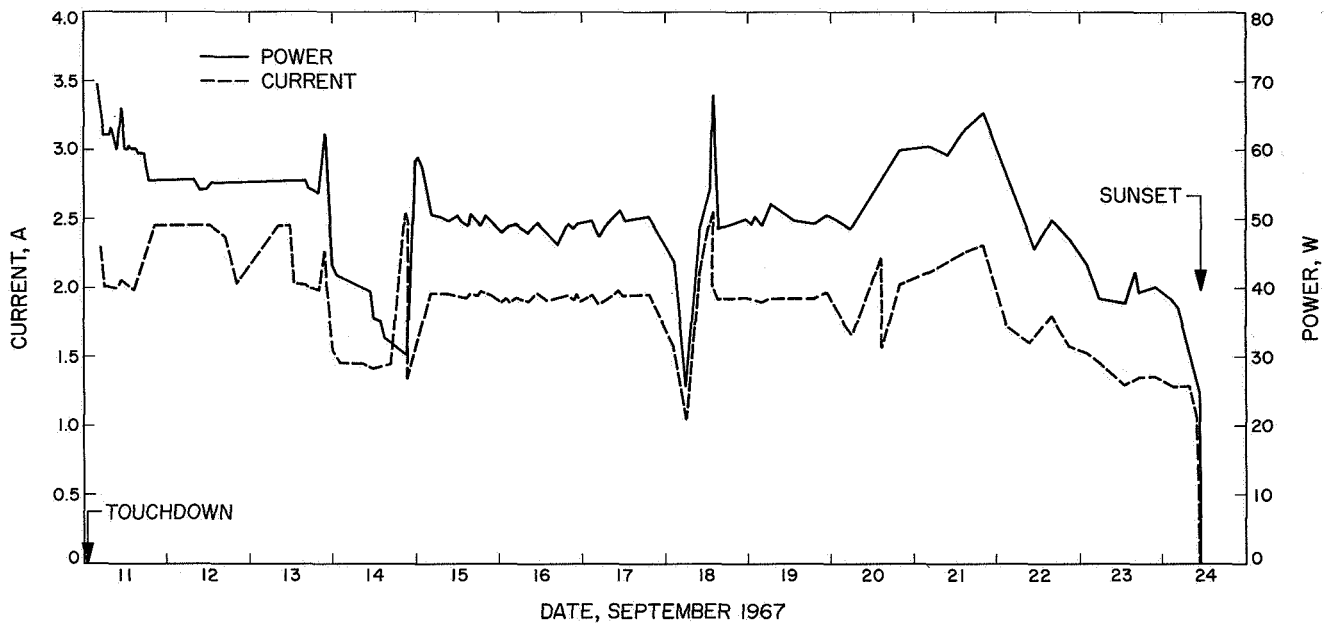


Fig. IV-23. Solar panel output characteristics during lunar day

sun direction) during the lunar day. The solar panel/sun angle varied from 65 to 5 deg, reducing the output of the panel current to a maximum of 2.55 A. Figure IV-23 shows the solar panel current and the calculated power output of the panel during the lunar day.

Battery performance during the first lunar day is shown in Fig. IV-24. The battery reached a maximum charge of 163 A-hr before sundown.

The prime consideration during lunar night operation was to spend the battery energy wisely in order to accomplish the following:

- (1) Maintain the battery temperature at  $+20^{\circ}\text{F}$  as long as possible by dissipating power in Compartment A until the battery was depleted to 45 A-hr. The 45-A-hr limit was determined from the results of lunar night survival tests. It represented (1) the energy storage level necessary to supply the spacecraft constant load requirements during cooldown and warmup of the battery to and from the temperature at which it would cease to provide power (zero-volt level), and (2) the minimum energy level necessary to prevent cell reversal.
- (2) Prevent the battery temperature from dropping below  $-175^{\circ}\text{F}$ . In tests performed at JPL, three batteries survived after exposure to a simulated lunar night environment at a temperature of  $-175^{\circ}\text{F}$ .

The *Surveyor V* spacecraft battery did survive the lunar night and appeared to be in good condition upon reawakening the second lunar day.

## E. Propulsion

The propulsion subsystem supplies thrust force during the midcourse correction and terminal descent phases of the mission. The propulsion subsystem consists of a vernier engine system and a solid-propellant main retro-rocket motor. The propulsion subsystem is controlled by the flight control system through preprogrammed maneuvers, commands from earth, and maneuvers initiated by flight control sensor signals.

### 1. Vernier Propulsion

The vernier propulsion subsystem supplies the thrust forces for midcourse maneuver velocity vector correction, attitude control during main retrorocket motor burning, and velocity vector and attitude control during terminal descent.

*a. Vernier propulsion description.* The vernier engine system consists of three thrust chamber assemblies and a propellant feed system, as shown in the schematic of Fig. IV-25. The feed system is composed of three fuel tanks, three oxidizer tanks, a high-pressure helium tank, propellant lines, and valves for system arming, operation, and deactivation.

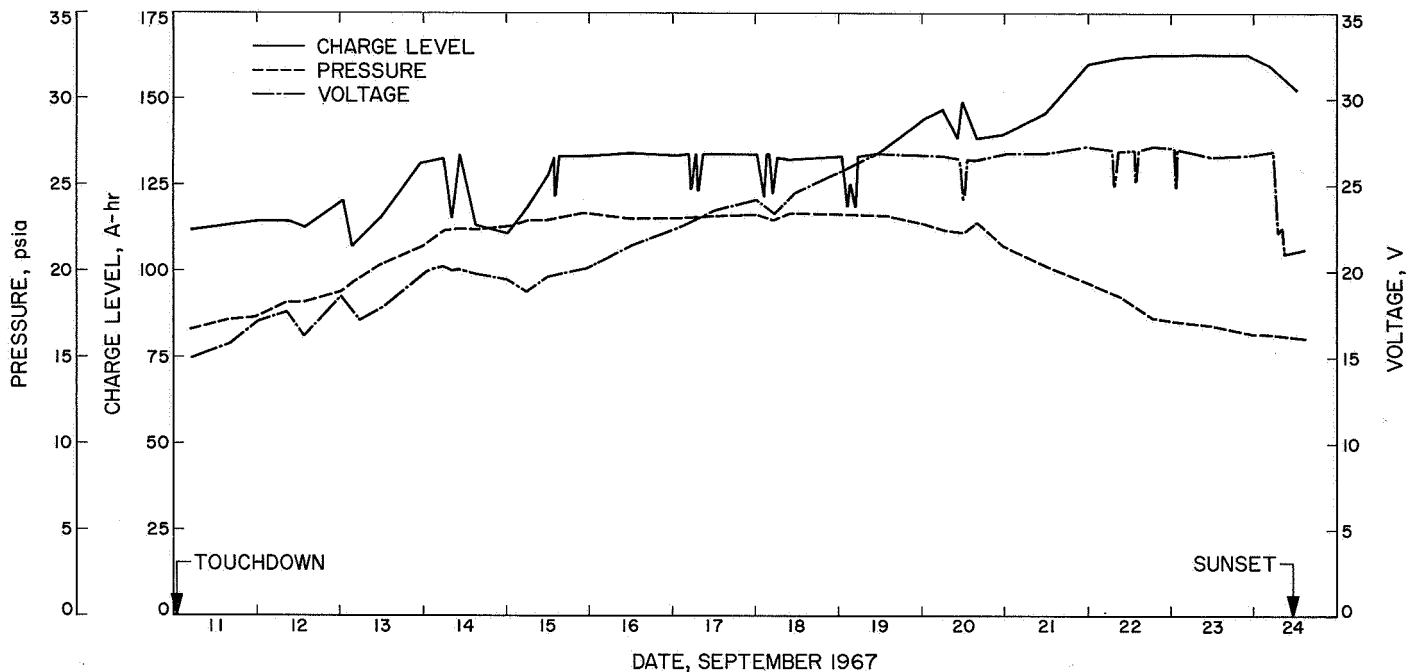


Fig. IV-24. Battery performance during lunar day

Fuel and oxidizer are contained in six tanks of equal volume, with one pair of tanks for each engine. Each tank contains a teflon expulsion bladder to permit complete and positive expulsion and to assure positive control under zero-*g* conditions. The oxidizer is nitrogen tetroxide ( $N_2O_4$ ) with 10% by weight nitric oxide (NO) to depress the freezing point. The fuel is monomethyl hydrazine monohydrate ( $MMH \cdot H_2O$ ). Fuel and oxidizer ignite hypergolically when mixed in the thrust chamber. The total minimum usable propellant load is 178.3 lb. The arrangement of the tanks on the spaceframe is illustrated in Fig. IV-26. Propellant freezing or overheating is prevented by a combination of active and passive thermal controls, utilizing surface coatings, multilayered blankets, and electrical and solar heating. The propellant tanks are thermally isolated to insure that the spacecraft structure will not function as a heat source or heat sink.

Propellant tank pressurization is provided by the helium tank and high-pressure valves assembly (Fig. IV-27). The high-pressure helium is released to the propellant tanks by activating a squib-actuated helium release valve. A single-stage regulator maintains the propellant tanks at a nominal working pressure of about 730 psi.\* Helium check and relief valves are located in a separate package

on the spaceframe and are connected by a single line to the helium tank and high-pressure valves assembly. This represents a slight modification of the system used on previous missions (*Surveyor I* through *IV*) in which the low-pressure valves were mounted directly on the high-pressure valves assembly. On the *Surveyor V* system, a filter was also added to the inlet part of each relief valve to protect against contamination. The check valves allow the flow of pressurizing helium to the propellant tanks but prevent the back flow of helium and propellant vapors from the propellant tanks to the pressure regulator or between fuel and oxidizer tanks. Helium relief valves relieve excess pressure from the propellant tanks in the event of a helium pressure regulator malfunction (such as occurred on this mission).

The thrust chambers (Fig. IV-28) are located near the hinge points of the three landing legs on the bottom of the main spaceframe. The moment arm of each engine is about 38 in. Engine 1 can be rotated  $\pm 6$  deg about an axis in the spacecraft *X-Y* plane for spacecraft roll control. The Engine 1 roll actuator is unlocked by the same command that actuates the helium release valve. Engines 2 and 3 are not movable. The thrust of each engine (which is monitored by strain gages installed on each engine mounting bracket) can be throttled over a range of 30 to 104 lb. The specific impulse varies slightly with engine thrust.

\*Specification requirements are: operating pressure, 700 to 755 psi; regulator lockup pressure, 795 psi maximum.

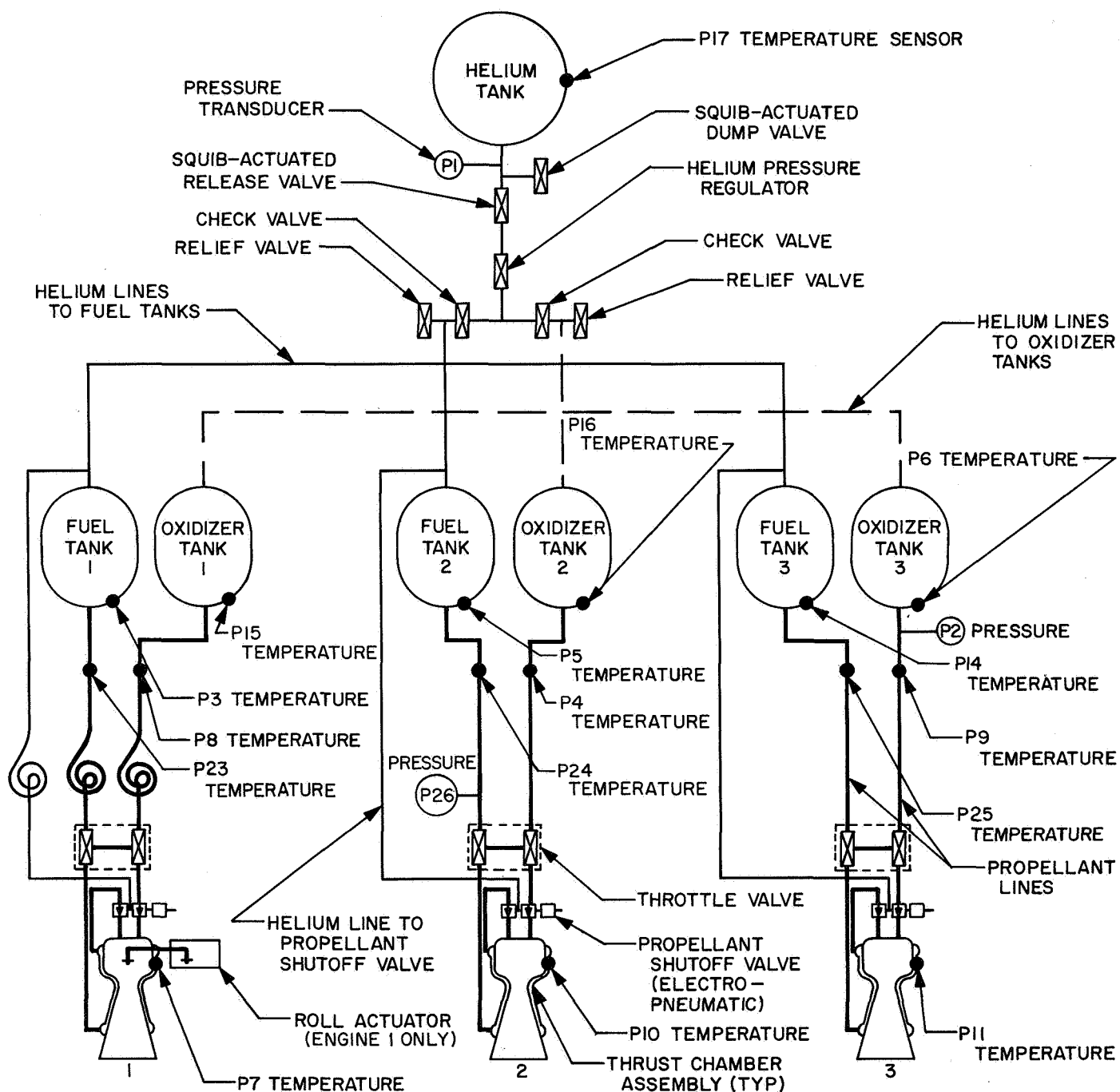


Fig. IV-25. Vernier propulsion system schematic including locations of pressure and temperature sensors

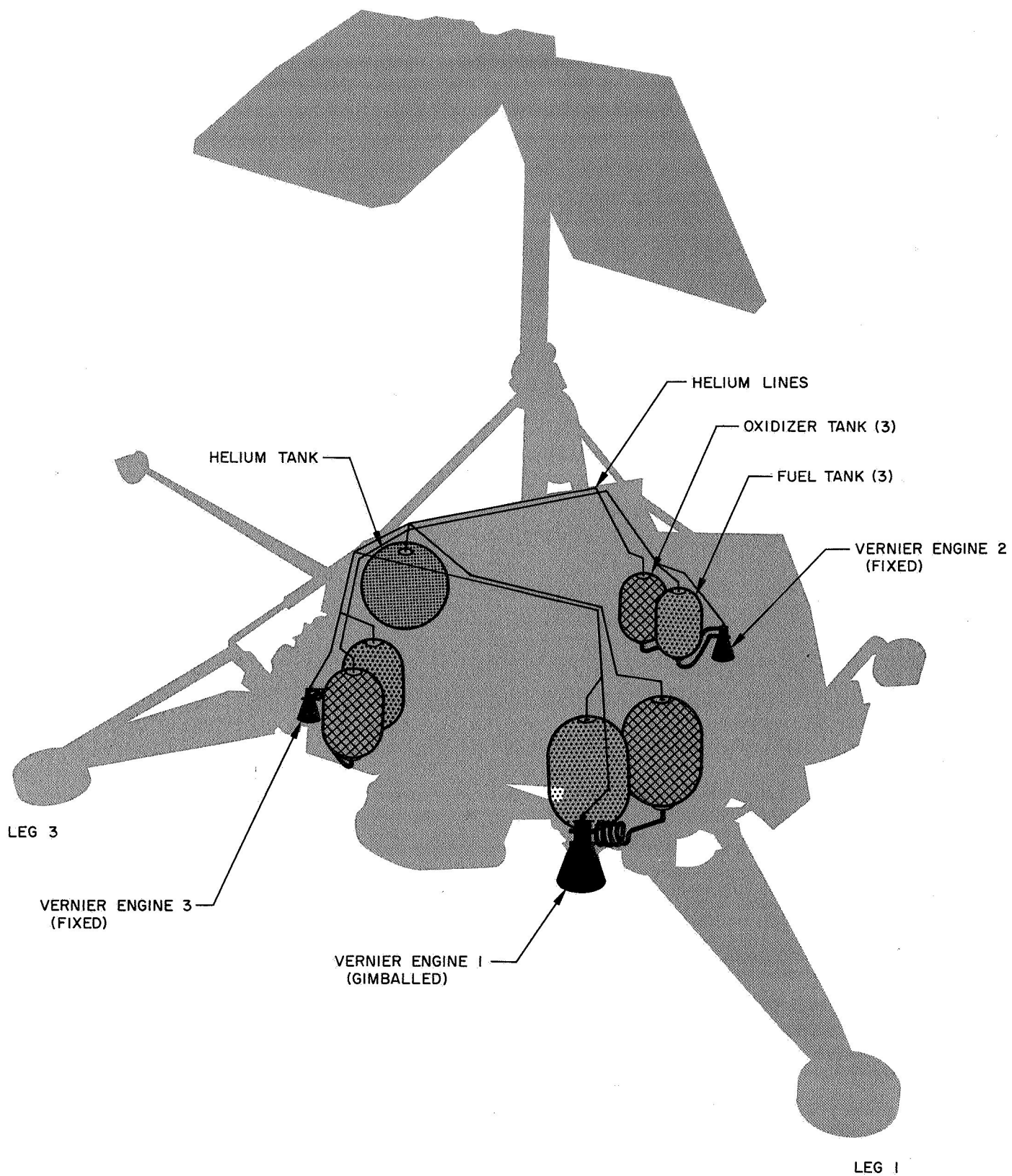


Fig. IV-26. Vernier propulsion system installation

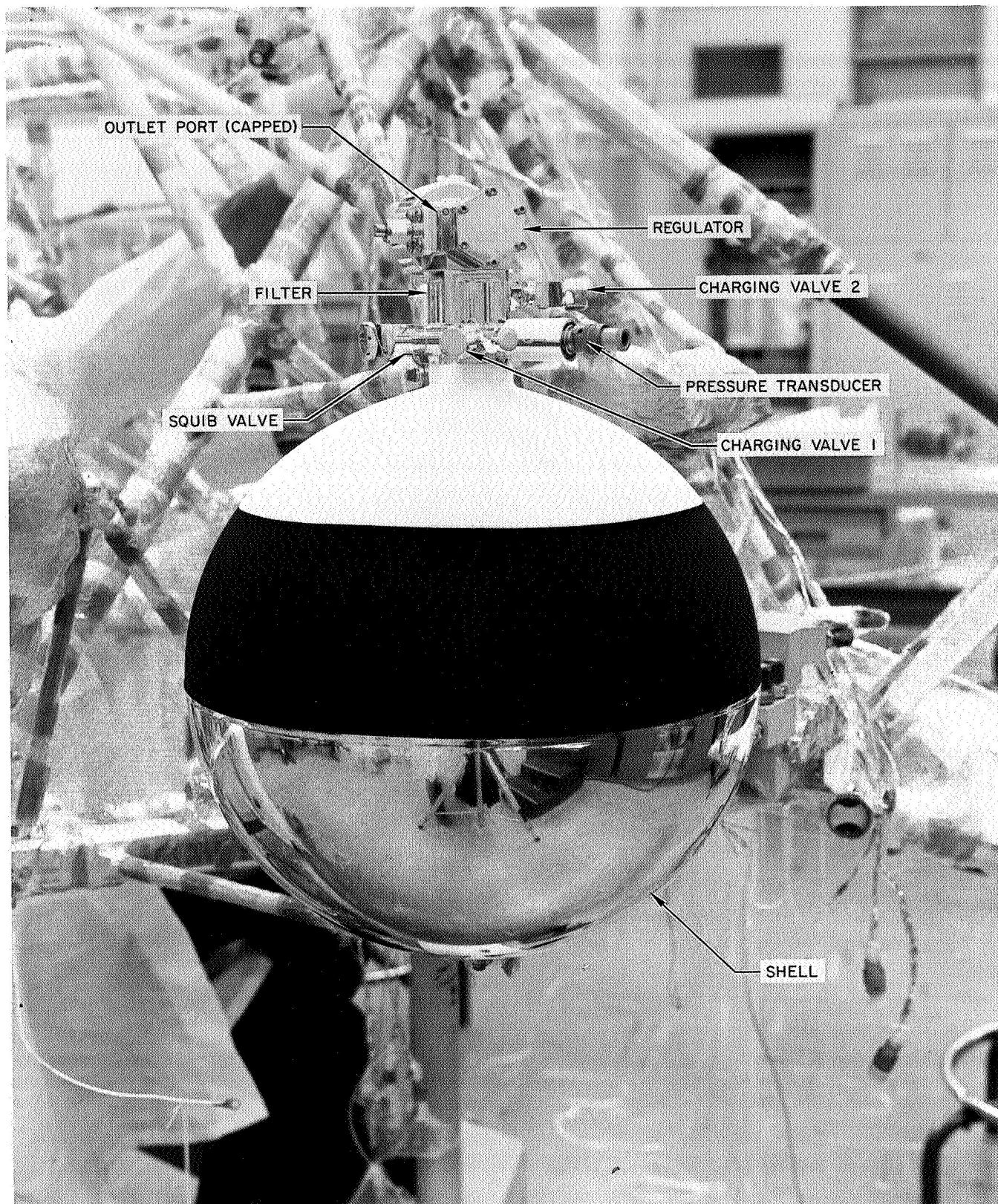
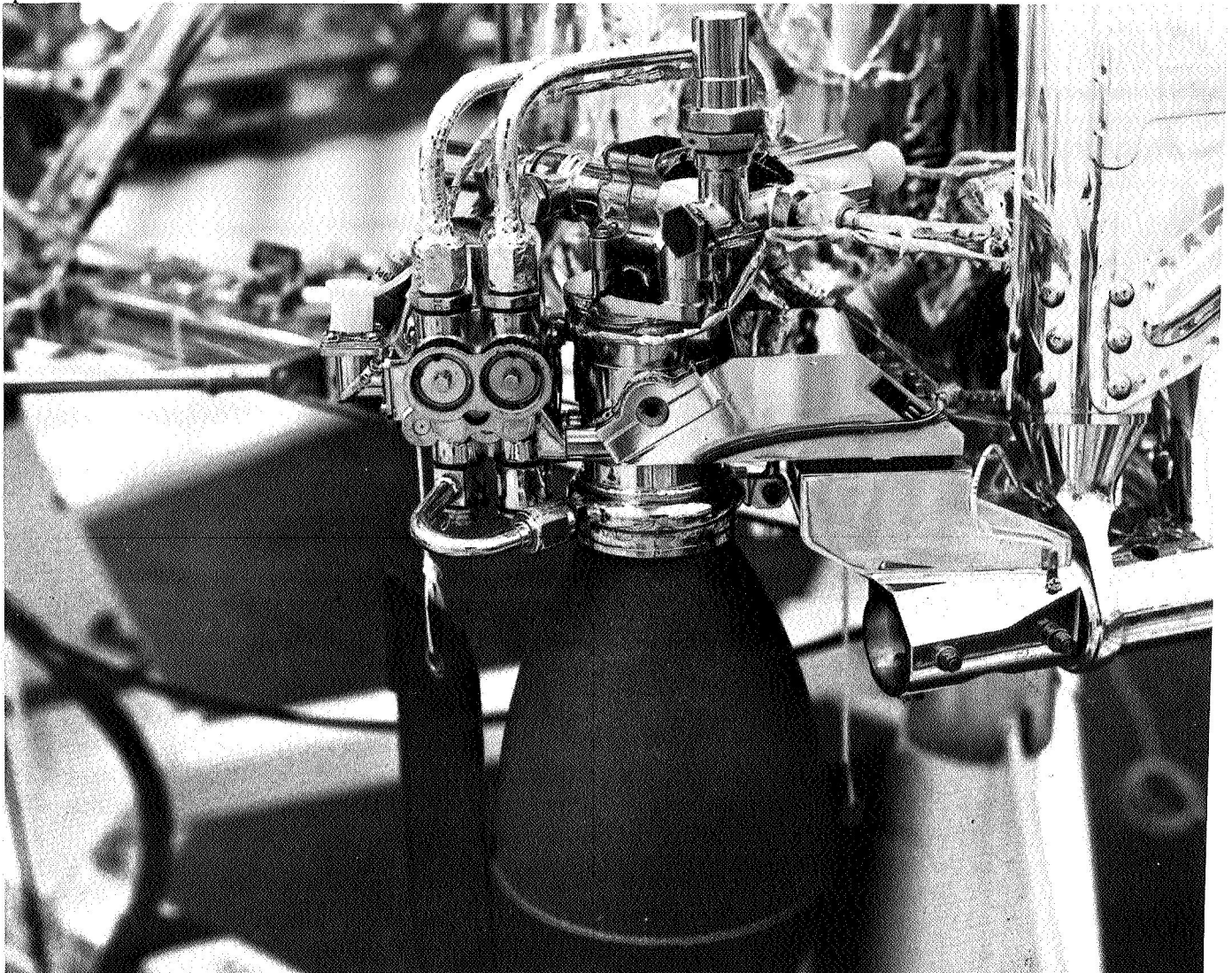


Fig. IV-27. Helium tank assembly





**Fig. IV-28. Vernier engine thrust chamber assembly**

Changes were made to obtain additional vernier propulsion system data on *Surveyor V* by adding a pressure transducer to Fuel Line 2 and temperature sensors to Fuel Lines 1 and 3.

*b. Vernier propulsion performance.* The *Surveyor V* vernier propulsion system successfully performed the necessary midcourse correction and terminal descent sequence. However, the terminal descent sequence required major modifications to be made during the flight because the helium regulator failed to lock up tight after midcourse correction. A postlanding vernier engine static firing experiment was also conducted successfully.

Vernier propulsion system parameters during launch and the pre-midcourse coast period were all normal and

well within the allowable range. After completion of the pre-midcourse attitude change maneuvers, vernier pressurization was commanded in accordance with the normal mission sequence. Vernier propellant tank pressurization is accomplished by firing the helium release squib and allowing high-pressure helium gas into the inlet port of the helium pressure regulator. The helium regulator allows a high flow rate of helium until the regulator outlet pressure reaches the normal regulation pressure ( $\sim 730$  psia). At this point the pressure forces on the regulator diaphragm overcome the spring forces and the regulator begins to close and restrict the flow rate. The regulator is normally completely closed at 770 psia and prohibits the flow of gas until the downstream pressure is decreased. Figure IV-29 shows the fuel and oxidizer tank pressures at vernier pressurization. Note that the

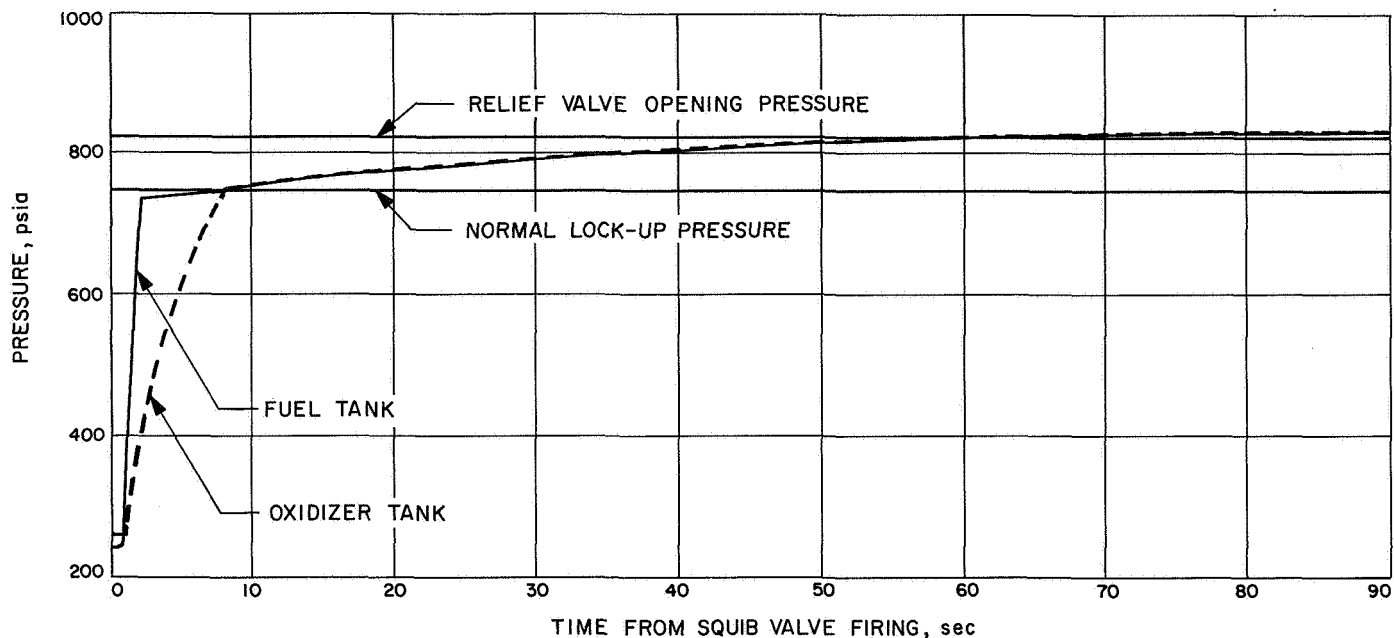


Fig. IV-29. Vernier propellant tank pressurization prior to Surveyor V midcourse correction

pressures rose rapidly to 750 psia and then continued to rise slowly until they reached 825 psia. Thus, it appears that the regulator functioned normally and attempted to completely stop the flow of gas to the propellant tanks when a pressure of 750 psia was reached. The regulator was unable to completely stop the flow of helium to the propellant tanks, and the pressures continued to rise until they reached the relief valve opening pressures. At this point the relief valve opens just enough to allow overboard leakage such that the tank pressure remains constant. Thus the spacecraft data agrees with what would be expected for a regulator which failed to lock up. The Surveyor V pressurization system functional parameters measured during test and flight are listed in Table IV-13.

The first midcourse correction (Vernier Firing 1) was executed normally about 2 min after vernier pressurization. The regulator leakage in the lock-up condition did not affect the midcourse correction. Vernier engine performance during the midcourse correction was normal, and start and shutdown transient performances were well within allowable limits.

After vernier cutoff, the propellant tank pressures returned to the relief valve settings. Overboard leakage was confirmed by a drop rate of 10 psi/min in the helium supply tank pressure. The helium supply tank pressure, beginning before midcourse correction, is shown in Fig. IV-30.

Three additional vernier firings were then performed in an attempt to clear and lock up the pressure regulator. A summary of all vernier firings is presented in Table IV-6. During each firing the flow of propellants from the tanks causes the pressure to drop until it reaches the regulation level, at which point the regulator opens and allows helium to flow and keep the pressure from dropping further. It was hoped that this repeated opening action would clear the seat area and allow the regulator to close completely. Vernier Firings 2 through 4 were executed for this purpose, but did not significantly reduce the

Table IV-13. Vernier pressurization system functional parameters during test and flight

	Flight acceptance test	Vernier system functional test	Surveyor V mission
Regulation pressures, psia			
Low flow	750	748	} 727 Failed to lock up
High flow	733	731	
Lock-up	762	755	
Relief valve pressures, psia			
Oxidizer opening	820	838	} 825
Oxidizer closing	802	814	
Fuel opening	818	839	} 825
Fuel closing	807	820	



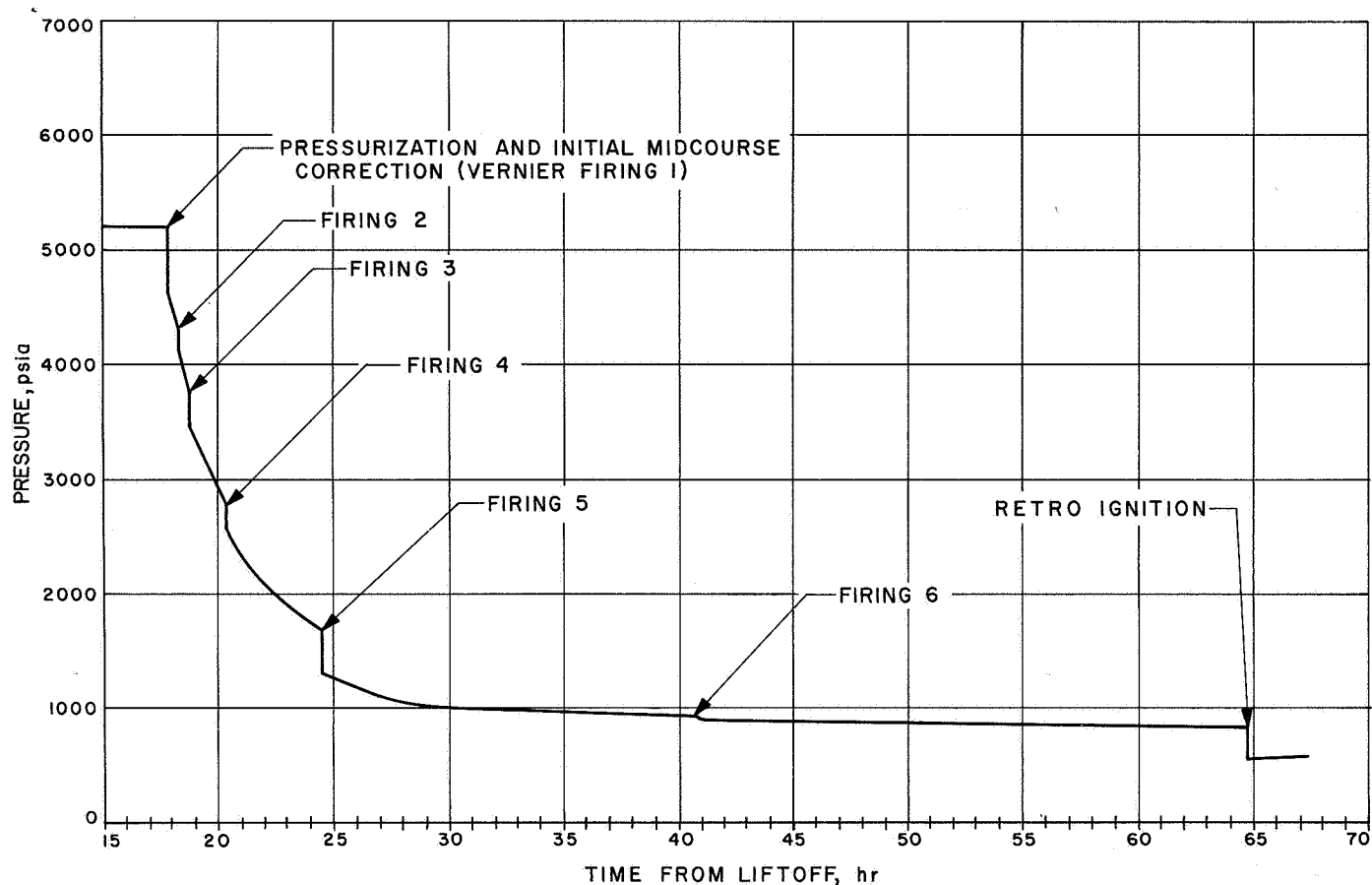


Fig. IV-30. Helium tank pressure decay following midcourse correction

helium leakage rate, and further attempts to stop the leakage were abandoned.

When the pressure regulator fails to lock up, the system slowly leaks gas overboard through the relief valves. Eventually, when the helium tank pressure drops to the relief valve setting, the overboard leakage will stop and the system will remain at just below the relief pressure from then on. (The *Surveyor V* system reached this point about 10 hr before terminal descent.)

The ability of the vernier engines to operate at low propellant feed pressures was evaluated in detail during the mission. Special engine flow tests simulating low propellant pressures were conducted at the JPL Edwards Test Station to determine the thrust control capability as a function of propellant feed pressure. The results are shown on Fig. IV-31. Note that, at propellant supply pressures between 550 and 500 psia, the oxidizer-to-fuel mixture ratio begins to vary significantly from the nominal 1.5 and, as a result, the thrust capability begins to drop

substantially. This characteristic and the loss of all thrust capability at a pressure of 450 psia are caused by a fuel pressure regulator in the engine which closes when the pressure in the engine's cooling jacket drops below 450 psia. The thrust characteristics calculated for each *Surveyor V* engine were very similar to those of the test engine shown on Fig. IV-31. A minimum operating propellant supply pressure of 500 psia was established from this data. Vernier Firing 5 was performed to lighten the spacecraft and reduce the vernier propellant requirements during terminal descent. Burning this additional propellant also increased the volume of gas inside the propellant tanks for the terminal descent sequence. A final midcourse correction (Firing 6) was made to alter the trajectory aim point to the preplanned location. This correction also slightly increased the volume of gas inside the propellant tanks. Since all the vernier firings were conducted before the helium tank pressure had leaked down to the propellant tank pressure, the final state of the propulsion system for the terminal descent was at 825 psia (the relief valve settings) for the propellant tanks and the helium tank. Because of the many vernier firings,

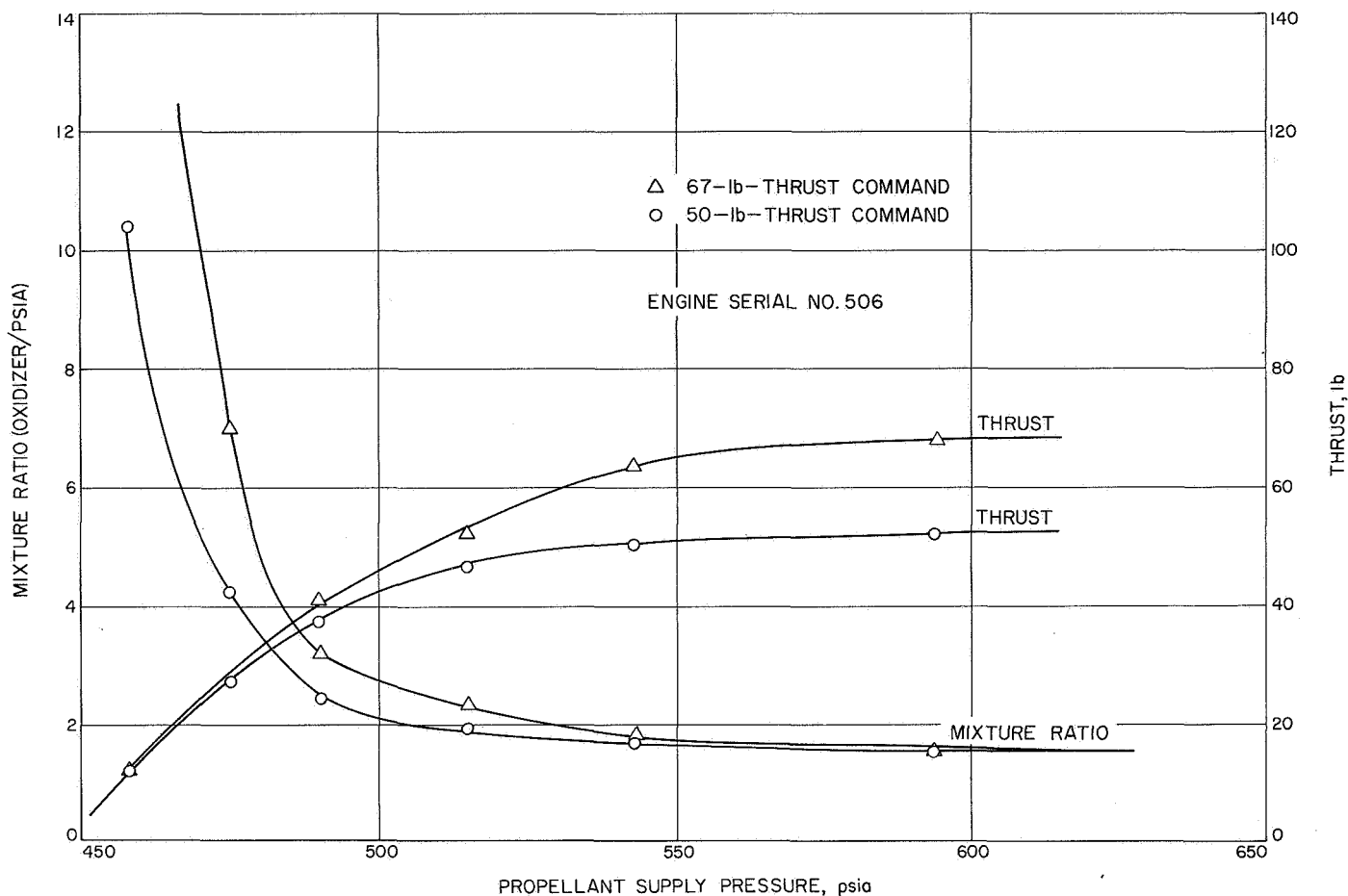


Fig. IV-31. Surveyor V vernier engine flow test results

the total gas volume was 3,240 in.<sup>3</sup>, which includes the 1,290-in.<sup>3</sup> volume of the helium tank.

Calculations made to determine the predicted drop in propellant supply pressure as propellants are used from the tanks are shown in Fig. IV-32. This prediction was verified before the Surveyor V lunar landing by a special test at the Hughes Aircraft Company propulsion test site. A complete vernier propulsion system on the S-6 test vehicle was loaded with alcohol (to simulate the fuel) and Freon (to simulate the oxidizer). The liquid volumes and pressures in each tank simulated the Surveyor V system. The S-6 engines were operated with a midthrust command until the propellant tank pressure dropped to 500 psia. The simulated propellants which flowed through each engine were caught and weighed. The total weight expelled was in good agreement with the analytical predictions (see Fig. IV-32). This data and the engine thrust capability for reduced supply pressures yielded a maximum allowable propellant usage during terminal descent

of 70 lb. This limit was used to determine the optimum burnout altitude and velocity. The actual propellant usage during the Surveyor V terminal descent and the final supply pressure are in good agreement with predictions and special test data as shown in Fig. IV-32.

The terminal descent sequence was also modified to maximize the vernier propellant available for the RADVS-controlled phase of the terminal descent. One important part of the modification was reducing the delay time between retro burnout and retro eject. A delay time of 5 sec was initially chosen, but reexamination of retro thrust tailoff characteristics showed that an 8-sec delay should be used. This was adopted. The 8-sec delay should be compared with the 12-sec delay normally allowed. The actual Surveyor V sequence is compared with a normal sequence in Fig. IV-8.

The vernier engine thrust command signals indicated thrust command saturations occurring just before the

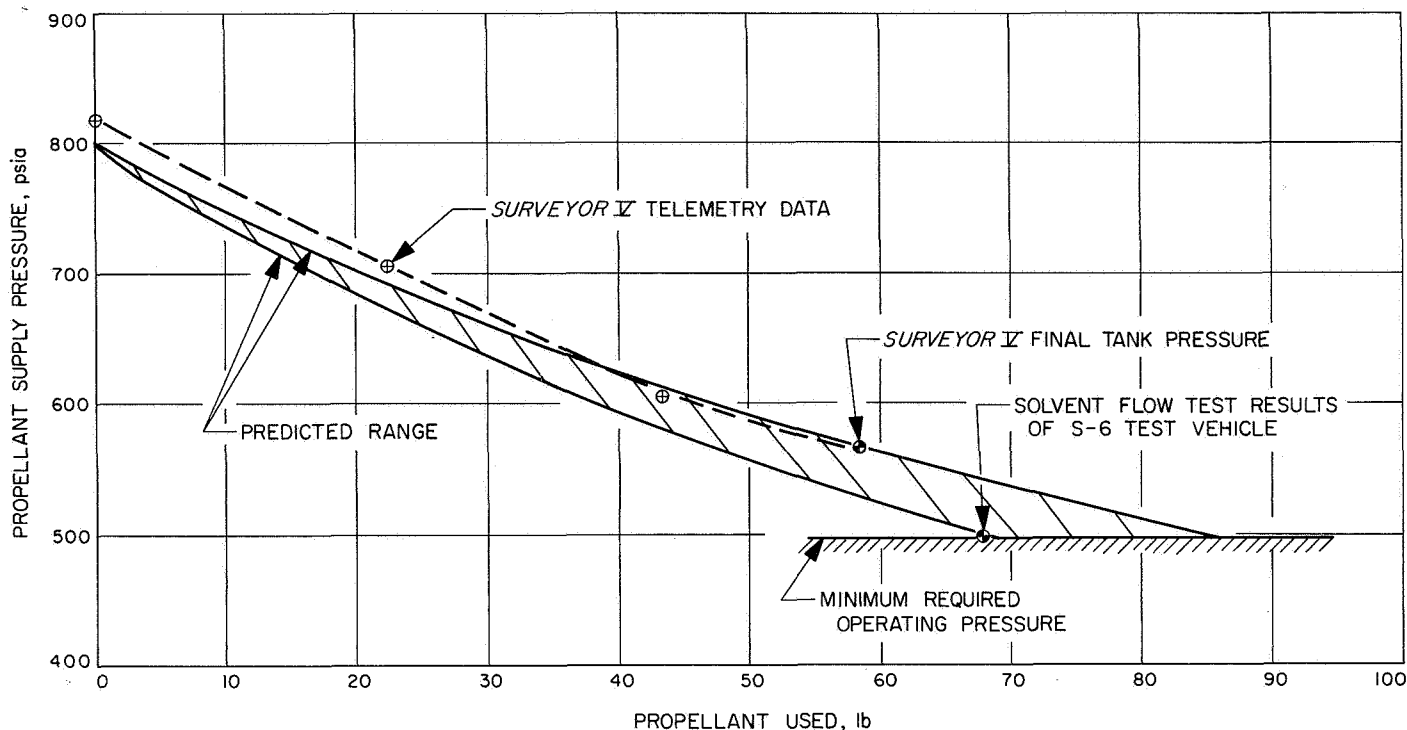


Fig. IV-32. Propellant supply pressure decay during terminal descent

10-ft/sec *mark* during terminal descent. This was caused by the low propellant supply pressure near the end of the terminal descent. This data indicates that the vernier engines were approaching the point where their thrust capability was severely degraded, which was as predicted based on the preterminal descent calculations.

An extensive review of the helium pressure regulator failure has been conducted. The results show that the most probable cause of the failure was contamination which damaged the helium regulator valve seat seal. This condition could result in an internal leak through the regulator, causing the outlet pressure to increase to a level which would cause the fuel or oxidizer relief valve to vent to space. Changes in the handling and checkout procedures for the helium pressurization system have been made. These changes will greatly reduce the probability of inducing contamination into the system and also provide for a lock-up performance test in the final phase of preflight vernier propulsion system testing.

Figure IV-33 shows propulsion system temperatures during the transit and lunar phases of the *Surveyor V* mission. Note that all temperatures remained within allowable limits during transit. Vernier system temperature profiles for the mission are included in Appendix D.

The temperatures experienced after landing were considerably higher than for previous spacecraft. The engine temperatures were particularly high.

A vernier static firing experiment was performed on September 13, about 53 hr after landing. Minimum vernier thrust (approximately 30 lb for each engine) was commanded for 0.55 sec. Figure IV-34 shows the vernier engine thrust profiles during the static firing experiment. A very limited amount of telemetry data was available during the firing; this made it necessary to use engine test data to construct the best estimate thrust profile through the limited *Surveyor V* data points. The 17 lb of thrust measured for Engine 2 was as expected, based on the initial engine temperature of 274°F. The oxidizer vapor pressure for this temperature is 1100 psia. Since the oxidizer tank pressure was only 750 psia at this time, the oxidizer side of the engine must have been filled with oxidizer vapor rather than liquid. Because of this, the oxidizer flow rate was well below normal, and resulted in the lower-than-normal minimum thrust level. Engine 2 temperature at ignition of 274°F was well above the 220°F maximum limit. This limit was set as the upper bound for normal operation. For this very short (0.55-sec) firing it was not necessary that the engines perform normally. Even if the hot engine had failed to ignite, it would not have endangered the spacecraft.

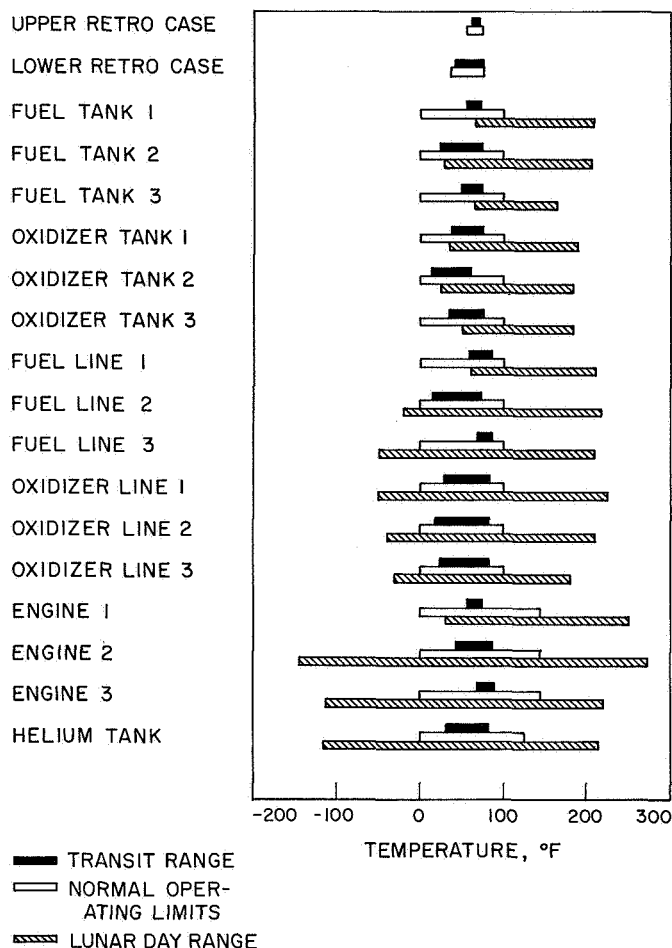


**Fig. IV-33. Propulsion system temperature ranges during transit and lunar day**

On September 18, about 7½ days after landing, oxidizer tank pressure dropped suddenly, as shown in Fig. IV-35. Concurrent with this pressure drop, large drops in Oxidizer Tank 1 and Line 1 temperatures occurred. Changes were also noted in the foil wrap of Oxidizer Tank 1, as shown in Figs. IV-36 and IV-37. These changes all were traceable to leakage of oxidizer through a tank O-ring seal. Special tests simulating the temperature profile experienced by Oxidizer Tank 1 showed that the O-ring seal material (Viton A) is severely attacked by the oxidizer at temperatures of 160°F and above. At normal temperatures (less than 85°F), which exist before launch and during the transit phase of the mission, very little degradation occurs. For this reason leakage caused by chemical attack is not of concern for the transit phase of future missions.

Figure IV-35 also shows a rapid drop in fuel pressure on September 22, about 11½ days after landing. Since

there were no temperature changes accompanying this pressure drop, it appears to be due to leakage from the gas side of the fuel system rather than the liquid side. The vernier engine solenoid valves, relief valves, and propellant tanks are all possible leakage points. Since they were all far above their normal operating limits (see Fig. IV-33), the leak could have occurred at any one of these locations. Since the leakage occurred under extreme environmental conditions, it does not represent a concern for the transit phase of future missions.

Except for the helium pressure regulator, all components of the vernier propulsion system performed well and, in many cases, under conditions far outside their normal operational limits.

## 2. Main Retrorocket Motor

The main retrorocket performs the major portion of the deceleration of the spacecraft during terminal descent.

**a. Retromotor description.** The main retromotor is a spherical solid-propellant unit with a partially submerged nozzle to minimize overall length (Fig. IV-38). The motor utilizes a carboxyl/terminated polyhydrocarbon composite-type propellant and conventional grain geometry.

The motor case is attached at three points on the main spaceframe near the landing leg hinges, with explosive nut disconnects for postburnout ejection. Friction clips around the nozzle flange provide attachment points for the altitude marking radar (AMR). The *Surveyor V* retro-rocket, including the thermal insulating blankets, weighed approximately 1400 lb. This total included 1251 lb of propellant. The thermal control design of the retrorocket motor is completely passive, depending on its own thermal capacity and insulating blanket (21 layers of aluminized mylar plus a cover of aluminized teflon). The prelaunch temperature of the unit is  $70 \pm 5^\circ\text{F}$ . At terminal maneuver, when the motor is ignited, the propellant will have cooled to a thermal gradient with a bulk average temperature of about 50 to 55°F.

The AMR normally triggers the terminal maneuver sequence. When the retro firing sequence is initiated, the retrorocket gas pressure ejects the AMR. The motor operates at a thrust level of 8,000 to 10,000 lb for approximately 39 sec at an average propellant temperature of 55°F.

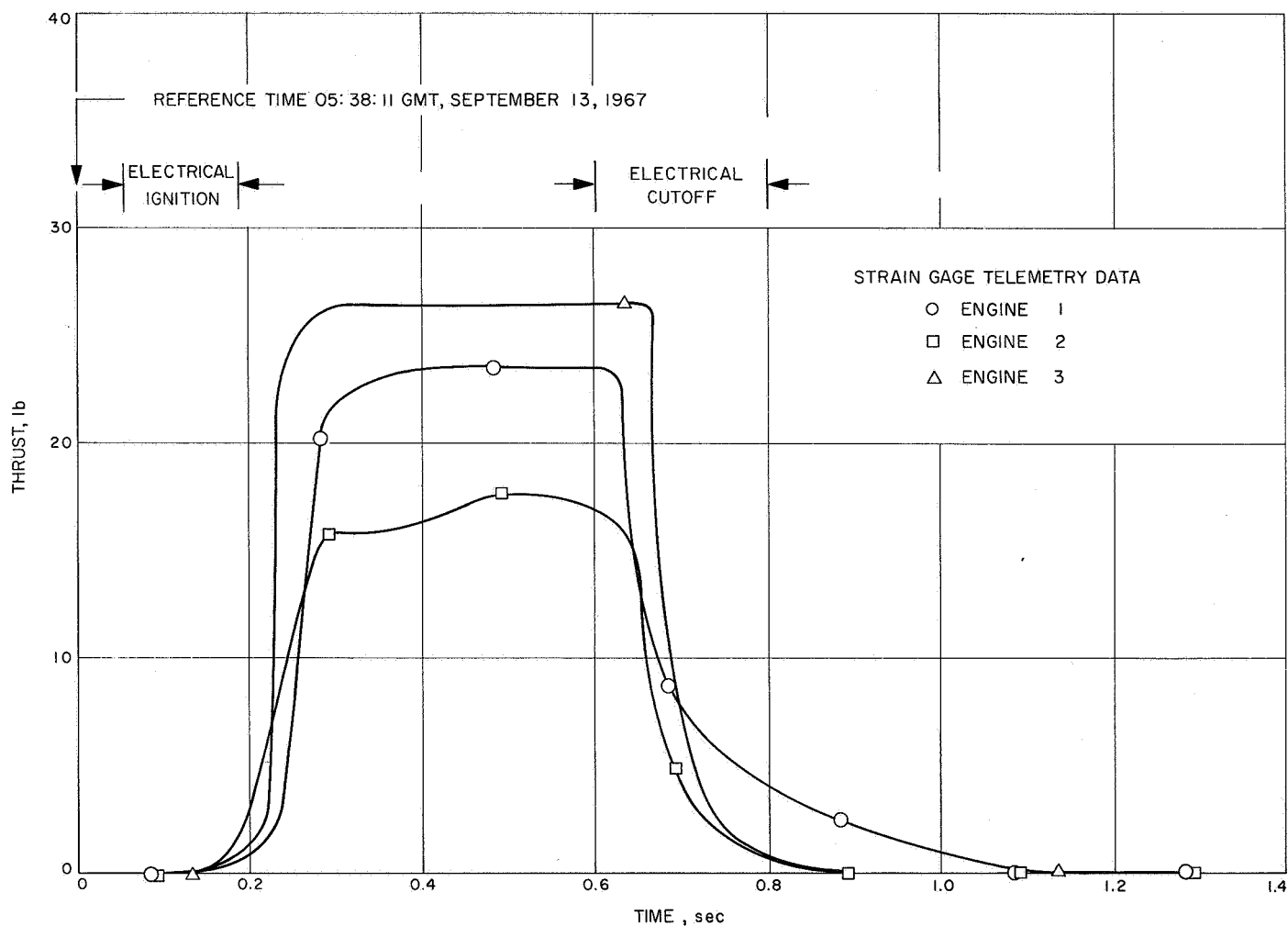


Fig. IV-34. Engine thrust during vernier static firing experiment on lunar surface

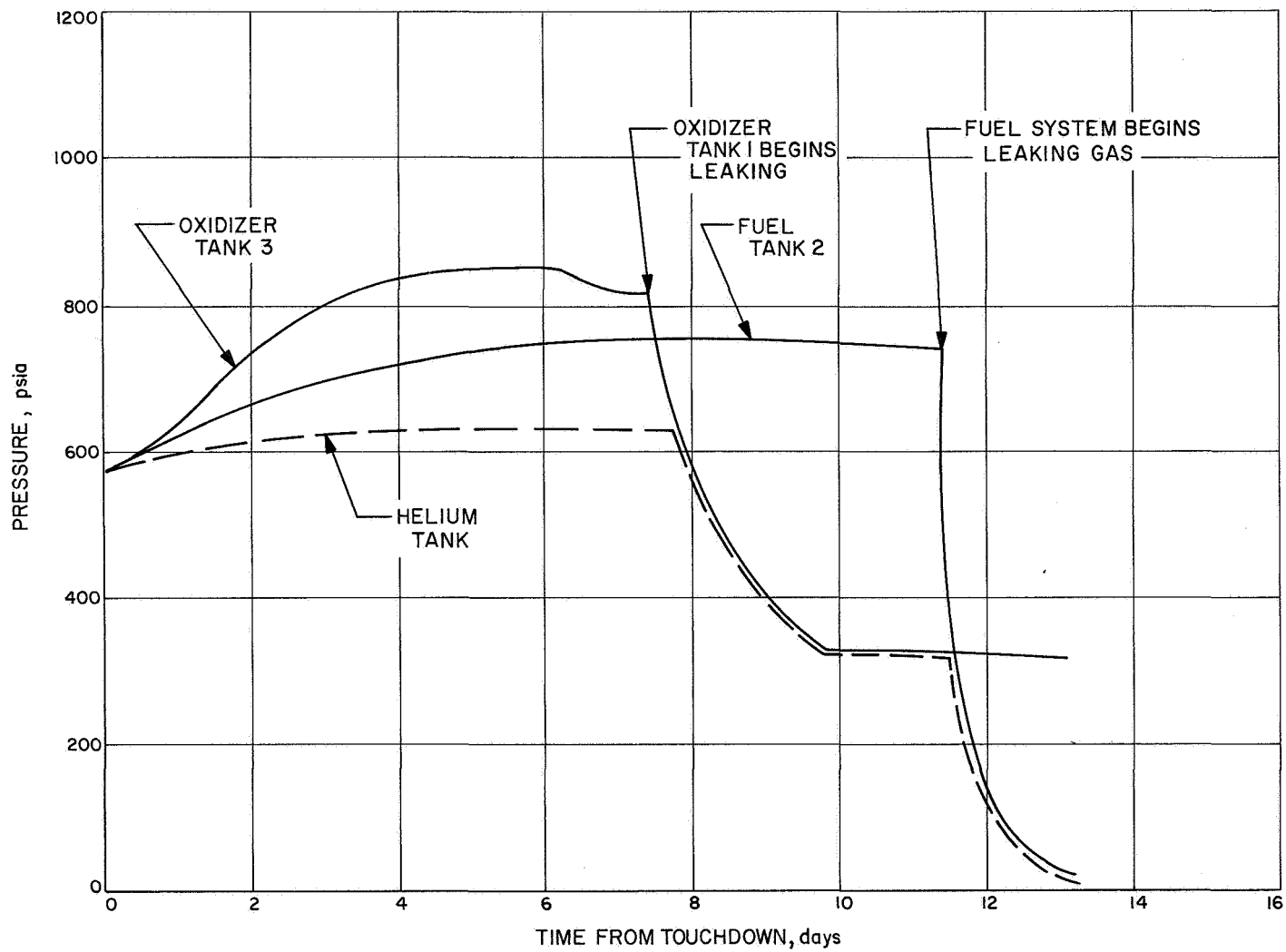
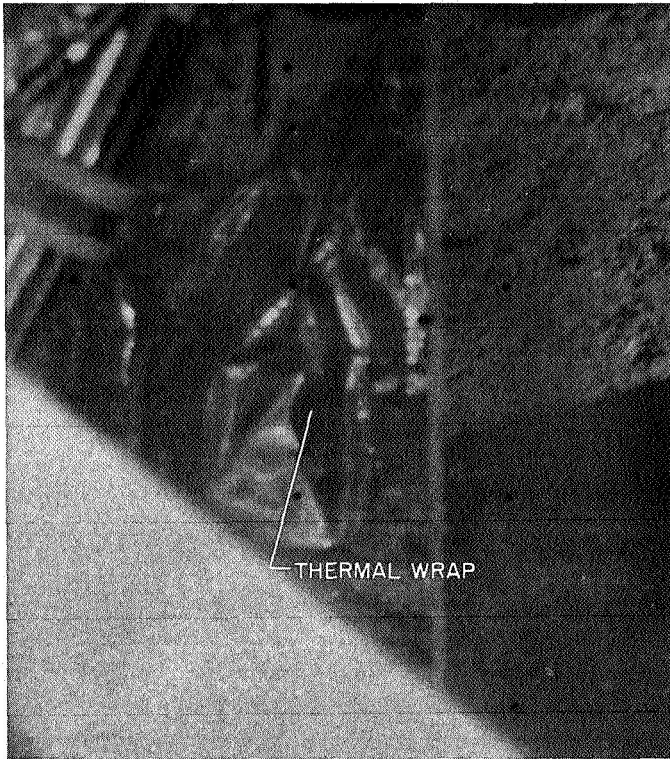
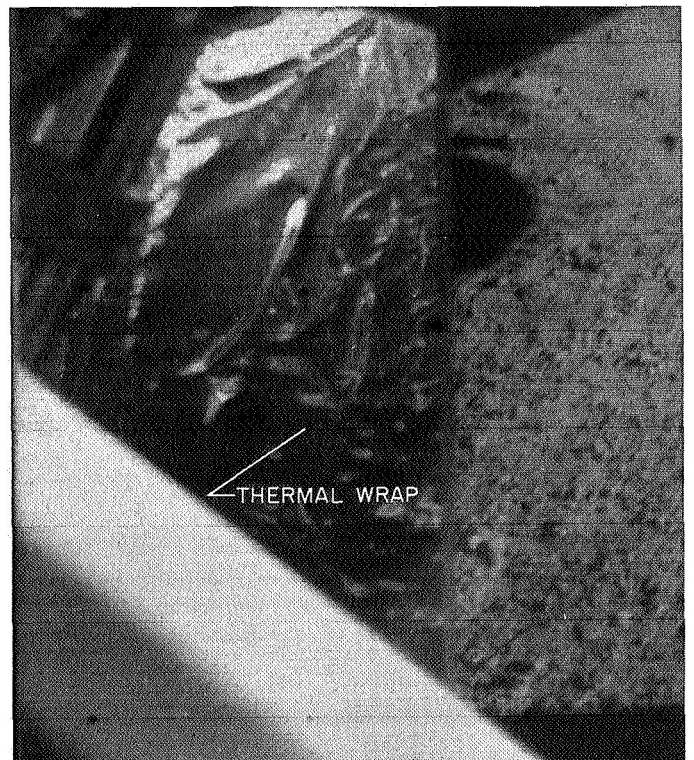


Fig. IV-35. Vernier propulsion system pressures during first lunar day



**Fig. IV-36. Oxidizer Tank 1 thermal wrap before oxidizer leak (September 12, 1967, 02:51:25.52 GMT)**



**Fig. IV-37. Oxidizer Tank 1 thermal wrap after oxidizer leak (September 21, 1967, 06:15:38.69 GMT)**

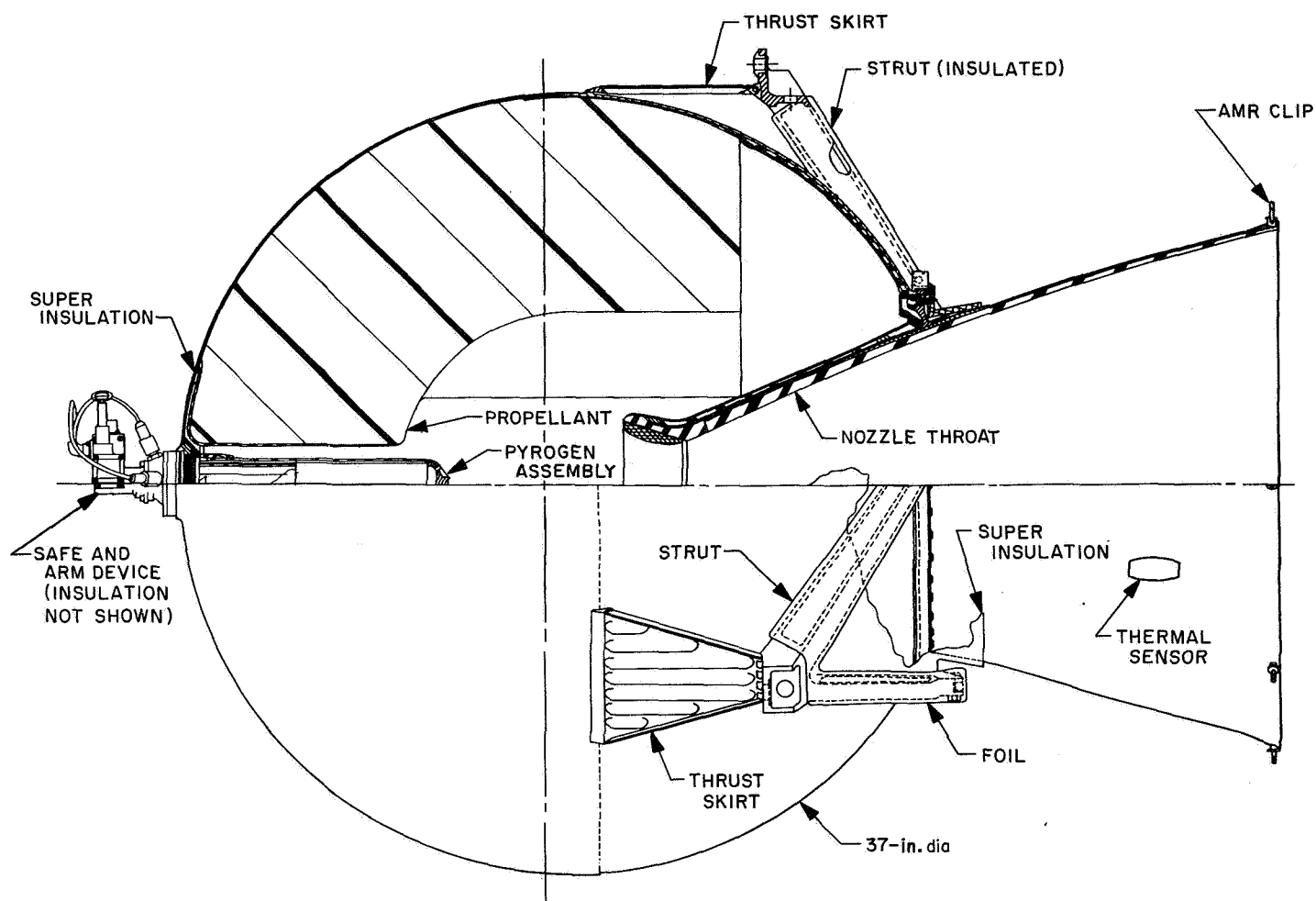


Fig. IV-38. Main retrorocket motor

**b. Retromotor performance.** Beginning at a launch bulk average temperature of approximately 70°F, the retromotor cooled at the predicted rate and arrived at an average temperature of 52.5°F at the time of ignition. At this temperature the burn time was predicted to be 39.06 sec. The postflight data analysis indicates a burn time of 38.56 sec or a difference of 1.3%. The maximum thrust developed was 9,950 lb against a prediction of 9,850 lb. The modulation of vernier engine thrust commands and the output of the gyros were small, which indicated a stable spacecraft during the main retro phase. The data also showed that the actual total impulse of the main retromotor was less than 0.1% below the predicted value.

Main retromotor ignition produced a short-duration disturbance torque of approximately 20 ft-lb. Following main retromotor ignition, all three vernier engines settled near their 50-lb-thrust condition and remained very

steady throughout main retromotor burning. This indicates that the retromotor did not experience any measurable thrust vector excursion or lateral center-of-gravity shift during operation. The maximum required corrective roll torque produced by Vernier Engine 1, after correcting the roll actuator position measurement for mounting bracket bending, was determined to be 12 in.-lb. Assuming that all this torque was produced by the main retromotor, the roll torque was well below the 90-in.-lb maximum moment allocated to the retromotor. Retromotor ejection from the spacecraft was very smooth and required no apparent corrective torque.

## F. Flight Control

The flight control subsystem provides spacecraft velocity and attitude control during transit from the time of spacecraft separation from the *Centaur* vehicle to



spacecraft touchdown on the lunar surface. The basic flight control functions include:

- (1) Attitude stabilization and orientation during transit.
- (2) Midcourse velocity correction based on ground commands.
- (3) Retro ignition and ejection and vernier descent control for soft-landing of the spacecraft.

### 1. Flight Control Description

The flight control subsystem consists of reference sensing elements, flight control and mode control electronics, and vehicle control elements functionally arranged as shown in Fig. IV-39.

The principal references used by the spacecraft are inertial, celestial, and lunar; each is sensed respectively by inertial, optical, and radar sensors. The control electronics process the reference sensor outputs, earth-based commands, and the flight control programmer and decoder outputs to generate the necessary control signals

for use by the vehicle control elements. The vehicle control elements consist of the attitude-control cold-gas-jet activation valves and gas supply system, the vernier engine throttleable thrust valves and controllable gimbal actuator, and the main retro igniter and retro case separation pyrotechnics.

The gas-jet attitude-control system is a cold gas system using nitrogen as a propellant. This system consists of a gas supply system and three pairs of solenoid-valve-operated gas jets interconnected with tubing (Fig. IV-40). The nitrogen supply tank is initially charged to a nominal pressure of 4600 psia. Pressure to the gas jets is controlled to  $40 \pm 2$  psia by a regulator.

Vehicle response in attitude, acceleration, and velocity is controlled as needed by various "control loops" throughout the coast and thrust phases of flight, as shown in Table IV-14. Upon separation of the spacecraft from the *Centaur*, stabilization of the spacecraft tipoff rates is achieved through activation of the gas jet system and use of rate feedback gyro control (*rate mode*). After rate

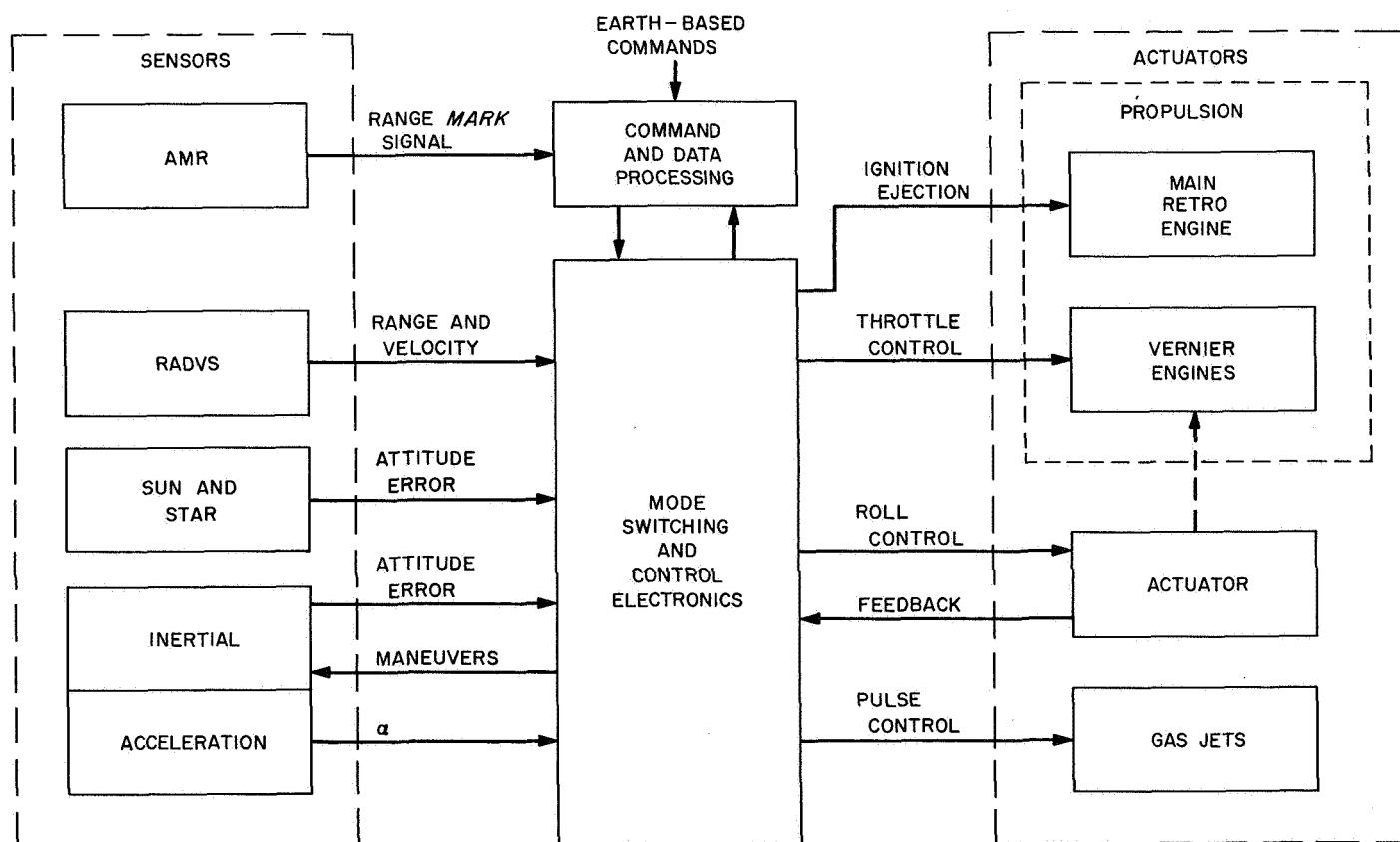


Fig. IV-39. Simplified flight control functional diagram

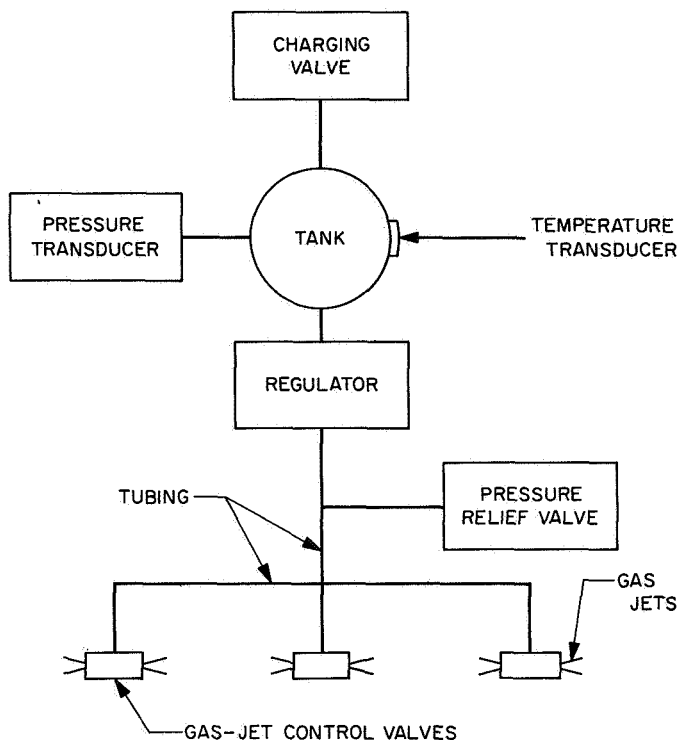


Fig. IV-40. Gas-jet attitude control system

capture, *inertial* mode is achieved by switching to position feedback gyro control.

Because of the long duration of the transit phase and the small unavoidable drift error of the gyros, celestial references are used to provide the desired attitude of the spacecraft. Following a 51-sec delay after spacecraft electrical disconnect from the *Centaur*, a flight control timer automatically initiates the sun acquisition sequence by commanding a negative roll maneuver. The sun is first acquired by the acquisition sun sensor, which has a 10-deg-wide by 196-deg-fan-shaped field of view that includes the spacecraft Z-axis and is centered about the minus X-axis. The roll command is terminated after initial sun acquisition, and a positive yaw command is automatically initiated which allows the narrow-view primary sun sensor to acquire and lock-on the sun. A secondary sun sensor, mounted on the solar panel, provides a backup for manual acquisition of the sun if the automatic sequence fails. On the *Surveyor V* spacecraft, a separation latch was incorporated in the flight control programmer which, upon initiation of the automatic sun acquisition sequence, inhibits subsequent false triggering of the automatic sun acquisition sequence.

Automatic Canopus acquisition and lock-on are normally achieved after initiation of a roll by command from

Table IV-14. Flight control modes

Control loop	Flight phase	Modes	Remarks
Attitude control loop			
Pitch and yaw	Coast	Rate Inertial Celestial	Gas jet matrix signals
	Thrust	Inertial Lunar radar	Vernier engine matrix signals
Roll	Coast	Rate Inertial Celestial	Leg 1 gas jet signals
	Thrust	Inertial	Vernier Engine 1 gimbal command
Acceleration control loop			
Thrust axis	Thrust (mid-course)	Inertial (with accelerometer)	Nominal 3.22 ft/sec <sup>2</sup> Minimum 4.77 ft/sec <sup>2</sup> Maximum 12.56 ft/sec <sup>2</sup>
	Thrust (terminal descent)	Inertial (with accelerometer)	
Velocity control loop			
Thrust axis	Thrust	Lunar radar	Command segment signals to 43-ft altitude Constant 5-ft/sec velocity signals to 13-ft altitude
Lateral axis	Thrust	Lunar radar	Lateral/angular conversion signals

earth. This occurs because the Canopus sensor angle is preset with respect to the primary sun sensor prior to launch for each mission. Star mapping for Canopus verification is achieved by commanding the spacecraft to roll while the spacecraft maintains sun lock.

The transit phase is performed with the spacecraft in the celestial-referenced mode except during initial rate-stabilization, midcourse and terminal descent maneuvers, and gyro drift checks, when the inertial mode is used.

Midcourse velocity correction capability is provided by means of the vernier engine throttle valves, a precision timer, and an accurate acceleration sensing device. The difference between the command acceleration level and the output from the accelerometer provides an error signal which is used to command the throttle valves for the required thrust level. The timer controls the duration of vernier thrusting in accordance with a time interval preset by earth command. For *Surveyor V*, the duration of the effective time interval which could be preset in the flight control was increased from 51 to 102 sec by incorporation of a new 10-Hz clock.

The terminal maneuver descent sequence has been described in detail in Section IV-A-15. The flight control subsystem provides initial orientation of the main retro-motor thrust axis and automatic sequencing after the lunar reference is first established by a signal from the AMR. Most of the approach velocity is removed by the solid-propellant retromotor during the initial phase of terminal descent. Spacecraft attitude during this phase is inertially stabilized using the gyros and differential throttling of the vernier engines.

During the vernier phase of descent, which follows main retro burnout and ejection, a sophisticated flight control technique is utilized that includes the use of radars to obtain range and velocities. The range information is used by the flight control subsystem during the vernier phase of descent to compute longitudinal velocity commands for controlling the total vernier engine thrust to achieve the desired descent profile (approximately constant acceleration). The velocity data is applied to the attitude control loop to produce a near-gravity turn during descent by aligning the spacecraft thrust axis with the velocity vector. The velocity data is also used to generate error signals for the velocity control loop.

## 2. Flight Control Performance

Flight control performance was completely satisfactory during all phases of the *Surveyor V* mission, which was unique because it included several extra vernier engine firings during transit, a terminal descent sequence which required modification after midcourse correction, and a vernier static firing after landing.

**a. Launch phase.** During the System Readiness Test conducted just before the countdown, it was necessary to raise the nose fairing inlet air temperature from 70 to approximately 75°F to allow the spacecraft gyros to run warmer and thereby meet specification values for gyro precession.

Spacecraft separation from the *Centaur* was normal. The spacecraft gyro data indicated that the following maximum angular rates (in deg/sec) occurred as a result of the separation sequence: pitch, +0.98; yaw, +0.21; roll, -0.10. Tipoff rates well within the specification limit of 3.0 deg/sec were also confirmed by *Centaur* data, which indicated nearly simultaneous extension of the three separation springs. The spacecraft reduced angular motion about each of the axes to  $\leq 0.1$  deg/sec in less than 20 sec.

**b. Sun acquisition.** A very nominal sun acquisition sequence was automatically executed. The acquisition sun sensor was illuminated after a negative roll of 342 deg, followed by a positive yaw turn of 18 deg which established primary sun sensor lock-on. The *sun-lock* signal was generated at a primary sun sensor pitch error of approximately -3.0 deg and a yaw error of -12.6 deg, which are within the expected lock-on field-of-view range of the sensor. The sun acquisition sequence required about 12 min.

**c. Star (Canopus) acquisition.** A *sun-and-roll* command was sent to the spacecraft about 6 hr after liftoff to initiate the star mapping and Canopus acquisition sequence. Analysis of star intensity signals resulted in positive identification of many stars, including Canopus, and the earth. Table IV-15 summarizes the objects that appeared in the field of view of the Canopus sensor. Following one complete roll turn and after light from the earth had passed the field of view, a *sun-and-star* command was sent to the spacecraft to enable automatic acquisition of Canopus by the spacecraft. The total time from start of the roll maneuver until automatic acquisition of Canopus was approximately 18 min.

The Canopus sensor performance was excellent during the mission. The *Surveyor V* sun filter value was calibrated at the *Surveyor III* and *IV* level of  $0.8 \times$  Canopus. The ratio of measured Canopus intensity to predicted intensity was approximately 1.08, which compares favorably with the *Surveyor III* ratio of 1.17 and the *Surveyor IV* ratio of 1.16.

**d. Midcourse maneuvers and velocity correction.** The maneuver combination selected to orient the spacecraft in the desired direction for the initial midcourse velocity correction consisted of a +71.9-deg roll followed by a -35.7-deg yaw. The actual maneuver magnitudes were verified as +71.914 deg of roll and -35.622 deg of yaw. An attempt was made to reduce the pointing errors by initiating each pre-midcourse attitude maneuver at the null point in the optical sensor control loop limit cycle. This attempt was successful, with the roll maneuver initiated within about 0.13 deg of null while the pitch and yaw optical errors were about 0.07 and 0.10 deg, respectively, for the yaw maneuver.

The initial midcourse velocity correction was successfully executed starting at about  $L + 17:48$ . The actual burn time was 14.22 sec compared to a commanded duration of 14.3 sec. Ignition was smooth with maximum pitch and yaw changes of -0.24 deg and +0.08 deg,

Table IV-15. Surveyor V star map results

GMT (September 8, 1967)	Roll angle, deg	Object in field of view	Angle from Canopus, deg		Peak telemetered intensity, V	Comment
			Indicated	Predicted		
14:10:06	0	—	—	—	—	
14:12:16	65	Zeta Ophiuchi	-114	-113.9	0.498	
14:12:47	80.5	{ Antares Tau Scorpii }	-98.5	-97.8 -96.3	0.795	{ Angle inaccurate owing to mutual interaction of objects
14:16:04	179	Canopus	0	0	3.793	
	—	Iota Orionis	—	48	—	Not identified owing to weak intensity
14:17:49	231.5	{ Alnitak Alnilam Mintaka }	52.5	52.0 52.9 53.9	0.737	{ Objects too close together to distinguish
14:18:03	238.5	Bellatrix	59.5	60.7	0.859	
14:18:31	252.5	Elnath	73.5	83.0	1.904	{ Angles of Elnath and Capella inaccu- rate owing to interaction with high intensity of earth
14:19:04	269	Earth	90	88	4.404	
14:19:28	281	Capella	120	100.6	1.8	
14:20:49	321.5	Polaris	142.5	144.2	0.532	
14:24:16	425	Zeta Ophiuchi	246	246.1	0.502	
14:24:46	440	Antares	261	262.2	0.805	
14:24:59	446.5	Tau Scorpii	267.5	263.7	0.610	
14:27:52	533	Canopus (lock-on)	0			

respectively. The additional midcourse corrections, conducted as a result of the helium leak, were also performed smoothly and spacecraft control was maintained at all times. A summary of all the corrections is contained in Table IV-6.

*e. Gyro drift measurements.* A large number of gyro drift measurements were made during the transit phase to obtain a good value of the gyro drift error for use in terminal maneuver calculations. Eight of these checks were made about all three axes; the other three were roll-axis-only checks. The following drift values (in deg/hr) were used in the terminal maneuver calculations: roll, +0.85; pitch, +0.6; yaw, -0.6.

For the first time on a mission, a 360-deg yaw turn was made several hours before terminal descent to determine the error in turning rate. The measured error was only 0.005 deg/sec, which is within the measurement accuracy, so no correction was applied in making the terminal maneuver. The Canopus roll had indicated no measurable roll rate error.

*f. Nitrogen gas consumption.* The calculated weight of the nitrogen contained in the attitude control system at launch was 4.58 lb, based on a telemetered tank pressure of 4708 psi and a tank temperature of 81.8°F.

Prior to the terminal maneuvers, 3.58 lb of nitrogen remained in the nitrogen tank, based on a pressure of 3122 psi and temperature of 46.3°F. This indicates that slightly in excess of 1 lb of nitrogen was used to perform spacecraft attitude maneuvers and stabilization up until that time in the mission.

*g. Terminal maneuvers and descent.* As in the case of the pre-midcourse maneuvers, an attempt was made to initiate the terminal maneuvers at the limit cycle null points. The first maneuver (+73.9 deg roll) was initiated within about 0.13 deg of null, while the pitch and yaw errors at the start of the second maneuver (+119.5 yaw) was 0.15 deg and 0.07 deg, respectively. The magnitudes of the maneuvers were verified to be as commanded.

The terminal descent sequence was modified from the nominal sequence by earth commands which stored the following magnitudes in flight control: (1) a longer-than-normal delay time of 12.3 sec between AMR *mark* and vernier ignition, and (2) a low total thrust level of  $152 \pm 8$  lb instead of the normal 200-lb level. In addition, a carefully timed tape was used to send earth commands, which overrode the flight control programmer and initiated retro ejection, vernier high thrust, and RADVS control.

Following AMR *mark*, all terminal descent events occurred at very close to predicted times (refer to Table



video signal. Their outputs are continuously summed and differenced. When the sum exceeds a fixed threshold and the difference simultaneously crosses zero with positive slope, the *mark* signal is generated. The sum threshold is set for an extremely low probability of marking on noise (false *mark*) throughout the operating time, while video integration plus a very substantial radar gain margin insures a high probability of marking successfully.

Two separate ground commands, whose timing is controlled, are required to fully activate the AMR. The first signal, called simply *AMR on*, commands on the primary power to the AMR, which includes all internal power except high voltage to the transmitter. The video signal is inhibited from reaching the marking circuits until the second command, thus eliminating any residual probability of false marking on noise during this warmup interval. The second signal, called *AMR enable*, commands on the transmitter high voltage and also removes the video inhibit. This enabling function is timed not only for favorable thermal conditions at the expected marking time but also to preclude premature marking on second-round echoes at much longer ranges.

AMR signals which are telemetered include three digital signals and three analog signals plus analog temperature data. The three digital signals (R-1, R-11, FC-64) are confirmations of on-board discrete events; they confirm, respectively, that prime power has been applied (*AMR on*), that high voltage and video enabling have been applied (*AMR enable*), and that the self-generated slant range trigger (*AMR mark*) has occurred. The three analog signals (besides temperature) are magnetron current (R-12), AGC voltage level (R-14), and late gate detected video voltage level (R-29). The AGC not only confirms receiver response to RF return, but is also useful in evaluating terrain reflectivity. The magnetron current confirms pulsing of the magnetron after *enable*, and is useful primarily as a transmitter failure mode indication. The late gate signal, primarily a receiver failure mode indication, normally confirms presence of gated video signal rising quickly to a peak at the time of *mark* and decaying quickly thereafter.

The AMR mounts in the retro rocket nozzle and is retained by friction clasps around the nozzle flange, with spring washers between the AMR and the flange. When the retro rocket is ignited, the gas generated by the ignitor develops sufficient pressure to eject the AMR from the nozzle. The AMR draws 22-V dc power through a break-

away plug that also carries input commands, the output *mark* signal, and telemetry information.

**b. AMR performance.** AMR performance was normal in all respects during the *Surveyor V* flight. AGC power (Fig. IV-42) remained at the threshold level from *AMR enable* (R-11) until approximately 50 sec prior to *AMR mark* (FC-64), then began increasing steadily and smoothly until *AMR mark* and then ejection. The fact that the AGC voltage remained in the threshold condition for a comparatively long time was due to the low level of the return pulse received which, in turn, was due to the large approach angle  $\theta$  of 46 deg. The threshold condition is normal for the AMR and does not represent a radar malfunction. When the AGC voltage rose out of threshold about 50 sec prior to *AMR mark*, it climbed rapidly to the *mark* signal generation level. The predicted curve does not take into account the AGC threshold condition; thus the predicted AGC voltage differs from the actual performance at signal levels below  $-91$  dbm.

The AMR was clearly pulse-length-limited in elevation and beam-width-limited in azimuth because of the comparatively large approach angle. The pulse-length-limiting condition is inversely proportional to the range cubed—rather than to the range squared as assumed for earlier flights. Predicted power at *mark* was  $-81.37$  dbm, based upon a predicted pulse width of 32.4 msec. The actual signal level at *mark* generation was about  $-81.3$  dbm. The prediction was based upon a lunar power reflection coefficient of  $-14.08$  db at  $\theta = 46$  deg.

AMR power output, as measured by magnetron input current, was normal and steady at an average of 2 W throughout AMR operation.

Temperatures of the AMR were within the expected range and compared favorably with those on the previous missions. Table IV-16 contains the last AMR temperatures telemetered prior to telemetry mode transfer. The listed temperatures are, therefore, representative of AMR temperatures just prior to AMR turn-on.

**Table IV-16. AMR temperatures ( $^{\circ}$ F) just before turn-on**

	<i>Surveyor I</i>	<i>Surveyor III</i>	<i>Surveyor IV</i>	<i>Surveyor V</i>
Antenna, edge	$-187$	$-200$	$-182$	<sup>a</sup>
Antenna, inside rear	$-12$	$0$	$-5$	$-6$
AMR electronics	$+16$	$+17.5$	$+14$	$+22$
<sup>a</sup> Not telemetered on this mission.				

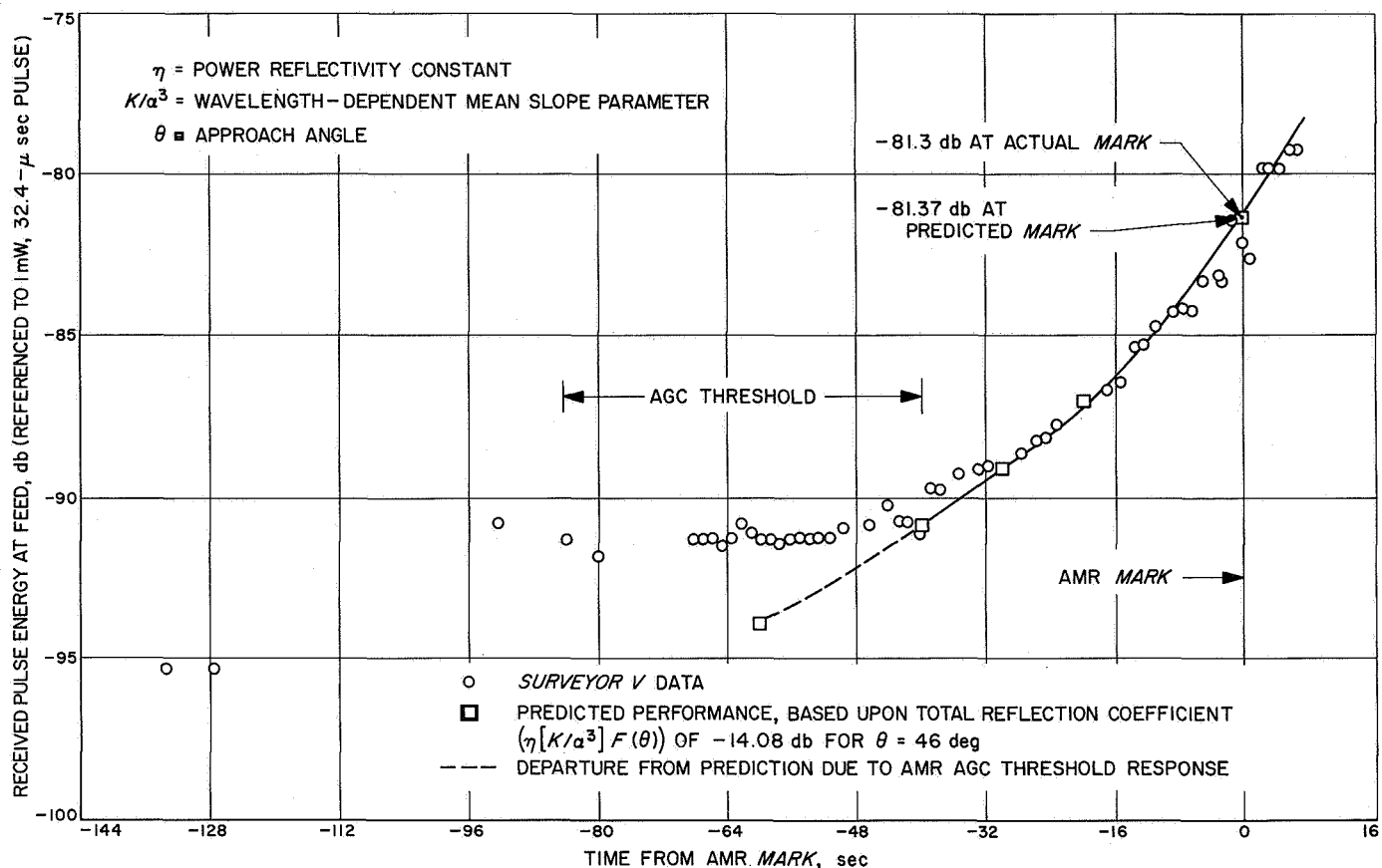


Fig. IV-42. Altitude marking radar AGC

## 2. Radar Altimeter and Doppler Velocity Sensor

The RADVS (Fig. IV-43) functions in the flight control subsystem to provide three-axis velocity, range, and altitude *mark* signals for flight control during the main retro and vernier phases of terminal descent. The RADVS consists of a doppler velocity sensor (DVS), which computes velocity along the spacecraft X, Y, and Z axes, and a radar altimeter (RA), which computes slant range from 40,000 to 13 ft and generates 1000-ft and 13-ft *mark* signals. The RADVS comprises five assemblies: (1) klystron power supply/modulator (KPSM), which contains the RA and DVS klystrons, klystron power supplies, and altimeter modulator, (2) altimeter/velocity sensor antenna, which contains Beams 1 and 4 transmitting and receiving antennas and preamplifiers, (3) velocity sensing antenna, which contains Beams 2 and 3 transmitting antennas and preamplifiers, (4) RADVS signal data converter (SDC), which consists of the electronics to convert doppler shift signals into dc analog signals, and (5) interconnecting waveguide. The RADVS is turned on at about 50 miles above the lunar surface and is turned off at about 13 ft.

*a. Doppler velocity sensor description.* The doppler velocity sensor (DVS) operates on the principle that a reflected signal has a doppler frequency shift proportional to the approaching velocity. The reflected signal frequency is higher than the transmitted frequency for the closing condition. Three beams directed toward the lunar surface enable velocities in an orthogonal coordinate system to be determined. The RADVS beam orientation is shown in Fig. IV-44.

The KPSM provides an unmodulated DVS klystron output at a frequency of 13.3 GHz. This output is fed equally to the DVS 1, DVS 2, and DVS 3 antennas. The RADVS velocity sensor antenna unit and the altimeter velocity sensor antenna unit provide both transmitting and receiving antennas for all three beams. The reflected signals are mixed with a small portion of the transmitted frequency at two points  $\frac{3}{4}$  wavelength apart for phase determination, detected, and amplified by variable-gain amplifiers providing 40, 65, or 90 db of amplification, depending on received signal strength. The preamp output signals consist of two doppler frequencies, shifted



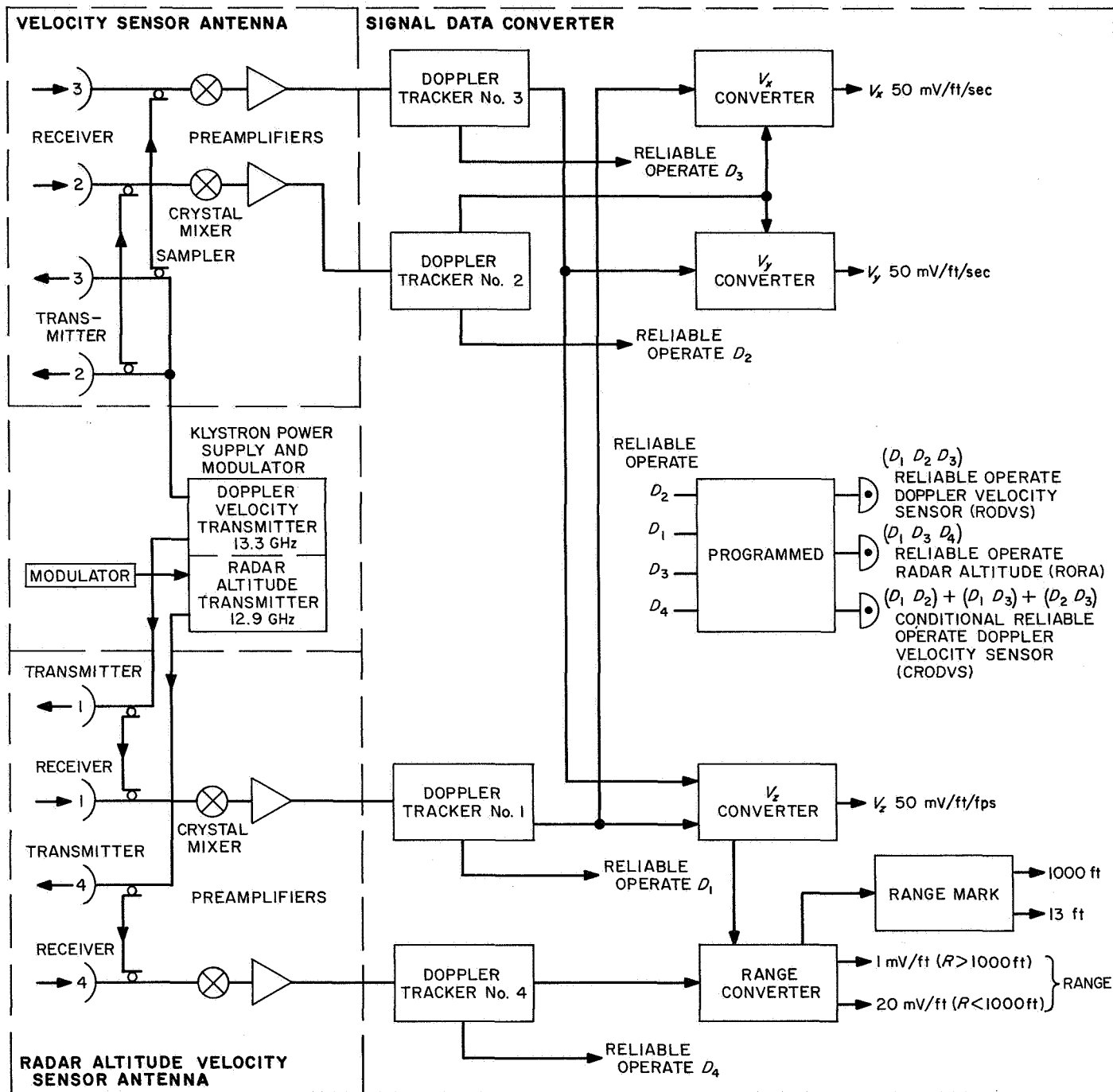


Fig. IV-43. Simplified RADVS functional block diagram

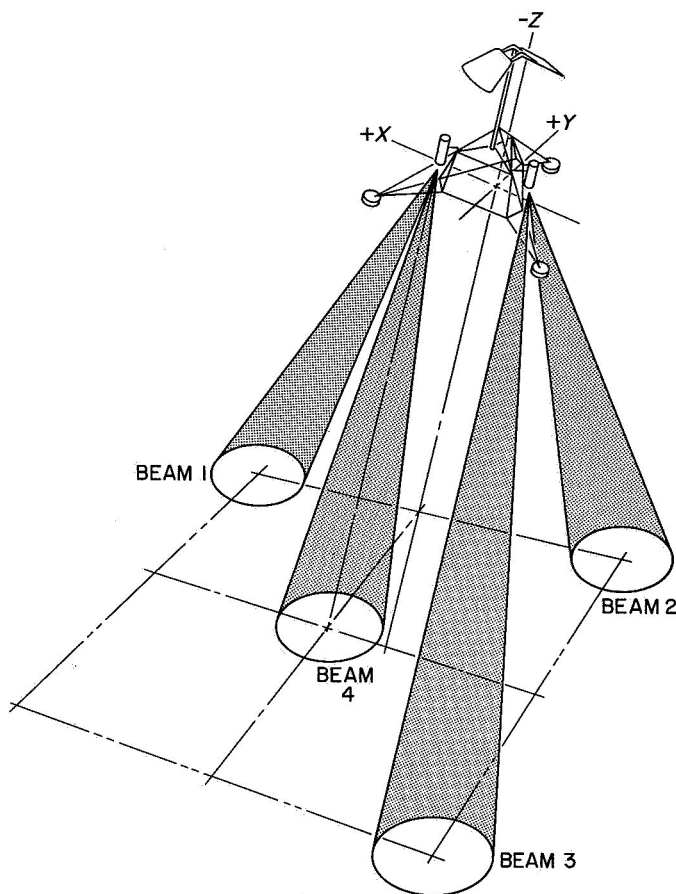


Fig. IV-44. RADVS beam orientation

by  $\frac{3}{4}$  transmitted wavelength, and preamp gain-state signals for each beam. The signals are routed to the trackers in the RADVS signal data converter.

The D1 through D3 trackers in the signal data converter are similar in their operation. Each provides an output which is 600 kHz plus the doppler frequency for approaching doppler shifts. If no doppler signal is present, the tracker will operate in search mode, scanning frequencies between 82 kHz and 800 Hz before retro burnout, or between 22 kHz and 800 Hz after retro burnout. When a doppler shift is obtained, the tracker will operate as described above and initiate a lock-on signal. The tracker also determines amplitude of the reflected signal and routes this information to the signal processing electronics for telemetry.

The velocity converter combines tracker output signals  $D_1$  through  $D_3$  to obtain dc analog signals corresponding to the spacecraft X, Y, and Z velocities;  $D_1 + D_3$  is also sent to the altimeter converter to compute range.

Reliability and reference circuits produce a *reliable operate doppler velocity sensor* (RODVS) signal if  $D_1$  through  $D_3$  lock-on signals are present beginning about 3 sec after main retro burnout. The RODVS signal is routed to the flight control electronics and to the signal processing electronics telemetry. The system is designed to produce a *conditional reliable operate doppler velocity sensor* (CRODVS) signal if only one or two, rather than all three, of the DVS beams are in lock. If the CRODVS signal occurs, the spacecraft will steer into the un-locked beam(s) to achieve lock-on of all beams and generation of RODVS. For *Surveyor IV* and later missions, the period of time that CRODVS was enabled has been extended to the 1000-ft mark to facilitate landings at increased approach angles. On earlier missions, CRODVS was disabled 1 sec after the three velocity trackers had achieved lock. When CRODVS is inhibited, the spacecraft switches to inertial attitude hold if beam lock is lost. Availability of CRODVS to 1000-ft altitude allows spacecraft maneuvering to reacquire lock, thus assuring greater probability of maintaining the programmed descent profile.

Cross-coupled sidelobe logic (CCSLL) is provided in the signal data converter to protect against false lock-on by a tracker of a sidelobe from another beam. The logic compares amplitude and frequencies between beams and breaks lock if the amplitude and bandwidth characteristics indicate that a cross-coupled sidelobe is being tracked. Prior to *Surveyor IV*, spacecraft had CCSLL provisions only for Beams 2 and 3. Later spacecraft have been provided with CCSLL between Beams 1, 2, and 3. Also, on the later spacecraft, the CCSLL has been disabled below 1000-ft altitude because the CCSLL is most effective at higher altitudes and may produce erroneous outputs near the lunar surface.

**b. Radar altimeter description.** Slant range is determined by measuring the reflection time delay between the transmitted and received signals. The transmitted signal is frequency-modulated at a changing rate so that return signals can be identified.

The RF signal is radiated, and the reflected signal is received by the altimeter/velocity sensor antenna. The received signal is mixed with two samples of transmitted energy  $\frac{3}{4}$  wavelength apart, detected, and amplified by 40, 60, or 80 db in the altimeter preamp, depending on signal strength. The signals produced are difference frequencies resulting from the time lag between transmitted and received signals of a known shift rate, coupled with an additional doppler frequency shift because of the spacecraft velocity.

The altimeter tracker in the signal data converter accepts doppler shift signals and gain-state signals from the altimeter/velocity sensor antenna and converts these into a signal which is 600 kHz plus the range frequency plus the doppler frequency. This signal is routed to the altimeter converter for range dc analog signal generation.

The range mark, reliability, and reference circuits produce the 1000-ft *mark* signal and the 13-ft *mark* signal from the *range* signal generated by the altimeter converter where the doppler velocity  $V_z$  is subtracted giving the true range.

The *range mark* and *reliable operate radar altitude* (RORA) signals are routed to flight control electronics. The signals are used to rescale the *range* signal, for vernier engine shutoff and to indicate whether or not the *range* signal is reliable. The RORA signal is also routed to signal processing for transmission to DSIF.

**c. RADVS performance.** On the *Surveyor V* mission, the RADVS performed very satisfactorily throughout the terminal descent sequence, which was modified to lower the main retro ignition (and burnout) altitude and shorten the RADVS-controlled phase. The shorter RADVS-controlled phase was required because of the helium leak, which reduced the total impulse that could be obtained from the vernier propulsion system.

The RADVS was turned on automatically for warmup 14 sec after the AMR 60-mile *mark* signal started the flight control programmer automatic sequence. Internal circuits in the RADVS then automatically applied high voltage to the DVS and altimeter transmitters 22.1 sec after RADVS turn-on. The velocity beam trackers locked on the reflected signals about 5 sec after RADVS high voltage turn-on to produce the *reliable operate* DVS signal. The altimeter tracker locked on after an additional 3.5 sec.

As a result of an earth command, which over-rode the automatic flight control sequence to produce an earlier than normal retro ejection, the RADVS-controlled descent phase was started only 11 sec (instead of the standard 14 sec) after retro burnout. The time from start of the RADVS-controlled descent until touchdown was only about 62 sec compared to a normal time of 135 sec. Spacecraft range decreased smoothly (Fig. IV-45), although Altimeter Beam 4 and Velocity Beam 3 trackers lost lock about 1 and 2½ sec, respectively, after retro case ejection.

This was apparently due to passing of the retro case through the beams and resulted in loss of the *reliable operate radar altimeter* (RORA) signal for about a 7-sec interval, during which time the RADVS switched to the *conditional reliable operate doppler velocity sensor* (CRODVS) signal and steered to reacquire beam lock. Resumption of RORA occurred upon beam relock. Acquisition of the descent contour Segment 3 (Fig. IV-9), which had been programmed in the spacecraft, was achieved 40 sec after start of RADVS control, when the spacecraft slant range from the lunar surface was only about 800 ft. After intercept of the descent contours, the RADVS controlled the spacecraft to closely follow the programmed range and velocity profile.

Reflectivity of the RADVS beam is shown in Fig. IV-46 in terms of IF amplifier output power level below telemetry saturation. The preamp gain state is also shown below the curve for each beam. Curves of the average reflectivity of *Surveyor III* are also shown for comparison. *Surveyor I* and *III* results were very similar. Evaluation of the data for the period of time prior to 30 sec before touchdown is difficult because of uncertainties in spacecraft attitude. However, the *Surveyor V* data shows close correlation with that of *Surveyor III* beginning 30 sec before touchdown, by which time the spacecraft had approached a vertical attitude and was undergoing relatively small attitude changes. Considerable care must also be exercised in evaluating points near gain switching because telemetry sampling of gain state is done less often (once every 1.2 sec) than sampling of reflectivity (once every 0.6 sec), and because the telemetry time constants are long enough so that data is unreliable near a gain switch. As was the case with *Surveyors I* and *III*, the fluctuation of Altitude Beam 4 reflectivity was much more pronounced than the data for the velocity beams. This was particularly true at lower altitudes where the spacecraft attitude was nearly vertical, and was due to the spectral nature of the beam.

The four beams were in saturation during the last few seconds of *Surveyor V* descent. This condition was also noted on previous missions and was expected. During the last few seconds there was some switching to Gain State 3, which also followed the pattern seen in previous landings. This condition occurs because the low spacecraft velocity near the lunar surface results in low doppler frequency of the return signal, and the preamplifier gain is less at low frequency (low-frequency rolloff). Under this condition, the gate matrix in the antennas switches to a higher gain state.

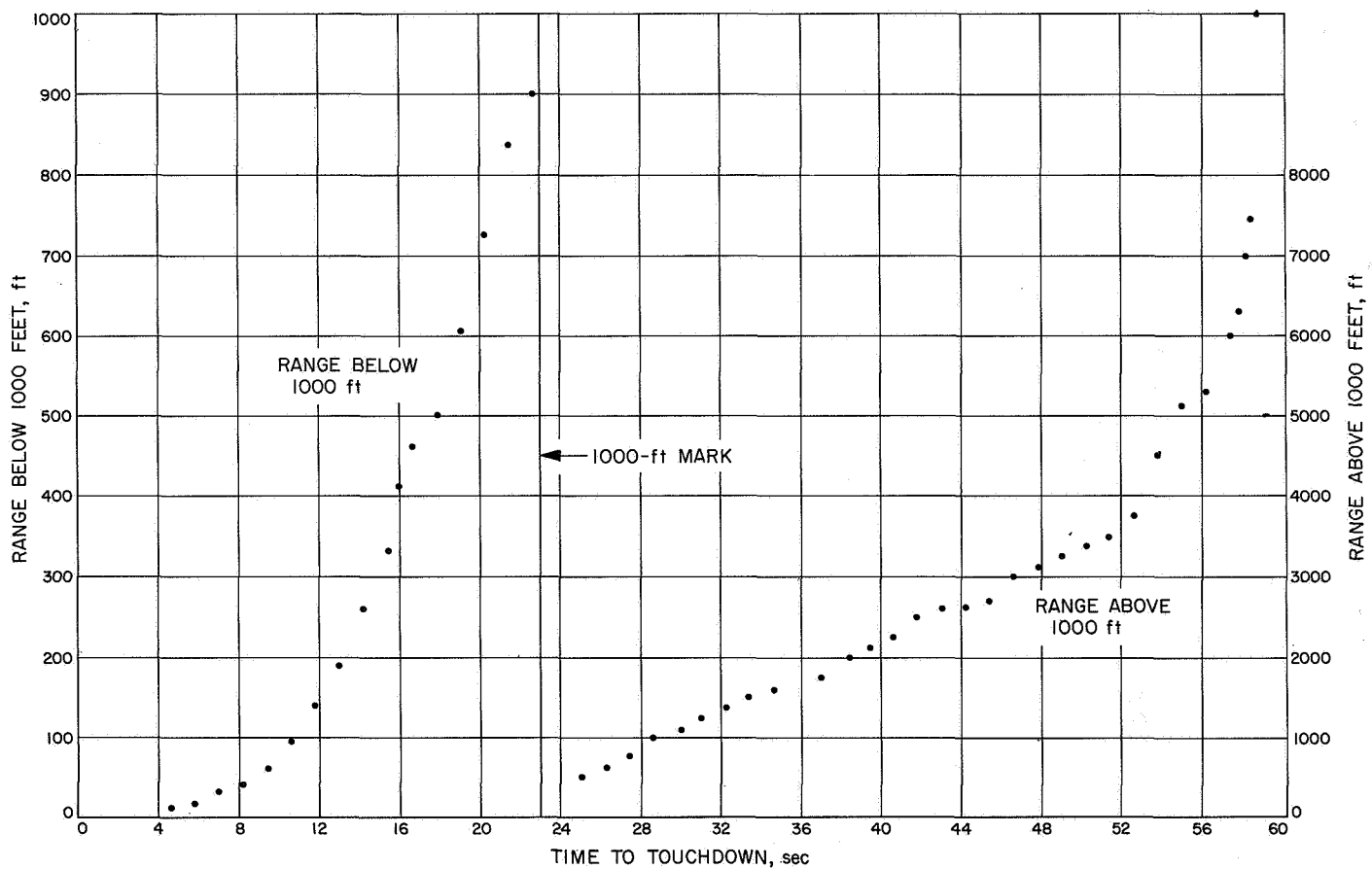


Fig. IV-45. Slant range vs time during terminal descent

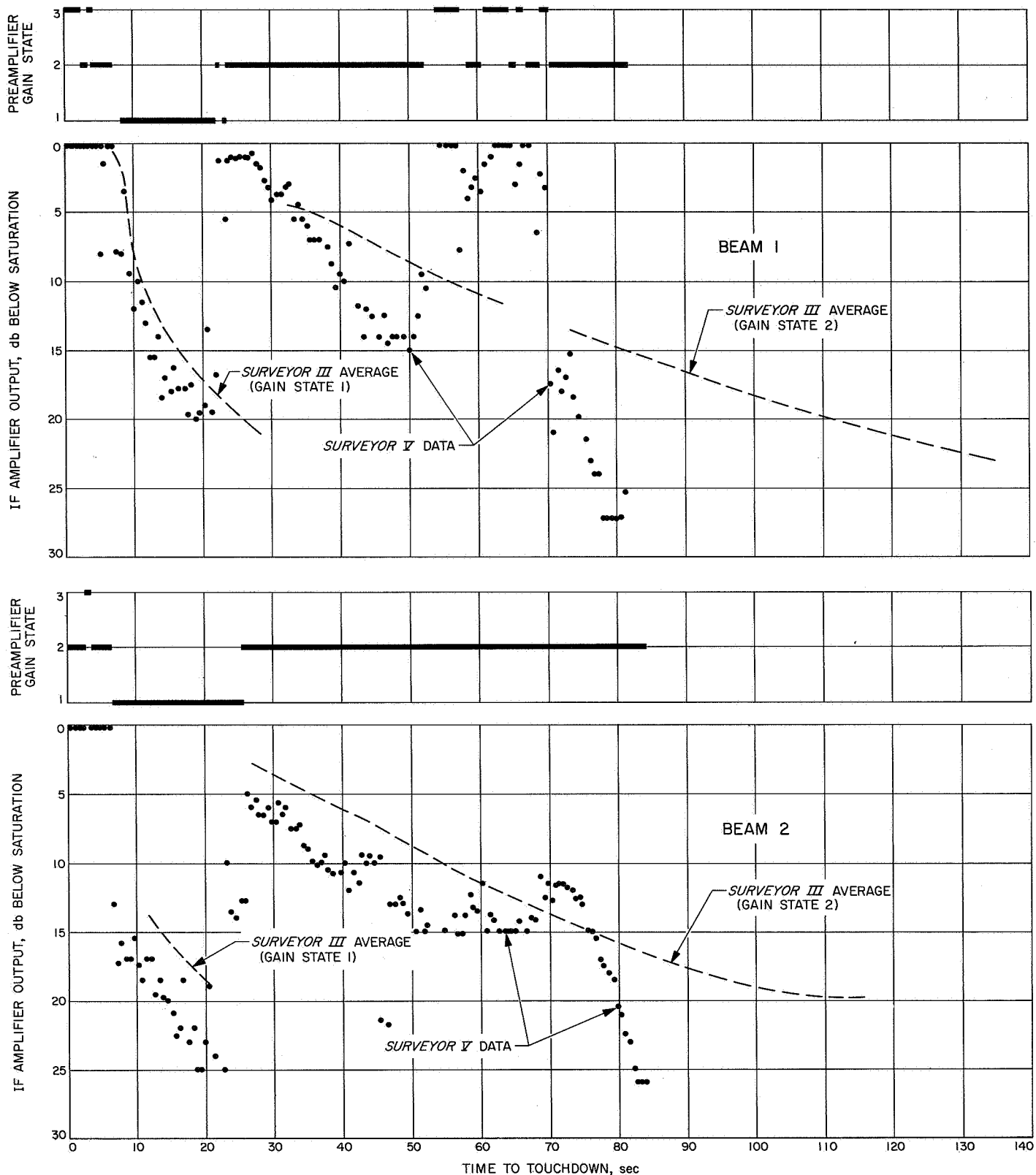


Fig. IV-46. Reflectivity of RADVS beams during terminal descent

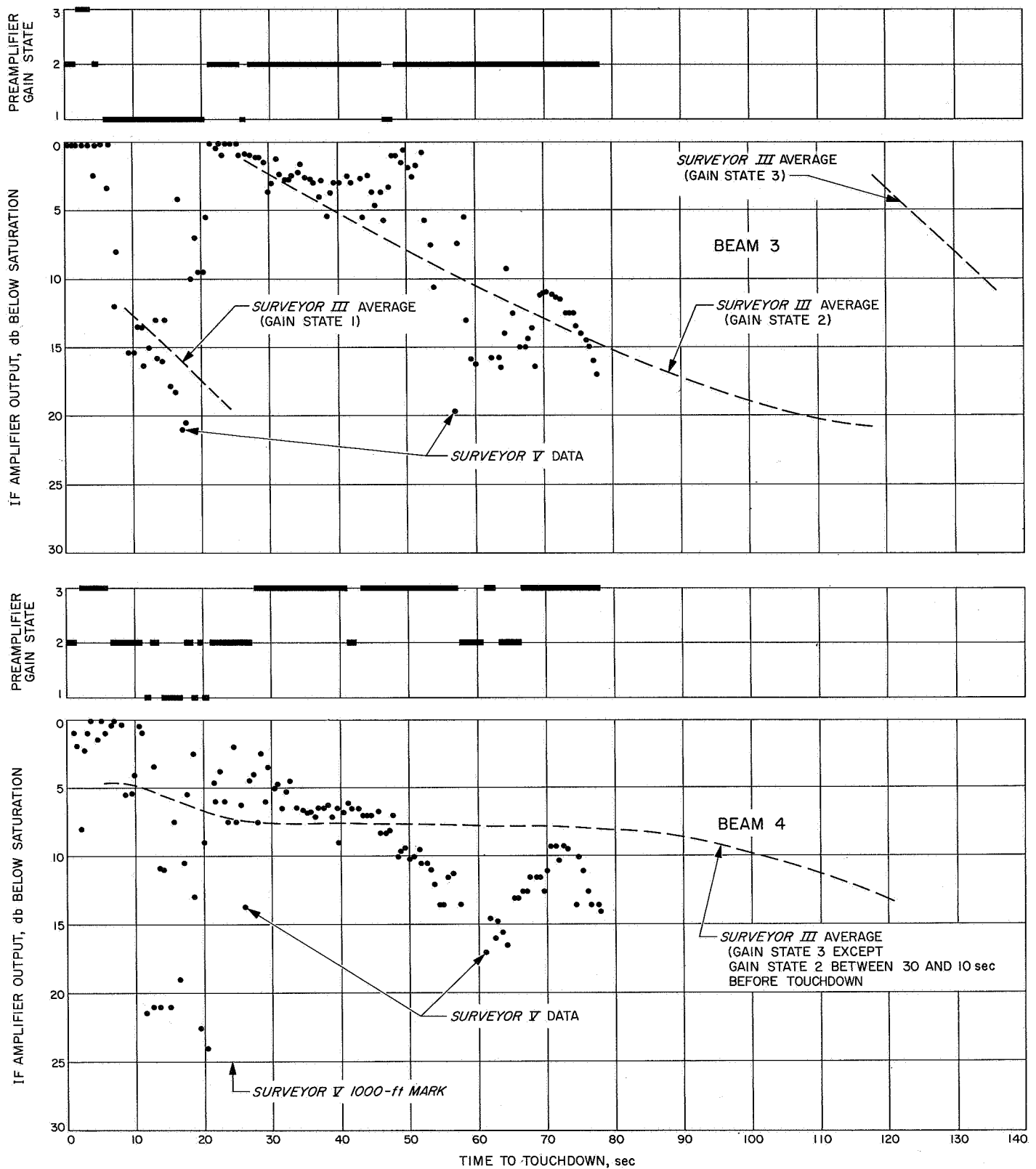


Fig. IV-46 (contd)

Figures IV-47 through IV-49 present plots of the velocity components along each of the spacecraft axes during terminal descent. As can be seen in Fig. IV-49, the longitudinal velocity component  $V_z$  came out of saturation (800 ft/sec) about 73 sec before touchdown. As a consequence of the lighter than normal spacecraft,  $V_z$  dropped very rapidly during the main retro phase and reached approximately 50 ft/sec at the beginning of RADVS control. As shown in Fig. IV-47, the X-component

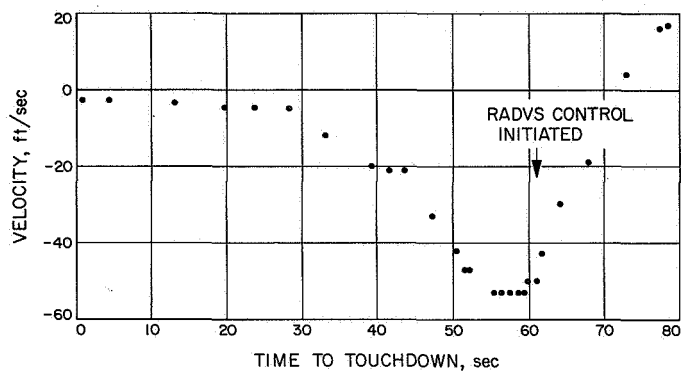


Fig. IV-47. X-component of velocity  $V_x$  during descent

of lateral velocity  $V_x$  increased to about 60 ft/sec before RADVS control, after which it decreased smoothly. The velocity component  $V_y$  (Fig. IV-48) was smaller at the

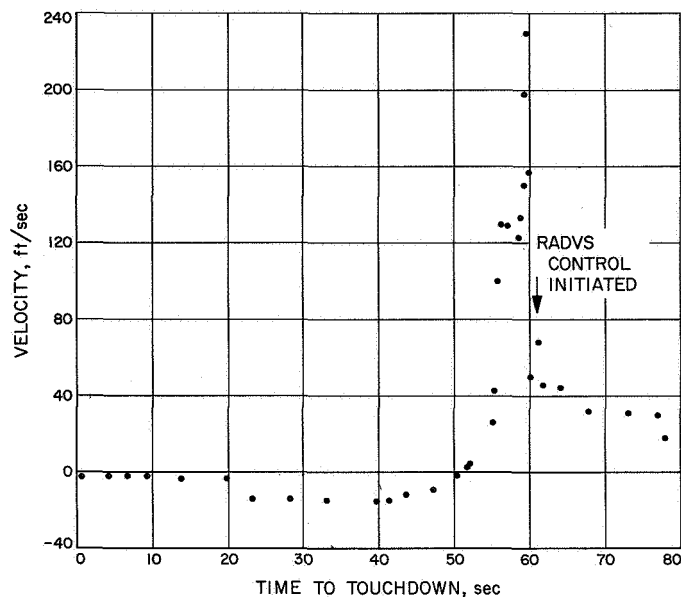


Fig. IV-48. Y-component of velocity  $V_y$  during descent

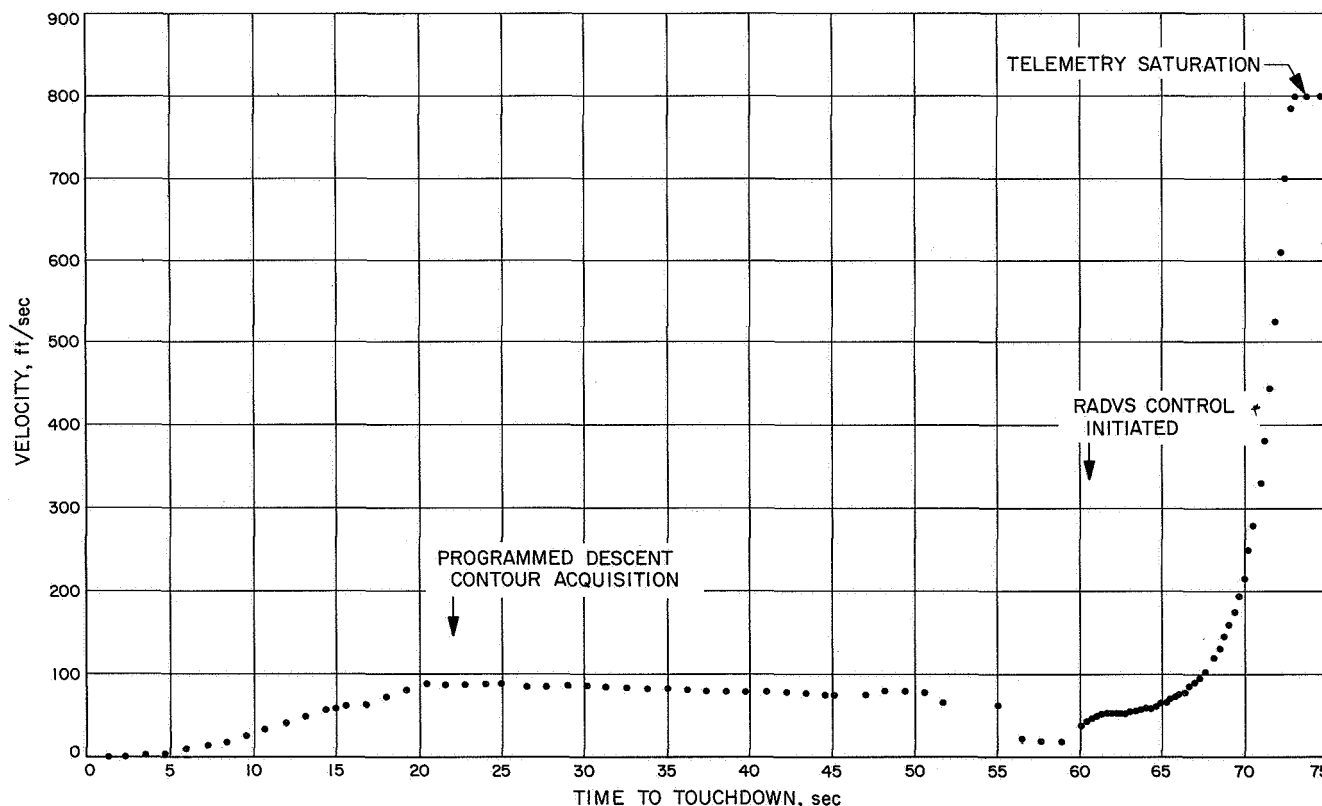


Fig. IV-49. Z-component of velocity  $V_z$  during descent



start of RADVS control, but the data indicated a sharp and unexpected increase to about 230 ft/sec about 4 sec after retro case ejection. Erratic behavior of the  $V_z$  signal was also noted during this time. (However, the anomalous  $V_z$  signal was not transmitted to flight control because RADVS was switched to CRODVS.) The explanation for the anomalous behavior of the  $V_y$  and  $V_z$  components is believed to be that the Beam 3 tracker locked on the retro case. If the case passed through the beam, it would have produced a low and increasingly negative doppler frequency, which the tracker could have locked onto because the tracker had lost lock and was searching in the lower end of its frequency sweep. The velocity components  $V_y$  and  $V_z$  did change in the direction which would be expected if case lock-on had occurred. Some shift in  $V_y$  may also have been due to the fact that the RADVS had switched to CRODVS, owing to loss of the beam lock, and was steering to reacquire the signals. Upon resumption of RORA,  $V_z$  had increased to 75 ft/sec and continued to increase slowly until it reached 87 ft/sec at 22 sec before touchdown, when the programmed descent contour was intercepted. It then decreased slowly

to about 5 ft/sec at the 13-ft mark. The final touchdown velocities of  $V_x$  and  $V_z$  were approximately zero.

## H. Telecommunications

The *Surveyor* telecommunications subsystem contains radio, signal processing, and command decoding equipment to provide (1) a method of telemetering information to the earth, (2) the capability of receiving and processing commands to the spacecraft, and (3) angle-tracking one- or two-way doppler for orbit determination.

### 1. Radio Subsystem

The radio subsystem utilized on the *Surveyor* spacecraft is shown schematically in Fig. IV-50. Dual receivers, transmitters, and antennas were originally meant to provide redundancy for added reliability. As presently mechanized, this is not completely true owing to switching limitations. Each receiver is permanently connected to its corresponding antenna and transmitter. The transmitters, which are capable of operation in two different

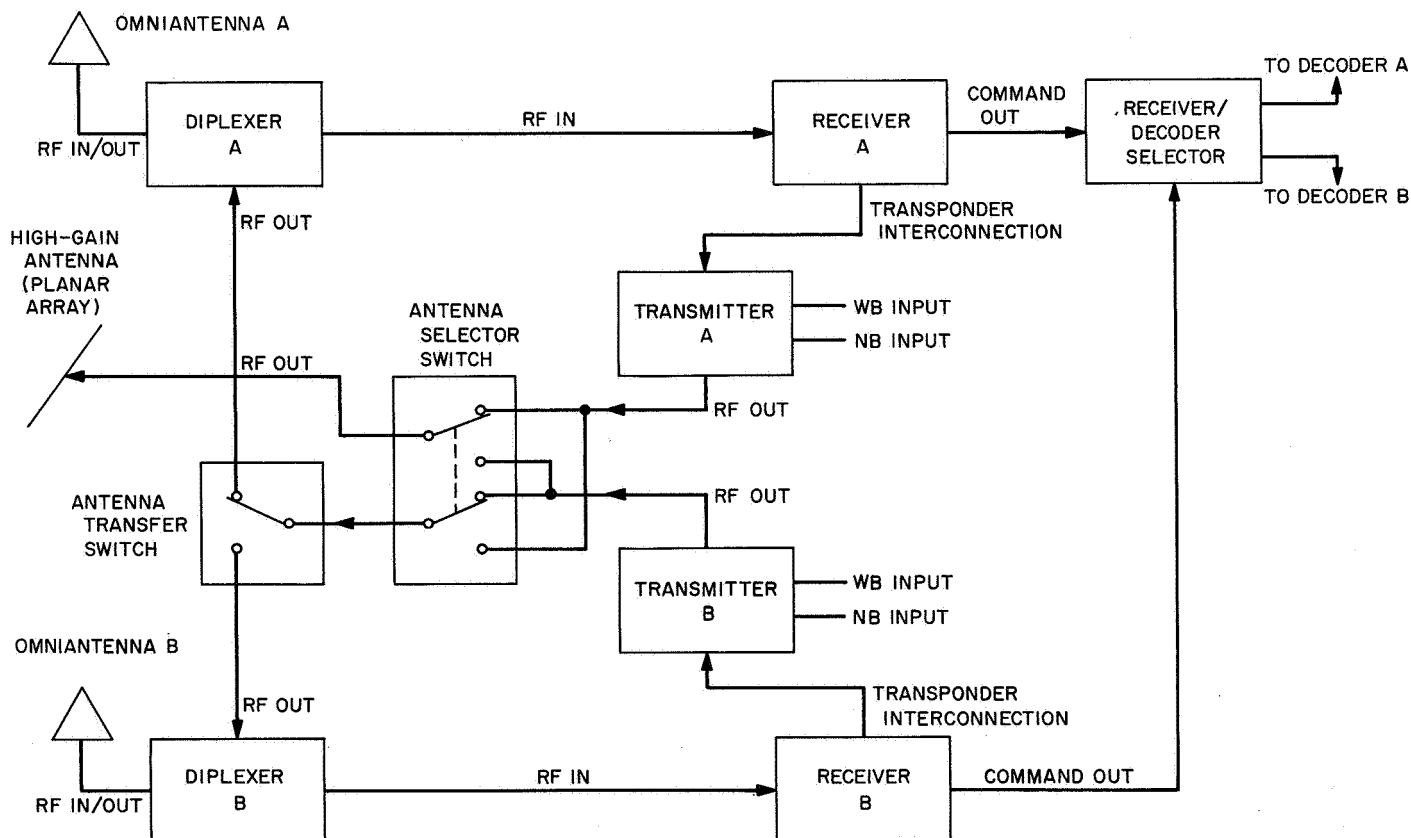


Fig. IV-50. Radio subsystem block diagram

power modes (100-mW low power, and 10-W high power), can each be commanded to transmit through any of the three antennas. The *Surveyor* radio system operates at S-band, 2295-MHz down-link, and 2113-MHz up-link.

**a. Receivers.** Both receivers are identical, crystal-controlled, double-conversion units, which operate continuously as they cannot be commanded off. Each unit is capable of operation in an automatic frequency control (AFC) mode, or an automatic phase control (APC) mode. The receivers provide two necessary spacecraft functions: the detection and processing of commands from the ground stations for spacecraft control (AFC and APC modes), and the phase-coherent spacecraft-to-earth signal required for doppler tracking (APC mode).

**b. Transmitters.** Transmitters A and B are identical units which provide the spacecraft-to-earth link for telemetry and doppler tracking information. The transmitters are commanded on, one at a time, from the ground stations. Each unit contains two crystal-controlled oscillators, wideband for TV and scientific information, narrowband for engineering data. Either unit can be commanded on at will, and, in addition, can operate from the receiver voltage-controlled oscillator (transponder mode) when coherent signals are required for two-way doppler tracking. The transmitters may be commanded to operate through any one of the spacecraft antennas as desired, and both are capable of providing either 100 mW or 10 W of output power.

**c. Transponders.** Two identical transponder interconnections permit each transmitter to be operated, on command, in a transponder mode. In the transponder mode, a transmitter is operated with the corresponding receiver voltage-controlled oscillator to provide coherent signals when two-way doppler tracking data is required.

**d. Antennas.** Three antennas are utilized on the *Surveyor* spacecraft. Two antennas are omnidirectional units which provide receive-transmit capability for the spacecraft. The third antenna is a high-gain, 27-db directional planar array used for transmission only of wide-band information.

**e. Radio subsystem performance.** The radio subsystem performed well during the *Surveyor V* mission and gave no indication of abnormal behavior. The transmitter went to high power upon command from the *Centaur* shortly before spacecraft separation. The spacecraft was acquired

by DSS 51, Johannesburg, about 33 min after liftoff, and the transmitter was commanded to low power after operating in the high-power mode about 21 min. During the initial coast phase, the inertially held attitude of the spacecraft X- and Y-axes caused the down-link signal to be lower than nominal when transmitting via Omni-antenna B. Therefore, at approximately 4 hr after launch, Transmitter B was commanded to transmit on Omni-antenna A. This change resulted in much stronger down-link signals. Transmitter B continued to transmit on Omni-antenna A until transfer to Omni-antenna B was effected a few minutes before the Canopus acquisition roll maneuver was commanded. The spacecraft continued transmitting on Omni-antenna B for the remainder of the mission.

Canopus lock was obtained about 6½ hr after launch. The up-link antenna pattern for Receiver B during the Canopus roll is shown in Fig. IV-51. The measured and predicted antenna patterns followed each other within expected tolerances. Peaks and nulls of the predicted and measured signal strength did not correspond exactly and resulted in a maximum deviation of approximately 6 db. The signal strength varied over a range of about 25 db during the roll maneuver.

Receiver A/Omni-antenna A performance for the flight is plotted in Fig. IV-52. In general, the signal strength to Receiver A was above the predicted level. The signal level varied up and down, as evidenced in Fig. IV-52. The larger variations can be identified with gyro drift checks and were expected because of the operating region within the omni-antenna pattern.

Receiver B/Omni-antenna B performance for the flight is plotted in Fig. IV-53. Prior to Canopus lock, received signal strength was considerably lower than predicted, as is evidenced in the large deviations shown graphically in the figure. As explained above, these large variations were due to spacecraft orientation. Prior to Canopus lock, the predicted signal strength is not expected to be valid and the large deviation between predicted and measured signal strength is of no concern. After Canopus lock, the received signal strength remained 4 to 5 db below the predicted levels. This differential is not understood at this time. However, similar variations have been noted on preceding flights. The cause of the difference is under investigation. The received signal strength remained well above the command threshold level of -114 dbm, and no difficulty in commanding the spacecraft was experienced during the entire transit to the moon.

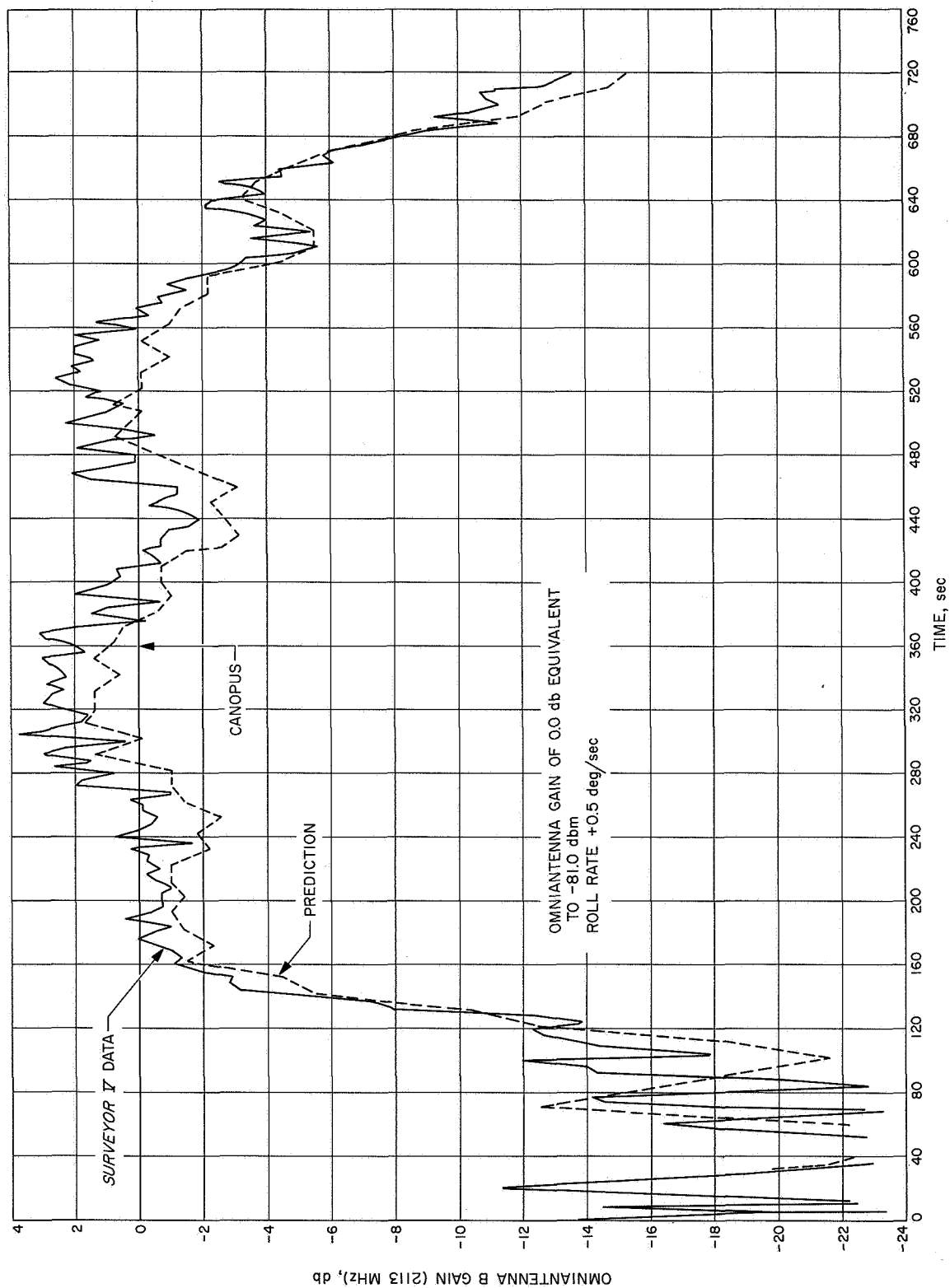


Fig. IV-51. Spacecraft Receiver B signal level during star verification/acquisition roll

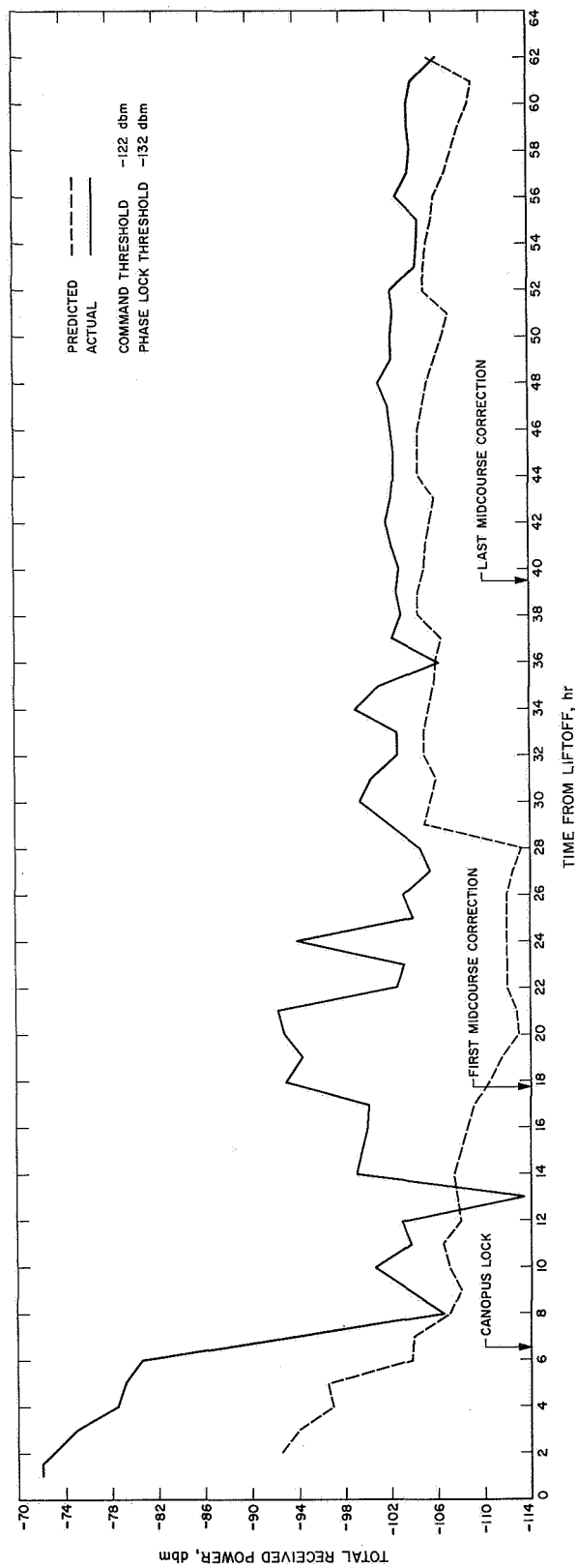


Fig. IV-52. Receiver A/Omniantenna A total received power during transit

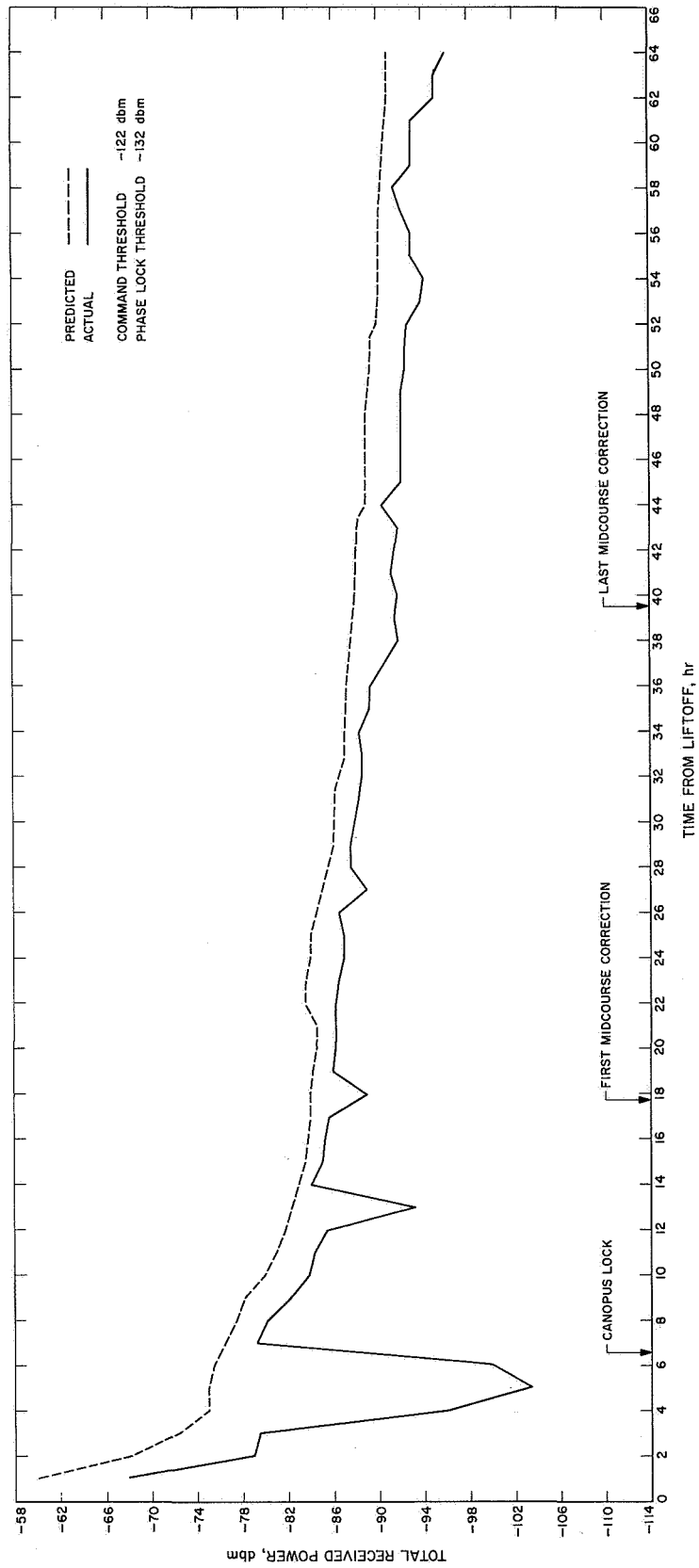


Fig. IV-53. Receiver B/Omniantenna B total received power during transit

A plot of down-link signal strength vs the predicted signal strength is shown in Fig. IV-54. Except for a short 2-hr period beginning 12 hr after liftoff and for the period of Canopus acquisition roll, predicted and measured signal levels remained within 1 db of each other. The 2-hr period mentioned above was experienced during a time when DSS 72, Ascension, was tracking the spacecraft. This station is equipped with a 30-ft parabolic antenna, and corresponding reduction in signal strength from that of the normal 85-ft DSIF antennas is expected. Toward the end of the transit phase, the down-link signal was slightly higher than the predicted value.

A summary of telecommunications performance values during the transit phase is presented in Table IV-17.

About 23 min after the *Surveyor V* spacecraft landed, Transmitter B high voltage was commanded off, high power having been on for about 78 min to insure adequate signal level during the entire terminal maneuver, descent, and postlanding interrogation phase. An 18.6-db decrease was observed between the high- and low-power modes, and good PCM data could not be obtained by DSS 11 in the low-power mode at the 137.5 bit/sec data rate. Transmitter A was turned on (for the first time since the prelaunch countdown) in high power, yielding a signal level of  $-127.4$  dbm at 1100 bit/sec. The DSIF received signal level increased by 4.8 db when Omni-antenna A was selected. The low signal level received via Omni-antenna B and the higher level obtained with Omni-antenna A had not been expected prior to terminal descent. However, the spacecraft tilt of about 20 deg on the lunar surface was in excess of that used in the prediction analysis.

A spacecraft telecommunications performance assessment was made with DSS 42 providing support. This assessment essentially exercises the system in all possible transmitting and command receiving configurations. It was clearly evident from assessment results that the subsystem was performing nominally in every respect.

In preparation for the vernier static firing which was performed on September 13, the A/SPP was repositioned with the Omni-antenna A up-link gain measuring  $-7.4$  db before and  $-8.4$  db after positioning. During the A/SPP stepping, 3- to 4-db peak-to-peak variations in spacecraft received AGC were noted. The fact that the measured gain was lower than the expected antenna gain of  $-1$  to  $-6$  db is attributed to the effect on the antenna pattern of the relative positioning of the solar panel and planar array, although the spacecraft-earth vector was such that there was no line-of-sight interference by the

solar panel. Spacecraft movement during firing was indicated by a shift in signal level of approximately 1 db, as indicated by both the spacecraft receiver AGC and the DSIF AGC. The firing time was so short (0.55 sec) that plume effects were neither expected nor observed.

On six different occasions during the lunar day, special telecommunications frequency tests were conducted with the support of DSS 61 and DSS 42. The purpose of the frequency test is to investigate the effects of temperature on the frequency characteristics of the spacecraft transmitters and receivers in the deep space environment. The approximate range of spacecraft receiver temperatures over which the tests were run was about 40 to 110°F. Analysis of the data is not complete. However, preliminary results show the data to be consistent with the *Surveyor IV* data taken during transit, and indicate completely normal operation of the *Surveyor V* RF system during lunar operations.

## 2. Signal Processing Subsystem

The *Surveyor* signal processing subsystem accepts, encodes, and prepares for transmission voltages, currents, and resistance changes corresponding to various spacecraft parameters such as events, voltages, temperatures, and accelerations.

The signal processor employs both pulse code modulation (PCM) and amplitude-to-frequency modulation telemetry techniques to encode spacecraft signals for frequency modulation (FM) or phase modulation (PM) of the spacecraft transmitter signals, and for recovery of these signals by the ground telemetry equipment. A simplified block diagram of the signal processor is shown in Fig. IV-55.

The input signals to the signal processor are derived from various voltage or current pickoff points within the other subsystems as well as from standard telemetry transducing devices such as strain gages, temperature transducers, and pressure transducers. These signals generally are conditioned to standard ranges by the originating subsystem so that a minimum amount of signal conditioning is required by the signal processor.

As illustrated in Fig. IV-55, some of the signal inputs are commutated to the input of the analog-to-digital converter (ADC) while others are applied directly to sub-carrier oscillators. The measurements applied directly are accelerometer and strain gage measurements which require continuous monitoring over the short intervals in which they are active.

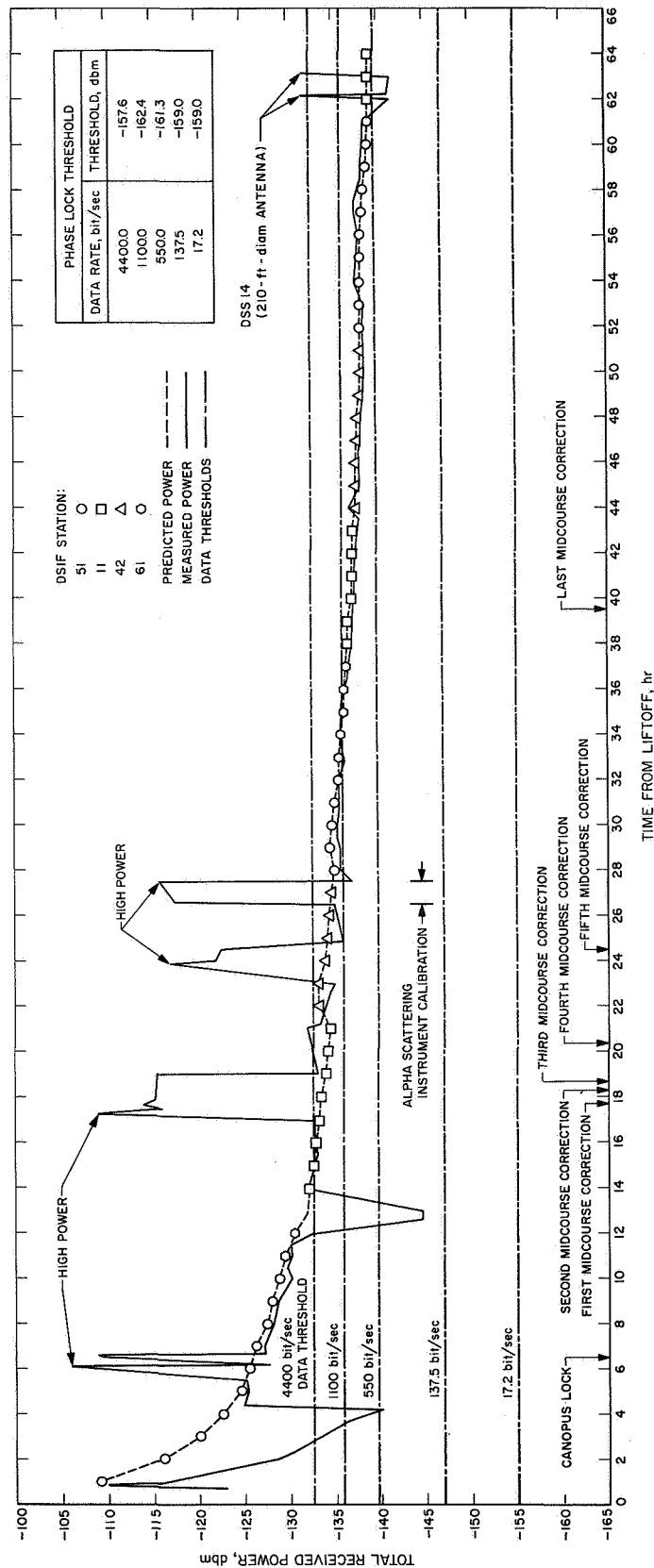


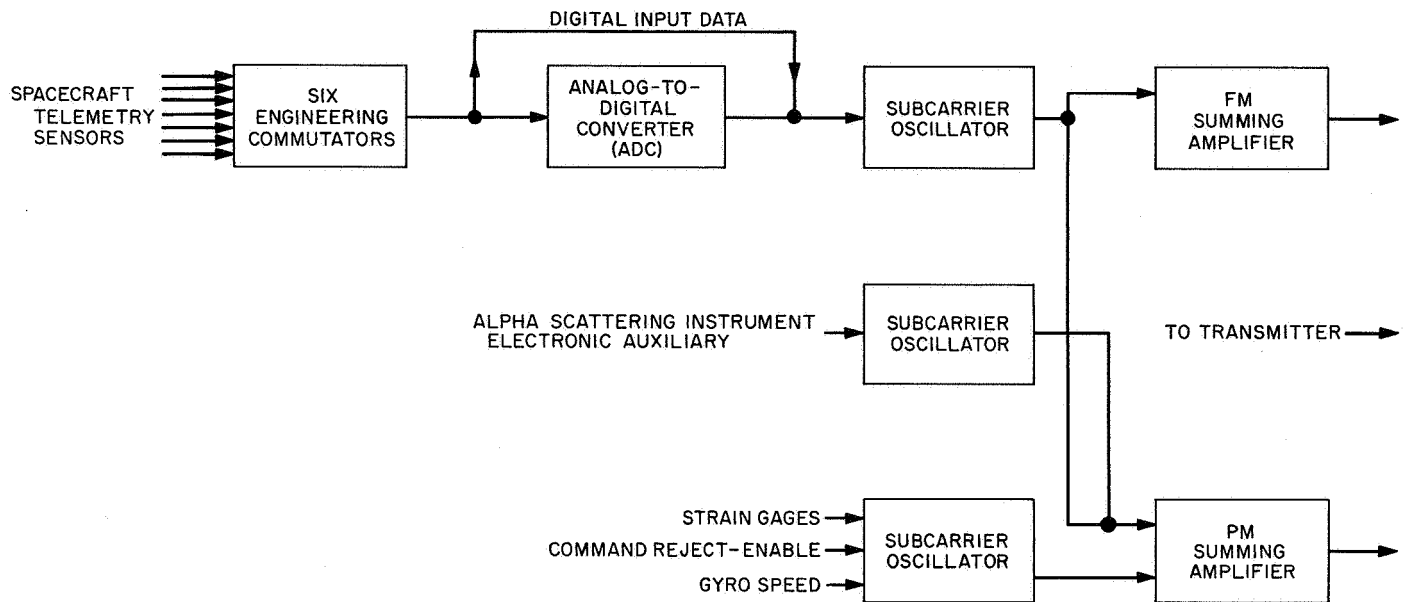
Fig. IV-54. DSIF received power during transit



Table IV-17. Telecommunications performance values<sup>a</sup> during transit

Mission phase	Parameter	Predicted		Observed
		Worst case	Nominal	
Coast (low power)	Bit error rate: for 1100 bit/sec for 550 bit/sec	$3 \times 10^{-3}$ at L + 17:00 $3 \times 10^{-3}$ at L + 40:00	$3 \times 10^{-3}$ at L + 32:00 $3 \times 10^{-3}$ at lunar distance	$1.1 \times 10^{-3}$ at L + 25:25 $0.9 \times 10^{-3}$ at lunar distance
	Spacecraft Receiver A input at lunar distance			
	Signal level, dbm	-114.0	-106.5	-106.0
	Command margin, db	0.0	7.5	8
	Spacecraft Receiver B input at lunar distance			
	Signal level, dbm	-95.4	-92.4	-96.0
	Command margin, db	18.6	21.6	18
	Star acquisition roll (4400 bit/sec, high power)			
	Spacecraft Receiver B phase lock	Continuous	Continuous	Continuous
	Duration of poor telemetry, sec	$\approx 160$		$\approx 80$
	Loss of star data	none	none	none
	Carrier signal level at Canopus lock, dbm	-121.3	-116.3	-116.4
First midcourse: roll	Carrier signal level variation, db		2.8	3.3
	Minimum PCM margin, db		15.2	17.0
	yaw			
	Carrier signal level variation, db		1.7	2.4
	Minimum PCM margin, db		15.8	17.4
	thrust			
	Carrier signal level variation, db			0.2
	Minimum PCM margin, db			19.3
Second midcourse: thrust	Carrier signal level variation, db			0.4
	Minimum PCM margin, db			17.2
Third midcourse: yaw	Carrier signal level variation, db		10.0	10.9
	Minimum PCM margin, db		5.8	9.4
	thrust			
	Carrier signal level variation, db			0.7
	Minimum PCM margin, db			8.7
	Sixth midcourse: roll			
	Carrier signal level variation, db		8.0	7.0
	Minimum PCM margin, db		5.4	6.5
	yaw			
	Carrier signal level variation, db		10.0	10.0
	Minimum PCM margin, db		3.7	5.9
	thrust			
	Carrier signal level variation, db			1.4
	Minimum PCM margin, db			15.9
Terminal (1100 bit/sec, high power)	Roll			
	Carrier signal level variation, db			3.6
	Minimum PCM margin, db		6.2	6.5
	Yaw			
	Carrier signal level variation, db			3.6
	Minimum PCM margin, db		5.6	6.5
Before ignition	Carrier signal level, dbm		$-129.0 \pm 2.0$	-127.9
	During descent			-2.5
	Minimum PCM margin with strain gages on, db			
	Touchdown			
	Carrier signal level, dbm		$-127.0 \pm 2.0$	-131.5
	Minimum PCM margin with strain gages on, db			-0.3

<sup>a</sup>All signal levels and margins are relative to an 85-ft DSIF antenna. Adjustment for the DSS 14 210-ft antenna is +7.5 db minimum.



**Fig. IV-55. Simplified signal processing functional block diagram**

The commutators apply the majority of telemetry input signals to the ADC, where they are converted to a digital word. Binary measurements such as switch closures or contents of a digital register already exist in digital form and are therefore routed around the ADC. In these cases, the commutator supplies an inhibit signal to the ADC and, by sampling, assembles the digital input information into 10-bit digital words. The commutators are comprised of transistor switches and logic circuits which select the sequence and number of switch closures. There are six engineering commutator configurations (or modes) used to satisfy the telemetry requirements for the different phases of the mission and one TV commutator configuration located in the TV auxiliary. The content of the telemetry modes is presented in Appendix C.

The ADC generates an 11-bit digital word for each input signal applied to it. Ten bits of the word describe the voltage level of the input signal, and the eleventh bit position is used to introduce a bit for parity checking by the ground telemetry equipment. The ADC also supplies commutator advance signals to the commutators at one of five different rates. These rates enable the signal processor to supply telemetry information at 4400, 1100, 550, 137.5, and 17.2 bit/sec. The bit rates and commutator modes are changed by ground commands.

The subcarrier oscillators are voltage-controlled oscillators used to provide frequency multiplexing of the

telemetry information. This technique is used to greatly increase the amount of information which is transmitted on the spacecraft carrier frequency.

The summing amplifiers sum the outputs of the subcarrier oscillators and apply the composite signal to the spacecraft transmitters. Two types of summing amplifiers are employed because of the transmitter's ability to transmit either a phase-modulated or a frequency-modulated signal.

The signal processing subsystem employs a high degree of redundancy to insure against loss of vital spacecraft data. Two ADC's, two independent commutators—the engineering signal processor (ESP) and auxiliary engineering signal processor (AESP)—and a wide selection of bit rates (each with the ADC driving a different subcarrier oscillator) provide a high reliability of the signal processing subsystem in performing its function.

From launch to touchdown on the *Surveyor V* mission, 325 commands effecting changes in the signal processor were received and properly executed by the signal processor. Table IV-18 shows representative prelaunch and in-flight values of the telemetered signal processing parameters. No signal processing anomalies were exhibited from launch to shutdown after sunset of the first lunar day.

**Table IV-18. Typical signal processing parameter values**

Parameter	Prelaunch	Flight
ESP reference volts (Mode 2), V	4.875	4.875
ESP reference volts (Mode 4), V	4.899	4.899
ESP reference return, V	0.000	0.000
ESP unbalance current (Mode 2), $\mu$ A	-7.649	-7.649
ESP unbalance current (Mode 4), $\mu$ A	-7.649	-7.649
ESP full-scale current calibration, % error from nominal	0.37	0.37
ESP mid-scale current calibration, % error from nominal	0.24	0.63
ESP zero-scale current calibration, % error from nominal	0.55	0.55
AESP full-scale current calibration, % error from nominal	0.12	0.12
AESP mid-scale current calibration, % error from nominal	-0.04	-0.04
AESP zero-scale current calibration, % error from nominal	0.43	0.33
AESP unbalance current, $\mu$ A	-2.062	-2.062
AESP reference volts, V	4.95	4.936

### 3. Command Decoding Subsystem

From liftoff to touchdown on the moon, the *Surveyor V* mission required a total of 704 earth commands. Thirty-two of these were quantitative commands (QC's) which provided the spacecraft with the quantitative information necessary for attitude and trajectory correction maneuvers; the other 672 were direct commands (DC's) which initiated single actions such as *extend omniantennas*, *AMR power on*, *A/D clock rate 1100 bit/sec*, etc.

These commands were received, detected, and decoded by one of the four receiver/central command decoder (CCD) combinations possible in the *Surveyor* command subsystem. The selection of the combination is accomplished by stopping the command information from modulating the up-link radio carrier for  $\frac{1}{2}$  sec. Once the selection is made, the link must be kept locked up continuously by either sending serial command words or unaddressable command words (referred to as fill-ins) at the maximum command rate of 2 word/sec.

The command information is formed into a 24-bit Manchester-coded digital train and is transmitted in a PCM/FM/PM modulation scheme to the spacecraft. When picked up by the spacecraft omniantennas, the radio carrier wave is stripped of the command PCM

information by two series FM discriminators and a Schmitt digitizer. This digital output is then decoded by the CCD for word sync, bit sync, the 5-bit address and its complement, and the 5-bit command and its complement (this latter only for DC's since the QC's contain 10 bits of information rather than 5 command bits and their complements). The CCD then compares the address with its complement and the command with its complement on a bit-by-bit basis. If the comparisons are satisfactory, the CCD then selects that one of the eight subsystem decoders (SSD's) having the decoded address bits as its address, applies power to its command matrix, and then selects that one of the 32 matrix inputs having the decoded command bits as its address to issue a 20-msec pulse which initiates the desired single action.

Those DC commands that are irreversible or extremely critical are interlocked with a unique command word. Ten of the DC's and all of the QC's are in this special category. None of these commands can be initiated if the interlock command word is not received immediately prior to the critical command.

The QC's, besides being interlocked, are also treated somewhat differently by the command subsystem. The only differences between the DC and QC are: (1) a unique address is assigned the QC words; (2) the QC word contains 10 bits of quantitative information in place of the 5 command and 5 command complement bits. Therefore, when this unique QC address is recognized, the CCD selects the flight control sensor group (FCSG) SSD and shifts the 10 bits of quantitative information into the FCSCG magnitude register. Hence, the QC quantitative bits are loaded as they are decoded.

The command decoding subsystem performed properly throughout flight and through touchdown. Furthermore, no substandard behavior was evidenced during lunar operations. The spacecraft has responded to 104,938 commands from launch to shutdown during the first lunar night.

### 1. Television

The television subsystem is designed to obtain photographs of the lunar surface, lunar sky, and portions of the landed spacecraft. For missions beginning with *Surveyor III*, the subsystem has consisted of a single television camera capable of panoramic viewing and a television auxiliary for processing commands and telemetry data.

## 1. Survey Camera

The survey television camera is shown in Fig. IV-56. The camera provides images over a 360-deg panorama and from +40 deg above the plane normal to the camera Z-axis to -60 deg below this same plane. The camera Z-axis is inclined 16 deg from the spacecraft Z-axis. Each picture, or frame, is imaged through an optical system onto a vidicon image sensor whose electron beam scans

a photoconductive surface, thus producing an electrical output proportional to the conductivity changes resulting from the varying reception of photons from the subject. The camera is designed to accommodate scene luminance levels from approximately 0.008 ft-lamberts to 2600 ft-lamberts, employing both electromechanical mode changes and iris control. Camera operation is totally dependent upon reception of the proper commands from earth. Commandable operation allows each frame to be

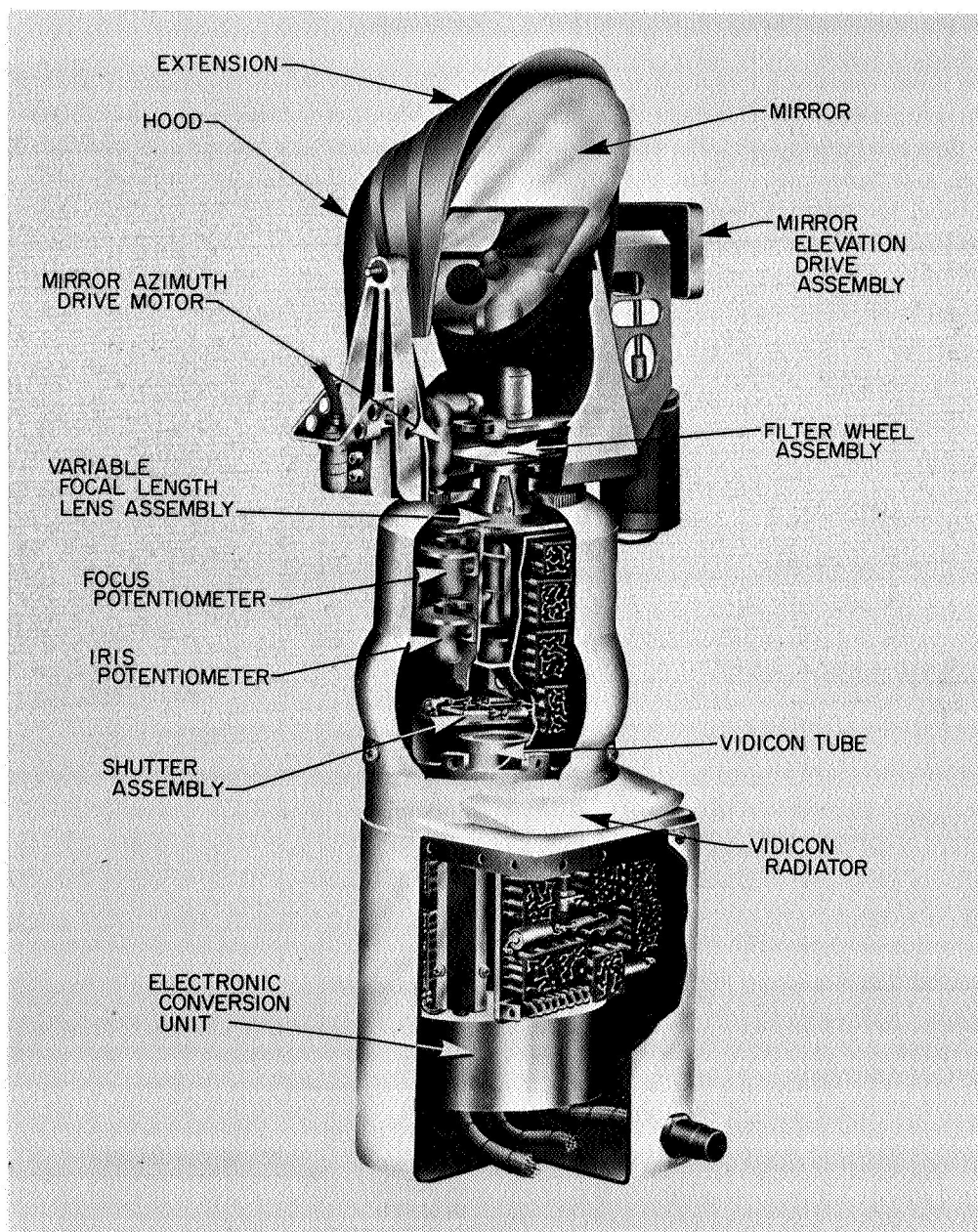


Fig. IV-56. Survey TV camera

generated by shutter sequencing preceded by appropriate lens settings and mirror azimuth and elevation positioning to obtain adjacent views of the subject. Functionally, the camera provides a resolution capability of approximately 1 mm at 4 meters and can focus from 1.23 meters to infinity.

Figure IV-57 depicts a functional block diagram of the survey camera and television auxiliary. Commands for the camera are processed by the telecommunications command decoder, with further processing by the television auxiliary decoder. Identification signals, in analog form, from the camera are commutated by the television auxiliary, with analog-to-digital conversion being performed within the signal processing equipment of the telecommunications subsystem. The ID data in PCM form is mixed in proper time relationship with the video signal in the TV auxiliary and subsequently sent to the telecommunications system for transmission to earth.

The survey camera contains a mirror, filters, lens, shutter, vidicon, and the attendant electronic circuitry.

The mirror assembly contains a mirror supported at its minor axis by trunnions. This mirror is formed by vacuum-depositing a Kanogen surface on a beryllium blank, followed by a deposition of aluminum with an overcoat of silicon monoxide. The mirrored surface is flat over the entire surface to less than  $\frac{1}{4}$  wavelength at  $\lambda = 550 \text{ m}\mu$  and exhibits an average specular reflectivity in excess of 86%. The mirror is positioned by means of two drive mechanisms, one for azimuth and the other for elevation.

The mirror assembly contains three filters (red, green, and blue), in addition to a fourth section containing a clear element for nonmonochromatic observations. The filter characteristics are tailored such that the camera responses, including the spectral response of the image

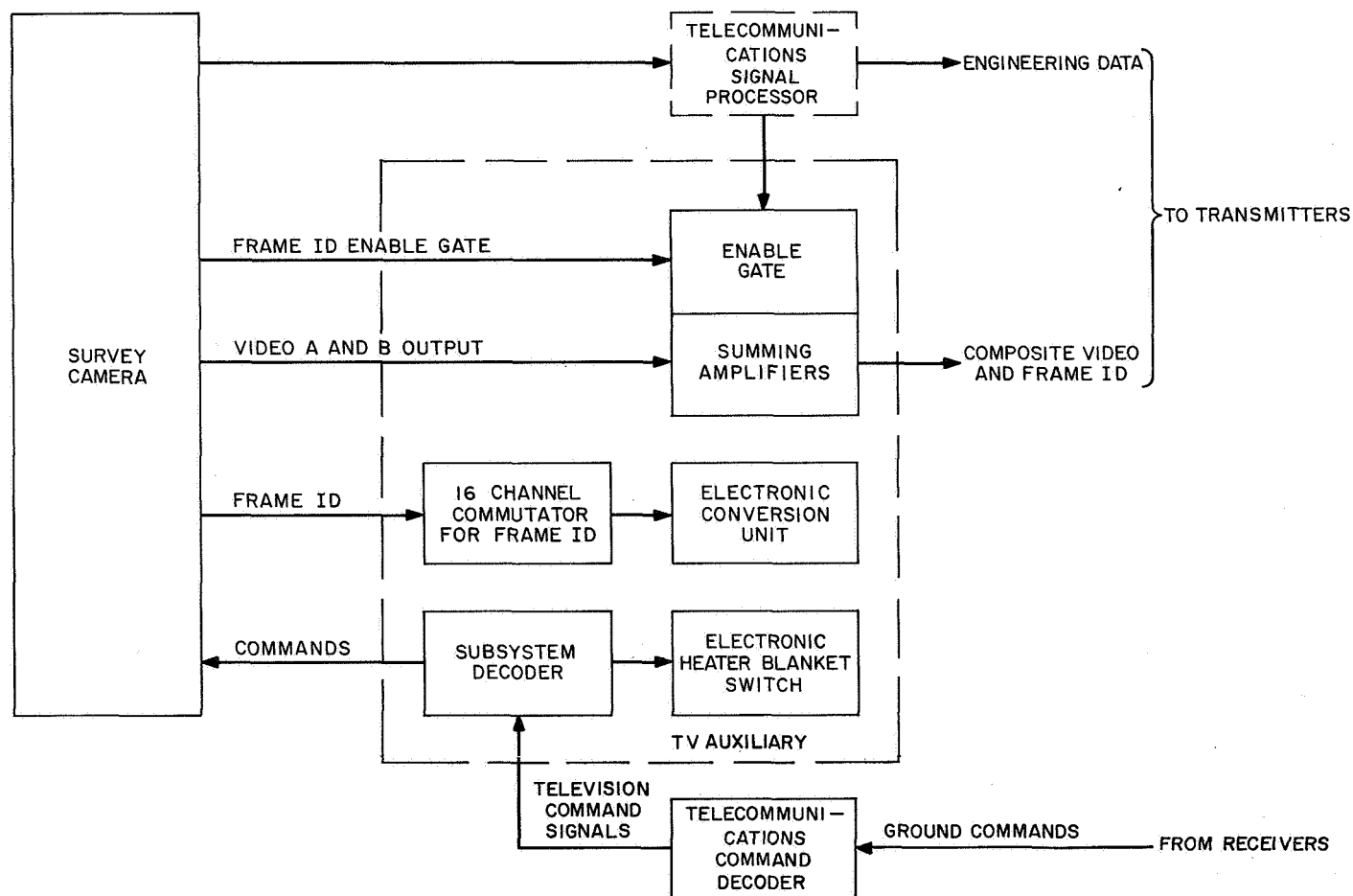


Fig. IV-57. Simplified survey TV camera functional block diagram

sensor, the lens, and the mirror match as nearly as possible the standard CIE tristimulus value curves. Color photographs of any given lunar scene can be reproduced on earth by combining three video photographs, each made with a different monochromatic filter element in the field of view.

The optical formation of the image is performed by means of a variable-focal-length lens assembly placed between the vidicon image sensor and the mirror assembly. The lens is capable of providing a focal length of either 100 or 25 mm, which results in an optical field of view of approximately 6.43 or 25.3 deg, respectively. Additionally, the lens assembly may vary its focus by means of a rotating focus cell from 1.23 meters to infinity, while an adjustable iris provides effective aperture changes of from  $f/4$  to  $f/22$ , in increments which result in an aperture area change of 0.5. While the most effective iris control is accomplished by means of command operation, a servo-type automatic iris is available to control the aperture area in proportion to the average scene luminance. As in the mirror assembly, potentiometers are geared to the iris, focal length, and focus elements to allow readout of these functions. A beam splitter, integral to the lens assembly, provides the necessary light sample (10% of incident light) for operation of the automatic iris.

Three modes of exposure control are afforded the camera by means of a mechanical focal plane shutter located between the lens assembly and the vidicon image sensor. In the *normal shutter* mode, upon earth command, the shutter blades are sequentially driven by solenoids across an aperture in the shutter base plate, thereby allowing light energy to reach the image sensor. The time interval between the initiation of each blade determines the exposure interval, nominally 150 msec.

In the second shutter mode (*open shutter* mode) the blades are positioned to leave the aperture open, thereby providing continuous light energy to the image sensor. This mode of operation is useful in the imaging of scenes exhibiting low luminance levels, including some of the brighter stars. The effective shutter time in this mode is 1.2 sec.

A third exposure mode, used for extremely low luminance levels such as stellar observations, lunar surface observation under earthshine illumination conditions, and faint solar corona observations, is referred to as the *integrate* mode. This mode is implemented by turning off the vidicon electron beam, opening the shutter, and then closing it after any desired exposure time. Scene

luminances on the order of 0.008 ft-lamberts are easily reproduced in this mode of operation, thereby permitting photographs under earthshine conditions. Detection of sixth-magnitude stars has been accomplished using this mode of operation with an exposure time of 5 min.

The transducing process of converting light energy from the object space to an equivalent electrical signal in the image plane is accomplished by the vidicon tube. A reference mark is included in each corner of the scanned format, which provides, in the video signal, an electronic level of the scanned image.

In the normal, or *600-line* scan mode, the camera provides one frame every 3.6 sec. Each frame requires nominally 1 sec to be read from the vidicon and utilizes a bandwidth of 220 kHz, requiring transmission over the high-gain (planar array) antenna.

A second scan mode of operation provides one 200-line frame every 61.8 sec. Each 200-line frame requires 20 sec to complete the video transmission and utilizes a bandwidth of 1.2 kHz. This *200-line* mode is used for transmission over one of the omniantennas.

Integral to the spacecraft and within the viewing capability of the camera are two photometric/colorimetric reference charts (Fig. IV-58). These charts, one on Omni-antenna B and the other adjacent to Footpad 2, are located such that the line of sight of the camera when viewing the chart is normal to the plane of the chart. Each chart is identical and contains a series of 13 gray wedges arranged circumferentially around the chart. In

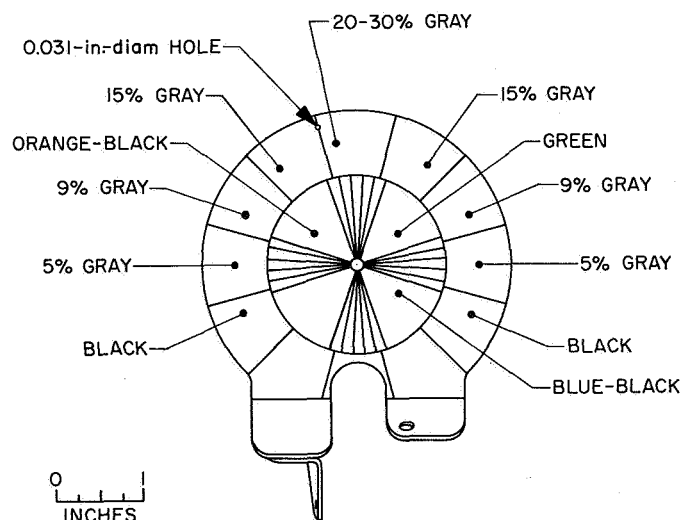


Fig. IV-58. TV photometric/colorimetric reference chart

addition, three color wedges, whose CIE chromaticity coordinates are known, are located radially from the chart center. A series of radial lines is incorporated to provide a gross estimate of camera resolution. Finally, the chart contains a centerpost which aids in determining the solar angles after lunar landing by means of the shadow information. Prior to launch, each chart is calibrated gonio-photometrically to allow an estimation of postlanding camera dynamic range and to aid photometric and colorimetric data reduction.

The survey camera incorporates heaters to maintain proper thermal control and to provide a thermal environment in which the camera components operate. The heater elements are designed to provide a sustaining operating temperature during the lunar night if energized. These consume 36 W of power when activated. A minimum temperature of  $-20^{\circ}\text{F}$  should be achieved prior to camera turn-on if operation is to be performed within known calibrations.

Two auxiliary mirrors were installed on the *Surveyor V* spacecraft for viewing obstructed areas of interest beneath the spacecraft. The larger of these was mounted for viewing of the area beneath Vernier Engine 3 and Crush Block 3; the smaller was mounted for viewing the alpha scattering instrument deployment area on the lunar surface.

## 2. Performance Characteristics

A premission calibration was performed on the survey camera with the camera mounted on the spacecraft. Each calibration utilized the entire telecommunication system of the spacecraft, thereby including those factors of the modulator, transmitter, etc., which influence the overall image transfer characteristics. The calibration data, in FM form, was recorded on magnetic tape for playback through the ground support equipment (GSE) at Goldstone and Pasadena. Thus the final calibration data recorded on the real-time mission film and tape equipment provides a complete system calibration.

The parameters which were calibrated included light transfer characteristics, color response, sine wave response, erasure characteristics, automatic iris tracking, geometric linearity, and camera pointing accuracy. Data was taken in both 600- and 200-line scan modes and in normal shutter, open shutter, and integrate exposure modes. The spacecraft television camera system has a 40% horizontal response at about 600 TV lines in the 600-line scan mode. The light transfer characteristics for the three

color filters are almost identical. This provides the capability of taking a set of color pictures without the necessity of changing iris position. Reduction of color data is then independent of accuracy or repeatability limitations in iris control.

## 3. Mission Performance

*Surveyor V* television camera performance was the best yet experienced on a mission, both in quality of pictures and in the extent of operations which could be conducted, unrestricted by camera problems. Picture quality was better because the camera characteristics exhibited the good dynamic range obtained on the *Surveyor I* mission as well as the good resolution obtained on the *Surveyor III* mission. A contributing factor was the cleanliness of the optical surfaces which resulted from the decision to launch with the camera mirror virtually closed.

During the first lunar day, the camera was operated from DSS 42, Canberra, in addition to DSS 11, Goldstone, resulting in a total of 18,006 pictures being taken. This number is greater than the combined number of pictures which were taken on the two previous successful missions (*Surveyors I* and *III*). The *Surveyor V* pictures include views of parts of the spacecraft, views of the area beneath the spacecraft using the auxiliary mirrors, panoramic narrow- and wide-angle surveys of the lunar landscape in azimuth and elevation, photometric surveys of specially selected objects, star surveys, focus ranging sequences for mapping of the surrounding lunar surface, shadow progressions, views through different filters for reconstruction of color pictures, and a solar corona sequence which lasted about 4 hr following sunset. Since it was of extreme interest to collect both spacecraft engineering data and television pictures during the first few hours following sunset, a unique camera commanding sequence was utilized for the first time on this mission. This sequence permitted the camera to integrate the solar corona images while the camera electronics were turned off. It was then only necessary to turn on the camera long enough to "read out" the stored image, thus allowing the engineering interrogation mode to be used at the rate of four out of every five minutes, and image integration to be done nearly five out of every five minutes.

Among other unique determinations obtained on this mission by use of the camera were: the displacement of the alpha scattering sensor head and the surface erosion resulting from the vernier static firing, the particle accumulation and distribution on the bar magnet, the vertical displacement of the spacecraft at the close of the first



lunar day due to sagging of the spacecraft, and the change in appearance of thermal surfaces due to oxidizer leakage from a propellant tank.

The camera operated without failure until about 14 hr before lunar sunset. After about 17,160 pictures had been taken and while the camera was being controlled by DSS 42, a camera electronics anomaly occurred which prevented control of focal length, focus, and filter wheel position. These functions were then fixed at the narrow angle (100 mm), 14.5 ft (stop 37), and green positions, respectively, and remained in these positions until the end of first lunar day operations. The anomaly occurred at 19.43 GMT on September 23, when the TV electronics temperature was  $+2^{\circ}\text{F}$  and the mirror baseplate temperature was  $+40^{\circ}\text{F}$ . These values are not below the operational limits, although it is of interest that the electronics temperature was falling rapidly before the anomaly occurred. Curves of the TV electronics and mirror baseplate temperatures during the first and second lunar days are contained in Fig. D-11 of Appendix D.

With the focus setting stuck at a position for an object distance of 14.5 ft, it was necessary to set the iris at  $f/22$  in order to achieve any useful degree of focusing on objects at infinity, such as for the solar corona and star surveys. Of course, this setting of the iris resulted in considerable attenuation of light as did use of the green filter. Yet, in spite of these handicaps, image integration mode of operation afforded sufficient flexibility in camera operations to result in a very successful series of corona pictures that spanned over 4 hr of additional camera operation.

On the second lunar day, the camera was found to be operative and supplied over 1000 additional pictures. The functional anomaly described above appeared no longer to exist until, again, just a few hours before lunar sunset. Since the second lunar day operations began with the camera electronics at  $130^{\circ}\text{F}$ , it appears that the anomaly was temperature-related.

Camera operation on the second lunar day was not normal in two respects: the 600-line video signal was low in amplitude, and the 200-line mode exhibited phase reversal as well as being low in amplitude. Only the failure of a single, identified resistor (R-9) or its wiring in the video preamplifier will result in these anomalies. It is believed that this failure resulted from the low temperature of the lunar night, which is below the camera design survival limit. The application of additional video signal amplification at the DSIF station resulted in pictures of

sufficient quality to provide useful spacecraft views as well as information of value for scientific purposes.

## J. Alpha Scattering Instrument

The alpha scattering technique of lunar surface chemical analysis takes advantage of the characteristic interactions of alpha particles with matter to provide information on the chemical composition. The energy spectra of the large-angle, elastically scattered alpha particles are characteristic of the nuclei doing the scattering. In addition, certain elements, when bombarded with alpha particles, produce protons, again with characteristic energy spectra. Consequently, these energy spectra and intensities of scattered alpha particles and protons can be used to determine the chemical composition of the material being exposed to the alpha particles.

The method has good resolution for the light elements found in rocks. (However, it can give only indirect information about hydrogen.) The resolution becomes poorer as the atomic weight increases (Fe, Co, and Ni cannot easily be resolved), even though the sensitivity is greater for heavy elements than for most light elements. The sensitivity for elements heavier than lithium is approximately 1 atomic percent.

The absence of an atmosphere on the moon makes practical the use, for such chemical analyses, of the relatively low-energy alpha particles from a radioactive source.  $\text{CM}^{242}$  ( $t_{1/2} = 163$  days,  $T_a = 6.11$  MeV) is the nuclide used in the *Surveyor* instruments. The use of low-energy alpha particles, however, restricts the information obtained to that pertaining to the uppermost few microns of material. The method is thus one of *surface* chemical analysis. Moreover, using practical source intensities, the rate of analysis is rather slow. A relatively complete analysis requires about one day. In spite of these disadvantages, the use of a radioactive source makes possible a relatively simple and compact instrument which may be deployed directly onto the lunar surface.

### 1. Instrument Description

The alpha-scattering instrument consists of a sensor head, which is deployed onto the lunar surface, and a digital electronics package located in a thermal compartment on the spacecraft. Associated equipment includes an electronic auxiliary, a deployment-mechanism/standard-sample assembly, and a thermally insulated electronics compartment. Figure IV-59 is a photograph of the instrument and its auxiliary hardware.



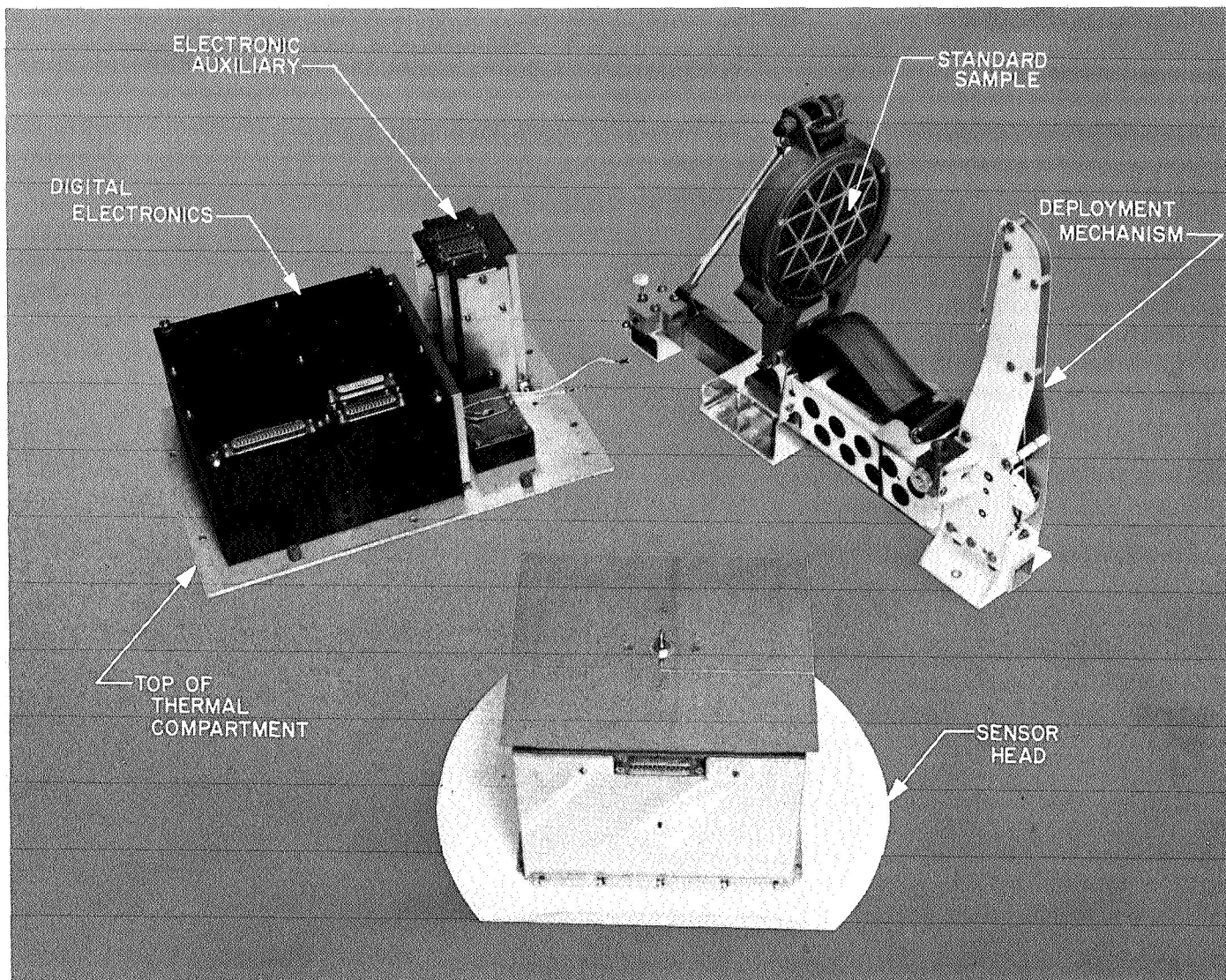


Fig. IV-59. Alpha scattering instrument components

The total weight of the alpha-scattering equipment, including mechanical and electrical spacecraft-interface substructure and cabling, is 29 lb. Power dissipation is 2 W, increasing to 17 W when heaters in the sensor head and electronics compartment are both active.

**a. Sensor head.** The sensor head is primarily a box ( $6\frac{3}{4} \times 6\frac{1}{2} \times 5\frac{1}{4}$  in. high), with a 12-in.-diameter plate on the bottom. The main purpose of the plate is to minimize the probability of the box sinking appreciably into a possibly soft lunar surface. Figure IV-60 shows a bottom view of the sensor head. In the bottom of the sensor head is a sample port,  $4\frac{1}{4}$  in. in diameter. Recessed  $2\frac{3}{4}$  in. above this circular opening is a set of six curium-242 alpha sources, collimated in such a way that the alpha particles

are directed through the opening. Across the face of each collimator is a thin, aluminum-oxide film to prevent recoils from the alpha source from reaching the sample area; a second film is mounted in front of each collimator for additional protection. Close to the alpha sources are two detectors arranged to detect alpha particles scattered back from the sample at an average angle of 174 deg from the original direction. These 0.031-in.<sup>2</sup> alpha detectors are of the silicon, surface-barrier type, with evaporated-gold front surface films. Thin films are mounted on collimation masks to protect the detectors from alpha contamination and excessive light.

The sensor head also contains four lithium-drifted silicon detectors (of approximately 0.155-in.<sup>2</sup> area each)

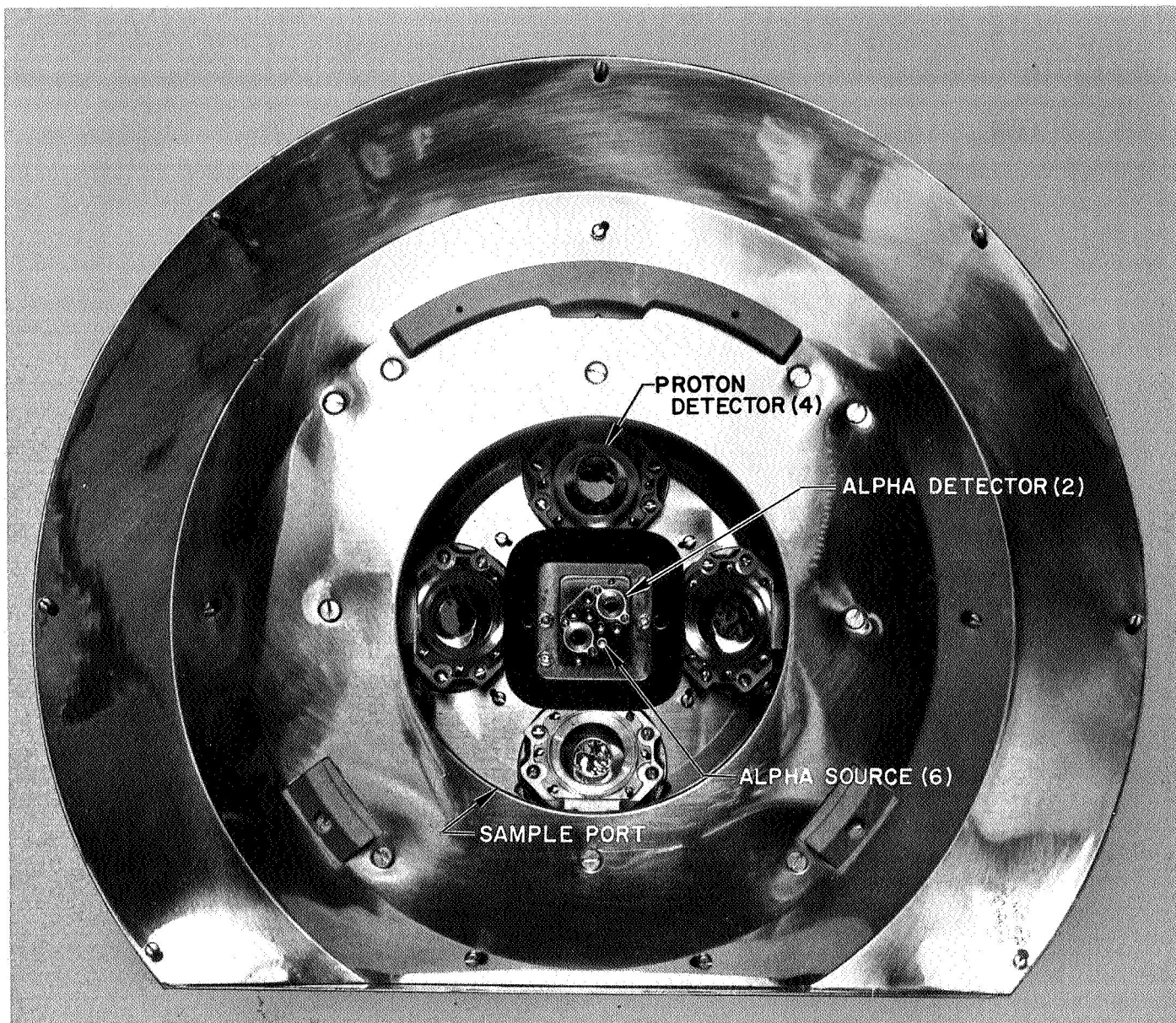


**Fig. IV-60. View of bottom of alpha scattering instrument sensor head**

designed to detect protons produced in the sample by the alpha particles. Gold foils, approximately 0.4-mil thick, prevent scattered alpha particles from reaching these detectors. Figure IV-61 is a diagrammatic side view of the sensor head, showing the configuration of sources, sample, and detectors.

Because the expected proton rates from the sample are low, and because these detectors are more sensitive to radiation from space, the proton detectors are backed by guard detectors. Most of the charged particles from space that strike a proton detector must first pass through

the corresponding guard detector, whereas protons from the sample are stopped in the proton detector. The electronics associated with the guard and proton detectors are arranged so that an event registered in both will not be counted as coming from the sample. This anticoincidence arrangement reduces significantly the background in the proton mode of the instrument.

Separate, 128-channel, pulse-height analyzers are used with the alpha and proton detectors. An output pulse from a detector is amplified and converted to a time-analog signal whose duration is proportional to the energy

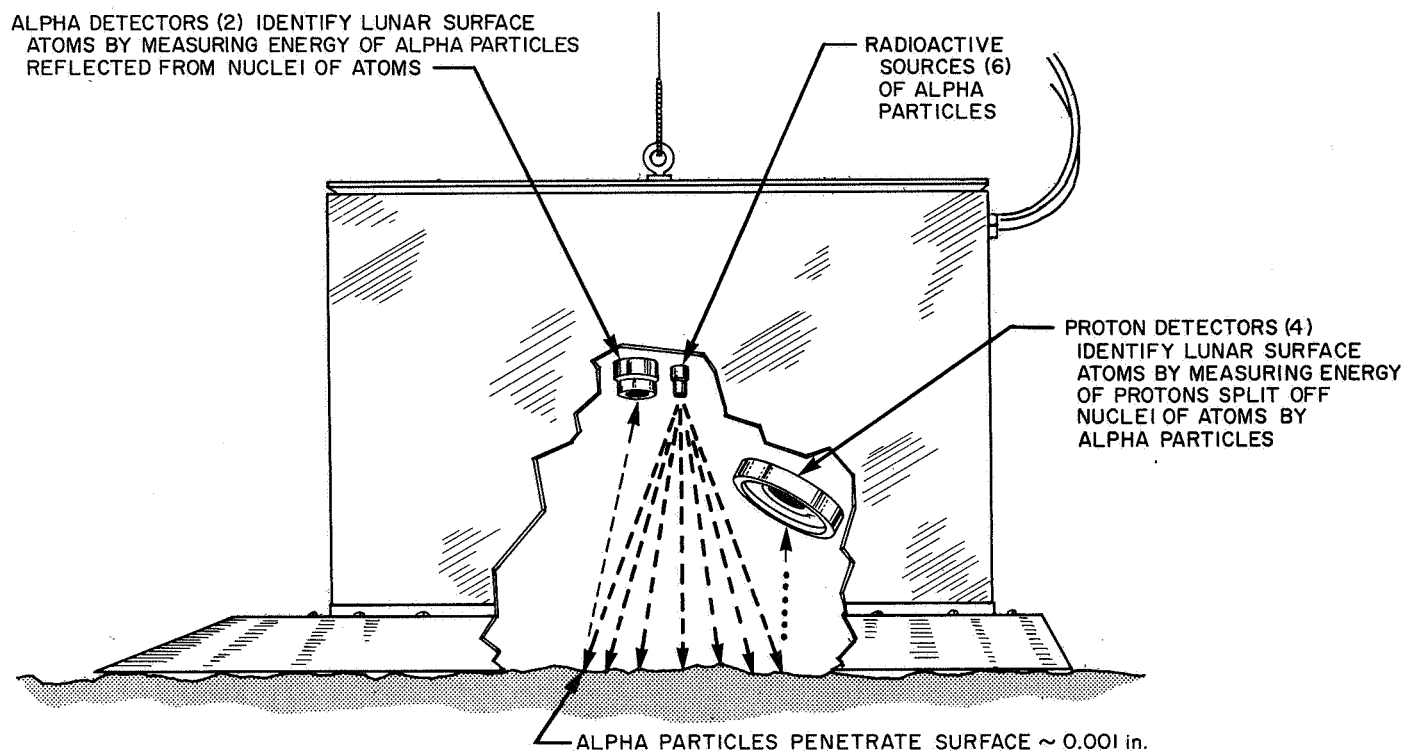


Fig. IV-61. Diagrammatic view of sensor head illustrating functional operation

deposited in the detector. The outputs of the two alpha detectors are combined before this conversion; a separate mixer circuit is used for the four proton-detector outputs. A ratemeter circuit is used to measure the frequency of events occurring in the guard (anticoincidence) detectors, but provides no information on the energy of such events.

In addition to the curium-242 sources, detectors, and associated electronics, the sensor head contains a platinum-resistance thermometer, a 5-W heater, and an electronic pulser. The pulser is used to calibrate the electronics of the instrument by introducing electrical pulses of two known magnitudes at the detector stages of the alpha and proton systems. This calibration mode is initiated by command from earth. Small amounts of alpha-radioactive einsteinium-254 are also used to calibrate the alpha and proton systems and, in addition, serve as real-time monitors. The einsteinium is located on the gold foil facing each proton detector and on the thin films mounted in front of the alpha detectors.

The external surfaces of the sensor head have been designed for passive thermal control. A second-surface mirror on top of the sensor head is used as a radiator to cool the sensitive components inside. The 5-W heater is

used at low temperatures. The operating temperature range specified for the sensor head is  $-40$  to  $+122^{\circ}\text{F}$ .

**b. Digital electronics.** The output of the sensor head is a signal (in time-analog form) that characterizes the energy of an event in either the scattered alpha or proton mode of the instrument. The signals from the sensor head are converted to 9-bit binary words by the digital electronics. Seven bits of each word identify which of the 128 channels represents the energy of the registered event. Two extra bits are added before transmission, one to identify the start of the word and one at the end of each word, as a parity check on transmission errors. Buffer registers provide temporary storage of the energy information for readout into the spacecraft telemetry system. The transmission rates are 2200 bit/sec for the alpha mode and 550 bit/sec for the proton mode. Measured events with energy greater than the range of the analyzers are routed to channel 126 (overflow channel).

The electronics package also contains power supplies and the logical electronic interfaces between the instrument and the spacecraft. For example, the output of an individual detector, together with its associated guard detector, can be blocked by command from earth. Also



via the electronics unit, the temperature of the sensor head, as well as various monitoring voltages, can be transmitted to earth.

*c. Electronic auxiliary.* The required electrical interfaces between the sensor head, digital electronics and spacecraft circuits are provided by an electronic auxiliary that provides command decoding, signal processing, and power management. Basic spacecraft circuits interfacing directly with the sensor head and digital electronics are (1) the central signal processor, which provides signals at 2200 and 500 bit/sec for synchronization of instrument clocks, and (2) the engineering signal processor, which provides temperature-sensor excitation current and commutation of engineering data outputs.

The electronic auxiliary provides two data channels for the alpha-scattering instrument. The separate alpha and proton channels are implemented using two subcarrier oscillators. Characteristics of these channels are defined in Table IV-19.

**Table IV-19. Characteristics of alpha scattering instrument data channels**

Characteristic	Alpha channel	Proton channel
Data input to electronic auxiliary	Digital (nonreturn to zero)	Digital (nonreturn to zero)
Input data rate	2200 bit/sec	550 bit/sec
Subcarrier oscillator center frequency	70,000 Hz	5400 Hz

The electronic auxiliary and the digital electronics are contained in Electronics Compartment C, which is attached to the upper part of the spaceframe. For passive control of temperatures at high sun angles the top of this compartment is painted white and the sides and bottom are insulated. A 10-W heater assembly, operated by means of the engineering signal processor, provides active thermal control at low temperatures. The operating temperature range specified for the electronic units in Compartment C is  $-4$  to  $+131^{\circ}\text{F}$ .

*d. Deployment mechanism/standard sample.* The deployment mechanism provides stowage of the sensor head, deployment to the background position, and to the lunar surface. The sensor head is mounted to the deployment mechanism by means of three support lugs on the bottom plate. Deployment mechanism clamps that engage these lugs are released during the deployment operation. Figure IV-62 illustrates the two-stage operation of the deployment mechanism. From the stowed position, the

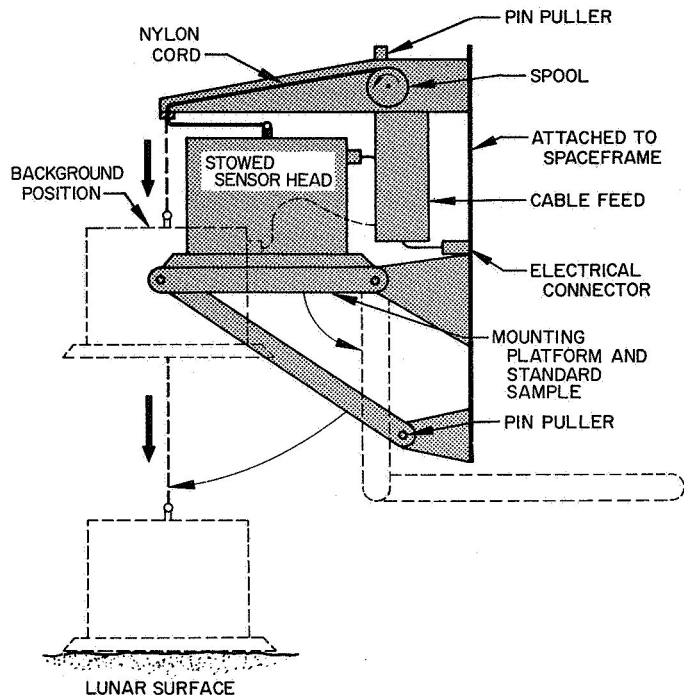


**Fig. IV-62. Alpha scattering instrument deployment mechanism**

sensor head is first released on command to a position 22 in. above the nominal lunar surface by activation of an explosive-pin-puller device. From the background position, the sensor head is then lowered directly to the lunar surface by activation of another explosive-pin-puller device. The deployment velocity is controlled by an escapement.

A sample of known composition is attached to the platform on which the sensor head is mounted in the stowed position. This standard-sample assembly covers the circular opening in the bottom of the sensor head during spacecraft transit and landing to minimize entrance of dust and light and to provide a means of assessing instrument performance shortly after the spacecraft lands on the moon. The standard sample and mounting platform move aside when the sensor head is deployed to the background position.

## 2. Alpha Scattering Instrument Data Handling

Two types of information relative to the alpha scattering experiment are transmitted from the spacecraft: engineering data and science data. The engineering measurements are used to monitor instrument voltages, temperatures, detector configuration, and background rates in the anticoincidence detectors. The seven parameters that are monitored are listed in Table IV-20.

**Table IV-20. Engineering parameters telemetered from alpha scattering instrument**

Telemetry channel	Parameter
AS-3	Sensor head temperature
AS-4	Compartment C (digital electronics temperature)
AS-5	Guard rate monitor
AS-6 (digital)	At least one alpha detector on
AS-7 (digital)	At least one proton detector on
AS-8	7-V monitor
AS-9	24-V monitor

The 9-bit digital words that characterize the energy of each of the analyzed alpha particles or protons comprise the science data. These data leave the instrument as separate alpha and proton bit streams and modulate separate subcarrier oscillators; they are then combined with the engineering data and transmitted by the spacecraft to earth. The composite signal from the spacecraft is recorded on magnetic tapes by an FR-1400 recorder at each DSIF station. These magnetic tapes, containing the raw data, comprise the prime source of alpha scattering information for use in postmission analysis.

For purposes of monitoring the experiment in real-time, the signal is separated at the DSIF station by discriminators and bit synchronizers into 2200-bit/sec alpha data and 550-bit/sec proton data. These reconstituted bit streams are presented to an on-site computer which establishes and maintains synchronization of the 9-bit data words and assembles, within its memory, four spectra of 128 channels each. The four spectra are: alpha parity-correct, alpha parity-incorrect, proton parity-correct, and proton parity-incorrect. In this manner, data is obtained at the stations in accumulations ranging in duration from 2 min during pulser calibration to a nominal 40 min during sample and background phases. The assembled spectra are transmitted via teletype to the SFOF for display and further computer processing.

Data analysis during the mission is performed so that proper control over the experiment may be exercised. The engineering data is simply displayed and compared with prelaunch measurements and predictions to assess the performance of the instrument and the functioning of commands.

The alpha and proton science data is also used to assess the performance of the instrument and is analyzed to determine the duration of the several operational phases.

This science-data analysis is conducted in the SFOF using a 7094 computer program.

### 3. Alpha Scattering Instrument Performance

The following table is a summary of the science-data accumulation time on the *Surveyor V* mission in each of the operational configurations based upon spectra assembled by the on-site computers and transmitted via teletype to the SFOF. (A total of 107 hr of data was recorded on the FR-1400 tape recorders during the 193 hr that the instrument was activated.)

Operational configuration	Accumulation time, min
Transit	20
Standard sample	75
Background	170
Lunar surface Sample I	1056
Lunar surface Sample II	4005
Calibration	281
Total	5607 (93½ hr)

The performance of the alpha scattering equipment and operational system during the *Surveyor V* mission was excellent.

All ten of the detectors in the sensor head functioned properly. Only once, during a period of rapidly changing temperatures, was there a suggestion of noise in the proton system. Sharp breakpoints in the sample spectra showed that the high quality of the curium-242 sources had been preserved. The films covering the sources and alpha detectors had survived the launch, midcourse maneuver, and touchdown operations. The electronics, calibration pulser, and einsteinium sources performed properly as evidenced by the sharpness of calibration peaks and agreement with prelaunch data. The guard detector and anticoincidence system worked as designed; guard monitor voltage and proton background spectrum agreed well with predicted values.

The digital electronics, instrument power supply, and electronic auxiliary performed as designed. Circuits used to monitor engineering parameters provided good data. Nearly 600 commands were transmitted to the alpha scattering instrument and, with one minor exception, all commands were executed correctly. The deployment mechanism functioned properly in spite of the approximate 20-deg tilt of the spacecraft. The sensor head positions on the lunar surface before and after static firing of the vernier engines are shown in Fig. IV-12.

The communications link from the spacecraft was excellent; a bit-error-rate of less than  $10^{-6}$  was estimated from the parity-incorrect spectra. In general, deviations from this high-quality data reception occurred only when the spacecraft was being tracked near the earth's horizon. Both of the major alpha scattering computer programs

and associated equipment gave excellent processing of the science data.

Preliminary scientific results of the *Surveyor V* alpha scattering experiment are presented in Part II of this report.



## V. Tracking and Data System

The TDS (Tracking and Data System) for the *Surveyor V* mission included selected resources of the AFETR (Air Force Eastern Test Range), the MSFN (Manned Space Flight Network), the DSN (Deep Space Network), and the NASCOM (NASA Communications System). This section summarizes the mission preparation, flight support, and performance evaluation of each element of the TDS.

The TDS support for the *Surveyor V* was considered less than nominal, but acceptable. With the exception of less than ideal near-earth support, all TDS requirements were met and in most cases exceeded. During the near-earth phase, acquisition and operational problems experienced by elements of the AFETR and MSFN placed the mission in a potentially serious position, in which corrective action could not have taken place in time to save an abnormal flight.

### A. Air Force Eastern Test Range

The AFETR performs TDS supporting functions for *Surveyor* missions during the countdown, launch, and near-earth phase of the flight.

The *Surveyor* mission requirements for near-earth-phase tracking and telemetry coverage are classified as

follows, in accordance with their relative importance to successful mission accomplishment:

Class I requirements consist of the minimum essential needs to ensure accomplishment of first-priority flight test objectives. These are mandatory requirements which, if not met, may result in a decision not to launch.

Class II requirements define the needs to accomplish all stated flight test objectives.

Class III requirements define the ultimate in desired support, and would enable the range user to achieve the flight test objectives earlier in the test program.

The AFETR configuration for the *Surveyor V* mission is presented in Table V-1. In addition to the land stations, three Range Instrumentation Ships (RIS *Coastal Crusader*, *Sword Knot*, and *Twin Falls*) and two C-130 Range aircraft (designated Audit 1 and 2) supported the mission.

Figure V-1 illustrates the positions of the Range Instrumentation Ships and aircraft and the planned coverage for *Surveyor V* on launch day. AFETR preparations for *Surveyor V* consisted of routine testing of individual facilities, followed by several Operational Readiness Tests.



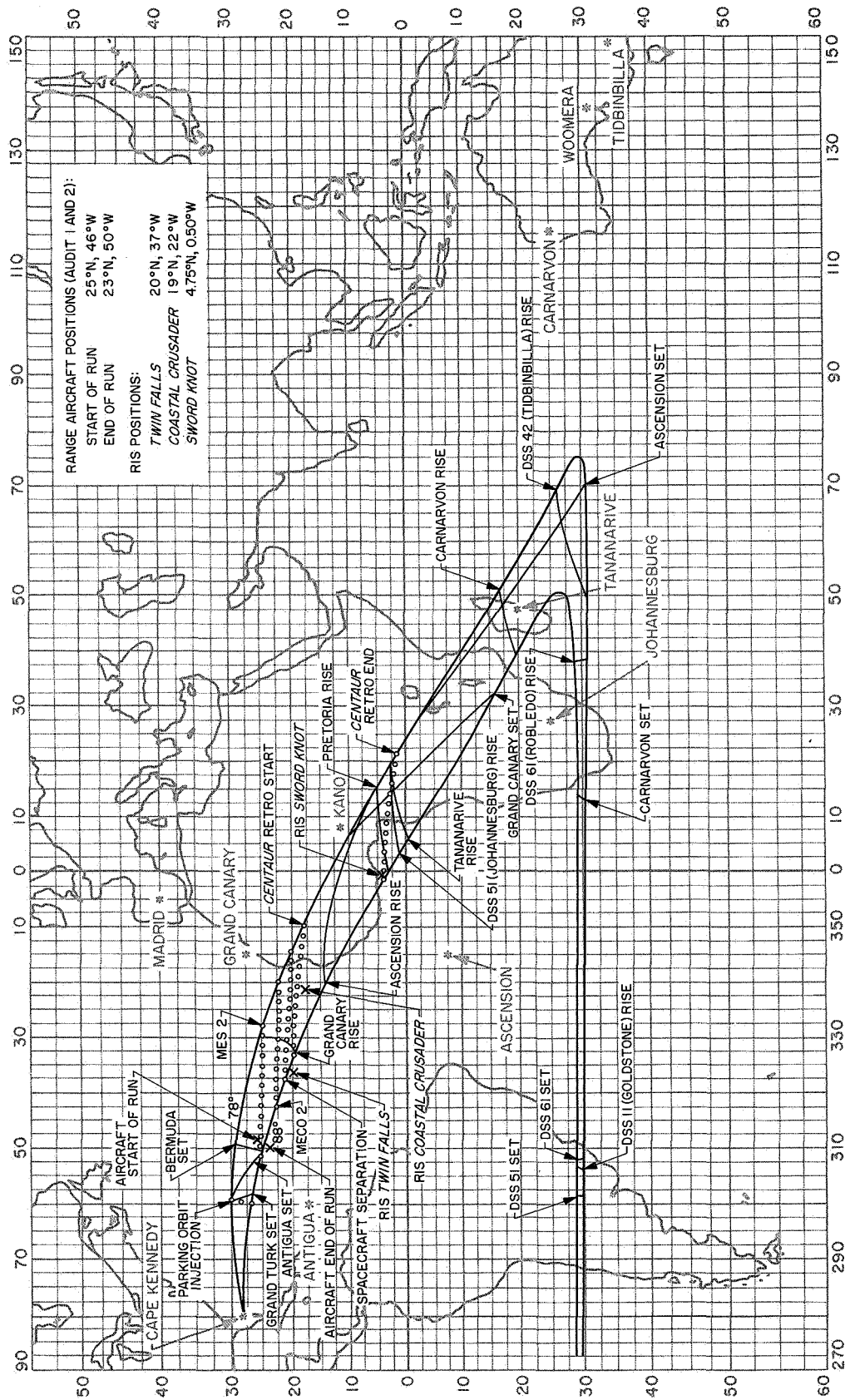


Fig. V-1. Planned launch phase TDS coverage for September 8, 1967

**Table V-1. AFETR configuration for Surveyor V mission**

Station		C-band tracking		Telemetry	
Number	Location	Capability	Antenna type	Capa- bility	Antenna type
0	Patrick AFB	beacon/skin	FPQ-6		
1	Cape Kennedy	beacon/skin	FPS-16		
19	Kennedy Space Center, Merritt Island (Tel 4)	beacon/skin	TPQ-18	VHF S-band	TAA-2A TAA-3A
3	Grand Bahama	beacon	FPS-16	VHF	LH tri- helix
		beacon/skin	TPQ-18	S-band	TAA-2
7	Grand Turk	beacon/skin	TPQ-18		
91	Antigua	beacon/skin	FPQ-6	VHF S-band	TLM-18 TAA-3A
Audit 1	Range aircraft			VHF	TAA-4
Audit 2	Range aircraft			VHF	TAA-4
UNI	RIS Twin Falls	beacon	FPS-16	VHF S-band	Rantec TAA5-12
WHI	RIS Coastal Crusader			VHF S-band	TAA-1 TAA5-24
YAN	RIS Sword Knot			VHF S-band	TAA-1 TAA5-24
12	Ascension	beacon	FPS-16	VHF	TLM-18
		beacon	TPQ-18	S-band	TAA-3A
13	Pretoria	beacon	MPS-25	VHF S-band	TLM-18 3-ft pa- rabola

### 1. Tracking Data (Metric)

The AFETR tracks the C-band beacon of the *Centaur* stage to provide metric data. This data is required during intervals of time before and after separation of the spacecraft for use in calculating the *Centaur* orbit, which can be used as a close approximation of the postseparation spacecraft orbit. The *Centaur* orbit calculations are used to provide early mission status evaluations and DSN acquisition information (in-flight predicts). C-band tracking data is also required during the parking orbit phase for determining acquisition information for down-range stations and theoretical DSN acquisition information. In addition, C-band tracking data is required following the *Centaur* retro maneuver in order to determine the final *Centaur* trajectory.

Estimated and actual radar coverages are shown in Fig. V-2. The Class I requirements were met only during the initial flight phase.

Complete and redundant C-band coverage was provided by the stations nearest the launch site (Cape

Kennedy, Kennedy Space Center, Patrick AFB, and Grand Bahama). However, the X-band radars at Cape Kennedy did not meet Range Safety commitments owing to signal dropouts from  $L + 71$  to  $L + 91$  sec on one radar and  $L + 72$  to  $L + 83$  sec on the other. The radars operated satisfactorily and the cause of the dropouts has not been determined.

The expected Grand Turk coverage interval was from  $L + 243$  to  $L + 568$  sec. The Grand Turk radar, although operational at launch, did not track because of an apparent acquisition problem with the radar target acquisition (RATAC) system. At liftoff, the radar was slaved in azimuth and range to the incoming acquisition data from Cape Kennedy and all appeared normal. At  $L + 60$  sec, the incoming range data jumped nearly 600 kiloyards. Acquisition data from Grand Bahama appeared to be identical to that from Cape Kennedy. Since RATAC data was not valid, manual look angles were selected but, by the time the change in operational mode could be accomplished, the vehicle had passed over the local horizon. Computer diagnostic tests were run immediately after the flight but the trouble could not be defined. Additional checks have been run with the help of Grand Bahama and Antigua, where the problem did not occur.

The Antigua radar was not operational during the entire launch window because of a hydraulic system pump failure. This condition had no impact on the actual launch azimuth, however. The inability of the Antigua radar to support probably would have caused a scrub for the day if a more southerly launch azimuth (as required for a later launch time) had been selected.

The *Twin Falls* failed to provide any metric tracking data because of an operator error. The pulse coder was improperly set, thus preventing a beacon response from the *Centaur*. Additional prelaunch procedures have been placed in effect to preclude recurrence of this problem. The lack of metric support from the *Twin Falls* placed the mission in a potentially serious position, in which corrective action could not have been taken in time to save an abnormal flight.

The Ascension radars did not acquire track because of the low elevation angles.

The Pretoria radar was late in acquiring track and experienced dropouts of long duration. The theoretical parking orbit interranger vector (IRV) with powered flight

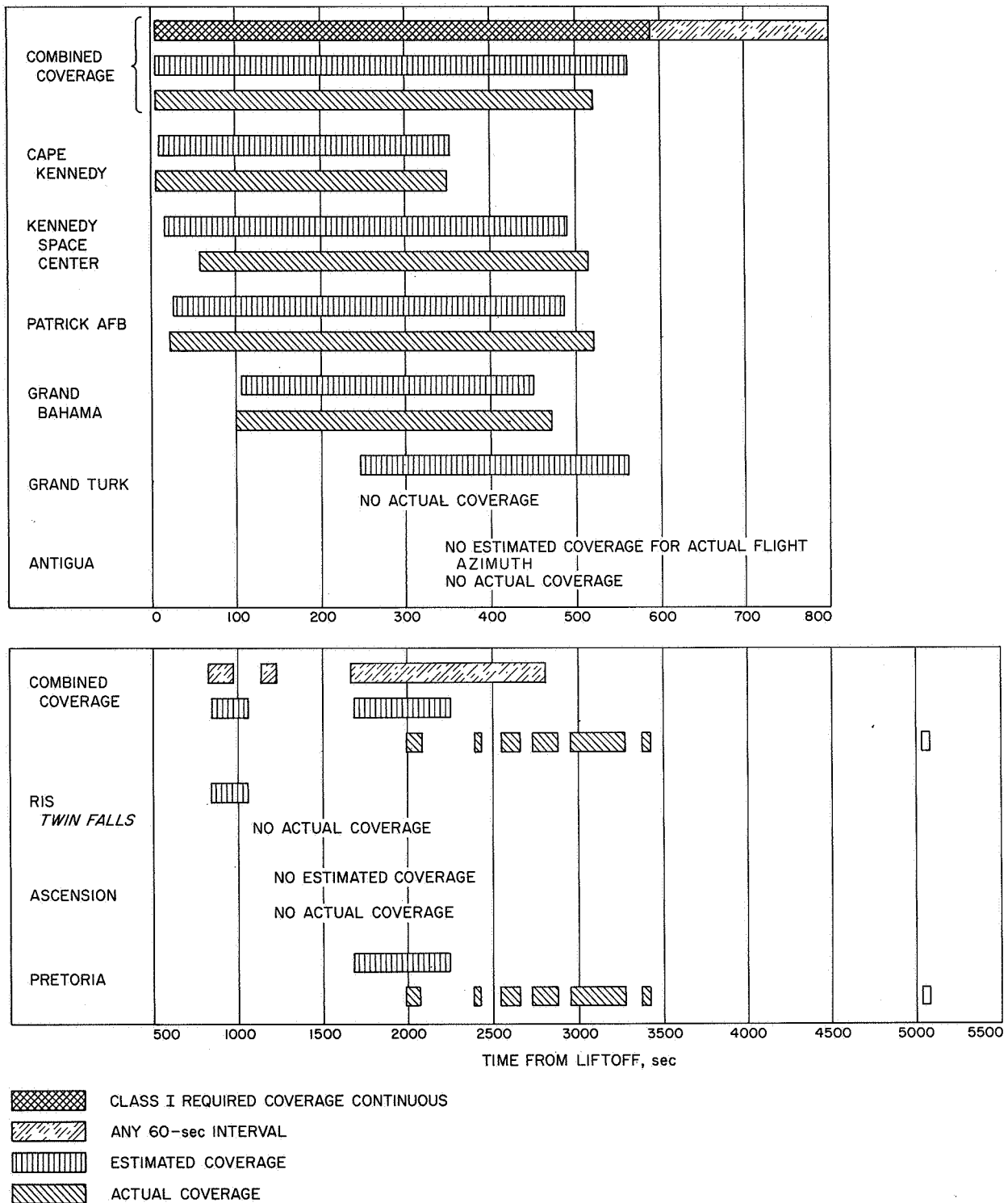


**Fig. V-2. AFETR C-band radar coverage**

constants deviated from tracking data by 3 to 5 deg in both azimuth and elevation. Initial auto track was obtained by slaving to the AT-36 60-ft wide-band telemetry antenna. It appears that the intermittent track was prob-

ably due to *Centaur* beacon characteristics resulting from tumbling of the vehicle after the retro maneuver. Carnarvon radar data had to be used for the postretro orbital parameters.

## 2. Atlas/Centaur Telemetry (VHF)

To meet the Class I telemetry requirements, the AFETR must continuously receive and record *Atlas* telemetry (229.9-MHz link) from before liftoff until shortly after *Atlas/Centaur* separation, plus *Centaur* telemetry (225.7-MHz link) until shortly after spacecraft separation. Thereafter, *Centaur* telemetry is to be recorded as station coverage permits until completion of the *Centaur* retro maneuver. In addition to the land stations, the AFETR provided RIS *Coastal Crusader*, *Sword Knot*, and *Twin Falls* as well as two telemetry aircraft (Audit 1 and 2).

Estimated and actual VHF telemetry coverages are shown in Fig. V-3. The two telemetry aircraft were on station but did not obtain usable data. Nevertheless, overall coverage was greater than predicted and all requirements were met, since continuous and substantially redundant VHF telemetry data was received and recorded beginning with the countdown through Pretoria loss of signal (LOS) at  $L + 5459$  sec.

## 3. Surveyor Telemetry (S-Band)

The AFETR is required to receive, record, and retransmit *Surveyor* S-band (2295-MHz) telemetry in real-time from spacecraft transmitter *high power on* until 2 min after continuous view by DSIF stations begins.

The AFETR S-band telemetry resources assigned to meet this requirement (Table V-1) were committed on a "best effort" basis, since the *Centaur* vehicle is not roll-attitude-stabilized and the aspect angle cannot be predicted.

Estimated and actual S-band coverages and receiver phase-lock times are shown in Fig. V-4. The requirement for receiving and recording Class I S-band telemetry was satisfied, since continuous coverage was obtained from spacecraft *high power on*, at about  $L + 1155$  sec to Pretoria LOS at  $L + 3180$  sec. Early evaluation of the S-band data indicated that perhaps good receiver lock was obtained but that the data may not be usable. Subsequent investigation revealed, however, that this was not the case.

Antigua received S-band data through *Centaur* first burn, although this was not expected because of expected masking of the antenna view by local terrain.

The RIS *Twin Falls* did not receive any S-band data because its view period occurred while the spacecraft transmitter was in the lower-power mode.

Since Pretoria has only a 3-ft S-band antenna, no coverage was estimated for that station, and the *Sword Knot* was positioned to be prime during the same interval as the Pretoria view period.

## 4. Surveyor Real-Time Telemetry Data

The AFETR retransmits *Surveyor* data (VHF or S-band) to Building AO, Cape Kennedy, for display and for retransmission to the SFOF. In addition, down-range stations monitor specific channels and report events via voice communication.

For the *Surveyor V* mission, existing hardware and software facilities were utilized to meet the real-time data requirements.

A summary of real-time telemetry data retransmission is presented in Table V-2.

Table V-2. Real-time telemetry data retransmission

Station providing data	Time selected for retransmission by TEL 4, sec from liftoff	Telemetry link	Communications path to TEL 4	Remarks
Kennedy Space Center (TEL 4)	-10	VHF	None required	Excellent quality. Building AO and DSS 71 received good data
Grand Bahama	+64	VHF	Subcable	Excellent quality. Building AO and DSS 71 obtained solid lock
Antigua	+542	VHF	Subcable	Excellent quality until signal began to break-up near LOS, at $L + 664$
RIS <i>Twin Falls</i>	+683	S-band	HF radio	No usable data received
RIS <i>Coastal Crusader</i>	+1032	S-band	HF radio/subcable relay via Antigua	No usable data received
RIS <i>Sword Knot</i>	+1424	S-band	HF radio via Ascension	Approximately $2\frac{1}{2}$ min of usable data received near LOS, at approximately $L + 1754$
Pretoria	+1855	S-band	HF radio via Ascension	Very little usable data received

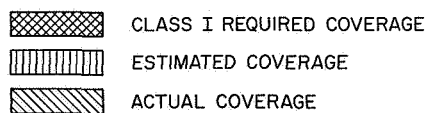
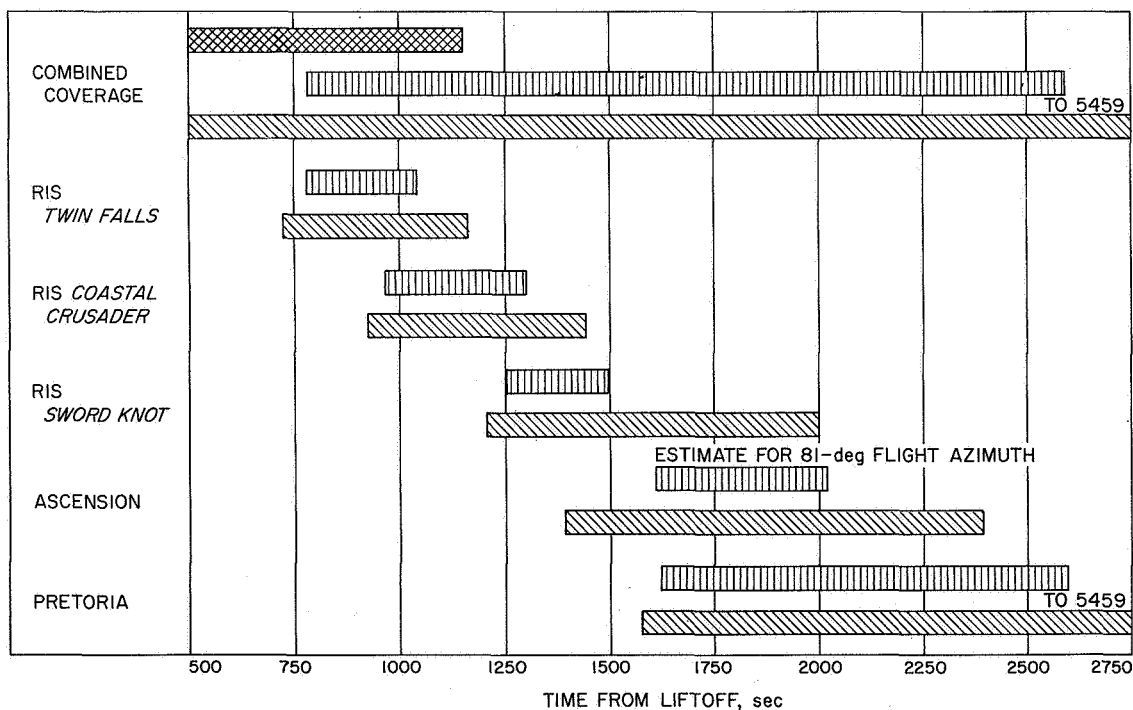
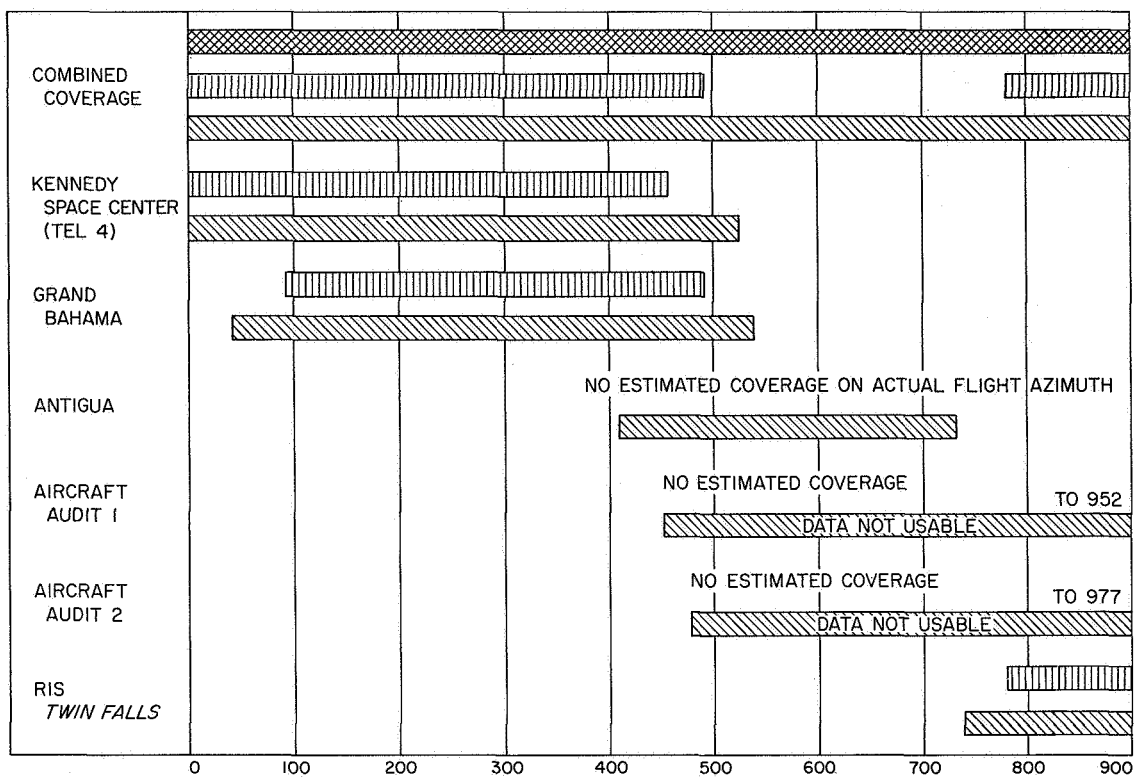


Fig. V-3. AFETR VHF telemetry coverage

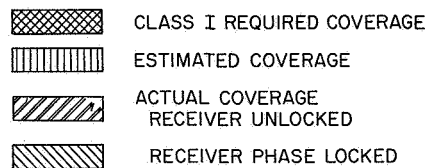
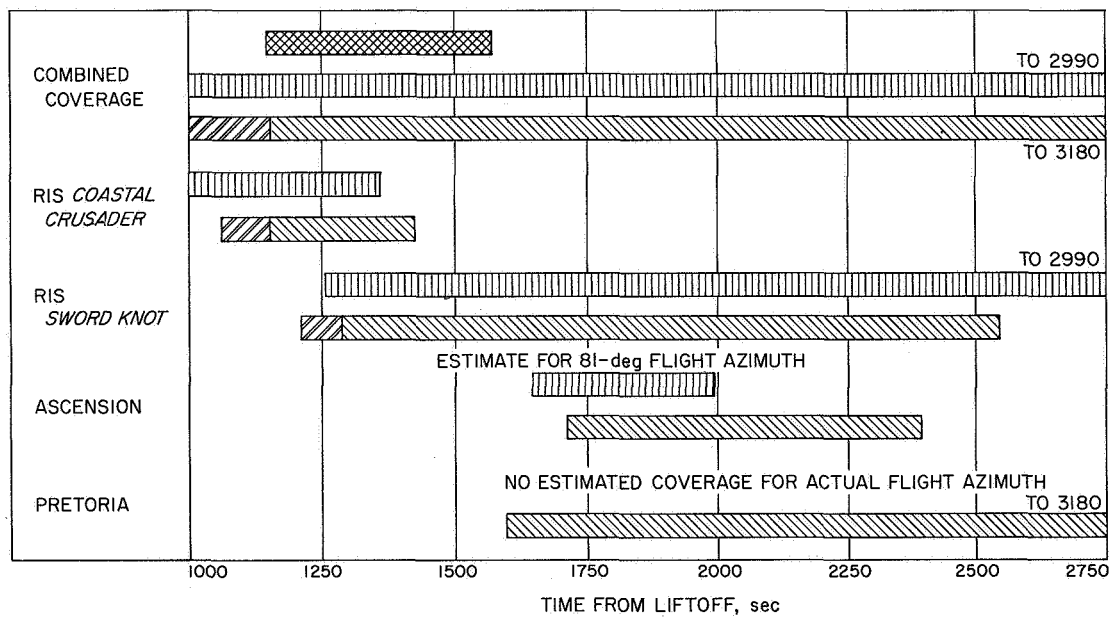
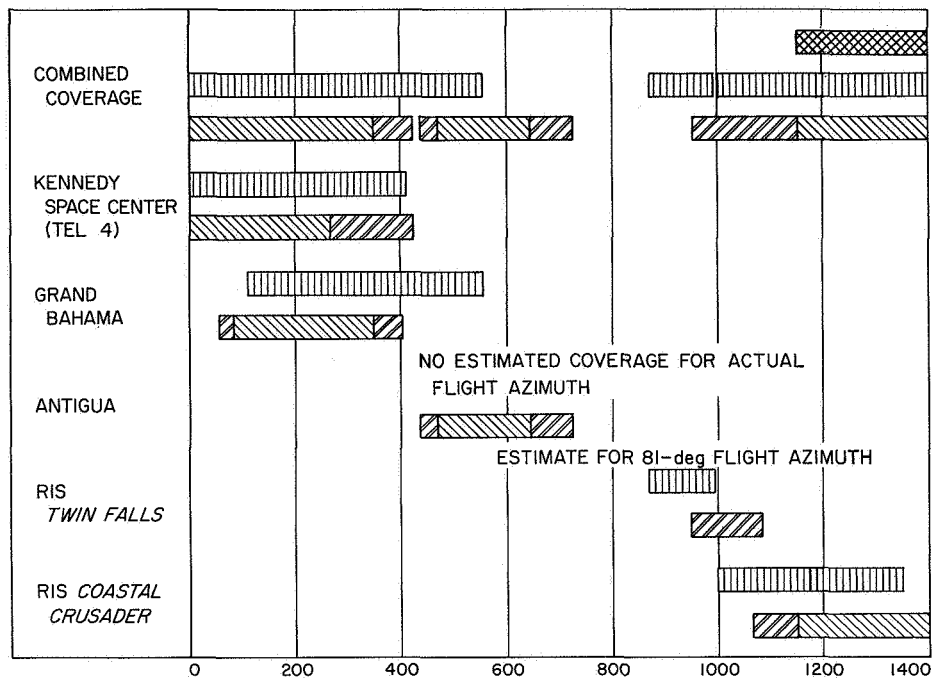


Fig. V-4. AFETR S-band telemetry coverage

Kennedy Space Center (Tel 4) provided good spacecraft data in real-time from the VHF link, beginning before liftoff. The switch to real-time VHF data from Grand Bahama was made at  $L + 64$  sec. Quality of the data was excellent. There was an overlap in coverage between Grand Bahama and Antigua; therefore, only a momentary dropout occurred when the subcable switch was made from Grand Bahama to Antigua data at  $L + 542$  sec. Antigua data was also excellent.

Real-time data from the *Twin Falls* was unusable because the ship was configured to retransmit S-band rather than VHF data. Inasmuch as the spacecraft was still on low power, the data source from the *Twin Falls* should have been the VHF link. However, the retransmission of VHF data from down-range ships and stations was deleted because of the good quality data received from the MSFN in real- and near-real-time.

No useful data were received from the *Coastal Crusader*. Indications are that the poor performance was caused by poor HF radio communications. The only communication path between the ship and TEL 4 at Cape Kennedy was by HF from the ship to Antigua, where the signal was demodulated with a Rixon receiver and then transmitted on the subcable to TEL 4. This path had been observed during the minus count and, although not consistently good, it had been usable. The HF communications path to the *Sword Knot* was excellent. However, when the switch from calibration signal to receiver was made, the time division multiplexer (TDM) at TEL 4 would not lock up. Parity errors were excessive, and only about  $2\frac{1}{2}$  min of useful real-time data was obtained. The lack of real-time spacecraft telemetry data from the *Twin Falls*, *Coastal Crusader*, and *Sword Knot* placed the mission in a potentially serious position because of the loss of real-time data for spacecraft performance evaluation before DSN acquisition.

Although AFETR had estimated no coverage from Pretoria, S-band data was provided to TEL 4, and the data from this station was retransmitted to DSS 71 and Building AO at  $L + 1855$  sec. The received data signal was not very good and the TDM could not maintain continuous lock for more than 6 to 8 frames.

AFETR and MSFN reported all Mark Events except Nos. 12, 22, and 23. The Mark Events read out and reported by AFETR and MSFN stations are presented in Table V-3. Refer to Appendix A, Table A-1, for a list of the Mark Events and event times determined postflight.

Table V-3. *Atlas/Centaur* Mark Event readouts

Mark Event No.	Time of Event (GMT)	Station reporting
	September 8, 1967	
Liftoff	07:57:01.257	Cape Kennedy
1	07:59:34.65	Cape Kennedy
2	07:59:38.05	Cape Kennedy
3	08:00:19.65	Cape Kennedy
4	08:00:49.9	Cape Kennedy
	08:00:49.9	Bermuda
5	08:01:07.62	Cape Kennedy
	08:01:07.7	Bermuda
6	08:01:11.05	Cape Kennedy
	08:01:10.0	Bermuda
7	08:01:20.5	Cape Kennedy
	08:01:20.3	Bermuda
8	08:06:48.4	Antigua
	08:06:48.3	Bermuda
9	08:06:51.0	Antigua
	08:06:51.3	Bermuda
10	08:08:15.2	Bermuda
11	08:08:06.0	Antigua
	08:08:05.6	Bermuda
12	Not reported	
13	08:13:32.2	Coastal Crusader
	08:13:32.2	Twin Falls
	08:13:32.2	Grand Canary
14	08:13:32.1	Coastal Crusader
	08:13:32.2	Twin Falls
	08:13:32.2	Grand Canary
15	08:15:25.2	Grand Canary
16	08:15:45.5	Grand Canary
17	08:15:55.7	Grand Canary
18	08:16:16.0	Coastal Crusader
19	08:16:21.0	Coastal Crusader
	08:16:22.2	Grand Canary
20	08:16:29.0	Coastal Crusader
	08:16:26.8	Grand Canary
21	08:17:29.8	Grand Canary
22	Not reported	
23	Not reported	
24	08:20:26.8	Grand Canary
25	08:24:37.2	Pretoria
26	08:26:16.5	Pretoria
	08:26:17.0	Sword Knot

## 5. Real Time Computer System (RTCS)

For the launch and near-earth phase of the mission, the RTCS provides trajectory computations based on tracking data and telemetered vehicle guidance data. The RTCS output includes:

- (1) The interrange vector (IRV), the standard orbital parameter message (SOPM), and orbital elements and injection conditions.
- (2) Predicts, look angles, and frequencies for acquisition use by downrange stations.

- (3) Injection conditions mapped to lunar encounter and I-matrices defining orbit determination accuracies for early trajectory evaluation prior to the highly refined orbits generated by the Flight Path Analysis and Command (FPAC) group.

The RTCS made the following computations from AFETR radar, MSFN radar, *Centaur* guidance telemetry, and DSN data. (Also refer to Sections II-D and VII.)

A parking orbit was computed using postinjection data from Bermuda. The solution was considered only fair by the RTCS because of the low elevation angle of the data used. An IRV and orbital elements were provided from this data. The SFOF confirmed that the elements appeared to be close to nominal.

*Centaur* guidance telemetry data was also used by the RTCS to compute a parking orbit solution. This solution appeared to be fairly close to nominal. An IRV, orbital elements, standard orbital parameter message, (SOPM), and an I-matrix were provided from this solution.

A theoretical transfer orbit was computed by the RTCS, using Bermuda data plus nominal *Centaur* second burn data. The solution indicated that the vehicle had slightly more energy than nominal. An IRV, orbital elements, and look angles for Grand Canary, Tananarive, and Carnarvon were provided from this computation. DSN predicts for DSS 72 and DSS 51 were also provided.

An initial transfer orbit was computed by the RTCS using Grand Canary data. The data span used was during the *Centaur* turnaround maneuver, preceding retro blowdown. No metric data was available for the coast period prior to *Centaur* turnaround. The Canary solution was considered only fair-to-poor because of the low elevation angle and the slight perturbation caused by *Centaur* lateral thrusting during the turnaround maneuver. An IRV, orbital elements, SOPM, lunar encounter conditions, and Carnarvon look angles were provided from this computation. DSN predicts for DSS 51 and DSS 42 were also provided.

Three radars were scheduled to provide postretro metric tracking data to the RTCS. The Tananarive radar did not track and the Pretoria radar tracked only intermittently, which left Carnarvon as the only radar providing usable postretro data to the RTCS. The RTCS used this data to compute a postretro orbit. The solution was considered fair. An IRV, orbital elements, SOPM, lunar

encounter conditions, and an I-matrix were provided from this solution.

Thirty-five minutes of DSS 51 data was used to compute an actual transfer orbit. This solution was considered only fair by the RTCS. An IRV, orbital elements, SOPM, lunar encounter conditions, and an I-matrix were provided from this solution. DSN predicts for DSS 51 and DSS 42 were also computed.

A second DSN solution, using DSS 51 data, was computed by the RTCS. This solution was also considered fair. An IRV, SOPM, orbital elements, and lunar encounter conditions were provided from this solution.

## B. Manned Space Flight Network

The Manned Space Flight Network (MSFN), managed by GSFC, supported the *Surveyor V* mission by performing the following functions:

- (1) Tracking of the *Centaur* beacon (C-band).
- (2) Receiving and recording *Centaur*-link telemetry.
- (3) Real-time retransmission of selected *Centaur*-link telemetry.
- (4) Providing real-time confirmation of certain Mark Events.

The GSFC tracking and telemetry facilities and equipment used in support of *Surveyor V* are listed in Table V-4. GSFC also supported the Operational Readiness Test (ORT) prior to launch.

**Table V-4. GSFC Network configuration**

Station	C-band radar	VHF telemetry	Real-time retransmission
Bermuda	X	X	X (telemetry data)
Grand Canary	X	X	
Tananarive	X	X	
Carnarvon	X	X	

### 1. Acquisition Aids.

Stations at Bermuda, Tananarive and Carnarvon are equipped with acquisition aids to track the vehicle and provide RF inputs to the telemetry receivers from AOS to LOS. Performance recorders are used to record AGC and angle errors for postmission analysis. The acquisition aid systems performed their required functions during the *Surveyor V* mission.



## 2. Telemetry Data.

Bermuda, Tananarive, and Carnarvon were also equipped to decommutate, receive, and record telemetry. The telemetry requirements placed on the MSFN were:

- (1) Bermuda, Tananarive, and Carnarvon were to receive and record the *Centaur* 225.7-MHz link from AOS to LOS.
- (2) Bermuda was to receive and record the *Atlas* 229.9-MHz link from AOS to LOS.
- (3) *Centaur* Mark Event readouts were required from Bermuda, Canary, and Tananarive in real-time or as near real-time as possible after the vehicle was in view of the station.
- (4) Bermuda was to display range safety parameters on the *Atlas* and *Centaur* links.
- (5) Bermuda, Tananarive, and Carnarvon were to provide magnetic tape recordings, strip chart recordings and Post-Launch Instrumentation Message (PLIM) data sheets.
- (6) Bermuda and Canary Island were to retransmit *Centaur* data in real- and near-real-time.

The predicted vs the actual VHF telemetry coverage is shown in Fig. V-5. The overall coverage was nominal. Owing to the flight azimuth and excessive range, no pre-

dictions for Carnarvon were made. However, Carnarvon did obtain usable data.

Real-time and near-real-time transmission of VHF data from Bermuda and Grand Canary were considered excellent. Bermuda transmitted guidance data from *Centaur* Channel 16 in real-time. The support provided during this mission represented the most intensive PAM/FM real-time and near-real-time data transmission yet attempted by Grand Canary. Three groups of data were transmitted, consisting of 15 IRIG channels and one 3-kHz carrier channel modulated by 800-bit/sec pulse-code-modulated (PCM) data. Seven selected post-lift-off time measurements were sent to Building AO, Cape Kennedy, in real-time. This worked very well, and resulted in an adequate analysis of second burn performance in real-time for the first time on a *Centaur* flight.

See Table V-3 for Mark Events reported by MSFN stations during the *Surveyor V* mission.

## 3. Metric Tracking Data (C-band)

The radar requirements placed on the MSFN for the *Surveyor V* mission were:

- (1) Provide C-band beacon tracking of the *Centaur* from AOS to LOS and range safety backup support to AFETR.

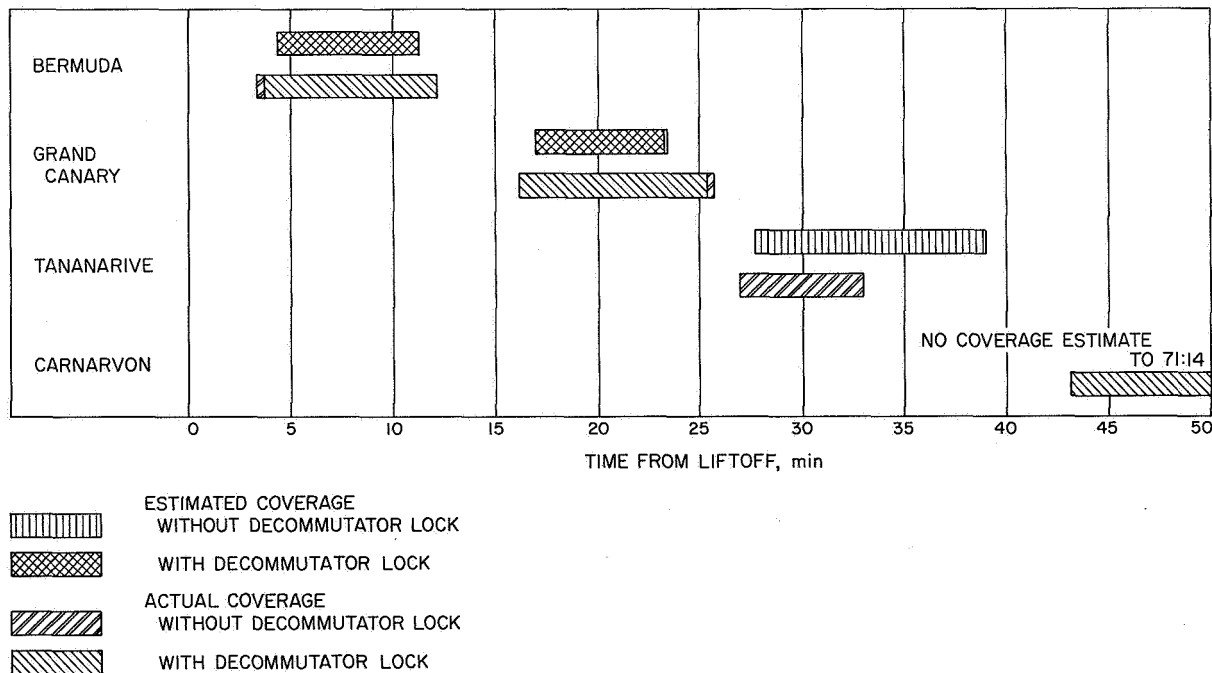


Fig. V-5. MSFN VHF telemetry coverage

- (2) Provide real-time transmission of high-speed and low-speed radar data to GSFC and RTCS.
- (3) Provide magnetic tape recording (at a minimum of 10 point/sec), strip chart recording, and PLIM data sheets.

The predicted vs the actual radar coverage is shown in Fig. V-6.

The Bermuda FPS-16 radar lost 33 sec of data because of an unfavorable aspect angle. A minor phasing problem was experienced by the FPS-16 shortly after acquisition. Although initial phasing was correct, the FPS-16 phasing operator thought he was incorrectly phased when the FPQ-6 radar at Patrick AFB caused interference. The operator rephased incorrectly, discovered the error in approximately 20 to 30 sec, then corrected his error. The Bermuda FPQ-6 radar lost 78 sec of data because of an equipment problem.

The Grand Canary radar acquired approximately 6 min late and provided about 2 min of pre-*Centaur* retro data, which was used to compute the transfer orbit. Although the acquisition message was received 30 sec prior to first view, operational procedures in use at the time prevented an early acquisition.

The Tananarive radar was operational on an engineering basis, but provided no C-band tracking data because

of confusion in operational procedures. The radar transmitter was turned on very late because the radar operator had misunderstood instructions and was waiting for Pretoria LOS.

The Carnarvon radar provided support on a limited basis because of a faulty klystron, which could only be operated on reduced power. The problem appears to reflect a logistics problem, since Carnarvon reportedly found a spare tube that was also incapable of full power output. The radar did provide post-*Centaur* retro data for orbit computations. LOS was due to the reduced power level and an unfavorable aspect angle.

#### 4. Computer Support, Data Handling, and Ground Communications

The GSFC Data Operations Branch (DOB) provides computing support for the MSFN stations during the pre-launch, launch and postinjection phases of the mission. Computer requirements were to provide MSFN station view periods for mission planning purposes and postflight reformatting of magnetic tape recordings of the radar data received from AFETR and MSFN.

The DOB provided all required support. The lateness of the acquisition message to Grand Canary was to have been expected because of the short time available to compute the data before Grand Canary rise.

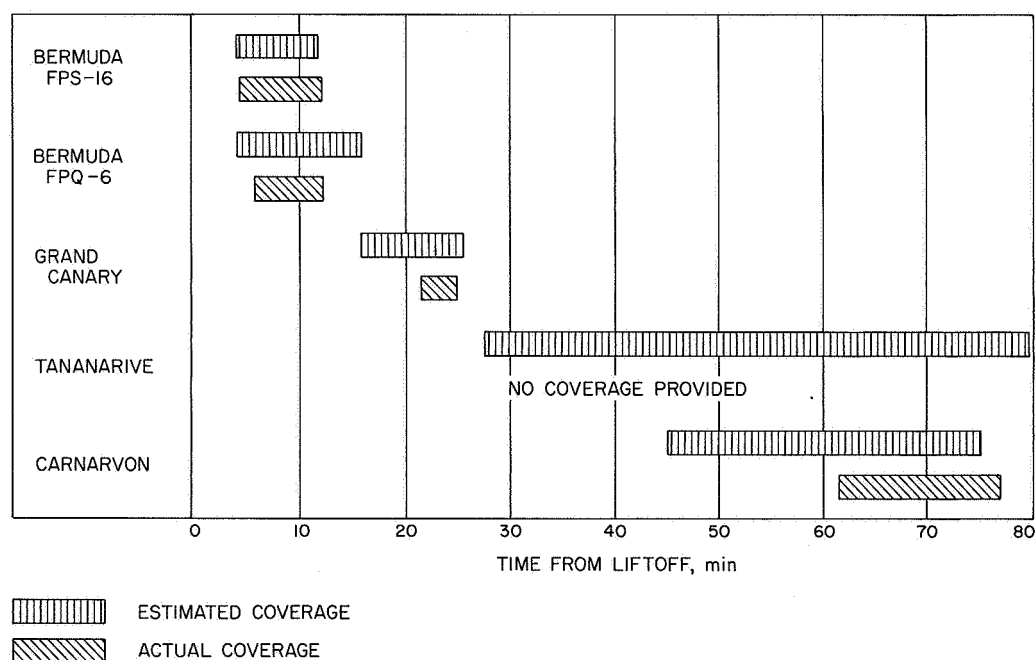


Fig. V-6. MSFN C-band radar coverage

The NASCOM Network provided 4 teletype, 8 voice, and 1 high-speed data circuits to the MSFN in support of the mission. Radio propagation forecasts were provided for all HF radio circuits commencing 8 hr before liftoff, and special coverage was implemented 6 hr before liftoff. Both voice and teletype circuits were activated via the AFETR.

### C. Deep Space Network

The DSN supports *Surveyor* missions with the integrated facilities of the Deep Space Instrumentation Facility (DSIF), the Ground Communications Facility (GCF), and the Space Flight Operations Facility (SFOF).

The DSN provides a command and telemetry link with the spacecraft upon initial acquisition of spacecraft signals by a DSIF station, enabling the DSIF station to control the spacecraft and furnish range rate data, angular tracking data, and real-time telemetry data to the SFOF. Continuous tracking and control is then provided throughout the remainder of the mission by the prime DSIF stations designated to support each *Surveyor* mission.

Following the accumulation of sufficient tracking data by the SFOF, an orbit is determined that predicts the future path of the spacecraft. This data allows the computation of a midcourse maneuver to compensate for injection errors. The DSIF, under the control of the MOS, commands the midcourse maneuver, after which engineering telemetry and tracking data is gathered and transmitted via the GCF to the SFOF, where the midcourse maneuver is evaluated and appropriate commands for the terminal maneuver are computed. After touchdown, in addition to receiving video and engineering and scientific telemetry data, the DSIF stations command the spacecraft during lunar operations.

#### 1. The DSIF

The following Deep Space Stations (DSS) were committed as prime stations for support of the *Surveyor V* mission:

DSS 11 *Pioneer*, Goldstone Deep Space Communications Complex (DSCC), Barstow, California

DSS 42 Tidbinbilla, Australia, near Canberra

DSS 61 Robledo, Spain, near Madrid

In addition to the basic support provided by prime stations, the following support was provided for the *Surveyor V* mission:

- (1) DSS 71, Cape Kennedy, provided facilities for spacecraft/DSIF compatibility testing, and also received and recorded telemetry data after liftoff. In addition, DSS 71 used its Command and Data Handling Console (CDC) and Telemetry and Command Processor (TCP) computer to process AFETR telemetry data for transmission to JPL.
- (2) DSS 14 *Mars*, Goldstone DSCC, Barstow, California, provided midcourse and terminal phase backup tracking and command support using its 210-ft-diameter antenna. At touchdown, the baseband telemetry output of the DSS 14 prime receiver was transmitted to the SFOF.
- (3) DSS 12 *Echo*, Goldstone DSCC, Barstow, California, provided backup telemetry coverage during terminal descent phase, and was used for a DSIF antennamapping experiment during postlanding operations.
- (4) DSS 51 (Fig. V-7), Johannesburg, South Africa, provided initial two-way acquisition and spacecraft commanding and tracking support during the transit phase.
- (5) DSS 72, Ascension Island, provided backup command support and early telemetry coverage.

For the September 8 launch date, DSS 51 was designated the initial two-way acquisition station.

The DSN was required to track the spacecraft and provide doppler and telemetry data as shown in Table V-5.

**Table V-5. DSN tracking data requirements**

Coverage and sampling rate	Data required
Track spacecraft from separation to first midcourse at 1-min sample rate (from initial DSIF acquisition to $L + 1$ hr, the sample rate is 1 sample per 10 sec)	Doppler (two- and three-way), antenna pointing angles, and telemetry
Track spacecraft from first midcourse to touchdown at 1-min sample rate	Doppler (two- and three-way), antenna pointing angles, and telemetry
Track spacecraft during midcourse maneuver and terminal maneuver executions at 1-sec sample rate, and transmit data at 10-sec sample rate	Doppler (two- and three-way or one-way), antenna pointing angles, and telemetry
Track spacecraft from touchdown to end of mission at 1-min sample rate during 1 hr following 10-deg elevation rise, during 1 hr centered around maximum elevation, and during 1 hr prior to 10-deg elevation set for DSS 11, 42, and 61	Doppler (two- and three-way) and telemetry

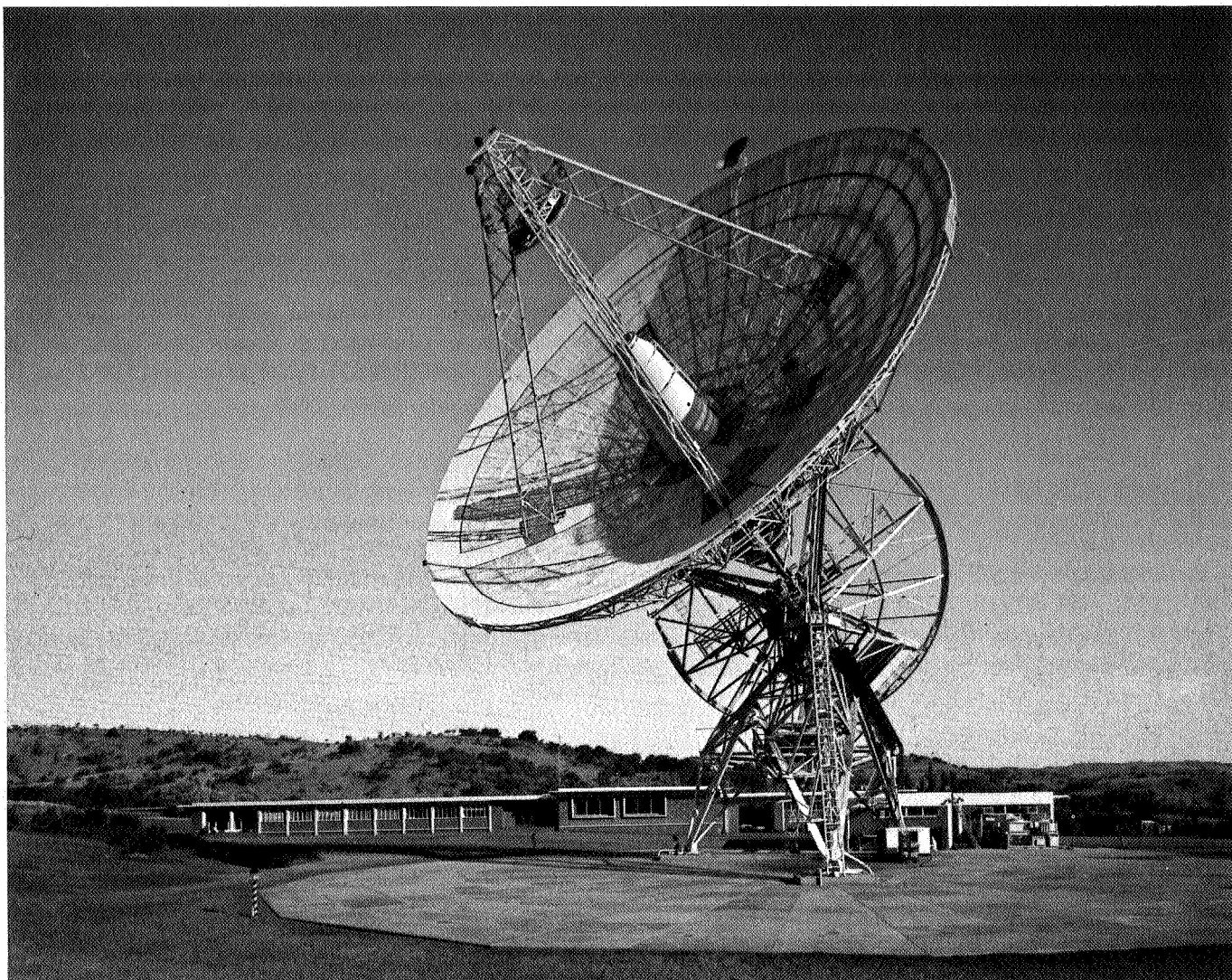


**Fig. V-7. DSS 51 antenna system at Johannesburg**

Data is handled by the prime DSIF stations as follows:

- (1) Tracking data, consisting of antenna pointing angles and doppler (radial velocity) data, is supplied in near-real-time teletype to the SFOF and post-flight in the form of punched paper tape. Two- and three-way doppler data is supplied full-time during transit, and also during lunar operations when requested by the *Surveyor* MOS. The two-way doppler function implies a transmit capability at the prime stations.
- (2) Spacecraft telemetry data is received and recorded on magnetic tape. Baseband telemetry data is supplied to the CDC for decommutation and real-time readout. The DSIF also performs precommunication processing of the decommutated data using an on-

site data processing (OSDP) computer. The data is then transmitted to the SFOF in near-real-time over high-speed data lines (HSDL).

- (3) Video data is received and recorded on magnetic tape. This data is sent to the CDC and, at DSS 11 only, to the spacecraft TV Ground Data Handling System (TV-GDHS, TV-11) for photographic recording. In addition, video data from DSS 11 is sent in real-time to the SFOF for magnetic and photographic recording by the TV-GDHS, TV-1. After lunar landing, the two DSS 11 receivers are used for different functions. One provides a signal to the CDC, the other to the TV-GDHS. (Signals for the latter system are the prime *Surveyor* Project requirement during this phase of a mission.)

- (4) Command transmission is another function provided by the DSIF. Approximately 280 commands are sent to the spacecraft during the nominal sequence from launch to touchdown. Confirmation of the commands sent is processed by the OSDP computer and transmitted by teletype to the SFOF.

The characteristics of S-band tracking systems are shown in Table V-6.

The maximum doppler tracking rate depends on the loop noise bandwidth. For phase error of less than 30 deg and strong signal (greater than  $-100$  dbm), tracking rates are as follows:

Loop noise bandwidth, Hz	Maximum tracking rate, Hz/sec
12	100
48	920
152	5000

a. *DSIF preparation testing.* A spacecraft compatibility test, configuration verification tests, system readi-

ness verification (SRV) tests, and an Operational Readiness Test (ORT) are conducted for each mission to verify that all prime stations, communication lines, and the SFOF are fully prepared to meet mission responsibility.

An RF compatibility test was conducted in July at DSS 71 verifying compatibility of the spacecraft with the DSIF.

Configuration verification tests, with all participating stations, were conducted in August and September and confirmed that the DSIF was in a functional configuration to meet mission requirements.

System readiness verification tests for all stations supporting the *Surveyor V* mission were conducted during the week prior to launch to verify readiness for the ORT and the mission. These tests include exercises involving a redesigned 7044 computer in conjunction with a communication process (CP) and DSS 11 and DSS 61. This was the first time this system was used to support a *Surveyor* mission.

**Table V-6. Characteristics for S-band tracking systems**

Antenna, tracking		Transmitter	
Type	85-ft parabolic	Frequency (nominal)	2113 MHz
Mount	Polar (HA-Dec)	Frequency channel	14b
Beamwidth $\pm 3$ db	$\sim 0.4$ deg	Power	10 kW, max
Gain, receiving	53.0 db, $+1.0$ , $-0.5$	Tuning range	$\pm 100$ kHz
Gain, transmitting	51.0 db, $+1.0$ , $-0.5$	Modulator	
Feed	Cassegrain	Phase input impedance	$\geq 50 \Omega$
Polarization	LH <sup>b</sup> or RH circular	Input voltage	$\leq 2.5$ V peak
Max. angle tracking rate <sup>a</sup>	51 deg/min = 0.85 deg/sec	Frequency response (3 db)	DC to 100 kHz
Max. angular acceleration	5.0 deg/sec/sec	Sensitivity at carrier output frequency	1.0 rad peak/V peak
Tracking accuracy ( $1\sigma$ )	0.14 deg	Peak deviation	2.5 rad peak
Antenna, acquisition		Modulation deviation stability	$\pm 5\%$
Type	2 $\times$ 2-ft horn	Frequency, standard	Rubidium
Gain, receiving	21.0 db $\pm 1.0$	Stability, short-term ( $1\sigma$ )	$1 \times 10^{-11}$
Gain, transmitting	20.0 db $\pm 2.0$	Stability, long-term ( $1\sigma$ )	$5 \times 10^{-11}$
Beamwidth $\pm 3$ db	$\sim 16$ deg	Doppler accuracy at $F_{rc}$ ( $1\sigma$ )	0.2 Hz = 0.3 m/sec
Polarization	RH circular	Data transmission	TTY and HSDL
Receiver	S-band		
Typical system temperature			
With paramp	270 $\pm 50^\circ$ K		
With maser	55 $\pm 10^\circ$ K		
Loop noise bandwidth	12, 48 or 152 Hz		
threshold ( $2B_{LO}$ )	$+0$ , $-10\%$		
Strong signal ( $2B_{LO}$ )	120, 255, or 550 Hz		
	$+0$ , $-10\%$		
Frequency (nominal)	2295 MHz		
Frequency channel	14a		

<sup>a</sup>Both axes.

<sup>b</sup>Goldstone only.

An Operational Readiness Test was conducted 1 day prior to launch and involved all DSIF committed stations, including DSS 11, 14, 42, 51, 61, 71, and 72. DSS 71 participated during the prelaunch countdown only, and DSS 14 was exercised during the test to back up DSS 11 during midcourse and terminal descent phases. Selected portions of the sequence of events were followed during the ORT, using both standard and nonstandard procedures.

The *Surveyor* on-site computer program (OSCP) integration tests, which are conducted to check out the OSCP and to verify that data can be transmitted from a DSIF station to the SFOF and processed, were reduced for *Surveyor V* to a short data flow test from each station. Such tests were conducted during the final countdown with each prime station (DSS 11, 42, and 61). Operational tests continued up until 38 hr prior to launch to provide additional training for operational personnel. An evaluation of station and net control support during the ORT indicated the readiness of the TDS.

**b. DSIF flight support.** The DSIF stations supported the *Surveyor V* mission with a high level of performance. Continuous tracking and telemetry coverage was provided, except for minor outages, from 23 min after liftoff on September 8 until 4 earth-days after lunar sunset, which occurred on September 24.

A number of minor equipment anomalies and procedural problems occurred, but were readily corrected by station personnel without affecting the mission.

All of the DSIF prime stations reported "go" status during the countdown. All measured station parameters were within nominal performance specifications, and communications circuits were up. *Surveyor V* was launched at 07:57:01 GMT on September 8, after a short delay due to an *Atlas* problem, with all essential elements of the DSN functioning nominally.

Figure V-8 contains a summary of DSIF support during the transit phase of the mission. This figure contains the periods each station tracked the spacecraft from liftoff until after touchdown and the number of commands transmitted by each station during each pass. (Also refer to the station view periods indicated in Fig. VII-2.)

One-way spacecraft signals were received by DSS 71 for 4 min and 39 sec after liftoff. DSS 71 also processed real-time AFETR telemetry with its CDC and TCP, although TCP computer problems occurred prior to

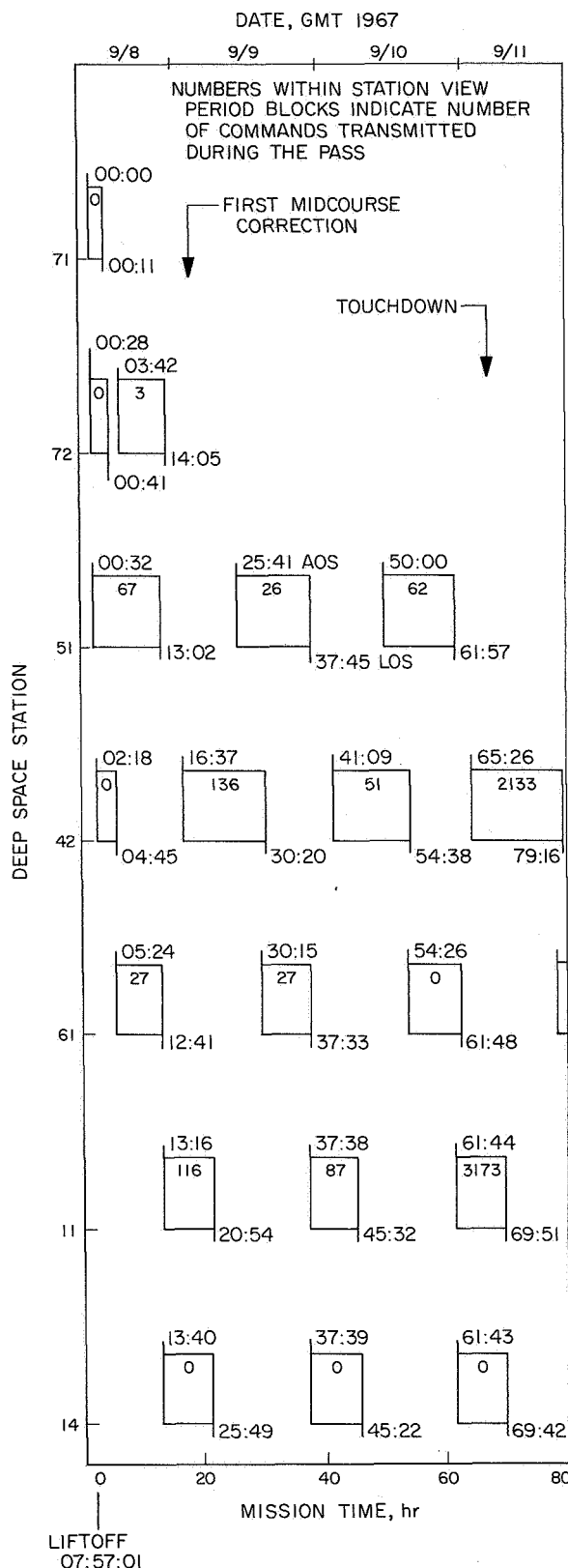


Fig. V-8. DSIF station tracking periods and command activity: transit phase

launch, causing DSS 71 data to be unusable. The backup data path via a dataphone circuit provided the required coverage, and no data was lost because of the computer outage.

DSS 72 performed initial one-way spacecraft acquisition at a very low elevation angle and tracked for 12 min during the launch pass.

DSS 51 achieved initial two-way acquisition 5 min, 11 sec after spacecraft rise over the station's horizon. Less than 7 min elapsed from the time of receipt of the first spacecraft signals until DSS 51 was prepared to command the spacecraft. DSS 51 tracked about 12 hr during the first pass, obtaining doppler data that was 89% valid.

From the time of initial two-way acquisition by DSS 51 until approximately 40 min before spacecraft main retro ignition, DSIF stations tracked *Surveyor V* in the two-way mode and, with minor exceptions, received high-quality doppler data. A loss of 70 min of two-way data occurred as a result of a dropping of up-link contact with the spacecraft by DSS 42 during the third pass, when DSS 11 was transferring receiving and commanding functions to DSS 42.

The signal levels received at the DSIF stations during the transit phase are shown in Fig. V-9. The received signal levels correspond very closely to the predicted levels. The predicted levels prior to Canopus acquisition are not given, as the spacecraft was not roll-stabilized during this period and the received signal level could vary over a wide range owing to variations in spacecraft antenna patterns. During star acquisition, midcourse correction, and terminal maneuver and descent, the spacecraft was in the high-power mode for which the received signal level is 20 db above that which exists in the low-power mode. Data bit rate changes occurred within 2 db of the predicted bit error rate thresholds. The periods during which gyro drift tests were conducted are shown at the top of the figure. Drifting of the spacecraft attitude during the gyro drift checks resulted in changes of  $\pm 3$  db in the received signal levels because of antenna pattern variations. Consistent with its 30-ft antenna, DSS 72 signal levels were approximately 10 to 12 db below signal levels received by the stations with 85-ft antennas.

The first midcourse was successfully commanded by DSS 11 during its first pass. DSS 14 also supported this phase using its 210-ft antenna. After the midcourse maneuver, telemetry data indicated a vernier propulsion

system helium leak due to a malfunctioning regulator valve. In an unsuccessful attempt to stop the leak, several additional spacecraft attitude maneuvers and vernier engine firings were commanded by the MOS using DSS 11 and 42.

The spacecraft terminal maneuvers and retro descent, which was nonstandard because of the helium leak, were successfully performed during the third DSS 11 pass. Spacecraft touchdown on the lunar surface was so gentle that none of the four receivers at the Goldstone complex (two each at DSS 11 and 14) lost one-way lock with the spacecraft.

At touchdown, the baseband telemetry output of the DSS 14 prime receiver was transmitted to the SFOF using the 96-kHz line. However, when the spacecraft strain gages were turned on prior to touchdown, this data became unprocessable. Since DSS 11 data was simultaneously sent to the SFOF using NASCOM high-speed data modems,\* good PCM data was available at touchdown.

Subsequent to the lunar landing, the DSIF provided 24-hr per day tracking coverage, with DSS 11, 42, and 61 providing postlanding mission operations support. Figure V-10 contains a summary of DSIF postlanding mission activity until spacecraft shutdown during the first lunar night on September 29, 1967 (the end of DSN committed coverage). This figure contains the periods each station tracked the spacecraft, the number of commands transmitted by each DSS during each pass, the number of TV pictures received by each DSS during each pass, and the number of hours of alpha scattering instrument data received by each DSS during each pass. The three prime stations committed to support alpha scattering operations received a total of 127 hr and 19 min of data.

In addition to normal support during the first lunar day, the DSIF conducted the following engineering experiments in accordance with prepared test descriptions.

- (1) DSS 85-ft antenna pattern measurement. This measurement was conducted at DSS 12 on September 17 and resulted in only three sets of radial measurements out to 10 deg from center being obtained because of time limitations. Subject to confirmation by later analysis, the data obtained appeared satisfactory.

\*A modem (modulator-demodulator) is a device for converting a digital signal to a signal which is compatible with telephone line transmission (e.g., frequency-modulated tone).



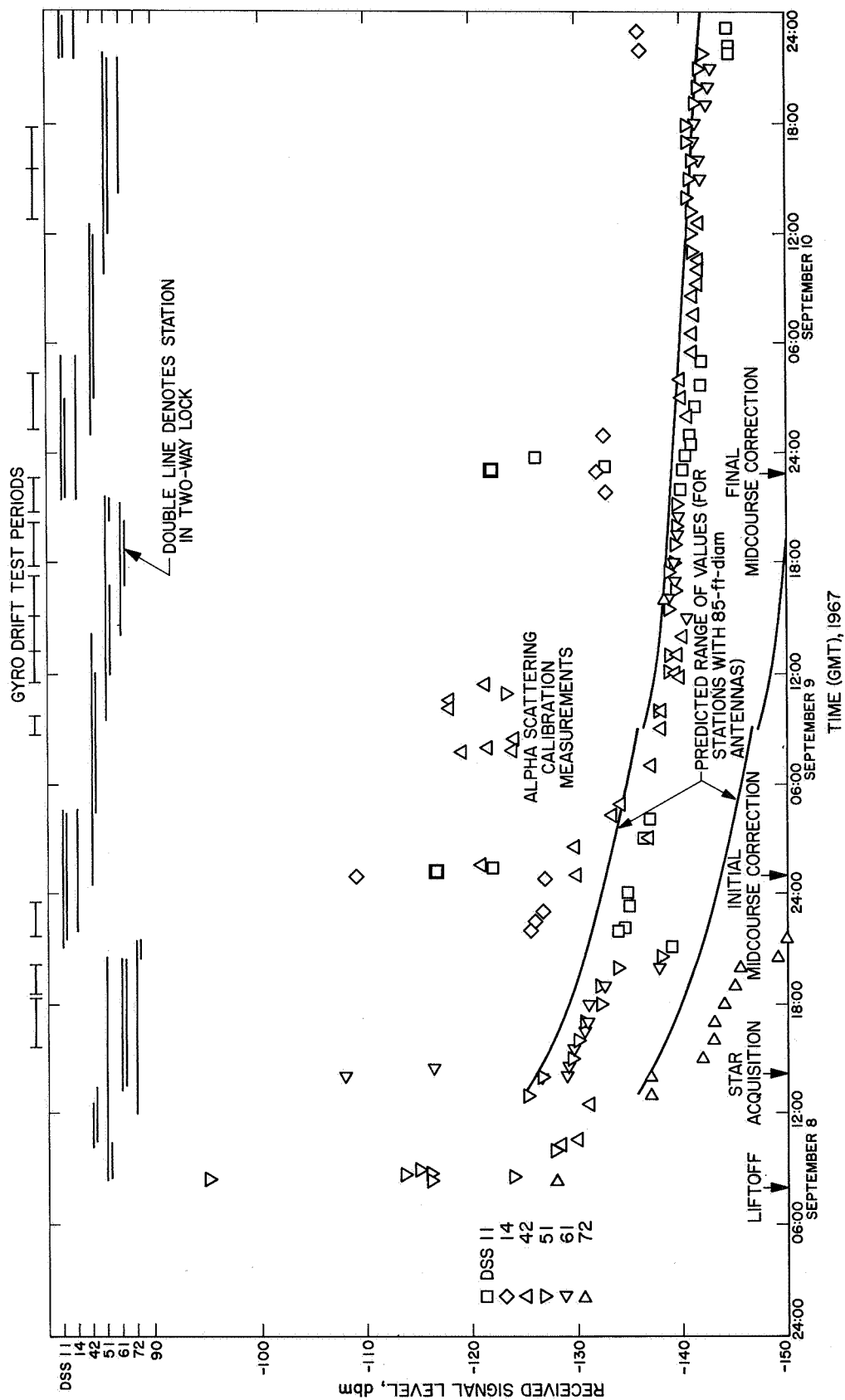


Fig. V-9. DSIF received signal level



- (2) Optimum antenna pointing for lunar surface operation. This experiment was conducted simultaneously with (1) above. Although good data was obtained, the results appeared to be inconclusive and the experiment is to be repeated on a later mission.
- (3) Doppler resolver counting. This experiment was conducted as opportunity permitted, by putting the spacecraft into the transponder mode, to obtain high-resolution two-way doppler data. Reduction of the experimental data shows good agreement with calculated values of doppler.

Attempts to reactivate *Surveyor V* during the second lunar day began at 08:00 GMT on October 15, 1967, using DSS 42. The spacecraft responded to the first series of commands, and good telemetry was received a short time later. Continuous tracking coverage was provided by the DSN for the remainder of the second lunar day except for a period from October 18 to 20, when DSS 11 and DSS 42 were required to support the *Mariner 1967* mission during Venus encounter. During this period, only DSS 61 was available for *Surveyor* support. Special coverage for the lunar eclipse on October 18 was provided by DSS 11 and by the MSFN station at Honeysuckle Creek (near Canberra, Australia), in conjunction with DSS 42. This coverage provided desired thermal data during the eclipse.

Continuous tracking coverage resumed on October 21 and continued until October 25, 48 hr after second lunar-day sunset. Coverage was provided after this time during the second lunar-night consisting of brief interrogations of the spacecraft, with the intervals between interrogations increasing from 4 hr to 24 hr over an eight-day period. This activity was terminated about 200 hr after sunset at 12:20 GMT November 1, 1967.

## 2. GCF/NASCOM

For *Surveyor* missions, the GCF transmits tracking, telemetry, and command data from the DSIF to the SFOF, and control and command functions from the SFOF to the DSIF by means of NASCOM facilities. The GCF also transmits simulated tracking data to the DSIF and video data and base-band telemetry from DSS 11, Goldstone DSCC, to the SFOF. The links involved in the system are shown in Fig. V-11. On the *Surveyor V* mission, for the first time, all communication circuits between the DSIF and SFOF were automatically switched using a communication processor (CP).

The GCF/NASCOM demonstrated a high degree of reliability during the ORT conducted before the mission. The performance of the NASCOM facilities in support of the *Surveyor V* mission was considered excellent, demonstrating a high degree of reliability.

**a. Teletype (TTY) circuits.** Teletype circuits (four available to prime stations) are used for transmitting tracking and telemetry data, commands, and administrative traffic. The *Surveyor V* mission utilized the CP for teletype circuit switching. The teletype circuits and the CP were exceptionally reliable, the weakest circuits (to DSS 51) showing approximately 98% reliability.

DSS 51 and 72 experienced outages on the high-frequency radio path circuits due to propagation problems. The JPL CP faulted twice during the ORT, once during the transit phase of the mission, and also during lunar operations. The GSFC CP and the Canberra and London circuits also caused minor outages during the mission.

During the ORT and the mission, the DSS 72 circuits handling tracking data and operational messages were routed via satellite with excellent results.

**b. Voice circuits.** The voice circuits are shared between the DSIF and the *Surveyor* Project for administrative, control, and commanding functions. The NASCOM voice circuits provided for the *Surveyor V* mission performed well except for several minor outages.

A voice circuit, via satellite to Ascension, then by HF radio through Pretoria to DSS 51, was activated as a backup during the mission launch phase. This circuit provided coverage during periods when the normal voice circuits failed and was used to back-feed the "Voice of *Surveyor*" to DSS 51.

The DSS 72 voice circuit was routed via satellite during both the ORT and the mission and performed exceptionally well.

**c. High-speed data lines (HSDL).** One HSDL is provided to each prime site for telemetry data transmission to the SFOF in real-time. This part of the communications system performed well during both the prelaunch testing and mission phases.

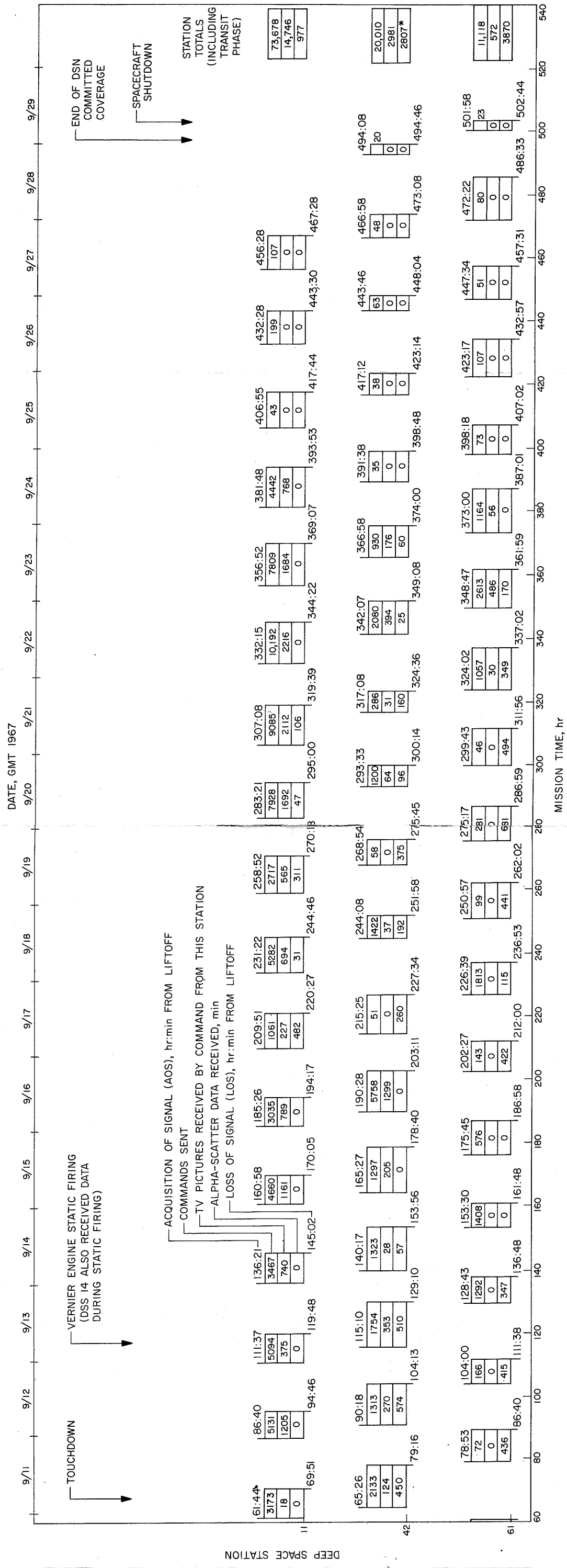


**Fig. V-10. DSIF station tracking periods and command activity: postlanding (first lunar day)**

\*OF THIS TOTAL, 48 min CALIBRATION DATA RECEIVED DURING TRANSIT



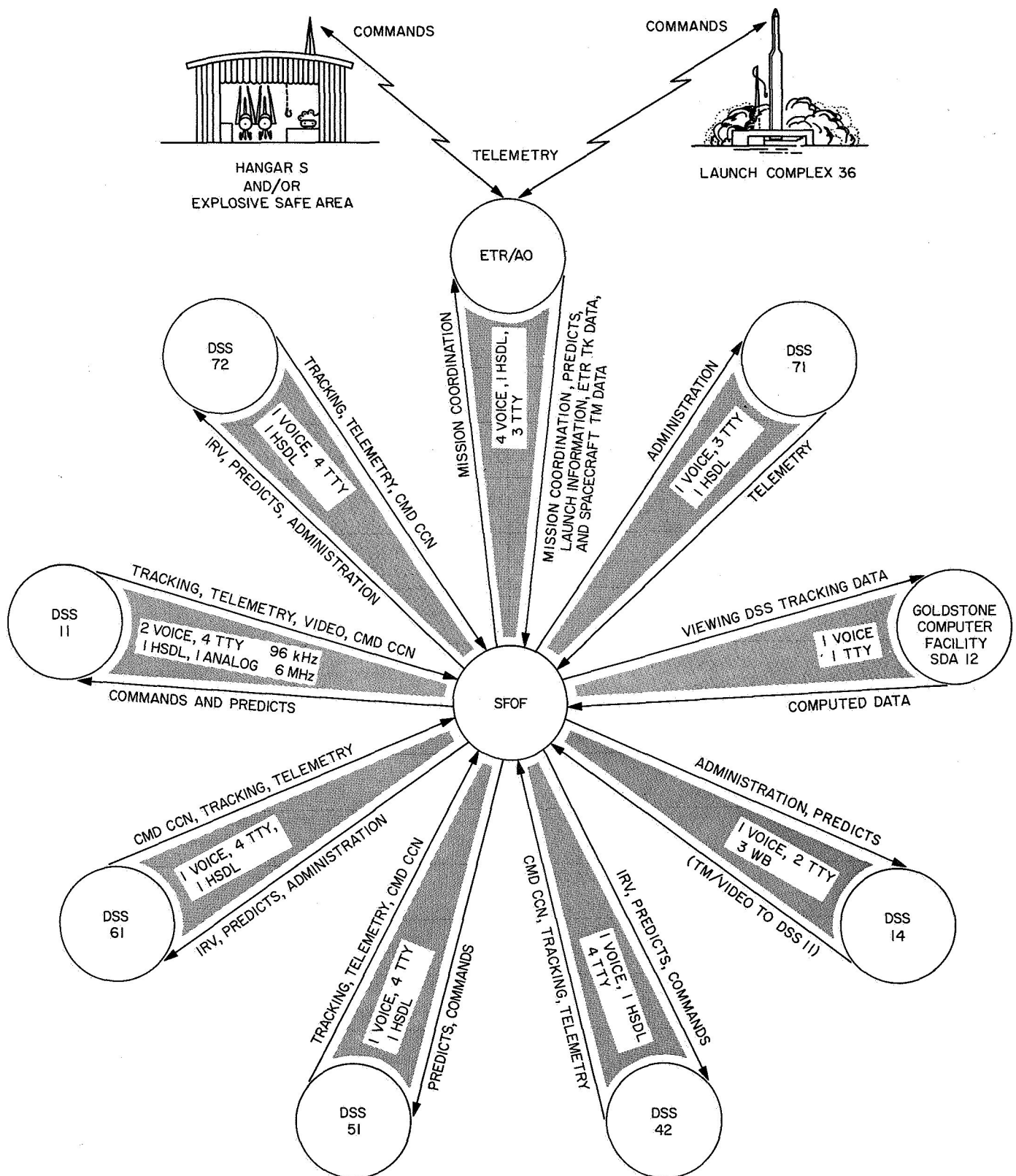


Fig. V-11. DSN/GCF communications links

The lines were used during testing to transmit simulation data to the stations and during the mission to back-feed various voice nets as required. The DSS 72 data circuit was routed via satellite during both the ORT and the mission. Performance was excellent.

Both modem types (NASCOM and Hallicrafters) were required during the *Surveyor V* mission. NASCOM modems were used for sending high-speed data from all stations except DSS 51, and reliability was very high. DSS 51 used the Hallicrafter modem, which performed reliably, the only circuit problems being due to propagation. Minor problems occurred during launch when several stations were active and modem switching was required in order for each station to perform data transfer tests.

**d. Wideband microwave system.** The wideband microwave link between DSS 11, Goldstone DSCC, and the SFOF consists of one 6-MHz simplex (one-way) channel for video and one 96-kHz duplex (two-way) data channel. The link performed with excellent reliability during the *Surveyor V* mission. An outage occurred during the transit phase, but this was during the early part of the checkout period prior to the DSS 11 pass and did not affect the performance of the mission.

### 3. DSN in SFOF

The DSN supports the *Surveyor* missions by providing mission control facilities and performing special functions within the SFOF.

**a. Data processing system (DPS).** The SFOF Data Processing System, under the control of the MOS, performs the following functions for *Surveyor* missions.

- (1) Computation of acquisition predictions for DSIF stations (antenna pointing angles and receiver and transmitter frequencies).
- (2) Orbit determinations.
- (3) Midcourse maneuver computation analysis.
- (4) On-line telemetry processing.
- (5) Command tape generation.
- (6) Simulated data generation (telemetry and tracking data for tests).

The DPS general configuration for the *Surveyor V* mission is shown in Fig. V-12 and consists of two PDP-7 computers in the telemetry processing station (TPS), two

strings of IBM 7044/7094 computers in the Central Computing Complex (CCC), and a subset of the input/output (I/O) system.

For *Surveyor V* a redesigned computer configuration in conjunction with a communication processing (CP) system was implemented which automatically switched teletype lines and allowed computer sharing in support of other concurrent space program missions. Its capabilities included switching, real-time monitoring, quick access message logging, and recall. Computer processor problems, although not significantly affecting the mission, did cause delays in providing SFOF user areas with incoming data.

The DPS performed in an excellent manner, with only minor hardware problems which did not detract from mission support. The two PDP-7 computers were used extensively to process high-speed telemetry data for the *Surveyor V* mission. This processing consisted of decommutating and transferring the data to the 7044 computer via the 7288 data channels, generating a digital tape for non-real-time processing, and supplying digital-to-analog converters with discrete data parameters to drive analog recorders in both the spacecraft analysis area and the space science analysis area.

The IBM 7044/7094 computer string dual configuration successfully processed all high-speed data received from the TPS and all teletype data received from the communications center, as well as all input/output requests from the user areas.

The input/output system provides the capability for entering data control parameters into the 7044/7094 computers and also for displaying computed data in the user areas via the various display devices. The input/output system performed adequately; many minor problems were reported, but were resolved in real-time without loss of data.

**b. DSN Intracommunications System (DSN/ICS).** The DSN/ICS provides the capability of receiving, switching, and distributing all types of information required for spaceflight operations and data analysis to designated areas or users within the SFOF. The system includes facilities for handling all voice communications, closed circuit television, teletypes, high-speed data, and data received over the microwave channels.

The DSN/ICS performed in an exceptional manner, with only minor anomalies.

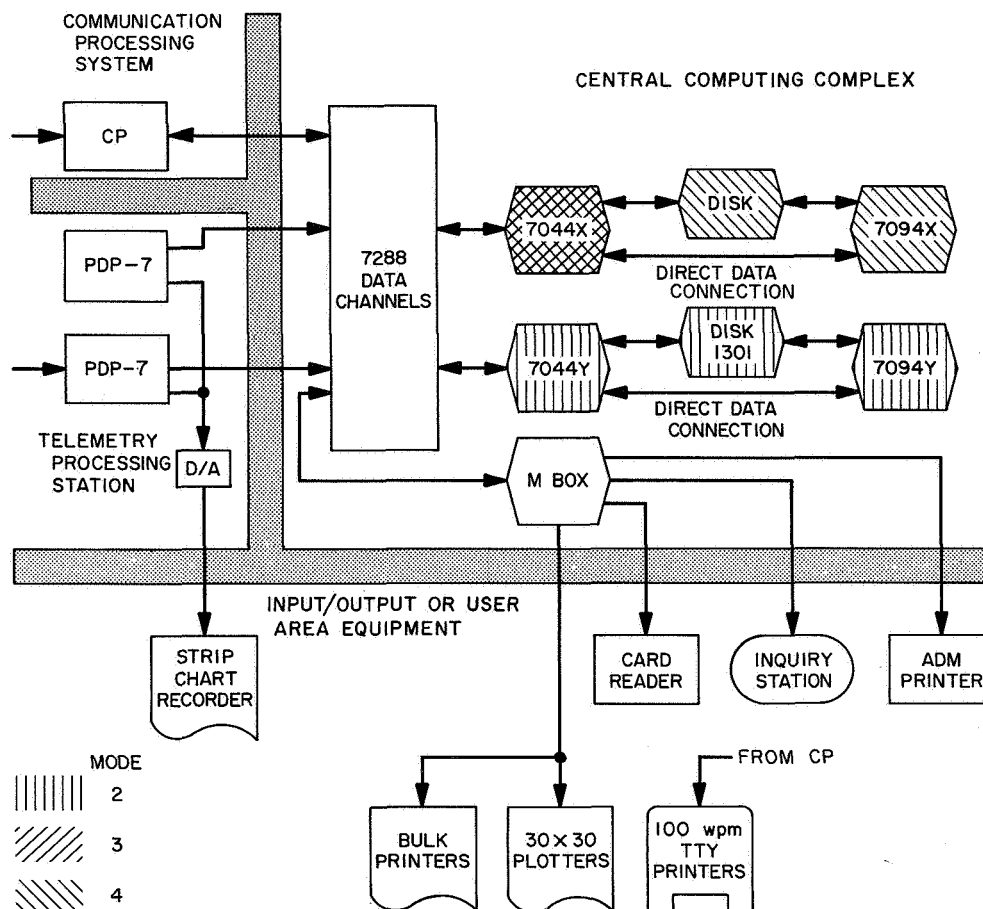


Fig. V-12. General configuration of SFOF data processing system

The television communications subsystem experienced minor equipment problems that were resolved in real-time. During the launch phase there was a shortage of TV monitors used for viewing teletype lines.

#### 4. DSN/AFETR Interface

The DSN/AFETR interface provides real-time data transmission capability for both VHF and S-band down-range telemetry from Building AO at Cape Kennedy to the SFOF. The nominal time of switchover from VHF to S-band telemetry is after spacecraft S-band transmitter high-power turn-on. The interface with the *Surveyor* Project is at the input to the CDC, Building AO, where it is sent to DSS 71 for processing by the CDC and the telemetry and command processor (TCP) computer. The output of the CDC is transmitted to the SFOF via the GCF/NASCOM. During the *Surveyor V* mission, this configuration was established as the prime link between the SFOF and AFETR to provide an interface similar to the data transmission links with prime DSIF stations. The

previously used link between Building AO and SFOF, via Bell modems, was retained as backup. A new interface, for Building AO and DSS 71 to receive AFETR real-time telemetry from TEL 4 at Kennedy Space Center, was exercised and performed very well.

In-flight spacecraft telemetry was received from the AFETR stations and relayed to the SFOF until approximately 40 min after liftoff.

Both the prime DSS 71 and the Bell modem backup systems provided good data during the mission, but due to the high quality of the Bell modem data, the DSS 71 data was not processed. The backup system was also used during the ORT to provide simulated telemetry data from the SFOF to Building AO and performed well.

DSIF tracking data for early orbit determination was successfully back-fed to the Real Time Computer System at the AFETR.



## VI. Mission Operations System

### A. Functions and Organization

The basic functions of the Mission Operations System (MOS) are the following:

- (1) Continual assessment and evaluation of mission status and performance, utilizing the tracking and telemetry data received and processed.
- (2) Determination and implementation of appropriate command sequences required to maintain spacecraft control and to carry out desired spacecraft operations during transit and on the lunar surface.

The *Surveyor* command system philosophy introduces a major change in the concept of unmanned spacecraft control: virtually all in-flight and lunar operations of the spacecraft must be initiated from earth. In previous space missions, spacecraft were directed by a minimum of earth-based commands. Most in-flight functions of those spacecraft were automatically controlled by an on-board sequencer which stored preprogrammed instructions. These instructions were initiated by either an on-board timer or by single direct commands from earth. For example, during the *Ranger VIII* 67-hr mission, only 11 commands were sent to the spacecraft; whereas for a standard *Surveyor* mission, approximately 300 commands

are sent to the spacecraft during the transit phase, out of a command vocabulary of 201 different direct commands. For *Surveyor V*, about 725 commands were sent during transit and over 100,000 commands were sent following touchdown.

Throughout the space flight operations of each *Surveyor* mission, the command link between earth and spacecraft is in continuous use, transmitting either fill-in or real commands every 0.5 sec. The *Surveyor* commands are controlled from the SFOF and are transmitted to the spacecraft by a DSIF station.

The equipment utilized to perform MOS functions falls into two categories: mission-independent and mission-dependent equipment. The former is composed chiefly of the *Surveyor* TDS equipment described in Section V. It is referred to as mission-independent because it is general-purpose equipment which can be utilized by more than one NASA project when used with the appropriate project computer programs. Selected parts of this equipment have been assigned to perform the functions necessary to the *Surveyor* Project. The mission-dependent equipment (described in Section VI-B, following) consists of special equipment which has been installed at DSN facilities for specific functions peculiar to the project.



The *Surveyor* Project Manager, in his capacity as Mission Director, is in full charge of all mission operations. The Mission Director is aided by the Assistant Mission Director and a staff of mission advisors. During the mission, the MOS organization was as shown in Fig. VI-1.

Mission operations are under the immediate, primary control of the Space Flight Operations Director (SFOD) and supporting *Surveyor* personnel. Other members of the team are the TDS personnel who perform services for the *Surveyor* Project.

During space flight and lunar surface operations, all commands are issued by the SFOD or his specifically

delegated authority. Three groups of specialists provide technical support to the SFOD in the flight path, spacecraft performance, and science areas.

### 1. Flight Path Analysis and Command Group

The Flight Path Analysis and Command (FPAC) group handles those space flight functions that relate to the location of the spacecraft. The FPAC Director maintains control of the activities of the group and makes specific recommendations for maneuvers to the SFOD in accordance with the flight plan. In making these recommendations, the FPAC Director relies on five subgroups of specialists within the FPAC group.

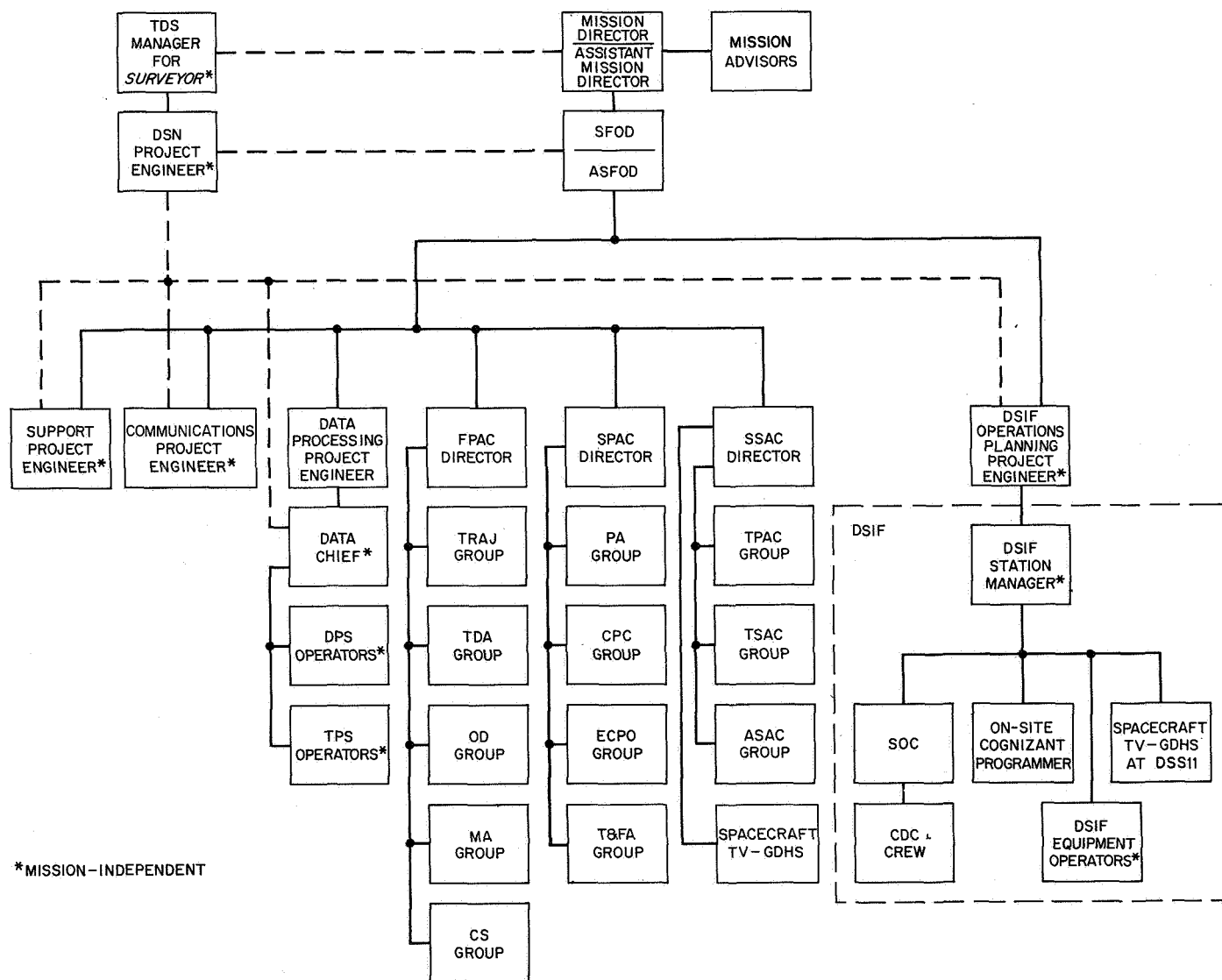


Fig. VI-1. Organization of the MOS during the *Surveyor V* mission

- (1) The Trajectory (TRAJ) group determines the nominal conditions of spacecraft injection and generates lunar encounter conditions based on injection conditions as reported by AFETR and computed from tracking data by the Orbit Determination group. The actual trajectory determinations are made by computer.
- (2) The Tracking Data Analysis (TDA) group makes a quantitative and descriptive evaluation of tracking data received from the DSIF stations. The TDA group provides 24-hr/day monitoring of incoming tracking data. To perform these functions the TDA group takes advantage of the Data Processing System (DPS) and of computer programs generated for their use. The TDA group acts as direct liaison between the data users (the Orbit Determination group) and the DSIF and provides predictions to the DSIF.
- (3) The Orbit Determination (OD) group, during mission operations, determines the actual orbit of the spacecraft by processing the tracking data received from the DSN tracking stations by way of the TDA group. Also, statistics on various parameters are generated so that maneuver situations can be evaluated. The OD group generates tracking predictions for the DSIF stations and recomputes the orbit of the spacecraft after maneuvers to determine the success of the maneuver.
- (4) The Maneuver Analysis (MA) group is the subgroup of FPAC responsible for developing possible mid-course and terminal maneuvers for both standard and nonstandard missions in real-time during the actual flight. In addition, once the decision has been made as to what maneuver should be performed, the MA group generates the proper spacecraft commands to effect these maneuvers. These commands are then relayed to the Spacecraft Performance Analysis and Command group to be included with other spacecraft commands. Once the command message has been generated, the MA group must verify that the calculated commands are correct.
- (5) The Computer Support (CS) group acts in a service capacity to the other FPAC subgroups, and is responsible for ensuring that all computer programs used in space operations are fully checked out before mission operations begin and that optimum use is made of the Data Processing System facilities.

## 2. Spacecraft Performance Analysis and Command Group

The Spacecraft Performance Analysis and Command (SPAC) group, operating under the SPAC Director, is basically responsible for the operation of the spacecraft itself. The SPAC group is divided into four subgroups:

- (1) The Performance Analysis (PA) group monitors incoming engineering data telemetered from the spacecraft, determines the status of the spacecraft, and maintains spacecraft status displays throughout the mission. The PA group also determines the results of all commands sent to the spacecraft. In the event of a failure aboard the spacecraft, as indicated by telemetry data, the PA group analyzes the cause and recommends appropriate nonstandard procedures.
- (2) The Command Preparation and Control (CPC) group is basically responsible for preparing command sequences to be sent to the spacecraft. In so doing they provide inputs for computer programs used in generating the sequences, verify that the commands for the spacecraft have been correctly received at the DSS, and then ascertain that the commands have been correctly transmitted to the spacecraft. If nonstandard operations become necessary, the group also generates the required command sequences. The CPC group controls the actual transmission of commands at the DSS by the *Surveyor* operations chief.
- (3) The Engineering Computer Program Operations (ECPO) group includes the operators for the DPS input/output (I/O) console and related card punch, card reader, page printers, and plotters in the spacecraft performance analysis area (SPAA). The ECPO group handles all computing functions for the rest of the SPAC group, including the maintenance of an up-to-date list of parameters for each program.
- (4) The Trend and Failure Analysis (T&FA) group consists of spacecraft design and analysis specialists who provide in-depth, near-real-time spacecraft performance analysis (in contrast to the PA group's real-time analysis). The group also manages the interface for the SCCF computer facility at Hughes Aircraft Company. The SCCF 1219 is used mainly for premission spacecraft ground testing but, during the mission, the T&FA group is provided two data lines to the SCCF 1219 via the TPS, which will accommodate telemetry rates up to 4400 bit/sec,

and eight incoming lines terminating at seven teleprinters and one line printer in the SPAC area. The T&FA group uses the system to process and display engineering data transmitted from the spacecraft. The group also includes draftsmen who perform wall chart plotting and maintain wall displays of spacecraft condition and performance.

### 3. Space Science Analysis and Command Group

The Space Science Analysis and Command (SSAC) group performs those space flight functions related to the operation of the TV camera and science instruments. SSAC is divided into the following operating subgroups:

- (1) The Television Performance Analysis and Command (TPAC) group analyzes the performance of the TV equipment and is responsible for generating standard and nonstandard command sequences for the survey TV camera.
- (2) The Television Science Analysis and Command (TSAC) group analyzes and interprets the TV pictures for the purpose of ensuring that the mission objectives are being met. The TSAC group is under the direction of the Project Scientist and performs the scientific analysis and evaluation of the TV pictures.
- (3) The Soil Mechanics Analysis and Command (SMAC) group prepares and recommends the commands to be sent to the soil mechanics/surface sampler instrument (SM/SS), and is also responsible for operating the SM/SS and analyzing its performance. This group was not utilized on the *Surveyor V* mission because an SM/SS instrument was not included on the spacecraft.
- (4) The Alpha Scattering Analysis and Command (ASAC) group prepares and recommends the commands to be sent to the alpha scattering instrument. This group is also responsible for conducting alpha scattering instrument operations during transit and lunar phases and for analyzing its performance.

The portion of the spacecraft TV Ground Data Handling System (TV-GDHS) in the SFOF provides direct support to the SSAC group in the form of processed electrical video signals and finished photographic prints. The TV-GDHS operates as a service organization within the MOS structure. Documentation, system checkout, and quality control within the system are the responsibility of the TV-GDHS Operations Manager. During operations

support the TV-GDHS Operations Manager reports to the SSAC Director.

### 4. Data Processing Personnel

The use of the Data Processing System (DPS) by *Surveyor* is under the direction of the Assistant Space Flight Operations Director (ASFOD) for Computer Programming. His job is to direct the use of the DPS from the viewpoint of the MOS. He communicates directly with the Data Chief, who is in direct charge of DPS personnel and equipment. Included among these personnel are the I/O console operators throughout the SFOF, as well as the equipment operators in the DPS and Telemetry Processing Station (TPS) areas.

Computer programs are the means of selecting and combining the extensive data processing capabilities of electronic computers. By means of electronic data processing, the vast quantities of mission-produced data are assembled, identified, categorized, processed and displayed in the various areas of the SFOF where the data are used. Their most significant service to the MOS is providing knowledge in real-time of the current state of the spacecraft throughout the entire mission. This service is particularly important to engineers and scientists of the technical support groups since, by use of the computer programs, they can select, organize, compare and process current-status data urgently needed to form their time-critical recommendations to the SFOD. (See Section V-C-3 for a description of the DPS.)

### 5. Other Personnel

The Communications Project Engineer (PE) controls the operational communications personnel and equipment within the SFOF, as well as the DSN/GCS lines to the DSIF stations throughout the world.

The Support PE is responsible for ensuring the availability of all SFOF support functions, including air conditioning and electric power; for monitoring the display of *Surveyor* information on the Mission Status Board and throughout the facility; for directing the handling, distribution, and storage of data being derived from the mission; and for ensuring that only those personnel necessary for mission operations are allowed to enter the operational areas.

The DSIF Operations Planning PE is in overall control of all DSIF stations; his post of duty is in the SFOF in Pasadena. At each station, there is a local DSIF station manager, who is in charge of all aspects of his DSIF

station and its operation during a mission. The *Surveyor* personnel located at each station report to the station manager.

## B. Mission-Dependent Equipment

Mission-dependent equipment consists of special hardware provided exclusively for the *Surveyor* Project to support the Mission Operations System. Most of the equipment in this category is contained in the Command and Data Handling Consoles (CDC) and spacecraft Television Ground Data Handling System (TV-GDHS), which are described below.

### 1. Command and Data Handling Console

*a. CDC equipment.* The Command and Data Handling Console comprises that mission-dependent equipment located at the participating Deep Space Stations that is used to:

- (1) Generate commands for control of the *Surveyor* spacecraft by modulation of the DSS transmitter.
- (2) Process and display telemetered spacecraft data and relay telemetry signals to the on-site data processor (OSDP) for transmission to the SFOF.
- (3) Process, display and record television pictures taken by the spacecraft.

The CDC consists of four major subsystems:

- (1) The command subsystem generates FM digital command signals from punched tape or manual inputs for the DSS transmitter, and prints a permanent record of the command sent. The major units of the command subsystem, which can accommodate 1024 different commands, are the command generator, the command subcarrier oscillator, the punched tape reader, and the command printer. Outgoing commands are logged on magnetic tape by the DSS and are relayed to the SFOF.
- (2) The FM demodulator subsystem accepts the FM intermediate-frequency signal of the DSS receiver and derives from it a baseband signal. The baseband signal consists of either video data or a composite of engineering subcarrier signals. Depending upon the type of data constituting the baseband signal, the CDC processes the data in either the TV data subsystem or the telemetry data subsystem.

(3) The TV data subsystem receives video data from the FM demodulator and processes it for real-time display at the CDC and for 35-mm photographic recording. In addition, telemetered frame-identification data is displayed and photorecorded. A long-persistence-screen TV monitor is mounted in the CDC. The operator, when requested, can thus evaluate the picture and, upon the SFOF's direction, initiate corrective commands during lunar television surveys.

(4) The telemetry data subsystem of the CDC separates the various data channels from the baseband signal coming from either the FM demodulator or the DSS receiver phase-detected output and displays the desired data to the operators. Discriminators are provided for each subcarrier channel contained in the baseband signal. In the case of time-multiplexed data, the output of each discriminator is sent to the pulse code modulation (PCM) decommutator and then relayed to both the OSDP computer for subsequent transmission to the SFOF and to meters for evaluation of spacecraft performance. In the case of continuous data transmissions, the output of the discriminator is sent to an oscilloscope for recording and evaluation. Alpha scattering experiment data is demodulated like other telemetry data, but is allowed to accumulate for periods of time in a SDS 920 computer in order to form spectrum information, which is then relayed to SFOF via teletype circuits.

The CDC contains built-in test equipment to insure normal operations of its subsystems. A CDC tester, consisting of a spacecraft transponder with the necessary modulation and demodulation equipment, insures day-to-day compatibility of the CDC and DSIF stations.

*b. CDC operations.* Table VI-1 lists the CDC mission-dependent equipment provided for support of *Surveyor V* at the DSIF stations. CDC's were located at DSS 11, 42, 51, 61, 71, and 72 and, during the mission, CDC operations were conducted at each of these stations. Table VI-2 lists the total number of commands transmitted, number of TV frames commanded and minutes of alpha scattering data accumulated in the telemetry and command processor (TCP) at each station during the transit phase and through the first lunar day's activities. (Refer to Figs. V-8 and V-10 for station activity during each pass including minutes of alpha scattering data received and recorded, all of which is not always accumulated in the station TCP.) Following is a brief summary of CDC

**Table VI-1. CDC mission-dependent equipment support of Surveyor V at DSIF stations**

DSS 11, Goldstone	Prime station with command, telemetry, TV and alpha scattering
DSS 42, Canberra	Prime station with command, telemetry, TV and alpha scattering
DSS 51, Johannesburg	Prime station for telemetry during cislunar phase
DSS 61, Madrid	Prime station with command, telemetry, TV and alpha scattering
DSS 71, Cape Kennedy	Station used for spacecraft compatibility tests and pre- and postlaunch telemetry data processing
DSS 72, Ascension	Backup station with command and telemetry
DSS 14, Goldstone	Station configured for command backup and telemetry reception via both the DSS 11 CDC and SFOF. Also used to record terminal descent and landing phase

**Table VI-2. Surveyor V command, TV and alpha scattering activity before shutdown during first lunar night**

Station	Commands transmitted	TV frames commanded	Alpha scattering data accumulated in station TCP, min
DSS 11	73,628	14,746	708
DSS 42	20,010	2,981	2,031
DSS 51	155	0	0
DSS 61	11,118	572	2,885
DSS 71	0	0	0
DSS 72	3	0	0

operations at each station before shutdown during the first lunar night.

- (1) DSS 11 Goldstone. The Pioneer station at Goldstone participated in 19 passes. Major mission events occurring at DSS 11 were midcourse maneuvers during the first and second passes and terminal descent during the third pass. After spacecraft landing, during the lunar day and into the lunar night, the station's activity emphasized the commanding of television pictures, although alpha scattering data was also accumulated and engineering interrogations were performed. Of the total TV frames obtained, 78% were commanded from this station, but only 13% of the total alpha scattering data was accumulated by this station.

The successful vernier static firing test was performed during the fifth pass. During the mission

problems were experienced with the TV generator, FM calibrator, command generator, input/output typewriter, and paper tape punch, but none of these had any effect upon the mission.

- (2) DSS 42 Canberra. Canberra participated in 21 passes. This station accomplished 18% of the TV commanding and 36% of the total alpha scattering accumulation time. CDC equipment problems during the mission occurred with the command generator, command printer, tape punch, low frequency oscillograph and film magazine of the photo recorder and a patch panel incorrectly seated. None of these problems had an effect upon the mission.
- (3) DSS 51 Johannesburg. DSS 51 participated in 3 passes during the transit phase and was not committed for use after touchdown. The initial acquisition by DSS 51 was accomplished very smoothly with everything normal. There were no CDC equipment problems during this mission.
- (4) DSS 61 Madrid. DSS 61 participated in 21 passes. Throughout the lunar day, alpha scattering operations comprised the primary activity with 51% of the total alpha scattering data accumulated by this station. Some television sequences were commanded; however, this represented only 3% of the total TV activity. The only CDC equipment problem occurred in the binary command comparator, a piece of test equipment, and this had no effect upon the mission.
- (5) DSS 71 Cape Kennedy. DSS 71 support for Surveyor V consisted of a DSIF/spacecraft compatibility test, the operational readiness test, the spacecraft prelaunch countdown, and approximately the first 40 min after liftoff. Data from the various AFETR tracking stations was routed to TEL-4\* until approximately 40 min after liftoff, and was then processed by DSS 71 and sent to the SFOF. There were no CDC equipment problems during this mission.
- (6) DSS 72 Ascension. DSS 72 was committed to back up DSS 51 for this mission. The station participated in two passes. During the second, three commands were transmitted to the spacecraft. There were no CDC equipment problems during the mission.

\*AFETR telemetry processing facility at Cape Kennedy.

## 2. Spacecraft Television Ground Data Handling System

The spacecraft Television Ground Data Handling System (TV-GDHS) was designed to record, on film, the television images received from *Surveyor* spacecraft. The principal guiding criterion was photometric and photogrammetric accuracy with negligible loss of information. This system was also designed to provide display information for the conduct of mission operations, and the production of user products, such as archival negatives, prints, enlargements, duplicate negatives, and a digital tape of the TV ID information for use in production of the ID catalogs.

The system is in two parts, TV-11 at DSS 11, Goldstone, and TV-1 at the SFOF in Pasadena. At DSS 11 is an on-site data recovery (OSDR) subsystem and an on-site film recorder (OSFR) subsystem. These subsystems are duplicated in the media conversion data recovery (MCDR) subsystem, and in the media conversion film recorder (MCFR) subsystem at the SFOF. The portion of the system used in real-time at the SFOF is comprised of the MCDR, the MCFR, the media conversion computer, the video display and drive subsystem (VDDS), and the FR-700 and HW-7600 magnetic tape recorders. (The HW-7600 recorder was used for the first time on the *Surveyor V* mission. The previously used FR-1400 was available as backup.) A film processor, the strip contact printer, and the strip contact print processor are used in near-real-time. The photographic subsystem used in non-real-time is comprised of several enlargers, a copy camera, two film processors, a film chip file, other photographic equipment, and film storage areas.

*a. TV-GDHS at DSS 11 (TV-11).* Data for the TV-GDHS is injected into the system at the interface between the DSS 11 receiver and the OSDR. In both the 200-line and the 600-line modes, the OSDR provides to the film recorder subsystem: (1) the baseband video signal, (2) the horizontal sync signal, (3) the vertical frame gate, (4) the resynchronized raw ID telemetry information, and (5) the time code. In 200-line mode, the OSDR also supplies a 500-kHz predetection signal to the DSS 11 FR-800 and FR-1400 magnetic tape recorders and to the SFOF via the microwave communication link. In 600-line mode, the OSDR provides: (1) a 4-MHz predetected signal to the DSS 11 FR-800 and to the SFOF via the microwave communication link, and (2) a baseband video signal to the DSS 11 FR-1400 magnetic tape recorder. In addition, for the *Surveyor V* mission the DSN provided an FR-900 recorder as backup to the FR-800 recorder.

The OSFR records the following on 70-mm film: the video image, the raw ID telemetry in bit form, the "human readable" time and record number, and an internally generated electrical gray scale. The film is then sent to the SFOF for development.

*b. TV systems at overseas DSIF stations.* In addition to the TV systems at DSS 11, Stations 61, 42, and 51, provide some TV recording capability for *Surveyor* missions. As described in Section VI-B, Stations 61, 42, and 51 all have 35-mm film recording capability in the Command and Data Consoles. They also provide FR-1400 and FR-800 recordings of video data received. In addition, for the *Surveyor V* mission, DSS 61 provided an FR-900 video recorder as a backup to the FR-800 recorder. The tapes and film from these stations are sent to TV-1 for processing and/or evaluation.

*c. TV-GDHS at the SFOF (TV-1).* The signal presented to the microwave terminal at DSS 11 is transmitted to the SFOF, where it is distributed to the MCDR and to the VDDS. The MCDR processes the signal in the same manner as the OSDR. In addition, the MCDR passes the raw ID information to the media conversion computer, which converts the data to engineering units. This converted data is used by (1) the film recorder, where it is recorded as human readable ID, (2) the wall display board in the SSAC area, (3) the disc file where the film chip index file is kept, and (4) the history tape.

The VDDS produces the signals to drive the scan converter and the signals to drive the various display monitors and the paper camera in the SSAC area. The VDDS also supplies the signals recorded by the FR-700 and the HW-7600 video magnetic tape recorders in the same manner as the FR-800 and the FR-1400 recorders at DSS 11. The scan converter converts the slow scan information from the spacecraft to a standard RETMA television signal for use by the SFOF closed circuit television and the public TV broadcasting stations.

The MCFR records on two different films. Both films are wet-processed off line. One of the negatives is used to make strip contact prints which are delivered to the users. Additionally, this negative is used to make a master positive for the production of a duplicate negative for the JPL Public Information Office (PIO) and a preliminary duplicate negative for the science users. The negative is then cut into chips which are entered into the chip file where they are available for use in making additional contact prints and enlargements.

**d. TV-GDHS performance.** On the *Surveyor V* mission a number of improvements were made to the operational system in TV-1 which provided better service to the scientific community. The modifications to equipment accomplished prior to the mission as well as continued personnel training programs allowed the TV-GDHS to perform the necessary pretracking countdowns much more smoothly than in the past. Although some film recorder problems were experienced, maintenance procedures and real-time trade-offs in usage allowed TV-1 to continue to provide the committed real-time products. No serious equipment failures were encountered in any system, and all minor ones were repaired in real-time. A film logistics problem was encountered prior to the first lunar day and, as a result, the experimenter data record (EDR) had to be delayed until the lunar night in order that the original negatives, duplicate positives, and PIO commitments could be continued. This problem showed a weakness in the logistics of the system. Actions are being taken to alleviate this problem for the next mission. Some problems were experienced in reading back the tapes from the overseas sites and made accurate evaluation of product completeness very difficult to establish. As of this report, all real-time and non-real-time products (six strip contact prints, a master positive, a PIO duplicate negative, and an EDR negative) have been produced and delivered to Project Science.

A total of 18,052 pictures were recorded by TV-1. Of these, over 14,246 were recorded in real-time and approximately 3,806 were from DSS 42 playbacks. From September 10, 1967 to September 26, 1967, 338 photo orders were received. These orders resulted in 4,620 pictures being produced. This was an average of 289 pictures a day.

Between September 11 and September 23, 166 mosaics were copied. This was an average of 13.8 mosaics a day. Paper negatives were also copied at an average of 13.8 a day. Three negatives of each mosaic were produced, for an average of 40.5 a day. The average production of mosaic paper positives was 110.5 per day, since eight copies were required of each mosaic.

The flexibility of the TV-GDHS was demonstrated during the second lunar day when the spacecraft camera was not producing a video signal with adequate signal-to-noise ratio. The TV-GDHS provided special support for an engineering evaluation of the problem by filtering and amplifying the signal to subdue the black level and enhance the white level. The result of this support was the production of photographs of fairly good quality but of

unknown calibration. This support provided valuable engineering information for pinpointing the problem and provided Project Science with considerable data which otherwise would have been lost.

In conclusion, the TV-GDHS very adequately supported the *Surveyor V* mission with real-time, scan-converted TV and photographic products. Problem areas that did show up did not jeopardize the real-time operation but gave an indication of improvements yet to be made.

## C. Mission Operations Chronology

Inasmuch as mission operations functions were carried out on an essentially continuous basis throughout the *Surveyor V* mission, only the more significant and special, or nonstandard, operations are described in this chronicle. Refer also to the sequence of mission events presented in Table A-1 of Appendix A.

### 1. Countdown and Launch Phase

No significant problems were reported in the early phases of the countdown, which proceeded normally down to the built-in hold at  $T - 5$  min. The count was not picked up as scheduled after the planned 10-min hold, however, because of an apparent anomaly in the *Atlas* launcher stabilization system. Following an additional 18-min hold, the countdown was resumed.

At 07:56 GMT ( $L - 1$  min), the FPAC Tracking Data Analysis (TDA) group started a computer run of  $L - 5$ -min predictions for initial DSIF acquisition, using computed center frequencies for Transmitter B and Transponder B supplied by SPAC, the actual launch azimuth of 79.517 deg, and station parameters. These  $L - 5$ -min predictions were completed by 08:03 GMT and sent to DSS 72 (Ascension Island), DSS 51 (Johannesburg), and DSS 42 (Tidbinbilla).

Liftoff ( $L + 0$ ) occurred at 07:57:01.257 GMT on September 8, 1967, with all systems reported in a "go" condition. Launch vehicle performance appeared to be nominal, with no significant anomalies on either the *Atlas* or *Centaur*. Following the parking orbit coast period, *Centaur* second burn occurred and the spacecraft was injected into a lunar transfer trajectory which was well within established limits. The required retro maneuver was successfully performed by the *Centaur*. A description of launch vehicle performance and sequence of events from launch through injection is contained in Section III.

Following separation at 08:16:27 GMT ( $L + 00:19:26$ ), the spacecraft executed the planned automatic sequences as follows. By using its cold-gas jets, which were enabled at separation, the flight control subsystem nulled out the small rotational rates imparted by the separation springs and initiated a roll-yaw sequence to acquire the sun. After a minus roll of 342 deg and a plus yaw of 18 deg, acquisition and lock-on to the sun by the spacecraft sun sensors was completed at 08:29:12 GMT. Concurrently with the sun acquisition sequence, the A/SPP stepping sequence was initiated to deploy the solar panel and position the roll axis. At 08:22:39 and 08:28:03 GMT, the solar panel and A/SPP roll axes, respectively, were locked in the proper transit positions. All of these operations were confirmed in real-time from the spacecraft telemetry.

Following sun lock-on, the spacecraft coasted with its pitch and yaw attitude controlled to track the sun and with its roll attitude held inertially fixed.

## 2. DSIF and Canopus Acquisition Phase

Both DSS 72 and DSS 51 received the  $L - 5$ -min predictions about 10 min before spacecraft rise. Using this data, DSS 72 acquired the down-link 1 min after *Surveyor V* rose above the horizon; DSS 51 achieved one-way lock 3 min later at 08:25:10 GMT, 28 min after liftoff. Good two-way communication was established at 08:30:11 GMT to complete the initial acquisition by DSS 51.

The first ground-controlled sequence ("Initial Spacecraft Operations") was initiated at 08:37 GMT ( $L + 00:40$ ) and consisted of commands for (1) turning off spacecraft equipment required only until DSIF acquisition, such as high-power transmitter and the solar panel deployment logic, (2) seating the solar panel and roll axis locking pins securely, (3) interrogating commutator Mode 1\* at the 550-bit/sec data rate established prior to launch, (4) increasing the telemetry sampling rate to 1100 bit/sec, and (5) performing interrogation of commutator Modes 4, 2, 6, and 5, in that order. All spacecraft responses to the commands were normal.

Initial spacecraft operations were completed at 09:00 GMT, with *Surveyor V* configured in low power, coast phase commutator on (Mode 5), and transmitting at 1100 bit/sec over Omnantenna B. During the operations, two objects, believed to be particles, passed through the field of view of the Canopus sensor. Therefore, it was recommended that the roll axis be held in the inertial mode and

the *cruise mode on* command not be sent to the spacecraft. (Cruise mode was commanded on five hours later at the completion of the star verification sequence.) It was also determined that there was no need to turn on Transponder A since Receiver A was already tracking the DSS 51 transmitter signal in the automatic-frequency-control mode.

The spacecraft continued to coast normally, with its pitch-yaw attitude controlled to track the sun and with its roll attitude held inertially fixed. Tracking and telemetry data was obtained by use of Transponder B and Transmitter B. (The spacecraft telemetry bit rate/mode profile for the complete transit portion of the mission is given in Fig. VI-2.)

The initial estimate of spacecraft orbit computed at Cape Kennedy by the Real Time Computer System based on *Centaur* C-band data indicated that lunar encounter would be achieved, even with no midcourse correction. The first estimate by the Orbit Determination (OD) group in the SFOF, completed at  $L + 01:45$ , based on 35 min of DSS 51 two-way doppler and angle data indicated that the maneuver required to land *Surveyor V* at the prelaunch aim point was well within the nominal midcourse correction capability. These results were further verified by the OD group following completion of their second and third orbit computations at  $L + 02:58$  and  $L + 03:58$ , respectively.

At 12:00 GMT, both DSS 51 and DSS 42 reported poor data quality and a low,  $-138$ -dbm signal level due to the spacecraft roll orientation; the earth/spacecraft vector was in a null region of Omnantenna B. The SPAC Performance Analysis (PA) group recommended selecting Omnantenna A rather than lowering the bit rate, since the 1100-bit/sec rate could be maintained and a check of RF transmission over Omnantenna A would be valuable for later operations. The command to switch omniantennas was sent at 12:19 GMT ( $L + 04:22$ ); signal strength rose to  $-125$  dbm, and data quality improved.

During the spacecraft interrogation prior to the star verification/acquisition roll maneuver, the solar panel switch tripped off to protect the battery, since battery voltage had built up to over 27 V. (This occurred eleven times during the early part of the flight and had been predicted as a result of premission solar-thermal-vacuum tests.) After time was allowed for the battery to discharge until voltage decreased below the solar panel switch trip level, the switch was commanded on and, at 14:10 GMT ( $L + 06:13$ ), DSS 61 (Robledo) commanded a positive spacecraft roll maneuver which initiated the star verification/acquisition

\*See Section IV-A (Table IV-1) and Appendix C for data content of telemetry modes.



sequence. This maneuver provides a measure of light intensity received from celestial objects passing through the Canopus sensor's field of view. The data is used for comparison with a precomputed star map for positive identification of the star Canopus. At the recommendation of the PA group, the following spacecraft configuration was used during the sequence: telemetry Mode 1 at 4400 bit/sec, Omnantenna B with Transmitter B in high power, and the transponder on. The first revolution was used for the verification part of the sequence.

The roll maneuver proceeded smoothly as the stars Zeta Ophiuchi; Antares and Tau Scorpii; Canopus; Alnitak, Alnilam, and Mintaka; Bellatrix; Elnath; the earth; and the stars Capella and Polaris were successively detected by the Canopus sensor and identified on the map in the SPAC area. The spacecraft continued to roll, and as Tau Scorpii passed from the field of view during this second revolution, the star acquisition mode was commanded on. When light from Canopus was sensed, *Surveyor V* ended the maneuver by automatically locking onto the star. (In both the *Surveyor I* and *II* missions, the Canopus intensity was above the upper threshold of lock-on range, necessitating manual acquisition; *Surveyors III* and *IV* locked on automatically.) Canopus acquisition occurred at 14:27:52 GMT ( $L + 06:30:51$ ) after the spacecraft had rolled through 533 deg for nearly 18 min.

At the end of the star verification/acquisition sequence, commands were sent to return the spacecraft to the cruise mode of flight control, select commutator Mode 5, lower the data rate to 1100 bit/sec, and return Transmitter B to low power. The spacecraft was coasting with pitch and yaw attitudes controlled by tracking the sun and the roll attitude controlled by tracking Canopus. *Surveyor V* was thus in a fixed attitude, a precise position from which midcourse maneuvers could be computed and executed.

The first midcourse conference was held at 15:00 GMT. Spacecraft data was provided by SPAC which showed that all subsystems were in good condition and operating properly. FPAC presented the results of computer runs to this time. Analysis of the *Surveyor V* trajectory indicated that a small midcourse correction at about  $L + 18:00$  would be the most desirable.

### 3. Pre-midcourse Coast Phase

The first gyro drift check was initiated 1 hr and 18 min after Canopus lock-on by commanding the spacecraft to inertial mode. The vehicle continued to coast as before, but with its attitude held inertially so that the sun and star

sensors continued to point at the sun and Canopus, respectively. During this period, an unscheduled interrogation of commutator Mode 4 was conducted in order to monitor alpha scattering instrument electronics and sensor head temperatures. At 18:16:28 GMT ( $L + 10:19:27$ ), the gyro drift check was terminated by commanding on cruise mode; 18 min later a second check was begun. Both of these checked the drift rate in the spacecraft's roll, pitch, and yaw axes. A gyro drift check of the roll axis only was also performed during this coast phase.

At 20:18:36 GMT, the bit rate was lowered to 137.5 bit/sec to permit DSS 72 tracking; the gain of the DSS 72 antenna, which is only 30 ft in diameter, would not permit higher data rates. Subsequently, the 17.2 bit/sec rate was commanded since DSS 72 was the only station tracking for about 15 min and the signal strength there was below the telemetry threshold of the higher rate. After transfer to DSS 11, the rate was returned to 1100 bit/sec.

At the final midcourse conference, the decision was made to perform a nominal  $L + 17$ -hr midcourse correction. Following the meeting, final computation of midcourse parameters was started by FPAC. (Refer to Section VII for a discussion of the factors considered in selecting the midcourse correction plan.) The Command Preparation and Control (CPC) group received the final midcourse guidance summary from FPAC at 23:44 GMT and immediately began real-time generation of the standard midcourse command tape message. The message was transmitted to DSS 11 at 00:05 GMT (September 9, 1967) and verified 15 min later.

Pre-midcourse engineering interrogation began at 23:41 GMT ( $L + 15:44$ ) with commutator Mode 4, followed by Modes 2 and 1 and a return to Mode 5. The pre-midcourse gyro speed check was then initiated, and the gyro spin rates in roll, pitch, and yaw axes were found to be nominal.

### 4. Midcourse Maneuver Phase

The midcourse correction sequence was initiated at 00:59:45 GMT ( $L + 17:02:44$ ) with an engineering interrogation in commutator Modes 4, 2, and 1. Telemetry readings indicated that the spacecraft was in satisfactory condition for midcourse operations. The interrogation was followed by commands to turn on Transmitter B high power and increase the telemetry sampling rate from 1100 to 4400 bit/sec. Starting at 01:32:57 GMT ( $L + 17:35:56$ ), the required roll (+71.8 deg) and yaw (-35.6 deg) maneuvers were executed to align the spacecraft axes in the

FOLDOUT FRAME

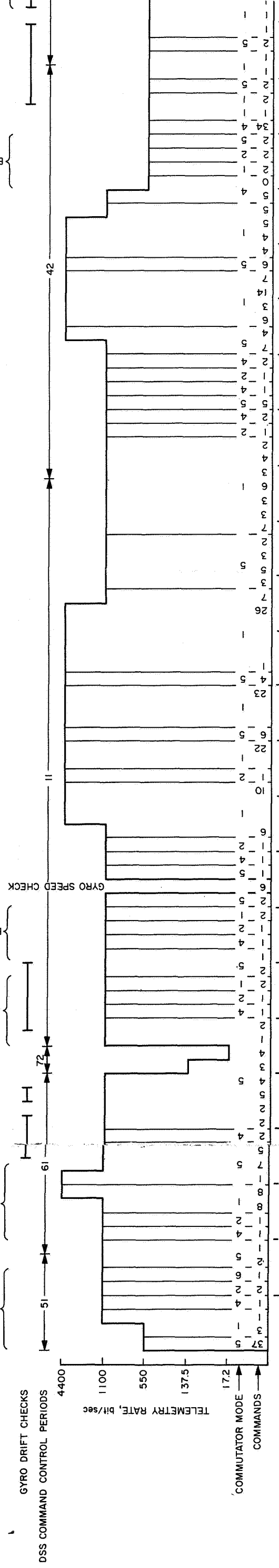
FOLDOUT FRAME

FOLDOUT FRAME

DAY  
SEPTEMBER 8, 1967

SEPTEMBER 9, 1967

GMT	MIN	SEC	HR	DAY
01.25	59	01	07	LIFTOFF
39	45	08	08	
46	51	19	08	
48	48	19	08	
52	49	52	08	
55	55	00	09	
00	00	30	13	
00	00	00	13	
47	46	47	13	
51	16	51	14	
12	54	12	14	
05	54	05	14	
30	30	32	15	
39	32	39	15	
45	52	15	15	
22	22	16	17	
26	26	26	18	
28	28	28	18	
34	34	28	20	
16	16	02	20	
02	02	36	21	
01	43	01	21	
06	41	06	21	
58	43	06	21	
47	47	24	22	
53	53	24	22	
56	56	43	22	
40	40	01	22	
33	40	33	23	
45	41	45	23	
46	46	46	23	
48	48	46	23	
53	53	55	23	
55	55	55	23	
48	48	23	02	
17	17	48	02	
20	20	23	02	
54	54	56	04	-ROLL
00	00	46	05	+ROLL
05	05	54	05	+YAW
09	09	33	05	+YAW
13	13	44	05	-ROLL
18	18	48	05	-YAW
19	19	01	05	-ROLL
19	19	03	05	-YAW
20	20	00	05	-ROLL
26	26	04	05	-YAW
32	32	52	06	
44	44	02	06	
05	05	53	06	
15	15	27	06	
29	29	12	06	
38	38	24	06	
50	50	29	06	
52	52	11	07	
54	54	30	07	+ROLL
58	58	31	07	+YAW
24	24	03	08	FIRING 5
26	26	10	08	
30	30	04	08	-YAW
33	33	51	08	-ROLL
40	40	35	09	
45	45	43	09	
21	21	03	09	
22	22	31	09	
55	55	12	10	
02	02	04	10	
05	05	48	10	
11	11	17	11	
32	32	51	11	
39	39	31	11	
44	44	25	12	
47	47	17	12	
00	00	00	12	
54	54	54	13	
59	59	29	13	



COAST PHASE I

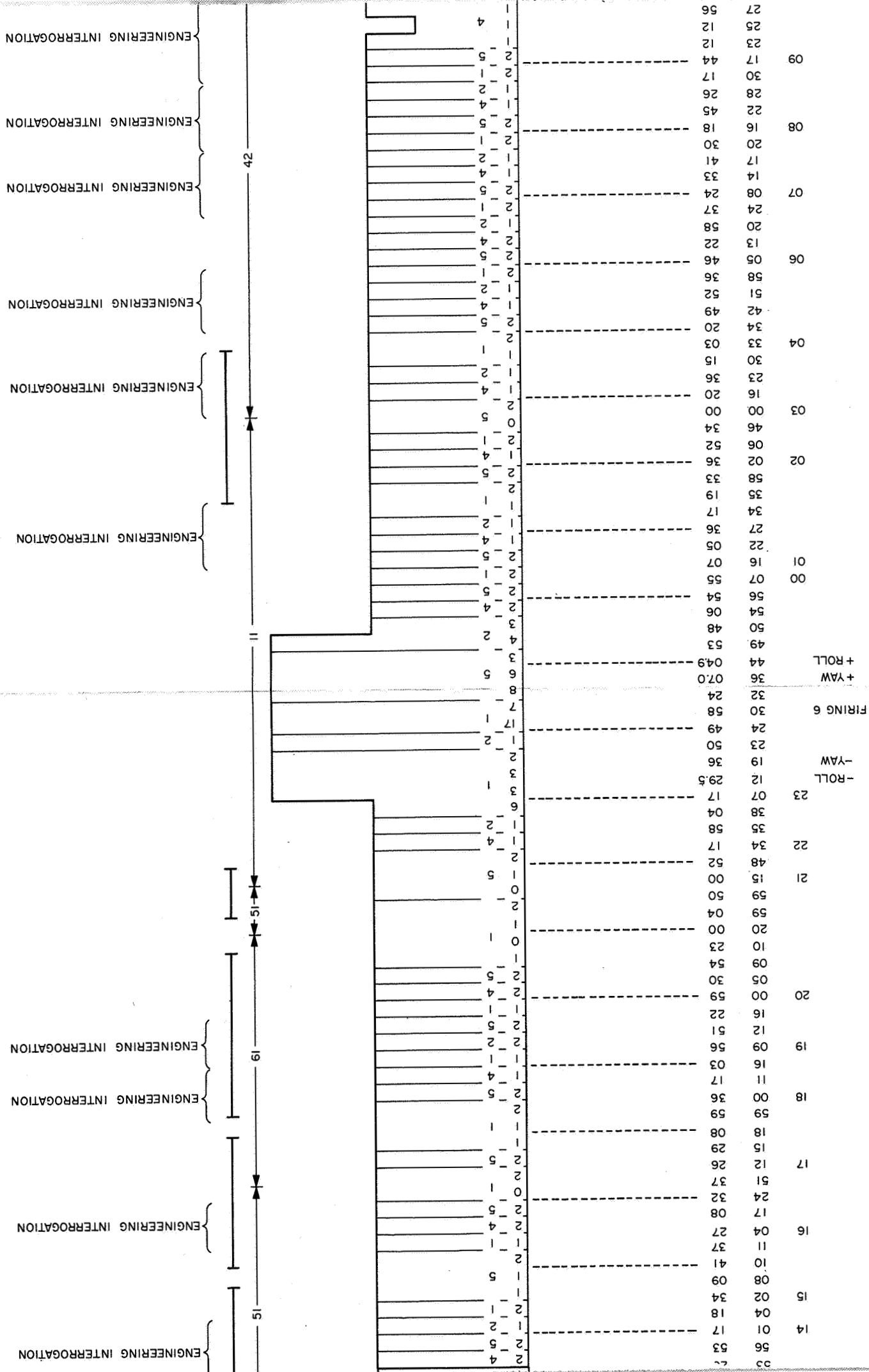
MIDCOURSE CORRECTION PERIOD I

ENGINEERING INTERROGATION

FOLDOUT FRAME

FOLDOUT FRAME 3

SEPTEMBER 10, 1967







desired direction for applying midcourse thrust. The attitude maneuvers were initiated at limit cycle nulls to reduce pointing errors. Following engineering interrogation in commutator Modes 2 and 1, the spacecraft was prepared for thrusting, including sending commands to (1) turn on propulsion strain gage power, (2) turn on inertial mode, (3) turn off cyclic loads and pressurize the vernier propulsion system, and (4) load the desired thrust time (14.25 sec) in the flight control programmer magnitude register. Midcourse velocity correction was executed at 01:45:02 GMT ( $L + 17:48:01$ ) on September 9 in accordance with the planned thrust time. All engines fired simultaneously, burned for 14.25 sec for a velocity change of 14.0 m/sec, then shut down automatically. The spacecraft remained stable throughout the thrusting period.

Following midcourse velocity correction, commands were sent to turn off various power sources used during the thrusting phase and to turn on commutator Mode 5. At 01:49:55 GMT ( $L + 17:52:54$ ), the spacecraft was returned to commutator Mode 1 for a check of all system pressures since a possible leak in the helium pressurization system had been detected and reported after vernier engine shutdown. A helium leak was verified at a rate of approximately 10 psi/min. The decision was made to perform a second midcourse correction in an attempt to reseal the helium regulator valve and stop the leak as quickly as possible (2500- to 3000-psi helium pressure is necessary for a standard terminal descent).

The reverse yaw maneuver (+35.6 deg) was performed, returning *Surveyor V* to sun lock-on, and the vernier engines were fired a second time at 02:12:02 GMT for 10.05 sec. The correction, along the sun line, changed the landing point to 1600 km east of the desired landing site, i.e., to 2.89 deg north latitude and 77.52 deg east longitude. Since the leak continued at an average 10.8 psi/min, a third midcourse correction (23.05 sec) along the anti-sun line was commanded at 02:39:50 GMT after a -180-deg yaw maneuver; the spacecraft's trajectory was thus altered to intercept a point 2685 km to the west, past the desired landing site and into lunar darkness, at 0.86 deg north latitude and 12.01 deg west longitude. This second attempt to reseal the regulator valve was also unsuccessful.

Pending the results of further analysis, the spacecraft was returned to a partial cruise-mode configuration, starting with a -180-deg post-midcourse yaw maneuver for sun lock-on. The telemetry rate was lowered from 4400 to 1100 bit/sec, Transmitter B was commanded from high to low power at 02:55:51 GMT ( $L + 18:58:50$ ), and commutator Mode 5 was selected.

SPAC recommended another vernier engine firing (the helium leak rate had averaged 6.9 psi/min for 1.5 hr following the third midcourse correction) to again attempt resealing the regulator valve and to prepare for a modified terminal descent by burning off propellant to reduce main retro burnout velocity. It was also necessary to return the spacecraft to the desired aim-point intercept course. FPAC computations for the pre-fourth-midcourse attitude maneuvers were being made based on a normal transit orientation, i.e., with sun and star lock. Therefore, at 04:00 GMT ( $L + 20:03$ ), a -71.9-deg roll maneuver was executed to reacquire Canopus. The spacecraft was then commanded to roll +68.5 deg and yaw +106.8 deg, and commutator Mode 1 was selected.

The fourth midcourse correction was initiated at 04:18:48 GMT using a manually controlled tape sequence comprising three vernier engine burns of 12.0-, 0.5-, and 0.5-sec duration, with the engines off for 1 sec during each of the two intervals between burning periods. Although the shock of the rapid firings appeared to have stopped loss of helium pressure, the stoppage was temporary; leakage indications resumed 5 min after the last of these vernier engine burns. Post-midcourse attitude maneuvers were executed in reverse order and opposite direction to achieve sun and Canopus lock-on, and the spacecraft was returned to flight control cruise mode at 05:07:51 GMT ( $L + 21:10:50$ ).

Mission Control and Project Management had been considering two quite different plans for the balance of the mission. Of these, the more desirable plan was to continue the attempt of a soft landing. Studies were in process to determine if this could be achieved by redesigning the terminal descent sequence. SPAC's propulsion specialist reported that the helium leak, which averaged 3.0 psi/min during this period, should stop when helium tank pressure decreased to the setting of the relief valves (approximately 825 psi) since the helium was being vented through these valves. It was also reported that an 825-psi pressure might be adequate for a nonstandard terminal descent but that more analysis was necessary, as well as ground tests, to derive the actual sequence.

The alternate plan was to fire the retro motor to place *Surveyor V* in earth orbit. If successful, this at least would have permitted some television and alpha scattering instrument operations in space and the accumulation of engineering data. Therefore, commutator Modes 2 and 4 were interrogated to obtain thermal data; Mode 5 was commanded back on, and, in preparation for a possible

earth-orbit decision, the survey camera electronics temperature control and the Compartment C heater (for alpha scattering instrument warmup) were commanded on at 05:46:48 GMT ( $L + 21:29:47$ ). Altitude marking radar (AMR) temperature control was turned off temporarily to conserve power. One hour later, Mission Control requested SPAC to turn off the Compartment C heater and the camera electronics temperature control and to turn the AMR temperature control back on. It had been determined that a decision to place the spacecraft in earth orbit could be delayed until after helium pressure reached 825 psi.

With only 42 hr left until predicted touchdown time, the operations groups intensified efforts to generate a terminal descent timing sequence for accomplishing a soft landing. Under direction of Project Management, the SFOD, and the Trend and Failure Analysis (T&FA) group, these efforts ultimately comprised subsystem and system analysis by SPAC, flow tests on the complete propulsion system on a spaceframe located at Hughes Aircraft Company's Placerita Canyon test facilities, thrust chamber assembly flow tests at JPL's Edwards test facility, terminal descent timing sequences on SC-6\* at Cape Kennedy, and extensive simulation runs on the flight control analog simulator in Hughes' facilities.

A fifth midcourse correction was recommended based on the need to further reduce retro burnout velocity and to maximize available helium at terminal phase by increasing gas volume (or ullage) in the propellant tanks. At 07:49:35 GMT ( $L + 23:52:34$ ), Transmitter B was commanded to high power. The 4400-bit/sec data rate and commutator Mode 1 were selected, and pre-midcourse attitude maneuvers were performed (+64.6-deg roll, +143.2-deg yaw). A 33.05-sec vernier engine firing was executed at 08:24:02 GMT in the positive, non-critical direction. Helium pressure at the end of the burn was 1235 psi. Post-midcourse attitude maneuvers returned the spacecraft to sun and Canopus lock-on, after which cruise mode, the 1100-bit/sec data rate, and low-power transmission were established. Helium was still leaking but at a rate of less than 1.5 psi/min; *Surveyor V* was otherwise in excellent condition.

### 5. Post-midcourse Coast Phase

In preparation for alpha scattering instrument operations to obtain calibration data and verify instrument operability, the Compartment C heater was turned on

\*Serial designation for the *Surveyor* spacecraft scheduled for the sixth *Surveyor* mission.

at 08:49 GMT. The data rate was lowered to 550 bit/sec at 09:22 GMT because of an excessive bit error rate. With the spacecraft transmitting in high power (commanded on at 10:33 GMT) and commutator Mode 4, command control was turned over to SSAC.

Alpha scattering instrument operations began at 10:36:48 GMT ( $L + 26:39:47$ ), when power to the instrument was commanded on, and ended at 11:27:43 GMT. During the approximately 51 min of operations, the Alpha Scattering Analysis and Command (ASAC) group received two 10-min accumulations of standard sample data, as well as data from seven 2-min pulser calibration runs. The runs were performed with the pulser calibration and alpha and proton detectors in various on/off configurations. This first in-flight operation of the instrument was completely successful.\*

After reassuming command control, SPAC returned the spacecraft to normal transit configuration—Transmitter B in low power, Compartment C heater off—and began an interrogation of commutator Mode 1 at 11:32:51 GMT ( $L + 27:35:50$ ) to check the condition of the helium pressurization system. Helium pressure had decreased to 1070 psi; the leak rate was still less than 1.5 psi/min. SPAC recommended use of commutator Mode 1 until the leak rate stabilized, with periodic interrogations of Modes 5, 4, and 2 to be scheduled as recommended by the group's thermal specialist. During the following hours from 11:39 to 21:48 GMT ( $L + 37:51$ ), 10 of these periodic interrogations and five gyro drift checks (one of the roll axis only) were performed. A gyro drift check also had been conducted prior to alpha scattering instrument operations.

When 12 hr of tracking data had been received following the fifth midcourse correction, the Maneuver Analysis (MA) group reported that the actual retro burnout velocity would be approximately 120 ft/sec assuming a vertical flight path. In addition, the Placerita Canyon tests indicated that 70 lb of usable vernier propellant would be available for the terminal phase. *Surveyor V*'s helium leak rate had dropped to less than 0.5 psi/min by this time, and it had been confirmed that a soft landing would be attempted using a revised descent sequence. A final midcourse correction was also required. Using 13 hr of tracking data from DSS 42, 51, and 61, the OD

\*Section IV-J describes the alpha scattering instrument. Section VII of Part II of this Mission Report also contains a description and presents the science results obtained during transit and lunar operations by the cognizant investigator team.

group reported that the computed orbit had been satisfactorily refined to permit maneuver computations. The correction was designed to further increase gas volume in the propellant tanks, lower retro burnout velocity to approximately 100 ft/sec at an altitude of 5000 ft, and correct a 267-km residual miss, moving the landing site from a mountainous area to the pre-midcourse aim point.

At 22:34 GMT ( $L + 38:37$ ), commutator Modes 4 and 2 were interrogated, and Mode 1 was reestablished. Transmitter B was then commanded to high power, and after the 4400-bit/sec data rate had been selected, the spacecraft executed a  $-76.0$ -deg roll and a  $-100.6$ -deg yaw. The sixth midcourse correction was commanded at 23:31:00 GMT and lasted for 5.45 sec. Subsequent to the vernier engine firing, helium pressure indicated 890 psi. Post-midcourse reverse attitude maneuvers were performed and cruise mode, commutator Mode 2, a telemetry rate of 550 bit/sec, and low power transmission were commanded. After an interrogation of commutator Modes 4 and 5, SPAC commanded on Mode 1. Helium pressure continued to decrease slowly, following the pressure-vs-time curve established earlier.

Three gyro drift checks—again, one of the roll axis only—and 15 periodic engineering interrogations were conducted between 01:16 and 18:00 GMT ( $L + 59:03$ ), September 10. During this period, the spacecraft was also commanded to turn on Vernier Oxidizer Tank 2 temperature control at 06:20 GMT, to change the data rate to 137.5 bit/sec at 09:25 GMT for a few minutes to get accurate readings of alpha scattering electronics and sensor head temperatures, and to turn on the Compartment A heater at 13:31 GMT for battery\* warmup and the Compartment C heater at 17:44 GMT for alpha scattering instrument warmup. Helium pressure reached 847 psi at approximately 14:00 GMT. From then on, the leak rate was too small to be measured.

For the first time in a *Surveyor* mission, a 360-deg attitude maneuver was performed specifically to determine the precession torquing-rate accuracy of the attitude control loop. Therefore, at 18:12:16 GMT ( $L + 58:15:15$ ) and at 18:22:52 GMT, respective yaw maneuvers of  $+179.9$  deg and  $+180.1$  deg were executed, after which cruise mode was reestablished. This test provided assurance that the contribution of gyro precession rate to pre-retro pointing error was minimal and within specification.

\*The "main" battery. *Surveyor V* carried the alpha scattering instrument in place of an auxiliary battery. (This configuration eliminated the need for power-mode cycling checks, which were performed on previous missions.)

During the next 3.5 hr (18:32 to 22:02 GMT), periodic engineering interrogations were conducted, camera electronics temperature control was turned on and, after a special commutator Mode 4 check, heater power to the alpha scattering instrument sensor head was turned on. By 22:02 GMT ( $L + 62:05$ ), SPAC had evaluated all gyro drift data and provided drift rate estimates to FPAC for use in terminal descent computations. Predicted retro motor burn time of 39.06 sec was also provided to FPAC. During this period, conferences were held to evaluate proposed terminal descent maneuvers and timing sequences. The final maneuver plan presented to and approved by the Mission Director contained the following items:

- (1) Use a roll-yaw sequence with Omnantenna B to optimize telecommunications performance.
- (2) Initiate the two-maneuver sequence no later than 26.5 min prior to retro ignition.
- (3) Transmit 1100-bit/sec PCM data.
- (4) Attempt to obtain strain gage data only if received signal level is at least  $-130.5$  dbm after terminal maneuvers are completed.
- (5) Turn off transponder prior to start of the maneuvers.

The recommended and approved terminal descent timing sequence was greatly revised from that of a standard descent. Basically, the sequence was modified to (1) adjust retro burnout altitude from 38,000 to about 4500 ft and spacecraft velocity at burnout to about 94 rather than the nominal 450 ft/sec by delaying retro ignition, and (2) initiate the RADVS-controlled descent phase earlier by overriding certain flight control signals with precisely timed earth commands. Timing desired for the final terminal descent earth commands (three) was provided to the PA group by the T&FA group at 22:15 GMT, while FPAC provided the predicted times for automatic descent events, the delay time between AMR *mark* and vernier engine ignition, and the desired time for the AMR backup command. Using this data, the PA group started preparing the final terminal descent command message. The message was sent to DSS 11 at 23:01 GMT.

The preterminal engineering interrogation of Modes 4, 2, and 1 was begun at 22:32 ( $L + 62:35$ ) and was followed by a return to Mode 5 and the gyro speed check. A VCXO check was then performed by commanding off transponder power for approximately 1.5 min. Spacecraft telemetry confirmed that *Surveyor V* was in good condition and ready for terminal descent.



## 6. Terminal Phase

The terminal phase began at 23:40 GMT ( $L + 63:43$ ), about an hour before retro ignition, with commands to turn off Compartment A heater power and to turn on the camera vidicon temperature control. Then Modes 6 (thrust phase commutator) and 4 were interrogated, Transmitter B was commanded to high power, the telemetry rate was increased from 550 to 1100 bit/sec, and power was turned on as required for monitoring vernier propulsion and touchdown forces by means of strain gages. The spacecraft transponder was turned off, and DSS 11 and 14 maintained the one-way tracking mode for the terminal maneuvers.

Terminal maneuvers were executed starting approximately 32.5 min prior to the predicted time of retro ignition. During the first maneuver, the spacecraft rolled  $+73.8$  deg. This was followed by a yaw maneuver of  $+119.6$  deg initiated at 00:16:21 GMT ( $L + 64:19:20$ ) on September 11. There was no need to perform a third maneuver since these two maneuvers (which oriented the retro thrust axis in the desired direction) resulted in optimum roll positioning—within RADVS and telecommunications constraints and for postlanding operations. The maneuvers were compensated for flight control sensor group deflections and gyro drift rates; they were also successfully initiated on limit cycle nulls to effectively reduce errors in the thrust vector direction.

In the remaining time before the automatic retro sequence, final preparations were made for terminal descent. For the first time in a *Surveyor* mission, the vernier engines were set at the 150-lb low-thrust level for the main retro phase. A longer-than-normal delay time of 12.325 sec between AMR *mark* and ignition of the vernier engines was stored in the spacecraft, and commutator Mode 6, retro sequence mode, AMR power, and thrust phase power were commanded on. The AMR was enabled at 00:43:01 GMT, 1 min and 50 sec before main retro ignition. From this point on, extremely close coordination was maintained among the men responsible for operational control of *Surveyor V*: the SFOD, SPAC Director, and Command Controller in the SFOF and the *Surveyor* Operations Chief and Command Console Operator at DSS 11.

At 00:44:37.85 GMT,\* when the spacecraft was about 60 mi (slant range) from the moon, the AMR *mark* signal occurred automatically. The DSS 11 command tape was

\*Terminal descent times given here have been corrected for 1.234-sec RF delay to indicate time at spacecraft.

started 0.12 sec earlier at the predicted AMR *mark* time. The AMR backup command, which normally is sent to arrive just after automatic *mark*, was significantly delayed according to plan and reached the spacecraft at approximately 00:44:45 GMT. The vernier engines ignited at 00:44:50.19 GMT; 1.07 sec later, at 00:44:51.26 GMT, the main retro motor ignited, ejecting the AMR. The spacecraft was approximately 150,000 ft in altitude above the moon at this time. RADVS power came on automatically as planned, followed by the RADVS *high voltage on* signal. Several seconds later, the doppler velocity sensor (DVS) beam trackers followed by the radar altimeter (RA) beam tracker automatically acquired the lunar surface. The spacecraft was stable and operating properly.

Main retro motor burnout occurred at 00:45:30.12 GMT, approximately 4100 ft in altitude above the lunar surface; the spacecraft had slowed from 8485 to about 79 ft/sec during the 38.8-sec burn time. The retro case was then ejected by earth command (which overrode the automatic flight control sequence), and the vernier engines were commanded (again, from earth) to the 200-lb thrust level. At 00:45:41 GMT, the spacecraft received the *emergency start programmed thrust* command from earth that initiated RADVS control of the vernier engines; i.e., steering was controlled by the three doppler velocity sensor beams while the radar altimeter continued to monitor distance to the moon. When the velocity reached 97 ft/sec at 00:46:21 GMT, the spacecraft intercepted the programmed descent contour and the vernier thrust level increased, after which the spacecraft followed the descent contour, slowing to 10 ft/sec at an altitude of about 51 ft, then to 5 ft/sec at about 15 ft. When the latter altitude was reached, the vernier engines cut off, and *Surveyor V* landed gently in the southwest part of Mare Tranquillitatis at 00:46:43.05 GMT ( $L + 64:49:41.80$ ) on September 11, 1967. (Refer to Section IV-A for a more complete description of the terminal descent sequence.)

## 7. First Lunar Day

*a. September 11 and 12.* Less than a minute after touchdown, the standard postlanding engineering assessment began. Thrust phase power, RADVS power, and all flight control power were commanded off. Engineering interrogations were then conducted which indicated that the spacecraft was in excellent condition. Touchdown and propulsion strain gage power were commanded off, and the required temperature controls to various subsystems were turned on. The legs were left unlocked since leg deflections at touchdown were small and since a vernier engine static firing later in the mission was under con-

sideration. Also for this reason, the helium was not dumped. (Helium pressure at landing was 575 psi.)

At touchdown, the signals in spacecraft Receivers A and B abruptly decreased 5.5 and 1.5 db, respectively, while the received signal level at DSS 11 decreased 4.6 db. These sudden decreases were indicative of spacecraft spin or tilt at touchdown. However, ground receiver lock was maintained, and good PCM and strain gage data was obtained. After reviewing strain gage data printed out in the SFOF, SPAC reported the following, very preliminary, information:

- (1) Spacecraft velocity at touchdown was approximately 13 ft/sec on a 7-psi static bearing strength surface. (The velocity had increased from about 5 ft/sec during free-fall after vernier engine cutoff at about 14 ft altitude.)
- (2) Leg 1 contacted the lunar surface first, followed by the contact of Leg 2 and the nearly simultaneous contact of Leg 3.
- (3) Initial estimates of peak landing loads on Legs 1, 2, and 3 were 1340, 1640, and 1600 lb, respectively (see Table IV-9 for final data).
- (4) The relative incidence angle between spacecraft and surface was at least 15 deg, indicating that *Surveyor V* had landed on a slope.

Strain gage and other pertinent touchdown data was provided to operations specialists, the Project Scientist, and cognizant Investigator Teams and Working Groups for further analysis and refinement of values. After analyzing additional data provided by subsequently received television pictures, scientists later reported that *Surveyor V* was located on the inner south wall of a small (30-ft-diameter), rimless crater. It was also found that Leg 1 touched down just outside the crater and that the other two legs touched down on the crater wall. The spacecraft then slid about 32 in. down the slope before coming to rest. Landing coordinates are estimated to be 1.41 deg north latitude and 23.18 deg east longitude, based on six weeks of postlanding tracking data. (Final *Surveyor V* science results are given in Part II of this Mission Report and are repeated herein only in a mission operations relationship.)

Engineering assessment continued, including commands to unlock and step the roll and polar axes of the A/SPP and to prepare the spacecraft for television operations. Command responsibility was then transferred to SSAC. The standard survey from Footpad 3 to Footpad 2

in the 200-line TV mode was conducted between 02:00 and 02:31 GMT. Eighteen high-quality pictures were received during this first and only (until the second lunar day) 200-line sequence.

Following completion of the postlanding assessment, SPAC began planar array and solar panel (A/SPP) stepping operations. Accomplishment of this sequence permits 600-line-mode television data transmission and insures that sufficient electrical power will be available for continued lunar operations. The sequence required more than the usual amount of time since initial A/SPP sun and earth acquisition is based on the assumptions of a horizontal landing site and the predicted spacecraft roll orientation; the deviation of *Surveyor's* actual attitude and orientation from the predicted was as yet undetermined. The sun eventually was acquired by the solar panel almost 30 deg in azimuth from the predicted position and about 4 deg higher in elevation. The earth was not acquired during planar array searches based first on a vertical spacecraft attitude and then on the 10- to 15-deg tilt indicated in the strain gage data. However, when a search was conducted calculated for a maximum slope of 20 deg, the received signal level increased to within 2 db of the predicted main lobe peak value. A crude tilt estimate of 18 deg was calculated at this point, and the spacecraft was immediately configured for television operations since the moon was now low on the horizon at DSS 11.

DSS 42 began 600-line-mode television operations, commanding the first picture at 05:29 GMT. Excellent pictures were received at that station and also, during the remaining 10 min of Goldstone view, at the SFOF, although the latter were degraded by noise due to the low Goldstone elevation angle. In contrast to television operations at DSS 11, pictures arriving from the moon at the overseas stations cannot be transmitted to the SFOF for real-time display on TV monitors and assessment by the Television Performance Analysis and Command (TPAC) and Television Science Analysis and Command (TSAC) groups. Therefore, following Goldstone set, as pictures were received by the Tidbinbilla station, the *Surveyor* Operations Chief at DSS 42 described them over the voice line connecting Australia and the SFOF. SSAC recommended or monitored changes in camera mirror azimuth and elevation as necessary. After receiving 51 600-line pictures, the station was directed to turn off the camera at 07:13 GMT and begin the alpha scattering experiment.

The alpha scattering instrument, still in the stowed position, was commanded on at 07:27 GMT. While monitoring incoming standard sample data, the DSS 42 data

analyst reported that the instrument's calibration pulser was on. This single instrument anomaly during the entire mission was also noted by the ASAC group in the SFOF, and a command was sent at 07:50 GMT to turn off the pulser. In preparation for subsequent operations, pictures of the area beneath the alpha scattering instrument were taken between 08:34 and 08:50 GMT during the second 600-line-mode television sequence. The alpha scattering experiment was then resumed. The ASAC group received data from a brief calibration followed by standard sample accumulation until 10:37 GMT, when stowed-position operations were concluded.

Prior to the mission, it had been planned that a vernier engine static firing test would be performed during the second postlanding Goldstone view period after fulfilling such prefiring requirements as taking more pictures of the area beneath the vernier engines, obtaining various temperature readings, and determining precise spacecraft attitude and roll orientation. One requirement was met when SPAC conducted a check, from 10:05 to 10:39 GMT, of the flight control and power modes to be used in the experiment.\* This was followed by A/SPP operations for attitude determination. After a precise sun sighting was obtained, the solar axis was unlocked at 11:49 GMT and planar array stepping began. The sequence was interrupted 10 min later to deploy the alpha scattering instrument to the background position. A command was sent at 12:14 GMT which moved away the supporting mechanism and standard sample, leaving the instrument properly suspended 22 in. above the lunar surface. After confirming that the instrument was accumulating background data, DSS 42 continued to step the planar array until a precise earth sighting was obtained at 12:44 GMT.

Based upon A/SPP fine positioning, it was calculated that *Surveyor V* was tilted 19.50 deg with the +X axis 24.51 deg clockwise from lunar east and the -Y axis 7.63 deg clockwise from the maximum negative slope gradient; i.e., Leg 1 was pointing approximately southwest and uphill, and Legs 2 and 3 were pointing roughly east and northwest, respectively, with about the same downhill tilt.

At 15:36 GMT, after station transfer to DSS 61, the alpha scattering instrument was lowered to the lunar sur-

face. The entire Robledo commanding period was devoted to the alpha scattering experiment. Pictures of the instrument on the surface were taken later, when DSS 11 assumed command responsibility and conducted television operations from 23:38 to 06:12 GMT on September 12. Station transfer to DSS 42 was accomplished, and television operations were continued by that station beginning at 06:56 GMT. Following TV operations, alpha scattering operations were initiated at 09:44 GMT. In general, this pattern of lunar operations was followed until shortly before lunar sunset, with exceptions as described in succeeding paragraphs. Although emphasis was usually placed on the alpha scattering experiment during Tidbinbilla and Robledo view periods, while Goldstone view periods were devoted primarily to television operations, significant video activity (other than shadow progression pictures) was conducted by the overseas stations for the first time in this *Surveyor* mission.

*b. September 13.* The vernier engine static firing had been rescheduled for September 13 (the third postlanding Goldstone pass), after a one-day postponement. (A dry run of the experiment was conducted on September 12.) By 03:34 GMT, television surveys of the areas beneath the engines were complete. In preparation for the experiment, flight control power was turned on for systems warmup, and the solar panel and planar array were stepped to safer positions. The rate mode was commanded on, nulling the gyros, and propulsion strain gage power, Transmitter A high power, and the 1100 bit/sec data rate were turned on. After turning on touchdown strain gage power and data channels and further configuring the spacecraft as required, SPAC commanded thrust phase power on and selected commutator Mode 1. Vernier engine ignition was commanded at 05:38:08 GMT. The engines fired for 0.55 sec, then shut down. Mode 5 was selected, and all flight control power, touchdown strain gage power and data channels, and propulsion strain gage power were commanded off. After lowering the telemetry rate to 137.5 bit/sec, DSS 11 returned Transmitter A to low power.

A/SPP attitude determination operations were conducted from 05:45 to 06:03 GMT to once again obtain precise sun and earth sightings. The extent to which vernier engine firing had caused a change in attitude and orientation was calculated. It was indicated that the spacecraft had turned slightly in a clockwise direction and was now tilted 19.71 deg with the +X axis 25.24 deg clockwise from lunar east and the -Y axis 9.85 deg clockwise from the maximum negative slope gradient. However, the changes in spacecraft attitude and orientation

\*Note that the alpha scattering experiment was in progress at this time. *Surveyor V* is designed to permit telemetry transmission in any one of commutator Modes 1 through 6, while simultaneously transmitting alpha- and proton-count telemetry in the phase-modulated subcarrier oscillator mode.

were less than the  $3\sigma$  uncertainty of the determinations ( $\pm 1.5$  deg for tilt,  $\pm 3$  deg for roll orientation). Television pictures revealed that the alpha scattering instrument had moved downhill about 4 in. but had not been harmed by the static firing. Pictures of the spacecraft, including Footpad 2 and the magnet assembly, and the lunar surface also showed the effects of vernier engine firing.

*c. September 14 and 15.* As lunar noon approached, temperatures of various spacecraft components increased as anticipated. *Surveyor V*'s location in a crater contributed to temperature rise since heat was less readily dissipated than it would have been had the spacecraft landed on a horizontal, open area. Between 10:00 and 21:15 GMT on September 14, the spacecraft was shut down seven times to permit cooling, especially of the battery and camera. The only other commanding operations performed during these hours were engineering interrogations.

On September 15, when the spacecraft was turned on and commutator Mode 4 selected at 00:17 GMT, it was found that the battery temperature had dropped sufficiently to continue lunar operations; however, the alpha scattering instrument remained off since temperatures were still too high for instrument operation. The elevation axis was unlocked at 00:20 GMT, and the planar array was stepped to partly shade Compartment A while extensively shading the camera. DSS 11 then assumed command responsibility and conducted television operations until 08:57 GMT; after station transfer, DSS 42 continued to take pictures for about 20 min.

At 11:48 GMT, SPAC initiated a telecommunications signal processing test. The test was halted when the battery temperature reached  $114.8^{\circ}\text{F}$ , and the spacecraft was shut down to allow the battery to cool. About 1.5 hr later, the spacecraft was turned on and a bit-error-rate test was initiated to check combined spacecraft/DSIF telemetry performance. After station transfer, DSS 61 also conducted this test. Following the test, the A/SPP was repositioned to optimize shading in Compartment A, leaving the camera slightly shaded. The spacecraft was then interrogated and commanded off at 22:46 GMT.

*d. September 16 and 17.* Prior to transfer from DSS 61 to DSS 11, the spacecraft was turned on at 01:02 GMT, September 16, following a 2-hr cooling period. Television operations from DSS 11 and 42 occupied the major portion of this day. During five of the engineering interrogations conducted between television sequences, the transponder mode was commanded on—twice from

Goldstone and three times from Tidbinbilla—to permit two-way doppler tracking. (Transponder A was also turned on prior to transfer to Robledo at 18:30 GMT.)

During this phase of a *Surveyor* mission, it is usually necessary to suspend operations until the sun passes the zenith and temperatures begin to decrease. However, SPAC specialists had devised planar array and solar panel shading patterns which prevented critical spacecraft temperatures from exceeding the operating limits and permitted operations to continue with only periodic shut-downs. DSS 42 was first directed to perform a brief A/SPP stepping sequence to shade the alpha scattering sensor head; the temperature quickly dropped to  $49^{\circ}\text{F}$ . After station transfer, SSAC commanded on instrument power at 18:40 GMT and reinitiated the alpha scattering experiment. A few hours later, SPAC directed DSS 61 to step the solar panel a few degrees to optimize Compartment A shading, then returned spacecraft control to SSAC. Alpha scattering operations were resumed. At 23:35 GMT, the sensor head heater was commanded on to maintain the proper operating temperature.

Lunar noon occurred at approximately 00:00 GMT on September 17. In order to maintain the shading patterns described above, it was not possible to keep the planar array pointed directly at earth. However, signal strength was adequate for television operations, and alpha scattering and television sequences were conducted throughout the day until 20:45 GMT when high battery temperatures were reached. The spacecraft was placed in standby mode twice, and A/SPP stepping was commanded to optimize shading. Three radial measurements of the 85-ft antenna pattern were made while the alpha scattering experiment was in progress at Goldstone. An optimum antenna pointing experiment was performed simultaneously with the antenna pattern measurements.

*e. September 18 to 20.* Several operations other than standard television and alpha scattering were conducted from September 18 to September 20. On September 18, two sets of calibration pictures ("glare tests") were taken at different times in preparation for solar corona sequences at lunar sunset. Also on this day the spacecraft was shut down four times for battery cooling. From this day on, as the sun angle decreased, there were no serious problems with high temperatures. During an engineering interrogation, it was noticed that the oxidizer pressure was dropping at a rate of 10 psi/hr and it was suspected that the oxidizer valve was cycling. However, later data indicated that Oxidizer Tank 1 was leaking. On September 19, the oxygen pressure, as well as helium pressure, continued

to drop. The leak, at this point in the mission, was not considered to be a serious problem. A spacecraft best-lock frequency test was performed on this day during the DSS 61 view period. Bit-error-rate tests were also conducted and the planar array was repositioned for optimum pointing. On September 20, a TV gain margin test was conducted from 16:40 to 18:05 GMT by DSS 42.

*f. September 21 and 22.* DSS 11 took a record 2110 pictures on September 21 from 03:58 to 12:01 GMT, the greatest number of frames ever received by one station during one pass. As sun elevation decreased, lighting improved, especially on the magnet assembly which had been in shadow for the greater part of the lunar operations. At 09:48 GMT, the first shadow progression sequence was started. These sequences were conducted with increasing frequency as the sun neared the horizon. After assuming command responsibility, DSS 42 continued alpha scattering operations which had been started by DSS 11. DSS 42 also conducted a shadow progression sequence, magnet survey, and an RF communications test before returning to alpha scattering operations. DSS 61 operations consisted of alpha scattering accumulations and a shadow progression sequence from 02:05 to 02:34 GMT on September 22. During the alpha scattering experiment, the planar array was repositioned to obtain improved signal strength. DSS 61 also performed a telecommunications signal processing test. DSS 11 activities on September 22 were devoted entirely to television operations.

*g. September 23.* Operations began with DSS 61 conducting alternate shadow progression sequences and alpha scattering data accumulations. These activities were interrupted briefly at 04:01 GMT when the command was sent to lock the landing gear. The legs apparently did not lock, and Legs 2 and 3 subsequently sagged, placing *Surveyor V* at a slightly increased tilt resting on the crushable blocks. A best-lock frequency test was performed by DSS 61 and later by DSS 42.

Television operations were conducted by DSS 11 from 05:30 to 15:39 GMT, interrupted only by engineering interrogations and two solar panel repositioning operations to optimize battery charge. Television was continued by DSS 42 until camera problems arose. During a shadow progression sequence, it was observed that the camera was not responding as commanded. The filter wheel and focus control could not be stepped, and the focal length could not be changed. There were no problems related to stepping the mirror, however, and the remaining pictures were taken as planned, only using the green filter, medium-distance focus, and narrow-angle focal length.

The alpha scattering experiment was concluded at 17:51:54 GMT on September 23, when the sensor head temperature reached  $-56^{\circ}\text{C}$  and DSS 42 commanded off power to the instrument. A total of 93.5 hr of alpha scattering instrument data had been accumulated including transit operations. The experiment was a complete success, giving scientists the opportunity, for the first time in history, to analyze the chemical composition of another celestial body using data obtained directly from its surface.

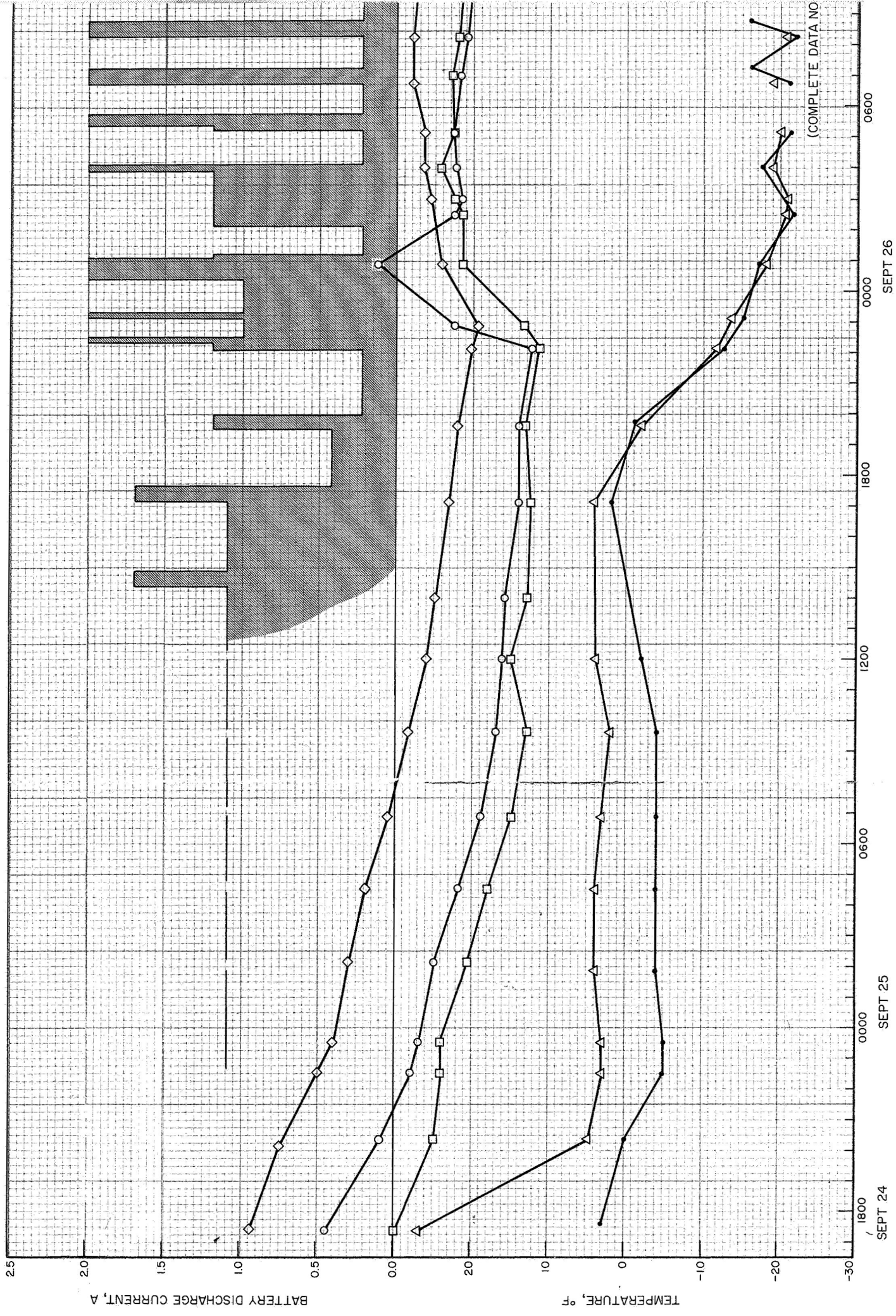
*h. September 24.* The sunset sequence was initiated at the start of the DSS 11 commanding period and consisted of narrow-angle surveys. At approximately 30 min before sunset, shadow progression sequences were started and continued until all direct sunlight had disappeared. Lunar sunset at the camera was 10:40 GMT; total spacecraft sunset (last light on the top of the antenna mast) was 10:56 GMT. Immediately thereafter, the camera was positioned for the solar corona experiment. The solar corona was observed for 3 hr and 40 min; then two earthshine pictures were taken of the Omnantenna B photo chart and one earthshine picture was taken of the lunar surface. The camera was turned off at 15:06:01 GMT. After the television sequence was concluded, engineering interrogations for spacecraft status and science thermal data continued.

*Surveyor V* transmitted 18,006 pictures to earth on the first lunar day. Television operations in the 600-line-mode comprised the following:

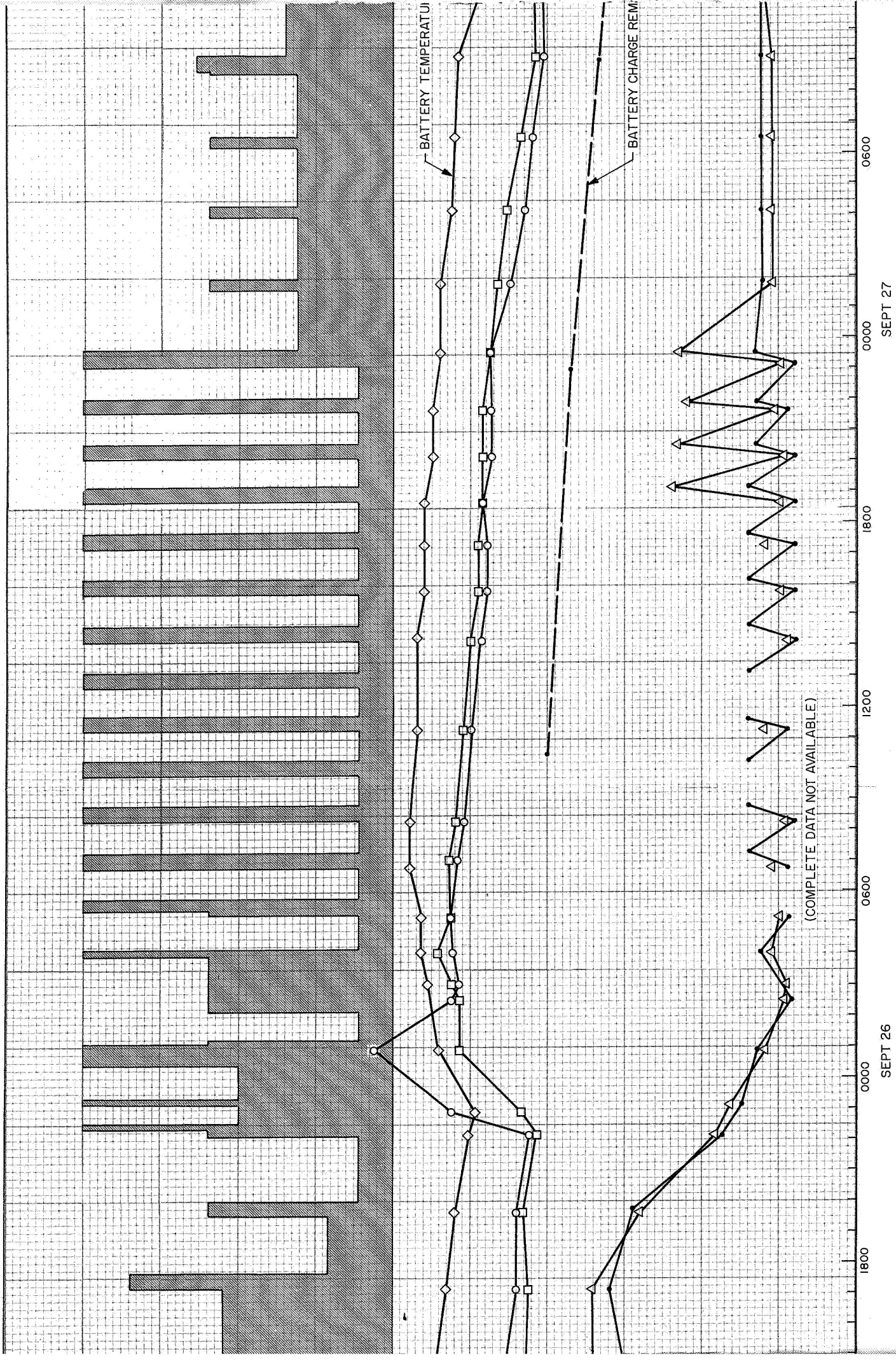
- (1) 360-deg wide-angle panoramas.
- (2) Narrow-angle surveys.
- (3) Special area surveys.
- (4) Focus ranging.
- (5) Photometric data collection.
- (6) Star and planet surveys.
- (7) Auxiliary mirror surveys.
- (8) Color surveys.
- (9) Magnet assembly surveys.
- (10) Shadow progression sequences.

*i. September 25 to 29.* Control of the spacecraft was turned over to the *Surveyor* Operations Chiefs for continuation of engineering interrogations once every 2.5 hr for 15 min. On September 25, one switch in each of the thermal compartments was stuck closed, and the command to dump the helium was sent in an attempt to





FOLDOUT FRAME



FOLDOUT FRAME

FOLDOUT FRAME 2





Fig. VI-3. Key spacecraft thermal and power parameters controlled during first lunar night operations before shutdown

FOLDOUT FRAME 3

FOLDOUT FRAME 4





vibrate the switches open. However, there was no indication that the command was acted upon, and it was determined that a defective transducer was at fault. Spacecraft control from the SFOF was resumed on September 26 and interrogations continued until temperatures and other parameters precluded further operations.

Figure VI-3 shows several key performance parameters during lunar night operations. The data is plotted from approximately 9 hr after sunset, when a steady-state spacecraft condition was achieved, until spacecraft shutdown at 06:35:58 GMT, September 29, 115 hr and 36 min after sunset. Figure VI-4 gives the predicted and actual spacecraft shutdown times and predicted revival times, with corresponding battery temperature profiles.

## 8. Second Lunar Day

*Surveyor V* was turned on by DSS 42 at 08:07 GMT, October 15, about 147 hr after sunrise at the landing site. The spacecraft responded immediately to the first series of commands following the 16-day (385.5 hr) shutdown. Engineering interrogations conducted after spacecraft turn-on and on October 16 revealed the following:

- (1) Battery temperature at spacecraft turn-on was 100°F higher than anticipated and was increasing at a rate of 3.5°F/hr.
- (2) When commands were sent to select telemetry rates of 17.2 and 137.5 bit/sec, the spacecraft transmitted data at 550 bit/sec instead.
- (3) Spacecraft Legs 2 and 3, which had sagged prior to lunar sunset, had returned to their normal positions as a result of rising temperatures. (Prior to sunset on the second lunar day, Leg 3 again sagged as the temperature dropped.)
- (4) The gyro temperatures were 100°F higher than on the first lunar day, confirming that a disintegration of the gyro thermal radiator had occurred as expected.

The alpha scattering instrument was turned on at 23:14 GMT on October 15. A few anomalies were noted in the detector status and in the analog-to-digital converter operation, but the instrument was otherwise operating well and returned many hours of useful data accumulations during the second lunar day until turn-off at 01:40 GMT, October 23. Since the data was noisy in part, the information received was useful primarily for engineering purposes with limited scientific value.

Comprehensive RF communications and signal processing assessments were carried out. A special test was conducted with *Surveyor V* placed in the terminal descent telemetry mode to resolve a data outage problem which occurred during terminal descent and again during the static firing experiment on the first lunar day. It was determined that the wide bandwidth used at DSS 14 was at fault. Other tests performed included best-lock frequency measurements as often as possible over DSS 61 and 42. Planar array and solar panel stepping operations were conducted as required for battery charging, attitude determination, and shading.

Television operations were initiated on October 16. It was discovered that camera focus, filter, and focal length controls were operating properly. The earlier anomaly was apparently temperature-related since these controls again stuck during the final video sequence on the second lunar day as they had at the onset of first lunar night. The first pictures received were quite gray and dark; the video signal was low in amplitude in both 600-line and 200-line modes, and the 200-line mode also exhibited phase reversal (the camera was deviating a maximum of 70 kHz vs a nominal 3 MHz). The spacecraft was placed in periodic standbys on October 16 and 17 because of high temperatures but, when possible during DSS 11 passes on these two days, experiments were run to enhance the video. The anomaly was traced to a resistor that had failed during the cold of the lunar night. By greatly amplifying the video signal at the TV ground data handling system at DSS 11, usable video images were obtained.

Pictures of Compartment A revealed that a radiator on a thermal switch had popped off. Subsequent searches failed to locate the missing mirror, and it was assumed that the mirror had slid off the compartment owing to spacecraft tilt and that it was in an area not visible to the camera.

A total eclipse of the sun by the earth occurred on October 18 at 10:28 GMT. Although the camera position precluded a view of the earth, excellent thermal data was obtained which reflected spacecraft cooling and warming as the earth's shadow passed across *Surveyor V*. Since the DSN was heavily committed to support the *Mariner V* encounter with Venus, special coverage for eclipse operations was provided by a MSFN facility at Honeysuckle Creek, Australia. Only DSS 61 was available on October 19 and 20, limiting *Surveyor V* activities to engineering and television interrogations and some alpha scattering operations. Full DSN coverage was reestablished on October 21,

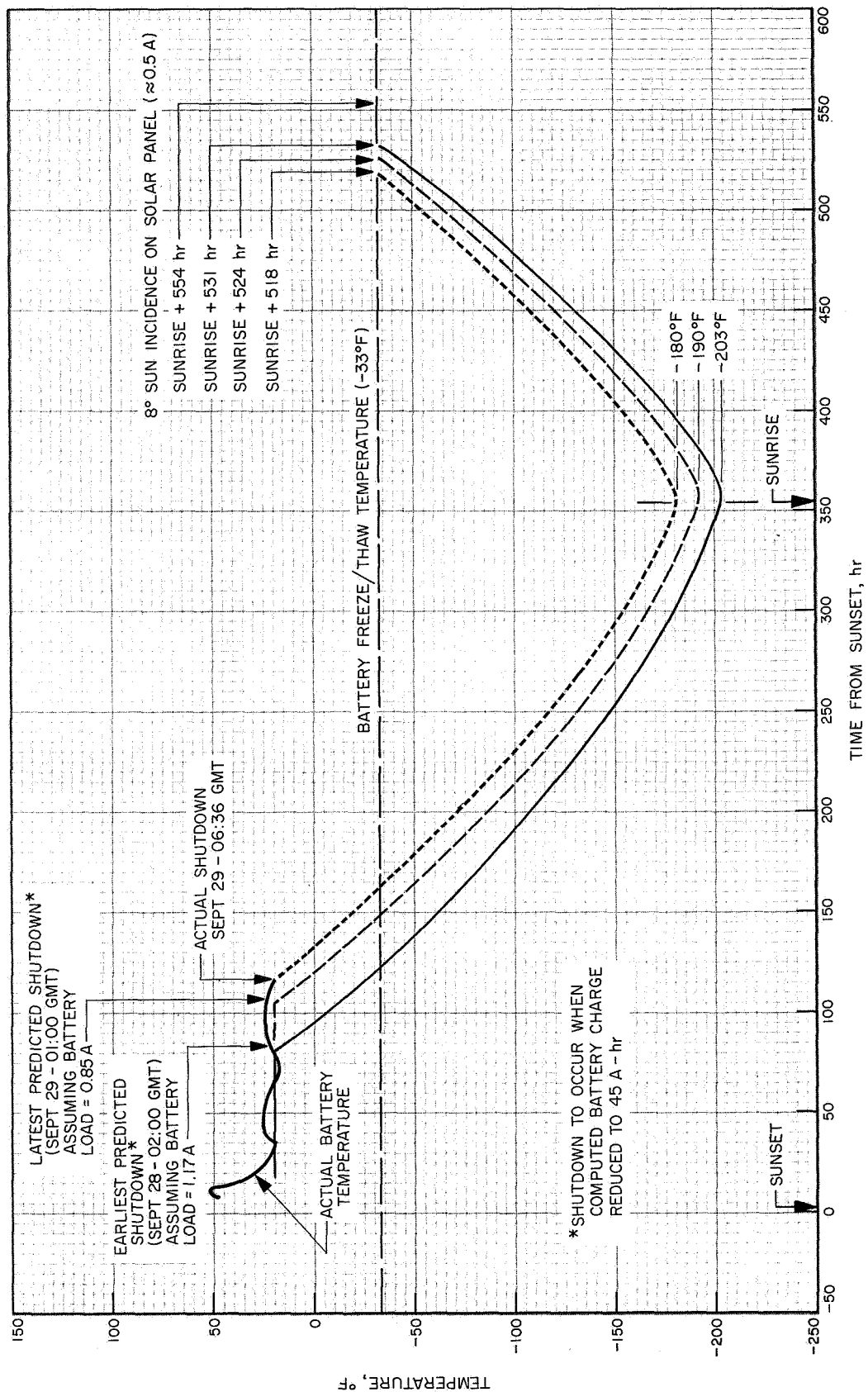


Fig. VI-4. Surveyor V lunar night survival plan and predicted battery temperature profile

and television operations were conducted at intervals until October 23 when the camera was turned off. *Surveyor V* transmitted 1048 pictures on the second lunar day, bringing the total pictures for the mission to 19,054.

A new technique was implemented in preparing the spacecraft for lunar night. After the battery was brought to the fully charged condition before sunset, solar panel energy was used to raise compartment temperatures in order to reduce power loads required during initial ther-

mal and power management after sunset. Sunset at the top of the solar panel occurred at 23:38 GMT, October 23. Spacecraft interrogations were conducted on 4-hr centers, then were increased to 8-, 12-, and finally 24-hr centers. *Surveyor V* was shut down on November 1 at 12:20 GMT, approximately 200 hr after lunar sunset.

The more important lunar operations sequences for both lunar days, other than routine engineering interrogations, are listed in Table A-2 of Appendix A.



## VII. Flight Path and Events

*Surveyor V* was injected first into a parking orbit and then into a nearly perfect lunar transfer trajectory. After the required midcourse maneuver was performed 17.8 hr after liftoff, the helium regulator did not reseal properly, thus allowing helium to escape into space through relief valves on the low-pressure side of the propellant pressurization system. Sunline and anti-sunline maneuvers were then made in quick succession in attempts to reseal the valve. Shortly thereafter, it was determined that soft landing might be accomplished in spite of drastically reduced helium pressure during the terminal descent if the helium volume and main retromotor burnout conditions were adjusted properly. These adjustments were achieved with three additional midcourse maneuvers. All six midcourse maneuvers were executed within a 22-hr period. Because terminal descent performance was very close to that predicted for the redesigned terminal sequence, soft landing was achieved. The current estimate of the landing site based on in-flight tracking data is 1.50 deg north latitude and 23.19 deg east longitude,\* which is about 32 km northwest of the aim point. This miss distance is not unduly large considering the large

uncertainty in the trajectory at the time of the final maneuver. The large uncertainty was due to the limited tracking time available between the last two maneuvers.

### A. Prelaunch

For *Surveyor V*, the landing site selected prior to launch for targeting of the launch vehicle ascent trajectory was in a mare area of the *Apollo* zone of interest at 0.83 deg north latitude and 24.00 deg east longitude. This site is a key *Apollo* landing site. It was selected for this mission mainly because it is accessible within the *Surveyor* unbraked incidence angle capability only from September to February and, therefore, schedule slips might have precluded reaching this site on a later mission. Furthermore, this site was predicted to be the most hospitable site available on the basis of surface smoothness. An unbraked impact speed was selected so that the Goldstone postarrival visibility would be maximized, while still satisfying the prearrival visibility constraints for all launch days in the launch period.

### B. Launch Phase

The *Surveyor V* spacecraft was launched from AFETR Launch Pad 36B at Cape Kennedy, Florida, September 8,

---

\*Based on preliminary analysis of postlanding tracking data, the landing site is at 1.41 deg north latitude, 23.18 deg east longitude.

1967, using an *Atlas/Centaur* (AC-13) boost vehicle. The launch was held until 18 min after opening of the launch window, the delay required to confirm adequate launcher stabilization pressure. Liftoff occurred at 07:57:01.257 GMT. Two seconds after liftoff, the launch vehicle began a 13-sec programmed roll that oriented the vehicle from a pad-aligned azimuth of 115 deg to a launch azimuth of 79.517 deg. At 15 sec, a programmed pitch maneuver was initiated which was completed at *Atlas* booster engine cutoff (BECO). Following booster section jettison the remainder of the flight to injection was guided by the *Centaur* inertial guidance system. The *Centaur* first burn injected the vehicle into a parking orbit having a 91-nm apogee and 85-nm perigee. The spacecraft was in the earth's shadow during the first 11.5 min of flight, but left the shadow during parking orbit coast and remained in sunlight during the remainder of the flight. After a 6.7-min coast, the *Centaur* burned a second time to inject the *Surveyor V* spacecraft into the desired lunar transfer trajectory. All event times for the launch phase were close to nominal. The launch phase sequence is discussed in greater detail in Section III, and actual event times for all phases of the mission are summarized in Table A-1 of Appendix A.

### C. Cruise Phase

Separation of *Surveyor V* from *Centaur* occurred at 08:16:26.8 GMT on September 8, 1967, at an approximate geocentric latitude and longitude of 21 and 344 deg, respectively. Automatic sun acquisition began about 1 min after separation and was completed after a maneuver of  $-342$  deg roll and  $+18$  deg yaw.

Predictions indicated *Surveyor V* would rise over the DSS 51 horizon at  $L + 00:28:09$ . DSS 51 received good one-way data at rise  $+ 39$  sec and good two-way data at rise  $+ 5$  min, 11 sec. Previous experience with the current acquisition procedure indicates that the above sequence was quite good. For instance, during the initial acquisitions of *Surveyors III* and *IV* by DSS 42 and DSS 72, respectively, good two-way data was first obtained at rise  $+ 6$  min, 55 sec and rise  $+ 6$  min, 38 sec.

From the time of two-way acquisition by DSS 51 until approximately 40 min before retro ignition, the DSN tracked the *Surveyor V* spacecraft in the two-way mode and, with minor exceptions, returned high-quality two-way doppler data. In fact, two-way doppler was obtained during each of the six midcourse maneuvers. One-way doppler was obtained during terminal descent and touchdown. The most serious loss of two-way doppler data

occurred during the second pass of DSS 42. For 70 min after handover from DSS 11, DSS 42 sent bad doppler data marked as good. It was supposed that the large doppler deviations reported by the near-real-time tracking data monitor were the result of the four midcourse maneuvers which the spacecraft had undergone by this time. It is for this reason that the error was not discovered sooner and that the data was lost. During the third pass of DSS 11 approximately two hours before retro ignition, the most significant digit of the doppler counter was lost for 32 min. All two-way tracking data taken during the *Surveyor V* mission was computer-monitored in near-real-time, which resulted in the early discovery of the lost digit in the doppler counter. This data was quickly recovered by hand-restoring the missing digit on punched cards. DSS 51 mislabeled approximately  $2\frac{1}{2}$  min of data at initial two-way acquisition during the launch pass. This data was mislabeled three-way, but the Orbit Determination Group recovered this data by changing the data condition code from three-way to two-way. DSS 72 transmitted no good doppler data during the launch pass, and this problem is currently under investigation. During the second pass of DSS 72, the antenna was initially positioned at 10-deg elevation, which delayed three-way acquisition to rise  $+ 1$  hr, 18 min. On the first pass of DSS 61, the maximum elevation angle was 16.9 deg. Because of this, the usefulness of the data is questionable. However, DSS 61 data did appear to be of better quality than it had been for the past three *Surveyor* missions.

A plot of the *Centaur* and *Surveyor V* trajectories, projected on the earth's equatorial plane, is provided in Fig. VII-1. The earth track traced by *Surveyor V* appears in Fig. VII-2. Specific events such as sun and Canopus acquisition and rise and set times for DSIF stations are also noted.

Prior to Canopus acquisition, the spacecraft was rolled to generate a star map. Then Canopus was acquired at  $L + 06:31$  with a net roll of  $+173$  deg. In normal cruise mode, the spacecraft  $-Z$  axis is aligned to the sun and the  $-X$  axis to the projection of Canopus on the spacecraft  $X-Y$  plane.

As shown in Fig. VII-3, the current best estimate of the uncorrected, unbraked impact point is in the southwest corner of the Sea of Tranquility at selenographic coordinates of 2.32 deg north latitude and 23.74 deg east longitude. The target point was 0.83 deg north latitude and 24.00 deg east longitude. The two points are approximately 45.9 km (28.5 miles) apart on the surface of the moon.

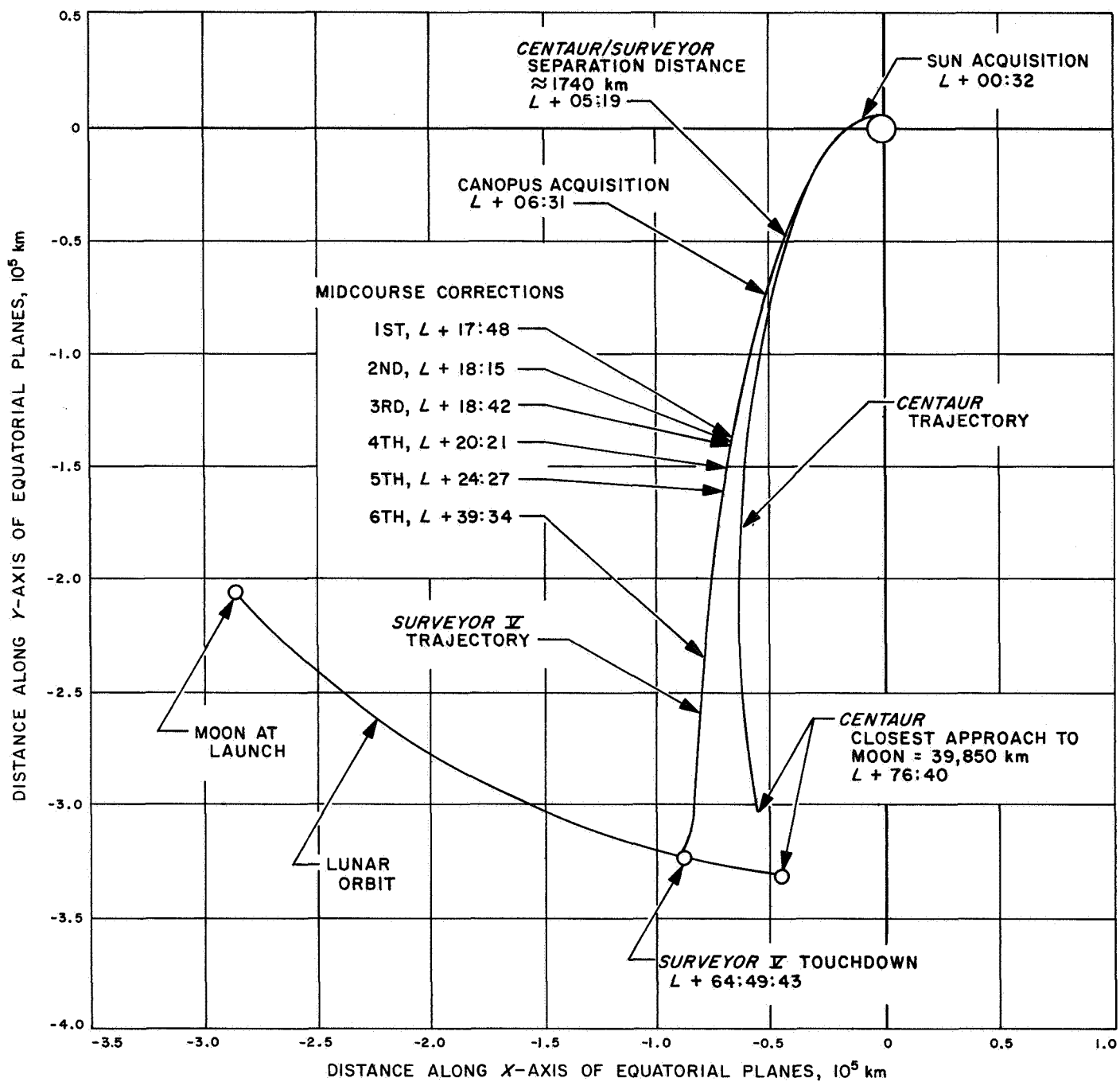


Fig. VII-1. Surveyor and Centaur trajectories in earth's equatorial plane



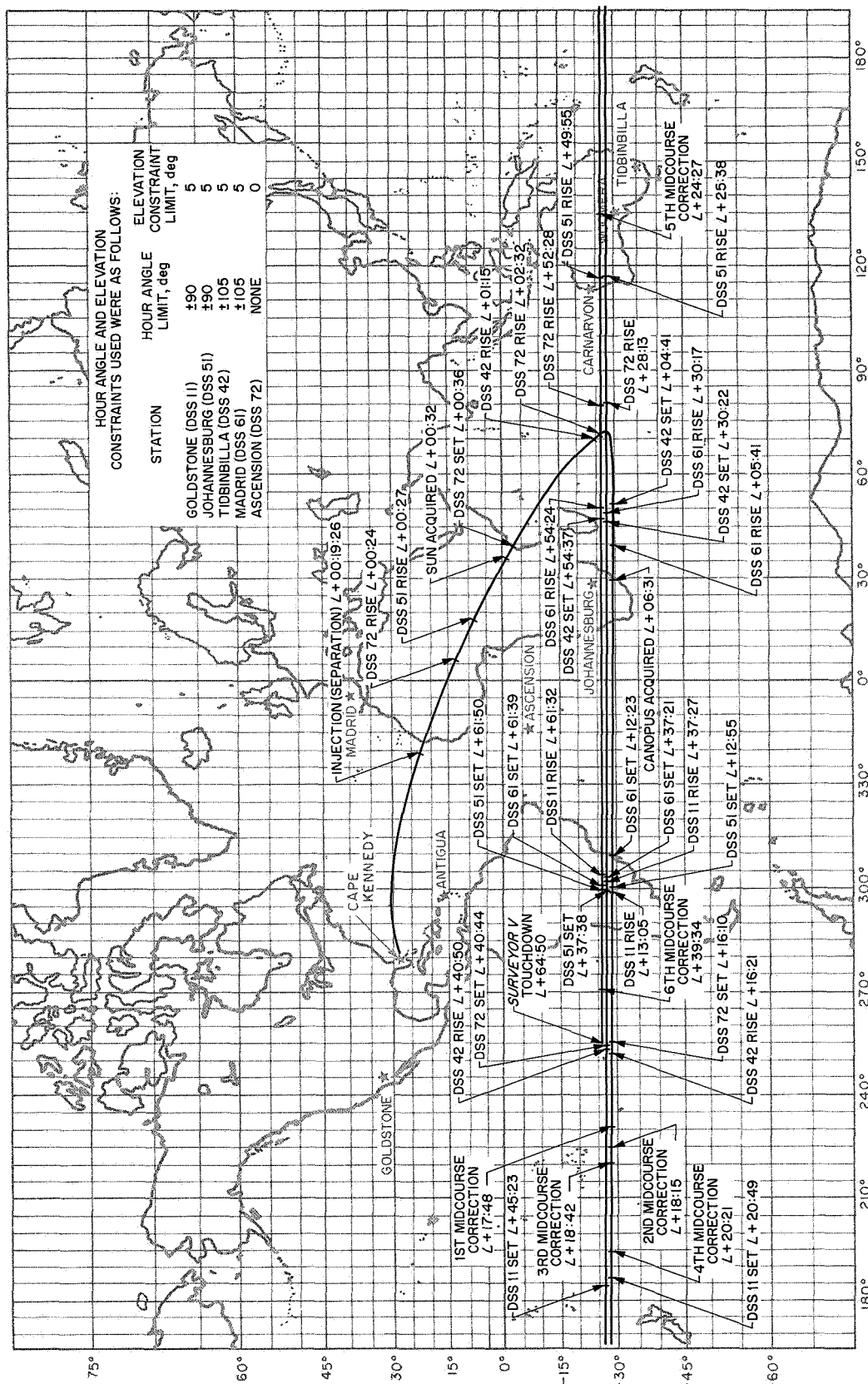


Fig. VII-2. Surveyor V earth track

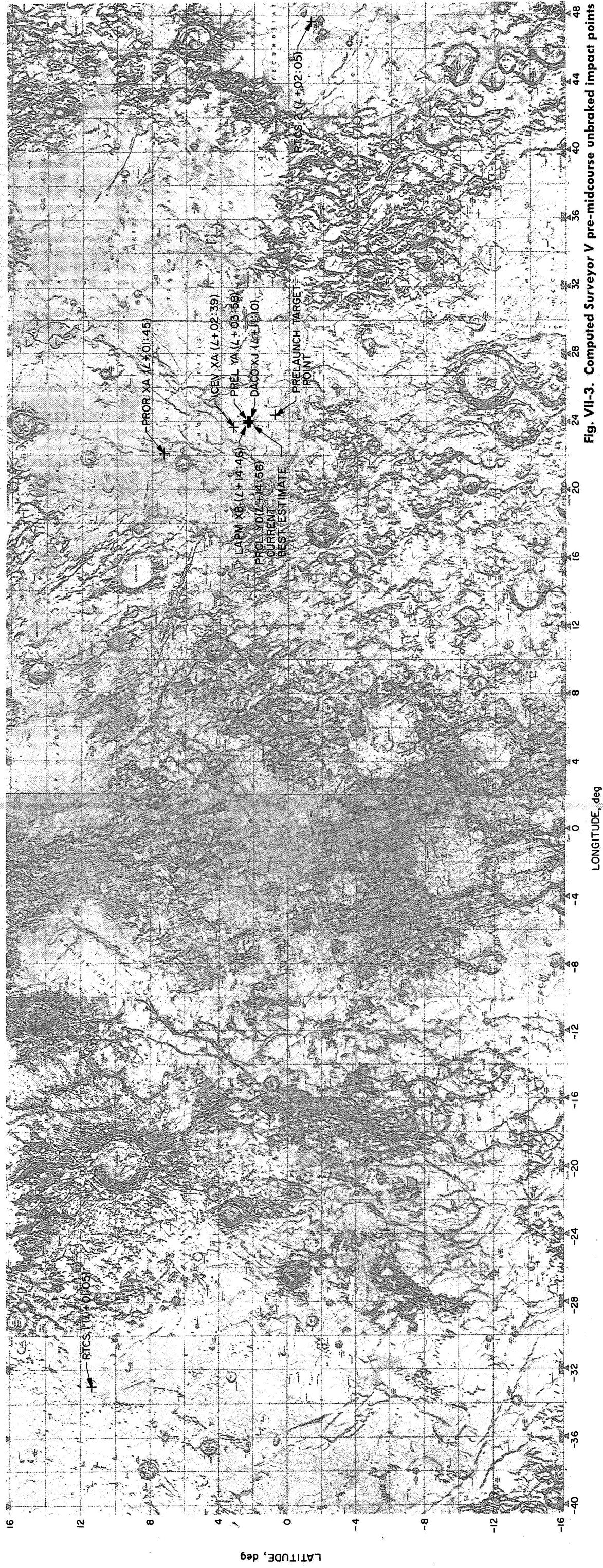


Fig. VII-3. Computed Surveyor V pre-midcourse unbraked impact points

Table VII-1. Surveyor V encounter conditions based on selected pre-midcourse orbit determinations

Orbit identification	Time computation completed (from liftoff)	Target statistics										Unbraked impact conditions			Data used
		B, km	B · TT, km	B · RT, km	TL, hr	SMAA (1σ), km	SMIA (1σ), km	THETA, deg	σ <sub>T</sub> IMPACT (1σ), sec	PHIP 99, deg	SVFIX R (1σ), m/sec	Lat, deg	Long, deg	GMT September 10	
RTCS 1	01:05	841.6	384.2	-748.8	63.0							11.19	327.06	23:16:32.2	Grand Canary radar
PROR XA	01:45	2866.8	2823.5	-496.8	63.12	123.19	27.63	98.15	48.184	3.927	0.6309	7.26	22.087	23:25:02.413	DSS 51 angular and two-way doppler
RTCS 2	02:05	3580.5	3579.7	74.8	63.01	30.82	5.92	71.76	10.202			-1.25	47.65	23:41:13.3	DSS 51 angular and two-way doppler
ICEV XA	02:39	2903.9	2891.5	-268.4	63.12	81.93	8.58	92.15	34.388	2.753	0.6233	3.21	23.68	23:25:07.173	DSS 51 two way doppler, and DSS 51, 42 angular
ICEV XB	02:58	2904.7	2896.3	-220.8	63.12	25.08	6.868	95.99	6.5323	0.6125	0.6187	2.36	23.78	23:25:13.901	DSS 51, 42 two-way doppler
PREL YA	03:58	2904.6	2896.2	-221.1	63.12	17.92	6.866	95.23	4.8304	0.4728	0.6186	2.36	23.78	23:25:13.842	DSS 51, 42 two-way doppler
DACO XJ	11:10	2903.8	2895.3	-222.2	63.12	3.172	2.071	67.87	0.68499	0.0789	0.6185	2.38	23.75	23:25:13.621	DSS 51, 42 and 72 two-way doppler
LAPM XB <sup>a</sup>	14:46	2903.2	2894.9	-219.7	63.12	8.811	3.651	78.00	1.7105	0.2268	0.6186	2.34	23.74	23:25:13.907	DSS 51, 42, 72 and 11 two-way doppler
PRCL YD <sup>b</sup>	26:56	2903.0	2894.7	-218.9	63.12	7.053	3.143	77.51	1.4345.	0.1848	0.6185	2.32	23.73	23:25:14.005	DSS 51, 42, 72, 11 and 61 two-way doppler
<div><div><sup>a</sup>Orbit used for midcourse computations.</div><div><sup>b</sup>Current best estimate.</div><div>TL Flight time from injection.</div><div>SMAA semimajor axis of 1σ dispersion ellipse.</div><div>SMIA semiminor axis of 1σ dispersion ellipse.</div></div> <div>THETA orientation angle of 1σ dispersion ellipse measured clockwise from TT axis in B-plane. σ<sub>T</sub> IMPACT 1σ uncertainty in predicted unbraked impact time. PHIP 99 99% velocity vector pointing error. SVFIX R 1σ uncertainty in magnitude of velocity vector at unbraked impact.</div>															



A few selected pre-midcourse (first) orbit computations mapped to the moon are also shown in Fig. VII-3. The numerical data for these selected pre-midcourse computations are presented in Table VII-1. Also shown are the results of the orbit determination from the Real Time Computer System (RTCS), Cape Kennedy, which were obtained at  $L + 01:05$  and  $L + 02:05$ . The initial computation of the spacecraft orbit by the RTCS was based on *Centaur* C-band data from Grand Canary. This orbit indicated lunar encounter would be achieved with no midcourse correction. The only data received from Grand Canary by the SFOF at JPL was *Centaur* C-band data for after the start of the retromaneuver sequence. Therefore, no orbit was computed by JPL based on this data.

The first estimate of the spacecraft orbit (PROR XA) based on DSN data only was completed by JPL at  $L + 01:45$ , using 35 min of DSS 51 two-way doppler and angle data. Although it was based on only 35 min of data, this orbit indicated that a lunar encounter would be achieved and that the correction required to hit the pre-launch target point was well within the nominal midcourse correction capability. These results were further verified by the ICEV XA and PREL YA orbit computations completed at  $L + 02:39$  and  $L + 03:58$ , respectively.

When sufficient data was received, the angle data was weighted out of the orbit solution. This was done first during the ICEV XB orbit computation. The resulting change of only 0.8 km in the  $B$  vector indicates an unusually good agreement between the doppler and angle data.

During the data consistency (DACO) orbit computation period, data was received from DSS 61 and DSS 72. Data from all DSIF stations received up to this time seemed to be consistent, and no significant biases were discovered. The LAPM XB orbit, on which the first midcourse correction was based, utilized all the two-way doppler data obtained until 3 hr, 16 min before midcourse correction, except for the DSS 61 data which was eliminated because of low elevation angles. When mapped to the moon, this solution predicted an unbraked impact point at 2.34 deg north latitude and 23.74 deg east longitude. For the current best estimate of the spacecraft pre-midcourse orbit (PRCL YD), all usable data taken by DSS 11, 42, 51, 61, and 72 from initial acquisition to start of the first midcourse maneuver was used.

#### D. Midcourse Maneuver Phase

A series of six midcourse corrections was performed during the *Surveyor V* mission. The initial correction was planned and executed in a nominal manner. However,

telemetry indicated that the vernier propulsion system helium regulator valve did not reseal tightly after the firing. This allowed helium from the supply tank to leak into the propellant tank manifold, and then to vent overboard when the manifold pressure reached the relief valve setting. Additional corrections were performed in an attempt to alleviate the problem. The problem persisted, but during this period, it was determined that a soft landing might be accomplished if the spacecraft weight, burnout velocity, and vernier propellant system gas volume were judiciously readjusted. The last midcourse corrections were performed to adjust the terminal descent parameters and also correct the trajectory to the desired landing location (approximately 32 km from where the spacecraft did land). A total of six corrections were made, with only the first and last corrections based upon orbit determination. A description of each of these maneuvers and associated rationale follows.

#### 1. First Midcourse Correction

The final aim point, selected prior to the first midcourse correction, was biased 0.12 deg northeast of the prelaunch target point in order to maximize the probability of landing in the area covered by high-resolution *Lunar Orbiter* photographs.

The first midcourse correction computed to enable the spacecraft to soft-land at the final aim point (0.916 deg north latitude and 24.083 deg east longitude) was 14.01 m/sec (corresponding to a burn time of 14.29 sec). The correction was executed upon an earth command at 01:45 GMT on September 9, 1967. This execution time of 17.5 hr after injection allowed 4 hr 34 min of pre-midcourse and 3 hr and 7 min of post-midcourse visibility from Goldstone. Figure VII-4 shows the prelaunch target site, the final aim point, the estimated soft-landing site, and the associated dispersions. The 99% ( $3\sigma$ ) dispersions are shown as an ellipse on the surface with a semimajor axis of 27.8 km and a semiminor axis of 18.5 km. The small ellipse is centered on the current best estimate of the landing site based on orbit determination (OD) and represents the  $3\sigma$  OD uncertainties in touchdown location.

Typical midcourse correction capability, as a function of the unbraked impact speed  $V_{imp}$ , is shown in Fig. VII-5. Typical *Centaur*  $3\sigma$  injection guidance dispersions and the effective lunar radius are also shown. The midcourse capability contours are in the conventional R-S-T coordinate system.\*

\*Kizner, W. A., *A Method of Describing Miss Distances for Lunar and Interplanetary Trajectories*, External Publication 674, Jet Propulsion Laboratory, Pasadena, August 1, 1959.

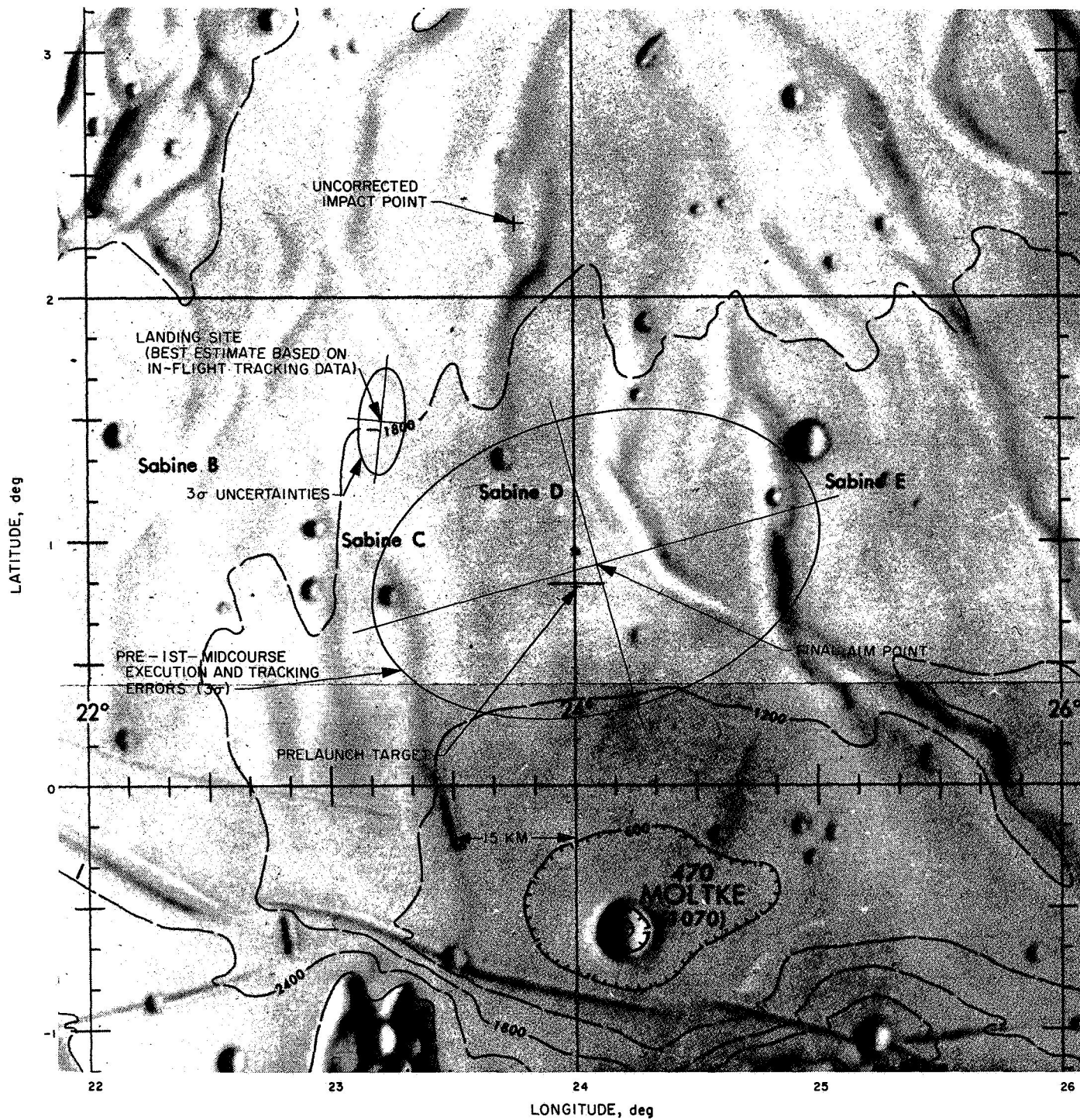


Fig. VII-4. Surveyor V landing location

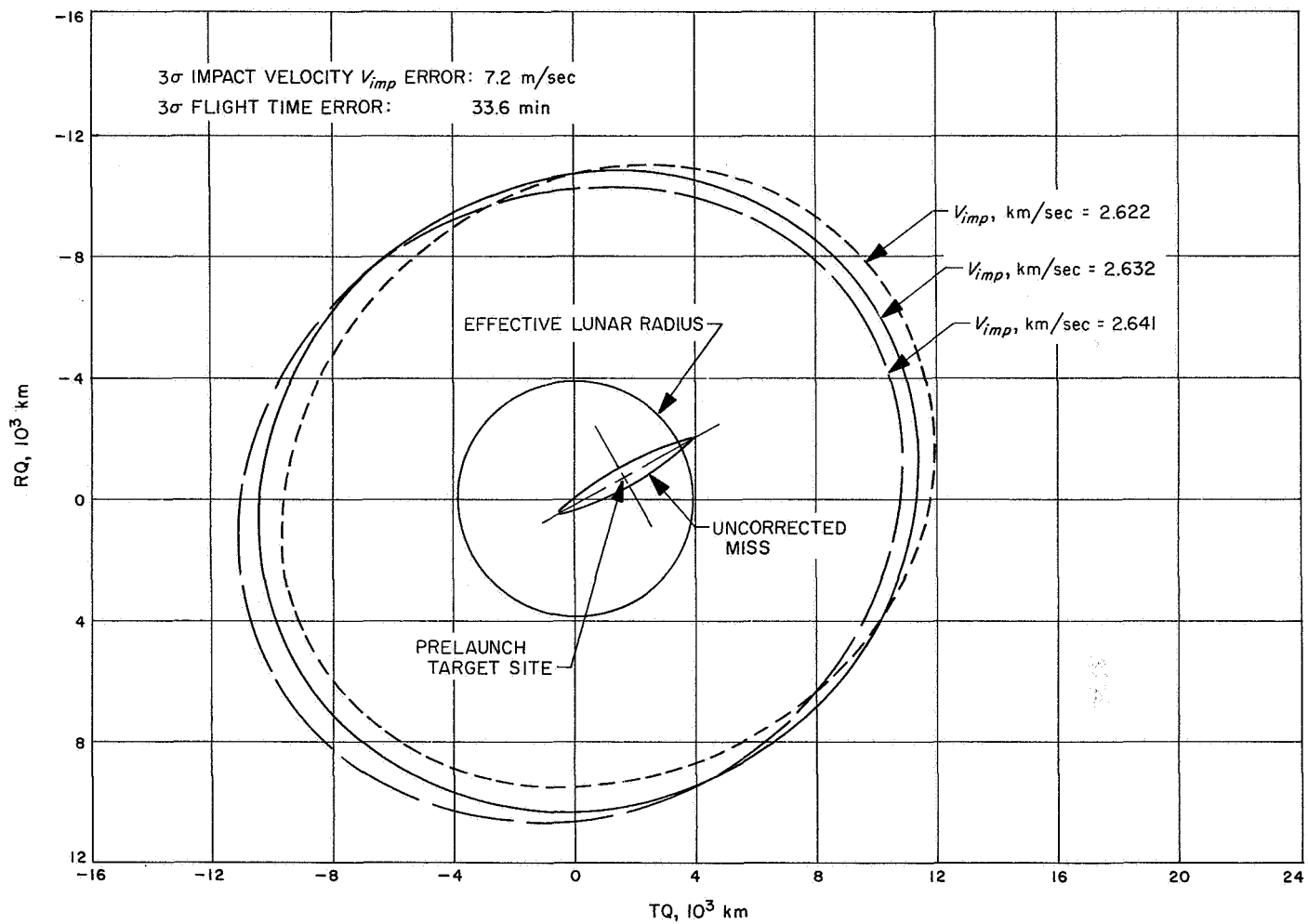


Fig. VII-5. Midcourse correction capability contours (for a correction 20 hr after injection)

The midcourse correction of 14.01 m/sec was selected to correct to the final aim point and to adjust other parameters. The velocity component in the critical plane, required to correct "miss only," was only 0.52 m/sec. The velocity component normal to the critical plane is referred to as the noncritical component since it does not affect the miss to the first order. The noncritical velocity component was  $-14.0$  m/sec. Figure VII-6 presents the variation in flight time, main retro burnout velocity, vernier propellant margin, and landing site dispersion with the noncritical velocity component  $\dot{U}_3$ . A value of  $-14.0$  m/sec was selected for the noncritical velocity component because (1) it was necessary to reduce spacecraft weight in order to provide adequate moment control at maximum thrust acceleration during terminal descent, (2) it was desired to reduce the main retro motor burnout velocity in order to increase the spacecraft performance margin

during terminal descent, and (3) it was desired to increase the Goldstone postarrival visibility time for lunar operations. The selected value satisfied all of the above objectives. As shown in Fig. VII-6, the resultant burnout velocity was reduced to 463 ft/sec, and the Goldstone postarrival visibility was increased by 31.2 min. If the maneuver strategy had been to correct "miss-plus-flight-time," the required noncritical component would have been  $-0.52$  m/sec, giving a total correction of 0.74 m/sec.

Since the final aim point was changed from the prelaunch target point, the above required correction does not properly evaluate the performance of the *Centaur* guidance system. Correcting 20 hr after injection to the prelaunch target point gives a miss-only requirement of 0.549 m/sec and a miss-plus-flight-time requirement of 0.740 m/sec, both remarkably small values.

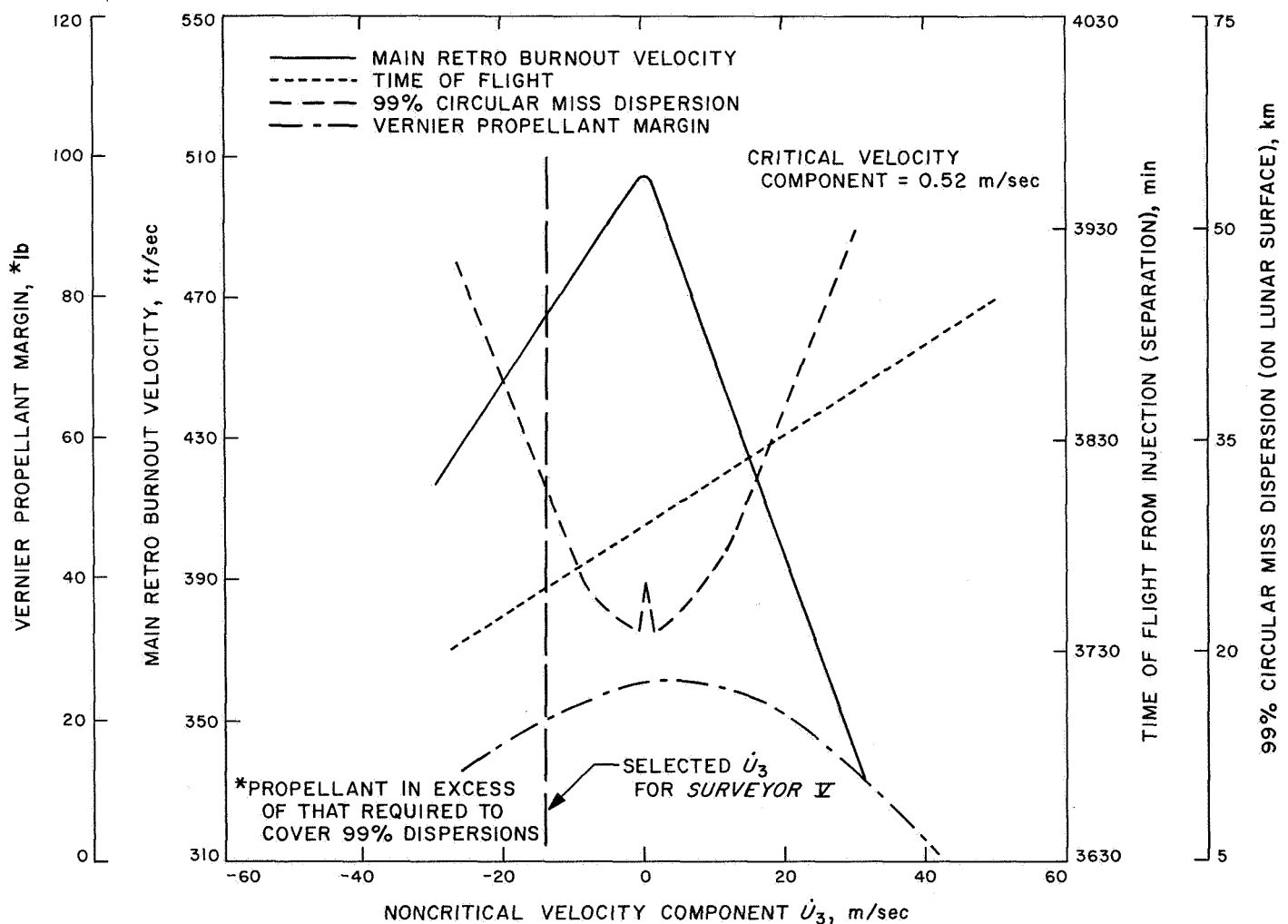


Fig. VII-6. Effect of noncritical velocity component on terminal descent parameters for first midcourse correction

The predicted results of the selected midcourse correction and other alternatives considered are given in Table VII-2. The possibility of not performing a midcourse correction was eliminated because it was required that the spacecraft land at a prime *Apollo* site. Execution of the midcourse correction during the second Goldstone pass would have doubled the required critical velocity component to 1.03 m/sec while reducing the landing site dispersions as shown in Table VII-2. However, this alternative was rejected because terrain evaluation indicated that it would not significantly increase the probability of soft landing, and a midcourse during the first pass would provide a high probability of landing in the *Lunar Orbiter* high-resolution picture area. The possibility of performing a correction along the spacecraft-sun direction was investigated and eliminated because the desired site could not be reached.

An analysis was made of eight pairs of pre-midcourse attitude rotations, any pair of which would have correctly oriented the spacecraft for the midcourse velocity correction. A combination of +71.84 deg roll and -35.64 deg yaw was chosen because it maximized the probability of mission success by providing maximum sun-lock time and continuous high antenna gain without requiring antenna

switching. The selected attitude rotations were compensated to achieve alignment of the actual thrust axis (determined prior to launch) with the desired midcourse vector. Also, the attitude rotations were initiated at limit cycle nulls in an attempt to further minimize pointing errors.

## 2. Second Midcourse Correction

The second correction was executed 27 min after the first correction as an emergency attempt to reseal the helium regulator valve which was observed to leak following the first correction. As time was critical, this correction was performed along the sunline with vernier engine ignition occurring while the spacecraft was in sun-lock. An engine burn time of 10.05 sec moved the spacecraft impact point from the desired site to the east 1600 km. The new impact location would have been 2.89 deg north latitude, 77.52 deg east longitude; the unbraked impact angle would have been of 81.5 deg.

Figure VII-7 shows the various impact points on the lunar surface of the trajectories resulting from injection and each midcourse correction. Table VII-3 provides execution times, attitude maneuvers, burn times, resulting impact points and unbraked impact incidence angles for each of the midcourse corrections.

Table VII-2. First midcourse correction alternatives comparison

Time of midcourse execution, Goldstone pass	Selected midcourse	Alternate considerations			
	First	No midcourse	First	Second	
Midcourse parameters					
Velocity magnitude, m/sec	14.01		14.01	14.04	14.04
Critical component, m/sec	0.52		0.56	1.03	1.03
Noncritical component, m/sec	—14.00		+14.00	—14.00	+14.00
Propellant weight, lb	11.64		11.64	11.66	11.66
First rotation, roll, deg	71.84		64.59		65.65
Second rotation, yaw, deg	—35.64		143.22		135.88
Landing site dispersions (mechanization plus tracking), 3σ					
Semimajor axis, km	27.8		34.8	13.0	12.8
Semiminor axis, km	18.5		14.3	7.5	7.4
Ellipse inclination, deg (positive TQ toward RQ)	—15.9				
Terminal parameters					
Aim point: north latitude, deg	0.916	2.33	0.916	0.916	0.916
east longitude, deg	24.083	23.74	24.083	24.083	24.083
Incidence angle, deg	46.4	46.0			
Unbraked impact speed, m/sec	2638.6	2633.4	2626		
Burnout velocity, ft/sec	463	505	428	464	429
Burnout altitude, ft	37,743				
Propellant margin, lb	20.0	26.1	22.8	19.9	22.8



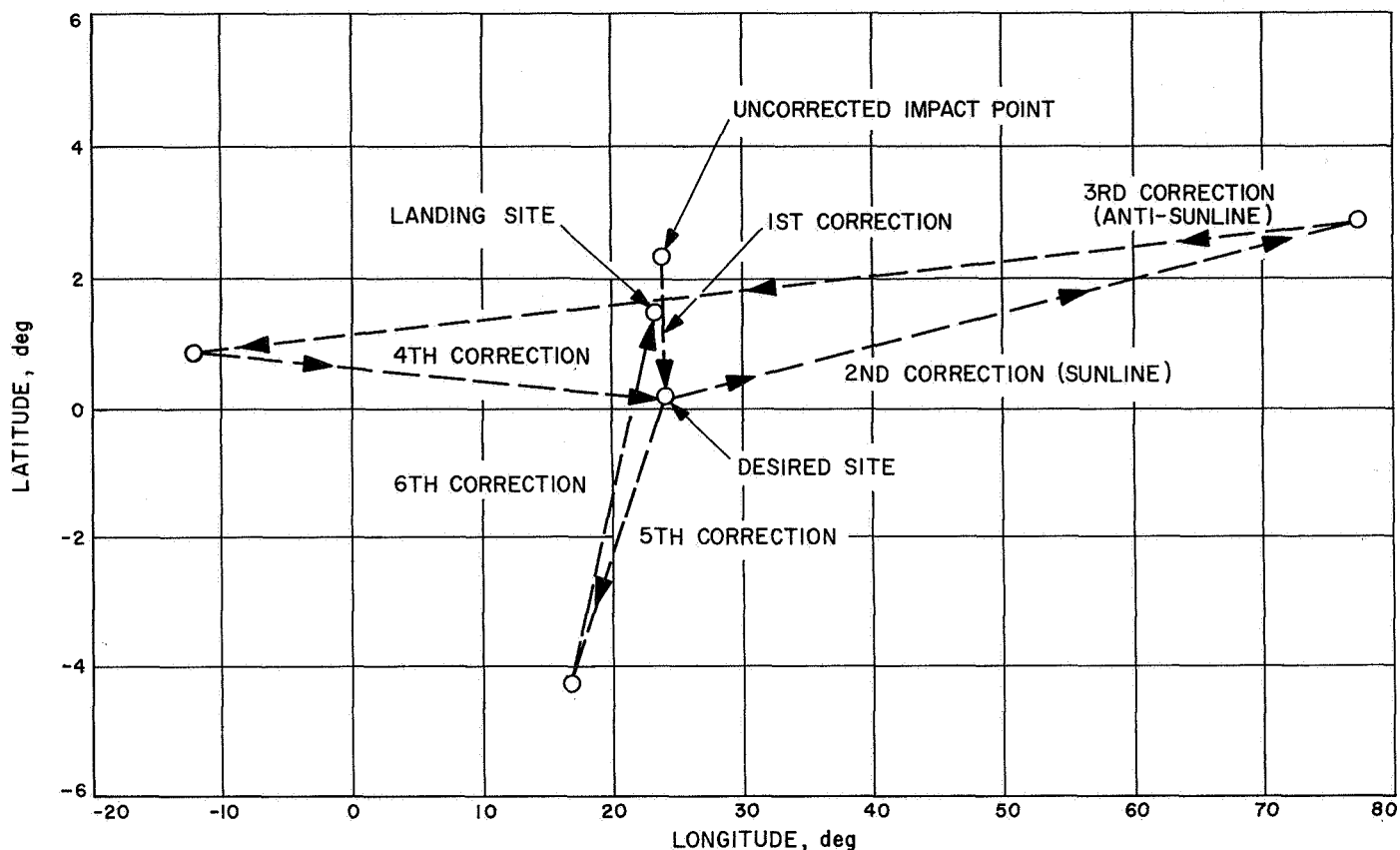


Fig. VII-7. Computed Surveyor V impact points for each midcourse correction

Table VII-3. Midcourse correction data

Midcourse correction	Ignition time, GMT (September 9, 1967)	Attitude rotations, deg	Burn time, sec	Prior impact point, latitude/longitude	Resultant impact point	Incidence angle, deg
First	01:45:02	Roll +71.8 Yaw -35.6	14.25	+ 2.33°N + 23.74°E	+ 0.917°N } + 24.083°E } <sup>a</sup>	46.4
Second (sunline)	02:12:02	None	10.05	+ 0.917°N + 24.083°E	+ 2.89°N + 77.52°E	81.5
Third (anti-sunline)	02:39:50	Yaw -180	23.05	+ 2.89°N + 77.52°E	+ 0.86°N - 12.01°E	20.7
Fourth	04:18:48	Roll +68.5 Yaw +106.8	13.0	+ 0.86°N - 12.01°E	+ 0.917°N } + 24.083°E } <sup>a</sup>	46.6
Fifth	08:24:02	Roll +64.6 Yaw +143.2	33.0	+ 0.917°N + 24.083°E	- 4.23°S + 16.83°E	46.7
Sixth	23:31:00	Roll -76.0 Yaw -100.6	5.45	- 4.23°S + 16.83°E	+ 1.50°N + 23.19°E	46.8

<sup>a</sup>Desired touchdown point.

### 3. Third Midcourse Correction

The third correction was made 27 min after the second correction in an additional attempt to reseal the helium valve. In order to prevent compounding the landing site

error, the spacecraft was yawed -180 deg before the engines were ignited for a burn period of 23.05 sec. This resulted in a velocity correction directly away from the sun, and moved the spacecraft impact point 2685 km to the west, past the desired landing site and across

the night-day terminator such that landing would have occurred in darkness. Impact would then have been at 0.86 deg north latitude, 12.01 deg west longitude, with an unbraked impact angle of 20.7 deg.

#### 4. Fourth Midcourse Correction

The fourth midcourse correction was executed 1 hr and 39 min after the third correction in an attempt to (1) reseal the helium regulator valve, (2) burn off propellant to reduce main retro motor burnout velocity, and (3) return to the desired landing site. A new trajectory was calculated which included the flight path changes due to the first three midcourse corrections. Based on the new trajectory, the critical velocity required to correct miss only was determined to be 8.30 m/sec. This was combined with a noncritical velocity component of +11.0 m/sec to increase time of flight and reduce burnout velocity. The total correction was determined to be 13.81 m/sec. The actual correction, modified in an attempt to reseal the helium valve, was conducted as a 12.0-sec burn followed by two 0.5-sec burns with 1-sec interruptions.

#### 5. Fifth Midcourse Correction

The fifth correction was executed 4 hr and 6 min after the fourth correction to further reduce the main retro burnout velocity and maximize usable propellant in the terminal phase by increasing gas volume in the propellant tanks. The spacecraft was reoriented to allow the velocity change to be in the positive noncritical direction, so as not to change the lunar impact point significantly, but to reduce the unbraked impact and retro burnout velocities. The engines burned for 33.0 sec following a roll-yaw attitude rotation sequence.

#### 6. Sixth Midcourse Correction

The sixth and final midcourse correction was conducted 15 hr and 7 min after the fifth correction and was based upon 13 hr of tracking. This correction was used to (1) adjust spacecraft weight and burnout velocity and further increase gas volume to optimal values, and (2) correct a 267-km residual miss to move the impact point from an area of mountainous terrain to the desired landing site. The critical velocity component required to correct the miss was determined to be 3.87 m/sec, and the noncritical component was calculated to be +3.6 m/sec. The total velocity change to the spacecraft was 5.32 m/sec.

Table VII-4 presents the injection and terminal conditions for the pre-midcourse, post-midcourse (fifth), and

post-midcourse (final) trajectories. Sufficient tracking data was not received between the first five midcourse corrections to reestablish the orbit. However, between the fifth and sixth corrections, the 2POM XD solution (see Table VII-5) was obtained based on 3 hr and 20 min, 9 hr and 18 min, and 3 hr and 15 min of tracking data from DSS 42, 51, and 61, respectively.

The first orbit computations of the final trajectory were completed approximately 8 hr after execution of the sixth midcourse correction. For the final (3POM XC) orbit computation during this period, approximately 3 hr of DSS 11 data and 5 hr of DSS 42 data were used. The initial values used for the orbit estimate were provided by the Trajectory Group, assuming a nominal maneuver mapped to the post-midcourse epoch. When these conditions were passed through the initial post-midcourse two-way doppler data from DSS 11, residuals of less than 1 Hz were computed. This was an early indication of a near-nominal maneuver execution. When the 3POM XC orbit was mapped to the moon, it indicated an unbraked impact point 25.8 km west and 14.8 km north of the final aim point. Based on the current estimate of the post-midcourse orbit (POST-2 orbit in Table VII-5), this is refined to be 17.6 km north and 26.8 km west of the final aim point.

#### E. Terminal Phase

Because of the helium leak it was necessary to redesign the nominal burnout conditions in order to effect a minimization of vernier propellant consumption. This necessitated extremely low burnout conditions. With this constraint, it was necessary that the actual burnout occur very near the predicted since the spacecraft could not accommodate the full 99% burnout dispersions. Figure VII-8 depicts the predicted nominal and actual burnout conditions and capability constraints for the *Surveyor V* terminal descent. Also shown are the more normal burnout conditions for the *Surveyor I* and *III* missions.

Following the fourth midcourse correction, it was determined that, by burning off sufficient propellant to maximize gas volume in the propellant tanks, approximately 35 lb of usable propellant could be reasonably expected for terminal descent with a possible maximum of 45 lb. Allowing for the propellant required for a modified main retro phase, which would utilize for the first time the optional low vernier thrust level and a short earth-commanded retro eject sequence, there remained about 13 to 23 lb for the vernier descent phase. Figure VII-9 presents graphically the vernier descent phase capability contours for these propellant values. Using this data, the

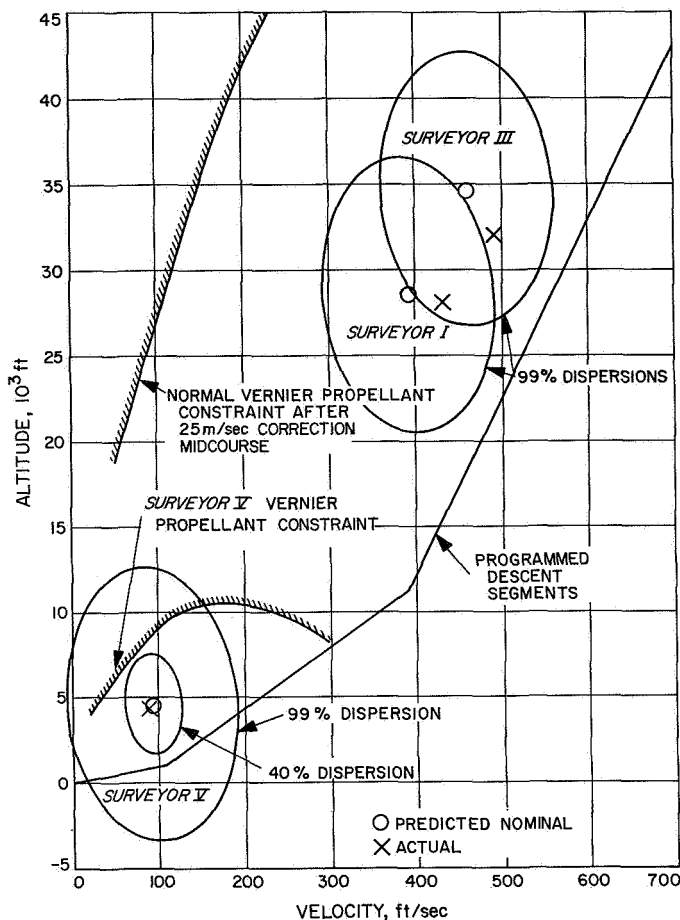


Fig. VII-8. Surveyor V main retro burnout conditions compared with previous missions

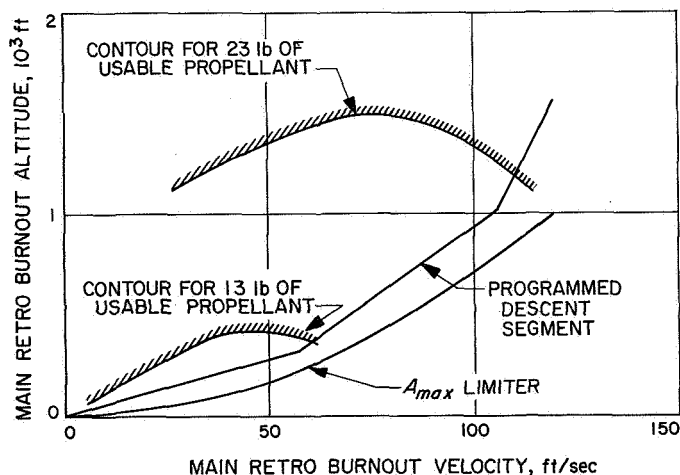


Fig. VII-9. Vernier descent phase capability contours—initial estimates

fifth midcourse correction was executed in the positive noncritical direction in order to (1) maximize usable pro-

pellant in the terminal phase and (2) reduce the unbraked impact and main retro burnout velocities. The correction was designed to provide a nominal main retro burnout velocity of  $\approx 50$  ft/sec, at an altitude that was to be determined later, assuming that a main retro thrust direction offset of 1.15 deg in the trajectory plane would lower the burnout velocity to the 50-ft/sec value and effect a near-vertical flight path angle at the beginning of the RADVS steering phase as shown in Fig. VII-10. Owing to the critical time factor, the computations for this maneuver were based on an assumed orbit obtained from the pre-midcourse orbit manually biased to reflect the subsequent corrections prior to the fifth maneuver. From this assumed orbit, the unbraked incidence angle was determined to be  $\approx 56$  deg.

Twelve hours after the fifth maneuver, tracking data indicated the actual unbraked incidence angle to be  $\approx 45$  deg and the unbraked impact velocity to be higher than expected. Based on these conditions, the burnout velocity would be  $\approx 120$  ft/sec, assuming that the retro thrust vector was biased to achieve a vertical flight path at burnout. In addition, based on vernier propulsion tests at Placerita Canyon, a new estimate of about 70 lb was obtained for the total usable vernier propellant which would be available for the terminal descent phase. With this additional capability a burnout velocity greater than the 50 ft/sec originally assumed was possible. Consequently, based on about 13 hr of tracking, a sixth midcourse maneuver consuming about 4.3 lb of propellant was executed to (1) further increase the gas volume in the propellant tanks, (2) lower the burnout velocity to  $\approx 100$  ft/sec at an altitude of 5000 ft, and (3) correct the residual miss of 267 km from the desired landing site. These burnout conditions were selected so that nominal burnout would be essentially centered within the possible burnout region defined by the vernier propellant constraint as shown in Fig. VII-8. In addition to the spacecraft weight adjustment accomplished as a result of the sixth maneuver, it was necessary to offset the retro thrust direction about 0.78 deg in the trajectory plane in order to achieve the desired burnout velocity and a near-vertical flight path angle at burnout. The effectiveness of offsetting the retro thrust vector to achieve the desired burnout velocity vector  $\bar{V}_{B/O}$  is illustrated in Fig. VII-10.

To obtain data for the final terminal phase orbit determinations, it was decided to use DSS 51, rather than DSS 61, together with DSS 11. It was believed that DSS 51 would yield better data, since DSS 61 would have low elevation angles. The final terminal phase computations were based on the 5POM XD orbit solution.

Table VII-4. Injection and terminal conditions for pre-midcourse and post-midcourse (fifth and sixth) trajectories

Coordinate system		Pre-midcourse injection conditions, September 8, 1967, 08:15:12.951 GMT										
Inertial Cartesian	X =	198.48565 km	Y =	6023.4380 km	Z =	2570.0137 km	DX =	-10.272135 km/sec	DY =	2.0979910 km/sec	DZ =	-3.2158004 km/sec
	R =	6551.8066 km	DEC =	23.095215 deg	RA =	88.112656 deg	VI =	10.966298 km/sec	PTI =	1.8612436 deg	AZI =	109.44002 deg
	R =	6551.8066 km	LAT =	23.095215 deg	LON =	337.60005 deg	VE =	10.553118 km/sec	PTE =	1.9341422 deg	AZE =	110.23461 deg
	C3 =	-1.4170543 km <sup>2</sup> /sec <sup>2</sup>	ECC =	0.97673275	INC =	29.840519 deg	TA =	3.7668428 deg	LAN =	316.13298 deg	APF =	124.20397 deg
Coordinate system		Pre-midcourse encounter conditions, September 10, 1967, 23:25:14.270 GMT										
Selenocentric	RAD =	1734.8998 km	LAT =	2.3229388 deg	LON =	23.736510 deg	VP =	2.6300633 km/sec	PTP =	-44.037751 deg	AZP =	84.711876 deg
	BTQ =	2663.5596 km	BRQ =	-1154.7721 km	B =	2903.1101 km						
	BTT =	2894.8402 km	BRT =	-219.00438 km	B =	2903.1126 km						
Coordinate system		Post-5th-midcourse injection conditions, September 9, 1967, 08:25:03.000 GMT										
Inertial Cartesian	X =	-72608.494 km	Y =	-170992.65 km	Z =	-99552.307 km	DX =	-0.18341951 km/sec	DY =	-1.3522584 km/sec	DZ =	-0.64966585 km/sec
	RAD =	210763.24 km	DEC =	-28.186422 deg	RA =	246.99249 deg	VI =	1.5113938 km/sec	PTI =	76.101267 deg	AZI =	82.218253 deg
	RAD =	210763.23 km	LAT =	-28.186423 deg	LON =	133.02898 deg	VE =	13.268311 km/sec	PTE =	6.3484601 deg	AZE =	270.21357 deg
	C3 =	-1.4981440 km <sup>2</sup> /sec <sup>2</sup>	ECC =	0.97200486	INC =	39.155774 deg	TA =	163.15704 deg	LAN =	320.85623 deg	APF =	121.02272 deg
Coordinate system		Post-5th-midcourse encounter conditions, September 11, 1967, 00:38:06.643 GMT										
Selenographic	RAD =	1734.8998 km	LAT =	-4.1150096 deg	LON =	15.900787 deg	VP =	2.6129615 km/sec	PTP =	-49.512494 deg	AZP =	88.139118 deg
	BTQ =	2590.5690 km	BRQ =	-774.43431 km	B =	2703.8484 km						
	BTT =	2701.2727 km	BRT =	118.03529 km	B =	2703.8503 km						
Coordinate system		Post-final-midcourse injection conditions, September 9, 1967, 23:49:00.000 GMT										
Inertial Cartesian	X =	-79403.169 km	Y =	-236876.77 km	Z =	-130327.68 km	DX =	-0.076667985 km/sec	DY =	-1.0507343 km/sec	DZ =	-0.47503746 km/sec
	RAD =	281781.42 km	DEC =	-27.549411 deg	RA =	251.46839 deg	VI =	1.1556734 km/sec	PTI =	76.684457 deg	AZI =	78.980499 deg
	RAD =	281781.42 km	LAT =	-27.549411 deg	LON =	265.88495 deg	VE =	17.991948 km/sec	PTE =	3.5836653 deg	AZE =	270.16233 deg
	C3 =	-1.4935712 km <sup>2</sup> /sec <sup>2</sup>	ECC =	0.97320145	INC =	29.510514 deg	TA =	167.44169 deg	LAN =	318.63568 deg	APF =	122.68167 deg
Coordinate system		Post-final-midcourse injection conditions, September 11, 1967, 00:45:15.329 GMT										
Selenographic	RAD =	1734.8997 km	LAT =	1.5018152 deg	LON =	23.251192 deg	VP =	2.6108076 km/sec	PTP =	-44.154648 deg	AZP =	85.031426 deg
	BTQ =	2766.9735 km	BRQ =	-1150.6664 km	B =	2996.6941 km						
	BTT =	2991.3850 km	BRT =	-178.34952 km	B =	2996.6969 km						



Table VII-5. Surveyor V encounter conditions based on selected post-first-midcourse orbit determinations

Orbit identification	Time computation completed (from liftoff)	Target statistics							Unbraked impact conditions					Data used	
		B, km	B • TT, km	B • RT, km	TL, hr	SMAA (1 $\sigma$ ), km	SMIA (1 $\sigma$ ), km	THETA, deg	$\sigma_T$ IMPACT (1 $\sigma$ ), sec	PHIP 99, deg	SVFIX R (1 $\sigma$ ), m/sec	Lat, deg	Long, deg		GMT, Sept. 10
2 POM XD <sup>a</sup>		2738.3	2735.3	127.8	40.19	10.40	10.13	170.0	7.9421	0.6943	0.6244	-4.24	16.828	00:37:38.795	DSS 42, 51 and 61 two-way doppler
2 POM YF <sup>b</sup>		2703.8	2701.3	118.0	40.20	23.03	18.84	47.84	16.407	1.394	0.6293	-4.12	15.90	00:38:06.637	DSS 11, 42, 51 and 61 two-way doppler
3 POMXC	47:34	2997.5	2993.5	-172.8	24.88	332.7	33.09	101.3	96.742	9.010	0.933	1.409	23.28	Sept. 11 00:45:13.321	DSS 11, 42 two-way doppler
5 POM XD <sup>c</sup>	61:34	2997.7	2992.4	-177.5	24.88	7.773	2.20	79.49	3.0671	0.1800	0.6234	1.488	23.28	00:45:15.325	DSS 11, 42 and 51 two-way doppler
FINAL YF <sup>d</sup>	64:20	2996.3	2990.9	-179.0	56.34	1.527	0.2345	96.12	0.55949	0.0238	0.6231	1.513	23.24	00:45:15.162	DSS 11 and 51 two-way doppler
POST-2 <sup>e</sup>	post- landing	2996.7	2991.3	-178.3	24.88	9.385	1.743	96.19	0.99209	0.1515	0.6232	1.502	23.25	00:45:15.315	DSS 11, 42 and 51 two-way doppler

<sup>a</sup>Orbit used for final (sixth) midcourse computations.  
<sup>b</sup>Current best estimate of trajectory prior to final midcourse correction.  
<sup>c</sup>Orbit used for terminal computations.  
<sup>d</sup>Orbit used to obtain unbraked impact time on which to base final descent sequence.  
<sup>e</sup>Current best estimate of post- (final) midcourse trajectory.

<sup>a</sup>Orbit used for final (sixth) midcourse computations.<sup>b</sup>Current best estimate of trajectory prior to final midcourse correction.<sup>c</sup>Orbit used for terminal computations.<sup>d</sup>Orbit used to obtain unbraked impact time on which to base final descent sequence.<sup>e</sup>Current best estimate of post- (final) midcourse trajectory.

- $\bar{V}_{ign}$  = VELOCITY AT MAIN RETRO IGNITION  
 $\Delta \bar{V}_R$  = VELOCITY CHANGE DURING MAIN RETRO PHASE  
 $\bar{V}_{BO}$  = MAIN RETRO BURNOUT VELOCITY  
 $G_L$  = LUNAR GRAVITY CONSTANT  
 $\Delta T_R$  = DURATION OF MAIN RETRO PHASE  
 $\delta$  = MAIN RETRO THRUST VECTOR OFFSET ANGLE

COMPLETE VECTOR DIAGRAM  
(NOT TO SCALE)

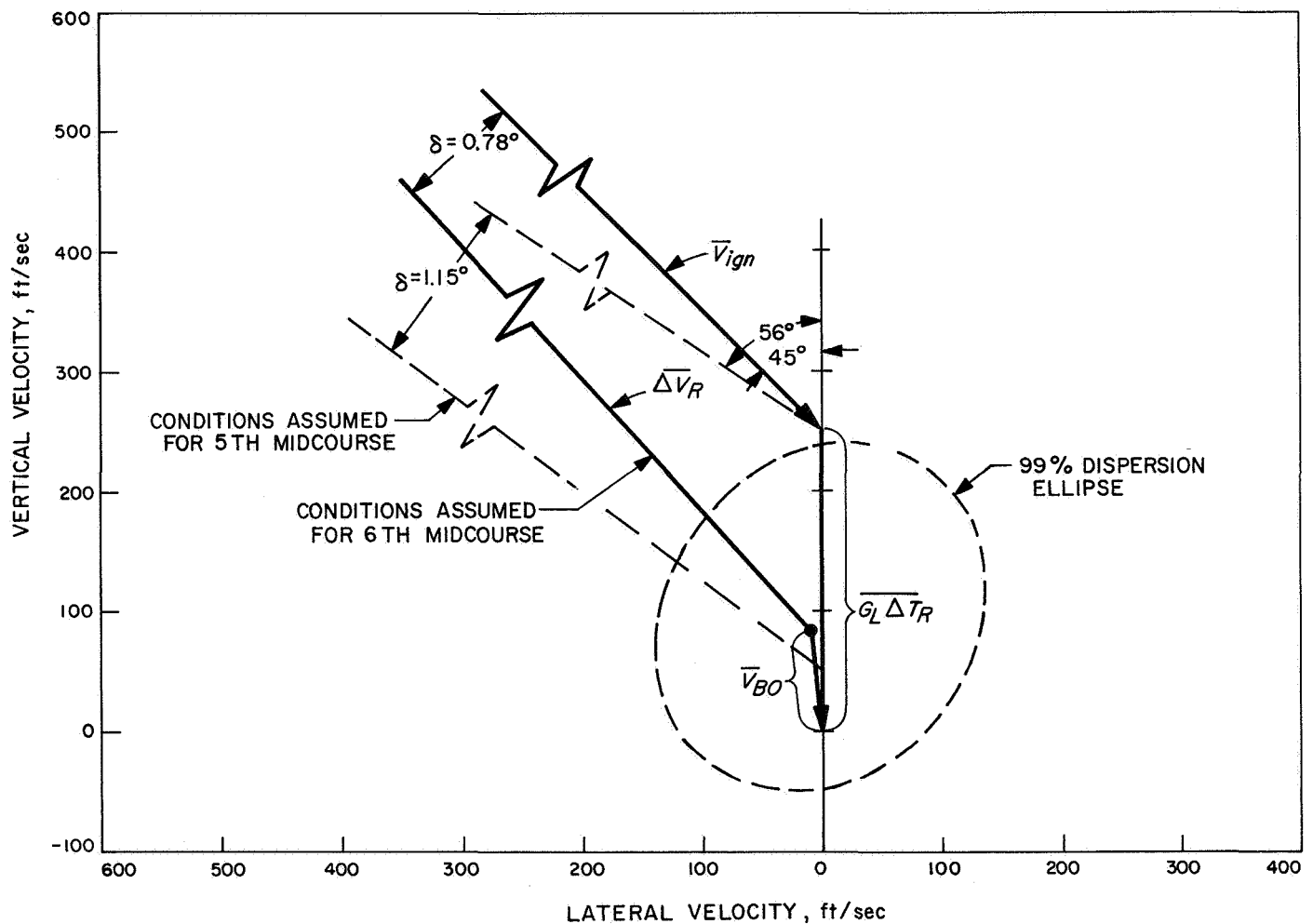
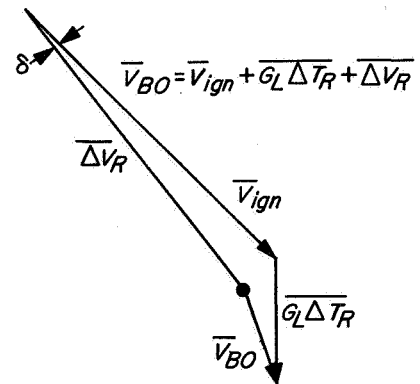


Fig. VII-10. Main retro phase velocity diagram

After this time, primary emphasis was placed on obtaining an estimate of unbraked impact time. Normally, the estimate of unbraked impact time is used primarily in calculating a backup signal for the spacecraft altitude marking radar (AMR). However, in order to accomplish the shorter retro eject sequence mentioned above, three key events were commanded from earth; namely, *retro eject*, *vernier high thrust*, and *enable RADVS steering*. The transmission times for these commands were based on the unbraked impact time estimate obtained from the final YE orbit computation. This solution was based on 2 hr, 15 min of two-way doppler data from DSS 11 and 2 hr, 24 min from DSS 51. Also, a priori information was used in the form of a covariance matrix based on data from the end of the sixth maneuver until 5 hr, 40 min before retro ignition.

A terminal attitude maneuver consisting of +73.83 deg roll and +119.60 deg yaw was initiated 33 min prior to retro ignition with 1.5 min allowed between rotations. The selection of the maneuver, using Omnantenna B, was based on an assessment of all possible maneuvers to provide satisfactory telecommunication performance during the terminal maneuver and terminal descent phases. Roll attitude of the spacecraft at retro ignition was constrained to be  $\approx 0$  deg\* by a problem with sidelobe

---

\*That is, the trajectory plane coplanar with the spacecraft X-Z-plane and the projection of the local vertical from the lunar surface being along the +X-axis.

crosscoupling of the RADVS. It was not necessary to negotiate a third rotation about the roll axis to satisfy this constraint since the yaw rotation resulted in a predicted roll attitude at ignition of  $\approx -5$  deg. The selected attitude rotations were compensated for a flight control sensor group deflection of 0.355 deg and for gyro drift rates which would have resulted in a 0.33-deg retro thrust vector offset. Also, it was attempted to initiate the attitude maneuvers at limit cycle nulls to further reduce pointing errors.

The terminal descent sequence is described in detail in Section IV-A. Table A-1 of Appendix A gives terminal phase event times. Initial touchdown occurred at 00:46:44.284 GMT on September 11, 1967, at a mission time of  $L + 64:49:43$ .

## F. Landing Site

The landing site of *Surveyor V* is at 1.50 deg north latitude and 23.19 deg east longitude (see Fig. VII-4), based upon final postflight orbit determination using data obtained in flight. This site is approximately 32 km from the final aim point. The  $3\sigma$ -miss ellipse about the computed touchdown location is defined by a semimajor axis of 6.9 km and a semiminor axis of 2.7 km, with the major axis in approximately a north-south orientation. Preliminary determination of the *Surveyor V* location using on-surface tracking data indicates that the landing site is at 1.41 deg north latitude and 23.18 deg east longitude.





**Appendix A**  
**Surveyor V Flight Events**

Table A-1. Mission flight events

Event	Mark No.	Mission time (predicted)	Mission time (actual)	GMT (actual)
Liftoff to DSIF acquisition <sup>a</sup>				
September 8, 1967 (Day 251)				
Liftoff (2-in. rise)		L + 00:00:00.00	L + 00:00:00.00	07:57:01.257
Initiate roll program		L + 00:00:02.00	L + 00:00:02.00	07:57:03.26
Terminate roll, initiate pitch program		L + 00:00:15.00	L + 00:00:15.00	07:57:16.26
Mach 1			L + 00:01:04.36	07:58:05.62
Maximum aerodynamic loading			L + 00:01:21.5	07:58:22.76
Atlas booster engine cutoff (BECO)	1	L + 00:02:33.49	L + 00:02:33.38	07:59:34.64
Jettison booster package	2	L + 00:02:36.59	L + 00:02:36.33	07:59:37.59
Admit guidance steering		L + 00:02:41.49	L + 00:02:41.25	07:59:42.51
Jettison Centaur insulation panels	3	L + 00:03:18.49	L + 00:03:17.97	08:00:19.23
Start Centaur boost pumps		L + 00:03:35.49	L + 00:03:34.81	08:00:36.07
Jettison nose fairing	4	L + 00:03:48.49	L + 00:03:47.75	08:00:49.01
Atlas sustainer engine cutoff (SECO)	5	L + 00:04:08.53	L + 00:04:06.40	08:01:07.66
Atlas/Centaur separation	6	L + 00:04:10.53	L + 00:04:08.33	08:01:09.59
Prestart Centaur main engines (chilldown)		L + 00:04:14.03	L + 00:04:09.9	08:01:11.2
Centaur main engines start (MES 1)	7	L + 00:04:20.03	L + 00:04:17.80	08:01:19.06
Centaur main engines cutoff (MECO 1)	8	L + 00:09:39.10	L + 00:09:47.06	08:06:48.32
100-lb thrust on	9	L + 00:09:39.10	L + 00:09:47.06	08:06:48.32
Vehicle destruct system safed by ground command			L + 00:10:01	08:07:02
100-lb thrust off	10	L + 00:10:55.10	L + 00:11:02.84	08:08:04.10
6-lb thrust on	11	L + 00:10:55.10	L + 00:11:02.9	08:08:04.2
100-lb thrust on	12	L + 00:15:46.68	L + 00:15:49.6	08:12:50.9
Start Centaur boost pumps		L + 00:15:58.68	L + 00:16:01.6	08:13:02.9
Prestart Centaur main engines (chilldown)		L + 00:16:09.68	L + 00:16:12.6	08:13:13.9
Centaur C1 main engine start (MES 2)	13	L + 00:16:26.68	L + 00:16:29.6	08:13:30.9
Centaur C2 main engine start (MES 2)	14	L + 00:16:26.68	L + 00:16:29.6	08:13:30.9
Centaur main engines cutoff (MECO 2)	15	L + 00:18:19.49	L + 00:18:23.8	08:15:25.1
Extend Surveyor landing legs command	16	L + 00:18:40.68	L + 00:18:43.8	08:15:45.1
Extend Surveyor omniantennas command	17	L + 00:18:51.68	L + 00:18:54.0	08:15:55.3
Surveyor transmitter high power on command	18	L + 00:19:11.68	L + 00:19:14.1	08:16:15.4
Surveyor/Centaur electrical disconnect	19	L + 00:19:17.68	L + 00:19:20.5	08:16:21.8
Surveyor/Centaur separation	20	L + 00:19:22.68	L + 00:19:25.6	08:16:26.9
Surveyor solar panel unlocked to begin stepping			L + 00:19:27	08:16:28
Start Centaur 180-deg turn	21	L + 00:19:27.68	L + 00:19:31.6	08:16:32.9
Start Surveyor sun acquisition roll			L + 00:20:10	08:17:11
Start Centaur lateral thrust	22	L + 00:20:07.68	L + 00:20:10.6	08:17:11.9
Cut off Centaur lateral thrust	23	L + 00:20:27.68	L + 00:20:30.6	08:17:31.9
Start Centaur tank blowdown (retro)	24	L + 00:23:22.68	L + 00:23:25.6	08:20:26.9
Solar panel locked for transit, start A/SPP roll axis stepping			L + 00:25:28	08:22:29
Cut off Centaur blowdown, 100-lb thrust on	25	L + 00:27:32.68	L + 00:27:35.6	08:24:36.9
A/SPP roll axis locked for transit			L + 00:28:35	08:25:36
Cut off Centaur electrical power, 100-lb thrust off	26	L + 00:29:12.68	L + 00:29:15.6	08:26:16.9
Complete Surveyor roll, begin sun acquisition yaw turn			L + 00:31:35	08:28:36
Surveyor primary sun sensor lock-on			L + 00:32:11	08:29:12
Initial acquisition and good two-way lock completed by DSS 51			L + 00:33:10	08:30:11

<sup>a</sup>The predicted values were computed postflight utilizing actual launch azimuth, tanked propellant weights, and atmospheric data which depend on day and time of liftoff.

Table A-1 (contd)

Event	Mission time (actual)	GMT (actual)
<b>Initial spacecraft operations to Canopus acquisition</b>		
Initial spacecraft operations		
1. Command Transmitter B from high to low power	L + 00:40:06	08:37:07
2. Command off A/D isolation amplifier, solar panel deployment logic, and Transmitter A high power	L + 00:45:20	08:42:21
3. Command step solar panel minus, then plus, to seat locking pin	L + 00:46:27	08:43:28
4. Command step roll axis plus, then minus, to seat locking pin	L + 00:47:24	08:44:25
5. Command on telemetry Mode 1 for interrogation at 550-bit/sec data rate	L + 00:48:39	08:45:40
6. Command on telemetry Modes 4, 2, 6, and 5 for interrogation at 1100-bit/sec data rate	L + 00:51:18 to L + 01:02:59	08:48:19 to 09:00:00
Command select Omniantenna A	L + 04:22:01	12:19:02
Command on telemetry Modes 4, 2, and 1 for interrogation at 1100-bit/sec data rate	L + 05:50:53 to L + 05:57:11	13:47:54 to 13:54:12
Star verification/acquisition		
1. Command on solar panel switch	L + 06:05:28	14:02:29
2. Command Transmitter B from low to high power	L + 06:06:27	14:03:28
3. Command select Omniantenna B	L + 06:07:30	14:04:31
4. Command on 4400-bit/sec data rate	L + 06:08:40	14:05:41
5. Command on cruise mode and manual delay mode, then command roll direction (positive)	L + 06:11:51	14:08:52
6. Command execution of positive roll (light sources successively detected by Canopus sensor: Zeta Ophiuchi; Antares and Tau Scorpii; Canopus; Alnitak, Alnilam, and Mintaka; Bellatrix; Elnath; earth; Capella; and Polaris)	L + 06:13:01	14:10:02
7. Command on star acquisition mode (after Tau Scorpii passed field of view during second revolution)	L + 06:28:35	14:25:36
8. Automatic Canopus acquisition	L + 06:30:51	14:27:52
9. Command on cruise mode	L + 06:33:09	14:30:10
10. Command on telemetry Mode 5 for interrogation at 4400-bit/sec data rate	L + 06:34:02	14:31:03
11. Command on 1100-bit/sec data rate	L + 06:35:39	14:32:40
12. Command Transmitter B from high to low power	L + 06:36:48	14:33:49
Command on solar panel switch	L + 07:11:25	15:08:26
<b>Pre-midcourse coast phase</b>		
Command on inertial mode (start first gyro drift check, all axes)	L + 07:48:51	15:45:52
Command on solar panel switch	L + 07:58:28, L + 08:45:14, and L + 09:19:16	15:55:29, 16:42:15, and 17:16:17
Command on telemetry Modes 4 and 5 for interrogation at 1100-bit/sec data rate	L + 09:25:15 and L + 09:29:49	17:22:16 and 17:26:50
Command on solar panel switch	L + 09:47:04	17:44:05
Command on cruise mode (end first gyro drift check)	L + 10:19:27	18:16:28
Command on solar panel switch	L + 10:36:28	18:33:29
Command on inertial mode (start second gyro drift check, all axes)	L + 10:37:27	18:34:28
Command on solar panel switch	L + 10:56:43, L + 11:37:24, and L + 12:10:37	18:53:44, 19:34:25, and 20:07:38
Command on cruise mode (end second gyro drift check)	L + 12:19:01	20:16:02
Command on 137.5-bit/sec data rate, then 17.2-bit/sec data rate	L + 12:21:35 and L + 12:46:25	20:18:36 and 20:43:26

Table A-1 (contd)

Event	Mission time (actual)	GMT (actual)
<b>Pre-midcourse coast phase (contd)</b>		
Command on solar panel switch	L + 13:41:54	21:38:55
Command on 1100-bit/sec data rate	L + 13:44:05	21:41:06
Command on sun acquisition mode (start third gyro drift check, roll axis only)	L + 13:46:57	21:43:58
Command on telemetry Modes 4, 2, 1, and 5 for interrogation at 1100-bit/sec data rate	L + 13:50:55 to L + 14:04:05	21:47:56 to 22:01:06
Command on cruise mode (end third gyro drift check)	L + 15:43:32	23:40:33
Pre-midcourse interrogation and gyro speed check		
1. Command on telemetry Modes 4, 2, 1, and 5 for interrogation at 1100-bit/sec data rate	L + 15:44:44 to L + 15:56:54	23:41:45 to 23:53:55
2. Command on gyro speed signal processor and check angular rate of gyro spin in roll, pitch, and yaw axes; command off gyro speed signal processor and return to telemetry Mode 5	L + 15:58:13 to L + 16:01:56	23:55:14 to 23:58:57
<b>Midcourse phase</b>		
	<b>September 9, 1967 (Day 252)</b>	
Command on telemetry Modes 4, 2, and 1 for interrogation at 1100-bit/sec data rate	L + 17:02:44 to L + 17:08:55	00:59:45 to 01:05:56
Command Transmitter B from low to high power	L + 17:18:19	01:15:20
Command on 4400-bit/sec data rate	L + 17:18:56	01:15:57
Pre-midcourse attitude maneuvers		
1. Command on cruise mode, then command roll maneuver direction (positive) and store roll magnitude of 143.8 sec (+71.9 deg)	L + 17:28:10	01:25:11
2. Command roll execution	L + 17:35:56	01:32:57
3. Command on sun acquisition mode, then store yaw magnitude of 71.4 sec (-35.7 deg)	L + 17:39:25	01:36:26
4. Command yaw execution	L + 17:41:05	01:38:06
Command on telemetry Modes 2 and 1 for interrogation at 4400-bit/sec data rate	L + 17:42:44 and L + 17:43:45	01:39:45 and 01:40:46
Command on propulsion strain gage power and inertial mode	L + 17:44:45	01:41:46
Command off thermal control power to the AMR and to vernier lines, Vernier Fuel Tank 2, and Vernier Oxidizer Tanks 2 and 3; then unlock Vernier Engine 1 roll actuator and pressurize the vernier system (helium)	L + 17:45:23	01:42:24
Midcourse correction		
1. Command on flight control thrust phase power	L + 17:46:16	01:43:17
2. Store magnitude of vernier engines burn time (14.25 sec, a velocity correction of 14 m/sec)	L + 17:46:30	01:43:31
3. Command execution of midcourse velocity correction	L + 17:48:01	01:45:02
4. Command standard emergency terminate midcourse velocity correction	L + 17:48:18	01:45:19
5. Command off flight control thrust phase power, propulsion strain gage power, and touchdown strain gage power	L + 17:48:33	01:45:34
Command on telemetry Mode 5	L + 17:49:33	01:46:34
Command on vernier lines and AMR temperature control	L + 17:51:05	01:48:06
Command on telemetry Mode 1 and observe all system pressures	L + 17:52:54	01:49:55
Attitude maneuver		
1. Command yaw maneuver direction (positive) and store yaw magnitude of 71.4 sec (+35.7 deg)	L + 17:55:50	01:52:51
2. Command yaw execution, returning spacecraft to sun lock-on	L + 17:56:50	01:53:51
Second midcourse correction		
1. Command on propulsion strain gage power, inertial mode, and thrust phase power	L + 18:07:39	02:04:40
2. Store magnitude of vernier engines burn time (10.05 sec)	L + 18:10:39	02:07:40

**Table A-1 (contd)**

Event	Mission time (actual)	GMT (actual)
<b>Midcourse phase (contd)</b>		
3. Command execution of second midcourse velocity correction (along the sun line)	L + 18:15:01	02:12:02
4. Command standard emergency terminate midcourse velocity correction	L + 18:15:13	02:12:14
5. Command off thrust phase power, propulsion strain gage power, and touchdown strain gage power	L + 18:15:38	02:12:39
Attitude maneuver		
1. Command on sun acquisition mode	L + 18:18:48	02:15:49
2. Command on telemetry Mode 5	L + 18:20:48	02:17:49
3. Store yaw magnitude of 360.2 sec (— 180.1 deg)	L + 18:22:19	02:19:20
4. Command on telemetry Mode 1	L + 18:23:22	02:20:23
5. Command yaw execution	L + 18:27:32	02:24:33
Third midcourse correction		
1. Command on propulsion strain gage power, inertial mode, and thrust phase power	L + 18:36:28	02:33:29
2. Store magnitude of vernier engines burn time (23.05 sec)	L + 18:41:39	02:38:40
3. Command execution of third midcourse velocity correction (along the anti-sun line)	L + 18:42:49	02:39:50
4. Command standard emergency terminate midcourse velocity correction	L + 18:43:15	02:40:16
5. Command off thrust phase power, propulsion strain gage power, and touchdown strain gage power	L + 18:43:34	02:40:35
Post-midcourse attitude maneuver		
1. Store yaw magnitude of 360.2 sec (— 180.1 deg)	L + 18:47:35	02:44:36
2. Command yaw execution, returning spacecraft to sun lock-on	L + 18:48:21	02:45:22
Command on sun acquisition mode	L + 18:56:23	02:53:24
Command on 1100-bit/sec data rate	L + 18:58:11	02:55:12
Command Transmitter B from high to low power	L + 18:58:50	02:55:51
Command on telemetry mode 5 for interrogation at 1100-bit/sec data rate	L + 18:59:53	02:56:54
Post-midcourse attitude maneuver		
1. Store roll magnitude of 143.8 sec (— 71.9 deg)	L + 20:02:59	04:00:00
2. Command roll execution, returning spacecraft to Canopus lock-on	L + 20:03:46	04:00:47
Pre-midcourse attitude maneuvers		
1. Command on cruise mode, then command roll maneuver direction (positive) and store roll magnitude of 137.0 sec (+ 68.5 deg)	L + 20:07:18	04:04:19
2. Command roll execution	L + 20:08:54	04:05:55
3. Store yaw magnitude of 213.6 sec (+ 106.8 deg)	L + 20:11:45	04:08:46
4. Command yaw execution	L + 20:12:32	04:09:33
Command on telemetry Mode 1	L + 20:16:43	04:13:44
Fourth midcourse correction		
1. Command on propulsion strain gage power, inertial mode, manual maneuver delay, and thrust phase power	L + 20:17:19	04:14:20
2. Command execution of fourth midcourse velocity correction (in direction placing the spacecraft back on aim-point intercept course), using the following manually controlled tape sequence:		
Engines on (12.0 sec)	L + 20:21:47.1	04:18:48.4
Engines off (1 sec)	L + 20:21:59.2	04:19:00.5
Engines on (0.5 sec)	L + 20:22:00.2	04:19:01.5
Engines off (1 sec)	L + 20:22:00.7	04:19:02.0
Engines on (0.5 sec)	L + 20:22:01.7	04:19:03.0
Engines off	L + 20:22:02.2	04:19:03.5
3. Command off thrust phase power, propulsion strain gage power, and touchdown strain gage power	L + 20:22:29	04:19:30
Post-midcourse attitude maneuvers		
1. Command on inertial mode, then store yaw magnitude of 213.6 sec (— 106.8 deg)	L + 20:59:37	04:56:38
2. Command yaw execution, returning spacecraft to sun lock-on	L + 21:01:12	04:58:13

Table A-1 (contd)

Event	Mission time (actual)	GMT (actual)
<b>Midcourse phase (contd)</b>		
3. Command on sun acquisition mode, then store roll magnitude of 137.0 sec ( $-68.5$ deg)	L + 21:06:00	05:03:01
4. Command roll execution, returning spacecraft to Canopus lock-on	L + 21:07:10	05:04:11
Command on cruise mode	L + 21:10:50	05:07:51
Command on telemetry Modes 2, 4, and 5 for interrogation at 1100-bit/sec data rate	L + 21:29:43 to L + 21:47:01	05:26:44 to 05:44:02
Command on Compartment C heater and survey camera electronics temperature control and command off AMR temperature control	L + 21:49:47	05:46:48
Command on telemetry Modes 4, 1, 4, and 5 for interrogation at 1100-bit/sec data rate	L + 22:08:52 to L + 22:41:23	06:05:53 to 06:38:24
Command off Compartment C heater and survey camera electronics temperature control, and command on AMR temperature control	L + 22:41:56	06:38:57
Command Transmitter B from low to high power	L + 23:52:34	07:49:35
Command on 4400-bit/sec data rate	L + 23:54:24	07:51:25
Command on telemetry Mode 1	L + 23:55:10	07:52:11
Pre-midcourse attitude maneuvers		
1. Command on cruise mode, then command roll maneuver direction (positive) and store roll magnitude of 129.0 sec ( $+64.5$ deg)	L + 23:56:09	07:53:10
2. Command roll execution	L + 23:57:29	07:54:30
3. Store yaw magnitude of 286.6 sec ( $+143.3$ deg)	L + 24:00:54	07:57:55
4. Command yaw execution	L + 24:01:30	07:58:31
Command on propulsion strain gage power and inertial mode	L + 24:21:37	08:18:38
Command off thermal control power to the AMR and to vernier lines, Vernier Fuel Tank 2, and Vernier Oxidizer Tanks 2 and 3; then unlock Vernier Engine 1 roll actuator and pressurize the vernier system	L + 24:22:44	08:19:45
Fifth midcourse correction		
1. Command on thrust phase power	L + 24:24:10	08:21:11
2. Store magnitude of vernier engines burn time (33.05 sec)	L + 24:25:34	08:22:35
3. Command execution of fifth midcourse velocity correction (in positive, noncritical direction)	L + 24:27:01	08:24:02
4. Command standard emergency terminate midcourse velocity correction	L + 24:27:37	08:24:38
5. Command off thrust phase power, propulsion strain gage power, and touchdown strain gage power	L + 24:28:00	08:25:01
Command on telemetry Mode 5	L + 24:29:09	08:26:10
Command on vernier lines and AMR temperature control	L + 24:31:42	08:28:43
Command on telemetry Mode 1	L + 24:33:04	08:30:05
Post-midcourse attitude maneuvers		
1. Command on inertial mode, then store yaw magnitude of 286.6 sec ( $-143.3$ deg)	L + 24:35:15	08:32:16
2. Command yaw execution, returning spacecraft to sun lock-on	L + 24:36:50	08:33:51
3. Command on sun acquisition mode, then store roll magnitude of 129.0 sec ( $-64.5$ deg)	L + 24:42:26	08:39:27
4. Command roll execution, returning spacecraft to Canopus lock-on	L + 24:43:34	08:40:35
Command on cruise mode	L + 24:47:26	08:44:27
Command on 1100-bit/sec data rate	L + 24:48:42	08:45:43
Command Transmitter B from high to low power	L + 24:50:02	08:47:03

Table A-1 (contd)

Event	Mission time (actual)	GMT (actual)
<b>Post-midcourse coast phase</b>		
Command on Compartment C heater (in preparation for alpha scattering instrument operations)	L + 24:52:12	08:49:13
Command on inertial mode (start fourth gyro drift check, all axes)	L + 25:11:31	09:08:32
Command on telemetry Mode 4	L + 25:24:02	09:21:03
Command on 550-bit/sec data rate	L + 25:25:30	09:22:31
Command on telemetry Mode 1 for interrogation at 550-bit/sec data rate	L + 25:58:11	09:55:12
Command on cruise mode (end fourth gyro drift check)	L + 25:59:50	09:56:51
Command on telemetry Modes 2, 5, and 4 for interrogation	L + 26:05:02 to L + 26:14:16	10:02:03 to 10:11:17
Alpha scattering instrument transit operations		
1. Command Transmitter B from low to high power	L + 26:36:26	10:33:27
2. Command on low-modulation-index subcarrier oscillator and phase-modulated presumming amplifier	L + 26:37:53	10:34:54
3. Command on alpha scattering instrument power and accumulate 10 min of standard sample data	L + 26:39:47	10:36:48
4. Command off Alpha Detectors 1 and 2 and Proton Detectors 1, 2, 3, and 4 (one 2-min pulser calibration run with calibration off)	L + 26:54:18	10:51:19
5. Command on calibration (one 2-min pulser calibration run)	L + 26:58:17	10:55:18
6. Command alpha ( $\alpha$ ) and proton (p) detectors on and off as follows (five 2-min pulser calibration runs):	L + 27:02:18 to L + 27:15:30	10:59:19 to 11:12:31
$\alpha$ Detector 1 on		
$\alpha$ Detectors 1 and 2 off; p Detector 1 on		
$\alpha$ Detector 2 on; p Detectors 1 and 2 off, p Detector 2 on		
$\alpha$ Detector 1 on; p Detectors 1 and 2 off, p Detector 3 on		
p Detectors 3 and 4 off, p Detector 4 on		
7. Command off calibration, then command on Proton Detectors 1, 2, and 3 and accumulate 10 min of standard sample data	L + 27:18:31	11:15:32
8. Command off alpha scattering instrument power	L + 27:30:42	11:27:43
9. Command off low-modulation-index subcarrier oscillator	L + 27:32:22	11:29:23
10. Command Transmitter B from high to low power	L + 27:33:33	11:30:34
11. Command off Compartment C heater	L + 27:34:49	11:31:50
Command on telemetry Mode 1 for interrogation	L + 27:35:50	11:32:51
Command on inertial mode (start fifth gyro drift check, all axes)	L + 27:42:30	11:39:31
Command on telemetry Modes 5 and 1 for interrogation	L + 27:47:24 and L + 27:50:16	11:44:25 and 11:47:17
Command on telemetry Modes 5 and 1 for interrogation	L + 28:57:53 and L + 29:02:53	12:54:54 and 12:59:54
Command on cruise mode (end fifth gyro drift check)	L + 29:18:28	13:15:29
Command on sun acquisition mode (start sixth gyro drift check, roll axis only)	L + 29:20:56	13:17:57
Command on telemetry Modes 4, 5, 2, and 1 for interrogation	L + 29:56:27 to L + 30:07:17	13:53:28 to 14:04:18
Command on telemetry Mode 5 for interrogation	L + 31:05:33	15:02:34
Command on cruise mode (end sixth gyro drift check)	L + 31:11:08	15:08:09
Command on inertial mode (start seventh gyro drift check, all axes)	L + 31:13:40	15:10:41



Table A-1 (contd)

Event	Mission time (actual)	GMT (actual)
<b>Post-midcourse coast phase (contd)</b>		
Command on telemetry Mode 1 for interrogation	L + 31:14:36	15:11:37
Command on telemetry Modes 4, 5, and 1 for interrogation	L + 32:07:26	16:04:27
	to	to
	L + 32:27:31	16:24:32
Command on telemetry Modes 5 and 1 for interrogation	L + 33:15:25	17:12:26
	to	to
	L + 33:18:28	17:15:29
Command on cruise mode (end seventh gyro drift check)	L + 33:21:07	17:18:08
Command on inertial mode (start eighth gyro drift check, all axes)	L + 34:02:58	17:59:59
Command on telemetry Modes 5, 4, and 1 for interrogation	L + 34:03:35	18:00:36
	to	to
	L + 34:19:02	18:16:03
Command on telemetry Modes 2, 5, and 1 for interrogation	L + 35:12:55	19:09:56
	to	to
	L + 35:19:21	19:16:22
Command on telemetry Modes 4, 5, and 1 for interrogation	L + 36:03:58	20:00:59
	to	to
	L + 36:12:53	20:09:54
Command on cruise mode (end eighth gyro drift check)	L + 36:13:22	20:10:23
Command on inertial mode (start ninth gyro drift check, all axes)	L + 37:02:04	20:59:05
Command on telemetry Mode 5 for interrogation	L + 37:02:49	20:59:50
Command on cruise mode (end ninth gyro drift check)	L + 37:51:51	21:48:52
Command on telemetry Modes 4, 2, and 1 for interrogation at 550-bit/sec data rate	L + 38:37:16	22:34:17
	to	to
	L + 38:41:03	22:38:04
Command Transmitter B from low to high power	L + 39:09:29	23:06:30
Command on 4400 bit/sec data rate	L + 39:10:16	23:07:17
Pre-midcourse attitude maneuvers		
1. Command on cruise mode, then store roll magnitude of 151.8 sec (—75.9 deg)	L + 39:15:17	23:12:18
2. Command roll execution	L + 39:16:50	23:13:51
3. Store yaw magnitude of 201.0 sec (—100.5 deg)	L + 39:21:18	23:18:19
4. Command yaw execution	L + 39:22:35	23:19:36
Command on telemetry Modes 2 and 1 for interrogation at 4400-bit/sec data rate	L + 39:26:49	23:23:50
	and	and
	L + 39:27:48	23:24:49
Command on propulsion strain gage power and inertial mode	L + 39:28:11	23:25:12
Command off thermal control power to the survey camera vidicon, to the AMR, and to vernier lines, Vernier Fuel Tank 2, and Vernier Oxidizer Tanks 2 and 3; then unlock Vernier Engine 1 roll actuator and pressurize the vernier system	L + 39:28:43	23:25:44
Sixth midcourse correction		
1. Command on thrust phase power	L + 39:29:06	23:26:07
2. Store magnitude of vernier engines burn time (5.45 sec)	L + 39:32:22	23:29:23
3. Command execution of sixth midcourse velocity correction	L + 39:33:59	23:31:00
4. Command standard emergency terminate midcourse velocity correction	L + 39:34:05	23:31:06
5. Command off propulsion strain gage power and thrust phase power	L + 39:34:22	23:31:23
Command on telemetry Mode 5	L + 39:35:23	23:32:24

Table A-1 (contd)

Event	Mission time (actual)	GMT (actual)
<b>Post-midcourse coast phase (contd)</b>		
Command on vernier lines and AMR temperature control	L + 39:36:18	23:33:19
Post-midcourse attitude maneuvers		
1. Command yaw maneuver direction (positive), then store yaw magnitude of 201.0 sec (+100.5 deg)	L + 39:38:00	23:35:01
2. Command yaw execution, returning spacecraft to sun lock-on	L + 39:39:06	23:36:07
3. Command off touchdown strain gage power	L + 39:44:01	23:41:02
4. Command on sun acquisition mode, then command roll maneuver direction (positive) and store roll magnitude of 151.8 sec (+75.9 deg)	L + 39:45:11	23:42:12
5. Command roll execution, returning spacecraft to Canopus lock-on	L + 39:47:04	23:44:05
Command on cruise mode	L + 39:52:06	23:49:07
Command on telemetry Mode 2	L + 39:52:52	23:49:53
Command on 550-bit/sec data rate	L + 39:53:48	23:50:49
Command Transmitter B from high to low power	L + 39:54:41	23:51:42
Command on telemetry Modes 4 and 5 for interrogation at 550-bit/sec data rate	L + 39:57:05 and L + 39:59:53	23:54:06 and 23:56:54
<b>September 10, 1967 (Day 253)</b>		
Command on telemetry Mode 1 for interrogation	L + 40:10:54	00:07:55
Command on telemetry Modes 5, 4, 2, and 1 for interrogation	L + 41:19:06 to L + 41:37:16	01:16:07 to 01:34:17
Command on inertial mode (start tenth gyro drift check, all axes)	L + 41:38:18	01:35:19
Command on telemetry Modes 5, 4, and 1 for interrogation	L + 42:01:32 to L + 42:09:51	01:58:33 to 02:06:52
Command on telemetry Modes 5, 4, 2, and 1 for interrogation	L + 42:49:33 to L + 43:33:14	02:46:34 to 03:30:15
Command on cruise mode (end tenth gyro drift check)	L + 44:36:02	04:33:03
Command on telemetry Modes 5, 4, 2, and 1 for interrogation	L + 44:37:19 to L + 45:01:35	04:34:20 to 04:58:36
Command on telemetry Modes 5 and 4 for interrogation	L + 46:08:45 and L + 46:16:21	06:05:46 and 06:13:22
Command on Vernier Oxidizer Tank 2 temperature control	L + 46:23:07	06:20:08
Command on telemetry Modes 2 and 1 for interrogation	L + 46:23:57 and L + 46:27:36	06:20:58 and 06:24:37
Command on telemetry Modes 5, 4, 2, and 1 for interrogation	L + 47:11:23 to L + 47:23:29	07:08:24 to 07:20:30
Command on telemetry Modes 5, 4, 2, and 1 for interrogation	L + 48:19:17 to L + 48:33:16	08:16:18 to 08:30:17
Command on telemetry Modes 5 and 4 for interrogation	L + 49:20:43 and L + 49:26:11	09:17:44 and 09:23:12
Command on 137.5-bit/sec data rate	L + 49:28:11	09:25:12
Command on 550-bit/sec data rate	L + 49:30:55	09:27:56

Table A-1 (contd)

Event	Mission time (actual)	GMT (actual)
Post-midcourse coast phase (contd)		
Command on telemetry Modes 2 and 1 for interrogation	L + 49:33:28 and L + 49:35:45	09:30:29 and 09:32:46
Command on telemetry Modes 5, 4, 2, and 1 for interrogation	L + 50:19:50 to L + 50:35:16	10:16:51 to 10:32:17
Command on telemetry Modes 5, 4, 2, and 1 for interrogation	L + 51:41:21 to L + 51:47:24	11:38:22 to 11:44:25
Command on telemetry Modes 5, 4, 2, and 1 for interrogation	L + 52:55:35 to L + 53:07:22	12:52:36 to 13:04:23
Command on sun acquisition mode (start eleventh gyro drift check, roll axis only)	L + 53:08:02	13:05:03
Command on Compartment A heater	L + 53:34:01	13:31:02
Command on telemetry Modes 5, 4, 2, and 1 for interrogation	L + 54:08:51 to L + 54:21:52	14:05:52 to 14:18:53
Command on telemetry Modes 5, 4, 2, and 1 for interrogation	L + 55:13:00 to L + 55:25:33	15:10:01 to 15:22:34
Command on cruise mode (end eleventh gyro drift check)	L + 55:27:12	15:24:13
Command on inertial mode (start twelfth gyro drift check, all axes)	L + 55:30:07	15:27:08
Command on telemetry Modes 5, 4, 2, and 1 for interrogation	L + 56:20:32 to L + 56:33:13	16:17:33 to 16:30:14
Command on telemetry Modes 5, 4, 2, and 1 for interrogation	L + 57:28:04 to L + 57:40:32	17:25:05 to 17:37:33
Command on Compartment C heater	L + 57:46:56	17:43:57
Command on cruise mode (end twelfth gyro drift check)	L + 58:02:41	17:59:42
Attitude maneuvers		
1. Command yaw maneuver direction (positive), then store yaw magnitude of 359.8 sec (+179.9 deg)	L + 58:13:36	18:10:37
2. Command yaw execution	L + 58:15:15	18:12:16
3. Store yaw magnitude of 360.2 sec (+180.1 deg)	L + 58:25:09	18:22:10
4. Command yaw execution, returning spacecraft to sun and Canopus lock-on	L + 58:25:51	18:22:52
Command on cruise mode	L + 58:33:13	18:30:14
Command on telemetry Modes 5, 4, 2, and 1 for interrogation	L + 58:35:08 to L + 59:04:00	18:32:09 to 19:01:01
Command on telemetry Modes 5 and 4 for interrogation	L + 59:34:36 and L + 59:38:10	19:31:37 and 19:35:11
Command on survey camera electronics temperature control	L + 59:40:24	19:37:25
Command on telemetry Modes 2 and 1 for interrogation	L + 59:44:50 and L + 59:52:00	19:41:51 and 19:49:01
Command on telemetry Mode 4 for interrogation	L + 60:15:33	20:12:34
Command on alpha scattering instrument sensor head heater power	L + 60:32:51	20:29:52
Command on telemetry Mode 1 for interrogation	L + 60:42:57	20:39:58
Command on telemetry Mode 5 for interrogation	L + 61:18:58	21:15:59

**Table A-1 (contd)**

Event	Mission time (actual)	GMT (actual)
<b>Post-midcourse coast phase (contd)</b>		
Command on telemetry Modes 4, 2, 1, and 5 for interrogation	L + 61:54:13 to L + 62:04:38	21:51:14 to 22:01:39
Preterminal interrogation, gyro speed check, and VCXO check		
1. Command on telemetry Modes 4, 2, 1, and 5 for interrogation at 550-bit/sec data rate	L + 62:35:55 to L + 62:41:39	22:32:56 to 22:38:40
2. Command on gyro speed signal processor and check angular rate of speed in roll, pitch, and yaw axes; command off gyro speed signal processor and return to telemetry Mode 5	L + 62:48:29 to L + 62:53:54	22:45:30 to 22:50:55
3. Command off transponder power to perform VCXO check, then command Transponder B power back on	L + 62:56:46 to L + 62:58:32	22:53:47 to 22:55:33
<b>Terminal phase</b>		
Command off Compartment A heater power	L + 63:43:33	23:40:34
Command on survey camera vidicon temperature control	L + 63:44:26	23:41:27
Command on telemetry Modes 6 and 4 for interrogation at 550-bit/sec data rate	L + 63:45:21 and L + 63:47:39	23:42:22 and 23:44:40
Command Transmitter B from low to high power	L + 63:54:40	23:51:41
Command on 1100-bit/sec data rate	L + 63:55:18	23:52:19
Command off summing amplifiers and command on phase summing amplifier B	L + 63:57:39	23:54:40
Command on telemetry Modes 2, 1, and 5 for interrogation at 1100-bit/sec data rate	L + 63:58:53 to L + 64:02:12	23:55:54 to 23:59:13
<b>September 11, 1967 (Day 254)</b>		
Command on propulsion strain gage power, touchdown strain gage power, and touchdown strain gage data channels	L + 64:03:30 to L + 64:06:07	00:00:31 to 00:03:08
Command off transponder power (one-way doppler)	L + 64:07:20	00:04:21
Terminal maneuvers		
1. Command on cruise mode, then command roll maneuver direction (positive) and store roll magnitude of 147.8 sec (+73.9 deg)	L + 64:11:57	00:08:58
2. Command roll execution	L + 64:15:14	00:12:15
3. Store yaw magnitude of 239.0 sec (+119.5 deg)	L + 64:18:24	00:15:25
4. Command yaw execution, aligning retro engine thrust axis in proper direction	L + 64:19:20	00:16:21
Command on phase-modulated presumming amplifier	L + 64:24:37	00:21:38
Command select nominal thrust bias (150-lb vernier thrust)	L + 64:26:18	00:23:19
Store retro sequence delay magnitude (12.325 sec between AMR mark and vernier engine ignition)	L + 64:27:48	00:24:49
Command on telemetry Mode 6 (thrust phase commutator)	L + 64:33:07	00:30:08
Command on retro sequence mode	L + 64:41:56	00:38:57
Command off thermal control power to vernier lines, Vernier Fuel Tank 2, and Vernier Oxidizer Tanks 2 and 3; command off temperature control to survey camera vidicon, survey camera electronics, and AMR; and command off Compartment C heater and alpha scattering instrument heater power	L + 64:42:11	00:39:12

Table A-1 (contd)

Event		Mission time (actual)	GMT (actual)
Terminal phase (contd)			
Command on AMR power		L + 64:42:59	00:40:00
Command on thrust phase power		L + 64:43:59	00:41:00
Command AMR enable		L + 64:46:00	00:43:01
	GMT (predicted)	Mission time (actual)	GMT (actual)
Terminal descent <sup>b</sup>			
1. AMR mark at 60-mi altitude and start of delay quantity countdown	00:44:37.73	L + 64:47:36.60	00:44:37.85
2. Emergency AMR mark command received at spacecraft		L + 64:47:43.92	00:44:45.17
3. Vernier engines ignition	00:44:50.05	L + 64:47:48.94	00:44:50.19
4. Main retro motor ignition	00:44:51.15	L + 64:47:50.01	00:44:51.26
5. AMR ejection		L + 64:47:50.07	00:44:51.32
6. RADVS power on for warmup		L + 64:47:50.60	00:44:51.85
7. RADVS high voltage on		L + 64:48:12.70	00:45:13.95
8. Reliable operation—doppler velocity sensor (RODVS) signal, following acquisition of lunar surface by doppler velocity sensor (DVS) beam trackers		L + 64:48:18.60	00:45:19.85
9. Reliable operation—radar altimeter (RORA) signal, following acquisition of lunar surface by radar altimeter (RA) beam tracker		L + 64:48:22.20	00:45:23.45
10. Main retro motor burnout (3.5g level sensed by inertia switch)	00:45:30.43	L + 64:48:28.87	00:45:30.12
11. Emergency retro case eject command received at spacecraft	00:45:38.43	L + 64:48:37.91	00:45:39.16
12. Vernier engine high thrust command received at spacecraft (200-lb thrust)		L + 64:48:38.49	00:45:39.74
13. RA beam tracker out of lock for 7 sec		L + 64:48:38.80	00:45:40.05
14. Emergency start programmed thrust command received at spacecraft (start RADVS-controlled descent; retro sequence mode off)	00:45:40.43	L + 64:48:39.91	00:45:41.16
15. DVS beam 3 tracker out of lock for 3 sec		L + 64:48:40.50	00:45:41.75
16. 1000-ft mark	00:46:14.44	L + 64:49:17.21	00:46:18.46
17. Programmed descent segment intercept and vernier thrust level increase	00:46:09.94	L + 64:49:19.85	00:46:21.10
18. 10-ft/sec mark	00:46:31.44	L + 64:49:34.61	00:46:35.86
19. 13-ft mark and vernier engines off	00:46:37.44	L + 64:49:40.21	00:46:41.46
20. Touchdown	00:46:39.14	L + 64:49:41.80	00:46:43.05
<sup>b</sup> Events are automatic unless a command is indicated. Time of occurrence of terminal descent events has been corrected for radio transmission delay to indicate time of occurrence at spacecraft.			

**Table A-2. Lunar operations<sup>a</sup>**

Date, 1967	Engineering (SPAC or DSIF)	Science (SSAC)	
		Television	Alpha scattering instrument
First lunar day			
Sept 11	Standard postlanding engineering assessment Initial postlanding solar panel and planar array (A/SPP) positioning Checkout of flight control and power modes to be used in vernier engine static firing experiment A/SPP positioning for attitude determination	Pad 3 to Pad 2 survey, 200-line mode 360-deg W/A panoramas (2) Mirror coverage of alpha scattering instrument	Data accumulation and calibration in stowed, background, and lunar surface positions
Sept 12	Dry run of static firing experiment	Special area and auxiliary mirror surveys Focus ranging: azimuths +36 and +18 deg N/A panorama: Segments 4, 5, 3, and 2 Photometric data collection (East-West)	Data accumulation and calibration
Sept 13	A/SPP positioning for safety during static firing experiment Static firing experiment (vernier engines on for 0.55 sec) A/SPP positioning for attitude determination	Special area surveys (3) Auxiliary mirror surveys (2) Star survey (unsuccessful): Venus, Rigel, Sirius, Canopus Mirror stepped to closed position for static firing experiment 360-deg W/A panorama N/A panorama: Segment 3 Periodic camera shutdowns due to high temperature	Data accumulation and calibration on second lunar sample
Sept 14	Spacecraft shutdowns (7) due to high temperature	Magnet surveys (2) Photometric data collection W/A color sequence of alpha scattering instrument Special area survey Auxiliary mirror survey 360-deg W/A panorama Star survey: Arcturus N/A panorama: Segments 4 and 3 Focus ranging: azimuth +108 deg	Data accumulation
Sept 15	A/SPP positioning to shade Compartment A and camera Spacecraft shutdowns (2) due to high temperatures Telecommunications signal processing test Bit error rate tests (2) to check combined spacecraft/DSIF telemetry performance	Photometric data collection 360-deg W/A panorama Color survey of magnet Special area survey Focus ranging: azimuths -90, -72, and -54 deg Star survey: Sirius Auxiliary mirror survey N/A panorama: Segments 2 and 5	No operations due to high temperature
aOther than routine engineering interrogations. All television sequences are 600-line mode unless otherwise noted. Wide angle and narrow angle are abbreviated W/A and N/A, respectively. DSIF two-way doppler tracking and resolver doppler counting was performed throughout lunar operations.			

Table A-2 (contd)

Date, 1967	Engineering (SPAC or DSIF)	Science (SSAC)	
		Television	Alpha scattering instrument
First lunar day (contd)			
Sept 16	A/SPP positioning to shade alpha scattering sensor head and Compartment A	Photometric data collection Color surveys of magnet (2) Crushable Block 1 area and auxiliary mirror surveys Focus ranging: azimuths —36, —18, 0, and +18 deg Star survey: Capella 360-deg W/A panorama N/A panorama: Segments 3, 4, and 5 W/A color sequence	Data accumulation and calibration
Sept 17 (lunar noon approximately 00:00 GMT)	A/SPP positioning to shade Compartment A Spacecraft shutdowns (2) due to high temperatures Radial measurements (3) of 85-ft antenna pattern (DSS 12) Optimum antenna pointing experiment	Magnet survey Photometric data collections (2) Crushable Block 1 area survey	Data accumulation and calibration
Sept 18	Spacecraft shutdowns (4) due to high temperatures Best-lock frequency test	Photometric data collection 360-deg W/A panorama Photometric data collection: Compartment B Magnet and auxiliary mirror surveys W/A color sequence W/A and N/A solar corona glare tests for calibration	Data accumulation and calibration
Sept 19	Best-lock frequency test Planar array positioning for optimum pointing	Star survey Photometric data collection Magnet, special area, and auxiliary mirror surveys 360-deg W/A panorama N/A color survey of lunar "rock"	Data accumulation and calibration
Sept 20	Bit error rate test TV gain margin test Best-lock frequency test	Photometric data collection Focus ranging: azimuths —144, —126, +124, and +108 deg 360-deg W/A panorama Star survey: Jupiter and Venus 360-deg N/A panorama Magnet and auxiliary mirror surveys Special area surveys (2)	Data accumulation and calibration
Sept 21	RF communications test	Photometric data collection 360-deg W/A panorama Magnet surveys (2) Special area and auxiliary mirror surveys Focus ranging: azimuths +90, +72, +54, and +36 deg W/A color survey Shadow progression sequences (3) 360-deg N/A panorama	Data accumulation and calibration

**Table A-2 (contd)**

Date, 1967	Engineering (SPAC or DSIF)	Science (SSAC)	
		Television	Alpha scattering instrument
First lunar day (contd)			
Sept 22	Planar array positioning to improve signal strength Telecommunications signal processing test	Shadow progression sequences (7) Magnet survey 360-deg W/A panoramas (2) W/A surveys (2): elevation —70 deg Special area surveys (2) Auxiliary mirror surveys (3) N/A panorama: lower half of Segments 1 and 5 Photometric data collection Focus rangings (2) 360-deg N/A panorama	Data accumulation and calibration
Sept 23	Landing gear commanded to lock; gear did not lock Best-lock frequency tests (2) Solar panel positioning to optimize battery charge	Shadow progression sequences (13) Auxiliary mirror surveys (2) 360-deg W/A panoramas (3) Magnet survey Crushable Blocks 1 and 3 areas survey Photometric data collection Magnet color surveys (2) 360-deg N/A panorama Star survey Special area survey Camera assessment and interrogation	Data accumulation and calibration Alpha scattering instrument turned off for lunar night
Sept 24 (lunar sunset: 10:56 GMT)	A/SPP final positioning for optimum attitude at sunrise on second lunar day Engineering interrogations for spacecraft status and science thermal data	Shadow progression sequences (10) N/A panoramas of horizon (4): Segments 1, 2, 3, and 4 Zero phase monitoring (camera pointed in same direction as sun-incidence) Solar corona experiment cycled with engineering interrogations Earthshine pictures (3) Camera secured for lunar night	
Sept 25 to Sept 29	Engineering interrogations for spacecraft status and science thermal data Spacecraft turned off for lunar night: 06:35 GMT, Sept 29		
Second lunar day			
Oct 15	Spacecraft turn-on: 08:07 GMT A/SPP positioning to charge battery, to shade Compartment A, and for attitude determination		Alpha scattering instrument turn-on: 23:14 GMT Data accumulation and calibration
Oct 16	Best-lock frequency tests (2) RF communications test Telecommunications signal processing test in low power A/SPP positioning to shade Compartment A	200-line and 600-line pictures to check camera (low amplitude video signal) Experiments to enhance video begun	Data accumulation and calibration



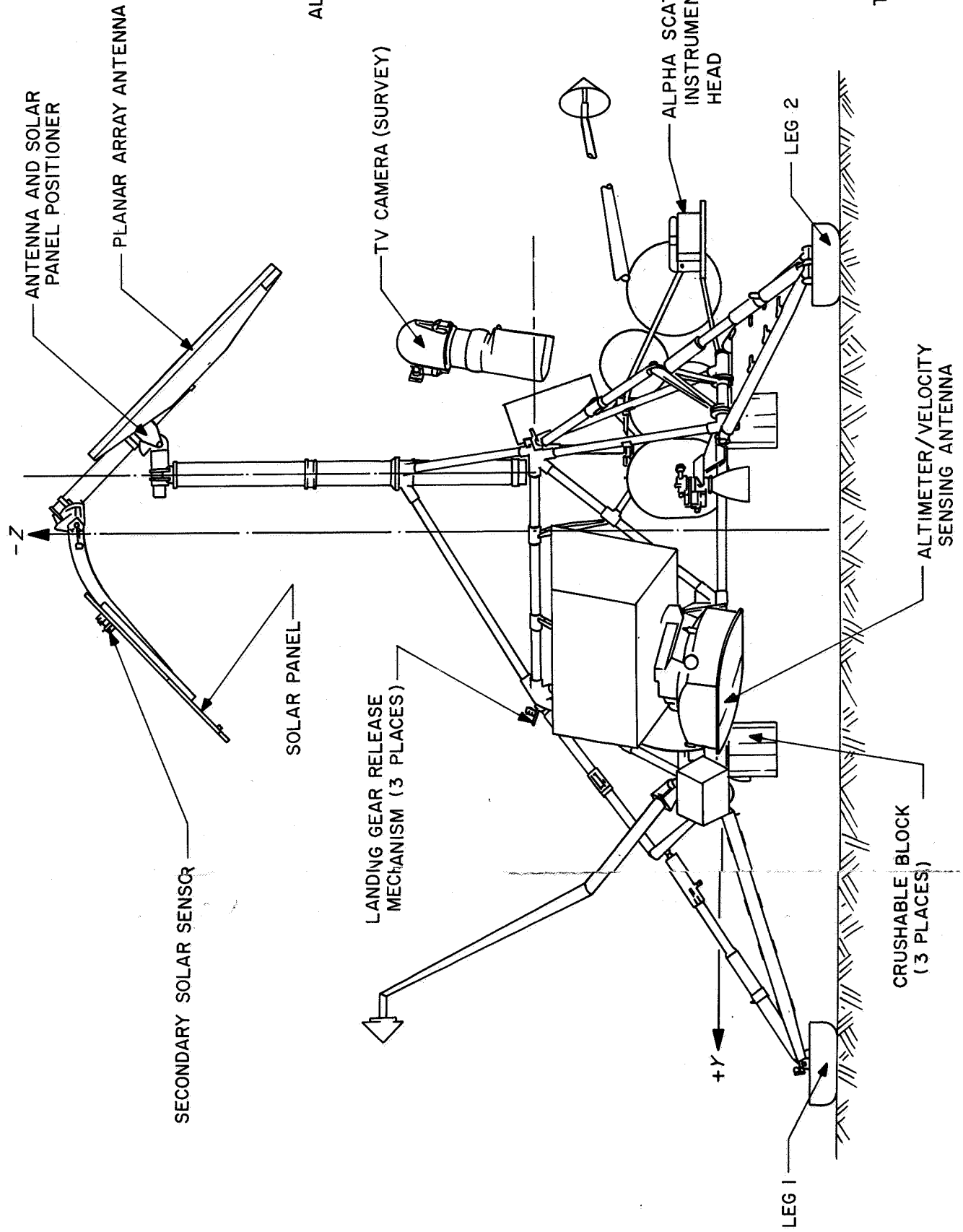
**Table A-2 (contd)**

Date, 1967	Engineering (SPAC or DSIF)	Science (SSAC)	
		Television	Alpha scattering instrument
Second lunar day (contd)			
Oct 17	Best-lock frequency tests (2) A/SPP positioning to shade Compartment A Spacecraft shutdowns (5) due to high temperature  Checkout of data link from Honeysuckle Creek, Australia, in preparation for eclipse operations	200-line (2) and 600-line pictures to check video signal	Data accumulation and calibration
Oct 18	Spacecraft shutdowns (2) due to high temperature and to DSN commitments to <i>Mariner V</i> Venus encounter A/SPP positioning for optimum attitude during eclipse Thermal data collection during eclipse period	Checks (2) of video signal	Data accumulation and calibration following eclipse
Oct 19	Spacecraft shutdown (1) due to high temperature Best-lock frequency tests (2) A/SPP positioning to shade Compartment A and to improve signal strength	Checks (2) of video signal	Data accumulation and calibration
Oct 20	Best-lock frequency tests (2) A/SPP positioning to charge battery Spacecraft shutdowns (3) to check solar panel switch and to increase battery charge rate	Checks (2) of video signal	Data accumulation and calibration
Oct 21	Attempt to lock landing gear (unsuccessful) DSS 14 telemetry test simulating terminal descent conditions Best-lock frequency test	N/A pictures of Vernier Engine 3, Crushable Blocks 1 and 3 areas, and Compartment A	Data accumulation and calibration
Oct 22	Best-lock frequency test Spacecraft shutdowns (6) to increase battery charging rate and to maintain compartment temperatures A/SPP positioning to charge battery	Pictures of various areas	Data accumulation and calibration
Oct 23 (lunar sunset: 23:38 GMT)	Engineering interrogations for spacecraft status and science thermal data	Pictures of various areas Camera secured for lunar night	Alpha scattering instrument turned off for lunar night
Oct 24 to Nov 1	Engineering interrogations for spacecraft status and science thermal data  Spacecraft turned off for lunar night: 12:20 GMT, Nov 1		

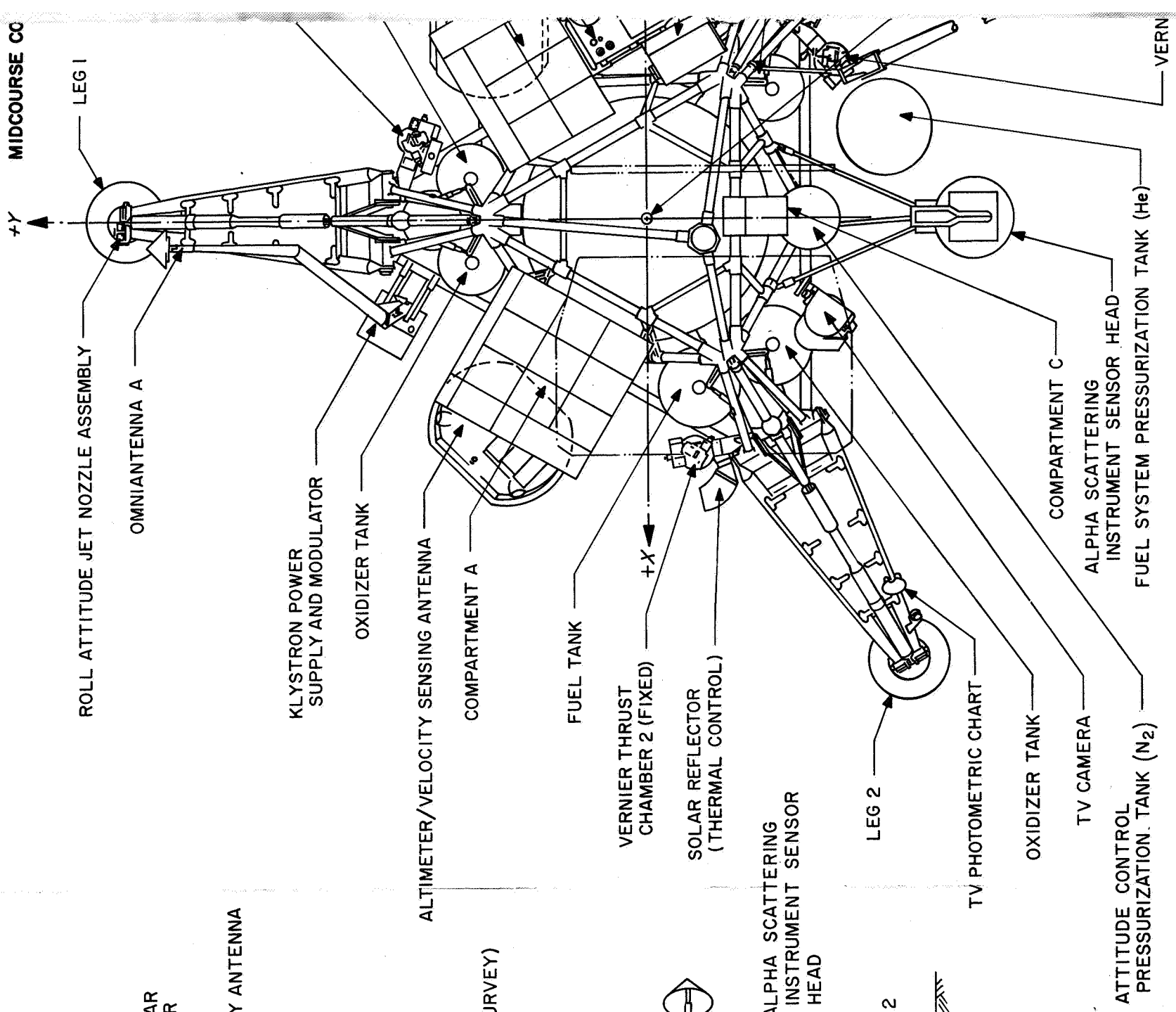
**Appendix B**  
***Surveyor V* Spacecraft Configuration**



# POSTLANDING CONFIGURATION



FOLDOUT FRAME 1

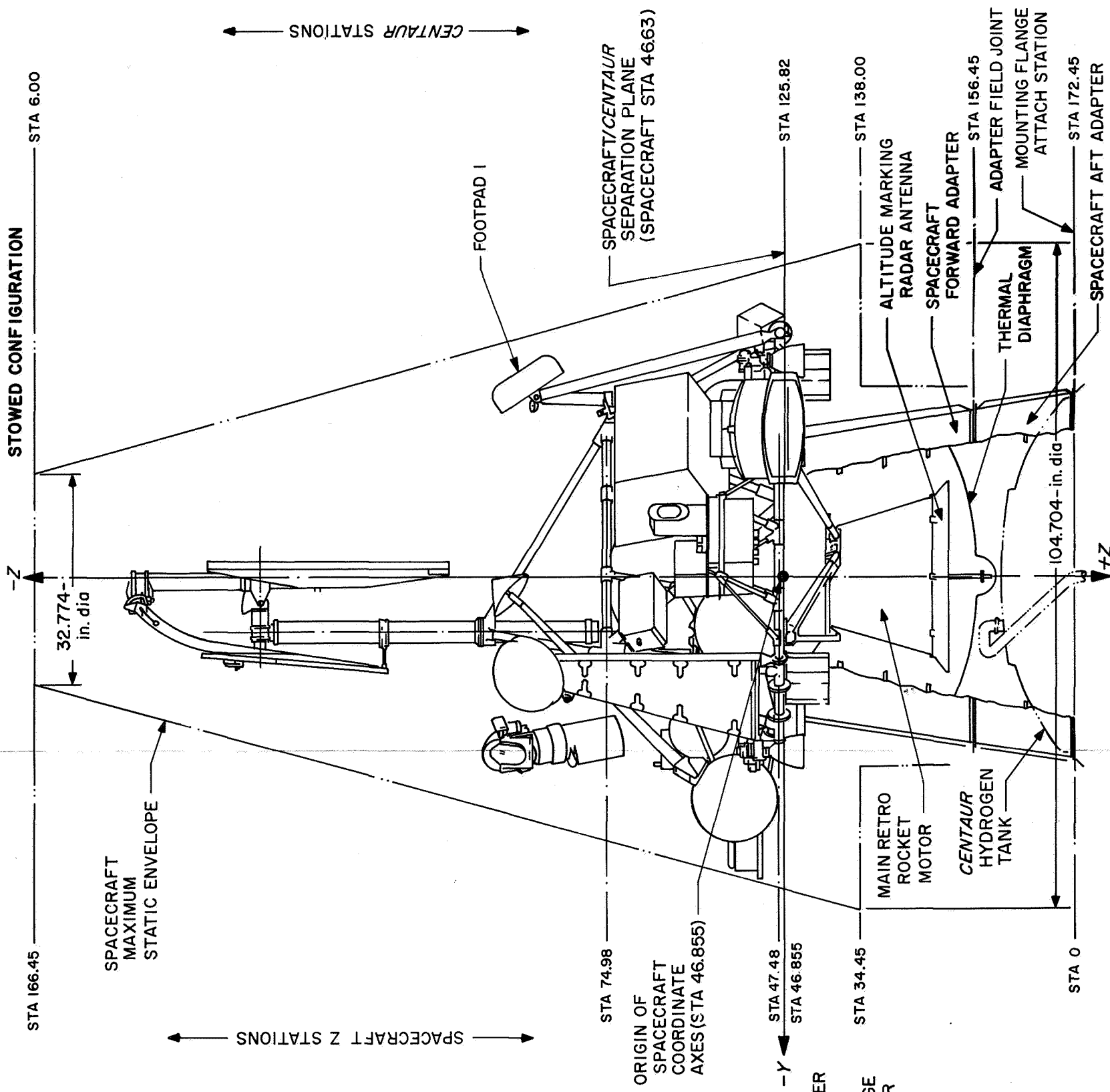
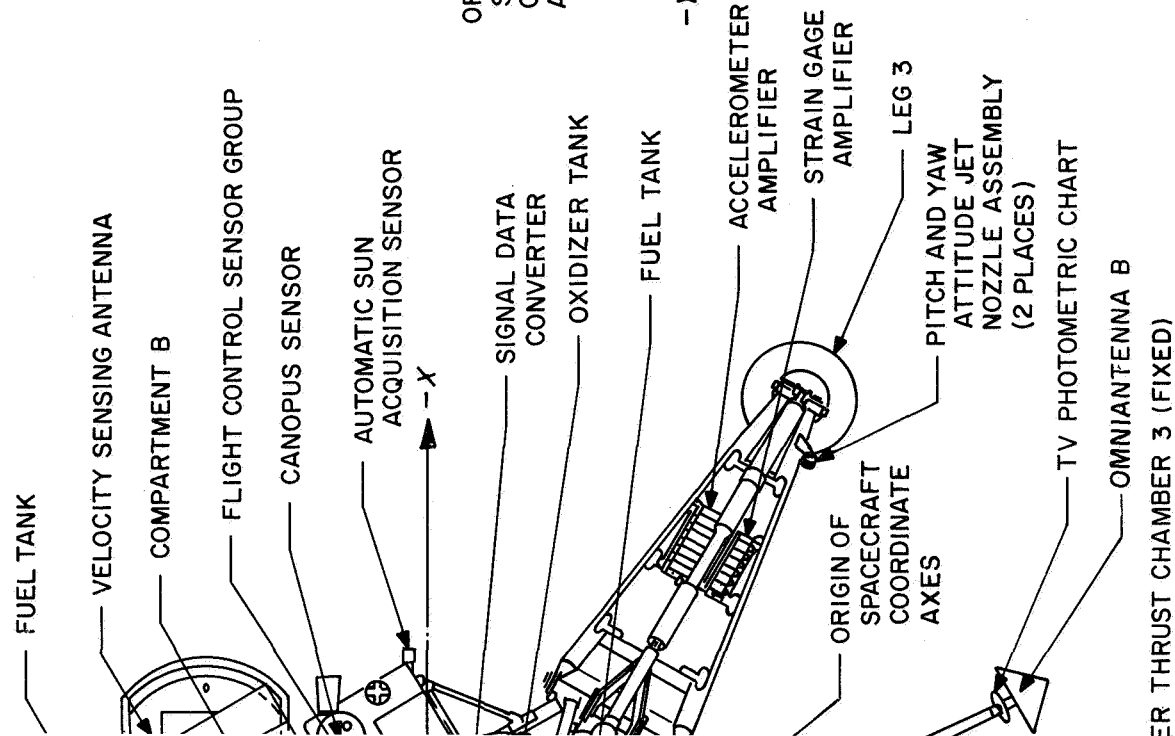


FOLDOUT FRAME 2

FIGURATION

NOTE:  
ANTENNA AND SOLAR PANEL  
POSITIONER HAS BEEN OMITTED  
FROM THIS VIEW FOR CLARITY

— VERNIER THRUST CHAMBER 1 (GIMBALLED)





**Appendix C**  
**Surveyor V Spacecraft**  
**Data Content of Telemetry Modes**

## ALPHA SCATTERING INSTRUMENT

CHAN	NAME	MODE 1 WORDS	MODE 2 WORDS	MODE 3 WORDS	MODE 4 WORDS	MODE C (5) WORDS	MODE T (6) WORDS
AS-3	SENSOR HEAD TEMP.				60		
AS-4	ELECTRONICS TEMP.				70		
AS-5	GUARD EVENT MONITOR				71		
AS-9	+24 VDC MONITOR				41		
<b>RADIO AND COMMAND DECODING (DATA LINK)</b>							
D-1	OWN 1 TRANSMITTER POWER				66		
D-3	OWN 2 TRANSMITTER POWER				11	57	
D-7	STATIC PHASE ERROR A				3,23,43,63,83	17	
D-8	RECEIVER A AGC				13,33,53,73,93	31	81
D-9	RECEIVER A AGC				17	31	79
D-10	TRANSMITTER A TEMPERATURE				2	6	30
D-13	TRANSMITTER A TEMPERATURE				12	30	37
D-16	RECEIVER A AFC				15,35,55,75,95	41	
D-17	RECEIVER B AFC						
<b>ELECTRICAL POWER</b>							
EP-2	3PV NON-ESSENTIAL VOLTAGE	90	90	48	7,37	59	69
EP-3	UNREGULATED BUS VOLTAGE	48	22	48	51	63	
EP-4	UNREGULATED OUTPUT CURRENT	22	22	48	22	45	9
EP-5	BOOST REG DIFFERENCE CURRENT				69	15	
EP-8	MAIN BATTERY TEMPERATURE	44	72	29	4	40	40
EP-9	BATTERY DISCHARGE CURRENT	72	29	29	29	29	29
EP-10	SOLAR CELL ARRAY CURRENT	59	59	29	8	26	20
EP-12	SOLAR CELL ARRAY TEMPERATURE	24	42	29	8	26	20
EP-14	BOOST REGULATOR TEMPERATURE	42	42	29	8	26	20
EP-17	REGULATED OUTPUT CURRENT	64	21	29	78	93	
EP-21	COMPARTMENT 8 HEATER CURRENT					35	
EP-22	BOOST REG. PREG. VOLTAGE					65	
EP-30	SOLAR CELL ARRAY REG. CURRENT					35	
EP-34	IRADIATED SOLAR CELL S.C. CURRENT					35	
EP-36	SOLAR CELL OPEN CRT. VOLTAGE	79	79			55	19
EP-37	FLIGHT CONTROL UNREGULATED CURRENT	32	32			19	
<b>FLIGHT CONTROL</b>							
FC-4	NITROGEN GAS PRESSURE	10,60				89	
FC-5	PRIM. SUN SENSOR PITCH ERROR	20,70				71	
FC-6	PRIM. SUN SENSOR YAW ERROR					99	
FC-8	SECONDARY SUN SENSOR CELL A	35	37			101	
FC-9	SECONDARY SUN SENSOR CELL B	37	37			105	
FC-10	SECONDARY SUN SENSOR CELL C	37	37			107	
FC-11	STAR INTENSITY SIGNAL	7,27,47,67				115	
FC-14	ACCELERATION ERROR	11,31,51,71,91					
FC-15	PITCH GYRO ERROR	12,62					
FC-16	YAW GYRO ERROR	12,62					
FC-17	ROLL GYRO ERROR	12,62					
FC-25	THRUST CMD TO VERNIER ENG 1	15,35,55,75,95					
FC-26	THRUST CMD TO VERNIER ENG 2	16,36,56,76,96					
FC-27	THRUST CMD TO VERNIER ENG 3	17,37,57,77,97					
FC-32	RETRO ACCELEROMETER	2,52					
FC-33	RETRO ACCELEROMETER	7,57					
FC-39	DOPPLER VELOCITY Vx	43,93					
FC-40	DOPPLER VELOCITY Vy	43,93					
FC-41	DOPPLER VELOCITY Vz	43,93					
FC-43	ROLL ACTUATOR SIGNAL	1,21,41,61,81					
FC-44	ROLL PRECISION COMMAND	41,91					
FC-45	FLIGHT CONTROL E/U TEMP 1	24					
FC-46	ROLL GYRO TEMPERATURE	60					
FC-47	CANOPUS SENSOR TEMPERATURE	17,37,57,77,97					
FC-49	PITCH PRECISION COMMAND	17					
FC-50	PITCH PRECISION COMMAND	17					
FC-51	YAW PRECISION COMMAND	17					
FC-52	PITCH GYRO TEMPERATURE	60					
FC-53	PITCH GYRO TEMPERATURE	60					
FC-55	YAW GYRO TEMPERATURE	60					
FC-70	ATTITUDE GAS JET 2 TEMP						
FC-71	ROLL ACTUATOR TEMPERATURE						
FC-77	FL. CONT. REFERENCE RETURN						
<b>MECHANICAL</b>							
M-3	SOLAR PANEL POSITION				71	57	
M-4	POLAR AXIS POSITION				98	91	
M-9	ELEVATION AXIS POSITION				87	91	
M-10	PLANAR ARRAY TEMPERATURE				14	38	
M-11	SOLAR PANEL STEP. MOTOR TEMP.				58	44	
M-12	ELEV. AXIS STEP. MOTOR TEMP.				64	106	
SPARE	(VOLTAGE)						
SPARE	(HIGH-ACC. TEMP)				5,25,45,65,85		
SPARE					80,90		
CHAN	NAME	MODE 1 WORDS	MODE 2 WORDS	MODE 3 WORDS	MODE 4 WORDS	MODE C (5) WORDS	MODE T (6) WORDS

\* COMPUTER ID NO. FOR PCM ANALOG SIGNALS/DIGITAL WORDS

## PROPULSION

CHAN	NAME	MODE 1 WORDS	MODE 2 WORDS	MODE 3 WORDS	MODE 4 WORDS	MODE C (5) WORDS	MODE T (6) WORDS
P-1	HELIUM PRESSURE	84	23			21	21
P-2	OXIDIZER PRESSURE	30	13			52	80
P-3	VERNIER LINES 2 TEMPERATURE	2	48			90	
P-4	VERNIER FUEL TANK 2 TEMP.					12	
P-5	VERNIER OXIDIZER TANK 2 TEMP.					70	
P-6	VERNIER LINES 1 TEMPERATURE	26	66			90	
P-7	VERNIER FUEL TANK 1 TEMP.	82	88			100	
P-8	VERNIER OXIDIZER TANK 1 TEMP.	40				50	
P-9	VERNIER LINES 3 TEMPERATURE					28	
P-10	VERNIER ENGINE 2 TEMPERATURE					4	
P-11	VERNIER FUEL TANK 3 TEMP.					54	
P-12	VERNIER OXIDIZER TANK 3 TEMP.					92	
P-13	VERNIER FUEL TANK 1 TEMP.					86	
P-14	VERNIER OXIDIZER TANK 1 TEMP.					7,37,57,97	
P-15	VERNIER FUEL TANK 2 TEMP.					1,41,71,101	
P-16	VERNIER OXIDIZER TANK 2 TEMP.					25,85	
P-17	VERNIER FUEL TANK 3 TEMP.					42	
P-18	VERNIER OXIDIZER TANK 3 TEMP.					84	
P-19	VERNIER ENGINE 1 STRAIN GAGE	13,33,53,73,93	13	13			
P-20	VERNIER ENGINE 2 STRAIN GAGE	14,34,54,74,94	14	14			
P-21	VERNIER FUEL LINE #1 TEMP	6,36	8	8			
P-22	VERNIER FUEL LINE #2 TEMP						
P-23	VERNIER FUEL LINE #3 TEMP						
P-24	VERNIER FUEL LINE #4 TEMP						
P-25	VERNIER FUEL LINE #5 TEMP						
P-26	VERNIER FUEL LINE PRESSURE	86	98				
<b>RADAR</b>							
R-2	RADVS-R AMPLITUDE			26			4,64
R-3	RADVS-D1 AMPLITUDE			28			4,64
R-4	RADVS-D2 AMPLITUDE			28			14,74
R-5	RADVS-D3 AMPLITUDE			46			34,94
R-6	AMR ANTENNA TEMPERATURE			54			
R-7	AMR ELECTRONICS TEMPERATURE			64			
R-8	RADVS KLY. UNIT TEMP.			8			28
R-9	DOPLER RADAR SENS. TEMP.			32			10
R-10	DOPLER RADAR SENS. TEMP.			94			22
R-12	AMR PWR OUTPUT (MAG CURRENT)			96			76
R-13	ALTIMETER RADAR SENS. TEMP.			96			59
R-14	ALTIMETER RADAR SENS. TEMP.			96			43
R-29	AMR LATE GATE SIGNAL			71			89
<b>SIGNAL PROCESSING</b>							
S-1	REFERENCE VOLTAGE			37			
S-2	COMMUTATOR UNBAL. CURR. (ESP)			31			
S-3	COMMUTATOR UNBAL. CURR. (AESP)			31			
S-5	ASP REFERENCE VOLTAGE					47	
S-8	MIL SCALE CURR. CALIB. (ESP)	92		92		81	
EP-19	MIL SCALE CURR. CALIB. (ESP)	32		32			
EP-20	ZERO SCALE CURR. CALIB. (ESP)	19		19			
EP-27	FULL SCALE CURR. CALIB. (AESP)					73	
EP-28	MID-SCALE CURR. CALIB. (AESP)					93	
EP-29	ZERO SCALE CURR. CALIB. (AESP)						
<b>TELEVISION</b>							
TV-16	SURV. CAM. ELECTRONICS TEMP.				16		
TV-17	SURV. MIRROR ASST. TEMP.				82		
<b>STRUCTURES (VEHICLE)</b>							
V-5	LANDING GEAR 1 DEFLECTION						
V-9	LANDING GEAR 3 DEFLECTION						
V-15	COMP. A TEMP. LOWER SUPPORT						
V-16	COMP. A TEMP. CANISTER CONT. RING						
V-18	COMP. A TEMP. SW. 5 IN FACE RAD.						
V-20	COMP. A TEMP. TRAY TOP CENTER						
V-21	COMP. B TEMP. LOWER SUPPORT						
V-22	COMP. B TEMP. SW. 4 IN FACE RAD.						
V-23	COMP. B TEMP. SW. 5 IN FACE RAD.						
V-25	COMP. B TEMP. SW. 8 IN FACE RAD.						
V-26	COMP. B TEMP. SW. 4 IN CONT. RING						
V-27	UPPER SPACEFRAME TENDON COMP. A						
V-29	WIRE HARN. TEMP. THERM TUNNEL						
V-30	SHOCK ABSORB 2 TEMPERATURE						
V-32	SHOCK ABSORB 2 TEMPERATURE						
V-33	UPPER SPACEFRAME TEMP. NO. 2						
V-35	UPPER SPACEFRAME TEMP. UNDER COMP. 3						
V-36	RETRO ATTACH POINT 1 TEMP.						
V-38	RETRO ATTACH POINT 2 TEMP.						
V-44	CRUSHABLE BLOCK TEMP.						
V-45	COMP. B TEMP. SW. 1 IN FACE RAD.						
V-46	COMP. B TEMP. SW. 5 IN FACE RAD.						
V-47	COMP. A TEMP. SW. 4 IN FACE RAD.						
V-49	COMP. A TEMP. SW. 3 IN FACE RAD.						







**Appendix D**  
**Surveyor V Spacecraft Temperature Histories**

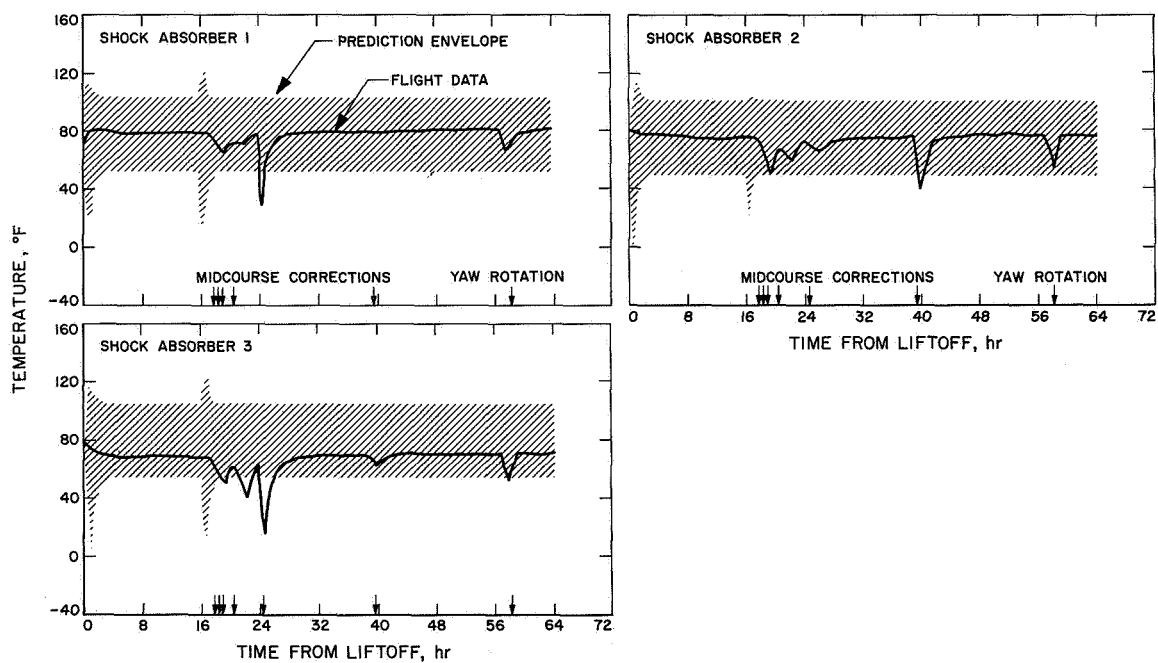


**Fig. D-1. Landing gear transit temperatures**

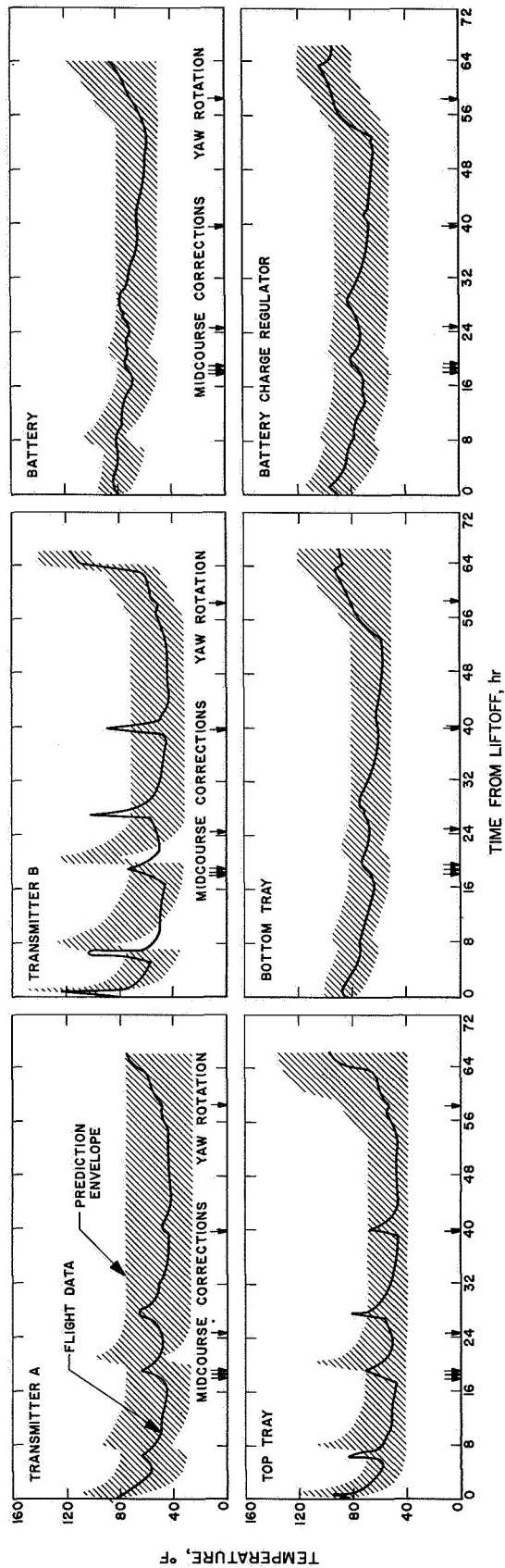


Fig. D-2. Compartment A transit temperatures

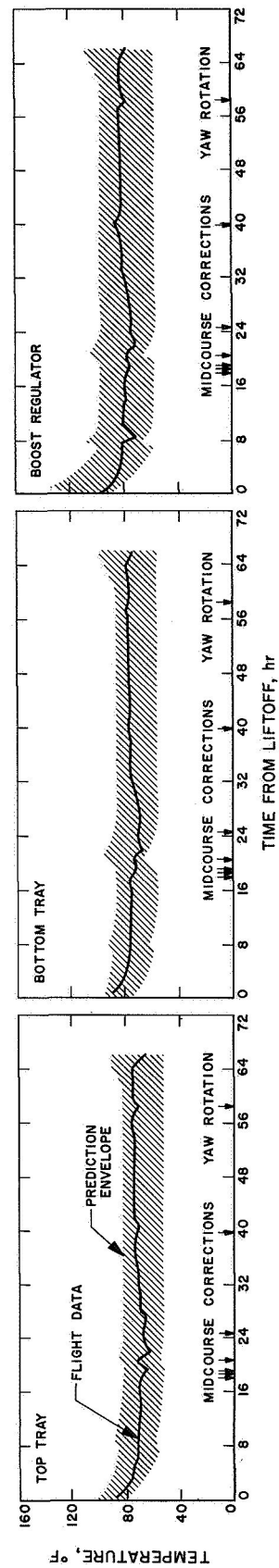
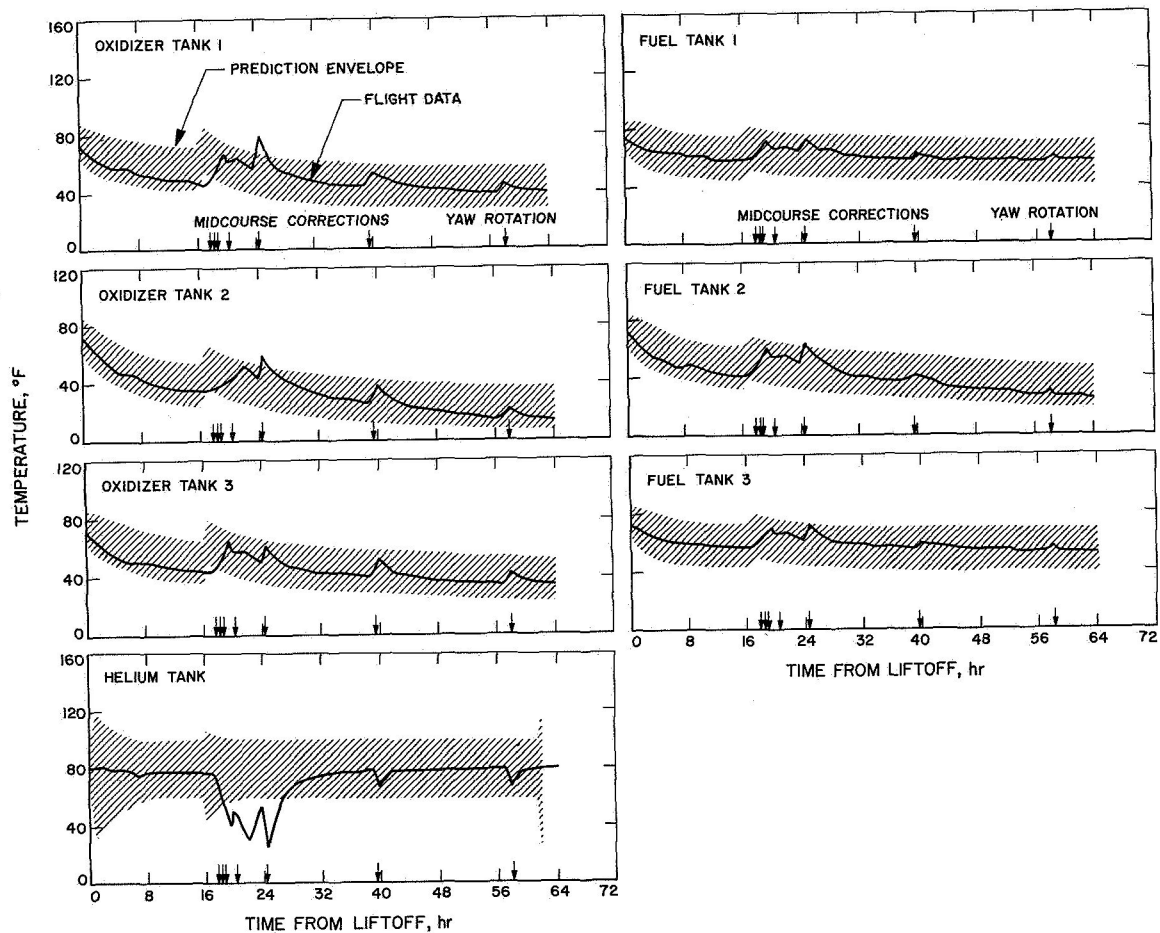


Fig. D-3. Compartment B temperatures



**Fig. D-4. Vernier propulsion system temperatures**

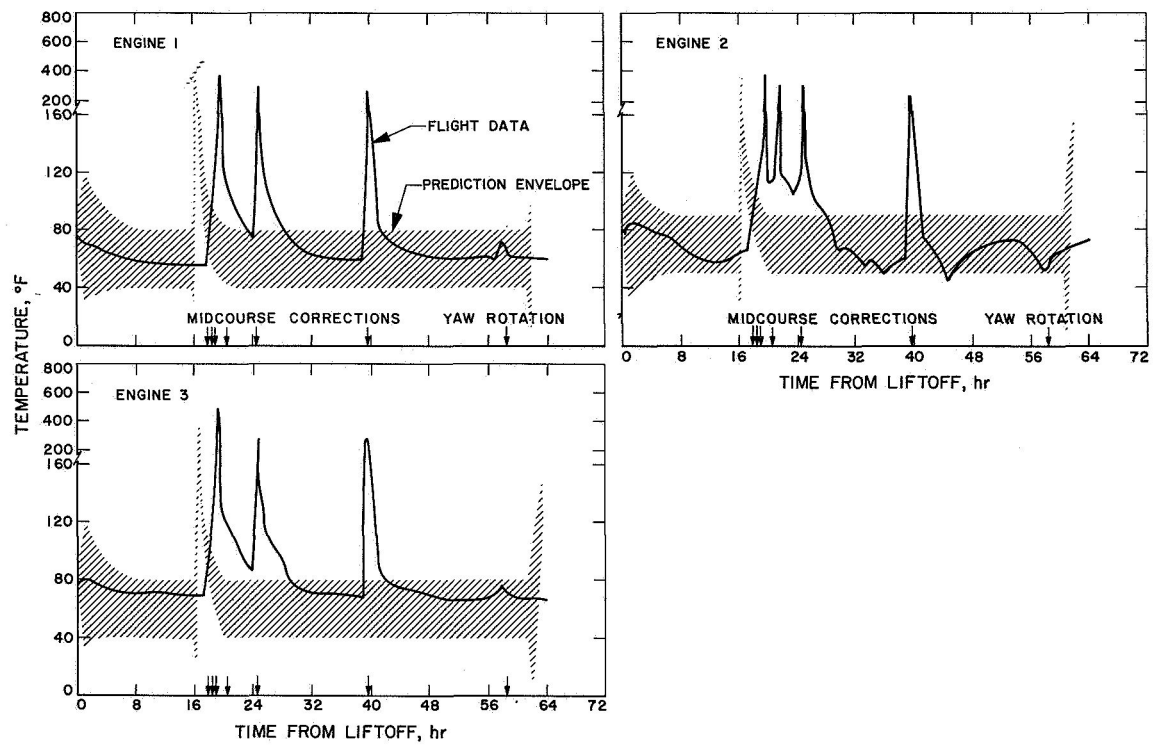


Fig. D-4 (contd)

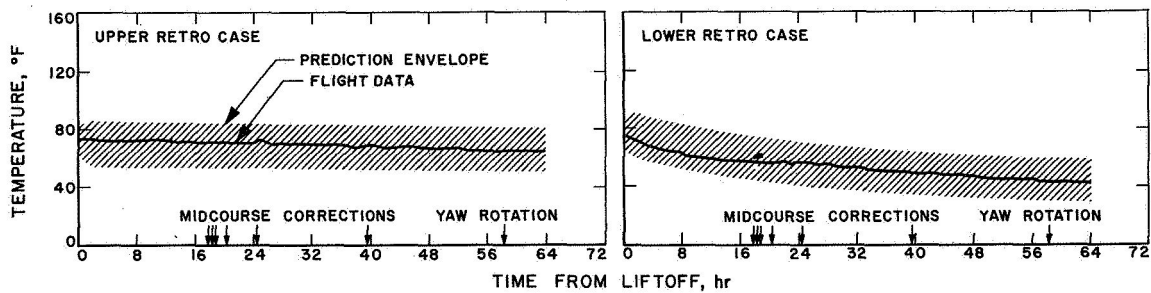


Fig. D-5. Main retrorotor transit temperatures

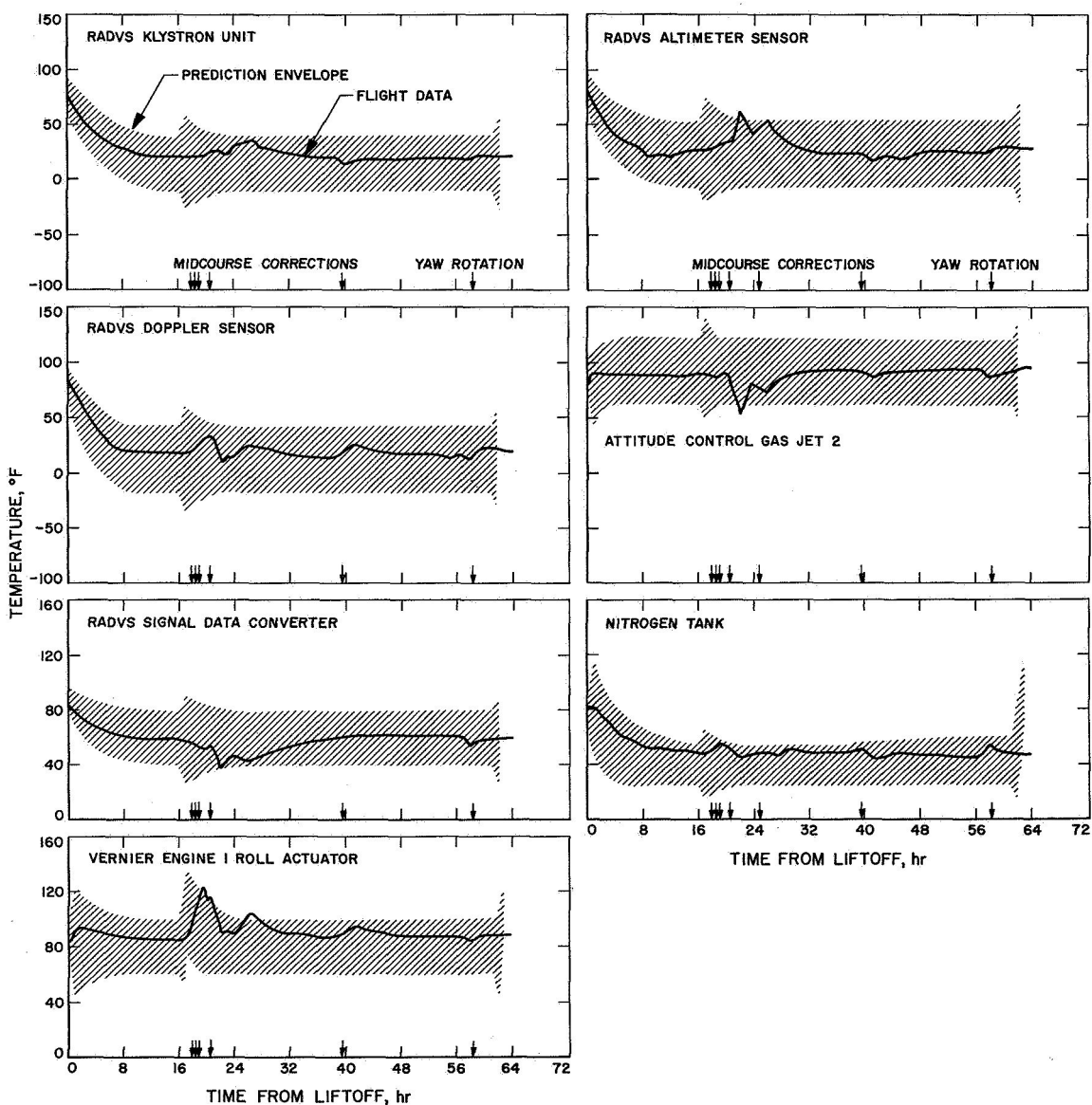


Fig. D-6. Radar and flight control temperatures



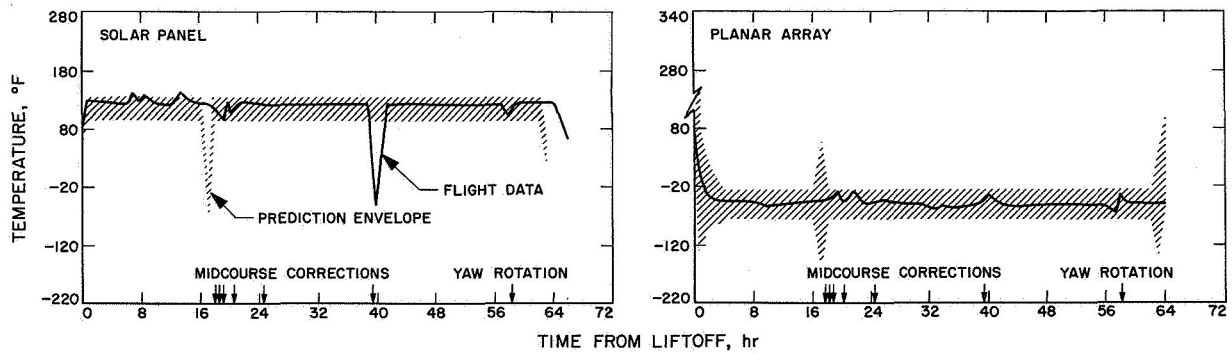


Fig. D-7. Solar panel and planar array transit temperatures

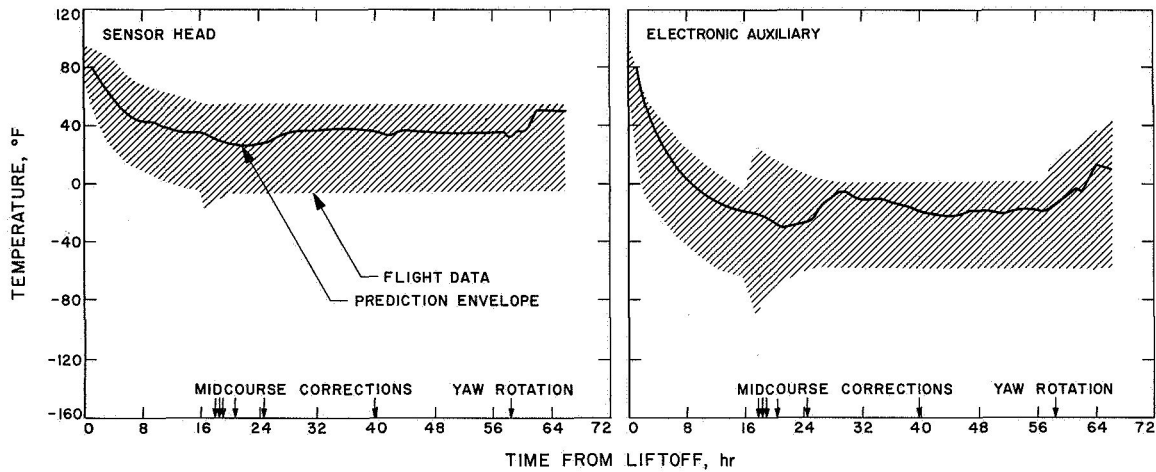


Fig. D-8. Alpha scattering instrument transit temperatures

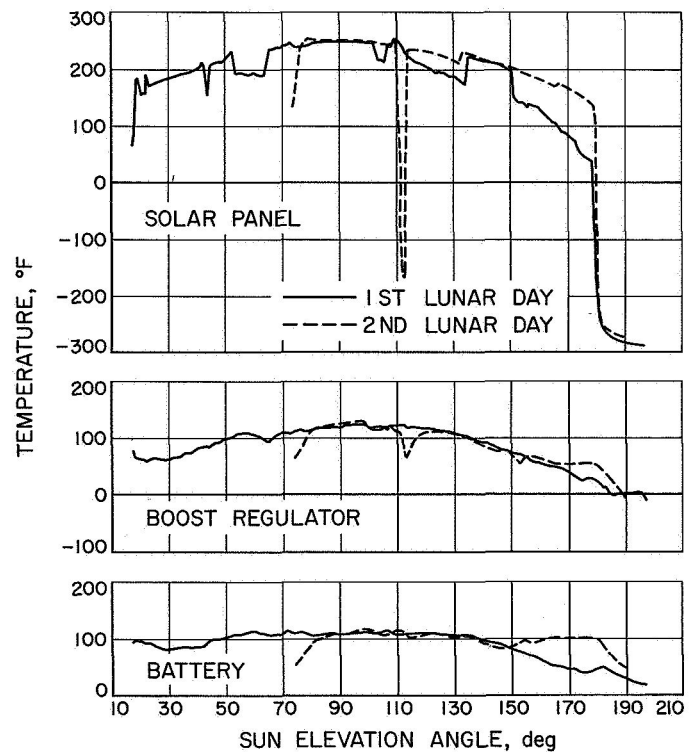
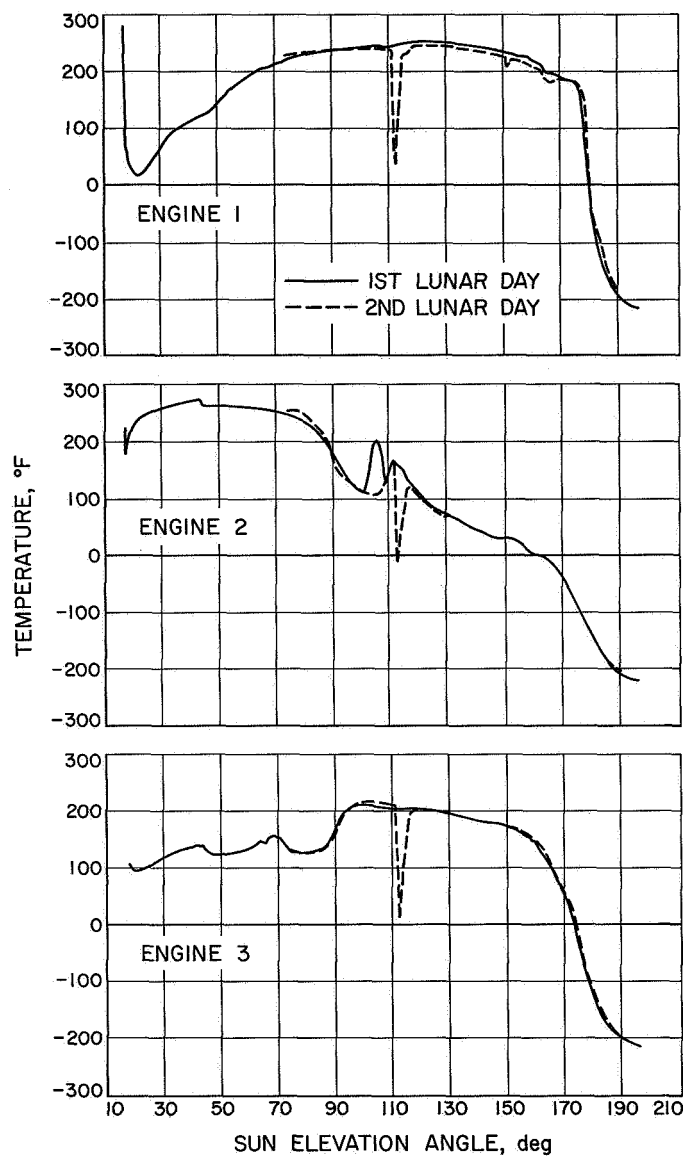
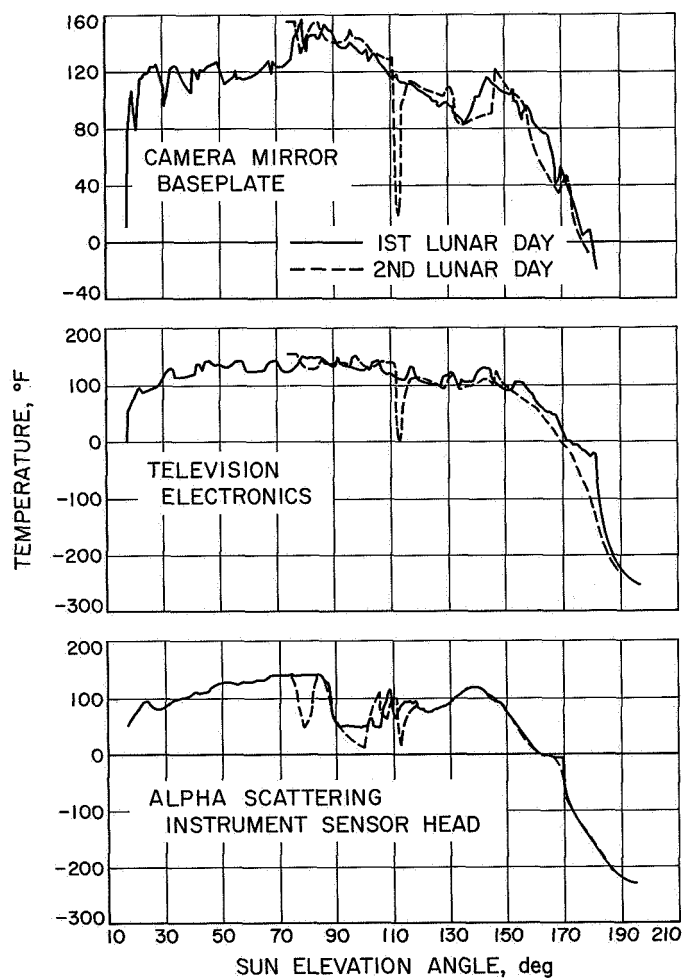


Fig. D-9. Electrical power subsystem postlanding temperatures



**Fig. D-10. Vernier propulsion subsystem postlanding temperatures**



**Fig. D-11. Television camera and alpha scattering instrument postlanding temperatures**

## Glossary

ABC	auxiliary battery control	FRB	Failure Review Board
AC	<i>Atlas/Centaur</i>	FRT	fine resolution tracking
A/D	analog-to-digital	CCF	Ground Communications Facility
ADC	analog-to-digital converter	GSE	ground support equipment
AESP	auxiliary engineering signal processor	GSFC	Goddard Space Flight Center
AFC	automatic frequency control	HSDL	high-speed data line
AFETR	Air Force Eastern Test Range	ICS	Intracommunications System
AGE	aerospace ground equipment	IF	intermediate frequency
AOS	acquisition of signal	I/O	input/output
APC	automatic phase control	IRIG	Inter-Range Instrumentation Group
A/SPP	antenna and solar panel positioner	IRV	interrange vector
BCD	binary coded digital	J-FACT	Joint Flight Acceptance Composite Test
BECO	booster engine cutoff	KPSM	klystron power supply modulator
BR	boost regulator	KSC	Kennedy Space Center
CCC	Central Computing Complex	LOS	loss of signal
CDC	command and data (handling) console	MAG	Maneuver Analysis Group
CDS	computer data system	MCDR	media conversion data recovery (subsystem)
CP	Command Preparation (Group)	MCFR	media conversion film recorder (subsystem)
CRT	Composite Readiness Test	MECO	main engine cutoff
CSP	central signal processor	MES	main engine start
CSTS	Combined Systems Test Stand	MSFN	Manned Space Flight Network
DC	direct command	NASCOM	NASA World-Wide Communication Network
DOD	Department of Defense	OCR	optimum charge regulator
DPS	Data Processing System	ODG	Orbit Determination Group
DSCC	Deep Space Communications Complex	ORT	Operational Readiness Test
DSIF	Deep Space Instrumentation Facility	OSCP	on-site computer program
DSS	Deep Space Station	OSDP	on-site data processing
DVS	doppler velocity sensor	OSDR	on-site data recovery (subsystem)
ECPO	Engineering Computer Program Operations (Group)	OSFR	on-site film recorder (subsystem)
EM	electromagnetic	OTC	overload trip circuit
EMA	engineering mechanism auxiliary	OVCS	operational voice communication system
ESF	Explosive Safe Facility	PA	Performance Analysis (Group)
ESP	engineering signal processor	PAM	pulse-amplitude modulation
FC	flight control	PCM	pulse code modulation
FCSG	Flight Control Sensor Group	PLIM	postlaunch instrumentation message
FPAC	Flight Path Analysis and Command	PU	propellant utilization

## Glossary (contd)

PUVEP	propellant utilization valve electronics package	SCAT	Spacecraft Analysis Team
PVT	Performance Verification Tests	SPAC	Spacecraft Performance Analysis and Command (Group)
QC	quantitative command	SSAC	Space Science Analysis and Command
RA	radar altimeter	SSD	subsystem decoder
RADVS	radar altimeter doppler velocity sensor	SSE	Standard Sequence of Events
RATAC	radar target acquisition (system)	STEA	system test equipment assembly
RETMA	Radio Electronics Television Manufacturing Association	STV	solar-thermal-vacuum
RFI	radio frequency interference	TCP	telemetry and command processor
RIS	range instrumentation ship	TDA	Tracking Data Analysis (Group)
RODVS	reliable operate doppler velocity sensor	TDM	time division multiplexer
RORA	reliable operate radar altimeter	TDS	Tracking and Data System
RTCS	Real Time Computer System, Cape Kennedy	T&DA	tracking and data acquisition
SDC	signal data converter	TelPAC	Television Performance Analysis and Command (Group)
SECO	sustainer engine cutoff	TPS	Telemetry Processing Station
SFOD	Space Flight Operations Director	TSAC	Television Science Analysis and Command (Group)
SFOF	Space Flight Operations Facility	TTY	teletype
SOCP	<i>Surveyor</i> on-site computer program	TV-GDHS	TV Ground Data Handling System
SOPM	standard orbital parameter message	VCXO	voltage-controlled crystal oscillator
SOV	solenoid-operated valves	VECO	vernier engine cutoff
SRT	System Readiness Test	VPS	vernier propulsion system

## Bibliography

### Project and Mission

- Surveyor A-G Project Development Plan*, Project Document 13, Vol. 1, Jet Propulsion Laboratory, Pasadena, January 3, 1966.
- Clarke, V. C., Jr., *Surveyor Project Objectives and Flight Objectives for Missions A through D*, Project Document 34, Jet Propulsion Laboratory, Pasadena, March 15, 1965.
- Willingham, D. E., *Lunar Surface Generation and Surveyor Landing Analysis*, Project Document 602-4, Jet Propulsion Laboratory, Pasadena, March 25, 1967.
- Macomber, H. L., *Surveyor E Mission Plan*, Project Document 602-30, Jet Propulsion Laboratory, Pasadena, August 25, 1967.
- Surveyor I Mission Report. Part I. Mission Description and Performance*, Technical Report 32-1023, Jet Propulsion Laboratory, Pasadena, August 31, 1966.
- Surveyor II Mission Report. Mission Description and Performance*, Technical Report 32-1086, Jet Propulsion Laboratory, Pasadena, April 1, 1967.
- Surveyor III Mission Report. Part I. Mission Description and Performance*, Technical Report 32-1177, Jet Propulsion Laboratory, Pasadena, September 1, 1967.
- Surveyor IV Mission Report. Part I. Mission Description and Performance*, Technical Report 32-1210, Jet Propulsion Laboratory, Pasadena, January 1, 1968.

### Launch Operations

- Macomber, H. L., *Surveyor Launch Constraints Document*, Project Document 43, Rev. 1, Jet Propulsion Laboratory, Pasadena, March 6, 1967.
- Macomber, H. L., *Surveyor Launch Constraints, Mission E—September 1967 Launch Opportunity*, Project Document 43, Rev. 1, Addendum No. 5, Jet Propulsion Laboratory, Pasadena, August 17, 1967.
- Centaur Unified Test Plan, AC-13/SC-5 Launch Operations and Flight Plan (Surveyor Mission E)*, Section 8.13B, Report AY62-0047, Rev. A, General Dynamics/Convair, San Diego, August 14, 1967.
- Test Procedure Centaur/Surveyor Launch Countdown Operations, AC-13/SC-5 Launch (CTP-INT-1001E)*, Report AA65-0500-008-04E, General Dynamics/Convair, San Diego, August 23, 1967.
- Atlas/Centaur-13 Surveyor-E, Operations Summary*, TR-567, Centaur Operations Branch, KSC/ULO, Cape Kennedy, September 1, 1967.
- Barnum, P. W., *JPL/ETR Field Station Launch Operations Plan, Surveyor Missions E, F and G*, JPL/ETR Field Station Document 690-11, Jet Propulsion Laboratory, ETR Field Station, Cape Kennedy, September 1, 1967.
- Atlas/Centaur-13 Surveyor-5, Flash Flight Report*, Report TR-569, Centaur Operations Branch, KSC/ULO, Cape Kennedy, September 13, 1967.
- Macomber, H. L., *Surveyor V Launch Phase Mission Analysis Report*, Section 312 Interoffice Technical Memorandum 312-862, Jet Propulsion Laboratory, Pasadena, December 8, 1967.

## Bibliography (contd)

### Launch Vehicle System

Shaffer, J., Jr., *Surveyor Spacecraft/Atlas-Centaur Launch Vehicle Interface Requirements*, Project Document 1, Rev. 3, Jet Propulsion Laboratory, Pasadena, September 1, 1967.

*Atlas Space Launch Vehicle Systems Summary*, Report GDC-BGJ67-001, General Dynamics/Convair, San Diego, February, 1967.

*Centaur Systems Summary*, Report GDC-BGJ67-003, General Dynamics/Convair, San Diego, April 1967.

*Centaur Technical Handbook*, Convair Division, Report GD/C-BPM64-001-2, Rev. C, General Dynamics/Convair, San Diego, March 20, 1967.

*Centaur Monthly Configuration, Performance and Weight Status Report*, Report GDC63-0495-49 General Dynamics/Convair, San Diego, August 21, 1967.

*Preliminary AC-13 Atlas-Centaur Flight Evaluation* (by staff of Lewis Research Center, Cleveland, Ohio), NASA Technical Memorandum X-52356, NASA, Washington, D.C., 1967.

*Atlas/Centaur AC-13 Flight Evaluation Report*, GDC-BNZ67-069, General Dynamics/Convair, San Diego, December 1, 1967.

### Spacecraft System

*Surveyor Spacecraft A-21 Functional Description*, Document 239524 (HAC Pub. 70-93401), 3 Vols., Hughes Aircraft Co., El Segundo, Calif., November 1, 1964 (with revision sheets).

*Surveyor Spacecraft A-21 Model Description*, Document 224847B, Hughes Aircraft Co., El Segundo, Calif., March 1, 1965 (with revision sheets).

*Surveyor Spacecraft Monthly Performance Assessment Report*, SSD 68252-11, Hughes Aircraft Co., El Segundo, Calif., September 21, 1967.

*Surveyor SC-5 Review Committee Report*, Report 2227.1/2177, Hughes Aircraft Co., El Segundo, Calif., September 29, 1967 (Revised October 27, 1967).

*Surveyor V Flight Performance Final Report*, SSD 68189-5, Hughes Aircraft Co., El Segundo, Calif., November 1967.

### Tracking and Data Acquisition

*Program Requirements No. 3400, Surveyor*, Revision 14, Air Force Eastern Test Range, Patrick Air Force Base, Fla., April 25, 1967.

*Operations Requirement No. 3400, Surveyor Launch*, Revision 9, Air Force Eastern Test Range, Patrick Air Force Base, Fla., August 3, 1967.

*Operations Directive No. 3400, Surveyor Launch*, Revision 1, Air Force Eastern Test Range, Patrick Air Force Base, Fla., August 14, 1967.

*Project Surveyor—Support Instrumentation Requirements Document*, Rev. 4, prepared by JPL for NASA, August 18, 1967.

## Bibliography (contd)

### Tracking and Data Acquisition (contd)

- Surveyor Project/Deep Space Network Interface Agreement*, Engineering Planning Document 260, Rev. 2, Jet Propulsion Laboratory, Pasadena, November 22, 1965.
- DSIF Tracking Instruction Manual (TIM), Surveyor Mission B* (4 volumes), Engineering Planning Document 391, Jet Propulsion Laboratory, Pasadena, August 1966 (with revision sheets for Mission E).
- Elliott, C. F., *Preflight Readiness Review of Tracking and Data System, Near Earth Phase, for Surveyor Mission E*, JPL/ETR Field Station Document 690-15, Jet Propulsion Laboratory ETR Field Station, Cape Kennedy, September 22, 1967.
- Elliott, C. F., *Report on Tracking and Data System, Near-Earth Phase, for Surveyor E*, JPL/ETR Field Station Document 690-16, Jet Propulsion Laboratory, ETR Field Station, Cape Kennedy, October 10, 1967.

### Mission Operations System

- Surveyor Mission Operations System*, Technical Memorandum 33-264, Jet Propulsion Laboratory, Pasadena, April 4, 1966.
- Space Flight Operations Plan—Surveyor Missions E, F and G*, Engineering Planning Document 180-S/ME, F and G, Jet Propulsion Laboratory, Pasadena, July 24, 1967 (and revision sheets through August 15, 1967).
- Goble, M. E., *Surveyor Lunar Operations Plan—Mission E*, Engineering Planning Document 486-ME (Project Document 602-1, Revision 2), Jet Propulsion Laboratory, Pasadena, August 10, 1967 (with changes of September 1, 1967).
- Goble, M. E., *Surveyor Lunar Operations Plan, Second Lunar Day—Mission E*, Engineering Planning Document 486-ME-A (Project Document 602-1, Revision 3), Jet Propulsion Laboratory, Pasadena, September 29, 1967.
- Surveyor Mission E Space Flight Operations Report*, Report SSD 78160, Hughes Aircraft Co., El Segundo, Calif., October 1967.
- Callan, R., *Space Flight Operations Memorandum—Surveyor V*, Project Document 602-38, Jet Propulsion Laboratory, Pasadena, November 15, 1967.

### Flight Path

- Davids, L., Meredith, C., and Ribarich, J., *Midcourse and Terminal Guidance Operations Programs*, SSD 4051R, Hughes Aircraft Co., El Segundo, Calif., April 1964.
- Cheng, R. K., Meredith, C. M., and Conrad, D. A., *Design Considerations for Surveyor Guidance*, IDC 2253.2/473, Hughes Aircraft Co., El Segundo, Calif., October 15, 1965.
- Surveyor Spacecraft/Launch Vehicle Guidance and Trajectory Interface Schedule*, Project Document 14, Rev. 3, Jet Propulsion Laboratory, Pasadena, November 30, 1966.

## Bibliography (contd)

### Flight Path (contd)

- Surveyor/Centaur Target Criteria—Surveyor Mission E*, Specification LS501486, Revision A, Jet Propulsion Laboratory, Pasadena, June 21, 1967.
- Fisher, J. N., and Gillett, R. W., *Surveyor Parking Orbit Trajectory Characteristics*, SSD 68219R, Hughes Aircraft Co., El Segundo, Calif., November 1966.
- Surveyor Station View Periods and Parking Orbit Trajectory Coordinates—Launch Dates July, August, September 1967*, SSD 68242-2, Hughes Aircraft Co., El Segundo, Calif., December 1966.
- Pavlick, T. J., *Pre-Injection Trajectory Characteristics Report—AC-13*, GDC-BKM67-055, General Dynamics/Convair, San Diego, July 1967.
- Dunn, H. S., *Surveyor Mission E Post-Injection Standard Trajectories*, SSD 68169-4 and Appendix A (SSD 78116), Hughes Aircraft Co., El Segundo, Calif., July 1967.
- Gans, J. F., *Surveyor Mission E Final Preflight Maneuver Analysis Report*, SSD 68230-3 and Appendix A (SSD 78123), Hughes Aircraft Co., El Segundo, Calif., August 1967.
- AC-13 Final Guidance Equations and Performance Analysis*, GDC-BKM67-059, General Dynamics/Convair, San Diego, August 1967.
- O'Connell, H. P., and West, M., *Firing Tables—AC-13, September Opportunity*, GDC-BKM67-051, and Appendix A, General Dynamics/Convair, San Diego, August 10, 1967.
- Surveyor V Flight Path Analysis and Command Operational Report*, SSD 74131, Hughes Aircraft Co., El Segundo, Calif., October 17, 1967.